Socioeconomic Differences and Secular Changes in Living Conditions in Late-Medieval and Postmedieval Luxembourg City

Dissertation

der Mathematisch-Naturwissenschaftlichen Fakultät

der Eberhard Karls Universität Tübingen

zur Erlangung des Grades eines

Doktors der Naturwissenschaften

(Dr. rer. nat.)

vorgelegt von

Anne Kremmer

aus Luxemburg Stadt /Luxemburg

Tübingen

2023

Gedruckt mit Genehmigung der Mathematisch-Naturwissenschaftlichen Fakultät der Eberhard Karls Universität Tübingen.

Tag der mündlichen Qualifikation:	16.06.2023
Dekan:	Prof. Dr. Thilo Stehle
1. Berichterstatter/-in:	Prof. Dr. Hervé Bocherens
2. Berichterstatter/-in:	Prof. Dr. Joachim Wahl

Table of Contents

1 Introduction 9

1.1 Aims of the study 11

1.2 Historical setting 13

1.3 Social stratification in Luxembourg City 16

1.4 The Franciscans, their church and their friary: Historical evidence 18

2 Materials and Methods 21

2.1 Methods 21
2.1.1 Statistical analyses 21

2.2 Material 22
2.2.1 Archaeological context 22
2.2.2 Body orientation and Position of the arms. 30
2.2.3 Data collection, preparation, and equipment 33
2.2.4 Representation and Preservation 35

3 Palaeodemography 39

3.1 Individual Data 39
3.1.1 Introduction 39
3.1.2 Age estimation 40
3.1.3 Sex estimation 51

3.2 Palaeodemography 62
3.2.1 Introduction 62
3.2.2 Methods 63
3.2.3 Results 66
3.2.4 Discussion 73
3.2.5 Conclusion 79

4 Growth 80

4.1 Introduction 80

4.2 Methods 80
4.2.1 Subadults 80
4.2.2 Adults 82

4.3 Results 84
4.3.1 Growth in Subadults 84
4.3.2 Body Height in Adults 87
4.3.3 Body Mass in Adults 88

4.4 Discussion and Conclusion 90
4.4.1 Growth 90
4.4.2 Achieved body height and weight 92
4.4.3 Conclusion 100

5 Physical adaptations to external stress 101

5.1 Bilateral asymmetry 102
5.1.1 Introduction 102
5.1.2 Methods 103
5.1.3 Results 103
5.1.4 Discussion and Conclusion 116

5.2 Indices of the postcranial skeleton 122
5.2.1 Introduction 122
5.2.2 Methods 124

5.2.3 Results 130
5.2.4 Discussion and Conclusion 150

5.3 Entheseal changes 155
5.3.1 Introduction 155
5.3.2 Methods 155
5.3.3 Results 157
5.3.4 Discussion and Conclusion 167

5.4 Reconstruction of habitual body posture 171
5.4.1 Introduction 171
5.4.2 Methods 171
5.4.3 Results 172
5.4.4 Discussion and Conclusion 174

6 Palaepathology 176

6.1 Joint diseases 176
6.1.1 Degenerative Joint disease and Osteoarthritis 177
6.1.2 Ankylosis of joints 201
6.1.3 Osteochondritis dissecans 202
6.1.4 Degenerative joint disease of the spine 204
6.1.5 DISH 225

6.2 Congenital defects 231
6.2.1 Introduction 231
6.2.2 Results and Discussion 231

6.3 Neoplastic disease 250
6.3.1 Introduction 250
6.3.2 Osteomata 251
6.3.3 Intraosseous ganglia 253
6.3.4 Malignant neoplasms 261

6.4 Miscellaneous Conditions 287
6.4.1 2016-082/403 287
6.4.2 2013-015/161 290
6.4.3 Ossified Thyroid 291

6.5 Trauma, Peri- and Postmortem procedures 293
6.5.1 Introduction 293
6.5.2 Methods 296
6.5.3 Results 296
6.5.4 Discussion and Conclusion 310

6.6 Infectious diseases 313
6.6.1 Periostitis 314
6.6.2 Osteomyelitis 320
6.6.3 Sinusitis and Otitis media 326

6.7 Non-specific indicators of stress 329
6.7.1 Enamel Hypoplasia 329
6.7.2 Cribra orbitalia and cribra cranii 344

6.8 Metabolic and endocrine disorders 353
6.8.1 Introduction 353
6.8.2 Methods 354
6.8.3 Results 358
6.8.4 Discussion 365
6.8.5 Paget's disease 375

6.9 Dental disease 378
6.9.1 Dental calculus 378
6.9.2 Caries 387

6.9.3 Periodontal disease 402
6.9.4 Periapical Lesions 409
6.9.5 Ante-mortem Tooth loss 415
6.9.6 Dental attrition 422

7 Stable Isotope Analysis 432

7.1 Introduction 432

7.2 Methods 434
7.2.1 Sampling strategy 434
7.2.2 Sample preparation, collagen extraction and isotope ratio measurements 436

7.3 Weaning Age Reconstruction 438
7.3.1 Introduction 438
7.3.2 Methods 440
7.3.3 Results 446
7.3.4 Discussion 459

7.4 Diet in late medieval and postmedieval Luxembourg City 465
7.4.1 Introduction 465
7.4.2 Methods 466
7.4.3 Results 466
7.4.4 Discussion 477

8 Conclusion 492

8.1 Physicial activity 493

8.2 Health and medical care 494

8.3 Diet and Nutrition 496

8.4 Living Conditions 498

9 Abstract 499

10 Zusammenfassung 501

11 Bibliography 504

12 List of Tables 557

13 List of Figures 560

14 Acknowledgments 569

APPENDIX I-V
on CD

Appendix I : Palaeodemography
Appendix II : Non-metric traits
Appendix III: Physical activity
Appendix IV : Isotope Analysis
Appendix V: Databases

1 Introduction

History and Archaeology are both concerned with understanding life in the past. But whilst historic sources mostly reflect the life of the privileged part of the population, archaeology, due to examining material remains, also aims to shed light on the part of the population that is usually not represented in historical sources. While the archaeological examination of urban settlements and cemeteries is concerned with the material and cultural aspects of past populations, it does not provide any direct insights into living standards. However, this gap can be closed through anthropological studies of human remains, which offer the most direct insights into past living conditions.

Indeed, environmental, cultural and social factors such as malnutrition, trauma, working conditions, hygiene etc. can leave traces on the human skeleton, allowing thus to establish living conditions for each individual examined (Sofaer 2005; Buzon 2012; Van de Vijver 2018).

The individual data such as biological age and sex estimations form the basis of all anthropological analysis. The age and sex distribution within a population helps to inform about the demographic profile. The age structure of a population, in particular child mortality as well as average age at death can provide important clues about a population's health (Herrmann *et al.* 1990; Grupe *et al.* 2015).

Differences between men and women may have underlying biological factors but can also offer a glimpse into past societies' social structure, division of labour and the social position of men and women in past societies (Kemkes-Grottenthaler 1997; Ulrich-Bochsler 1997; Callewaert *et al.* 2010; Shiau & Reynolds 2010a; Laffranchi *et al.* 2020).

Degenerative joint diseases, entheseal changes and metrical indices of bone robusticity can be used in an attempt to reconstruct the intensity and type of physical activity in the past (Weiss & Jurmain 2007; Shaw & Stock 2009; Havelková *et al.* 2013), whilst stressors such as cribra orbitalia and cranii, periosteal reactions or linear enamel hypoplasia can be indicative of exposure to infectious diseases and malnutrition during childhood and adulthood (Robb *et al.* 2001; Grupe *et al.* 2015; Scott & Hoppa 2018; Casna & Schrader 2022).

The study of the dental status such as dental attrition, caries prevalence and tooth loss among others can offer clues about what kind of diet was primarily consumed (Chazel *et al.* 2005; Šlaus *et al.* 2011; Vilkama *et al.* 2016).

Biological anthropology often makes use of other scientific methods to gain deeper insights into specific areas of research such as using stable isotope analysis to gain deeper knowledge on diet and nutrition or migration and mobility or DNA analysis to reconstruction family relationships on graveyards or to investigate origins of disease for example (Grupe *et al.* 2015). Considering the overall information gathered from each individual, comparisons can then be made within the population or to other populations from the same or from different time periods in order to detect similarities or differences (see studies by Lewis and Gowland 2007 on child health in medieval and post-medieval Britain; Palubeckaitė et al. 2002 on medieval and post-medieval prevalence of enamel hypoplasia). That way, it can be established how and why living standards changed over time or whether there was a social stratification within a cemetery or burial complex. In order to track changes in living conditions over time, while reducing the risk of interpopulation differences, it would be ideal to conduct such studies on cemeteries which remained in use continuously from the Middle-ages until post-medieval times (for example St Benet's Sherehog (Miles *et al.* 2008) or Ellwangen-Jagst in Germany (Kairies 2021)).

Combining archaeological data on funerary practices and results from anthropological analyses, will allow to study the effects of social status within a population.

The reconstruction of socio-economic status between and within burial groups plays a central role to further our understanding of everyday life of past societies. Material features such as grave goods are most commonly used to distinguish between high and low status burials, but with the advent of Christianity in Europe and the abolition of grave goods in the burial rites, other factors such as burial depth and location need to be considered as well (Pearson 1999).

Therefore, in the absence of grave goods among Christian burials, it is still possible to estimate social status of individuals buried in a graveyard based on their burial position relative to the church. In fact, graves closest to the church altar and inside the church were the most sought after and most expensive, which resulted in church burials being predominantly reserved for clerics and rich citizens who could afford a burial place there and cemetery burials being reserved for the rest of the population (Effros 1997; Müldner & Richards 2007a; Augenti & Gilchrist 2011; Yoder 2012; Quintelier *et al.* 2014; Vossler-Wolf 2016; Widmaier 2016; Nater 2018). Oftentimes, burials in monasteries or friaries were also more sought after and therefore more expensive than simple parish burials. Affluent lay families would financially fund a friary or monastery in exchange for burial within the monastic precinct. This way they could ensure that the friars would pray for their departed and it would at the same time demonstrate their social rank and religious piety to the rest of the society (Mays 2009). However, whilst generally

burial in a friary was associated with a cost, different burial locations within the monastic complex incurred different fees, as has been reported in historical documents from the Carmelite friary in Aalst (De Groote *et al.* 2011; Quintelier *et al.* 2014).

1.1 Aims of the study

This study aims to further investigate secular changes and socio-economic differences in living standards through the analysis of 391 stratified inhumations excavated between 2008 and 2017 at the place Guillaume II in the city center of Luxembourg, and which belong to the late medieval/post-medieval Franciscan friary founded in ~1255 AD. Several dated burial phases allow to track changes in living condition from the late medieval to early modern times whilst a comparison between church and cloister burials to cemetery burials offers a glimpse into the living conditions of individuals of different social status. For all interpretations it must be kept in mind however, that the individuals buried in the Knuedler burial complex do not represent a biologically grown population as the burial complex is composed of friars as well as citizens of Luxembourg City. Furthermore, the citizens interred in the Knuedler burial complex might also just represent a specific part of Luxembourg's population as this is only one of several documented grave yards that were in use at that time (d' Hollosy & de Meulemeester 1999; Nothwang *et al.* 2004; Rehbach & Bis-Worch 2006; Rehbach 2008; Trautmann & Trautmann 2011) and the few grave goods uncovered suggest a rather high social status of the deceased (Bis-Worch 2011). The reconstruction of overall living conditions relies on the investigation of three major aspects: pathological load and medical care, reconstruction of dietary patterns and nutritional status and lastly reconstruction of physical activity.

Therefore, the different chapters of the thesis will aim to answer the following research questions:

1. What is the demographic composition of the population in terms of age and sex distribution? What is their life expectancy and child mortality?
2. What is the growth profile of the population and what can adult height and weight reveal about living conditions?
3. What can dental status and stable isotope analysis reveal about dietary patterns and nutritional status as well as weaning practices in this population? Is there a difference in dietary patterns between the sexes?

4. What can the exposure to environmental stressors such as linear enamel hypoplasia, *cribra orbitalia* but also exposure to infectious diseases, trauma and general pathological load reveal about hygiene and medical care in Luxembourg City? Was there a difference in men and women? Is there a link between child mortality and occurrence of environmental stressors?
5. What kind and what intensity of workload were these people exposed to? Are the indicators used for reconstruction of physical activity (e.g., bone robusticity, bilateral asymmetry, entheseal changes and degenerative changes of the joints and spine) influenced by age and/or sex?
6. Are there diachronic trends in the above-described parameters that might indicate change of living conditions over time?
7. Are there differences in the above-described parameters between church/cloister and cemetery burials which might indicate differences in socio-economic status between individuals of the two burial locations?
8. How do the demographic parameters, pathological data and dietary data of the Knuedler cemetery, compare to those of other cemeteries in the city? Were the living conditions of those buried in the Knuedler cemetery different from those of rural Luxembourgish sites and European sites?

Lastly, an attempt will be made to interpret the results of the anthropological analysis in light of the historical context of Luxembourg City.

Therefore, in order to reach a more comprehensive conclusion about living conditions in Luxembourg City between the late 14th -late 18th century it is important to be able to interpret the results of the anthropological study in the light of the political landscape of the time and the implications it had on Luxembourg City and its citizens.

1.2 Historical setting

During roman times, a small castellum was situated on the crossing of two consular roads in what is today the center of Luxembourg City. In 963 AD this castellum was first mentioned as Lucilinburhuc in an exchange charter between Siegfried, count of the Ardennes, and the St-Maximin abbey in Trier. Siegfried built his castle on the rocky promontory called "Bock" and shortly after, a small settlement developed around the castle. At the start, Siegfried's other territories were dispersed along the rivers Moselle, Alzette, Sauer and in the Ardennes. But under one of his descendants, Conrad I (1040-1086AD), the accumulation and concentration of further territories was started and grew steadily under his successors over the next centuries and with it the settlement around the castle (Pauly 2011; Thewes 2017).

In 1244 AD, countess Ermesinde II of Luxembourg officially presented the town charter to Luxembourg City (Pauly 2011), and a few years later around 1250 AD, the Franciscan monastery, to which the graves analysed in this work belong, is founded still outside of the city gates (Beck & Beck 2000; Bis-Worch 2011). In the 14th century, count Henri VII of Luxembourg is crowned king of Germany and after him, a further 3 members of the dynasty of Luxembourg, were crowned kings of Germany and two, namely Charles IV (1355-1378 AD) and Sigismund (1433-1437 AD), were eventually elected emperor of the Holy Roman Empire (Pauly 2011; Thewes 2017). Based on documents detailing the incomes of the "denier du feu" and dating between 1311-1495 AD it was possible to calculate an estimate for the inhabitants of the city. For the beginning of the 14th century, about 5000 people (915 households) were estimated to have lived in Luxembourg City and this number increased to over 7000 (1409 households) towards the middle of the 15th century. This indicates a steady increase in citizens over time and indeed, no epidemics that could have had an impact on population growth, such as the plague, have been explicitly reported in Luxembourg City for that time period (Pauly 1994). This would change in the second half of the 15th century however, where the number of houses fell to an all-time low of 140 in 1485AD. This decrease in houses can be attributed to several factors, including the numerous plague epidemics recorded for the town, migration, political troubles or impoverishment of the citizens (Pauly 1994, 2020).

In 1443, the city of Luxembourg experienced its first direct siege and conquest by Philip le Bon, the duke of Burgundy. With this conquest, the duchy of Luxembourg became a province of the Netherlands and due to the strategic position of the duchy between the borders of all the

major forces at the time, became also directly involved in many of the political turbulations of the time (Trausch 1993; Pauly 2011; Thewes 2017).

During the 16th and 17th century, after the Netherlands had passed from the Bourbon dynasty to the Habsburgs, the duchy and especially Luxembourg City, were frequently involved in the struggles for power between Habsburg Spain, the French Valois and the French Bourbons (Pauly 2011; Thewes 2017). Within three years, the duchy was conquered twice by the French and was in return reconquered twice by the Habsburgs (Pauly 2011) and suffered 5 sieges (Trausch 1993). During this time, the fortress of Luxembourg City was gradually expanded and ultimately became one of the most coveted strongholds in Europe, earning its nickname "Gibraltar of the North" in the process (Thewes 2017).

However, with a growing fortress also came a growing number of military personnel stationed in the city. In 1655 for example, 1170 individuals associated with the military were living in the upper town of Luxembourg City. Officers and soldiers usually also brought their wives, children, and servants with them. In the absence of barracks inside the city walls, military personnel was housed in the private residences of the towns' citizens, which was regarded as a duty that every citizen had to adhere to (Thewes 2011, 2013). In 1672, the construction of several new barracks was begun, but the number of soldiers that were living among the towns' people was still very high. Townhouses were usually quite small and many of the inhabitants were rather poor and had their own families. A record from 1681, states that a butcher named Jacques Nehr, who himself had a wife, a valet and five children, was housing eight soldiers and their families, amounting to a total of 17 military people, within their 3-room home. These living arrangements generally led to a very tense relationship between the military personnel and the citizens of Luxembourg, especially because on many occasions the soldiers' behaviour towards their hosts was fairly disrespectful, with reports of destruction of property and theft, of drunken escapades by the soldiers etc. accumulating (Thewes 2013). Only in 1684 AD, after the siege and subsequent conquest of the city by the French king Louis XIV did the situation improve slightly. The French engineer Vauban, next to extending the fortifications of the town considerably, also build more barracks for military personnel to live in (Thewes 2013, 2017).

Figure 1 Map of Luxembourg City around 1560AD (by Jacques Deventer) sourced from Trausch (1993), modified by A. Kremmer to show the location of the Franciscan friary (blue arrow)

However, problems within the city are not only caused by the crowded living conditions. In the 16th century, the Dutch revolt led to a vastly increased presence of officers and soldiers on the roads in the duchy and in Luxembourg City, as well as to decreased harvests and food shortages. Citizens across the duchy were forced to feed and house stationed and passing soldiers for free and were subjected to substantial fiscal charges to support the high costs of food supplies for the army (Weis 2004). Amidst all this, Luxembourg City was rocked multiple times, from the mid 15th to the early 18th century, by plague epidemics, causing the local elite to flee the city and leading to food shortages and famines among those who stayed behind (Pauly 2020).

Luxembourg remained under French rule for 13 years after which it passed back to the Spanish Habsburgs.

In 1715, the duchy passed to the Austrian branch of the Habsburgs, after which ensued nearly a century of peace (Thewes 2017). However, Luxembourg City remained a garrison town and although the number of soldiers stationed in the city decreased, tensions between misbehaving soldiers and citizens persisted. Soldiers were not required to live in the barracks but could also lodge with the regular towns people. However, over the course of the 18th century, it was possible to forego the duty of housing military personnel by paying a fee. Therefore, only affluent people, aristocrats and certain professions such as clerics or lawyers were exempt from the duty of providing housing to the military (Thewes 2013).

In 1795, French revolutionaries besiege and finally conquer the city. They close the Franciscan friary and convert it into barracks, which marks the end of use for the cemetery under study in this thesis. The friary is finally dismantled in 1815 and the place Guillaume II is being remodeled into its present appearance (Beck & Beck 2000; Bis-Worch 2011).

1.3 Social stratification in Luxembourg City

Based on analyses of reports from the 13th to the beginning of the 16th century, documenting wine sales and payment of taxes in the city by quarters, it was possible to determine more affluent areas in the city. Most of the affluent citizens, magistrates and wine sellers were living around today's "marché aux poisons" close to the old Saint-Michel church, but wine sales were also quite high in all of the old town, where a lot of magistrates had their residences as well. The quarter called "Acht", where the Franciscan monastery under study was situated, was bigger in size than the two previously described and was occupied by a more socio-economically mixed population. Several magistrates were reported to have lived there as well

as some prominent wine sellers, but also a lot of less affluent citizens. The quarters of the less affluent citizens involved in more manual professions were situated in the lower part of town, like the Grund, Pfaffenthal or Clausen (Pauly 1994).

The distribution of several houses belonging to nobility or affluent citizens across all of the upper town during the late 16th and 17th century indicates, that the area was predominantly inhabited by a society of higher social standing (Philippart 1994).

Luxembourg City counted thirteen professional associations. In 1778, 245 members of these associations were exempt from tax due to poverty. Two thirds of all members did not own any property in town. Whilst the majority of affluent citizens belonged to the provincial council in the 17th century, in the 18th century, many simple citizens managed to make considerable profit by selling and marketing their products to the numerous citizens and military personnel. In the 18th century, the city of Luxembourg counted around 8500 citizens and 7000 military. These merchants gradually rose in fortune and in social rank an began to separate themselves more and more from the ordinary citizens, founding private clubs etc. instead of attending communal festivities (Thewes 1994)

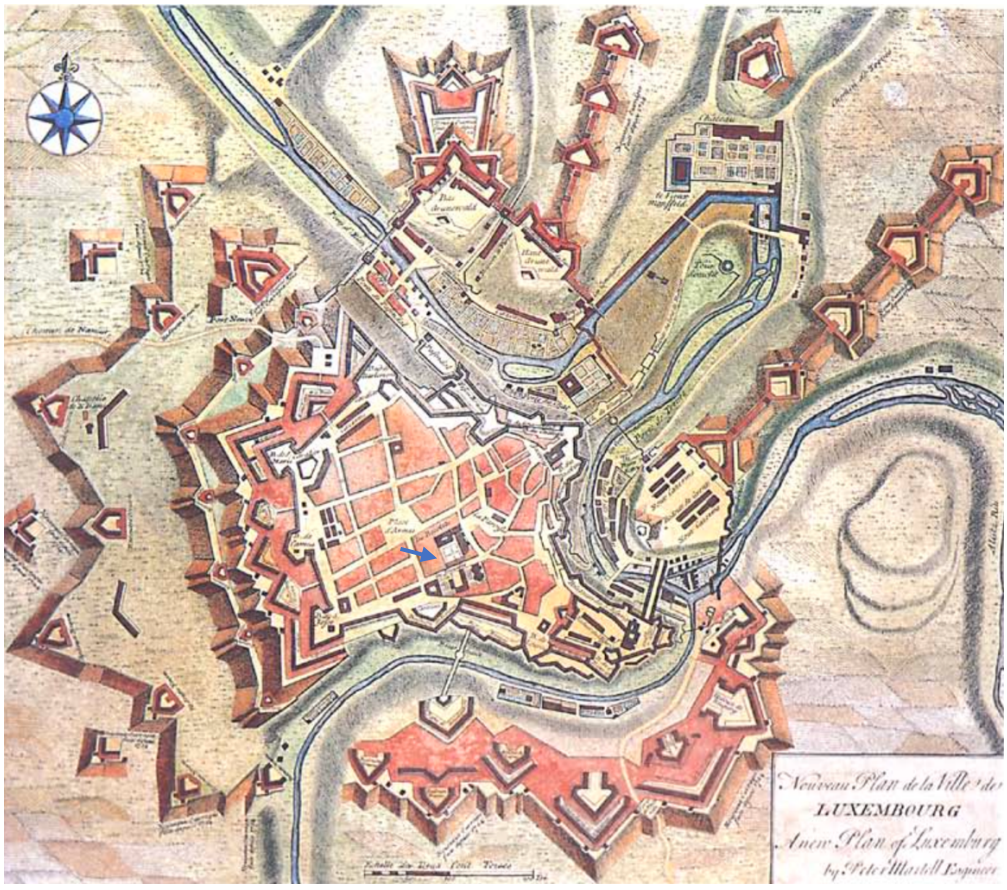

Figure 2 Map of Luxembourg city with focus on the fortifications from the mid 18th century (by Peter Martell, London ~1745) sourced from Trausch (1993), modified by A. Kremmer to show the location of the Franciscan friary (blue arrow)

1.4 The Franciscans, their church and their friary: Historical evidence

Life in Luxembourg has always been dominated by the church (Reuter 1966; Schmitt 1994). This has also been evident on medieval and early postmedieval panoramic views of the city that highlighted numerous churches (Schmitt 1994). The Franciscan friary from the Knuedler was therefore only one of several monasteries and churches in the city of Luxembourg. The churches of Saint-Ulric, Saint-Nicolas and Saint-Michel formed the three parishes of Luxembourg City (Schmitt 1994). However, historical records suggest that the church of the Franciscan friary on the Knuedler played the most central role in religious worship in Luxembourg City, as the majority of services and major religious events were held there (Reuter 1966).

The first arrival of the Franciscans in Luxembourg is still somewhat unclear since all official documents of the foundation of the friary were lost either during the fire 1554AD or sometime later around 1569-1588, when the management of the friary was forcefully ceded to the city council of Luxembourg. However, the first mention of the presence of Franciscans in Luxembourg was found in a document dating back to 1262AD certifying a donation from the knight Theoderich von Zolver to the Franciscans in Luxembourg. Since there is no mention of the Franciscans in the will of Ermesinde, countess of Luxembourg, from 1247AD, it is assumed that the foundation and construction of the friary must have taken place somewhen between 1250 and 1260AD.

At its foundation, the friary had been constructed outside the city walls on roughly one acre of land but soon after, likely due to multiple donations, the property grew until it reached the second ring of the city walls. As the city kept growing, the construction of a third city wall was started in 1340 AD which then also included the Franciscan friary within the city walls.

By the 15th century, due to the city's continued expansion, the Franciscan friary was then situated in the city center. In this century, the church of the friary was extended considerably making it the biggest and most luxurious church in the city at the time with 5 altars and measuring 48.50m in length. Therefore, many of the towns wealthier families and local aristocracy chose to be buried at the Franciscan friary, with some of them even commissioning their own burial chapels either within or near the church (e.g. the chapel of P. E. de Mansfeld, governor of the duchy of Luxembourg (1604AD) or the Beck family chapel (1648AD) (Reuter 1966). Most notably, in 1544AD, after the destruction of the Munster Abbey in Pfaffenthal, the body of John the Blind was transported to the church of the Franciscan monastery before it was

buried again in the newly built Neumünster abbey in 1618 (Schmitt 1994). And thus, the church became the center of religious life in Luxembourg City, with most of the main religious services and events as well as funerals carried out by the friars, which occasionally caused disputes with the regular clergy (Beck & Beck 2000). Furthermore, the Franciscans took on the role of garrison chaplains (Reuter 1966).

On the 11th of June 1554AD, gunpowder that had been stored in the church's attic by the fortress authorities caught fire and caused a massive explosion which engulfed half the city in flames. This led to a general redesign of the town center with several streets being expanded (Pauly 2011, 2022a, b) and in the same year, the Franciscans rebuild their church using mainly the friaries wealth and that of a few wealthy families (Reuter 1966; Beck & Beck 2000).

Until 1569AD, the Franciscans, who had since their arrival been dependent on the diocese of Trier and Cologne, were Friar Minor Conventuals, which is one of three branches within the wider Franciscan order that follows the least strict interpretation of pauperism, which allows them to accumulate institutional wealth but no personal wealth. However, after complaints about greediness and lack of discipline by several cities in the Habsburg Netherlands, by order of the Vatican, all Franciscans, including the friars in Luxembourg City, were forced to adopt the observant rule, enforcing the vows of pauperism, and forbidding the institutional accumulation of wealth. After this, the town administration took over the financial organisation of the Franciscan friary and the relations to Trier and Cologne were severed. As a result, a large part of the resident friars left the convent and were replaced by friars from Walloon and Flemish friaries. For many years a language barrier caused a rift in the relations between the new French speaking Franciscans and the Germanic-speaking town's citizens. Nevertheless, over time the friars found new wealthy benefactors and their reputation rose again and from 1640AD onwards the friars adopted voluntarily the recollect rule, the strictest form of pauperism, leading to a gradual decrease of their gardens and fields but also leading to a steady growth in friars from 11 to about 40-50 (Reuter 1966).

On the 27th of March 1606AD, only about 50 years after the renovation of the old church, misfortune struck again when a storm with gale-force winds blew off the roof of the church, which first sparked the idea to simply build a new church (Pauly 2011). In 1660AD the construction of the new church was then finally begun, and while the old church was built parallel to the rue Notre-Dame, the orientation of the new church was turned by 90°. The construction of the new church was completed 7 years later in 1667AD and of all the former chapels associated with the old church, only that of the former governor count of Mansfeld was

kept intact but the tombstones from the old church were transferred to the new church (Reuter 1966).(Figure 3)

However, in December 1683AD, disaster struck again when the French troops, amidst a conflict between France and the Habsburg Netherlands, bombed the city and caused severe damage in town, but the Franciscan friary suffered only minor damage. After a two months siege under Vauban, Luxembourg City capitulated to the French troops in June 1684AD, after which the French helped generously with the reconstruction of the city and the friary (Reuter 1966; Beck & Beck 2000). After the restauration, the church was the largest and most imposing church in town which held all major services, held the representative funeral services of the imperial family and the funerals of the town's nobility and wealthy citizens (Reuter 1966; Bis-Worch 2011). In 1778AD, by order of the provincial council, the cemetery of the Franciscan friars was officially closed (Reuter 1966) and after the city's conquest in 1795AD by the French revolutionary troops, the friars were evicted from their convent and the buildings were converted into military barracks (Thewes 1994). Until its complete destruction in 1830AD, the friary did not solely offer religious services but had also served throughout the centuries as meeting place for the majority of the guilds and civic associations of the town (Bis-Worch 2011).

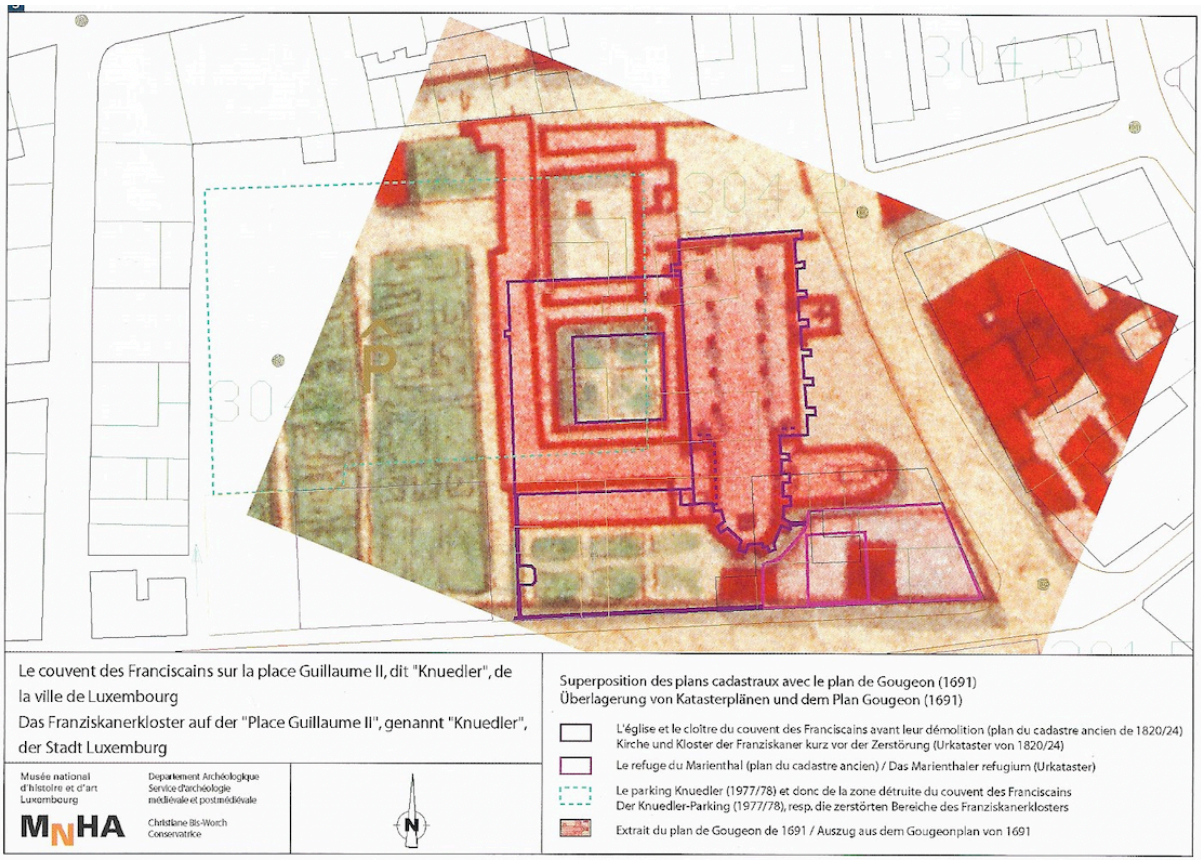

Figure 3 Superimposition of the outlines of the remnants of the friary buildings from old cadastral maps (1820/24) on the drawing of the friary on the plan de Gougeon from 1691 (sourced from Bis-Worch (2011)

2 Materials and Methods

2.1 Methods

All recording methods and the analytical concept underlying each study are listed in the relevant chapters and the Methods section. This section will only introduce the statistical tests used in all single studies.

2.1.1 Statistical analyses

Before any statistical analysis, the assumptions were checked, to select the appropriate test. As assumptions were never entirely fulfilled due to presence of outliers and/or non-normal distribution, non-parametric tests were used when comparing continuous variables.

For evaluation of paired data, the Wilcoxon-signed ranks test was used. This is the non-parametric equivalent of the Paired Student's T-test and allows to detect any relevant differences between two variables that were recorded for the same participants (Field 2009) and was used in this study to compare right- to left-side bone measurements of the same individuals for example.

For comparisons between two groups, such as between sex, burial location and burial layer, the non-parametric equivalent of the Student's T-test, namely the Wilcoxon/Mann-Whitney U test was used. The Kruskal-Wallis test, the non-parametric equivalent of the ANOVA, was used to compare groups with more than two factor levels such as Age and occasionally distance to church. When significant, the Kruskal-Wallis test was followed up by pairwise Wilcoxon tests with "Hochberg" correction to detect which of the groups presented the significant difference. If useful, effect size was calculated to determine whether a significant p-value was actually meaningful and to what extent.

$$r = \frac{Z}{\sqrt{N}}$$

Z = z-score of the test statistic
N = Total sample size
(Field 2009)

The values of the r statistic were interpreted by Cohen's criteria: values between 0.1 and 0.3 indicate a small effect size, values between 0.3 and 0.5 indicate a moderate effect size and values >0.5 a large one.

Comparisons between two or more groups presenting count data were made using the Fisher's exact test or Pearson's chi square test, depending on the number of groups under study. If necessary, pairwise nominal comparisons were used to determine which groups showed the significant difference. For all statistical tests, significance was set at $p<0.05$.

The number of individuals that was entered into the statistical analyses followed the research criteria of each chapter and therefore varies by analysis.

All statistical analyses were conducted in RStudio 2022.07.0 "Spotted Wakerobin"and graphs were either created in RStudio as well or in Microsoft Excel.

2.2 Material

2.2.1 Archaeological context

The burials analysed in this study belong to 391 individuals from inside the cloister and church area of a former Franciscan friary and the adjacent cemetery. The friary was formerly situated in between the rue Notre-Dame and the rue du Fossé, on the square that is today officially called Place Guillaume II in Luxembourg City. Nowadays, no remains of the friary or its cemetery are visible on the square anymore as all the buildings were dismantled in 1815AD and the stones used to erect the city hall that is still standing on the square today. Nevertheless, the memory of the former friary has been conserved in the informal name of the square, "Knuedler", which stems from the Luxembourgish word "Knued", meaning knot and referring to the typical knots of the friar's habits (Bis-Worch 2011).

The very first excavations on the "Knuedler" in 1977 was an emergency excavation before the construction of an underground parking space below the square. During these excavations, 3 decorated tombstones were recovered in the southern wing of the cloister, all dating between 1636-37AD. One tomb stone belonged to Jean Poncelet and his wife Marguerite Fuchs, the other also belonged to a Jean Poncelet, likely the father of the former Jean Poncelet, who was already mentioned on his tomb stone. Judging by the decorative motifs, Jean Poncelet's father worked for the military. The last tomb stone belonged to Jean Ventsch and was decorated with his coat of arms. Historical sources attest a Jean Ventsch as alderman of the city between 1619-1636 AD and it seems likely that he was the father of the friar minor Dominique Ventsch (Mousset 1999).

The next excavation campaign on the "Knuedler" took place between 2008 and 2011, carried out by the Centre National de la Recherche Archéologique (CNRA) under the direction of Mme. Christiane Bis-Worch. The excavation concentrated on the southern area of the "Knuedler" and revealed several walls of the first church erected between 1250-60AD to which belonged several decorated tomb stones dating between the 15th and 17th century. The archaeological analysis so far could confirm what was already known through historical documents, namely that the first church was built parallel to the rue Notre-Dame and had two entry ways, the main one oriented towards rue Notre-Dame. Furthermore, the excavations revealed that the building was a typical Franciscan church with two naves and a strongly elongated monks' chancel.

Several foundations of the second church that was built between 1660-67AD were also uncovered, confirming that the building at been erected at a 90-degree angle to the first church, and was parallel to the rue du Fossé, the chancel facing towards rue Notre-Dame (Bis-Worch 2011).

Of the 391 individuals analysed in this study, 321 were recovered in this excavation campaign and of those, 273 were found on the cemetery outside the church walls and 48 were found inside the first church.

As can be seen in Figure 4, 3 major burial Layers could be identified (green, yellow, blue) and within those, another 3 burial horizons each were located. This shows that the level of the cemetery had been raised twice over the span of its use (Bis-Worch 2011). The green skeletons (n=89) symbolise the lowest layer, the yellow ones (n=76) the one in the middle and the blue ones (n=132) the upper and thus the youngest layer. Three radiocarbon dates were obtained from the cemetery graves, one for each major layer (Table 1). The dates for the lower and middle layer overlapped considerably (2008-78/1340$_{middle_layer}$: 1483-1650cal AD (95%); 2008-78/1334$_{lower_layer}$: 1446-1528cal AD (55%)/1553-1634cal AD (40.4%)). These two tooth samples were pretreated, collagen extraction was performed, and they were analysed by Beta Analytic Inc. The elemental analysis and isotopic measurements were carried out in a Thermo-Finnegan Delta mass spectrometer, no more specifics were given on the report. The modern reference standard was 95% the ^{14}C signature of the international standard NIST SRM-4990C (oxalic acid) and quoted errors were reported as 1σ counting statistics. The graves from the upper Layer were thought to likely date to around and after the construction of the second church since 30 burials were rotated by 90 degrees facing now south and in the direction of the altar of the second church. To confirm this hypothesis, a femur sample of one individual (2008-

78/838), for which pretreatment and collagen extraction had already been conducted by the author at the Biogeology working group at the University of Tübingen (full protocol description in chapter on Stable Isotope Analysis), was send to the ETH Zürich Ion Beam Physics Laboratory for radiocarbon dating. The sample yielded a calibrated date of 1662-…AD (95.5%) confirming the aforementioned theory.

Next to the 321 individuals, numerous bone stray finds and bones in grave fill were collected, and three ossuaries were excavated, which are all not part of this study. The majority of the archaeological finds has not been analysed in detail yet but are listed in the find books of the excavation and consist generally of ceramics, mortar, metal and glass fragments, with a few identified objects. A more detailed analyses of some well-preserved objects from the upper layer showed an array of finely decorated baroque-era amulets, crosses and rosaries hinting at a rather high social status of those buried on the cemetery (Bis-Worch 2011).

Before the start of the expansion works for the underground parking space below the "Knuedler", another excavation campaign was started in 2013 and lasted until 2015. In order to minimise the risk of damage to the still buried remains of the Franciscan friary, the construction of the parking space was carried out by forepoling, a method which is often used in tunnel construction, where the vault is stabilised at the same time as the tunnel is being excavated. Therefore, a deep whole had to be dug to build a ramp down to the excavation level, which necessitate the detailed excavation of the area where the ramp was going to be build as that would ensue the complete destruction of any archaeological remains. Therefore, this excavation campaign was focused on this area which covered the northern part of the friary buildings. The rest of the square was investigated by 3x3m surveys at the locations where the pilons of the future parking were going to be positioned. (Figure 5) The campaign was organised by Mrs Bis-Worch from the CNRA and carried out by the archaeology firm Archeodunum SA with the help of an excavation team from Archeoconstructions. The preliminary analysis by Archeodunum revealed 3 construction phases in the large excavation area. From the first and oldest phase, the remains are very scarce, but their architecture suggests that they did not belong to the friary. The second phase contained a building that was modified several times and of which mainly a cellar with mortar floor and a fireplace have been preserved. Additional finds included gallo-roman tiles which had been likely foraged from a yet undiscovered roman building and reused in the construction of the building of phase 2. A third phase was characterised by well-founded walls, which likely separated the second cloister of the friary from the church square of the 17th century. No tombs were unearthed in that excavation area. 27 surveys were undertaken across the square and revealed mainly structures

of the 17th century church but also remains of the cloister and friary buildings from the 13th to 17th century onwards. A detailed interpretation of most of the features was not possible as of yet (Thorimbert & Hervé 2015). The human remains were only recovered from these surveys and were represented by numerous stray finds and bones in grave fill, 4 ossuaries and 48 inhumations, of which only 23 could be studied. The remaining 25 inhumations could not be located anywhere in the archives of the CNRA. The majority of the missing 25 inhumations were those buried inside the 17th century church. Dating of the remaining 23 inhumations was undertaken with the help of 7 radiocarbon dates by Beta Analytics Inc. (Table 1), field notes and a Harris matrix kindly provided by Archeodunum SA. Most finds consisted of ceramic and glass fragments, metal objects, rosaries, animal bones and remains of wood likely from coffins, which have all not been studied so far. Among the most interesting finds are a game of nine men's Morris engraved in an architectural structure as well as two exploded bombs dating to the siege by the French troops in 1683-1684AD (Thorimbert & Hervé 2015).

The last excavation campaign started in 2016 and is still ongoing. It consisted solely of 19 surveys, of which 4 contained human remains. Survey III yielded only 2 individuals, survey IV had 10 individuals, survey VIII had 26 individuals and survey XX had 8 individuals that could be analysed. Individuals from survey XX were oriented north-south, situated inside the church and therefore belong to the new church of the 17th century. Attribution of the individuals from the other surveys was not as clear. Therefore, samples from the upper and lower layer of survey VIII were sent for radiocarbon dating at the Ion Beam Physics Laboratory at the ETH Zürich. This revealed that the lowest of the 4 burial layers in that survey dated between 1301-1403cal AD (95.45%). The sample of the upper layer however dated from 1179-1272cal AD (95.45%). This means that this sample which was collected by the author likely did not belong to an inhumation from that layer but rather represented semi articulated grave fill (os coxa, femur, tibia: connection not noted) likely originally from the founding era of the friary. Attribution of the human bones as inhumations was done with the help of the find books and notes on the find tags. Therefore, no upper bound date could be determined for survey VIII. However, through study of the field notes and a preliminary, schematic, and hand-drawn survey map (both kindly provided by the CNRA), a preliminary attempt was made by the author to understand the relationship of the burials from the 2016 surveys to those from the other campaigns by understanding their association to certain structures and burial position.

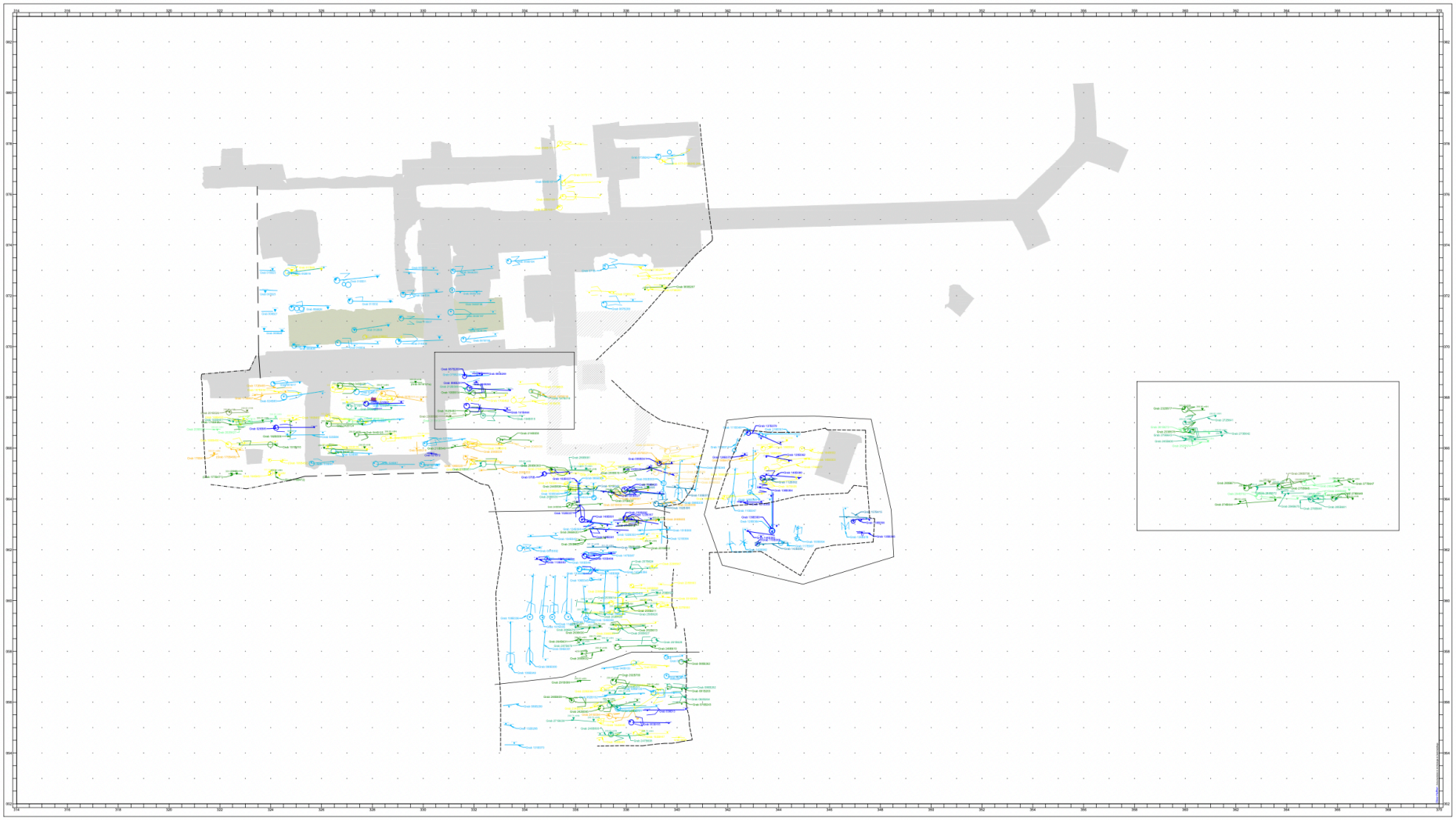

Figure 4 Excavation map of the excavation campaign 2008-2011 (kindly provided by Mme Bis-Worch of the INRA)

It was concluded that, except for the individuals from survey XX, those from all Layers of the remaining survey were likely buried before the establishment of the 17th century church, however this attribution remains hypothetical and should be confirmed through further radiocarbon analyses and an in-depth study of the archaeological structures. However, the responsible archeologist also stated that, except for survey XX, the inhumations from the 2016 campaign could likely be attributed to the first church and associated monastic buildings (oral communication, Bis-Worch). In the same way, the positioning of the surveys from the 2016 campaign in relation to the burials and structures from the previous campaigns was established, as no excavation map of this campaign is available to date. It was concluded that all individuals from the 2016 campaign were buried within the friary complex, either within the church or the cloister area, as opposed to the cemetery. (Figure 6)

The unfinished archaeological investigation especially of campaign 2016 but also of that of 2013-15 did not allow for a more detailed division into individuals buried inside one of the two churches or inside the cloister. Therefore, for the anthropological analysis, it was decided to group all those buried within the friary complex together under the label “cloister” or “church” with both terms used interchangeably throughout the thesis, and those outside the friary complex as “cemetery”. As such, all burials from campaigns 2013-15 and 2016 as well as 48 individuals from campaign 2008-11 were labeled as buried in the “cloister”. The remaining individuals from campaign 2008-11 were labeled as coming from the cemetery.

Since it was not possible for the author of this study to put all the different burial layers across all surveys and campaigns in relation to each other, a simple division into individuals likely associated most closely to the 17th century (Layer 1) and those older than the 17th century church (Layer 2) was undertaken for the anthropological analysis, however, it cannot be excluded that there is a slight overlap in the two “Layers”. In campaign 2016 individuals from survey 10 were attributed to “Layer 1” the rest to “Layer 2”, in campaign the division was based on the Harris matrix and radiocarbon dates (see catalog for Layer attribution) and in campaign 2008-11 the yellow and green individuals were attributed to Layer 2 and the blue ones to Layer 1. Thus, Layer 2 covers a span from the 14th to mid 17th century and Layer 1 covers a span of roughly mid 17th to 18th (1778AD) century. A more precise division would require more radiocarbon dating and a full and detailed archaeological analysis of all the structures and finds, which has not taken place yet.

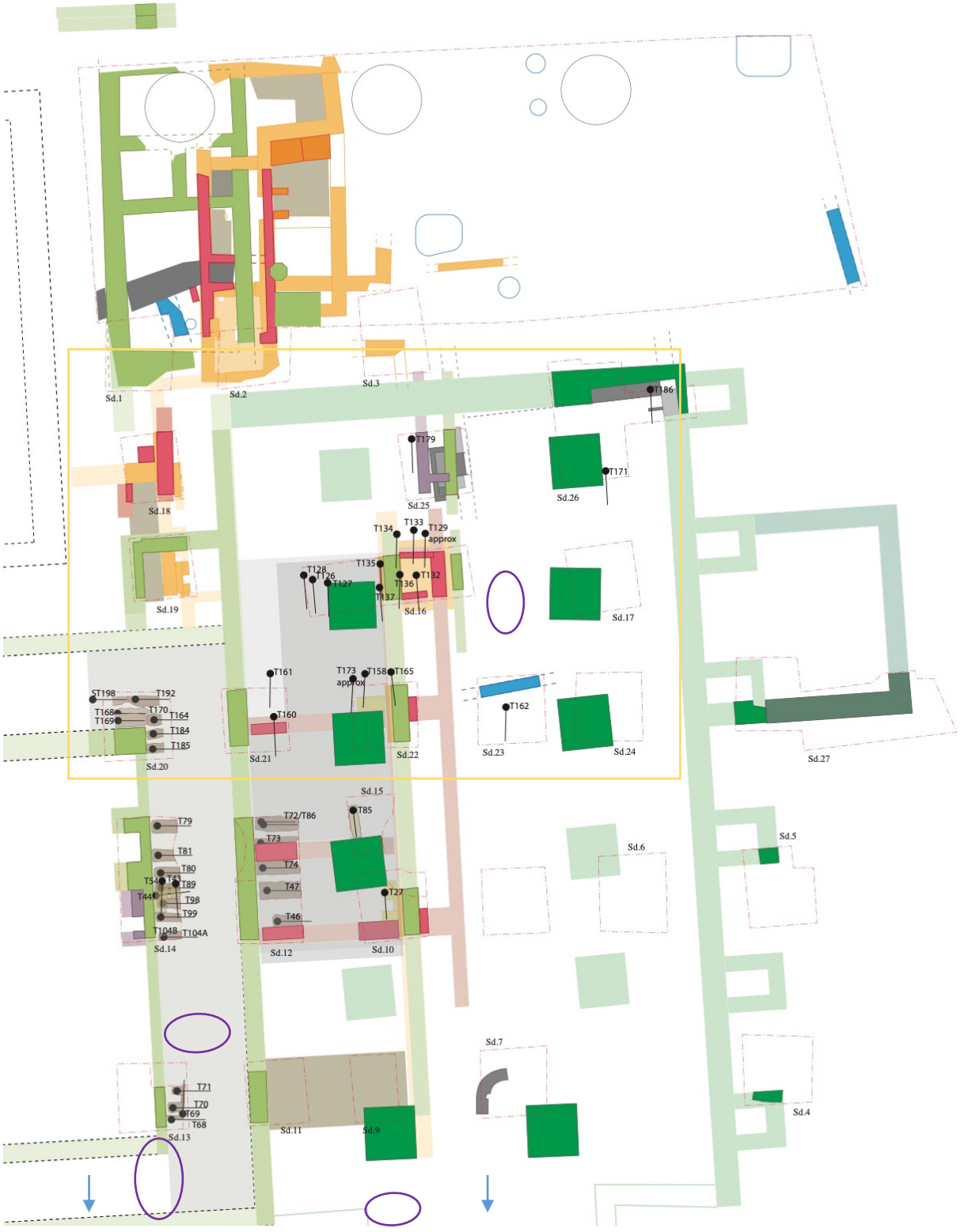

Figure 5 Excavation map of the excavation campaign 2013-15 (kindly provided by Archeodunum SA), modified by A.Kremmer to indicate approximate placement of the 4 surveys with inhumations from campaign 2016 (mauve ovals) and indicating the position of campaign 2008-11(pale blue arrows) (skeletons from 2013-15 missing (yellow rectangle

Table 1 Radiocarbon dates for samples from all three excavation campaigns

Labcode	Inventory ID	Bone	Cal 1 sigma	Company
KNUDLER 1	2013-015/128	Femur right	1477-1642cal AD (95.4%)	Beta Analytics Inc.
KNUDLER 2	2013-015/240	Humerus	1445-1524cal AD (61.6%) 1558-1632cal AD (33.8%)	Beta Analytics Inc.
KNUDLER 3	2013-015/177	Molar 1 upper left	1635-1684cal AD (45.8%) 1736-1805cal AD (40.1%) 1935- Post AD 1950 (8.6%) 1530-1538cal AD (0.9%)	Beta Analytics Inc.
KNUDLER 4	2013-015/161	Canine/Incisor	1802-1938cal AD (65.5%) 1680-1739cal AD (27.1%) 1745-1763cal AD (2.8%)	Beta Analytics Inc.
KNUDLER 5	2013-015/359	Canine lower left	1445-1524cal AD (61.6%) 1558-1632cal AD (33.8%)	Beta Analytics Inc.
KNUDLER 6	2013-015/353	Canine lower right	1482-1646cal AD (95.4%)	Beta Analytics Inc.
KNUDLER 7	2008-78/1340	Canine lower right	1485-1650cal AD (95.4%)	Beta Analytics Inc.
KNUDLER 8	2008-78/1334	Premolar 1 lower left	1446-1528cal AD (55%) 1553-1634cal AD (40.4%)	Beta Analytics Inc.
KNU-23	2016-082/453	Femur right	1301-1403cal AD (95.45%)	ETH Zürich
KNU-24	2016-082/366	Femur right	1179-1272cal AD (95.45%)	ETH Zürich
KNU-87	2008-78/838	Femur left	1662-…cal AD (95.45%)	ETH Zürich

Figure 6 Superimposition of the reconstruction from archaeological vestiges of the first Franciscan church (green) with the cemetery area (red) and the outline of the friary buildings and 17th century church and Marienthal refugium from cadastral maps (1820/24) (mauve) and the Mansfeld chapel (green dashes) sourced from Bis-Worch (2011), modified by A. Kremmer to show approximate location of inhumation areas of campaign 2008-11 (blue rectangle) to campaign 2013-15 (yellow rectangle) and 2016 (pink rectangle)

2.2.2 Body orientation and Position of the arms.

The orientation of the inhumation graves from all three campaigns was determined by the author of this study using the burial maps, field notes and photographic documentation. The vast majority was buried on their back in extended position with the head in the west, facing east (n=341) (Figure 7). This is founded in the belief that during resurrection, Jesus would return in the east and thus, Christians were usually buried with their head in the west and facing east so that they could witness his return (Pearson 1999; Augenti & Gilchrist 2011; Nater 2018). Four males (juvenile-mature II), located in the cemetery, were buried with the head in the east facing west. Priests were often buried with the head in the east facing west as they were required to watch over their commune (Effros 1997; Pearson 1999; Nater 2018), which means that these four individuals might have been clerics. Except for 3 individuals, those facing north (n=14) and those facing south (n=32) could be securely associated with the church of the 17th century as they are now oriented towards the new church altar. Those inside the cloister area were generally facing south and those on the cemetery were facing north. It must be noted here that not all individuals from "Layer 1" in the cemetery were facing north, however, as they were attributed by the excavation firm to the same layer (blue) as the others, it is assumed that those still buried east-west were buried either shortly before or during the construction of the new church. One individual on the cemetery was buried lying on the left side with knees bent (Figure 8).

Due to some individuals being left partially in profile or destroyed by previous works such as pipes, it was not possible to reconstruct burial orientation for all individuals analysed.

Burial position

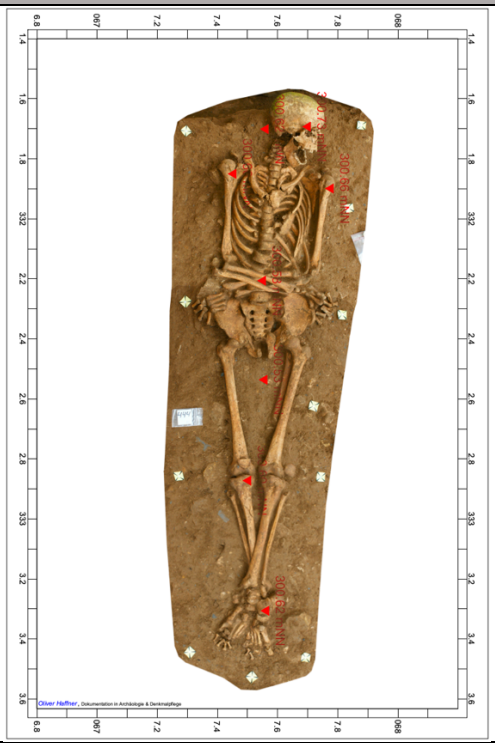

Figure 7 Example of a typical burial oriented west-east with arms folded over abdomen (2008-78/885; 161B444) by Oliver Haffner provided by CNRA (scale 1:10)

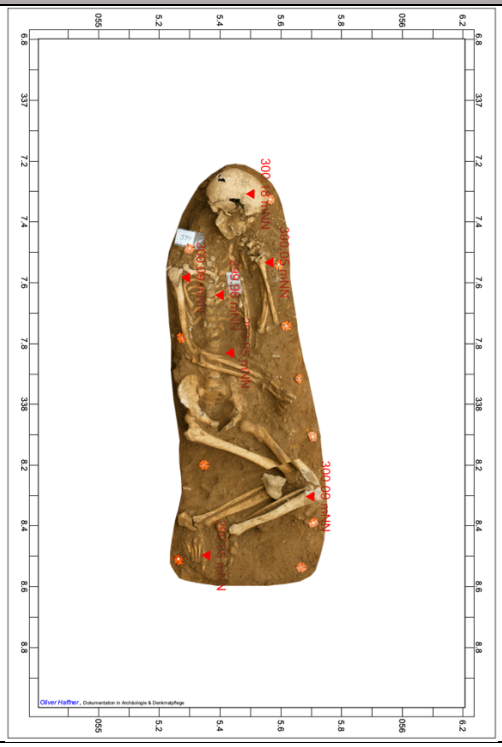

Figure 8 The individual resting on the left side with bent knees, oriented west-east (2008-78/1340; 241B594) by Oliver Haffner provided by CNRA (scale 1:10)

As some authors claim that it is possible to approximately date individuals by the position of their arms in the grave (Scholkmann 2009; Tagesson 2015), the position of the arms of the individuals was reconstructed by the author based on field notes and photographic documentation and the classification by Tagesson (2015) was used (Figure 9). Arm position could not be determined for 186 individuals. Of the remaining 205, 3 showed arms stretched out next to the body (A), 48 showed arms folded in the lap (B), 80 had their arms folded over the abdomen (C) (at least one possibly had their hand folded (field notes by Thorimbert)), 72 had their arms crossed over their chest (D) and 1 possibly had the arms stretched along the body, hands resting on the pelvis (E) (Figure 10). For one further individual, classification into either A or E was not possible.

The distribution of arm positions A-E was evaluated via a Fisher's exact test to estimate differences between burial location, burial layer and sex. Significance was taken at $p<0.05$. Whilst the distribution was fairly similar between Layer 1 and Layer 2 ($p=0.6349$) (Figure 11) as well as between cemetery and cloister burials ($p=0.2375$) (Figure 12) there was a significant difference between males and females ($p=0.0175$) (Figure 13). Whilst arm positions of type C were more common in males, in females, type D was dominant.

Whilst in some cases a clear chronological change in position of the arms was observable (Tagesson 2015), others could not detect a clear change (Düring 2014). The latter was also the case here as all arm positions except for A and E were similarly represented in each burial layer and in each burial location. However, the burial types C and D were always most common and according to Scholkmann (2009), Tagesson (2015) and Kenzler (2015) state that arms folded over the chest (D) and abdomen (C) or hands folded over the lap (B) only became more prominent from the late medieval times onwards, whereas arms extended next to the body were more prominent in the early and high middle ages. This would be in line with most of the radiocarbon dates obtained for the Knuedler cloister and cemetery that fall predominantly into the late medieval and postmedieval periods. Interestingly, this study seemingly revealed a difference in arm position between the sexes, where females were preferentially buried with arms crossed over the chest.

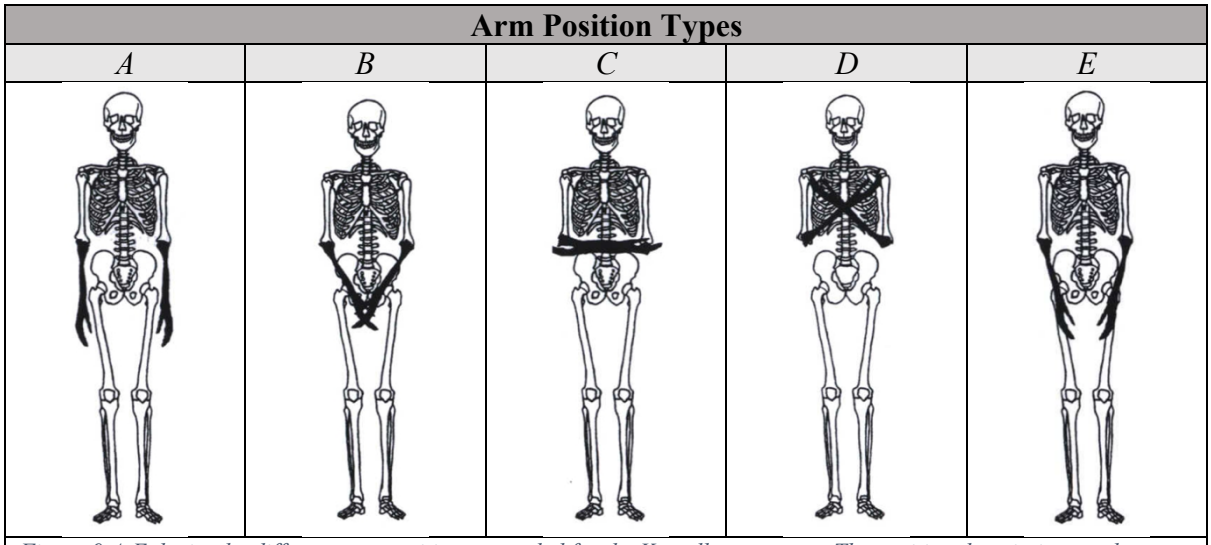

Figure 9 A-E depict the different arm positions recorded for the Knuedler cemetery. The position descriptions and labelling are recorded after Tagesson (2015) but the illustrations are sourced from Eibl (2015)

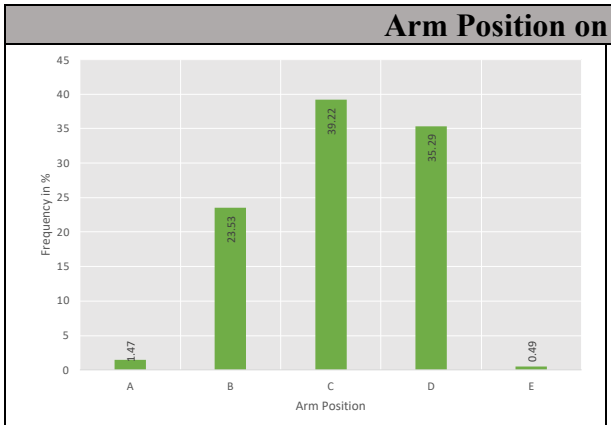

Figure 10 Frequency of arm positions overall

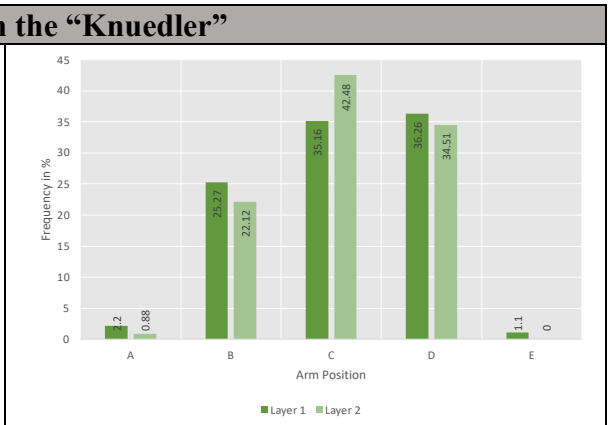

Figure 11 Frequency of arm positions by Layer

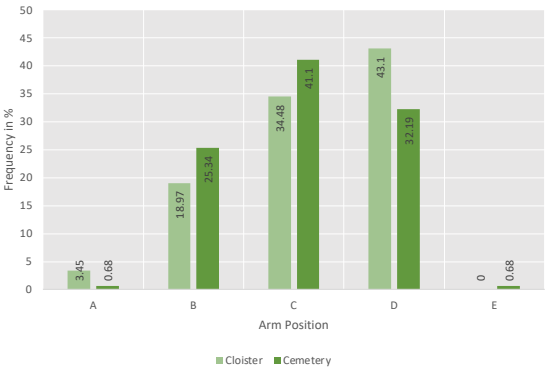

Figure 12 Frequency of arm positions by burial location

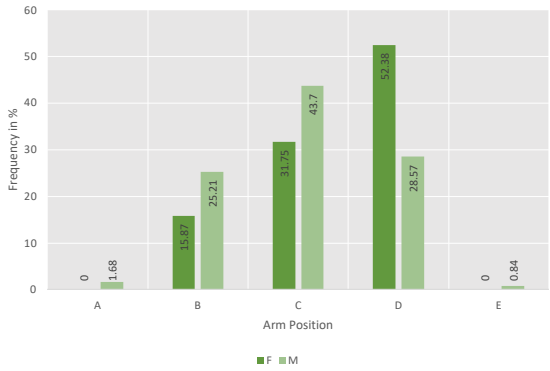

Figure 13 Frequency of arm positions by sex

2.2.3 Data collection, preparation, and equipment

As all skeletons analysed in this thesis come from 3 different excavation campaigns (2008-078; 2013-015; 2016-082), they had been stored in different archives of the INRA (Institut National de Recherche Archéologique), of Luxembourg. After going through the find and field books as well as the available excavation maps, a list of possible graves to analyse, was established. Next, several trips to the different archives were undertaken to sort through the inventory boxes to retrieve the human bones. Stray finds, ossuaries and bones from grave fill were not included in this study. Unfortunately, not all skeletons from the grave list could be retrieved. Reasons for why the graves are missing, were manifold. About 50 graves from the 2013-015 campaign, which concerned nearly all individuals buried in the second friary church as well as those buried in the northern part of the cloister, were not stored with the remaining graves from this campaign and could not be found in any of the archives and the excavation firm also did not know about the whereabouts of these skeletons. Several skeletons from the 2008-078 campaign could not be retrieved, probably due to missing or misplaced find tags. Some of those could be reconstructed by comparison of the skeleton inside the box to the in-situ photographs of the graves but boxes without and with false inventory numbers were not considered in this study. A few graves from the 2016-082 campaign were also missing. Possibly, since in that campaign the grave fill and grave contents sometimes had the same inventory number, the content of these few, mostly incomplete graves, had been stored among the bones from the grave fills.

After the retrieving process, all skeletons first had to be cleaned. This process was conducted at the INRA in Luxembourg by the author of this thesis. Since none of the skeletons had been cleaned before, the encrusted dirt had to be removed using a water-wetted soft-bristled brush. When the soil was hard to remove, a toothbrush and/or a wooden stick or wooden clay-modelling tools were used, and plant roots were extracted as well. The different skeletal

elements were then spread out onto trays and left to dry for 6h at a maximum of 36°C inside a large oven with circulating airflow. After that, the bones were left to finish drying and to cool off before being sorted into new plastic boxes.

The skeletal analysis took place at the University of Tübingen. Therefore, the boxes were transported to Tübingen in several rounds of ~80 boxes each. After analysis, the previous boxes were transported back to Luxembourg and put back into storage. During analysis, every bone element of an individual was drawn onto a skeletal sheet for the respective inventory number, where also basic sex and age estimations were noted. The sheet was based on a selection of those used for Grevenmacher which had been conceived by Trautmann (2012). However, the majority of information was directly entered into digital databases in Microsoft Excel. If multiple individuals were recorded in one grave or had the same inventory number, a letter in the order of the alphabet was added at the end of the original inventory. In the end, a total of 391 individuals were retained for anthropological analysis. Skeleton 2016-082/366, recorded in the field notes as grave, was later found to be grave fill. However, the bones of this individual (right os coxa, right and left femora, right tibia) were likely belong to the same individual, which is why the individual was included in the statistical analysis. Non-metric traits were recorded and are discussed in the Appendix II. For the metrical analysis, a selection of 72 postcranial measurements was recorded, a list of which can be found in the Appendix V. To maximise sample size, all postcranial bones that showed fresh breaks were glued back together with wood glue (Ponal) as it is water-soluble and does not damage bone structure. Broken cranial bones were only glued together in order to better visualise pathological lesions or trauma. As cranial measurements were not pertinent to this study, they are not presented. All measurements were taken using the measurement devices recommended by the respective authors by which they were established. Fe13, Sc1, Sc2, SCOX and DCOX were measured with the spreading caliper, long bone lengths and diaphyseal breadths were measured with an osteometric board, circumferences were measured with a tape measure and the remaining measurements were taken with a Bluetooth digital calliper.

Pathological lesions and examples of non-metric traits were photographically documented using a white photographic tent to mute shadows and a Nikon D5300 camera with magnification lenses for close-up shots. Radiographs of pathological bone lesions were taken at the Department of Anthropology of the DAI (Deutsches Archäologisches Institut) (black background) using a voltage of 80kv (by the author of this thesis), and on the CT-scanner (Model: Nikon XT H 450) of the Department of Palaeontology at the University of Tübingen

(white background) (by Mrs. C. Kyriakouli and the author of this thesis) using a voltage between 145-195kv depending on the bone. CT-scans were performed at the Crona clinic with the help of Dr. S. Afad on a medical CT-scanner (Siemens SOMATOM Force) using a voltage of 120kv, and on the CT-scanner of the Department of Palaeontology, with the help of Mrs. C. Kyriakouli, Dr. G. Ferreira and Mr. A. Tröscher.

2.2.4 Representation and Preservation

2.2.4.1 Introduction

One of the first steps of anthropological analysis is to determine the representation, and preservation of analysed skeletal remains. Representation describes the completeness of a skeleton, meaning how many bones of the skeleton could be recovered, whereas preservation describes the condition of the bone surface. It is important to get an overview on the overall preservation of a skeletal assemblage to gauge the quality of the ensuing anthropological evaluation (Grupe *et al.* 2015). Bone preservation and representation of a skeleton are strongly dependent on taphonomic processes. The taphonomic process begins with the death of an organism and lasts until its recovery. It is divided into 3 stages: Necrology (death of the organism), Biostratinomy (covers all the steps between death and burial such as weathering, disarticulation, scavenging etc.), and lastly Diagenesis (post depositional processes that occur after burial and last until recovery of the remains, such as effects of soil fauna and microorganisms, effects of temperature, biochemical composition of soil and pH, root etching, soil movement etc.) (Grupe & Harbeck 2015). In the case of Christian burials, where burial of remains takes place very soon after death, skeletal preservation is mainly influenced by burial environment and therefore by the afore mentioned diagenetic processes. Overall, cold, dry and alkaline pH burial environments such as calcareous soils, promote bone preservation and warm, moist and acidic pH environments such as sandy soils promote bone demineralisation and destruction (White & Folkens 2005; Nikulka 2016). Furthermore, soil movement and pressure but also weathering processes can cause post-mortem bone deformations and fractures which then need to be distinguished from perimortem fractures, through their typically irregular and sharp-edged fracture margins.

Additionally, plant roots can cause surface modifications on bones, leaving characteristic etchings, or they can penetrate the bone completely sometimes causing post-mortem breakage (White & Folkens 2005; White *et al.* 2012). Lastly, human disturbances such as reburial or construction works can cause damage to human remains and lead to loss of bone elements.

2.2.4.2 Methods

As recommended by Grupe et al. (2015), the degree of completeness was expressed as a percentage value. Therefore, the presence of all bones in an area was summed up and transformed into a percentage value relative to all bones that compose the respective skeletal area. An average percentage value was calculated for each skeletal area and the total representation of the skeleton was estimated by calculating the average of the sums of all skeletal areas. The bones that make up each skeletal area can be found in Table 2. For the skeletal area of the skull, the auditory ossicles (*malleolus, stapes and incus*) were not taken into account as they could not be reliably recorded as absent or present when the external and internal auditory canals (*meatus acusticus externus/internus*) were still intact.

Table 2 Composition of skeletal areas used in analysis of representation

Composition of the skeletal areas	
Area	*Bones*
Skull	2x Parietal, 1x Frontal, 1x Occipital, 2x Temporal, 2x Nasal, 2x Lacrimal, 2x Concha nasalis inferior, 1x Vomer, 1x Ethmoid, 1x Sphenoid, 2x Zygomatic, 2x Palatine, 2x Maxilla, 1x Mandible, 1x Hyoid
Shoulder girdle	2x Scapula, 2x Clavicle
Arms	2x Humerus, 2x Radius, 2x Ulna
Hands	7x Carpals, 5x Metacarpals, 5x Proximal phalanges, 4x Medial phalanges, 5x Distal phalanges
Thorax	7x Cervical vertebrae, 12x Thoracic Vertebrae, 5x Lumbar Vertebrae, 24x Ribs, 1x Sternum
Pelvic girdle	2x Os ischium, 2x Os pubis, 2x Os ilium, 1x Sacrum, 1x Ossa coccyges
Legs	2x Femur, 2x Tibia, 2x Fibula, 2x Patella
Feet	6x Tarsals, 5x Metatarsals, 5x Proximal Phalanges, 4x Medial Phalanges, 5x Distal Phalanges

Next, for each skeleton, the average percentage value of representation of each skeletal area and of the whole skeleton were lumped into larger percentage spans: 1-25%, 25-50%, 50-75% and 75-100%, and 0 being not preserved. This last step was undertaken to increase comparability to other archaeological sites.

Finally, surface preservation was rated after the criteria listed in Table 3. Next to studying the surface texture of the bone, a metal probe was used to determine the sounds described in the definitions.

Table 3 Description of bone preservation stages after Trautmann (2012)

Bone Surface Preservation		
Stage	*Definition*	*Description*
0	Brittle	Bone structure is very unstable and is mostly held together though adhesive dirt. Falls apart under contact with water. Working with the bone requires hardening or leaving some of the dirt in place.
1	Fragile	Bone is noticeably decalcified, with rough and cracked surface structure, localised flaking of the compact bone and widespread destruction of the cancellous bone. Bone tends to break easily and, when hit with a metal probe, it sounds like cardboard.
2	Solid	Bone not or slightly decalcified. Bone surface structure is intact, compact bone is dense, cancellous bone is mostly preserved. Bone does not break easily, is resistant to water and, when hit with a metal probe, it sounds like wood
3	Hard	Bone hardened post-mortem by mineral deposition. Bone resistant to water, does not break easily and, when hit with metal probe, it sounds like burned ceramics

2.2.4.3 Results

The average skeletal representation of the human remains from the Knuedler cemetery lies around 42.46%. At 59.93%, 55.40% and 53.77% respectively, the arms, legs and shoulder girdle are the best-preserved skeletal areas, whereas hands (26.57%) and feet (16.02%) were the worst preserved. The skull was on average also not well represented (37.06%), which was mostly because the majority of crania were fractured, and smaller and more delicate bones such as the ethmoid the nasal conchae, lacrimals etc. were either not preserved or had not been recovered (Figure 14). The same trend can be observed when looking at representation categories. Most of the arms and shoulder-girdle areas were preserved between 75-100% and most of the pelvic girdle and leg were preserved between 50-100%. Among the shoulder and pelvic girdle as well as the arms, percentage of preservation was mostly lowered when all the bones were missing entirely (Figure 15).

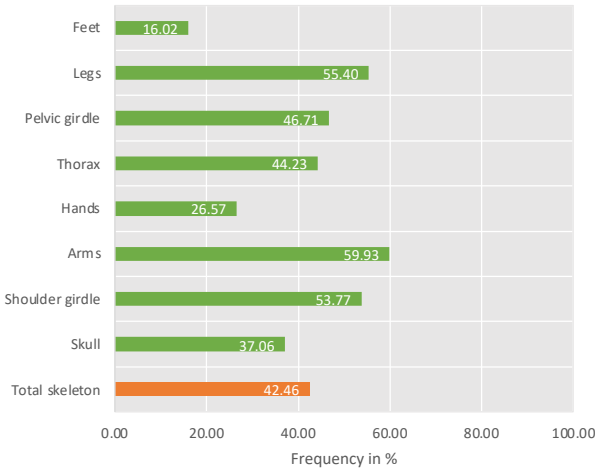

Figure 14 Average representation of the whole skeleton and by skeletal area

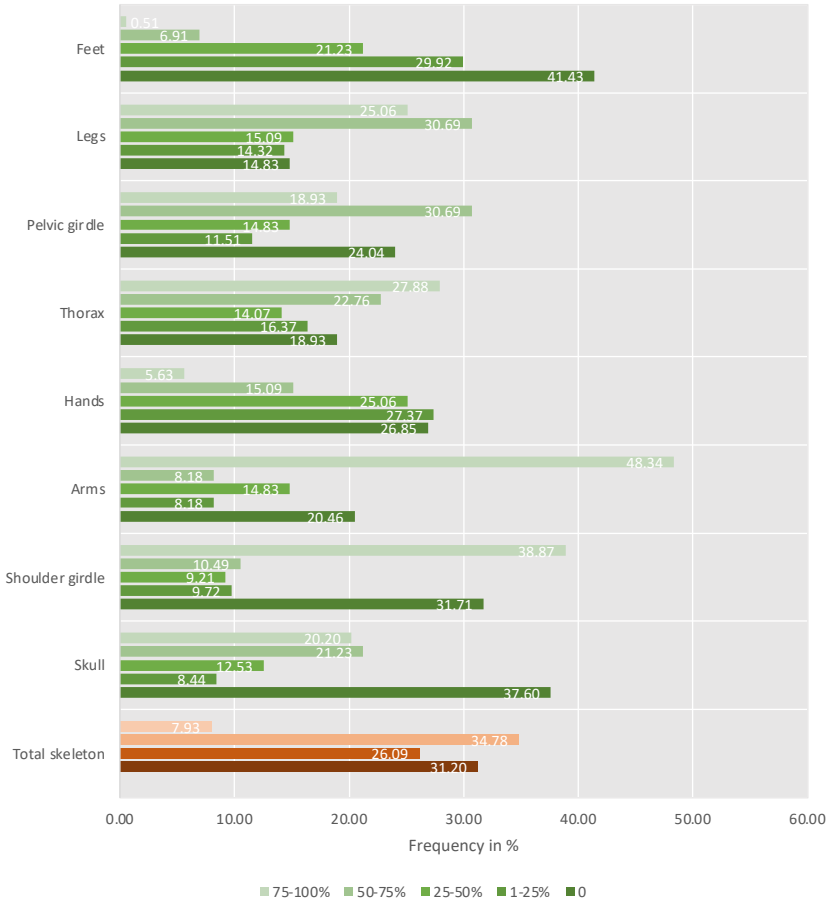

Figure 15 Representation classification for the whole skeleton and by skeletal area (dark red: 1-25%, dark orange: 25-50%, orange: 50-75%, light orange: 75-100%)

Bone preservation is predominantly good at the Knuedler cemetery, with most individuals falling in the solid (48.08%) and hard (27.11%) group. Only about 1/4th of the skeletons had to be classified as either brittle or fragile (Table 4).

Table 4 Bone preservation status of the Knuedler cemetery

Bone Surface Preservation			
Preservation	*Description*	*Nr.*	*Frequency*
0	Brittle	17	4.35 %
1	Fragile	80	20.46 %
2	Solid	188	48.08 %
3	hard	106	27.11 %

2.2.4.4 Discussion and Conclusion

The average percentage of representation for the skeletons from the Knuedler cemetery (42.46%) is very similar to that from Grevenmacher, a medieval rural site from Luxembourg (45.1%). When considering average representation of the different skeletal areas, it becomes

clear that the differences between Grevenmacher and the Knuedler cemetery lie mainly in the representation of the skull and pelvic elements, which were missing more frequently in the Knuedler cemetery than in Grevenmacher (Trautmann 2012). The overall preservation of the skeletons in the Knuedler cemetery was slightly better than that of the St. Esprit cemetery, which is also located in Luxembourg City. In both cemeteries only ~7% of skeletons were 75-100% preserved, but in St. Esprit ~36% of records had only <5% of skeletal elements preserved (Nothwang & Rehbach 2006) whereas in the Knuedler cemetery, only ~1% had this stage of representation. Compared to Ellwangen-Jagst (Kairies 2021), skeletal representation at the Knuedler cemetery is not very good. At Ellwangen, the majority of skeletons is preserved to 75-100% and preservation 0-25% is overall lowest, whereas in the Knuedler cemetery preservation between 75-100% is lowest. Differences in skeletal representation and preservation between sites can be due to different burial environments but also due to different excavation techniques and conditions. Calcareous soil promoted good skeletal preservation in Ellwangen-Jagst (Kairies 2021). As was noted in the field notes from the Knuedler excavation campaigns, the bedrock is sandstone and several of the overlying soil layers have a sandy component, which promotes bone demineralisation. Furthermore, all excavation campaigns at the Knuedler were rescue excavations and surveys, and skeletons were not entirely recovered when they extended beyond the excavation margins.

3 Palaeodemography

3.1 Individual Data

3.1.1 Introduction

Sex and age estimation form the basis of all anthropological analysis. The age and sex distribution within a population helps to inform about the demographic profile. Furthermore, regarding metric and pathological evaluation, it is important to always consider possible sex- and age specific differences in the degree or form of their expression.

The majority of sex estimation methods is based on functional traits of the pelvis and general robusticity of the skeleton (Grupe *et al.* 2015).

Age estimation relies primarily on indications of wear and tear on the skeleton in adult individuals and on skeletal developmental markers in subadults (Grupe *et al.* 2015). It has to

be noted however, that due to the variability of age-related changes in the skeleton, it is only possible to estimate physiological age, as opposed to chronological age, of an individual (Wahl 2007; Grupe *et al.* 2015). Environmental factors such as illness, diet or physical activity, but also genetic predisposition can cause age-related changes to start at a different age than expected (Ferembach, D.; Schwidetzky, I.; Stloukal 1979; Herrmann *et al.* 1990), and Ferembach et al. (1979) emphasise that biological sex also seems to play an important role in the occurrence of age-related bone changes.

There are several methods and indicators to estimate age and sex of an individual and to reach the best accuracy, it is recommended to use as many of the methods as possible. Therefore, accuracy of age and sex estimation does not only depend on the accuracy of the methods used but also on skeletal preservation and representation (White & Folkens 2005; Wahl 2007).

The following section briefly presents the methods used for age- and sex estimation and aims to give an overview of the sex- and age distribution of individuals buried in the Knuedler cemetery. The age- and sex estimations presented here form the basis for all the following anthropological analyses.

3.1.2 Age estimation

3.1.2.1 Methods

3.1.2.1.1 *Age ranges*

Due to the aforementioned variability of age-related skeletal changes, it is not possible to determine the exact age of death of an adult individual. Therefore, the individuals are classified into age ranges that allow for a certain variability of age-related changes on bones.

In this study, age ranges were defined after Martin & Saller (1957) and among adults the classification in 10-year ranges by Hermann et al. (1990) was adopted. A description of the age ranges and the codes used in all subsequent analyses can be found in Table 5.

Individuals that fell within two of the defined age ranges were added to the younger age range for all subsequent analyses. As such, individuals aged 25-34y were added to the young adult category of 20-29 years, those aged 35-44y were added to the adult category of 30-39 years and those aged 45-54y were added to the mature I group of 40-49 years. Individuals aged 40+ were evaluated within the 40–49-year age group and those aged 50+ were evaluated within the 50–59-year group. This decision was taken as the majority of the morphological age-related features suggested that they probably belonged in the younger age group, but no definite age-

range could be determined due to a few features being indicative of older age. Individuals where only epiphyseal closure could be confirmed, were addressed as Adultus (20+) and were not considered in age-specific analyses. Only for the calculation of the mortality tables, all individuals were distributed among all their possible age groups.

Table 5 Age categories used in all analyses of this study

Age categories									
Neonatus	Infans I	Infans II	Juvenile	Adult		Mature		Senile	Adultus
Neonatus	Infans I	Infans II	Juvenile	Young Adult	Adult	Mature I	Mature II	Senile	Adultus
0-1	1-6	7-14	15-20	20-29	30-39	40-49	50-59	60+	20+

3.1.2.1.2 Subadult Age Estimation

Since subadults pass through characteristic developmental stages at short intervals, it is possible to narrow down age estimations to smaller age ranges (Schutkowski 1989).

3.1.2.1.2.1 Dental mineralisation and eruption

The most commonly used method for age estimation among subadults concerns dental mineralization and eruption. As both these processes are mostly unaffected by environmental factors (Demirjian 1986) they are considered to be very reliable indicators for subadult age. Dental mineralization starts already in utero, beginning at the occlusal surface of the crown and continuing towards the formation of the crown, the neck and finally the root (Schaefer *et al.* 2009). By the time of birth, the crowns of the deciduous teeth have already developed within the jaw and over the course of the first 3 years of life, the tooth roots finish developing as well. The first teeth to erupt are the deciduous incisors at around 6-9 months and at about 2.5-3 years, the full deciduous dentition has erupted. At approximately 6 years, the first permanent molar starts erupting followed by the permanent incisors at about 7 years, and by around 12 years, the complete permanent dentition except the 3rd molar has erupted. At around 14-15 years, the roots of the 2nd permanent molar will have completed mineralization (Schour & Massler 1941; Ubelaker 1978; Smith 1991; AlQahtani *et al.* 2010). The eruption of the 3rd permanent molar is very variable but in most cases it happens in early adulthood (Ubelaker 1978; Herrmann *et al.* 1990). Probably the most widely used model for age estimation from dental mineralization and eruption is that by Ubelaker (1978), but Schour and Massler (1941) also still remains in use. Volkmann (2006) reviewed several dental age estimation methods and concluded that

Ubelaker (1978) yielded the most accurate results. However, in the meantime, another method by AlQahtani (2010) was developed, which in a review yielded slightly more accurate results than Schour and Massler (1941) and Ubelaker (1978) (AlQahtani *et al.* 2014). Therefore, all three methods were used in this study. In order to complement and possibly refine the results obtained from the three afore-mentioned methods, the dental mineralisation and eruption charts by Smith (1991) and Anderson et al. (1976) were applied as well.

3.1.2.1.2.2 Postcranial measurements

Another fairly reliable option to estimate age of subadults is to measure long bone lengths (Herrmann *et al.* 1990). It has to be noted though that studies body height of modern populations have found differences in body height at the same ages between different populations, suggesting that long bone length growth is rather variable (Grupe *et al.* 2015). Therefore, it is recommended to apply methods developed on a population that is timewise and geographically close to the one that is being analysed. As such, the methods described in Scheuer and Black (2000), which are all based on modern populations consistently underaged the subadults from the Knuedler cemetery, when compared to the dental eruption ages. In the end, the reference tables developed by Stloukal und Hanáková (1978) developed on early medieval Slavic skeletal series were used in this study as they produced the best agreement with dental age. The long bone measurements were taken after the recommendations in Welte & Wahl (2010). Additionally, a metric method developed by Kunos (1999) on the sternal end of the first rib was used as well but yielded rather inconsistent results when compared to age estimation based on dental eruption and long bone lengths.

3.1.2.1.2.3 Epiphyseal fusion

Finally, the status of epiphyseal fusion of the postcranial and cranial bones can also be used for subadult age estimation even though it is influenced by environmental factors such as disease or nutritional status, and is therefore considered to be less accurate (Cardoso 2007; Grupe *et al.* 2015). Fusion of the bone elements of the skull can be used for children up to 7 years, when the pars basilaris of the occipital bone has fused with the partes lateralis (Scheuer & Black 2000). Furthermore, the fusion of sphenobasilar symphysis is often considered as an important marker to distinguish between late juvenile and young adult age (Grupe *et al.* 2015). However, more recent studies have shown that the timing of fusion for the symphysis is actually really variable with complete fusion having been observed already in 13 year old girls (Schaefer *et al.* 2009). The epiphyseal fusion of the long bones, shoulder, and pelvic girdle as well as of

hands and feet is an important tool for age estimation in older children and juveniles as some of the epiphyses do not close until early adult hood. In this study, the model from Schaefer et al. (2009) was used as a reference to estimate age via epiphyseal closure. Furthermore, a method based on the fusion of the head and tubercle of the first rib was also employed (Kunos *et al.* 1999).

3.1.2.1.3 Adult Age Estimation

In order to narrow down the age ranges as much as possible and improve estimation accuracy, several methods were used in adult age estimation.

3.1.2.1.3.1 Epiphyseal Fusion

First of all, an individual was considered adult when the epiphyses that close before 20 years of age were all fused.

Since the iliac crest and the sternal end of the clavicle only fuse around 20-24 years, their fusion status was used in adult age estimation as well (Szilvássy 1988; Schaefer *et al.* 2009).

3.1.2.1.3.2 Cranial Suture Closure

A commonly used age estimation method is cranial suture closure. This is based on the assumption that over the course of an individual's life, the cranial sutures close gradually with increasing age (Meindl & Lovejoy 1985a). However, it has to be kept in mind that the method is thought to be quite unreliable, which is further supported by the fact that there is not one universally used system but rather a variety of different models. Many studies found varying degrees of correlation or even no relation at all, between suture closure and age (Acsádi & Nemeskéri 1970; Masset 1982; Perizonius 1984; Key *et al.* 1994; Hershkovitz *et al.* 1997; Galera *et al.* 1998; Obert *et al.* 2010). Furthermore, several studies found sex-based differences in suture closure timing (Key *et al.* 1994; Hershkovitz *et al.* 1997; Galera *et al.* 1998; Sahni *et al.* 2005; Gocha *et al.* 2015), whilst others did not (Acsádi & Nemeskéri 1970; Perizonius 1984; Meindl & Lovejoy 1985b; Wolff *et al.* 2012; Chiba *et al.* 2013). And some found differences in closure rates between populations (Meindl & Lovejoy 1985b; Hershkovitz *et al.* 1997), whilst others did not (Perizonius 1984; Key *et al.* 1994; Chiba *et al.* 2013). Lastly, there are also contradicting views on the effects environmental factors, such as mastication, disease or trauma on suture closure, with some authors confirming and others refuting effects on suture closure timing (Moss 1960; Martinez-Lage *et al.* 1984; Kanisius & Luke 1994; Byron *et al.* 2004; Sun *et al.* 2004; Herring 2008).

With that in mind, in this study, ecto- and endocranial suture closure was recorded after Meindl & Lovejoy (1985) and ectocranial suture closure was also recorded after Herrmann et al. (1990). As recommended by Key et al. (1994), endocranial suture closure was only used to indicate whether an individual was likely above or under 50 years of age.

3.1.2.1.3.3 Dental wear stages

Dental wear describes the mechanical wear of teeth due to contact with objects such as food items or other foreign substances but also due to tooth-on-tooth contact through malocclusions or bruxism. The degree to which dental abrasion is expressed is not only dependent on the food items consumed but also on individual factors such as size of the tooth, thickness of enamel or force of mastication (Grupe *et al.* 2015). The longer teeth are exposed to these environmental factors, the more the enamel is being worn down, which is the principle on which the age estimation methods on dental wear adheres to. Considering the different nature of these environmental factors and their variability, it is evident however, that the intensity and degree of progression of dental wear is also strongly variable and highly dependent on these external factors. As such, caution must be applied when using dental wear as age estimation method, which is why it was used only as a complement to other methods in this study. In this study, two methods were used for age estimation using dental wear: the one by Lovejoy (1985) and that by Miles (1963) which was sourced from Brothwell (1981).

3.1.2.1.3.4 Pubic symphysis

As an individual ages, the surface structure of the pubic symphysis changes. At a young age, the surface presents distinct horizontal ridges without margins, and over time these ridges start flattening, the surface gradually becomes more irregular and margins with lipping become more prominent. Several methods have been developed to match these changes to age ranges. In this study, the method by Suchey and Brooks (1990) has been used.

3.1.2.1.3.5 Auricular surface scoring on the os coxa

This age estimation method is based on age-related changes to the surface configuration and texture of the auricular surface of the ilium. In very young individuals, the auricular surface appears fine grained and is marked by distinct transverse ridges. Over the years, the ridges disappear gradually, and the surface appears coarser. Furthermore, bone spurs may develop around the margins, apex and on the retro auricular area, and porosity gradually develops on the auricular surface (Lovejoy *et al.* 1985). In this study the scoring method by Lovejoy et al.

(1985) was used in which the characteristics observed for transverse organization, texture, apical and retro auricular activity as well as porosity are matched to descriptions of their appearance at certain age ranges. Based on the estimated age ranges for each characteristic feature, an overall age range for the individual is then determined.

3.1.2.1.3.6 Acetabulum

With age, degenerative changes also become apparent in the hip joint. Therefore, Calce (2012) devised an age estimation method based on the degree of expression and development of degenerative changes of 4 features within the acetabulum. When all traits have been scored on a three-point scale, the overall acetabular score is matched to one of three large age spans, which allow for a rough distinction between adults, matures and seniles.

3.1.2.1.3.7 Ribs

Other age estimation methods, which also rely on the formation of degenerative changes, concern the ribs. As a person ages, the costal cartilage which connects the ribs to the sternum starts gradually ossifying. The ossification process generally begins at the sternal rib ends. Therefore, Isçan & Loth (1986) devised a method to score the degree of ossification of the costal cartilage at the sternal rib ends, in particular the 4th rib, and matched those scores to age ranges. Kunos (1999) developed a similar method based solely on the first rib but also including different aspects of the rib head and tubercle. Both these methods were also employed for age estimation of the skeletons from the Knuedler cemetery.

3.1.2.1.4 Results

Of the 391 individuals analysed in this study, age could be estimated for 346 (88.49%) individuals whereas for 45 (11.51%) individuals, an age estimation was not possible beyond the fact that, based on epiphyseal fusion, they were all at least adult (Figure 16).

Overall, the majority of individuals reached their age at death in the adult category (30-39y) (n=70), matures I (40-49y) (n=57), matures II (50-59y) (n=59) and seniles (60+) (n=56) were approximately represented equally and made up the next most represented age categories. Subadults and young adults were least represented. (Figure 16)

When looking at frequencies of the larger age categories and without considering individuals whose age could not be determined more precisely (adultus), it becomes clear that the majority of individuals died between the age of 40-59y (mature) followed by 20–39-year-olds (adult), 0–19-year-olds (Subadult) and seniles (60+). (Figure 17)

Age Distribution

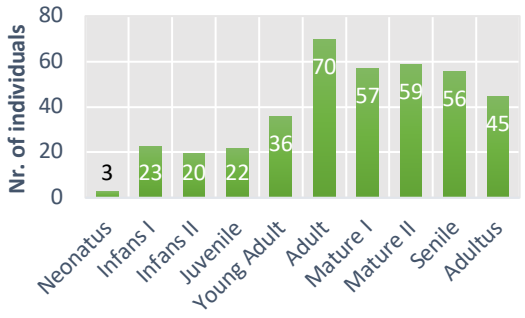

Figure 16 Number of individuals in each age category

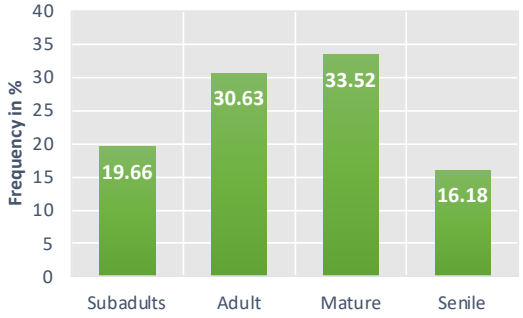

Figure 17 Frequency of individuals for the 20-year span age categories without adultus

When comparing only adult age groups by burial location, it becomes evident that the age distribution between the cemetery and cloister are statistically significantly different (p=0.0475). In the cemetery, mortality is higher in young adults, adults and matures I and lower in matures II and seniles than in the cloister.

No statistically significant difference in age frequency distribution could be detected between the two burial layers (p=0.4228).(Table 6)

Table 6 Age Distribution By Layer and Location

Age Distribution of Adults								
		n	**Young Adult**	**Adult**	**Mature I**	**Mature II**	**Senile**	**p-value**
Location	cemetery	194	28 (14.43%)	55 (28.35%)	42 (21.65%)	34 (17.53%)	35 (18.04%)	**0.0475**
	cloister	84	8 (9.52%)	15 (17.86%)	15 (17.86%)	25 (29.76%)	21 (25.00%)	
Layer	Layer 1	121	14 (11.57%)	34 (28.10%)	29 (23.97%)	24 (19.83%)	20 (16.53%)	0.4228
	Layer 2	157	22 (14.01%)	36 (22.93%)	28 (17.83%)	35 (22.29%)	36 (22.93%)	

3.1.2.1.4.1 Infant mortality

In the overall sample, 17.40% (n=68) of individuals were subadult, which corresponds to 0.77% of neonates, 5.88% of infans I, 5.12% of infans II and 5.63% juvenile.

Among cloister burials, Subadults made up 17.79% (n=21) of the population, with Neonates represented at 1.69% (n=2), infans I at 2.54% (n=3), infans II and juveniles at 6.78% (n=8) each. Among cemetery burials, Subadults made up 17.23% (n=47) of the population, with Neonates represented at 0.37% (n=1), infans I at 7.33% (n=20), infans II at 4.40% (n=12) and

juveniles at 5.13% (n=14). Whilst in the cemetery the majority of Subadults died between 1-6 years (infans I), in the cloister infans I, II and juveniles did not show a difference in mortality. When separating Subadults by burial Layer, they made up 11.87% (n=19) of the population in Layer 1 and 21.22% (n=49) of the population in Layer 2. In Layer 1 there were 0.62% (n=1) of Neonates, and 3.75% (n=6) of infans I, II and juveniles each. In Layer 2 there were 0.87% (n=2) Neonates, 7.36% (n=17) infans I, 6.06% (n=14) infans II, and 6.93% (n=16) juveniles.

3.1.2.1.5 Discussion and Conclusion

The age distribution observed in the Knuedler population is similar to, but does not reflect that of a typical medieval or postmedieval urban or rural population, when compared to 9 urban German sites and 4 rural Luxembourgish sites. Most strikingly, the percentage of Subadults is quite low compared to that of other urban and rural sites and the percentage of seniles is relatively high. The high mortality of children, especially in towns but also in rural communities, can be explained by the group's high susceptibility to nutritional deficiencies and infectious disease (Hühne-Osterloh 1989; Hühne-Osterloh & Grupe 1989; Lewis 2002; Lewis & Gowland 2007), a tendency which was also reflected in 18th century church registers from Berlin where infant mortality was clearly higher in the lower social classes but adult mortality did not differ significantly (Schultz 1991). In particular, the stress caused by weaning can put a child's organism at risk, as with the cessation of lactation, the immunological protection of the breastmilk vanishes, the exposure to new food items exposes them to new pathogens and the unvaried weaning diet can cause nutritional deficiencies (Katzenberg *et al.* 1996; Dittmann & Grupe 2000; Lewis 2002; Pearson *et al.* 2010; Beaumont *et al.* 2015). Either, the part of the population from Luxembourg City buried in the Knuedler cemetery was not exposed to these mortality risks in childhood, hinting at fairly good living conditions, or other factors, such as funerary practices, taphonomic processes or excavation bias (Lewis & Gowland 2007), are at the root of the child deficit observed among the Knuedler burials.

When dividing the Knuedler burials into cemetery and cloister burials, the age distribution between the two areas is markedly different. In the cloister, infans II and juveniles are slightly more represented than in the cemetery and infans I are much less frequent than in the cemetery. A similar trend, albeit on a greater scale, was also observed between cloister/church and cloister garth burials in the Carmelite friary of Aalst, where cloister and church burials, thought to represent burials of friars and affluent citizens, presented way less subadults than cloister garth burials, where it is assumed that part of the ordinary town and lay population was buried (De

Groote *et al.* 2011). In both cloister and cemetery burials from the Knuedler, subadults are underrepresented compared to other urban sites such as Emden (Stech 2009), Ellwangen (Kairies 2021), Lübeck (Caselitz 1982) , Frankfurt (Martens & Alt 2019), Bernau (Hornig 2002) or Kiel (Helmuth 1966). Even compared to Luxembourgish rural sites, such as Givenich (Rehbach *et al.* 2009), Grevenmacher (Trautmann 2012), or Fentingen (Rehbach *et al.* 2005; Nothwang & Rehbach 2006), the number of subadults in the Knuedler sample is comparatively low. Monastic sites such as Ihlow (Timmermann 2009), Schleswig (Caselitz 1983), Leipzig (Schott 1960), Hude (Caselitz 1981), Bern (Ulrich-Bochsler & Meyer 1993) and Aalst (De Groote *et al.* 2011) showed generally less subadults, especially less infans I while in some monasteries the amount of juveniles and infans II was quite similar to that from the Knuedler, and especially to the cloister burials. Compared to Luxembourgish urban monastic sites, the Knuedler cemetery showed less infans I than St. Esprit (Rehbach 2008), a Clarissan convent in Luxembourg City, but more than at Luxembourg Hospice Civil (Nothwang *et al.* 2004), burials of the same Clarissan convent that moved to the Pfaffenthal mid-17th century. The burials form Luxembourg Neumünster (d' Hollosy & de Meulemeester 1999), a Benedictine monastery, showed a similar amount of infans I, II, and juveniles compared to the Knuedler burials. According to Grupe et al. (2015) juveniles between 10-14 years show generally the lowest risk of death and, in a naturally grown population as found in urban and rural settlements, should therefore be least represented and serve as an indicator for overall good health of a population. As Table 7 shows, this is the case among most of the urban and especially among the rural sites. In the monastic sites where subadults were present, usually the younger ones (infans I and II) are least frequent. Timmermann (2009) explains this by the fact that novices usually started around 15 years and that those who were not physically strong enough might not have survived their first year under the harsh fasting rules of the monasteries. Since monasteries would primarily bury their own members, juveniles would be overrepresented in comparison to younger subadults. In the Knuedler friary, juveniles showed a similar representation to that of infans I and II.

Furthermore, the burials from the Knuedler cemetery showed less matures and seniles than those from the cloister, suggesting that overall individuals buried in the cloister reached an older age. According to Schott (1964), the mortality peak among high medieval cemeteries ranges between 40-59 years. The amount of seniles overall in the Knuedler cemetery is fairly high compared to most urban, rural and monastic sites. However, the overall adult age distribution and in particular that of the cemetery resembles most that found in Kiel and Luxembourg Neumünster, whereas that of the cloister resembled that of Fentingen and

Givenich, which are thought to belong to upper-class individuals (Nothwang & Rehbach 2006; Rehbach *et al.* 2009), and especially that of cloister burials from a Dominican convent in Bern. Overall, the age distribution of both cemetery and cloister burials shows most affinities with other urban monastic burials. Especially when comparing the cloister burials from the Knuedler site to the cloister burials from Bern, the age distributions show a striking similarity characterised by a very low number or even absence of infans I and a slightly higher presence of infans II and juveniles and a large amount of seniles. Except for Bern and Aalst however, the other monastic sites all present more mature than adult individuals. The site Grund/Wenzelsmauer in Luxembourg shows an age distribution that is quite distinct from all other sites including the Knuedler cemetery, lacking young subadults and seniles completely with a predominance of adult individuals. Since it is thought that Grund/Wenzelsmauer represents primarily a soldiers' cemetery (Trautmann & Trautmann 2011), this age distribution pattern is not surprising.

To conclude, the age distribution in the Knuedler cemetery and cloister, which is heavily weighted towards the older age categories and is comparatively lacking in subadults, suggests that the individuals buried there had rather high living standards. Overall, the age distribution is representative of an urban monastic burial ground where friars and a portion of the town's population were buried together. The child deficit observed in the cemetery might have several causes. Special funerary practices might have been enacted by the friary (Lewis & Gowland 2007), the sandy and thus rather acidic soil composition favoured the decomposition of children's bones and/or there was a special burial area for children, as was the case on many medieval cemeteries (Lewis & Gowland 2007), that has not been found yet during the different archaeological sondages.

Table 7 Comparison of age distributions between the Knuedler cemetery and 9 urban German sites, 6 European monastic sites and 8 Luxembourgish rural and monastic sites

Age distribution compared to other sites										
Urban populations										
Age group	*Knuedler overall*	*Emden*	*Ellwangen LM*	*Ellwangen PM*	*Lübeck Dom Paradies*	*Kiel*	*Frankfurt*	*Bernau*	*Hettstedt Gymnasium*	*Völklingen PM*
Infans I	7.5	15.7	13.21	24.87	18.4	12.1	10.7	22.2		
Infans II	5.8	8.1	9.91	24.88	13.1	20.6	10.7	15.1		
Juvenile	6.4	4.8	10.38	14.63	7.9	8.5	8.6	14.3	8.8	2.8
Adult	30.6	29.5	51.42	21.95	21.1	31.6	27.9	7.1	41.2	57.0
Mature	33.5	35.4	14.15	11.22	34.2	14.6	40.0	19.1	48.5	37.4
Senile	16.2	6.5	0.94	1.46	5.3	12.6	2.1	8.7	1.5	2.8
Monastic populations										
Age group	*Knuedler cloister*	*Knuedler cemetery*	Leipzig Franciscans	Ihlow Cistercians	Hude Cistercians	Schleswig Dominicans	Bern Dominicans	Aalst Carmelites church	Aalst Carmelites cloister	Aalst Carmelites cloister garth
Infans I	3.8	8.7	0	0.5	0	0	0	8.3	6.7	26.7
Infans II	7.6	5.0	0	3.0	0	4.2	~14.5			
Juvenile	7.6	5.8	0	10.6	0	12.5				
Adult	21.9	34.4	38.3	32.7	27.3	33.3	~38	62.5	53.3	48.3
Mature	38.10	31.5	57.4	49.2	72.7	41.7	~23.5	26.0	40.0	21.7
Senile	20.00	14.5	4.3	4.0	0	8.3	~24	3.1	0	3.3
Luxembourgish sites										*Hospital*
Age group	*Knuedler overall*	Givenich	Diekirch	Grevenmacher	Fentingen	Luxemburg Neumünster	Luxemburg St. Esprit	Grund/ Wenzelsmauer	Luxembourg Hospice civil	*Regensburg Minoritenweg*
Infans I	7.5	22.4	18.9	18.8	21.9	15.8	17.7	0	5	9.5
Infans II	5.8	14.9		10.8	6.3		6.5	0	0	4.1
Juvenile	6.4	3.0	8.2	2.8	0	7.9	6.5	17.4	0	7.6
Adult	30.6	14.9	44.0	33.5	21.9	30.9	24.2	69.6	25	34.9
Mature	33.5	55.2	23.3	30.1	46.9	28.1	41.1	13	40	34.9
Senile	16.2	13.4	5.6	4.0	3.1	17.3	4.0	0	30	9.0

Knuedler = Kremmer (hic)
Emden = Stech (2009)
Ellwangen LM/PM = Kairies (2021)
Lübeck = Caselitz (1982)
Frankfurt = Martens & Alt (2019)
Kiel = Helmuth (1966)
Bernau = Hornig (2002)
Hettstedt Gym./Völklingen PM = Roβbach (2015)

Leipzig Franciscans = Schott (1960)
Ihlow Cistercians = Timmermann (2009)
Hude Cistercians = Caselitz (1981)
Schleswig Dominicans = Caselitz (1983)
Bern Dominicans = Ulrich-Bochsler & Meyer (1993)
Aalst Carmelites = De Groote et al. (2011)
Regensburg Minoritenweg = von Heyking (2012)

Givenich = Rehbach et al. (2009)
Diekirch = sourced from Trautmann (2012)
Grevenmacher = Trautmann (2012)
Fentingen = Nothwang & Rehbach (2006)
Luxemburg Neumünster = d'Hollosy & de Meulemeester (1999)
Luxemburg St. Esprit = Rehbach (2008)
Grund/Wenzelsmauer = Trautmann & Trautmann (2011)
Luxembourg Hospice civil = Nothwang et al. (2004)

3.1.3 Sex estimation

3.1.3.1 Methods

3.1.3.1.1 Subadults

Sex estimation is not recommended for subadults before puberty as the sexually dimorphic features that are present in adults have not yet (fully) developed. Nevertheless, there exist several morphological and metric methods to estimate subadult sex primarily based on mandible and iliac shape or discriminant functions of long bones and the ilium (Schutkowski 1989, 1990, 1993; Molleson *et al.* 1998; Loth & Henneberg 2001; Cardoso & Saunders 2008). All these methods were applied to the subadults from the Knuedler cemetery, but the results were very ambiguous, with different methods yielding different sex estimates. There are new methods to determine sex in children (e.g. amelogenin markers of dental enamel, DNA analysis etc.) (Dash *et al.* 2020) but those are quite costly and time consuming.
So, it was decided that no sex estimation would be considered in any further analyses for neonates, infans I and infans II. Sex estimation was only applied to juveniles, considering the adult sex estimation methods.

3.1.3.1.2 Adults

3.1.3.1.2.1 Sexually dimorphic features of the cranium and postcranium

Sex estimation of adults is primarily based on sexually dimorphic morphological features of the cranium and pelvis. Most of the methods rely on the fact that certain features are more prominently expressed in men as they are generally more robust than women. The morphological features of the pelvis are considered to be the most reliable for sex estimation as the female pelvis is generally smaller but wider than the male pelvis due to its adaptation to pregnancy and birth (Grupe *et al.* 2015). In this study the method by Ferembach et al. (1979) was used to assess sexually dimorphic traits of the pelvis and cranium. Additionally, morphological traits of the os pubis were assessed according to Phenice (1969).

3.1.3.1.2.2 Metric methods

Three metric methods were also used for sex estimation of the Knuedler individuals. This was done on one hand to improve and complement the morphological estimations and on the other hand to allow at least tentative sex estimations in cases where no morphological features were

preserved. The first method concerns the pelvis. An open-source software based on discriminant functions called DSP V2 (Murail *et al.* 2005; Brůžek *et al.* 2017) was used to estimate biological sex from a series of measurements of the os coxa. Several studies have tested the validity of the DSP software and all concluded that over 90% of individuals were sexed correctly by the software (Mestekova *et al.* 2015; Brůžek *et al.* 2017; Quatrehomme *et al.* 2017). Furthermore, cut-off value-based sex estimation methods for humeral and femoral head diameters were used (Milner & Boldsen 2012). In order to securely identify the sex of those individuals lacking the sexually dimorphic morphological traits on the cranium and pelvis, metric sexing functions based on long bone (humerus, femur, radius, tibia, fibula) (Spradley & Jantz 2011) and tarsal (calcaneus, talus) (Steele 1976) measurements were used. These functions are based on cut off points, meaning if the result of the function lies above the cut-off point, the individual will be classified as male and if it lies below, the individual will be classified as female. For metric sexing approaches, it is recommended that an accuracy of at least 75% be reached in order to attempt sex estimation. With a classification accuracy of >85% the individual can be reliably classified. In order to be able to reliably classify those individuals where only metric sexing was possible, the accuracy of these discriminant functions was tested on those individuals from the Knuedler sample that could be morphologically sexed. Not all functions performed equally well in the accuracy tests. Among the most reliable functions for metrically determining an individual's sex are those of the humerus, femur and radius described in Spradley and Jantz (2011) and that of the talus and the combined function for talus and calcaneus described in Steele (1976). The functions for tibia, fibula, clavicula (Spradley and Jantz 2011) and calcaneus (Steele 1976) can only securely classify males. These latter functions should therefore not be used on their own for classifying individuals whose sex could not be determined morphologically. Therefore, all individuals for which sexing was only possible through the latter functions will remain classified as indeterminate, while those, that could be sexed using the former functions will be attributed to their metrically determined sex. (For accuracy test results: see Appendix I)

3.1.3.1.3 Classification Categories

Based on the accuracy of the sex estimation methods used and based on how many traits could be scored and/or yielded conclusive or inconclusive estimates, all adult individuals were assigned as Male (M), maybe Male (M?), possibly Male (M??), Female (F), maybe Female (F?), possibly Female (F??) or Indeterminate (Indet). The sex of subadults was entered as Indet

into the database. For subsequent analyses, all M, M?, M?? were grouped together under Male (M) and all F, F?, F?? were grouped together under F. Indeterminate individuals were not considered in sex-specific analyses.

3.1.3.1.4 Masculinity Index

The masculinity index expresses the proportional relationship between men and women in a population. According to Hermann et al. (1990) all individuals whose sex could be determined are included in the formula, which includes all those from the juvenile to the senile age group. In order to follow the age groups defined in Hermann et al. (1990) the masculinity index was calculated on the age groups instead of the mortality tables. The masculinity index is calculated using the following formula:

$$Masculinity\ index\ (MI) = \frac{Males\ x\ 100}{Females}$$

MI cut-off point	Ratio description
MI = 100	Balanced male to female ratio
MI < 100	Females > Males
MI > 100	Males > Females

3.1.3.2 Results

As Figure 18 shows, there were more males (62.62%; n=196) than females (37.38%; n=117) buried in the Knuedler cemetery and sex could not be determined for 78 individuals, 50 of which were subadults. For 8 indeterminate individuals age could be determined and for 20 neither sex nor age could be estimated. As Figure 18 reveals, a reliable sex estimation was possible for the majority of males (n=121/40) and females (n=58/41), and only 20 females and 24 males were classified as possibly male (M??) or possibly female (F??) respectively. Age estimations of individuals of indeterminate age start at the F?/M? category because for most of them, only metric sex estimation was possible. Overall, males showed one clear mortality peak among adults whilst matures I, matures II and seniles showed approximately the same values. Females showed two smaller mortality peaks, one among young adults and one among matures I.

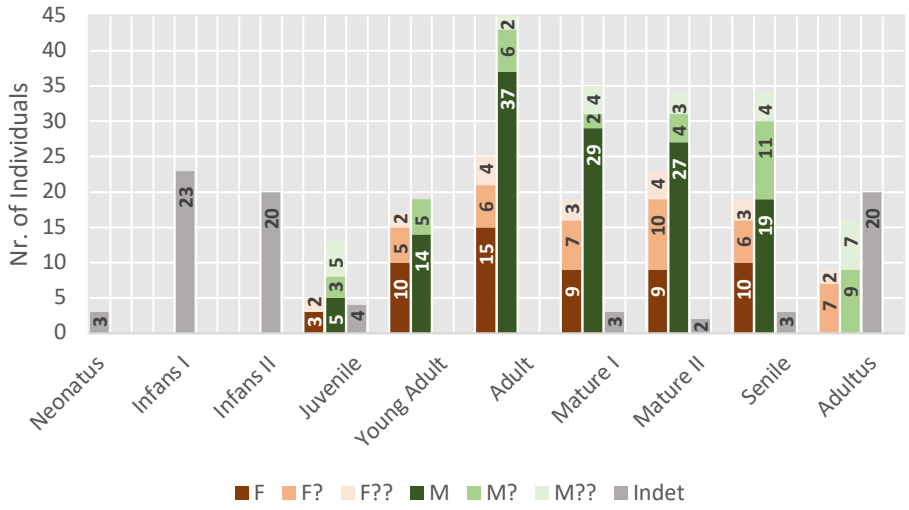

Figure 18 Number of individuals by age and sex

When separating only the adult individuals by Sex, Layer and Burial location, it becomes apparent that in both Layers, females from the cloister show a similar pattern of mortality than those from the cemetery (L1: p=0.8926; L2=0.9529). In Layer 1 females from the cloister have a mortality peak among matures II and those from the cemetery have theirs among matures I. In Layer 2 however, both females from the cemetery and those from the cloister have their mortality peak among adults, followed by two smaller ones among seniles and young adults. In contrast, in Layer 1 mortality is lowest among seniles and young adults.

The mortality pattern in Layer 2 between males and females is quite different with men having their mortality peaks in the mature II (cloister) and senile (cemetery) age ranges whereas that of females lies in the adult age range. The mortality pattern between cloister and cemetery burials of males from Layer 2 is fairly similar (p=0.3526) but in the cemetery, the mortality peak among seniles is not as pronounced as adults also show a small increase in mortality compared to matures I and II

When comparing females to males within Layer 1, both sexes show completely different trends among cemetery and church burials. Whereas in females, there is no difference between the burial locations, in males the mortality peak of cemetery burials lies clearly in the adult age group whereas that of the cloister clearly lies in the senile age group. Therefore, among males from Layer 1, the cloister burials show a completely opposite pattern of mortality to that from the cemetery burials (p=0.0001)

Mortality peaks for Adults by Sex, Layer and Burial Location

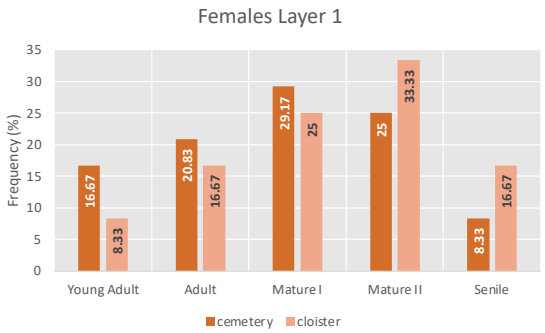

Figure 19 Mortality peaks of women from Layer 1 by Burial Location (p=0.8926)

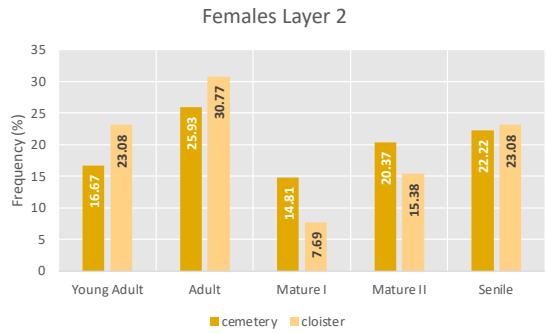

Figure 20 Mortality peaks of women from Layer 2 by Burial Location (p=0.9529)

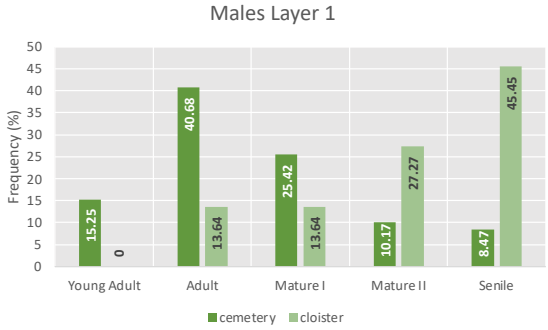

Figure 21 Mortality peaks of men from Layer 1 by Burial Location (p=0.0001)

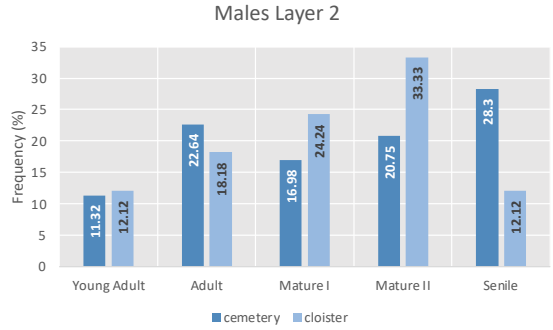

Figure 22 Mortality peaks of men from Layer 2 by Burial Location (p=0.3526)

3.1.3.2.1 Masculinity index

The masculinity index (MI) (167.5) lies clearly above 100 and therefore reveals that there was overall a surplus of men buried in the Knuedler cemetery.

$$MI = \frac{196\ x\ 100}{117} \rightarrow 167.5 \rightarrow M > F$$

Since cloister burials and cemetery burials likely represent individuals of different social status, with those buried in the cloister, likely consisting of Franciscan friars and the upper social classes, and those from the cemetery consisting mainly of the general population, the masculinity index was also calculated by burial location. This analysis revealed that among cloister burials, the MI is much higher than that of cemetery burials, indicating that the surplus in males was far greater in cloister burials than in cemetery burials.

$$MI_{cloister} = \frac{63\ x\ 100}{30} \rightarrow 210 \rightarrow M > F$$

$$MI_{cemetery} = \frac{133\ x\ 100}{87} \rightarrow 152.9 \rightarrow M > F$$

To determine whether the proportion of men to women changed over time, the MI was calculated for both burial Layers and interestingly, the surplus in males was greater in the younger Layer 1 than in the older Layer 2.

$$MI_{Layer\ 1} = \frac{95\ x\ 100}{38} \rightarrow 250 \rightarrow M > F$$

$$MI_{Layer\ 2} = \frac{101\ x\ 100}{79} \rightarrow 127.9 \rightarrow M > F$$

Even though it reduces the sample size in each group considerably, the MI was also calculated for each burial location by Layer. Strikingly, the MI of the cemetery in Layer 2 is quite balanced, whereas in the cloister in Layer 2 and 1 and especially in the cemetery of Layer 1, there was a clear surplus of men.

$$MI_{Layer\ 1_cem} = \frac{68\ x\ 100}{24} \rightarrow 283.3 \rightarrow M > F$$

$$MI_{Layer\ 2_cem} = \frac{65\ x\ 100}{63} \rightarrow 103.2 \rightarrow M \cong F$$

$$MI_{Layer\ 1_cl} = \frac{27\ x\ 100}{14} \rightarrow 192.9 \rightarrow M > F$$

$$MI_{Layer\ 2_cl} = \frac{36\ x\ 100}{16} \rightarrow 225 \rightarrow M > F$$

3.1.3.3 Discussion and Conclusion

If a graveyard were to represent the composition of the living population, based on modern data, one would expect to find a rather balanced ratio of men to women, with a biologically

determined slight surplus of men (Kemkes-Grottenthaler 1997). Kemkes-Grottenthaler (1997) places the expected masculinity index for a biologically grown population between 103 and 113.

However, many studies have found that medieval and postmedieval burials tend to be characterised by a surplus of men and the reasons for this are not entirely clear yet (Jungklaus 2009). Several hypotheses to explain this trend have been brought forward so far. Schott (1964) for example suggests that a high surplus in men is characteristic for cemeteries in towns or cities with a lot of immigration, as it was mostly men that moved to another town for work reasons. Voland (1984) even goes as far as suggesting infanticide or neglect of young girls as a possible cause for the lower number of females. Since females were of lower social value, boys were favoured over girls and parental investment was directly focussed on them. Furthermore, socio-cultural circumstances, such as different burial practices for women have also been discussed in literature. As such, most excavations of cemeteries are conducted in surveys, which might cause a loss of women, if they were buried predominantly in an area that was not excavated (Kemkes-Grottenthaler 1997; Ulrich-Bochsler 1997; Nater 2018), a factor that needs to be particularly considered in the interpretation of the Knuedler cemetery data, since the site was excavated primarily through surveys. With an MI of 167.5 and 196 (62.62%) men to 117 (37.38%) women, the Knuedler burial site shows a clear surplus in males. Compared to most other urban and rural sites, this MI can be considered to be high and resembles most that of both burial phases of the "Dom Kirchhof" in Lübeck (Boenisch & Bräuer 1986) that of Diekirch (Trautmann 2012) and that of Fentingen (Nothwang & Rehbach 2006). Since the Knuedler burial complex belonged to a friary, a comparison of the MI to other monastic cemeteries seemed warranted. Among the monastic sites however, the MI was mostly much higher (Schott 1960; Caselitz 1981, 1983; Ulrich-Bochsler & Meyer 1993), clearly indicating the presence of mechanically grown populations consisting primarily of resident monks and a selection of male and female workers and seldomly a selection of lay people (Timmermann 2009). Among the Knuedler burials, the surplus in men was much higher in the cloister (210) than in the cemetery (152.9). This corresponds to a trend that several studies have pointed out, namely that the presence of men was much more prominent in church burials than in cemetery burials, which was likely due to the higher position of men in society (Caselitz 1981; Ulrich-Bochsler 1997). Whilst clerics and rich benefactors were buried in the church, women were often considered not worthy enough for this burial space, likely due to their "innate sin" and often also their inability to amass riches, high social standing or higher ecclesiastical functions on their own (Ulrich-Bochsler 1997). At Aalst, a similar difference in

MI was observed between cloister and cloister garth burials, the latter of which were considered to contain lay folk and possibly lay brothers, and the former primarily monks. In church burials, there was also a male surplus, but it was smaller than in the cloister and even cloister garth, which the authors suggested might be explained by the fact that the church burials were considered expensive and therefore contained members of the benefactor families, including their children and wives (De Groote *et al.* 2011). This pattern was also observed in the Knuedler burial complex, even though here, the cloister sample also contains a few church burials. Overall, among the other Luxembourgish sites, the MI of the Knuedler cemetery and cloister resembles most closely that of Diekirch, Fentingen and Luxembourg Neumünster (d' Hollosy & de Meulemeester 1999), a Benedictine abbey at first close to and later inside Luxembourg City. Diekirch dates much earlier than the Knuedler site, namely to the early to high middle ages, where a surplus in males is often the norm on cemeteries (Ulrich-Bochsler 1997). The burials from Fentingen all stem from the inside of the church, reflecting the surplus of males among church burials. (Table 8) Therefore, the surplus in males, which is generally higher than that found in urban and rural cemeteries but lower than that in monastic settings, can best be explained through burial of a mixture of monks or friars with a selection of towns people. The higher number of men among the cloister burials suggests that primarily friars were buried in this area, but the few women and children suggest that rich benefactors were likely also buried there as well alongside their families. Another possible explanation would be the presence of nuns, especially as in 1681 AD, the Marienthal refugium, a nunnery, was established close to the Knuedler friary (Reuter 1966).

Furthermore, the MI in Layer 1 (250) was strikingly higher than in the older Layer 2 (127.9), which seems to stand contrary to the general observations that the sexual divide in burial practices receded in postmedieval times and that the presence of both sexes became more balanced (Ulrich-Bochsler 1997). In order to find out whether the presence of men increased in both burial areas over time, the MI was also calculated for each burial location by Layer. Interestingly, the number of men increased a lot relative to that of women in cemetery burials from Layer 2 (103.2) to Layer 1 (238), whereas that in the cloister seemed to decrease slightly (Layer 2: 225, Layer 1: 192.9). The trend observed in the cloister might reflect that observed by Ulrich-Bochsler (1997) for Bernese material, suggestive of a change in burial practices for women from the medieval to postmedieval times, in which it became possible for women to also acquire the rights for church burials. But of more interest is the stark increase in male-to-female ratio between cemetery burials of Layer 2 and Layer 1. In the older Layer 2, the male-to-female ratio was quite balanced, lying in the bounds suggested by Kemkes-Grottenthaler

(1997) for a normal biologically grown population. However, the MI from the cemetery in Layer 1 was the highest estimated for all burial locations and Layers of the burial complex. Therefore, the frequencies of ages at death for male and female adults were determined for each burial location by Layer. Females show a similar trend of age-at-death frequency between burial locations within each Layer, but the trends differ between the Layers. In Layer 1 (Figure 19) women from the cloister had their mortality peak in the mature II (50-59y) and those from the cemetery in the mature I (40-49y) age group, meaning they lived longer than women from Layer 2 (Figure 20) who had their mortality peak in adult age (30-39y), and thus closer to childbearing age. This might either suggest improved living conditions for the women from late medieval to postmedieval times, but, with the construction of the Marienthal refugium in 1681 next to the friary (Reuter 1966), it might also reflect an increased presence of nuns that were not exposed to the risks posed by birthing.

Considering males however, the differences between the layers and burial locations are much more striking. In Layer 2 (Figure 22), men from the cloister had a similar peak age-at-death than men from the cemetery, with the peak in the cemetery lying in the mature II age category and that of the cloister in the senile age category. The values from both Layer 1 and 2 of females and Layer 2 of males are consistent with those of other contemporaneous sites (see Table 7). The high mortality among male seniles in the cloister hints at the presence of friars or males of high social standing in this burial location.

In Layer 1 (Figure 21) however, males from the cemetery show a completely different pattern of age distribution than those from the cloister. While that from the cloister is very similar to that observed in cloister burials from Layer 2, the peak age-at-death among cemetery burials lies in the adult (30-39y) age group. Together with the high masculinity index for this burial location in Layer 1, this means that there were a lot of adult men buried in the cemetery. The reasons for this predominance of adult men cannot be pinned down exactly, but several possibilities should be discussed. For one, it is possible that, over time, the function of the cemetery changed so that more friars were also buried on the cemetery and less women were accepted. Another possibility would be that a burial segregation between men and women took place, and that the burial location of women was simply not excavated. However, all these possible explanations do not account for the high number of adult males. In this case it would be useful to also consider the historical context for the interpretation. The peak adult age at-death suggests that most of these males died at an age where they were fit for military service. In fact, in 1684 AD Luxembourg suffered a several month-long siege by the French army under the command of Vauban. After the successful capture of the city by Vauban, military tensions

remained high between the former occupants the Habsburgs and the new occupants the French, especially between 1700-1714 during the War of the Spanish succession, until the city was ceded again to the Habsburgs in 1715 during the Peace of Rijswijk (Pauly 2011). Therefore, it is possible that the high number of adult men partly reflects those that died during the siege of 1684 AD, but this interpretation remains just a hypothesis.

In conclusion, the sex distribution in the Knuedler burial complex mostly resembles that of other urban friaries and monasteries, with burials likely comprising monastic as well as lay folk. Wealthy benefactors and their families were likely buried alongside friars in the cloister, and the town citizens were predominantly buried in the cemetery. In Layer 1 the high number of adult men suggests either a change in burial practices or might be the consequence of the 1684 AD siege by the French.

Table 8 Masculinity Indices (MI) from the Knuedler cemetery compared to other European and Luxembourgish urban and monastic sites

Masculinity Index compared to other sites										
Urban populations										
Site	*Knuedler overall*	*Emden*	*Ellwangen*	*Ellwangen*	*Lübeck Dom Paradies*	*Lübeck Dom Kirchhof*	*Lübeck Dom Kirchhof*	*Kiel*	*Frankfurt*	*Petershausen*
Period	Mid 14th-18th C	10th-19th C	LM	PM	1173-1299	13th-15th C	16th-18th C	1350-1571	~15th-18th C	PM
MI	167.5	109	110.4	133.3	83	168	182	125.7	283.3	51.9
Monastic populations										
Site	*Knuedler cloister*	*Knuedler cemetery*	*Leipzig Franciscans*	*Ihlow Cistercians*	*Hude Cistercians**	*Schleswig Dominicans*	*Bern Dominicans**	*Aalst Carmelites church&*	*Aalst Carmelites cloister&*	*Aalst Carmelites cloister garth&*
Period	Mid 14th-18th C	Mid 14th-18th C	1227-1550	1228-1529	1232-1536	1239-1529	13th-16th C	16th-18th C	16th-18th C	16th-18th C
MI	210	152.9	353	180.7	1100	464	533.3	122.5	500	182.4
*Luxembourgish sites**										*Hospital*
Site	*Knuedler overall*	*Givenich*	*Diekirch*	*Grevenmacher*	*Fentingen*	*Luxemburg Neumünster*	*Luxemburg St. Esprit*	*Grund/ Wenzelsmauer*	*Luxembourg Hospice civil*	Regensburg Minoritenweg
Period	Mid 14th-18th C	11th-15th C	8th-10th	8th-15th C	10th-15th C	13th-18th C	12th-17th C	16th-18th C	16th-1792	12th-17th C
MI	163.4	86.4	160.5	107.5	155.6	172.3	68.5	375.0	Only Females	117.9

Knuedler = Kremmer (hic)
Emden = Stech (2009)
Ellwangen LM/PM = Kairies (2021)
Lübeck = Caselitz (1982)
Frankfurt = Martens & Alt (2019)
Kiel = Henke (1972)
Lübeck Kirchhof = Boenisch & Bräuer (1986)

Leipzig Franciscans = Schott (1960)
Ihlow Cistercians = Timmermann (2009)
Hude Cistercians = Caselitz (1981)
Schleswig Dominicans = Caselitz (1983) sourced from Stech (2009)
Bern Dominicans = Ulrich-Bochsler & Meyer (1993)
Aalst Carmelites = De Groote et al. (2011)
Regensburg Minoritenweg = von Heyking (2012)

Givenich = Rehbach et al. (2009)
Diekirch = sourced from Trautmann (2012)
Grevenmacher = Trautmann (2012)
Fentingen = Nothwang & Rehbach (2006)
Luxemburg Neumünster = d'Hollosy & de Meulemeester (1999)
Luxemburg St. Esprit = Rehbach (2008)
Grund/Wenzelsmauer = Trautmann & Trautmann (2011)
Luxembourg Hospice civil = Nothwang et al. (2004)

* = only Adults (20+y) in the MI
& = calculated from raw data by the author of this study
MI = Masculinity Index

3.2 Palaeodemography

3.2.1 Introduction

Palaeodemography can provide information on the distribution, size, structure, and development of past populations. Principal demographic parameters, such as life expectancy and probability of death, which can inform on the general health status of a population, rely primarily on accurate age- and to a lesser degree on sex estimations and are calculated using models derived mostly from the field of modern demography (Grupe *et al.* 2015). However, all these calculations and reconstructions rely on the principle that the population under study is stable, stationary, healthy, biologically grown, belongs to the same cohort (have the same year of birth) and is represented in its entirety (Acsádi & Nemeskéri 1970; Grupe *et al.* 2015; Wahl 2022). However, these premises are very rarely given when dealing with archaeological material (Kölbl 2004). The first basis for these premises to hold true would be, that at least the entire cemetery was excavated for there to be a chance that it offers a balanced cross-section through the once living population, as specific burial practices such as segregation of men and women, grouping of children's graves etc. might lead to underrepresentation of certain members of the population (Wahl 1994; Ulrich-Bochsler 1997; Grupe *et al.* 2015). However, this is mostly not the case and certainly was not for the Knuedler burial complex. As shown in the previous section, an accurate age- and/or sex estimation was sometimes not possible. Furthermore, the Knuedler cemetery does not meet the criterion of the assemblage constituting a single cohort due to its large span of use (mid 14th-late 18th C). The premise of a stationary population presumes that there was none or only very minimal immigration or emigration (Acsádi & Nemeskéri 1970; Kölbl 2004; Czermak 2011). The fact that the Knuedler cemetery is situated in a town and especially its capacity as a garrison town where immigration and emigration of military personnel with their families is historically documented (Thewes 2013), already suggests that the population was not stationary. Additionally, the assumption that the population under study should be stable and healthy, ignores that wars, epidemics famines etc. certainly had an influence on mortality (Grupe *et al.* 2015; Wahl 2022). In fact, a few sieges, and epidemics, which led to an increase in deaths, are historically documented for Luxembourg City (Pauly 2011, 2020). The models all work under the premise that the mortuary assemblage reflects a biologically grown living population, however, the structure of the mortuary assemblage generally differs considerably from the living population. The structure of the mortuary assemblage could only represent the living population if the entire living population

suddenly died all at the same time, which is extremely rare (Grupe *et al.* 2015). In an ideal living population, the number of neonates and young children is highest, and the number of individuals decreases gradually with age. In a hypothetical archaeological mortuary assemblage however, the number of neonates and young children is high due to the high risk of mortality in these age groups in the past. Furthermore, the amount of matures and seniles should be higher than the amount of juveniles and adults as the mortality risk increases. Therefore, a mortuary assemblage would reflect a different population structure than the living population (Grupe *et al.* 2015). Additionally, since the Knuedler burial complex belonged to a Franciscan friary where both friars and towns people were buried, it likely does not reflect a biologically grown population, which is also suggested by the very imbalanced male-to-female sex ratio.

Lastly, the Knuedler cemetery is only one of several cemeteries in Luxembourg City (see. Grund/Wenzelsmauer, Hospice civil, St. Esprit, Luxembourg Neumünster etc.) which is why the burials cannot reflect the entire population of the city. Therefore, any palaeodemographic estimations should be interpreted with caution, keeping in mind that none of the basic principles for demographic modelling are fulfilled. Notwithstanding the previously mentioned violations of the principles, a palaeodemographic analysis is still attempted for the Knuedler burial complex as the results can at least indicate a general trend for the population. However, due to the Knuedler cemetery being just one of several in town, no attempt was made to reconstruct population size or growth rate.

3.2.2 Methods

3.2.2.1 Mortality Tables

As the calculation and definitions of mortality tables form the basis for most of the following palaeodemographic calculations, they will be addressed first. The calculation of the mortality tables was adapted to archaeological material by Acsádi and Nemeskéri (1970). The calculations are all based on the age estimation of the skeletons and follow the aforementioned premises (Acsádi & Nemeskéri 1970; Czermak 2011), therefore representing a snapshot of an entire living population. However, most of these premises are not given for archaeological burials and cemeteries (Kölbl 2004; Wahl 2022), which is why the data generated by and from these mortality tables can only be regarded as approximations and need to be interpreted carefully.

In this study, the mortality tables were calculated in 5-year age groups. All individuals that spanned several of the age groups were sorted equally into each of the groups, leading to decimal figures in the D_x (group size in years) column.

The following formulas are used to calculate the mortality tables (originally from Acsádi and Nemeskéri (1970) and sourced directly from Grupe et al. (2015)):

Table 9 Formulas for the calculation of mortality tables

	Calculation of the mortality tables
x	Age group in years
a	Size of the age groups in years
D_x	Number of individuals that died in the specific age groups
d_x	Respective proportion of individuals that died in the specific age groups in ‰
l_x	Relative proportion of survivors in age group x. At birth l_x must unavoidably be 1000‰. For the next age groups, the following formula applies $l_x = l_{x-1} - d_{x-1}$
q_x	Probability of death in ‰ for age group x. $q_x = {}^{d_x}/_{l_x} X1000$ In the highest age group q_x = 1000‰, as no individual can reach a later age.
p_x	Probability of survival in ‰ for age group x. $p_x = 1000 - q_x$ In the highest age group p_x = 0, as no individual can survive to this group.
L_x	Number of lived years in total. $L_x = \frac{a \times (l_x + l_{x+1})}{2}$
T_x	Number of years left to live for age group x. $T_x = T_{x-1} - L_{x-1}$ and $T_0 = \sum L_x$
e_x	Average life expectancy for age group x. $e_x = {}^{T_x}/_{l_x}$

3.2.2.2 Representation

Ideally the skeletal series should be representative of the whole population for any further interpretation of the mortality tables and the resulting calculations to be approximately reliable (Jungklaus & Krippner 2016). There are two formulas that can be used to estimate the representation of the skeletal series under study.

The formulae by Bocquet and Masset (1977) ignore children under 5 years of age and group all adults together due to the oftentimes inaccurate age estimation ranges for adults. Both

formulae need to have their conditions fulfilled for the skeletal series to be representative. The first formula calculates the ratio of children aged 5-9 to that of children aged 10-14. In a representative population, the amount of 5–9-year-olds should be at least twice as high as that of 10–14-year-olds, which are considered to have survived all childhood risks. In the second formula, the ratio of all subadults aged 5-14 to all adults aged 20+y is calculated and for the skeletal series to be representative, the ratio should be equal to or greater than 0.1. This is based on the premise that all adults have survived the risks of childhood and adolescence.

$$\frac{D_{5-9}}{D_{10-14}} \geq 2$$

$$\frac{D_{5-14}}{D_{20+}} \geq 0.1$$

For the sake of completeness, the formula by Weiss (1973) was used as well to determine the representation of the skeletal series. This formula uses the relative proportion of survivors in a certain age group (l_x) and is based on the premise that 10–14-year-olds had the lowest mortality risk overall and that juveniles (15-19y) had a lower mortality risk than neonates.

$$Q_x = 1 - \frac{l_{x+1}}{l_x}$$

where $Q_{10} < Q_{15}$ and $Q_0 > Q_{15}$

3.2.2.3 Probability of death

The probability of death reflects the percentage of individuals that died within a specific age group.There are two possibilities to estimate the probability of death which oftentimes lead to different results. The first possibility is to simply note the estimate q_x calculated already for the mortality tables. This estimate includes all individuals in the sample that could be aged, including those aged less than 5 years. This method for estimating probability of death faces the problem that all estimates include children less than 5 years which are thought to have a higher mortality risk than the other groups.

The second option is to calculate probability of death during the first year of life and during the first 5 years of life following a formula by Bocquet and Masset (1977) which ignores the recorded values for those aged 0-4 years.

According to Grupe et al. (2015), if the observed value q_x for children 0-4 years in the mortality table is lower than the calculated value ${}_5q_0$, the skeletal series under study presents with a child deficit.

$$_1q_0 = 0.568 \text{ x } \sqrt{\log10\ (200\frac{D_{5-14}}{D_{20+}})} - 0.438 \quad \pm 0.0016$$

$$_5q_0 = 1.154 \text{ x } \sqrt{\log10\ (200\frac{D_{5-14}}{D_{20+}})} - 1.014 \quad \pm 0.041$$

3.2.2.4 Life expectancy

Life expectancy (e_0) defines the average of the years that an individual has left to live from birth onwards. There are two ways to estimate life expectancy. The first method would be to use the values at e_x already estimated in the mortality tables. This has the advantage that the average life expectancy was calculated for each age group of the population. However, this formula yields slightly incorrect results as a possible child deficit is not considered. Therefore, a formula by Bocquet and Masset (1977) can be used which only considers adults aged 20+ and children aged 5-14 years to estimate life expectancy at birth, ignoring the number of excavated children aged 0-4 years and thereby circumventing the problems caused by child deficit (Grupe *et al.* 2015).

$$e_0 = 78.721 \text{ x } \log_{10}\sqrt{\frac{D_{20+}}{D_{5-14}}} - 3.384 \quad \pm 1.503$$

3.2.3 Results

3.2.3.1 Representation

In order to estimate how reliable, the following demographic parameters are, the representation of the Knuedler skeletal series was calculated in a first step. According to the formula of Bocquet and Masset (1977), there should be at least twice as many children ages 5-9 years than those aged 10-14 years and the ratio of 5–14-year-olds to adults should be equal or higher than 0.1. None of the two conditions were fulfilled, which is likely due to the small number of subadults in the sample. By adding 7 children to the age group 5-9, both conditions would be fulfilled (2,04 respectively 0,11).

$$\frac{D_{5-9}}{D_{10-14}} = 1{,}43 \qquad \neg \geq 2 \qquad \rightarrow \text{condition not fulfilled}$$

$$\frac{D_{5-14}}{D_{20+}} = 0{,}09 \qquad \neg \geq 0.1 \qquad \rightarrow \text{condition not fulfilled}$$

According to the formulas by Weiss (1973), the ratio of 5–9-year-olds to 0–4-year-olds should be greater than that of 15–19-year-olds to 20–24-year-olds (condition 2) and the ratio of 10–14-year-olds to 15–19-year-olds should be smaller than that of 15–19-year-olds to 20–24-year-

olds (condition 1). For the Knuedler skeletal series, only condition 1 is fulfilled but condition 2 is not.

$$Q_0 = 1 - \frac{l_{5-9}}{l_{0-4}} = 0.04859$$

$$Q_{10} = 1 - \frac{l_{15-19}}{l_{10-14}} = 0.03235$$

$$Q_{15} = 1 - \frac{l_{20-24}}{l_{15-19}} = 0.05378$$

Condition1: $Q_{10} < Q_{15}$: 0.032 < 0.053 → condition fulfilled
Condition2: $Q_0 > Q_{15}$: 0.048 ¬> 0.054 → condition not fulfilled

Since none of the conditions after Bocquet and Masset (1977) and only one condition after Weiss (1973) are fulfilled, the demographic parameters that will be calculated in and derived from the mortality tables need to be considered carefully during interpretation.

3.2.3.2 Life expectancy and probability of death

All mortality tables used for the life expectancy and probability of death calculations can be found in Appendix I. For the comparisons of life expectancy and probability of death by sex, only adult individuals that were strictly 20+ years old were included, all those that would have to count partially to the juveniles as well were left out in order to get a full number total.

3.2.3.2.1 Life expectancy

3.2.3.2.1.1 Overall and by Sex

Overall, the mortality tables indicate a life expectancy at birth (e_0) of 40.20 years and at 20-24 years one (e_{20-24}) of 26.33 years (Tab1A1) When considering only adult males and females, life expectancy rises to 27.09 for males (Tab2A1) and drops to 26.07 for females (Tab3A1).
The life expectancy graphs show a a nearly linear relationship with age, with life expectancy declining gradually until old age (Figure 23). The average life expectancy of men is only noticeably higher in the 0–4-year age group, after that, it becomes very similar to that of females (Figure 24).

Life expectancy overall and by Sex

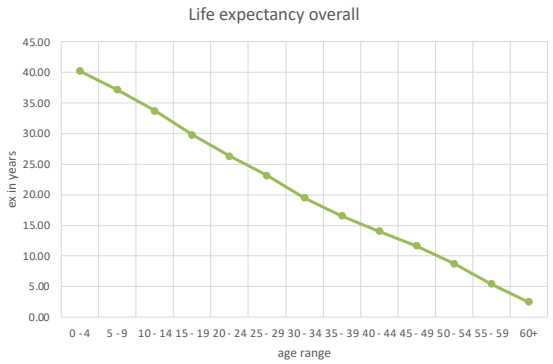

Figure 23 Life expectancy overall

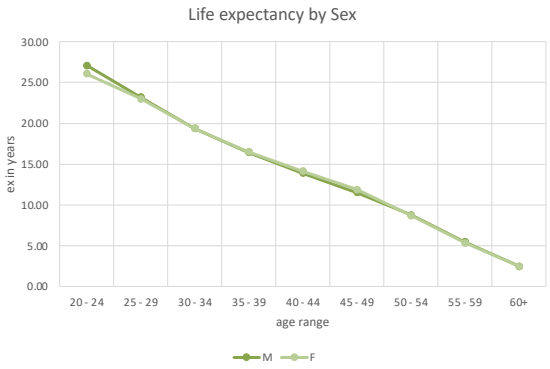

Figure 24 Life expectancy by sex

3.2.3.2.1.2 By Burial Location

In the cemetery, a life expectancy at birth of 39.5 years and at 20-24y one of 25.05 years was observed (Tab7A1). In the cloister, a life expectancy at birth of 42.61 years and at 20-24y one of 29.30 years was observed (Tab4A1). For males in the cemetery, life expectancy at 20-24y lay at 25.20 years (Tab8A1) whereas that of males in the cloister reached 30.97 years (Tab5A1). Females in the cemetery had an average life expectancy of 25.84 years at 20-24 years old (Tab9A1) and that of 20–24-year-old females from the cloister reached 26.80 (Tab6A1). Both males and females from the cloister showed a higher life expectancy than men and women from the cemetery until about 50-54 years of age (Figure 25, Figure 26). In the cemetery, men have overall a higher life expectancy than women but in the cemetery, the trend is reversed and the difference between the sexes is not as marked (Figure 26).

Life expectancy by Burial Location

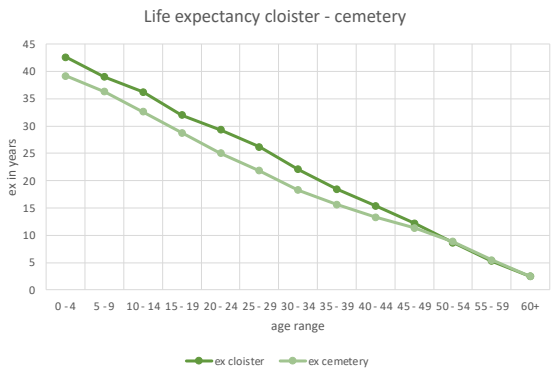

Figure 25 Life expectancy by burial location

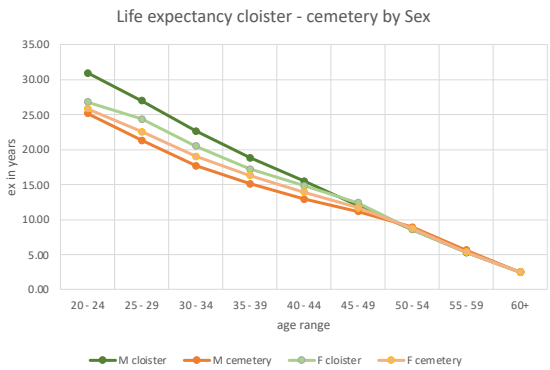

Figure 26 Life expectancy by burial location and sex

3.2.3.2.1.3 By Burial Layer

In burial Layer 1, a life expectancy at birth of 41.51 years and at 20-24y one of 25.37 years was observed (Tab10A1). In Layer 2, a life expectancy at birth of 39.27 years and at 20-24y one of 27.02 years was observed (Tab13A1). For males in the Layer 1, life expectancy at 20-24y lay at 25.24 years (Tab11A1) whereas that of males from Layer 2 reached 28.93 years (Tab14A1). Females in the Layer 1 had an average life expectancy of 26.36 years at 20-24 years old (Tab12A1) and that of 20–24-year-old females from Layer 2 reached only 25.92 (Tab15A1). Overall, life expectancy starts off higher at birth in Layer 1 than in Layer 2 but among 20–24-year-olds, this trend reverses until the 50–54-year age group when life expectancy in both layers assimilates (Figure 27). Males from Layer 1 have overall a lower life expectancy than those from Layer 2 until the 45–49-year age group where the values from both locations become very similar (Figure 28). Females from Layer 1 and 2 have very similar a very similar life expectancy but that of Layer 1 drops slightly starting around 35-39 years. In Layer 1, life expectancy starts off higher in females and the trend reverses around 40-44 years, while in Layer 2 the opposite trend could be observed (Figure 28).

Life expectancy by burial Layer

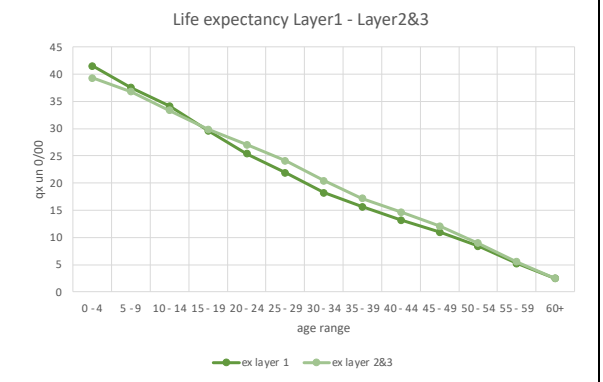

Figure 27 Life expectancy by burial layer

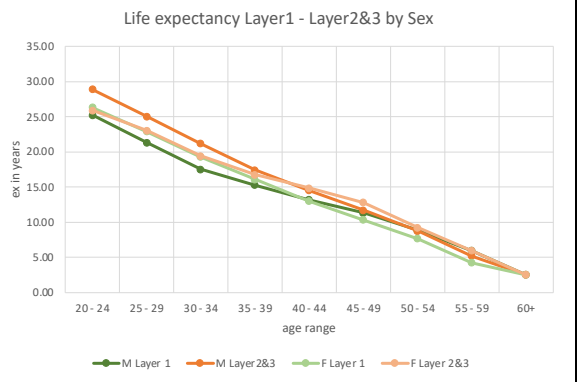

Figure 28 Life expectancy by burial layer and sex

3.2.3.2.2 <u>Probability of death</u>

3.2.3.2.2.1 Overall and by Sex

Overall, the mortality tables indicate a probability of death at birth (q_0) of 4.86% and at 20-24 years still one ($q_{20\text{-}24}$) of 7.19%, which is considered quite low. Only from 30 years onwards, the probability of death exceeds 10% (q_{30424} = 10.88%) (Tab1A1). Adult females ($q_{20\text{-}24}$ = 7.57%) had a higher probability of death than males ($q_{20\text{-}24}$ = 4.31%). Both males and females reach a probability of death higher than 10% from 30 years onwards (Tab2-3A1). Overall, and

among both sexes, probability of death increases slowly until 50 years of age, after which a stark increase occurs (Figure 29, Figure 30).

Probability of death overall and by sex

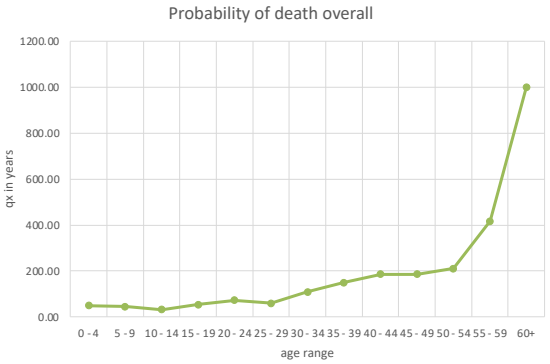

Figure 29 Probability of death overall

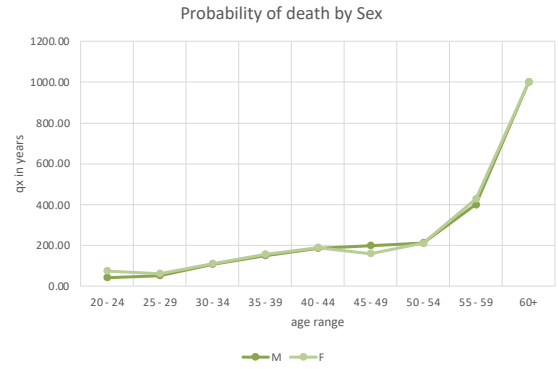

Figure 30 Probability of death by sex

3.2.3.2.2.2 By Burial Location

In the cemetery, a probability of death at birth of 5.50% and at 20-24y one of 7.41% was observed (Tab7A1). In the cloister, a probability of death at birth of 3.39% and at 20-24y one of 6.67% was observed (Tab4A1). Individuals from the cemetery surpassed 10% probability of death after 30 years and those from the cloister only after 34 years. For males in the cemetery, probability of death at 20-24y lay at 4.80% (Tab8A1) whereas that of males in the cloister reached 3.45% (Tab5A1). Females in the cemetery had an average probability of death of 6.91% at 20-24 years old (Tab9A1) and those from the cloister reached 9.63% (Tab6A1). Overall, probability of death from the cloister and cemetery are quite similar until 25-28 years, after which life expectancy becomes more elevated in the cemetery before attaining similar values again around 50-54 years (Figure 31). Both males and females from the cemetery have a higher probability of death than those from the cloister. In cloister, probability of death is lower in men and the opposite trend occurs in the cemetery (Figure 32). Probability of death increases quite gradually until 50-54 years of age after which it increases starkly.

Probability of death by burial location

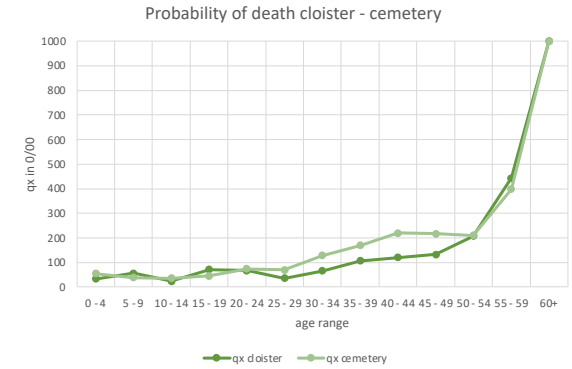

Figure 31 Probability of death by burial location

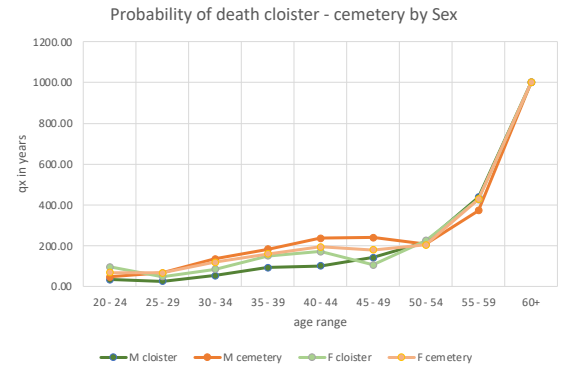

Figure 32 Probability of death by burial location and sex

3.2.3.2.2.3 By Burial Layer

In burial Layer 1, a probability of death at birth of 2.52% and at 20-24y one of 6.34% was observed (Tab10A1). In Layer 2, a probability of death at birth of 6.47% and at 20-24y one of 7.85% was observed (Tab13A1). In Layer 1, individuals surpassed 10% probability rate after 30 years, which occurs earlier than among individuals from the cloister where it happens after 35 years. For males in the Layer 1, probability of death at 20-24y lay at 4.56% (Tab11A1) whereas that of males from Layer 2 reached 4.07% (Tab14A1). Females in the Layer 1 had an average probability of death of 6.05% at 20-24 years (Tab12A1) old and that of 20–24-year-old females from Layer 2 reached 8.37% (Tab15A1). Overall, probability of death is quite similar between Layer 1 and Layer 2, with values from Layer 2 exceeding those from Layer 1 slightly between 5-24 years and from 25-59 years the trend reverses (Figure 33). The same trend observed for burial layers overall also applies to males and females from the two layers. Mostly, men from Layer 1 have a higher probability of death than men from Layer 2 but probability of death among females does not differ much from that of Layer 1 until after 50 years where values of females from Layer 1 become noticeably higher than those from males from Layer 1 and 2, and females from Layer 2 (Figure 34).

Probability of death by Burial Layer

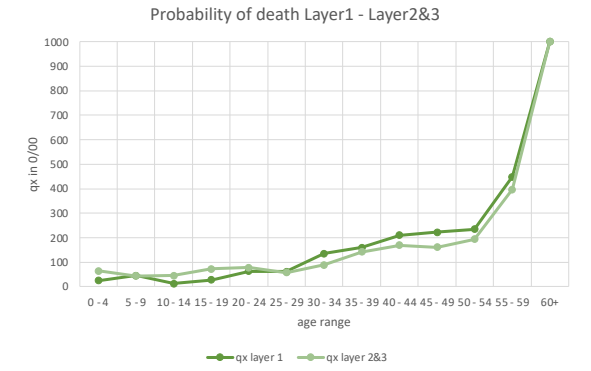

Figure 33 Probability of death by burial layer

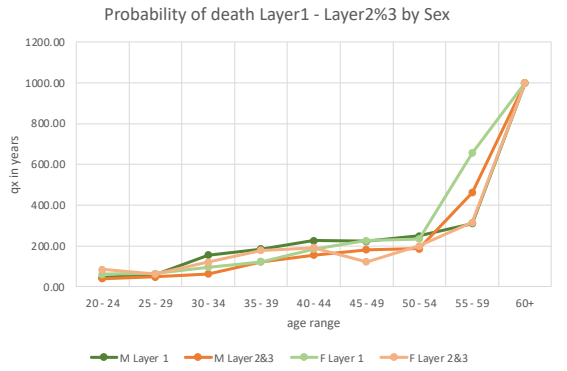

Figure 34 Probability of death by burial layer and sex

3.2.3.2.3 Life expectancy

In order to avoid any potential problems caused by a child deficit, life expectancy was also estimated using the formula by Bocquet and Masset (1977). This formula estimates a life expectancy of ~38.55 years at birth for the whole Knuedler burial complex. This value is slightly lower (1.65y) than that established via the mortality table ($e_{0\text{-}4}$ = 40,2).

$$e_0 = 38.55 \qquad \pm 1.503$$

3.2.3.2.4 Probability of death

Probability of death at birth and within the 5 first years from birth, was also estimated after Bocquet and Masset (1977), which allows for an estimation with minimal influence of a possible child deficit. Therefore, a comparison of the percentage of probability of death with and without potential child deficit, could reveal whether the skeletal series presents a child deficit. If both estimates are the same or very similar, there is no child deficit but if the estimates vary considerably, there is a child deficit. Subtracting the estimate with child deficit from that without child deficit, the percentage and number of missing children missing children in the 0–4-year age group can be determined.

According to these formulas, probability of death at birth lay at 19.34% and between 0-5 years it lay at 26.88%, which means that roughly less than 20% of the members of this population died during the first year and nearly 27% within the 5 first years from birth.

According to the calculated mortality tables, only 4.86% of the children died between 0-5 years, which suggests a child deficit. A $_5q_0$ value of 26.88% means that, in the 0–5-year age group, ~20% of children were missing, which suggests a $D_{0\text{-}4}$ value of 136.

$_1q_0 = 0.19338 \quad \pm 0.0016$
$_5q_0 = 0.26878 \quad \pm 0.041$

3.2.4 Discussion

3.2.4.1 Representation

For a palaeodemographic analysis to be reliable, the skeletal series under study should fulfil several criteria, namely that the skeletal assemblage under study should be stable, stationary, biologically grown, be representative of the entire population and ideally belong to the same cohort (Acsádi & Nemeskéri 1970; Drenhaus 1977; Herrmann *et al.* 1990; Grupe *et al.* 2015). Since archaeological material seldomly fulfils these criteria, over the years, several studies have questioned the reliability and usefulness of these methods applied to archaeological material (Langenscheidt 1985; Wood *et al.* 1992; Waldron 1994; Kölbl 2004). As already mentioned before, the Knuedler burial complex does not seem to fulfil these criteria either. Due to partial excavation, specific burial practices such as a burial segregation of men and women might have led to a noticeable imbalance of the sexes, a grouping of children or shallow children's graves might lead to a child deficit etc. (Wahl 1994; Ulrich-Bochsler 1997; Grupe *et al.* 2015). Furthermore, it is possible that the skeletal assemblage does not represent a biologically grown and stable population. For a population to be stable, birth rates and death rates should be balanced. However, if friars were also buried in the Knuedler complex, which is very likely, they would represent a group that had never contributed to birth rates, thus creating an imbalance in birth and death rates. Hence, it was necessary to verify whether the population buried in the Knuedler cemetery was representative of a biologically grown population. According to the formulae by Bouquet and Masset (1977), a stable and biologically grown population should show at least 2 times more 5–9-year-olds than 10–14-year-olds and the 5–14-year-olds should make up at least 10% of the population relative to all adults. In the Knuedler assemblage, both criteria are not met. However, at 0.09, the ratio of 5–14-year-olds to adults is very close to the required threshold of 0.1. Weiss' (1973) formula is based on the premise that 10–14-year-olds had the lowest mortality risk overall and that juveniles had a lower mortality risk than neonates. In the Knuedler assemblage, the first premise was fulfilled but the second one was not. Therefore, the Knuedler assemblage did not fulfill the majority of the representation criteria, which suggests that the population was not stable nor biologically grown.

An example of a representative skeletal assemblage would be the burials from inside the church in Emden (Stech 2009). Contrary to expectations, this population fulfilled the criteria even though the burial location suggested that only a very specific part of the population would have been buried there. Generally, in the later Middle Ages, church burials were reserved for important clerical figures and wealthier, often male, individuals. Only later, was the family of wealthy citizens also buried inside the church (Illi 1992; Ulrich-Bochsler 1997). Like the Knuedler cemetery, the cemetery of Ellwangen-Jagst had also been only partially excavated, which was listed as one of the reasons why the representation criteria were only partially fulfilled (Kairies 2021). The skeletal series from the Ihlow monastery (Timmermann 2009) and Regensburg Minoritenweg (Von Heyking 2012) did also not fulfill the representation criteria, which was likely due to the fact that both formed mechanically grown populations as the former belonged to a monastery and the latter to a hospital. Since the Knuedler burial complex belonged to a Franciscan friary, the individuals there might also not have represented a biologically grown population. Therefore, all further interpretations of the data need to be considered carefully.

3.2.4.2 Child deficit and child mortality

One of the main criteria that a population has to fulfil in order to be considered representative of a living population is the relationship of subadults to adults. Acsádi and Nemeskéri (1977) postulate that ideally, a cemetery should present between 45-60% of subadult individuals and about 40-55% of adults, and that neonates should never make up less than 20% of the population. This based on the assumption that child mortality was considerably higher in the past, as young children and especially neonates whose immune system has not yet fully developed, were under greater risk of dying from infectious disease, nutritional deficiencies often related to weaning stress etc. (Goodman & Armelagos 1989; Katzenberg *et al.* 1996; Dittmann & Grupe 2000; Lösch 2009; Pearson *et al.* 2010). However, many archaeological skeletal series do not fulfil these criteria (Kölbl 2004). In fact, based on the mortality table, the Knuedler skeletal assemblage presented only 16.75% of subadults. Therefore, based on a comparison of estimates for probability of death between 0-5 years from the mortality table and those derived from a calculation by Bocquet and Masset (1977), a child deficit of ~20% among 0–4-year-olds was confirmed for this skeletal series. Social, cultural and biological factors as well as archaeological determinants such as preservation and recovery, may influence infant representation in a skeletal series (Goodman & Armelagos 1989; Ulrich-Bochsler 1997; Kölbl 2004; McFadden *et al.* 2022). If children were buried in shallow graves they might have

been already disturbed and destroyed before the archaeological excavation of the cemetery (Cave & Oxenham 2007). A partial excavation of the burial complex might have as a consequence that not all children were excavated if they were buried in a specific area of the cemetery that was not excavated (e.g. the so called "Traufkinder"/"eaves-drip-burials", mostly perinates or neonates that had likely not been baptised and are thought to have been buried under the eave of the church in hopes of a post-humous baptism through consecrated rain water from the roof (Lindenhofer 2012; Hausmair 2020)), or barred from burial on the cemetery entirely due to religious practices, such as unbaptised children being often excluded from burial in Christian cemeteries or the possibility that some religious institutions might not have accepted child burials (Wahl 1994; Ulrich-Bochsler 1997; Lewis 2007; Obertová *et al.* 2008; Hausmair 2017; McFadden *et al.* 2022). Furthermore, due to their more porous structure, smaller size and lower mineral content, children's bones might decompose faster than adult bones, leading in return to an underrepresentation of subadults (Buckberry 2000; Scheuer & Black 2000; Lewis 2007; Djurić *et al.* 2011). However, several studies also suggest that most of the time there is no actual child deficit and that the assumption that the number of children must lie around 45-60% due to their increased mortality risk, is simply not true (Dollhopf 2002; Kölbl 2004). Parental care and access to adequate health care might, for instance, have an influence on child mortality (Oxenham, M., & Willis 2017; McFadden *et al.* 2022), and since social status usually regulates access to health care, the number of subadults might also be influenced by socioeconomic status of the population under study (McFadden *et al.* 2022). However, several studies have proposed and even shown, that the number of subadults is above all else influenced by fertility rates, wherein small numbers of subadults would indicate low fertility of the population (Kölbl 2004; McFadden *et al.* 2022). It is however impossible to pin down the causes for the very low number of subadults in the Knuedler skeletal assemblage. On the one hand, the cemetery has only been partially excavated increasing the risk of missed burial groups, furthermore, it is known that the first church of the cloister was transformed into friary buildings in the mid-17th century when a new church was built (Bis-Worch 2011), which might have led to a destruction of burial groups close to the church walls or inside the first church. On the other hand, the burial complex belonged to a friary, which means that certainly, friars, which most likely did not contribute to the fertility and birth rates, were also buried at the site, which is already suggested by the significant surplus in males. This hypothesis was also used to explain the low percentage of subadults in the Ihlow monastery skeletal sample (Timmermann 2009). In short, any or several of these factors might have led to the observed underrepresentation of children in the Knuedler skeletal assemblage.

3.2.4.3 Life expectancy and probability of death

According to Grupe et al. (2015), life expectancy and probability of death are the most important parameters calculated in the mortality table, as they make good proxies to estimate the overall health status of a population. In the Knuedler assemblage, overall life expectancy at birth lies at 40.20 years (corrected for child deficit: 38.55y) and at 26.33 years among 20–24-year-olds (M: 27.09y; F: 26.07y). A comparison to urban, rural and monastic sites revealed that the life expectancy at birth of the Knuedler cemetery most closely resembles that of other monastic burials. As such, individuals buried at the Cistercian monasteries of Ihlow (Timmermann 2009) and Hude (Caselitz 1981) showed a life expectancy at birth of 39.0 respectively 42.3 years and those buried in the Dominican convent in Schleswig had a life expectancy at birth of 37.5 years (Table 10). Timmermann (2009) argued that the underrepresentation of subadults and overrepresentation of older adults, likely caused the elevated life expectancy at birth suggesting that the high life expectancy would be indicative of better living conditions in the monasteries. As reasons for better living standards in monasteries she lists the relative absence of everyday stress factors due to a regulated working day, a regular supply of food and the protection that a secluded life style likely offered in regard to infectious diseases among others (Timmermann 2009). The burials recovered around the monastery church in Petershausen (Konstanz) showed a life expectancy at birth of 41 years for males and 39 years for females for the burials dating to the early postmedieval period (Berszin 2009) (Table 10). In all these cases, the high life expectancy at birth is influenced by the low number of subadults and the relatively high number of older adults, which was also the case in the Knuedler cemetery. According to Berszin (2009) this age-at-death distribution was likely caused by the fact that the individuals buried in such close proximity or inside the church were either clerics, monks or probably rather wealthy lay folk. This suggests that their higher social status possibly allowed them access to better healthcare, which in return might have led to more individuals surviving into old age and less individuals dying in childhood. The same interpretation can likely be applied as well onto the Knuedler burial complex. In fact, when calculating life expectancy at birth for the two burial areas of the Knuedler burial complex it becomes evident that life expectancy at birth is slightly higher among cloister (42.61y) than among cemetery (39.5y) burials, which might suggest a higher living standard for the former. In the 20-24 age group, the difference in life expectancy between cloister (29.30y) and cemetery (25.05y) was even more marked. This difference in life expectancy might therefore indicate a difference in social status of the people buried in the two inhumation areas. This

would not be very surprising as burials within a church or within the cloister area were often reserved for monks/friars, high-ranking clerics and high-ranking members of society and their families (Ulrich-Bochsler 1997).

But even so, life expectancy at birth is still higher in the Knuedler cemetery area, than in regular urban and rural cemeteries and even higher than burials inside parish churches, with the exception of Lingen (1250-1541 AD) urban cemetery where a life expectancy at birth of 43.7 years was observed (Caselitz & Heine 1979) (Table 10). It is also generally thought that burials in a monastery, even on their cemetery, were also more sought after and therefore not affordable to everyone (Ulrich-Bochsler 1997), which might explain the differences observed between regular cemeteries and the one from the Knuedler friary.

At 20-24 years, the average life expectancy (26.33 years) of the Knuedler skeletal assemblage, together with the other monastic sites, starts resembling that found in urban and rural cemeteries and church burials (calculated on an age cohort of 20-29 y), resembling most closely that of the cloister burials from the Dominican monastery in Bern (Ulrich-Bochsler & Meyer 1993). The Knuedler burial complex and Petershausen also showed a difference in life expectancy at birth between men and women, with men having overall a higher life expectancy than females (Berszin 2009), which might be related to the fact that women did not have the same recognition in past societies and might have been treated differently and that they were exposed to the risk of dying in child birth at a rather young age (Schultz 1982; Ulrich-Bochsler 1997). However, some studies point out that the risk of dying during child birth is often overestimated (Kemkes-Grottenthaler 1997) and that the risk of dying in child bed is ultimately more influenced by insufficient nutritional intake and too much exertion than by the number of births (Acsádi & Nemeskéri 1970). This trend was true for cloister burials and burials from Layer 2 but not for cemetery burials and burials from Layer 1, where men tended to have a lower life expectancy than women, which was likely influenced by the large number of adult males buried in the cemetery in Layer 1.

In order to be able to compare the Knuedler assemblage to another site from Luxembourg City, a new mortality table in 10-year steps was calculated for both the Knuedler and St. Esprit skeletal series. The table for St. Esprit was calculated based on raw data from the final report by Rehbach (2008). Following the new calculations, life expectancy at birth until 10 years of the Knuedler skeletal series was 40.5 years, at 21-30 years it was 26.8 years (Tab16A1). At St. Esprit, life expectancy at birth until 10 years was 33 years and 23.6 years at 21-30 years (Tab17A1) (Figure 35). Therefore, the health status of individuals buried in St. Esprit was likely slightly lower than that of Knuedler individuals.

As a general observation on the life expectancy at birth values obtained for the Knuedler sample, it has to be pointed out that the high values observed are likely strongly influenced by the very low number of subadults in the assemblage. Since it is unclear what caused this child deficit in the Knuedler assemblage, the life expectancy estimates can only be regarded as a general trend.

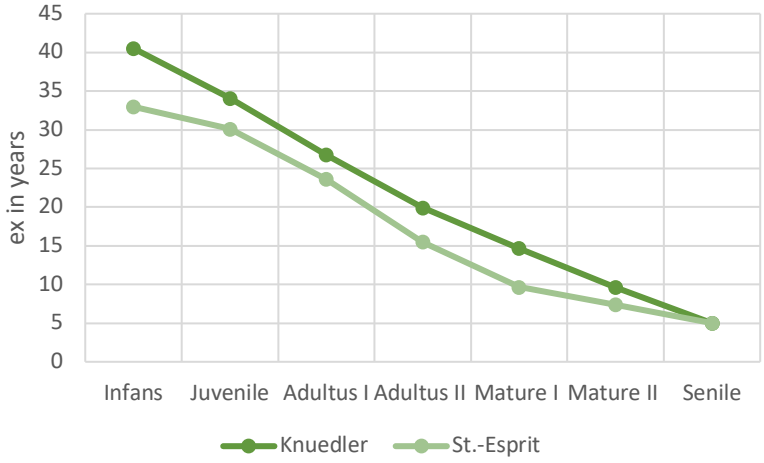

Figure 35 Life expectancy for 10-year steps for the Knuedler ad St. Esprit burial grounds

Regarding probability of death, which is very closely linked to life expectancy, the lowest value was observed in 10–14-year-olds (3.24%) and 5–9-year-olds (4.44%). Bocquet and Masset (1977), Strott (2006) as well as Grupe et al. (2015) argue that infans II and juveniles are least exposed to factors that increase mortality risk and should therefore show the lowest probability of death. This trend was also observed in other roughly contemporaneous skeletal samples such as in Emden (Stech 2009) and in Minoritenweg (Von Heyking 2012), a medieval hospital in Regensburg. Among the monastery burials of Ihlow (Timmermann 2009), probability of death was highest among infans I and in burials from rural Grevenmacher (Trautmann 2012) individuals between 15-19 years showed the lowest probability of death. When comparing the Knuedler cemetery to St. Esprit, probability of death was lowest in the juvenile age category whereas in St. Esprit it was lowest in the young adult age group. As in high- and late medieval Ellwangen-Jagst (Kairies 2021) and Minoritenweg (Von Heyking 2012), a small peak in probability of death was observed in the 20-24 year age group. For the differences between the sexes, the same trends apply that were already discussed in the section on life expectancy.
In the Knuedler sample, the low probability of death at birth, the slight increase after 30 years and then suddenly and strongly after 50 years is likely influenced by the low number of

subadults and fairly high number of mature II and seniles. A similar trend was observed by von Heyking (2012) for the burials at Minoritenweg. She argues that the high number of seniles is not unusual for a hospital as the patients were likely old and hospitals often adopted the function of a care home for the elderly (Jungklaus 2017). The increased presence of elderly individuals in a cemetery could therefore be indicative of effective health care (Kairies 2021).

Table 10 Comparison of life expecancy at birth and 20 years to other European urban, rural and monastic sites

Comparison of Life expectancy at birth and at 20-24 years				
Site	*Period*	e_0	e_{20}	*Study*
Urban sites				
Emden*	10th-19th C	29.4	21.2	Stech (2021)
Ellwangen%	LM	26.4	14.0	Kairies (2021)
Ellwangen%	PM	20.3	16.8	Kairies (2021)
Kiel (Gertrudenfriedhof)	1350-1571	28.6	23.5	Helmuth (1966)/Henke (1972)
Lübeck Dom	1173-1299	30.8		Caselitz (1982)
Lingen	1250-1541	43.7		Caselitz & Heine (1979)
Monastic sites				
Knuedler%	mid-14th-18th C	40.2/*40.5*	26.33/*26.8*	Kremmer (hic)
St. Esprit	12th-17th C	33.0	23.6	Kremmer (hic)&
Bern Dominicans	13th-16th C		25.0	Ulrich-Bochsler & Meyer (1993)
Schleswig Dominicans church*	1239-1529	29.8		Caselitz (1983)
Schleswig Dominicans cemetery	1239-1529	37.6		Caselitz (1983)
Ihlow Cistercians	1228-1529	39.3	23.3	Timmermann (2009)
Hude Cistercians	1232-1536	42.3		Caselitz (1981)
Petershausen	PM	39/41		Berszin (2009)
Hospital				
Minoritenweg%	12th-17th C	35.8	22.6	Von Heyking (2012)
Rural sites				
Grevenmacher%	8th-15th C	30.5	20.8	Trautmann (2012)
Treskow	11th-15th C	27.5		Jungklaus et al. (2001)
Tasdorf	13-16th C	29.0		Jungklaus &Niemitz (2001)
Diepensee	13th-14th C	29.8		Jungklaus (2008a,b)

* Burials inside church
% e_x calculated in 5 year steps, other sites in 10 year steps
& Calculated by the author on raw data from Rehbach (2008)
Italic nb = calculation in 10-year steps
LM = late medieval
PM = postmedieval

3.2.5 Conclusion

In conclusion, the low probability of death and high life expectancy at birth from the Knuedler friary are in line with those observed for other monastic sites and suggest that the people buried at the Knuedler friary had an overall good health status with adequate access to health care and the means to provide themselves with adequate nutrition. However, as the skeletal series cannot be considered representative, these interpretations must be considered with care.

4 Growth

4.1 Introduction

Together with age and sex estimation, height estimation constitutes one of the main aims of anthropological investigation. Since modern studies have found that body height, although mainly genetically predetermined, is also influenced by environmental factors such as climate, nutrition, physical activity etc. and that especially in poorer countries differences in stature are quite evident between different socioeconomic groups (Bogin 1999a, 2001; Davey Smith *et al.* 2000; Kreiter *et al.* 2000; Ozmen *et al.* 2013), stature is often used in anthropological studies to estimate overall population health (Goodman *et al.* 1992; Betsinger *et al.* 2021).
Several studies on archaeological skeletal material have found associations between stature and mortality, showing that lower stature is often associated to higher mortality (Alter *et al.* 2004; Kemkes-Grottenthaler 2005), whilst other studies have focused on the association of body height and mass and socioeconomic status (Lantzsch & Schuster 2009; Siegmund 2010a; Vercellotti *et al.* 2011; Schoch *et al.* 2012; Kaupová *et al.* 2013; Weiss *et al.* 2019) or have investigated the impact of nutrition and disease on body height (Mays *et al.* 2009; Geber & Murphy 2012). In this light, it was the aim of this study to firstly create a growth curve for the subadults to see whether they followed a normal growth pattern and to detect any growth disturbances during childhood. Secondly, adult body height, body mass and BMI were calculated and compared between the Layers and social groups in order to determine whether any of these factors had a significant influence on body height and whether anthropometric measures could be used to characterise different social groups on the site. Lastly, the results from the Knuedler cemetery should be compared to other Luxembourgish and European sites in order to understand whether they follow the general trends prevalent across Europe during the late medieval and postmedieval times.

4.2 Methods

4.2.1 Subadults

All bone measurements of subadults were recorded following the definitions in Welte and Wahl (2010). Only long bone measurements were used in this study as the measurements for skull cap thickness and thickness of the cruciform eminence could not be recorded for many of the

subadults present. Growth curves were therefore reconstructed based on the long bone lengths and circumferences, and in the case of the radius, distal diaphyseal width, to investigate differences in growth rate of lengthwise and appositional growth.

Body height was estimated from all available long bone lengths using the discriminant functions of Telkkä et al. (1962) sourced from Hermann et al. (1990). In order to use discriminant functions based on the same population, the formulas by Telkkä et al (1962) for individuals aged 10-15 years were also applied to those aged 16-20. Telkkä et al. (1962) present separate formulas for males and females. For those individuals that could not be sexed, the average of the height reconstructions for males and females was used, but for those that could be sexed, the formulas for the corresponding sex were calculated. To increase sample size, body height reconstructions were not limited to one single bone, instead height reconstructions from all available bones were used. Furthermore, since body height reconstructions based on different bones also yield slightly different results, the average of all body height reconstructions for all available bones was taken for each individual as final body height.

Data processing also followed the recommendation by Welte and Wahl (2010). In order to maximise sample size in each age group, the measurements of one individual were included in all age groups included in the determined age range of the individual. This means that an individual aged 1-2 years was added to the 1-year age group and to the 2-year age group, an individual aged 11-13 years was added to the 11-year age group, the 12-year age group and the 13-year age group etc., as the measurements recorded for these individuals might be representative of all these age groups. This procedure helped to avoid potential misclassifications of measurements if having to choose just one of the possible age groups. Table 11 indicates the number of individual measurements in the respective age group for each long bone measurement and body height. Based on these classifications, a growth curve in annual steps was established for each bone measurement and body height. In the line plots (= growth curves), the dots represent the average measurements of each age group in millimeter (mm) for the long bone measurements and in centimeter (cm) for body height, and the lines connect these averages to visualise the overall trend in the data. The growth curves were established for each bone and the dark green line represents the bone lengths whereas the light green line represents the circumferences/widths. The lengths are plotted on the primary y-axis on the left and the circumferences/widths are plotted on the secondary y-axis on the right but both values are plotted on the same x-axis (Age in years). Additionally, the standard deviation of the measurements within each age group was calculated and added to the line plot in the form of error bars. Finally, a velocity curve, a curve representing the amount of additional bone

growth by year, was calculated by subtracting the average of the previous age group from that of the following age group. For example, additional growth between 0 and 1 years was calculated by subtracting the average of the 0-year age group from that of the 1-year age group etc. The plotting of the velocity curve is the same as that already described for the growth curve. The velocity curve is an effective tool to estimate growth spurts within a population.

Table 11 Number of individuals in each age category for each measurement (due to overlapping age estimations, several age groups share the same participants)

Number of individuals within each age group							
Neonate and Infans I							
Measurement	*0*	*1*	*2*	*3*	*4*	*5*	*6*
H3	3	5	6	4	2	4	5
H6	4	7	6	4	3	5	7
R7	2	3	4	3	2	2	3
R8	3	3	4	4	3	3	3
F10	0	2	5	4	3	2	2
F13	2	7	6	5	4	6	6
T14	2	2	3	4	4	4	4
T16	2	3	4	5	4	4	4
Height	3	5	6	4	4	4	5
Infans II							
Measurement	*7*	*8*	*9*	*10*	*11*	*12*	*13*
H3	3	6	3	2	1	1	1
H6	4	7	5	5	3	3	3
R7	2	3	2	3	2	1	1
R8	3	5	2	2	1	1	1
F10	1	3	4	5	4	2	3
F13	2	5	6	7	4	4	5
T14	1	4	6	7	3	0	0
T16	1	4	6	7	3	0	0
Height	3	6	6	7	4	2	3
Juvenile							
Measurement	*14*	*15*	*16*	*17*	*18*	*19*	
H3	1	3	5	4	3	2	
H6	2	2	7	7	6	4	
R7	1	4	8	8	7	4	
R8	2	4	7	5	6	3	
F10	3	5	9	8	6	6	
F13	6	7	12	11	9	8	
T14	1	5	10	11	9	7	
T16	3	5	11	11	9	8	
Height	3	5	10	11	9	7	

H = humerus
R = radius
F = femur
T = tibia
The numbers behind the letters represent the measurements after Welte and Wahl (2010)

4.2.2 Adults

Since there is still no universal consensus on which height reconstruction formulas to use, the discriminant functions by Pearson (1899), Bach (1965) for females, Breitinger (1938) for males, Trotter and Gleser (1952) ("American White") and Ruff (2012) were used in this study. This was done in order to render this skeletal assemblage from Luxembourg City comparable

to several contemporaneous European sites all while still using the most up-to-date formulas. The formulas developed by Pearson (1899) are based on a reference population by Rollet (1888) from France and the formulas are particularly useful for height estimations of archaeological material as this reference population dates before the onset of the acceleration, which describes, among other things, the increase of anthropometric parameters such as stature. The formulas by Breitinger (1938) were developed on in-life measurements of German athletes and those by Bach (1965) were based on in-life measurements for female athletes from the DDR. As Rösing (1988) and Siegmund (2010) already pointed out, the formulas by Bach (1965) and Breitinger (1938) do not produce accurate height estimations as they tend to overestimate actual height. Since those formulas are most often used in German studies however, it was necessary to calculate them for this study as well so that a comparison to German medieval and postmedieval sites would be possible. The formulas by Trotter and Gleser (1952) were developed on a reference population of fallen American soldiers from the second World War with known live size as well as on the skeletal remains from the Terry collection in St. Louis. Ruff et al. (2012) developed their formulas on archaeological reference skeletons, which makes these formulas particularly suited for height reconstructions of archaeological skeletal remains. Ruff et al. (2012) determined body height of 501 individuals (male: 268, female: 233) spanning the complete Holocene period and many geographical regions, with the modified Fully method. The regression formulas for the single bones were then based on these reconstructed heights and yielded good results for all time periods and geographical regions tested. Even though more formulas are available by Trotter and Gleser (1952) and Ruff et al. (2012), only those based on maximum humeral (H1), radial (R1), femoral (F1) and tibial (T1b) length were used in this study so that all calculations include the same number of individuals and measurements. The formulas by Bach (1965) and Breitinger (1938) rely partially on different measurements which were not recorded in this study. Therefore, the height estimations after Bach (1965) are based on H1, F1 and T1b and those by Breitinger (1938) only on F1 and T1b). Where possible, height reconstructions were based on femoral measurements, in absence of femoral measurements they were substituted by tibia, humerus or radius, in the order as they are listed. When left- and right-side measurements were possible, an average of the height estimations for the right and left side were taken. Within site comparisons were only conducted for Pearson (1988), Trotter and Gleser (1952) and Ruff et al. (2012), but Breitinger (1938) as well as Bach (1965) were only used for comparisons to other sites. Body mass was estimated using the formulae from Auerbach and Ruff (2004) and Ruff et al. (2012). Whenever possible F19 was used in the calculations and was substituted by

F18. When right and left side could be measured, an average value of both sides was calculated. Height and body mass reconstructions were not performed on pathologically altered bones.
In order to account for both body height and weight, BMI was calculated using the following formula:

$$BMI = \frac{Weight\ (kg)}{Stature\ (cm)^2}$$

The body height and weight values estimated from the formulas provided by Ruff et al. (2012) were used for the BMI estimations as both formulas were developed by the same authors and on the same reference populations. BMI was also calculated based on height reconstructions after Trotter and Gleser (1952) and weight reconstructions after Auerbach and Ruff (2004) as this combination allowed for some comparisons to other sites.
The BMI values of each individual were then attributed to the following categories as recommended by the World Health Organisation (WHO 2010) (Table 12):

Table 12 BMI classification after WHO (2010)

Range	Category - WHO	Category – short
<18.5	Underweight	UW
18.5-24.9	Normal weight	NW
25.0-29.9	Overweight/Pre-obesity	OW
>30.0	Obesity	OB

4.3 Results

4.3.1 Growth in Subadults

All growth curves of all long bones and of reconstructed body height show, as expected, a steady increase in size by age. All growth curves show a stark increase in size or height from 0 to 1 year of age. Between 1 and 2 years, the curve starts flattening and this trend continues between 2 and 3 years, which likely corresponds to a period of growth stagnation. After 3 years the curve becomes steeper again, meaning that the growth rate increased. Between 6 and 7 years the curve got steeper again, representing another episode of accelerated bone growth. (Figure 36, Figure 38, Figure 40, Figure 42, Figure 44)
The curves of additional growth by annual steps represent growth velocity, which means that they indicate how much a bone (in mm) or the body (in cm) has grown either in length or in circumference/width from one age group to the next. These velocity curves show several peaks,

episodes of increased growth, which occurred more or less around the same ages across all measurements. The first peak occurs between 0 and 1 year of age. After that, growth velocity decelerates until the next smaller peak which occurs around 3-4 years. After a short period of growth deceleration, the next larger peak is reached at around 6-7 years in bone lengths as well as circumferences/widths and body height. After another period of decreased bone growth, another peak can be observed in all velocity curves, except that of the tibia because the data is missing, around the age of 11 years and another, more prominent peak occurred around the age of 13-14 years. Only in reconstructed body height, the peak around 11 years is more prominent than that around 13-14 years. (Figure 37, Figure 39, Figure 41, Figure 43, Figure 45) For most bones, the velocity curves of the length and circumference/width follow the same pattern and show peaks in the same age groups. However, in the humerus, appositional growth of the diaphyseal circumference occurred slightly shifted regarding the length wise growth. Whilst lengthwise growth showed two velocity peaks, one at around 10 and one at around 13 years, appositional growth only showed one at around 11 years. (Figure 37) All bones present a further albeit smaller peak in growth velocity around 17 and 18 years, but this peak is strongly influenced by one particularly tall individual which achieved a final body height of ~185cm.

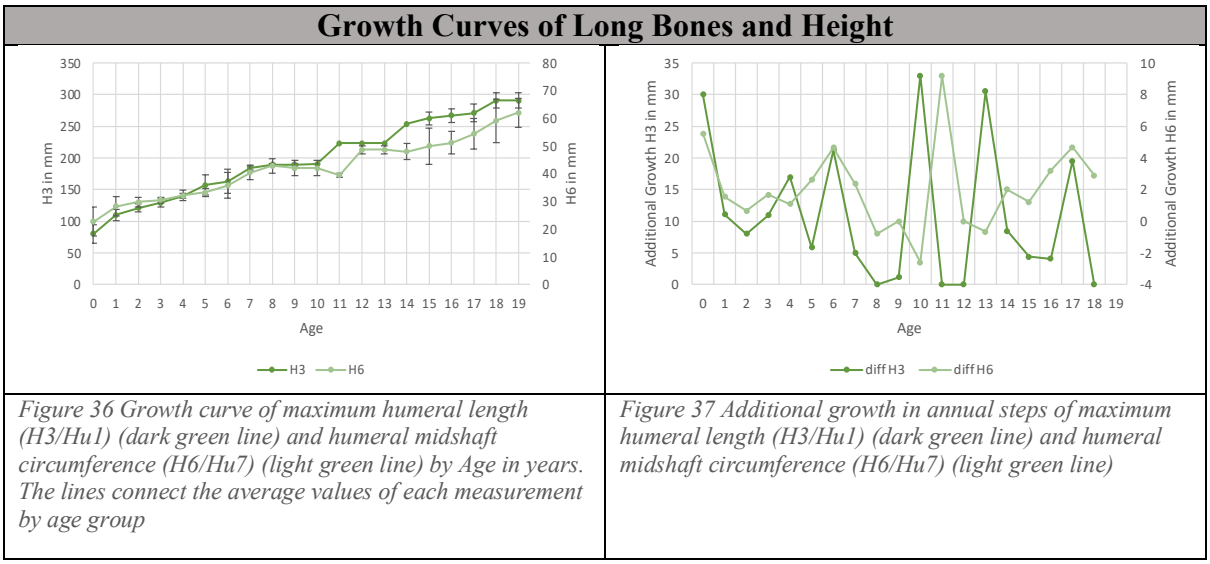

Figure 36 Growth curve of maximum humeral length (H3/Hu1) (dark green line) and humeral midshaft circumference (H6/Hu7) (light green line) by Age in years. The lines connect the average values of each measurement by age group

Figure 37 Additional growth in annual steps of maximum humeral length (H3/Hu1) (dark green line) and humeral midshaft circumference (H6/Hu7) (light green line)

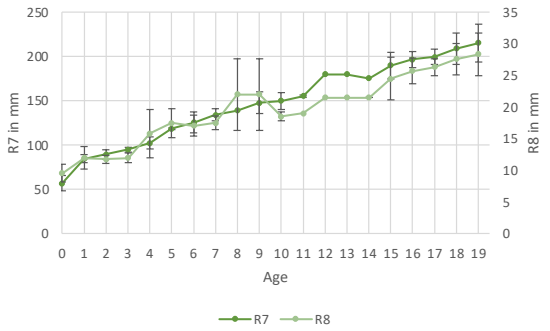

Figure 38 Growth curve of maximum radial length (R7/Ra1) (dark green line) and maximum breadth of distal diaphysis (R8/Ra5(6)) (light green line) by Age in years. The lines connect the average values of each measurement by age group

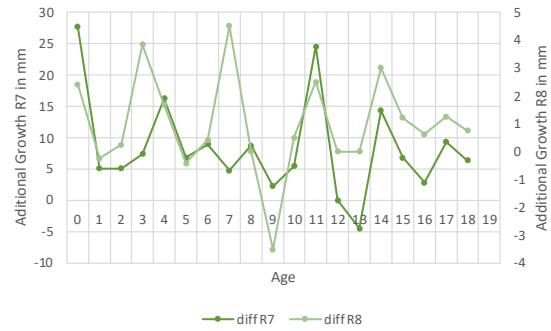

Figure 39 Additional growth in annual steps of maximum radial length (R7/Ra1) (dark green line) and maximum breadth of distal diaphysis (R8/Ra5(6)) (light green line)

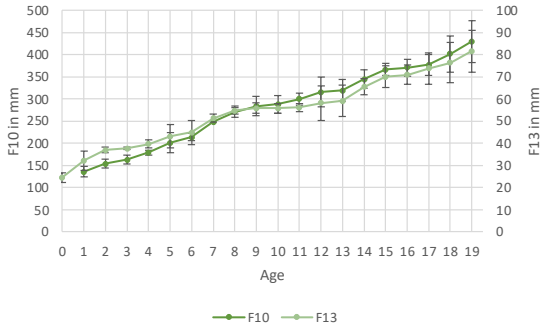

Figure 40 Growth curve of maximum femoral length (F10/Fe1) (dark green line) and femoral midshaft circumference (F13/Fe8) (light green line) by Age in years The lines connect the average values of each measurement by age group

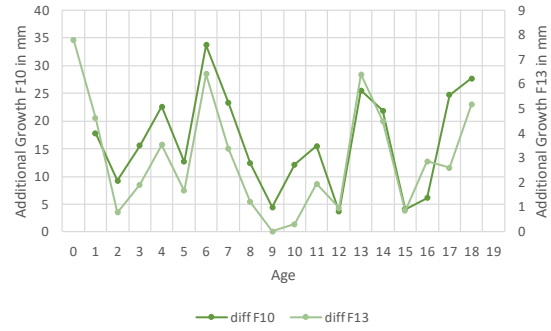

Figure 41 Additional growth in annual steps of maximum femoral length (F10/Fe1) (dark green line) and femoral midshaft circumference (F13/Fe8) (light green line)

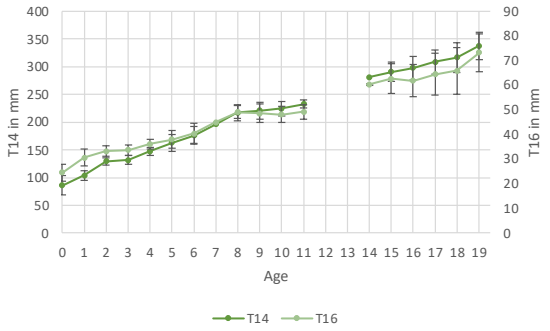

Figure 42 Growth curve of maximum tibial length (T14/Ti1) (dark green line) and tibial least circumference (T16/Ti10b) (light green line) by Age in years. The lines connect the average values of each measurement by age group

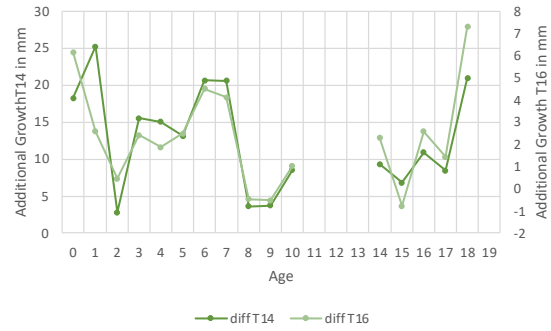

Figure 43 Additional growth in annual steps of maximum tibial length (T14/Ti1) (dark green line) and tibial least circumference (T16/Ti10b) (light green line)

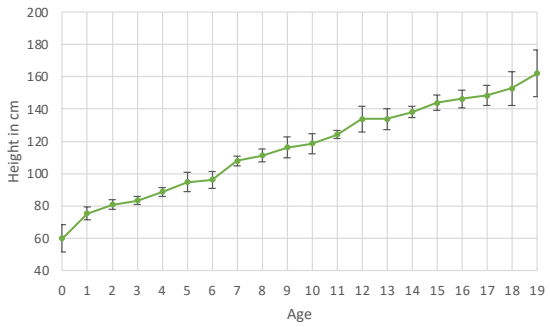

Figure 44 Growth curve of reconstructed body height by Age in years. The lines connect the average values of each measurement by age group

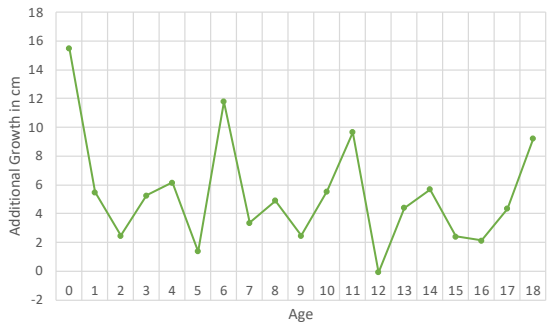

Figure 45 Additional growth in annual steps reconstructed body height

4.3.2 Body Height in Adults

Overall, the formulas by Ruff et al. (2012) and Pearson (1988) yield the smallest height reconstructions. Both the formulas by Pearson (1988) and Ruff et al. (2012) can be considered to match actual achieved height of the Knuedler population most closely since they are both based on reference populations dating before the onset of the acceleration of human development, which is thought to have started in the mid-19th century. All formulas showed that there is a significant difference in height between males and females with males being on average taller than women. According to Pearson (1899), average female height was 154.22 cm (min: 145.98, max: 163.38) and average male height was 166.89 cm (min: 156.91, max: 179.54). After Trotter and Gleser (1952) average female height amounted to 157.71 cm (min: 146.97, max: 169.52) and male height amounted to 170.62 cm (min: 159.11, max: 185.77). Following the formulas by Ruff et al. (2012) females achieved an average height of 155.80 cm (min: 144.70, max: 168.78) and males an average height of 166.74 cm (min: 152.71, max: 184.97). Among both men and women, no significant differences in reconstructed body height could be detected among the age groups nor between the burial locations. But on average, females were slightly taller in the cemetery and males slightly taller in the cloister. Heights were also more widespread in the cemetery than in the cloister for both men and women, with men from the cemetery having 21.08cm difference between the highest and lowest estimated height, in women from the cemetery this difference lay at 17.40 cm, in men from the cloister at 17.93 cm and in females from the cloister at only 10.79cm, suggesting that especially the female population from the cloister was likely more homogenous than that from the cemetery. Overall, among both males and females, there is a trend of increasing stature by burial Layer with those from Layer 1 being on average taller than those from Layer 2. Height reconstructions based on formulas after Pearson (1899) and Ruff et al. (2012) did not show any significant

difference between burial layers among the two sexes. However, males from Layer 1 were significantly taller than those from Layer 2 when formulas by Trotter and Gleser (1952) were used. (Table 13) Although only results of the Mann-Whitney-U/Wilcoxon tests are presented in this study for all groups, those groups where a comparison by a parametric test was possible, were also tested using the parametric test and those yielded the same results as the non-parametric tests. For completeness, the average values for height reconstructions for females after Bach (1965) and for males after Breitinger (1938) will be mentioned here as they will be used later for comparisons to other sites. A significant difference in height between men and women was also recorded based on those formulas, with women sporting an average height of 161.35 cm and males a height of 169.37 cm.

Table 13 Within site comparisons of body height reconstruction (cm) after Pearson (1899), Trotter and Gleser (1952) and Ruff et al. (2012)

Adults		**Body Height Reconstruction**										
Factor		**variable**	**n**	**Pearson (1988)**			**Trotter and Gleser (1952)**			**Ruff et al. (2012)**		
				mean	**median**	**p-value**	**mean**	**median**	**p-value**	**mean**	**median**	**p-value**
Total			248	162.27	163.09		165.96	166.96		162.63	162.62	
Sex		F	86	154.22	153.99	**<0.0001**	157.71	157.10	**<0.0001**	155.80	155.47	**<0.0001**
		M	155	166.89	167.03		170.62	170.49		166.74	166.88	
Age	F	YA	14	154.18	154.46	0.9751	157.71	157.75	0.9714	156.07	156.44	0.9773
		Adult	20	154.61	153.51		158.22	156.79		156.45	155.13	
		Mature I	14	154.18	154.43		157.41	157.53		15.23	155.40	
		Mature II	18	154.51	154.0		157.94	157.23		156.41	155.34	
		Senile	12	153.36	152.32		156.51	155.82		154.87	153.64	
	M	YA	14	167.86	168.12	0.8235	172.49	172.28	0.4895	168.82	169.34	0.4180
		Adult	43	166.87	166.19		170.50	170.24		166.66	165.66	
		Mature I	31	165.44	165.25		168.72	168.79		164.83	164.30	
		Mature II	28	167.12	167.03		170.69	170.23		167.45	167.12	
		Senile	29	167.86	168.12		171.49	172.08		167.94	167.98	
Location	F	Cemetery	71	154.30	154.10	0.7457	157.79	157.41	0.7457	155.87	155.60	0.9682
		Cloister	15	153.85	153.37		157.34	156.85		155.46	154.93	
	M	Cemetery	112	166.67	166.78	0.2465	170.37	170.30	0.3091	166.41	166.88	0.2066
		Cloister	43	167.46	167.22		171.29	171.10		167.61	167.97	
Layer	F	1	30	155.06	154.75	0.1213	158.87	158.46	0.0937	156.99	156.68	0.0772
		2	56	153.77	153.71		157.09	156.80		155.16	154.32	
	M	1	74	167.54	167.29	0.0753	171.54	171.07	**0.02940**	167.64	167.94	0.0704
		2	81	166.30	165.48		169.79	168.99		165.92	165.32	

4.3.3 Body Mass in Adults

Overall, the body mass reconstructions after Auerbach and Ruff (2004) yielded slightly heavier weights than those after Ruff et al. (2012). As expected, both formulas indicated that males (A&R(2004): avg.: 69.58kg, min: 50.76kg, max : 84.21kg; Ruff et al. (2012) avg.: 68.50kg, min : 52.35kg, max : 83.86kg) weighed significantly more than females (A&R (2004): avg.: 58.74kg, min : 46.76kg, max : 69.96kg; Ruff et al. (2012) avg.: 57.56kg, min : 45.09kg, max :

67.78kg). No significant differences in weight existed between the age groups. Males from Layer 1 were significantly heavier than those from Layer 2 and the opposite trend was visible in females albeit non-significant. According to both formulas, females from the cemetery were significantly heavier than those from the cloister. Men showed the same trend than women, but significance was only reached with the formulas by Ruff et al. (2012). (Table 14)

Table 14 Within site comparisons of body mass (in kg) reconstructions after Auerbach and Ruff (2004) and Ruff et al. (2012)

Adults		**Body Mass Reconstruction**							
Factor		**variable**	**n**	**Auerbach and Ruff (2004)**			**Ruff et al. (2012)**		
				mean	**median**	**p-value**	**mean**	**median**	**p-value**
Total			193	65.50	65.83		64.38	64.63	
Sex		F	72	58.74	59.21	**<0.0001**	57.56	58.06	**<0.0001**
		M	120	69.58	69.36		68.50	68.05	
Age	F	YA	12	58.39	59.87	0.1757	56.71	59.12	0.1485
		Adult	18	57.18	56.77		55.65	55.34	
		Mature I	12	62.22	62.19		61.07	59.59	
		Mature II	15	57.62	55.78		57.21	55.31	
		Senile	11	58.69	59.34		58.01	58.41	
	M	YA	13	71.70	73.16	0.1836	70.79	68.06	0.3021
		Adult	34	69.88	69.99		68.79	70.10	
		Mature I	27	68.66	68.54		67.21	66.86	
		Mature II	24	69.30	68.84		68.59	68.06	
		Senile	20	68.71	68.17		67.57	67.17	
Location	F	Cemetery	59	59.31	59.34	**0.0357**	58.10	58.34	**0.0419**
		Cloister	13	56.17	56.73		55.10	54.86	
	M	Cemetery	89	70.16	70.16	0.0503	69.20	68.55	**0.0496**
		Cloister	31	67.90	68.30		66.49	66.58	
Layer	F	1	25	58.20	58.22	0.7584	56.97	56.31	0.5153
		2	47	59.03	59.22		57.88	58.10	
	M	1	58	71.17	70.29	**0.0090**	70.28	69.62	**0.0194**
		2	62	68.09	68.46		66.84	67.13	

The calculation and classification of the BMI showed that overall (n=187), most females displayed normal weight (81.69%, n=58) followed by those with overweight (15.49%, n=11) and only one female each was underweight (1.41%, n=1) or obese (1.41%, n=1). Most men were of normal weight (59.48%, n=127) but compared to females, the proportion of overweight individuals (40.52%, n=47) was higher in men. Men did not show any underweight or obese individuals. As such, the Fischer's exact test showed that the distribution of BMI classes within males differed significantly from that of females (p=0.0002). On average, males (24.58) also had a higher BMI than females (23.72) (p=0.0046). Within both sexes, no significant differences could be detected in BMI class distribution between the burial layers and locations (Figure 47, Figure 46) as well as among the age groups. When considering BMI average however, females from the cemetery (23.92) displayed a significantly higher BMI than those from the cloister (22.64) (p=0.0193). The same trend was observable in males but was not

statistically relevant (cloister: 23.94, cemetery: 24.80, p=0.0835). No significant differences were detected in average BMI between males and females of Layer 1 and 2. BMI based on height reconstructions after Trotter and Gleser (1952) and weight reconstructions after Auerbach and Ruff (2004) yielded similar results except that the difference between males and females was not significant. More males fell into the normal weight category, whilst slightly more females turned out to be overweight. This discrepancy shows that BMI reconstructions need to be considered with care as they might yield quite different results depending on the formulas they are based on.

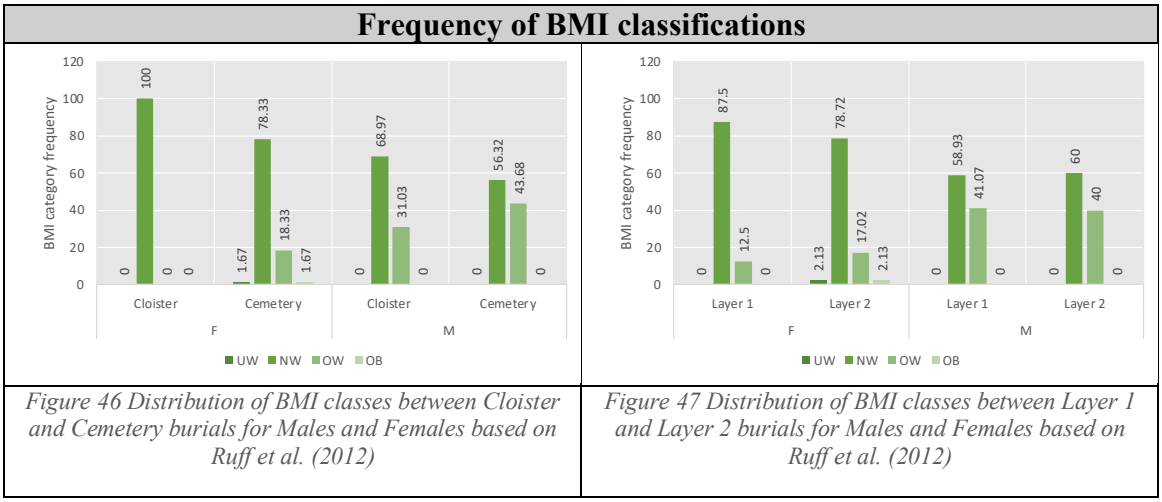

Figure 46 Distribution of BMI classes between Cloister and Cemetery burials for Males and Females based on Ruff et al. (2012)

Figure 47 Distribution of BMI classes between Layer 1 and Layer 2 burials for Males and Females based on Ruff et al. (2012)

4.4 Discussion and Conclusion

4.4.1 Growth

According to Bogin (2001), the growth process from birth to adulthood can be divided into 5 phases: the infancy stage ranging from birth to ~3 years, followed by the childhood stage from 3 to ~5 years, the juvenile stage from 7 to 10 years in girls and 7 to 12 years in boys and ends with the adolescent stage. Each growth phase is characterised by distinct rates in growth velocity (Bogin 2001).

A total of 5 growth peaks could be observed in the growth velocity curves of the subadults of the Knuedler cemetery. As explained by Bogin (2001), directly after birth, a rapid growth velocity occurs which marks the start of the infancy stage of the growth phase. Towards the end of the infancy stage, growth velocity decelerates slightly. The trend observed in both the growth and velocity curves of the Knuedler sample for children between birth and about 3 years of age corresponds to the infancy stage described by Bogin (2001). From birth to 1 year of age there is a stark increase in growth, followed by a noticeable reduction in growth velocity around

2-3 years before growth picks up pace again around 3-4 years. Of particular interest is the low growth velocity around 2-3 years. Stech (2009) observed a similar phase of growth stagnation around 3 years in subadults from the church in Emden, northern Germany and Hühne-Osterloh (1997) observed also a growth retardation around 3 years of age among medieval subadults from Schleswig. Most likely this growth stagnation or at least retardation can be attributed to the weaning process. In fact, Hühne-Osterloh (1997) argue that in Schleswig this was the case since Grupe (1986) was able to narrow down weaning age in this population to 0.5-2 years based on trace element analysis. The change from breastfeeding to weaning foods, even if gradual, puts the child's organism under significant pressure, as new food items expose the child to new pathogens and oftentimes the weaning foods are not very nutritious compared to breastmilk, which might lead to episodes of malnourishment if the child's nutritional requirements are not met (Katzenberg *et al.* 1996; Dittmann & Grupe 2000; Miszkiewicz 2015). And whilst in modern societies, weaning foods are often supplemented or naturally high in proteins, vitamins and other nutrients (Asma *et al.* 2006), in the middle ages, weaning foods mostly consisted of pap, mainly bread soup, made from bread, butter and broth (Kühnel 1986). Therefore, it is possible that the weaning stress, caused a growth stagnation or retardation (Wurm 1987). This would then indicate that the children buried in the Knuedler cemetery were weaned around 2-3 years of age. These results will be further considered in following chapters dealing with the weaning process. The light growth spurt observed between 3-4 years among subadults from the Knuedler cemetery might then be tentatively interpreted as an episode of catch-up growth to make up for the growth retardation during the weaning period.

The next growth peak that can be observed in the Knuedler cemetery falls around 7-8 years and according to Bogin (2001), corresponds to the mid-growth spurt which marks the end of the childhood growth phase. The juvenile growth phase is marked by the slowest growth rate since birth (Bogin 2001). A deceleration of growth can also be observed in this phase for the subadults from Knuedler. A further two growth velocity peaks could be observed in the Knuedler growth curve. Whilst the second of these peaks, which occurs around 13-14 years, most likely represents the adolescent growth spurt, the cause for the first peak at around 11 years is not entirely clear. As Trautmann (2012) suggested, this earlier peak might either represent children that entered the adolescent growth spurt earlier than others due to better nutritional conditions during life or they might represent differences between the sexes. As Bogin (2001) states, in girls, the juvenile growth phase usually ends around 10 years already and that in boys only around 12. This means that the adolescent growth spurt occurs earlier in girls than in boys. Unfortunately, the fragmentary preservation of most subadult remains did

not allow for a clear sex estimation in these age groups, which is why the latter theory cannot be accounted for in this study. However, it was possible to check the distribution of burial locations (cloister vs. cemetery) among the individuals composing the two growth peaks, but the distribution was rather balanced so that socioeconomic differences in growth spurt occurrence can likely be discarded.

Overall, the growth curve from the Knuedler cemetery resembles that of other contemporaneous sites such as Grevenmacher from Luxembourg, Emden from Germany and a series from Schleswig from Germany. This suggests that the trends observed in the curve are valid despite the small number of subadults that could be included (n=58).

4.4.2 Achieved body height and weight

Even though final body height is predominantly genetically determined, it is also influenced by environmental factors (Bogin 1999b; Silventoinen *et al.* 2000, 2003; Silventoinen 2003; Kemkes-Grottenthaler 2005; Rizzoli 2008; Siegmund 2010b). Today, in Western societies, it is estimated that about 20% of stature variation is caused by environmental factors. In poorer countries however, the influence of environmental factors is thought to be more extensive and body height is thought to vary with socioeconomic status (Silventoinen 2003). Nutrition and diseases are the factors that have most influence on bone growth and therefore on adult body height (Bonjour *et al.* 2001; Silventoinen 2003; Rizzoli 2008). In fact, dietary intake can directly or indirectly affect bone metabolism leading to delays or accelerations in bone resorption or bone remodeling rate by influencing osteoblast and osteoclast activity (Rizzoli 2008). Sufficient protein, vitamin D, calcium, phosphorus and other trace element intake are thought to promote bone growth, whereas a lack or shortage of those nutrients can lead to bone growth retardation (Kreiter *et al.* 2000; Bonjour *et al.* 2001; Branca & Ferrari 2002; Rizzoli 2008; Mays *et al.* 2009; Ozmen *et al.* 2013). Therefore final body height mirrors mainly the nutritional and likely socioeconomic status of individuals during their childhood (Bogin 1999b; Davey Smith *et al.* 2000; Komlos 2005; Siegmund 2010b). In fact, Vercellotti et al. (2011) found that in an Italian medieval population, men of higher social status were distinctly taller than men of low social status but found no status-based differences in body size in women. The same pattern was later also observed in a study on medieval inhabitants of Alba in Italy (Weiss *et al.* 2019). But Siegmund (2010a) did not find an association between social status and stature. Henceforth, it was the aim to test whether individuals buried in the cloister, which are thought to be of higher social status, achieved a higher adult body height than those from the cemetery, but no statistically significant differences were detected between the groups. Males

from the cloister, based on formulas from Pearson (1899), were on average only 0.79cm taller than those from the cemetery and females from the cloister were on average 0.45cm smaller than those from the cemetery. This suggests that individuals buried in the cemetery did not experience a more adverse nutritional provision than those buried in the cloister, which in return indicates that the social divide between the two groups might not have been very prominent. However, it also has to be kept in mind, that there are biological mechanisms to correct for slowed growth. As such, catch-up growth has often been observed in modern populations to correct for delayed or slowed growth in childhood (Mummert *et al.* 2011) and might even lead to delayed closure of epiphyses (Rosenstock 2014). Therefore, possible differences in nutritional status between individuals from the cemetery and cloister might not be directly reflected in adult body height. As Harris lines are thought to represent catch-up growth (Mays 1985), it might be interesting for future studies, to X-ray some long bones from the cemetery and cloister to detect any Harris lines, but this type of analysis was outside the scope of this thesis. However, due to bone remodeling, Harris lines are often not retained in the skeleton for a long time anyway and are therefore also a rather unreliable proxy for identifying catch-up growth (Mummert *et al.* 2011).

Siegmund (2010a) and Bogin (1999b) also suggest that adult body height might be affected by climatic conditions either directly or indirectly. On the one hand, according to Allen and Bergman's rule, stature body shape and body proportions are influenced directly by climate as the body adapts in order to cope with different climatic conditions. In order to get rid of excess heat, populations living closer to the equator generally display longer limbs and a rather slender build whereas those living further north and in high altitude have rather short and stocky limbs in order to conserve body heat (Pearson 2000). On the other hand, climatic conditions also influence harvest outcomes, which in return have an impact on food availability, especially among rural populations that are directly dependent on agriculture (Siegmund 2010b). In urban centers, due to a flourishing market system, episodes of bad harvests were often not felt as badly as in the countryside because food items could be imported from further away (Adamson 2004; Ervynck 2004; Van Neer & Ervynck 2004). On the other hand, urbanisation brought also a host of health risks such as increased exposure to infectious diseases due to crowded living conditions, garbage accumulation and water pollution (Armelagos *et al.* 2005; Galea & Vlahov 2005; LaDeau *et al.* 2015; Betsinger *et al.* 2020, 2021), and additionally, as can be witnessed in urban areas of lower-income countries today, the poor were likely also not exempt from food shortages (Joshi *et al.* 2019). Comparisons of stress indicators between past urban and rural populations have yielded very mixed results, with some studies supporting that

individuals from rural areas were healthier overall than urban dwellers (Gamble 2020) whereas other studies have found the exact opposite pattern (Palubeckaitė *et al.* 2002; Walter & DeWitte 2017; Nagaoka *et al.* 2019; Ives & Humphrey 2020) and others did not find any differences at all (Alter 2004; Mays *et al.* 2008; Schoch *et al.* 2012; Kaupová *et al.* 2013; Primeau *et al.* 2018).

Therefore, the adult body height from Layer 1 and Layer 2 from the Knuedler cemetery was compared to the adult body height of other roughly contemporaneous northern European rural, urban and monastic communities (Table 15). When compared to other urban sites, females from both Layers fall below the estimated average height and males fall just around the average, following reconstructions based on formulas by Pearson (1899). However, only 3 urban sites, one of them being the Knuedler cemetery and the other two being Ellwangen-Jagst and St. Esprit monastery which also is also located in Luxembourg City, could be compared according to the formulas by Pearson (1899), which means that these observations are not representative. However, it is clear, that individuals from the Knuedler cemetery are very similar in height to those from the St. Esprit cemetery, which is not surprising as both are located in the same city. However, individuals from the St. Esprit cemetery are on average smaller than those from the Knuedler cemetery, which might suggest, that the St. Esprit cemetery harboured individuals of a lower social status than those buried on the Knuedler cemetery. Using the formulas by Bach (1965) and Breitinger (1938) comparisons to 9 different medieval and postmedieval German sites are possible. In this instance females from both Layers fall above the average female height and males from Layer 2 fall just below and those from Layer 1 just above the mean of men. Using the formulas by Trotter and Gleser (1952), it was possible to compare the Knuedler site to Ellwangen-Jagst in Germany, to 6 sites from the Netherlands and to Spitalfields in England. In this case, the females from Luxembourg fall clearly below the average whereas men fall just around the average. This suggests that women from Luxembourg City were closer in height to German urban women than to Dutch women, which were on average taller, and that Luxembourgish men fall within the average height of urban men from the Netherlands and Germany. Compared to rural sites, the urban sites yield consistently slightly higher average heights, especially in men. Females from the Knuedler cemetery are of a similar height and the females from St. Esprit are even smaller than those from rural Luxembourgish sites, whereas men from the Knuedler cemetery are ~1-2cm taller than men from the rural sites. Men and women from the Knuedler cemetery are taller than those from rural German sites. These comparative results suggest that especially urban men were exposed to less stressors in childhood that might have inhibited growth. However, since the height differences are so small,

statistical comparisons on raw data between the urban and rural sites would be needed, to test whether the differences observed are of statistical relevance. When comparing the Knuedler cemetery to purely monastic sites however, at the monastic sites both men and women were noticeably taller, and overall, monastic sites showed noticeably higher average stature in both sexes compared to urban and rural sites. This is likely due to the fact that monks and nuns entered monastic life often at a young age already, profiting from the privileged living conditions that often prevailed in monastic institutions, but it is unclear in how far this influenced overall health of the monks and nuns (Mays 2009; Timmermann 2009). Even though the Knuedler cemetery belonged to a friary, the cemetery and likely also the friary grounds were open for lay burials of the towns people, which is why average health and therefore stature would be rather representative of that of an urban population.

Furthermore, several studies have found a decrease of stature from the early medieval to postmedieval times (Wurm 1985; Steckel 2004; Maat 2005; Siegmund 2010b; Arcini *et al.* 2014). Therefore, a comparison of stature between all burials from before ~1650AD and after ~1650AD was carried out for the Knuedler sample but generally, no significant differences were found between both Layers. However, it is noticeable that males and females are consistently taller in Layer 1 than in Layer 2. Therefore, the temporal trend of a decreasing stature could not be observed in this sample.

Table 15 Comparison of adult stature with rural, urban and monastic sites across northern Europe

Stature									
Period	**Site**	**Country**	**Pearson (1899)**	**Pearson (1899)**	**Bach (1965)**	**Breitinger (1938)**	**Trotter & Gleser (1952)**	**Trotter & Gleser (1952)**	**Publication**
Sex			*F*	*M*	*F*	*M*	*F*	*M*	
Rural populations									
8th-15th C	Grevenmacher	Luxembourg	156.4	166.2	161.1	169.3	160.9	170.8	Trautmann (2012)
10th-15th C	Fentingen	Luxembourg	154.0	167.0					Rehbach et al. (2005), Nothwang & Rehbach (2006)
11th-15th C	Givenich	Luxembourg	154.0	163.0					Rehbach et al. (2009), Weidig et al. (2009)
13th-14th C	Diepensee	Germany			163.0	170.0			Jungklaus (2008a, b)
11th-15th C	Treskow	Germany			164.0	170.0			Jungklaus et al. (2001)
13th-16th C	Tasdorf	Germany			160.7	168.7			Jungklaus & Niemitz (2001a)
13th-15th C	Dahmsdorf	Germany			156.7	164.9			Melzer (2005)
Average			*154.8*	*165.4*	*160.6*	*168.2*			
Urban populations									
10th-18th C	Emden	Germany			162.8	171.9			Stech (2009)
1350-1571	Kiel Gertrudenfriedhof	Germany				168.8			Helmuth (1966)

Stature									
1173-1299	Lübecker Dom	Germany			157.8	169.8			Caselitz (1982)
13th-16th C	Bernau	Germany			161.0	169.0			Hornig (2009)
13th-16th C	Liebenwalde	Germany			154.0	165.0			Jungklaus (2004)*
13th-16th C	Templin	Germany			160.5	169.8			Büttner (2006)
13th-16th C	Strausberg Dominikaner	Germany			160.3	162.5			Jungklaus (not published)*
Late medieval	Ellwangen-Jagst	Germany	157.4	162.5	163.4	170.7	162.1	171.8	Kairies (2021)
Postmedieval	Ellwangen-Jagst	Germany	156.6	168.0	160.8	169.6	160.6	170.9	Kairies (2021)
12th-17th C	Regensburg Minoritenweg	Germany			160.8	169.6			Heyking (2012)
12th-17th C	St. Esprit	Luxembourg	152.5	163.4					Rehbach & Bis-Worch (2006), Nothwang et al. (2006), Rehbach et al. (2007), Rehbach & Nothwang (2007), Rehbach (2008), Rehbach & Nothwang (2009)
14th-mid-17th C	Knuedler	Luxembourg	153.77	166.30	161.0	168.9	158.87	171.54	Kremmer (hic)
mid-17th-18th C	Knuedler	Luxembourg	155.06	167.54	162.1	170.0	157.09	169.79	Kremmer (hic)
1265-1433	Delft	Netherlands				170.5	163.2	171.8	Onisto et al. (1998)
1275-1572	Dordrecht	Netherlands				170.6	160.8	172.5	Maat et al. (1998)&
1433-1652	Delft	Netherlands				168.9	162.2	170.8	Onisto etal. (1998)
1455-1572	Gorinchem	Netherlands				169.7	160.7		Maat & Mastwijk (2000)
1600-1824	Breda	Netherlands				171.3	160.6		Maat & Mastwijk (2000)
1725-1828	Alkmaar	Netherlands				170.0	159.9	170.6	Baetsen (2001)
1700-1850	London, Spitalfields	England					157.0	169.0	Molleson & Cox (1993)[6]
Average			*155.1*	*166.5*	*160.4*	*169.3*	*160.3*	*171.0*	
Monastic populations									
1228-1529	Ihlow Cistercians				164.4	172.5			Timmermann (2009)
1170-1563	Barthe Premonstratensian Sisters				165.1	174.2			Burkhardt (2001)
1232-1536	Hude Cistercians				170.4	173.3			Caselitz (1981a)
1227-1543	Leipzig Franciscans					167.2			Schott (1960)*
Average					*166.6*	*171.8*			

*Sourced from Timmermann (2009)
& Sourced from Baetsen (2001)

Comparisons of body mass to other European medieval and postmedieval sites proved more difficult as studies on this measurement are not as prevalent as those on stature. Nevertheless, it was possible to compare body mass from the Knuedler cemetery to a rural and an urban site in Denmark (Parker 2019), two medieval Italian sites (Vercellotti *et al.* 2011; Weiss *et al.* 2019) and several medieval Swiss, Austrian, German and Swedish sites (Siegmund 2010a) (Table 16). An overall comparison of the rural and urban sits seems to suggest that urban and rural

women were of similar weight, but urban men were on average heavier than rural men. However, since the rural sample only consists of two different sites, the observed difference needs to be considered with care. When comparing only regionally close sites, it becomes clear that in Denmark, the rural population weighed less than the urban population, but in Luxembourg the opposite trend was observed. Within the urban samples, men and women from both the high- and low-status burials from the Knuedler cemetery fall within the urban range. When comparing high- and low status burials, both Italian sites (Vercellotti *et al.* 2011; Weiss *et al.* 2019) showed significant differences between the social groups. At both Italian sites and Grevenmacher, males from high status burials had higher body mass than those from low-status burials (Vercellotti *et al.* 2011; Trautmann *et al.* 2017; Weiss *et al.* 2019). At Trino Vercellese, this trend was also visible within women (Vercellotti *et al.* 2011) but in Alba and Grevenmacher, body mass of women did not differ much between the two social groups (Trautmann *et al.* 2017; Weiss *et al.* 2019). A significant difference was also detected between high- and low-status burials from the Knuedler cemetery. However, here females from high-status burials were heavier than those from low-status burials but men from high-status burials were lighter than those from low-status burials. As Parker (2019) noted, increased body weight is not necessarily due only to higher body fat but might also reflect increased muscularity. This might then also be reflected in increased BMI caused by higher muscularity and shorter stature among poorer individuals. Siegmund (2010b) however did not find any statistically relevant differences between social classes regarding body mass. Furthermore, males showed significantly higher body mass in Layer 1 (postmedieval) than in Layer 2 (late medieval/early postmedieval) but females showed the opposite trend albeit non-significant. Siegmund (2010b) analysed body mass and BMI over the course of the Middle Ages and did not find a significant increase or decrease over time and concluded that there was more variation within the different time periods than between them, suggesting that mainly living conditions had an influence on body weight. Possibly, the increase in body weight observed in men from Layer 2 to Layer 1 might therefore indicate an improvement of living conditions over time.

Table 16 Comparison of adult body mass with rural, urban and mixed sites across northern Europe

Body Mass					
Period	**Site**	**Country**	**Auerbach and Ruff (2004)**	**Auerbach and Ruff (2004)**	**Publication**
Sex			*F*	*M*	
Rural populations					
	Tirup	Denmark	53.7	66.1	Parker (2019)
	Grevenmacher high-status	Luxembourg	62.2	71.3	Trautmann et al. (2017)
	Grevenmacher low-status	Luxembourg	62.3	68.8	Trautmann et al. (2017)
Average			*59.4*	*68.7*	
Urban populations					
	Black Friars	Denmark	56.7	68.0	Parker (2019)
8th-13th C	Trino Vercellese High-status	Italy	56.81	70.91	Vercellotti et al. (2011)
8th-13th C	Trino Vercellese low-status	Italy	54.98	66.51	Vercellotti et al. (2011)
7th-18th C	Alba high-status	Italy	65.0	76.8	Weiss et al. (2019)
7th-18th C	Alba low-status	Italy	65.2	75.4	Weiss et al. (2019)
14th-18th C	Knuedler high-status	Luxembourg	59.31	67.90	Kremmer (hic)
14th-18th C	Knuedler low-status	Luxembourg	56.17	70.16	Kremmer (hic)
Average			*59.2*	*70.8*	
Mixed sites					
Medieval	Europe mix	Europe	60.2	73.8	Siegmund (2010b)

Regarding BMI, a comparison of males and females from the rural (Tirup) and urban (Black Friar) individuals from Denmark revealed that both groups had very similar proportions of BMI classifications. In Tirup 8.3% of male individuals were underweight, 86.1% normal weight, 5.6% overweight and 0 obese and 0 female individuals were underweight or obese, 80.3% were normal weight and 19.7% were overweight. The urban Black Friar site yielded very similar results with 1.4% of males being underweight, 89.2% being of normal weight, 9.4% being overweight and 0 obese, and 0.6% of females being underweight and obese, 72.4% being of normal weight and 26.5% being overweight (Parker 2019). Female BMI distribution is very similar to that from the Knuedler cemetery, but male BMI distribution differs considerably, with the Knuedler cemetery displaying proportionately more overweight individuals. However, when using the BMI based on Auerbach and Ruff (2004) and Trotter and Gleser (1952), male values become also very similar to those of the Danish sites. A comparison of the Knuedler cemetery to a set of mixed medieval European sites was also possible using BMI based on Auerbach and Ruff (2004) and Trotter and Gleser (1952). Overall, the same trend is visible among the medieval mixed European sites that has already been observed for the Danish and Luxembourgish sites, namely that proportionately more women are of normal weight than overweight but that men tended to be overweight more frequently than women. But whilst in

the Danish and Luxembourgish sites, normal weight was still vastly predominant, among the European mixed sites, overweight was nearly as common as normal weight. When comparing average BMI values, males from Black Friars (23.8) and Tirup (23.3) show lower values compared to males from the Knuedler cemetery (24.58/24.01), but males from the mixed European sites (24.2) show similar values, and females from Tirup (21.3) and Black Friars (22.5) also show on average lower values than females from the Knuedler cemetery (23.72/23.71), whilst females from the mixed European sites (23.2) show more similar values. When combining the two Danish sites and comparing BMI distribution and values by time period (medieval vs. postmedieval) however, both male and female values and distributions approach those found in the Knuedler cemetery between Layer 1 and Layer 2 (Figure 48, Figure 49, Figure 50, Figure 51). For both the Danish and Luxembourgish sites, females display lower BMI on average than males, with many more females falling within the normal weight range than males do. This trend does not change much between the medieval and postmedieval periods. Regarding average values, Parker (2019) detected a statistically significant increase in BMI from the medieval to the postmedieval period in both men and women. Siegmund (2010b) on the other hand detected a significant decline in BMI from the early to the late medieval period, suggesting that this was due to a decline in child and adolescent care. On the Knuedler cemetery, a decrease was observed among females and an increase was observed among men but both trends did not turn out statistically relevant. The fact that no statistically relevant trend can be observed between Layer 1 and Layer 2 from the Knuedler cemetery, suggests that no significant changes in nutritional habits occurred over time. A direct comparison between the Danish and Luxembourgish sites however needs to be considered carefully since height, as well as weight estimations were conducted using different formulae. While at the Danish sites height was reconstructed using the revised Fully method after Raxter et al. (2006) and was only complemented by reconstructions on the femur by Ruff et al. (2012) (Parker 2019), at the Knuedler site, the BMI is based on height reconstructions after Ruff et al. (2012) and Trotter and Gleser (1952) using mainly the femur and substituting with the other remaining bones. At the Danish sites, body weight is estimated using an average of the femoral head-based methods after Ruff et al. (1991), Grine (1995) and McHenry (1992) as well as iliac breadth after Auerbach and Ruff (2004) (Parker 2019), but for the Knuedler cemetery, BMI was based on weight reconstructions after Ruff et al. (2012) and Auerbach and Ruff (2004).

BMI comparison over time

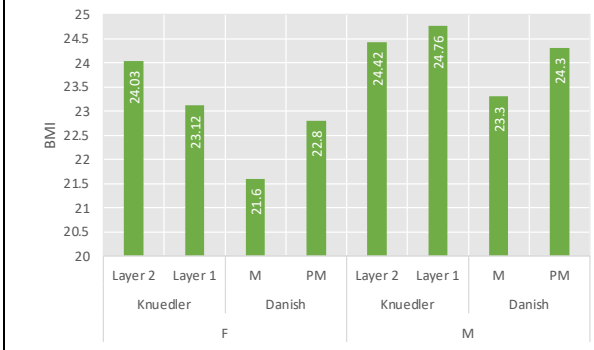

Figure 48 Comparison of average BMI by period between Danish sites and the Knuedler cemetery (Layer 2 = late medieval-early postmedieval, Layer 1 = postmedieval, M = medieval, PM = postmedieval) (KNU after Ruff et al. 2012)

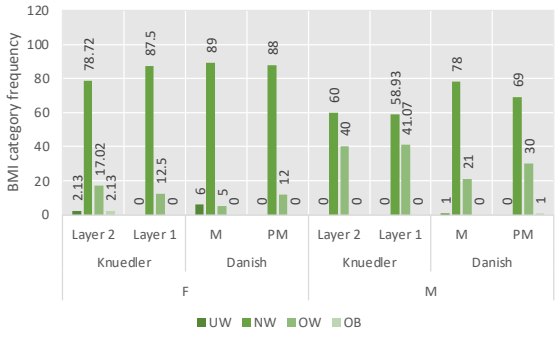

Figure 49 Comparison of BMI class frequencies by period between Danish sites and the Knuedler cemetery (Layer 2 = late medieval-early postmedieval, Layer 1 = postmedieval, M = medieval, PM = postmedieval) (KNU after Ruff et al. 2012)

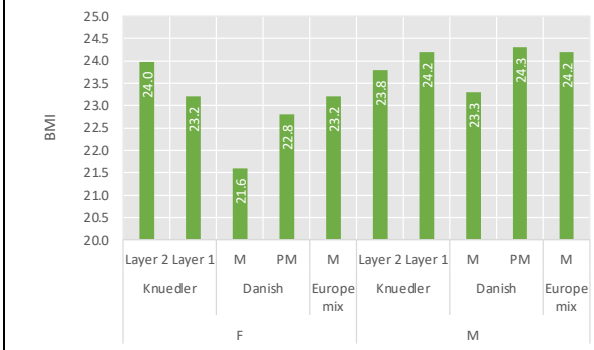

Figure 50 Comparison of average BMI by period between Danish sites and the Knuedler cemetery (Layer 2 = late medieval-early postmedieval, Layer 1 = postmedieval, M = medieval, PM = postmedieval) (KNU and Europe mix after Auerbach and Ruff (2004) & (Trotter and Gleser (1952))

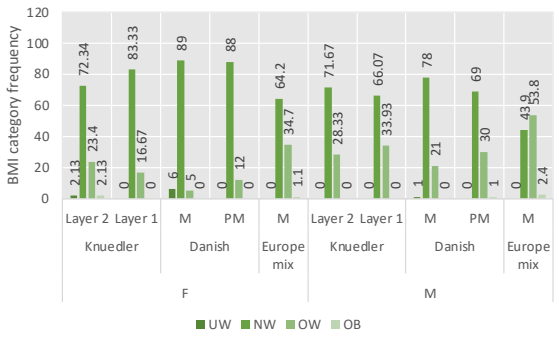

Figure 51 Comparison of BMI class frequencies by period between Danish sites, a mix of European sites and the Knuedler cemetery (Layer 2 = late medieval-early postmedieval, Layer 1 = postmedieval, M = medieval, PM = postmedieval) (KNU and Europe mix after Auerbach and Ruff (2004) & (Trotter and Gleser (1952))

4.4.3 Conclusion

To conclude, the growth rate of subadults in Luxembourg City follows the 5 phases described in Bogin (2001) and is very similar to that observed in other contemporaneous populations. Furthermore, the growth stagnation around 2-3 years of age might be a consequence of stressful weaning practices, a trend that was also observed in Emden and in Schleswig.

As expected, adult body height and weight differ significantly between the sexes with males being taller and heavier than women. Stature did not vary significantly with social status, but weight did. Males from the cemetery were on average heavier and had a higher BMI than those from the cloister, suggesting that they were either of a more muscular built or were simply bigger than those from the cloister. Regarding BMI, stature and body mass, the individuals from Luxembourg City fell right within the range of European late- and postmedieval urban populations. Direct comparisons to other sites are not only complicated by the use of different

formulas for estimating height and weight but are also strongly influenced by the genetic influence on adult body height, which might lead to vastly different adult heights between populations, that have nothing to do with socioeconomic status, disease burden or nutritional status.

5 Physical adaptations to external stress

In the following chapter, an attempt will be made to reconstruct activity patterns among the people buried in the "Knuedler" cemetery from Luxembourg City. Since biomechanical stresses experienced over extended periods of time can leave traces on the bones, an in-depth analysis of these traits which might have been affected through mechanical loading has been carried out.

In a first step, since increased physical stress on the bones might lead to increased use and therefore increased bone formation in the dominant limb, bilateral asymmetry was assessed for all postcranial measurements. Directional asymmetries, allowed for a reconstruction of overall handedness and preferential use patterns. Absolute asymmetries were used to explore the overall scope of asymmetry in all measurements, with higher absolute asymmetries suggesting increased mechanical loading on specific areas of the bone on one body side.

Secondly, since bone shape and robusticity are often influenced by mechanical loading patterns, postcranial indices were analysed in order to characterise the prevalent bone shape and robusticity among the different groups in the cemetery and detect any differences between the groups. Lateralisation of shape and bone robustness were then also assessed.

Thirdly, enthesial changes, which are characterised by traces left on the bone surface due to physical stress at tendon and ligament attachment sites, were recorded for all adult individuals. The degree of expression of these enthesial changes can inform about specific muscle use and therefore the degree of mechanical stress put on a specific part of the body or bone.

Finally, the occurrence and prevalence of tibial squatting facets was assessed. As the name of the trait already suggests, these facets most likely originate through frequent squatting and might therefore be used as an indicator for changes, differences, or similarities in regular physical activities between the sexes, age groups, social classes and over time.

5.1 Bilateral asymmetry

5.1.1 Introduction

While at first glance the human skeleton seems mostly symmetrical, a closer look reveals metric and non-metric differences in symmetry. There are three types of asymmetries that may occur in nature. Fluctuating asymmetries are small differences that reflect the individual's ability to react to environmental or genetic developmental noise (Van Valen 1962; Palmer 1994; Tomkins & Andrews 2001). Antisymmetry represents a significant amount of difference from symmetry that occurs randomly and shows no side preference (Van Valen 1962), whilst directional asymmetries constitute larger differences that are systematically more pronounced on one side and are thought to occur as the result of an adaptive reaction to environmental factors and in particular to mechanical loading, as bones adapt to the mechanical loads they are exposed to, following the principles of Wolff's law (Roy *et al*. 1994; Steele & Mays 1995; Tomkins & Andrews 2001; Rhodes & Knüsel 2005; Auerbach & Ruff 2006; Özener 2007). As such, the most severe asymmetries are observed in athletes. Handball players for example display significant humeral retrotorsion in their throwing arm (Pieper 1998), whilst professional tennis players show considerable cortical hypertrophy of the distal humeral diaphysis (Jones *et al*. 1977) and increased length in the playing arm (Haapasalo *et al*. 1996) and many cricketers present with asymmetry in humeral robusticity, in humeral and ulnar rigidity as well as asymmetry of the humeral diaphysis (Shaw & Stock 2009).

Directional asymmetries can provide information on the amount of mechanical load a body has been exposed to and might be used to make inferences on habitual movements but cannot be used to reconstruct specific activities (Stirland 1993). Most asymmetries develop already during bone growth since growth is easily affected by these environmental stressors (Steele & Mays 1995; Anderson & Trinkaus 1998; Auerbach & Ruff 2006).

The majority of studies so far have focussed on differences in asymmetries between and within pre-industrial and/or modern populations (Sakaue 1998; Auerbach & Ruff 2006; Weiss 2009). However, during the late medieval and postmedieval period, with increasing urbanisation and a shift from agricultural towards more sedentary occupations such as trade, a reduction of bilateral asymmetry would be expected.

The aim of the following chapter is to determine the patterns of asymmetry present within the late medieval to postmedieval urban population from Luxembourg City.

5.1.2 Methods

All 53 measurements were converted into percentage directional asymmetries (%DA) and subsequently into absolute asymmetries (%AA) using the following formula:

$$\%DA = \frac{(R - L)}{(R + L)/2} \times 100$$

R represents the measurement of the right and L the one of the left bone. (Steele & Mays 1995; Mays *et al*. 1999; Čuk *et al*. 2001; Mays 2002; Plochocki 2004; Auerbach & Ruff 2006; Blackburn & Knüsel 2006; Auerbach & Raxter 2008; Weiss 2009; Reeves *et al*. 2016)
Representing the asymmetric differences as percentages of directional asymmetry makes the data of all measurements from all elements comparable to each other, regardless of the size differences of the raw measurements. Positive values correspond to right- biased, negative values to left-biased asymmetries and 0 indicates symmetry between the two sides.
Absolute asymmetries (%AA) were calculated as the absolute value of %DA (|%DA|) and represent the absolute degree of asymmetry irrespective of side. This will allow to determine the actual amount of bilateral asymmetry in a measurement which is why this measure was preferred over %DA in this study in the group comparisons
All comparisons between the sexes, age groups, burial locations and layers were conducted on %DA and %AA of all measurements but results and discussion for %DA, except those of the entire sample, can be found in Appendix III. Appendix III also presents and discusses the results for handedness estimation and crossed symmetry in the sample. Only statistically significant results are presented.

5.1.3 Results

5.1.3.1 Bilateral and directional asymmetry in women and men

The results of Wilcoxon signed ranks tests ($p<0.05$) for direct pairwise comparisons of right and left bone measurements, the mean and median values and the standard deviation (sd) of the raw measurements by side are reported for males and females in Table 17. N represents the total number of individuals from the samples considered in the test for each measurement. The measurements for which the results of the Wilcoxon signed ranks tests are significant ($p<0.05$), are marked in bold. They show a statistically significant amount of directional asymmetry. For the %DA, a positive value for mean and median stands for a right biased asymmetry whereas

a negative value indicates that the asymmetry is left biased. A non-significant result ($p>0.05$) means no relevant asymmetry.

The results of the Wilcoxon signed ranks tests, which were carried out separately for males and females, indicate that within males and females, there is a high degree of bilateral asymmetry in the arm bones, namely the humerus and to a slightly lesser degree, also the radius and ulna, whereas only a few measurements of the leg bones show a significant bilateral asymmetry. This pattern was especially prevalent in men, where a nearly half (49%) of the measurements show a significant amount of bilateral asymmetry, as opposed to females (34%). Females only showed 21% of significant asymmetry in arm bones, and men 36%. Noteworthily, all scapular and all humeral measurements except one (Hu4), showed significant asymmetry in men. The leg bones on the contrary in men only showed 11% asymmetrical measurements and those of females 13%. Overall, the majority of measurements was right-biased but the lower limb showed more left biased ones than the upper limbs, suggesting that the majority of individuals was right-handed and that the population displayed a typical pattern of cross symmetry. More detailed analyses of %DA, handedness and cross symmetry are discussed in Appendix III. By checking the outliers of each measurement, it became clear that all tibial measurements of individual 2008-78/1486, a mature female from layer 2 consistently came up as outliers in the histogram of pairwise differences. The right tibia seems to be significantly smaller across all measurements than the left one. This pattern is so distinct, that it can also be observed on the in-situ photograph of the individual. This photograph also confirms that both tibiae analysed belonged to the same individual. Since no other bones of this individual showed a similar pattern and no noteworthy pathological changes were recorded, the outlier was kept in the sample for the evaluation and accounted for as natural variation.

Table 17 Raw measurements with results of Wilcoxon signed ranks tests for males and females

Measurement	Sex	Side	max	min	mean	median	sd	%DA	V	p-value	n
Sc2	F	L	98	90	93.67	93.50	2.73	-0.17	9	0.7656	6
		R	97	91	93.50	93.00	2.59				6
	M	L	111	94	104.19	104.00	4.78	-1.23	**86.5**	**0.0036**	16
		R	110	91	102.94	103.50	5.17				16
Sc12	F	L	36.07	29.38	33.17	33.60	1.73	1.17	51	0.1415	18
		R	35.72	31.16	33.54	33.72	1.37				18
	M	L	44.2	28.59	38.29	38.32	2.64	0.67	**383**	**0.0359**	49
		R	44.36	33.85	38.74	38.80	2.16				49
Sc13	F	L	26.81	23.04	24.74	24.78	1.19	-0.04	80	0.8276	18
		R	27.31	22.37	24.74	24.71	1.48				18
	M	L	31.14	23.91	27.86	27.83	1.62	1.83	**177.5**	**0.0052**	38

Measurement	Sex	Side	max	min	mean	median	sd	%DA	V	p-value	n
		R	38.13	24.97	28.62	28.68	2.26				38
Cl1	F	L	144	116	133.00	133.00	8.04	-0.86	**333.5**	**0.0124**	15
		R	146.5	116	131.87	132.00	8.12				15
	M	L	163	132	146.68	146.50	7.81	-1.14	34	0.2985	30
		R	165	131	145.03	143.75	7.83				30
Cl4	F	L	11.51	6.83	8.80	8.65	1.17	1.86	437	0.7217	40
		R	11.31	7.2	8.79	8.59	1.10				40
	M	L	17.31	7.65	10.59	10.35	1.47	2.03	1,293	0.2909	77
		R	19.2	7.41	10.67	10.60	1.57				77
Cl5	F	L	13.68	9.3	10.95	10.85	1.10	-0.05	81	0.0594	40
		R	13.7	9.69	11.15	11.00	1.04				40
	M	L	16.33	8.54	12.84	12.84	1.54	0.67	575	0.7813	77
		R	17.08	8.26	13.10	13.00	1.57				77
Cl6	F	L	36	28	32.53	32.00	2.09	1.29	85	0.0980	40
		R	36	29	32.88	33.00	1.95				40
	M	L	48	30	38.99	39.00	3.55	1.72	**253**	**0.0024**	76
		R	50	32	39.66	39.00	3.59				76
Hu1	F	L	312	264	293.36	292.00	11.88	1.57	**10**	**0.0003**	22
		R	319	268	297.98	295.50	11.46				22
	M	L	356	290	323.45	323.00	14.01	1.10	**52.5**	**0.0000**	43
		R	359.5	301	327.01	325.50	13.72				43
Hu3	F	L	46.5	41	44.08	44.50	1.55	0.90	**19.5**	**0.0366**	20
		R	48	41.5	44.48	44.50	1.65				20
	M	L	60	46	50.88	51.00	2.97	0.91	**75.5**	**0.0103**	33
		R	59	47.5	51.39	51.00	2.88				33
Hu4	F	L	61.5	48.5	53.67	53.50	3.27	0.63	74	0.2522	23
		R	61	49.5	54.00	53.00	3.10				23
	M	L	72	54	62.01	62.50	3.46	0.27	173.5	0.3420	43
		R	69	54	62.19	62.50	3.61				43
Hu5	F	L	22.85	17.54	20.48	20.61	1.40	1.77	**232**	**0.0170**	40
		R	23.58	18.31	20.83	20.67	1.27				40
	M	L	27.45	17.84	22.51	22.43	1.66	3.26	**335.5**	**0.0000**	75
		R	28.47	17.36	23.24	23.10	1.59				75
Hu6	F	L	18.5	13.86	15.98	16.14	1.22	1.43	**221**	**0.0113**	40
		R	19.14	13.85	16.21	16.16	1.18				40
	M	L	21.88	15.85	18.29	18.04	1.36	2.05	**631.5**	**0.0000**	75
		R	23.37	15.95	18.69	18.41	1.63				75
Hu7	F	L	68	53	60.03	60.00	3.77	1.16	**52**	**0.0044**	40
		R	69	55	60.70	60.00	3.44				40
	M	L	81	60	67.47	67.00	4.31	1.76	**154.5**	**0.0000**	74
		R	82	62	68.66	68.00	4.25				74
Hu9	F	L	40.87	33.18	37.83	38.53	2.10	0.60	73	0.8900	17
		R	41.54	33.38	37.81	38.29	2.27				17
	M	L	48.36	37.83	44.12	44.12	2.16	1.00	**83**	**0.0004**	32
		R	49.22	39.63	44.72	44.74	2.20				32
Hu10	F	L	44.8	35.81	40.43	40.73	2.02	-0.07	107	0.3536	23

Measurement	Sex	Side	max	min	mean	median	sd	%DA	V	p-value	n
		R	43.85	34.63	40.68	41.02	2.01				23
	M	L	52.97	42.95	46.54	46.40	2.36	1.36	**250**	**0.0043**	44
		R	51.85	42.42	47.00	46.96	2.35				44
Ra1	F	L	236.5	199.5	215.52	213.50	9.68	1.42	**29**	**0.0003**	26
		R	243	202	218.60	217.50	9.96				26
	M	L	262	216	239.03	238.00	12.21	1.10	**131.5**	**0.0000**	49
		R	264	216	241.63	241.00	11.34				49
RaW32	F	L	22.96	19.36	20.97	20.89	0.94	-0.74	62.5	0.2487	13
		R	22.88	19.32	20.83	20.57	1.13				13
	M	L	26.41	20.81	23.36	23.21	1.21	0.72	108	0.1462	26
		R	26.23	21.47	23.52	23.49	1.13				26
Ra4	F	L	16.67	10.35	13.65	13.86	1.40	1.59	333	0.1413	42
		R	15.93	11.21	13.86	13.87	1.29				42
	M	L	18.1	11.89	15.32	15.45	1.51	4.04	**424**	**0.0000**	81
		R	19.5	13.24	15.94	15.88	1.47				81
Ra4a	F	L	18.83	11.2	15.16	15.33	1.60	1.38	309.5	0.1184	42
		R	18.59	12.3	15.35	15.25	1.56				42
	M	L	20.67	13.68	16.84	16.72	1.58	2.90	**608.5**	**0.0000**	81
		R	21.86	14.12	17.33	17.33	1.62				81
Ra5	F	L	11.91	9.07	10.41	10.30	0.69	1.19	**260.5**	**0.0172**	42
		R	11.97	9.32	10.53	10.58	0.68				42
	M	L	14.09	9.75	12.11	12.22	0.88	1.83	**856.5**	**0.0004**	81
		R	14.71	10.13	12.33	12.34	0.90				81
Ra5a	F	L	13.15	9.28	10.70	10.55	0.89	-0.65	526	0.3548	42
		R	12.31	9.05	10.62	10.55	0.75				42
	M	L	14.94	9.95	12.19	12.09	1.11	-0.40	1,724	0.7667	81
		R	15.08	9.99	12.14	12.17	1.00				81
Ra6	F	L	32	23.5	29.13	29.00	1.96	0.22	136.5	0.9753	32
		R	33	23	29.19	29.50	1.93				32
	M	L	37.5	29	33.27	33.00	2.29	0.72	130	0.0565	51
		R	38	29	33.50	33.50	2.10				51
Ul1	F	L	252	218	236.93	238.00	7.46	0.30	56.5	0.0725	21
		R	252.5	221.5	237.62	237.50	6.78				21
	M	L	277	235	254.59	252.50	11.35	0.98	**45.5**	**0.0029**	27
		R	277	235	257.11	258.00	11.66				27
Ul11	F	L	13.64	8.42	11.04	11.12	1.13	4.22	**182.5**	**0.0002**	46
		R	14.88	9.25	11.52	11.51	1.24				46
	M	L	16.5	11.31	13.50	13.41	1.16	3.44	**1,000**	**0.0005**	84
		R	17.89	11.49	13.98	13.76	1.29				84
Ul12	F	L	16.97	11.2	14.59	14.63	1.25	2.67	**254**	**0.0011**	47
		R	17.85	12.7	14.98	15.02	1.27				47
	M	L	20.78	13.31	17.24	17.28	1.40	2.29	**1,061.50**	**0.0013**	84
		R	21.62	14.62	17.64	17.49	1.48				84
UlW35	F	L	20.76	14.21	17.72	17.89	1.63	0.76	189.5	0.3820	30
		R	21.52	14.35	17.86	18.10	1.74				30
	M	L	25.42	16.59	20.17	20.09	1.66	2.53	**288.5**	**0.0001**	55

Measurement	Sex	Side	max	min	mean	median	sd	%DA	V	p-value	n
		R	24.7	16.16	20.69	20.44	1.76				55
UlW36	F	L	21.15	16.06	18.33	18.01	1.26	4.13	**6**	**0.0000**	25
		R	22.16	15.85	19.11	18.90	1.53				25
	M	L	24.55	18.52	21.07	20.65	1.32	2.08	**104**	**0.0010**	35
		R	24.29	18.76	21.51	21.20	1.32				35
Fe1	F	L	459	376	419.85	418.00	19.29	-0.21	473.5	0.1360	46
		R	456	375	418.87	418.00	19.90				46
	M	L	502	414	458.65	459.00	22.26	-0.25	**1,530**	**0.0292**	73
		R	502.5	411	457.36	458.00	21.59				73
Fe2	F	L	454	374	416.46	415.00	19.00	-0.29	565	0.0819	45
		R	453	372	415.29	416.00	19.79				45
	M	L	500	412	455.25	456.00	21.79	-0.23	1,410.50	0.0516	71
		R	497	410	454.17	455.00	21.05				71
Fe3	F	L	441.5	366.5	405.17	404.00	15.81	-0.15	181	0.3802	32
		R	440	368	404.56	402.50	15.98				32
	M	L	482	400	442.36	444.00	21.06	-0.24	802	0.1935	57
		R	485	399	441.29	442.00	20.63				57
Fe4	F	L	428	355.5	395.61	395.00	15.81	-0.32	**269**	**0.0179**	31
		R	427	355	394.35	393.00	16.25				31
	M	L	470.5	387	432.70	435.00	20.34	-0.21	827	0.2099	57
		R	471	388.5	431.78	433.00	19.68				57
Fe6	F	L	32.02	23	25.79	25.40	1.82	-0.76	993	0.1872	61
		R	30.92	21.96	25.60	25.19	1.88				61
	M	L	35.91	24.54	28.87	28.48	2.12	0.23	1,735	0.2747	93
		R	36.33	24.02	28.95	28.55	2.23				93
Fe7	F	L	31.45	22.31	25.89	25.62	1.96	-0.58	807	0.5816	58
		R	30.81	22.14	25.73	25.52	1.89				58
	M	L	31.8	22.61	28.02	28.27	1.96	-1.57	**2,746**	**0.0004**	92
		R	32.15	23.72	27.58	27.36	1.93				92
Fe8	F	L	95	74	80.95	80.00	4.75	-0.72	**410**	**0.0056**	58
		R	92	73	80.34	80.00	4.32				58
	M	L	101	78	88.96	89.00	4.92	-0.34	1,116.50	0.2097	93
		R	102	78	88.66	88.00	4.91				93
Fe9	F	L	35.49	24.59	29.76	29.85	2.56	0.30	664.5	0.3790	59
		R	35.8	25.39	29.82	29.69	2.22				59
	M	L	36.51	26.71	31.86	31.83	2.37	-0.21	2,041	0.9807	94
		R	37.23	25.44	31.80	31.74	2.48				94
Fe10	F	L	29.59	20.99	24.06	23.68	1.93	-0.26	832	0.4435	58
		R	28.53	19.36	24.00	23.85	1.96				58
	M	L	32.66	22.4	27.01	26.98	2.02	0.05	1,896	0.7980	94
		R	32.24	21.92	27.03	26.99	2.03				94
Fe13	F	L	103	81	92.29	93.00	5.35	0.42	156	0.1718	49
		R	103	82	92.65	93.00	5.05				49
	M	L	116	94	104.49	103.00	5.51	0.38	**321.5**	**0.0402**	77
		R	119	94	104.91	105.00	5.83				77
Fe18	F	L	46.89	38.92	42.69	42.97	1.99	0.88	**185**	**0.0015**	43

Measurement	Sex	Side	max	min	mean	median	sd	%DA	V	p-value	n
		R	46.26	39.27	43.06	43.44	1.95				43
	M	L	52.96	42.87	48.62	48.72	2.51	0.30	943.5	0.0807	72
		R	54.83	43.49	48.76	48.97	2.52				72
Fe19	F	L	47.52	38.55	42.54	42.51	2.03	0.36	284.5	0.0594	43
		R	47.03	38.92	42.69	42.83	1.91				43
	M	L	53.15	42.62	48.13	48.15	2.52	0.67	**747**	**0.0015**	74
		R	55.08	43.43	48.45	48.57	2.50				74
FeHmax	F	L	46.93	39.35	43.22	43.39	1.95	0.77	**138.5**	**0.0013**	39
		R	47.13	39.51	43.56	43.75	2.02				39
	M	L	53.46	42.94	49.08	49.10	2.66	0.26	886.5	0.1154	69
		R	55.13	43.76	49.20	49.27	2.63				69
Fe21	F	L	81	64	73.37	74.00	3.35	0.34	129	0.2388	39
		R	80.5	64	73.63	73.00	3.43				39
	M	L	103	74	82.45	82.00	4.75	0.22	**295.5**	**0.0496**	61
		R	104	74	82.64	82.00	4.87				61
Ti1	F	L	368.5	281	333.46	335.00	19.59	-0.12	236.5	0.6888	37
		R	366	286.5	332.95	333.00	17.78				37
	M	L	409	320	364.33	363.50	21.30	-0.41	**895.5**	**0.0128**	60
		R	410	320	362.85	359.50	21.46				60
Ti1b	F	L	370.5	283	333.59	334.00	19.62	-0.09	238.5	0.8596	37
		R	366	288	333.24	334.00	18.89				37
	M	L	409	313	363.12	364.00	21.36	-0.13	771.5	0.4543	62
		R	411	322	362.60	360.50	20.51				62
Ti3	F	L	84	62.5	68.79	69.00	4.07	0.14	111	0.4163	33
		R	82	62	68.86	69.00	3.58				33
	M	L	85	69	76.57	76.50	3.14	0.05	510.5	0.7437	65
		R	85	70	76.61	76.50	3.14				65
Ti6	F	L	52	44	47.70	47.00	2.43	0.53	108	0.1420	33
		R	53.5	44	47.97	48.00	2.78				33
	M	L	61	46	53.35	53.25	3.05	1.01	108	0.1420	48
		R	59	47	53.90	54.00	3.01				48
Ti8	F	L	31	21.58	25.70	25.48	2.06	0.56	348.5	0.2909	48
		R	33.91	21.24	25.87	25.82	2.32				48
	M	L	33.13	24.1	29.35	29.61	2.15	-0.36	1,551.50	0.5058	85
		R	33.26	25.58	29.22	29.19	1.88				85
Ti8a	F	L	35.15	22.96	28.82	28.75	2.42	1.87	**212.5**	**0.0048**	48
		R	37.8	23.41	29.39	29.16	2.79				48
	M	L	38.53	27.62	33.16	33.20	2.13	0.44	1,283	0.7126	82
		R	38.45	28.2	33.30	33.18	2.13				82
Ti9	F	L	24.22	17.85	20.25	20.08	1.76	-1.08	374	0.7400	44
		R	23.4	17.56	20.01	20.00	1.41				44
	M	L	26.35	18.18	22.58	22.78	1.72	0.23	1,266	0.6442	81
		R	27.55	19.52	22.62	22.53	1.58				81
Ti9a	F	L	27.03	19.52	22.33	22.05	1.93	1.26	**260.5**	**0.0452**	48
		R	26.98	19.66	22.59	22.77	1.65				48
	M	L	28.89	21.87	25.00	24.93	1.78	0.54	1,063.50	0.0814	82

Measurement	Sex	Side	max	min	mean	median	sd	%DA	V	p-value	n
		R	31.16	21.39	25.14	25.15	1.91				82
Ti10	F	L	85	66	75.24	75.00	5.00	-0.58	260	0.1835	45
		R	89	67	74.80	75.00	4.86				45
	M	L	94	73	84.07	84.00	4.96	0.36	530	0.2962	81
		R	94	73	84.37	84.00	4.81				81
Ti10a	F	L	98	70	82.83	82.50	5.65	0.72	**67**	**0.0094**	46
		R	100	74	83.43	83.00	5.89				46
	M	L	108	83	93.58	94.00	4.98	0.42	723	0.0734	81
		R	110	83	93.99	94.00	5.24				81
Ti10b	F	L	78	60	68.16	69.00	4.04	0.32	99	0.0779	49
		R	82	60	68.39	69.00	4.16				49
	M	L	86	68	75.52	76.00	3.83	0.25	364	0.3791	82
		R	85	68	75.71	75.50	3.75				82
Fi1	F	L	362	308	333.68	337.00	16.52	-0.36	33	0.2357	11
		R	355.5	303	332.45	334.00	15.73				11
	M	L	394	343	366.86	366.75	16.15	-0.51	47	0.0520	14
		R	394	341	365.00	361.75	16.48				14

bold *= p<0.05*

5.1.3.2 Differences in Absolute asymmetry between women and men

The significant results of the Mann-Whitney U tests (p<0.05) for differences between males and females, the directional and absolute asymmetries, and the mean, median and standard deviation of the %AA for the pooled sample are shown in Table 18. Means and medians are calculated using N, the total number of individuals from the sample considered in the test for each measurement. Only statistically significant values represent directional asymmetry, and only significant measurements have been presented in Table 18.

After testing for differences in absolute asymmetries between males and females, 6 measurements showed significantly higher degrees of asymmetry in women then in men, namely Hu1, Hu4, Ra6, Ti3, Ti6 and Ti8a. Since 4 of those measurements involve joints, this might hint at a slightly differential physical load or movement patterns in females than in males. Due to these differences between males and females, all further comparisons were conducted for males and females separately.

Table 18 Significant %AA between males and females.

Measurement	Sex	max	min	mean	median	sd	W	p-value	n
Hu1	F	3.83	0.00	1.70	1.46	0.96	620	0.0422	22
	M	3.89	0.00	1.24	1.06	0.83			43
Hu4	F	5.31	0.00	2.15	1.94	1.48	684	0.0103	23
	M	5.97	0.00	1.34	0.82	1.50			43

Measurement	Sex	max	min	mean	median	sd	W	p-value	n
Ra6	F	10.10	0.00	2.52	1.82	2.42	1040	0.0317	32
	M	6.67	0.00	1.68	1.48	1.93			51
Ti3	F	8.70	0.00	1.65	1.44	1.64	1339	0.0446	33
	M	3.68	0.00	1.17	1.29	0.93			65
Ti6	F	10.31	0.00	2.66	2.25	2.00	1017.5	0.0295	33
	M	8.00	0.00	2.02	1.83	2.04			48
Ti8a	F	14.88	0.10	4.47	3.84	3.09	2583	0.0030	48
	M	10.16	0.00	2.87	2.27	2.33			82

5.1.3.3 Difference in asymmetry patterns between age groups

A Kruskal-Wallis test was used to determine whether there is any difference in the degree of asymmetry in males and females between the age groups. Differences were calculated between adults (20-39 years), mature (40-59 years) and senile individuals (60+ years). In order to maximise sample size in each group, young adults and adults as well as mature I and II were grouped together for this analysis.

Regarding absolute asymmetry (%AA) only three measurements (Hu7, Fe1 and Fe2) show differences in females and one (RaW32) shows differences in males. The only difference in joint measurements occurs in men adults having higher degrees of asymmetry than matures and seniles, but post-hoc pairwise Wilcoxon tests did not turn out significant.

In females however, Fe1, Fe2 and Hu7 show the same pattern, with matures having a higher degree of asymmetry than adults and seniles, (Posthoc: Hu7: A>M, $p<0.03$; Fe1: A<M>S, $p>0.03$; Fe2: /). (

Table *19*)

Table 19 %AA between the three age groups in males and females

Measurement	Sex	Age	max	min	mean	median	sd	X^2	p-value	n
Hu7	F	Adult	7.02	0.00	1.70	1.70	1.97	**7.0915**	**0.0289**	16
		Mature	7.14	0.00	2.18	1.77*	1.82			19
		Senile	0.00	0.00	0.00	0.00*	0.00			5
	M	Adult	5.88	0.00	2.09	1.48	1.92	0.0810	0.9603	30
		Mature	8.00	0.00	2.12	1.48	1.98			31
		Senile	8.92	0.00	2.62	1.55	2.73			13
RaW32	F	Adult	5.66	0.98	3.46	3.56	2.06	2.5243	0.2830	5
		Mature	3.97	0.15	1.54	1.63	1.41			7
		Senile	2.32	2.32	2.32	2.32	-			1

Measurement	Sex	Age	max	min	mean	median	sd	X^2	p-value	n
	M	Adult	4.17	0.00	2.69	3.32	1.62	**6.0178**	**0.0494**	10
		Mature	3.19	0.12	1.41	1.39	1.03			13
		Senile	1.86	0.09	0.78	0.39	0.95			3
Fe1	F	Adult	1.65	0.00	0.54	0.48*	0.39	**10.1678**	**0.0062**	21
		Mature	4.17	0.00	1.32	1.21*&	1.05			15
		Senile	0.75	0.00	0.33	0.35&	0.32			8
	M	Adult	2.73	0.10	0.81	0.76	0.65	1.1209	0.5710	30
		Mature	2.04	0.11	0.79	0.76	0.55			29
		Senile	2.30	0.00	0.65	0.33	0.71			12
Fe2	F	Adult	1.66	0.00	0.58	0.45	0.43	**6.7568**	**0.0341**	20
		Mature	3.47	0.11	1.20	1.07	0.93			15
		Senile	0.96	0.00	0.48	0.49	0.28			8
	M	Adult	2.23	0.00	0.83	0.66	0.60	0.01879	0.9907	29
		Mature	3.39	0.00	0.87	0.63	0.71			28
		Senile	2.32	0.00	0.90	0.62	0.85			12

bold=significant bias

5.1.3.4 Difference in asymmetry patterns between socio-economic groups

As mentioned already in the previous chapters, church/cloister and cemetery burials are thought to reflect different social classes. The cemetery burials are presumed to be belong to people of a lower social class than those buried inside the church and the monastery complex. Furthermore, even within the cemetery, it is often assumed that people buried farther away from the church were also of a lower social class than those who could afford to be buried closer to the church. In order to detect any differences between people from different social classes in Luxembourg City, burials were separated into 2 categories based on their position in relation to the church: those buried inside the church or the cloister and those buried on the cemetery. In a second step, for the statistically significant measurements, burials from within the church were compared to the burials from close to church as well as those from the middle and far back of the cemetery. Lastly, with the aim to detect any changes over time, all burials were compared across the different layers detectable in the site. For all analyses, only the statistically significant differences are displayed.

5.1.3.4.1 Difference between cemetery and cloister burials

Generally, there is no clear pattern in asymmetry in %AA between cloister and cemetery burials across all measurement sections. In females, Ra5, Fe6, Fe8 and Fe9 show a significant

difference in degree of asymmetry and in males Cl6 and Fe6. Cl6, Ra5, Fe6 in males and Fe9 display higher degrees of absolute asymmetry in the cloister sample and Fe6 in females as well as Fe8 display more asymmetry in the cemetery (Table 20).

Table 20 %AA between cloister and cemetery burials in males and females

Measurement	Sex	Location	max	min	mean	median	sd	X^2	p-value	n
Cl6	F	Cemetery	8.96	0.00	2.64	2.82	2.85	130	0.6588	32
		Cloister	11.76	0.00	3.06	2.99	3.61			9
	M	Cemetery	17.28	0.00	2.43	2.30	3.28	**365.5**	**0.0291**	57
		Cloister	13.04	0.00	4.78	2.67	4.36			19
Ra5	F	Cemetery	12.22	0.10	2.52	1.86	2.55	**78**	**0.0144**	32
		Cloister	9.29	1.63	4.83	3.46	3.09			10
	M	Cemetery	12.14	0.00	3.94	3.54	2.82	761	0.3274	58
		Cloister	8.92	0.00	3.26	3.31	2.40			23
Fe6	F	Cemetery	10.18	0.12	3.05	2.41	2.27	**445**	**0.0468**	47
		Cloister	3.35	0.15	1.78	1.60	1.02			14
	M	Cemetery	7.65	0.04	2.29	2.00	1.80	**531**	**0.0241**	71
		Cloister	10.13	0.04	3.42	2.94	2.27			22
Fe8	F	Cemetery	5.41	0.00	1.56	1.26	1.51	**424**	**0.0308**	44
		Cloister	1.31	0.00	0.61	0.57	0.63			14
	M	Cemetery	5.71	0.00	1.24	1.12	1.27	596	0.0907	71
		Cloister	6.67	0.00	1.88	1.21	1.63			22
Fe9	F	Cemetery	9.86	0.07	2.54	2.15	2.38	**113**	**0.0010**	47
		Cloister	11.43	1.89	4.87	3.74	2.81			12
	M	Cemetery	13.42	0.09	3.15	2.54	2.51	705	0.4399	72
		Cloister	8.37	0.63	3.34	2.87	2.16			22

bold=significant bias

5.1.3.4.2 Difference between distance to church

In a next step, those values that displayed statistically significant differences in %AA were also examined by their distance to church. By comparing cloister burials, those close to, midway to and those far from the church, potential differences in bilateral asymmetry in relation to proximity to the church can be detected. Only Fe8 and Fe9 of women show any statistically relevant differences in relation to proximity to church. Although the Kruskal-Wallis test for Fe8 indicated a significant difference in degree of asymmetry by distance to church, the pairwise Wilcoxon tests could not detect any relevant differences between the pairs. Nonetheless, there is an overall trend towards a higher degree of asymmetry in the burials further away from church. For Fe9, the pairwise Wilcoxon tests revealed that people buried

inside the cloister area had significantly more asymmetry than those buried in the middle or farther away This means that there is a decreasing trend in bilateral asymmetry intensity the further away people are buried from the church. (

Table 21)

Table 21 %AA between burials from, close to, midway to and far from the church in males and females

Measurement	Sex	Location	max	min	mean	median	sd	W	p-value	n
Fe8	F	Cloister	1.31	0.00	0.61	0.57	0.63	**8.4491**	**0.0376**	14
		Close	3.21	0.00	0.85	0.00	1.14			11
		Far	5.41	0.00	1.87	1.36	1.66			9
		Mid	4.88	0.00	1.76	1.26	1.56			24
	M	Cloister	6.67	0.00	1.88	1.21	1.63	3.7053	0.2951	22
		Close	3.39	0.00	1.18	1.08	1.16			15
		Far	3.28	0.00	1.28	1.21	1.10			18
		Mid	5.71	0.00	1.23	1.10	1.41			38
Fe9	F	Cloister	11.43	1.89	4.87	3.74*&	2.81	**11.8143**	**0.0080**	12
		Close	9.62	0.13	3.36	2.69	2.95			11
		Far	9.86	0.13	2.34	1.33*	2.98			9
		Mid	9.50	0.07	2.28	2.26&	1.90			27
	M	Cloister	8.37	0.63	3.34	2.87	2.16	1.0079	0.7993	22
		Close	5.05	1.04	2.51	1.84	1.33			15
		Far	13.42	0.09	3.34	2.80	3.14			18
		Mid	8.85	0.09	3.30	2.55	2.56			39

bold=significant bias

5.1.3.4.3 Difference between cemetery and cloister burials by Layer

In order to account for any influence of burial time on the comparisons between cloister and cemetery burials, individuals from Layer 1 were compared between the two burial locations separately of those from Layer 2.

People from Layer 1 experienced higher degrees of absolute asymmetry in three measurements. Cl6 and Fe9 show higher %AA values in the among the cloister burials than in the cemetery and vice versa for measurement Ul11. Individuals from Layer 2 only exhibited higher degrees of asymmetry among cemetery burials, namely in the measurements UlW36 and Ti1. (Table 22)

Table 22 %AA between burials from the cloister and the cemetery in Layer 1 and 2

Measurement	Layer	Location	max	min	mean	median	sd	W	p-value	n
Cl6	1	Cemetery	10.53	0.00	1.99	0.00	2.76	**176.5**	**0.0195**	39
		Cloister	12.66	0.00	3.73	2.99	3.35			15
	2	Cemetery	17.28	0.00	2.97	2.67	3.34	312	0.4660	51
		Cloister	13.04	0.00	4.63	2.60	4.85			14
Ul11	1	Cemetery	22.27	0.54	7.48	6.24	5.50	**581**	**0.0019**	41
		Cloister	16.67	0.00	3.70	2.67	3.86			19
	2	Cemetery	21.96	0.30	6.95	6.43	5.02	435	0.5114	54
		Cloister	21.30	0.09	7.72	6.55	5.40			18
UlW36	1	Cemetery	11.96	0.06	3.59	2.85	3.21	52	0.8195	16
		Cloister	5.26	0.30	3.28	3.99	1.92			7
	2	Cemetery	10.41	0.04	4.30	3.51	3.05	**236**	**0.0014**	26
		Cloister	4.95	0.00	1.38	0.87	1.46			11
Fe9	1	Cemetery	9.86	0.07	3.11	2.65	2.35	**313**	**0.0187**	49
		Cloister	11.43	1.46	4.56	3.57	2.59			20
	2	Cemetery	13.42	0.09	2.81	2.26	2.57	468	0.2757	71
		Cloister	7.44	0.63	3.21	2.70	2.21			16
Ti1	1	Cemetery	2.78	0.00	0.99	0.78	0.81	194	0.8668	25
		Cloister	2.79	0.00	0.97	0.74	0.88			15
	2	Cemetery	7.10	0.00	1.14	0.92	1.16	**374**	**0.0468**	49
		Cloister	1.64	0.00	0.57	0.56	0.43			11

bold=significant bias

5.1.3.5 Difference in asymmetry patterns over time

Lastly, with the aim to detect any changes over time, all burials were compared across two different time periods. Burials from Layer 1 represent the late postmedieval and burials from Layer 2 represents the early postmedieval and late medieval periods.

5.1.3.5.1 Difference by Sex

The majority of differences in %AA is found in males. Three measurements, Cl5, Ra6 and Fe4 and display a higher median %AA in Layer 1, whereas Hu1 and Ra5 show higher median %AA in Layer 2. Amongst the women, only Ti10a and Ti10b show any statistically significant difference between the layers, with Layer 2 having a higher median %AA than Layer 1. The results for the statistically significant measurements are shown in Table 23.

Table 23 %AA between Layer 1 and 2 in males and females

Measurement	Sex	Layer	max	min	mean	median	sd	W	p-value	n
Cl5	F	1	19.13	0.66	6.00	4.26	5.19	218	0.4859	16
		2	14.41	0.19	4.86	3.27	4.20			24
	M	1	13.33	0.49	5.30	4.52	3.69	**477**	**0.0069**	37
		2	17.10	0.71	7.98	7.53	4.33			40
Hu1	F	1	2.86	0.00	1.57	1.93	1.04	52	0.6948	9
		2	3.83	0.68	1.79	1.41	0.93			13
	M	1	3.89	0.31	1.57	1.50	0.91	**317.5**	**0.0295**	19
		2	2.76	0.00	0.97	0.98	0.68			24
Ra5	F	1	9.29	0.19	3.70	2.83	2.93	262	0.1677	16
		2	12.22	0.10	2.68	2.02	2.75			26
	M	1	12.14	0.00	4.45	4.10	2.92	**1062**	**0.0207**	38
		2	11.75	0.00	3.13	2.72	2.37			43
Ra6	F	1	10.10	0.00	2.58	0.88	3.79	85.5	0.3231	10
		2	5.31	0.00	2.49	3.20	1.57			22
	M	1	4.32	0.00	1.05	0.00	1.37	**219**	**0.0430**	23
		2	6.67	0.00	2.20	1.56	2.18			28
Fe4	F	1	1.92	0.00	0.67	0.44	0.59	127.5	0.7508	14
		2	2.82	0.00	0.72	0.37	0.82			17
	M	1	1.89	0.00	0.58	0.45	0.51	**265**	**0.0305**	25
		2	3.08	0.11	0.91	0.79	0.67			32
Ti10a	F	1	6.90	0.00	1.04	0.60	1.80	**135**	**0.0321**	14
		2	10.17	0.00	2.17	1.67	2.15			32
	M	1	6.45	0.00	2.18	2.08	1.56	910.5	0.3777	38
		2	7.65	0.00	1.96	1.17	1.75			43
Ti10b	F	1	3.28	0.00	0.60	0.00	0.99	**152.5**	**0.0210**	15
		2	6.45	0.00	1.74	1.44	1.81			34
	M	1	4.26	0.00	1.24	1.27	1.25	900.5	0.5338	38
		2	6.45	0.00	1.11	1.24	1.38			44

bold=significant bias

5.1.3.5.2 Difference by Location

Since %AA showed some significant differences between the layers and between burial location, it was decided to also check for any differences between the layers within each of the two burial locations, namely the cloister complex and the cemetery. Only measurements which showed statistically significant differences are reported in Table 24.

Only a total of 6 measurements showed significant differences between the layers. Two measurements amongst the cloister burials, Hu3 and Ul11, had a lower median %AA in Layer 1 than in Layer 2, and one measurement, Fe6, showed a higher median %AA in Layer 1 than in Layer 2. Amongst the cemetery burials, Ra5 showed a higher median %AA in Layer 1 and Ra6 as well as Ti6 showed higher median %AA in Layer 2.

Table 24 %AA between Layer 1 and 2 in cloister and cemetery burials

Measurement	Location	Layer	max	min	mean	median	sd	W	p-value	n
Hu3	Cemetery	1	4.26	0.00	1.58	1.02	1.50	116.5	0.5571	14
		2	4.60	0.00	1.70	1.21	1.50			19
	Cloister	1	1.98	0.00	0.88	1.10	0.88	**18.5**	**0.0195**	9
		2	2.90	0.00	1.79	2.02	0.78			11
Ra5	Cemetery	1	12.14	0.00	4.22	4.09	2.92	**1,275.5**	**0.0224**	40
		2	12.22	0.00	2.88	2.43	2.61			52
	Cloister	1	9.29	0.39	4.45	4.05	2.97	186	0.1540	16
		2	8.57	0.00	3.12	2.36	2.21			18
Ra6	Cemetery	1	10.10	0.00	1.67	0.00	2.63	**299**	**0.0098**	26
		2	6.25	0.00	2.45	2.90	1.71			37
	Cloister	1	3.45	0.00	0.94	0.00	1.33	36.5	0.4715	7
		2	6.67	0.00	1.98	1.48	2.49			13
Ul11	Cemetery	1	22.27	0.54	7.32	5.96	22.27	1,159	0.6988	42
		2	21.96	0.30	7.19	6.46	21.96			55
	Cloister	1	16.67	0.00	3.70	2.67	16.67	**81**	**0.0055**	19
		2	21.30	0.09	7.72	6.55	21.30			18
Fe6	Cemetery	1	10.18	0.04	2.71	2.38	2.16	1,804	0.6328	49
		2	8.58	0.00	2.44	2.00	1.94			73
	Cloister	1	10.13	0.86	3.45	2.92	2.03	**250**	**0.0285**	22
		2	6.84	0.04	2.17	1.54	1.95			16
Ti6	Cemetery	1	3.02	0.00	1.41	1.83	1.06	**268**	**0.0461**	19
		2	8.00	0.00	2.51	2.11	2.01			45
	Cloister	1	7.55	0.00	2.56	2.60	2.25	73.5	0.4071	11
		2	10.31	0.00	2.27	0.95	3.12			11

bold=significant bias

5.1.4 Discussion and Conclusion

5.1.4.1 Patterns of asymmetry by sex

According to most studies, males and females generally display the same direction of asymmetries in upper and lower limb measurements, but there are differences in the extent of

asymmetry of certain measurements. In males, the humeral and femoral cross-sectional properties, diameters and circumferences tend to be larger than in females (Stock & Pfeiffer 2004; Auerbach & Ruff 2006; Auerbach & Raxter 2008; Battles 2009), but in females, bilateral asymmetry of bone-, and especially humeral-, length is generally larger than in males (Hiramoto 1993; Auerbach & Ruff 2006; Gloux 2007; Auerbach & Raxter 2008). However, a study on 200 individuals from the Sassari cemetery in Sardinia, found that the humeral lengths are more asymmetrical in males (Gualdi-Russo 1998). The results from the Wilcoxon signed ranks tests of the Knuedler burials broadly reflect the above mentioned results from the other studies based on the same measurements, except for long bone lengths, which are more asymmetrical in males than in females. Overall, the higher humeral length bilateral asymmetry in males follows the pattern observed in the study by Gualdi-Russo (1998), but regarding absolute asymmetry, humeral length asymmetry is higher in females than in males, a pattern also observed in (Sakaue 1998; Čuk *et al*. 2001; Auerbach & Ruff 2006; Gloux 2007; Auerbach & Raxter 2008). Furthermore, all measurements, except for distal epiphyseal breadth (Hu4) of the humerus are significantly asymmetrical in both sexes, but the measurements of the humeral head only display significant differences in males. This, in combination with only males showing significant bilateral asymmetry in all scapular and most humeral measurements, especially those of the glenoid cavity, suggests that mechanical loading of the shoulder joints was different in males than in females, and they might have carried out different kinds of tasks, such as carrying heavier loads or work involving lifting the arms for an extended time. Though significant for both sexes, the midshaft and circumferential measurements of the humerus show stronger asymmetry in men than in women, as shown by the higher p-values, which corroborates the results found in studies by Auerbach & Ruff 2006, Auerbach & Raxter 2008, Battles 2009, Stock & Pfeiffer 2004 and Čuk *et al*. 2001. However, regarding femoral measurements, only the medio-lateral midshaft diameter shows more asymmetry in men, but the midshaft circumference is more asymmterical in women. And while proximal width, the transverse diameter of the head and the distal epiphysis are more asymmetrical in men, the vertical and maximum head diameters are more asymmetrical in women. Statitcally significant differences between men and women were detected in 3 arm and 3 leg measurements, with femlaes displaying the highest asymmetry scores, which might suggest that females engaged more in activities involving the elbow and the lower legs. Upper limbs systematically present a right-biased asymmetry and femoral lengths are mainly left-biased, a trend observed in all afore-mentioned studies. Several studies suggest that the greater amount of asymmetry,

especially in cortical thickness and diaphyseal breadths observed in men is the cause of increased mechanical loading resulting from larger musculature during and after development (Round *et al*. 1999; Auerbach & Ruff 2006; Abdel Fatah *et al*. 2012). Comparisons between modern and archaeological populations seem to support the idea that differences in mechanical loading are the most probable underlying cause for differences in bilateral asymmetry. In the past, differences in asymmetry between men and women were more pronounced than they are today, suggesting that men carried out different and more strenuous tasks than women (Auerbach & Ruff 2006; Battles 2009), an assumption which seems to be reflected also in the individuals buried in this cemetery.

5.1.4.2 Patterns of asymmetry By Age

As bones remodel constantly throughout adult life and are constantly exposed to mechanical forces, it would stand to reason to assume that bilateral asymmetry would increase with age, which is also supported by a study by Pfeiffer (1980). These studies showed an increase in asymmetry of external humeral measurements, mainly diaphyseal diameter with age, likely caused by appositional growth stimulated by the day-to-day exposure to mechanical forces (Pfeiffer 1980). But a study by Heaney et al. (1997) reached the opposite conclusion and found that, even though the cortical area, the shaft diameter and the neck angle of the femur increase with age, the diameter and the cortical thickness and density of the upper limb decrease significantly (Heaney *et al*. 1997). Furthermore, Stirland (1993) observed a decrease in asymmetry with age in 9 of 11 humeral measurements among individuals from Norwich and the Mary Rose Tudor ship, and a study on prehistoric Californians by Ruff and Jones (1981) showed a clear decrease in humeral and tibial midshaft diameters with age. In many modern populations, the elderly do not engage in as strenuous tasks anymore as the youth. This decrease in mechanical load on the bones means that the rate of bone loss will outrun that of bone gain (Ruff & Jones 1981; Garn *et al*. 1992; Stirland 1993), which in return might lead to a decrease in bilateral asymmetry.

In this study, only a few measurements showed differences in absolute asymmetry between the age groups. Generally, there is a tendency of increasing absolute asymmetry from adult to mature and a decreasing tendency from mature to senile age groups, except in absolute asymmetry of the humeral circumference in females, which showed higher degrees of asymmetry in adults and the lowest in seniles.

This result is somewhat surprising since the majority of studies that focused on shaft diameters and circumferences recorded a clearer decrease in asymmetry with age (Ruff & Jones 1981; Stirland 1993; Heaney *et al*. 1997). Maybe this clear lack of change is either just random variation or due to the relatively small sample sizes in each of the age groups for some of the measurements. The age-related change in bilateral asymmetry of the scapular glenoid fossa, could be due to age-related or degenerative remodelling of the joint surfaces.

5.1.4.3 Patterns of Asymmetry by socio economic status

Differences in the degree and pattern of bilateral asymmetry between different groups of a single population are most likely the result of differential activity-related mechanical loading of the bones (Stirland 1993; Blackburn & Knüsel 2006). Stirland (1993) for example found that soldiers from the Mary Rose ship exhibited less asymmetry in the humeri than the poor from Norwich, an occurrence that was attributed to different loading patterns rather than to differences in activity intensity in both groups. Only the humeral head of the soldiers was significantly more asymmetrical than that of the Norwich paupers, likely due to the frequent use of the long bow in the former (Stirland 1993).

The degree of asymmetry has frequently been linked to different kinds and intensities of mechanical loading. Since it is expected that different social classes engage in different activities and are thus exposed to different types and intensities of mechanical loading, there could be detectable differences between the social classes present in this burial complex. Indeed, three leg bone measurements showed significant directional asymmetry between cemetery and cloister burials, with men showing higher %AA in the cloister than in the cemetery and females vice versa. This suggests that maybe individuals from the cloister and from the cemetery regularly engaged in activities with different use of the legs. The fact that femoral midshaft measurements show a different pattern in the degree of asymmetry between cemetery and cloister burials than one proximal shaft measurement, might suggest a different loading pattern on the leg bones in the two burial locations. Furthermore, a higher degree of asymmetry in the clavicular circumference and radial midshaft diameter among the cloister burials hints at a heavier load on these bones, possibly also caused by different kinds of regular tasks.

In rural Grevenmacher, Luxembourg, burials from within the cloister exhibited less bilateral asymmetry than those from the cemetery (Trautmann 2012), whereas in Luxembourg City the

opposite was true but due to differences in investigative methods, these results are not directly comparable.

5.1.4.4 Patterns of Asymmetry over time

Compared to studies examining pre-industrial populations, the overall degree of asymmetry is lower in this sample from Luxembourg, which might be due to a reduction of mechanical loading of the bones caused possibly by the reduction of heavy manual labour through gradual industrialisation (Auerbach & Ruff 2006; Waidhofer 2013; Hiramoto 1993; Battles 2009). Alternatively, the low overall asymmetry might also suggest that generally, the citizens of Luxembourg, or at least those buried at the Franciscan friary were engaged in less strenuous daily tasks as would be expected for example of merchants. Additionally, there are not many statistically significant differences between the layers regarding. Women from Layer 2 seem to have experienced a higher load of stress on the tibiae, mainly regarding the shaft. Among men, no clear pattern can be observed between statistically significant bilateral asymmetry patterns among the layers. The low number of significant asymmetries and the absence of a clear pattern suggests that there were no systematic differences in mechanical stresses on the bones between the late medieval/ early postmedieval period. This comes as no surprise as most likely, the nature of activities carries out did not change much over time, as the industrial revolution, and thus the automation of many physical tasks only began around 1760 in Great Britain and really only started to take off in Continental Europe in the 19th century, well after the closure of this cemetery (Hobsbawm 1962; Milward & Samuel 2013).

5.1.4.5 Conclusion

The formation of bilateral asymmetries relies entirely on the fact that bone is sufficiently malleable to react on environmental stimuli by adapting its shape (Lazenby 2002; Battles 2009). Understanding the two major bone growth mechanisms, namely endochondral ossification and appositional growth, is vital for any further interpretation of bilateral asymmetry pattern between bones (Carter *et al*. 1996).

Longitudinal bone growth, like bone development, proceeds via endochondral ossification. The growth plate is located between the metaphyses and the epiphyses of long bones and can be divided into 5 zones. In the zone nearest to the epiphysis, cartilage cells proliferate and expand towards the zones closer to the diaphysis, through which they proceed to gradually hypertrophy, degenerate, calcify and finally ossify. This way, the epiphysis is gradually pushed away from the diaphysis, resulting in longitudinal growth. This process continues until the

plates fuse with the bone shaft and epiphyses between 15 and 20 years, depending on the bone. Therefore, longitudinal bone growth is usually not much influenced by external factors and after the fusion process is complete, bone lengths do not change much anymore. (Carter *et al*. 1996; Sumner & Andriacchi 1996; White *et al*. 2012). This means that the asymmetry patterns observed in long bone lengths are likely not influenced by outside environmental factors after bone growth stopped, meaning that the factors that led to an asymmetrical development in the bone lengths likely occurred during childhood already. Since males display more bilateral asymmetry in all long bone lengths, this suggests that maybe males generally started regular manual activities already in childhood, or at least before bone growth was complete.

Appositional growth refers to the circumferential growth of bones and only starts once the hyaline cartilage models have completely ossified and the perichondrium has been replaced by periosteum. The bone forming cells which enable the circumferential growth are contained in the cambium, the inner layer of the periosteum. Together with the endosteum which covers the walls of the medullary cavity, the periosteum is responsible for increasing cortical thickness and overall shaft circumference during development. Appositional growth continues throughout most of adult life, but much slower than in childhood (Carter *et al*. 1996; White *et al*. 2012), and is often influenced by biological processes and mechanical loading (Carter *et al*. 1996; Sumner & Andriacchi 1996), thereby following the concept of Wolff's law (1892), which states that the structure of bones adapts depending on the biomechanical stressors it is exposed to (Wolff 1892a). Many studies could confirm the basic principles laid out in Wolff's original work, but in the meantime, several improvements for Wolff's law have already been proposed (Bertram & Swartz 1991), such as the mechanostat model, which starts with the premise that bone adapts constantly to everyday stimuli in order to allow the individual to conduct a healthy life without any pain or discomfort, and factors in the threshold value for bone production and resorption based on daily stimuli, the intensity of those stimuli and the changes each intensity causes in the bone (Frost 2000). Therefore, the asymmetries observed in diameters, joints and circumferences can have either started to develop already in childhood, but were likely mainly formed during adult hood, after bone growth had already stopped. The rather high rates of bilateral asymmetry in men and women in the upper limbs suggests that both sexes, engaged in manual labour, which was either regular and/or hard enough to cause differential appositional bone growth in the left and right body sides, causing bone growth to be more prominent in the dominant arm in order to strengthen the bone against all the mechanical loads put upon them.

Unfortunately, although some studies exist on bilateral asymmetries in professional athletes, it is not possible in this case, to pinpoint an exact pattern of activity for the men and women buried in this cemetery. The fact that only females showed bilateral asymmetry in midshaft measurements of the tibia, suggests that they might have engaged in physical activities that would have put more load on the lower legs, such as prolonged kneeling or squatting.

Differences in bilateral asymmetry patterns are highest between the sexes. Generally, no consistent patterns can be observed regarding differences in bilateral asymmetry between the burial locations and layers and the age groups. This suggests that there were no traceable systematic differences in mechanical loading on bones, between the groups analysed.

5.2 Indices of the postcranial skeleton

5.2.1 Introduction

Nowadays, with the availability of radiography and CT-scanning, digitally obtained cross-sectional geometric data is largely preferred over the external bone measurements in biomechanical analyses (Ruff 2000, 2007; Wescott 2006). However, due to the large number of bones in this sample and time constraints, it was not feasible to subject all humeri, femora, and tibiae to either CT-scanning or radiography. Therefore, while maybe not as precise as direct cross-sectional measurements, external measurements were used in this study. This decision was supported by the fact that several studies have shown that robusticity reconstructions based on external measurements of long bones yielded similar results to those on direct cross-sectional data, and that therefore, these measurements can be used as substitutes to cross-sectional data for inferring changes or differences in mechanical load on the bones (Larsen 1981; Cole 1994; Ruff 1994; Bridges *et al.* 2000; Stock & Shaw 2007). For example, a study by Cole (1994) using external measurements to examine changes in long bone shape, robusticity, and sexual dimorphism between hunter-gatherers and horticulturalists in the Northern Plains, was later supported by a study from Ruff et al. 1994 on the cross-sectional data of the same individuals, which yielded very similar results. Another study by Larsen 1981, which detected a significant difference in antero-posterior and medio-lateral external dimensions between prehistoric hunter-gatherers and horticulturalists in Georgia, was later supported by results on cross-sectional data of the same groups (Ruff *et al.* 1984). Furthermore, a study by Bridges et al. (2000) found that the femur midshaft shape index calculated from external measurements showed nearly the same patterns of change among ancient populations

from Illinois than the cross-sectional data of the same groups. Further studies have set out to and have finally also proven the strength of the relationship between external and cross-sectional dimensions (Jungers & Minns 1979; Pearson 2000; Stock & Shaw 2007). Stock and Shaw (2007) for instance argue that the product of the antero-posterior and medio-lateral diameters standardised to body mass and bone length, could be used as reliable proxies for *J*, which represents the torsional strength of a bone.

Some indices of the postcranial skeleton can therefore be used to infer physical adaptation of bones to environmental stressors, mainly mechanical loading. This relies entirely on the premise that bone is flexible enough to adapt its shape to environmental stimuli. (Lazenby 2002; Battles 2009), a concept already established by Julius Wolff who wrote in 1892: "Every change in the form and function of bones, or of their function alone, is followed by certain definite changes in their internal architecture and equally definite secondary alteration in their external conformation, in accordance with mathematical laws" (Wolff 1892a). In short, his means that the structure and therefore the shape of bones adapts to the biomechanical stressors it is exposed to, mainly by bone resorption or apposition in the affected areas. Whereas single bone measurements only inform about one single part of the bone, bone indices provide a ratio of measurements from different bone parts to each other, thus helping to characterise the shape of the bone, namely whether it is rather broad compared to the length, whether the diaphysis is rather flat or rounded etc.

The following study aims to determine the dominant bone shapes in the population and aims to investigate whether bone shape and robusticity differ between the sexes, the burial layers, and locations, and among the age groups, as differences in bone shapes might hint at different regular physical activities being carried out by the groups, due to differential mechanical loading on the bone. By comparing the burial layers, a potential shift in mechanical loading patterns and thus in activities could be tracked over time, whereas the different burial locations might inform about differential labour division among social classes. In order to take into account, the role of ageing in bone formation and resorption all indices will also be compared by age group. In a second step, differences in lateralisation of bone shapes and robusticity will be explored throughout the sample. Since mainly diaphyseal morphology is thought to be influenced by external stressors and epiphyseal morphology is thought to be mainly influenced genetically (Trinkaus *et al.* 1994; Pearson 2000; Lieberman *et al.* 2001), only indices of the bone diaphysis were calculated for this study.

5.2.2 Methods

Both the bone length-thickness indices as well as the robusticity indices of the long bones describe the robustness of an individual, or at least the robustness of the respective body parts of an individual.

a. Length-Thickness Index

$$L_Th = \frac{MC}{ML} * 100$$

L_Th = length to thickness index	*MC = midshaft circumference*	*ML = maximum length*

In the following study, the length-thickness index was calculated solely for the femur and humerus as these are thought to be most affected by external environmental stressors such as mechanical loading.

For the same reason, the robusticity index was only calculated for the humerus and femur but for the tibia as well.

The bone robusticity index was calculated according to the following formula:

b. Robusticity Indices

$$ROBU = \frac{(APWM\ +\ MLWM)}{ML} * 100$$

APWM = antero-posterior midshaft diameter
MLWM = medio-lateral midshaft diameter
ML = maximum length
(Boyd & Boyd 1989; Larsen 1997; Mazza 2019)

However, several studies established, that bone robusticity is also influenced not only by bone length but also by body mass (Ruff *et al*. 1991; Pearson 2000; Lieberman *et al*. 2001; Wescott 2006; Stock & Shaw 2007; Holt *et al*. 2018; Laffranchi *et al*. 2020). Therefore, in order to control for this influence as well, the robusticity index for the femur and humerus was additionally standardised for bone length and body mass and calculated after the formula suggested by Stock and Shaw (2007), where maximum femoral length is additionally multiplied by body mass calculated on transverse femoral head diameter (Fe19) which acts as a proxy for body mass. This formula was also esteemed to be the best alternative to the

calculation of the polar second moment of area *(J)*, which is usually calculated using cross-sectional data (Stock & Shaw 2007; Laffranchi *et al*. 2020), and which informs about torsional and average bending rigidity of the bone. In short, this index informs about the bone strength. Greater index values indicate greater levels of mechanical loading. Body mass was estimated by averaging the results of the three formulas by Ruff et al. (1991), McHenry (1992) and Grine (1995), as recommended by Ruff et al. (1997), Auerbach and Ruff (2004) and Siegmund (2010) (Ruff *et al*. 1997; Auerbach & Ruff 2004; Siegmund 2010a).

$$FMR = \frac{(APWM * MLWM)}{(ML * BM)} * 100$$

FMR = femoral midshaft robusticity
APWM = antero-posterior midshaft diameter
MLWM = medio-lateral midshaft diameter
ML = maximum length
BM = body mass (calculated after Ruff et al. 1997)
(Stock & Shaw 2007; Laffranchi *et al.* 2020)

$$HMR = \frac{HD_{max} * HD_{min}}{BM * HML} * 100$$

HMR = humeral midshaft robusticity
HD_{max} = humeral maximum midshaft diameter (Hu5)
HD_{min} = humeral minimum midshaft diameter (Hu6)
BM = body mass (calculated after Ruff et al. 1991)
HML = humeral maximum length (Hu1)
(Stock & Shaw 2007; Laffranchi *et al.* 2020)

c. Femoral and Humeral Midshaft shape

$$FMS = APWM/MLWM$$

FMS = femoral midshaft shape
APWM = antero-posterior midshaft diameter
MLWM = medio-lateral midshaft diameter
(Stock & Shaw 2007; Laffranchi *et al.* 2020)

$$HMS = HD_{max} * HD_{min}$$

HMS = humeral midshaft shape *HD_{max} = humeral maximum midshaft diameter (Hu5)* *HD_{min} = humeral minimum midshaft diameter (Hu6)* *Stock and Shaw, 2007; Laffranchi et al., 2020)*

In accordance with the majority of recent studies on bone robusticity (Wescott 2006; Stock & Shaw 2007; Mazza 2019; Laffranchi *et al*. 2020), femoral and humeral midshaft shape (FMS/HMS) were also calculated. These indices are thought to characterise bone midshaft shape and the direction of the forces that were applied to it. For the femur this would mean that values > 1 indicate greater anteroposterior loading, values < 1 would correspond to greater mediolateral bending forces applied to the diaphysis and values around 1 would suggest that the bending forces applied to the bone were equal in both planes. Greater anteroposterior loading is considered indicative of increased mobility because the bone shape, which means an elongated antero-posterior diameter in relation to the medio-lateral one, hints at a stronger use of the muscles attached to the linea aspera, which are involved in locomotion. For the humerus, values < 1 should not occur, but as for the femur, values around 1 indicate equally applied forces along the two diaphyseal perpendicular planes and values >1 correspond to greater bending forces along the axis HD (Hu5), which would suggest that manual repetitive unidirectional movements were carried out on a regular basis (Mazza 2019; Laffranchi *et al*. 2020). HMS and FMS are often used as proxies for the shape indices l_x/l_y and l_{max}/l_{min} derived from cross-sectional data and based on cortical thickness (Stock & Shaw 2007; Laffranchi *et al*. 2020). However, according to Stock and Shaw 2007, HMS and FMS did not show as good a correlation to their cross-sectional counterparts as did FMR to *J*, regularly underestimating cortical thickness values. Generally, externally derived data on bone shape and robusticity should not be compared directly to those collected using cross-sectional data due to external measurements not being able to fully reconstruct inner bone morphology and thus regularly underestimating the effects of bending forces on bones. This means for this study that, if high index values are being detected on average, likely the individuals buried on this cemetery experienced high degrees of bending forces to the respective bones, either compatible with increased locomotion and/or strenuous and repetitive physical activities. However, if no high values are being detected, it will not necessarily mean that the population was not exposed to any more or less significant environmental stressors.

But HMS and FMS are not the only ways to describe the shape. The platymeric and pilastric indices of the femur and the cnemic index of the tibia for instance describe the shape of the

cross-section of the respective bone. The platymeric and cnemic indices describe the shape of the cross-section at the proximal diaphysis and the pilastric index the shape at the midshaft. Changes in the cross-sectional shape of a bone are often caused by physical stress and the subsequent adaptation of the bone to the increased mechanical load.
The indices are calculated as follows:

a. Platymeric Index

$$PLATY = \frac{FAPSD}{FMLSD} * 100$$

FAPSD = femur antero-posterior subtrochanteric diameter
FMLSD = femur medio-lateral subtrochanteric diameter
(Senol & Yucel 2019)

For the platymeric index of the femur, the bone is classed into 4 groups describing the shape at the subtrochanteric diaphyseal region, based on the values determined through the index calculation. Very low values indicate that the region is rather flat, meaning the medio-lateral diameter is notably larger than the antero-posterior one. The higher the index values, the more the antero-posterior and medio-lateral diameters grow alike in size, giving the bone a more rounded appearance in that area. The cut-off values and shape descriptions of the platymeric index can be found in Table 25.

Table 25 Cut-off values and shape descriptions of the platymeric index

Hyperplatymeria (very flattened)	<75.0
Platymery (flattened)	75.0-84.9
Eurymery (rounded)	85.0-99.9
Stenomery (rounded-elongated)	>100.0

b. Pilastric Index

$$PIL = \frac{FAPMD}{FMLMD} * 100$$

FAPMD = femur antero-posterior midshaft diameter
FMLMD = femur medio-lateral midshaft diameter
(Stock & Shaw 2007; Senol & Yucel 2019)

The pilastric index describes the shape of the femur at midshaft. The higher the values obtained through the index calculation, the higher is the value of the antero-posterior diameter compared to that of the medio-lateral diameter, giving the midshaft a more antero-posteriorly elongated shape. The smaller values indicate a more rounded to flattened shape of the area. The values are strongly influenced by the degree of expression of the linea aspera, the stronger it is expressed, the higher the index will be. The pilastric index is essentially the same as FMS, but due to the multiplication by 100 in order to fit it into one of the following categories, it becomes easier to visualise and understand the actual shape of the cross-section. The cut-off values and their shape descriptions for the pilastric index can be found in Table 26.

Table 26 Cut-off values and shape descriptions of the pilastric index

No pilaster	<100
light. Pilastric/linea aspera weak	100-109.9
Intermediate/normal	110-119.9
Advanced/prominent	>120

c. Cnemic Index

$$CNEM = \frac{TMLND}{TAPND} * 100$$

TAPND = tibia antero-posterior diameter at nutrient foramen
TMLND = tibia medio-lateral diameter at nutrient foramen
(Lovejoy *et al.* 1976)

The cnemic index describes the shape of the tibial diaphysis at the nutrient foramen, which is located in the proximal third of the shaft. The higher the index values are, the more rounded is the shape of the shaft, however as the values get smaller, the shaft shape becomes more flattened, meaning the antero-posterior diameter becomes more prominent in relation to the medio-lateral one. The cut-off values and their shape descriptions for the pilastric index can be found in Table 27.

Table 27 Cut-off values and shape descriptions of the cnemic index

hypercnemia	<54.9
Platycnemia (flattened)	55-62.9
mesocnemia (moderate)	63-69.9
eurycnemia (rounded)	>70.0

Finally, in order to investigate differences in bilateral asymmetry of the indices, all values of these indices were then also converted into percentage directional asymmetries (%DA) using the following formula:

$$\%DA = \frac{(R - L)}{(R + L)/2} \times 100$$

R = measurement of right bone
L = measurement of left bone
(Steele & Mays 1995; Mays *et al.* 1999; Čuk *et al.* 2001; Mays 2002; Plochocki 2004; Auerbach & Ruff 2006; Blackburn & Knüsel 2006; Auerbach & Raxter 2008; Weiss 2009; Reeves *et al.* 2016)

Next, the %DA were converted into %AA, by calculating the absolute values of each %DA. Like with the raw measurements in the previous chapter, representing the asymmetric differences as percentages of directional asymmetry makes the data of all measurements from all elements comparable to each other, regardless of the size differences of the raw measurements.

The first part of this study is dedicated to the general analysis of bone robusticity and shape by body side, comparing the sexes, age groups, burial layers, and locations. Significant differences in bone shape or robusticity between these groups would hint at differential loading patterns and thus differences in physical activity or locomotion between the groups. The second part of the analysis focusses on the bilateral asymmetry of the indices, where differences between the afore mentioned groups could also suggest differences in physical stress mechanisms or intensity to the bone. As already mentioned in the previous chapter, right-left asymmetries are nearly always present but are exacerbated by the influence of external stressors to the bone, as it is assumed that the main limb, which for most people is the right arm or left leg, is heavier involved in the carrying out of the physical activity. For this study, only individuals for which the indices could be calculated for both the right and left body sides were included. Since the

previous analysis showed most variability in bone robusticity to be present between the sexes, the following analysis were all carried out for males and females separately.

5.2.3 Results

5.2.3.1 Differences in diaphyseal shape patterns

In the following part of the study, diaphyseal shape patterns of the tibial and femoral diaphysis will be explored using the pilastric, platymeric and cnemic indices. As these indices directly characterise bone shape by classifying them into a category based on index value, they can be used to compare the distribution of these categorised bone shapes among the different groups.

5.2.3.1.1 Differences between men and women

As can be observed in Table 28, only the femoral cross-sectional shape shows any differences between some of the groups. In males, an eurymeric (L: ~41&; R: ~41%) and platymeric (L: ~49%;R: ~44%) shape seems to be most common, whereas women tend to have rather hyperplatymeric (L: ~26%; R: ~32%) to platymeric (L: ~41%; R: ~40%) bone shapes, which means that generally, women have a more flattened bone cross-sectional shape at the subtrochanteric region than men. Overall, the femora in this sample predominantly show a platymeric shape, followed by a eurymeric one, which means that generally, the subtrochanteric region of the femur tends to be slightly flattened to rounded in shape.

The pilastric index describes bone shape at the midshaft. This index only shows significant differences between men and women on the right body side, with females predominantly showing no pilaster (L: ~46%; R: ~52%), followed by the presence of a small pilaster (L: ~44%;R: ~34%). In men, a small pilaster (L: ~40%; R: ~39%) is most common, followed closely by the absence of a pilaster (L: ~37%;R: ~32%). However, contrary to women, a rather substantial proportion of men still present with a medium pilaster (L:~20%; R:~25%), meaning the antero-posterior diameter is noticeably larger than the medio-lateral one. The same trend can be observed on the left side; however, it does not show a significant difference between men and women. This means that, while women generally at a rather rounded or slightly flattened diaphyseal shape, men had generally a more rounded or antero-posteriorly elongated shape. It is important to note here, that stenomery (a very flattened cross-sectional shape at the subtrochanteric portion of the femoral diaphysis) as well as a prominent pilaster (a strongly enlarged antero-posterior diameter at midshaft), only occur very rarely in the sample. The

cnemic index of the tibia shows the exact same trend in men and women, namely a strong prevalence of eurycnemia (rounded shape at nutrient foramen) as opposed to mesocnemia (rounded but slightly more flattened shape at the nutrient foramen). Notably, platycnemic (flattened) and hypercnemic (very flattened) shapes are completely absent in this population.

Table 28 Prevalence of bone diaphyseal shapes among males and females

Index	Side	Shape	F	M	Total	X^2	p-value
PLATY	R	Hyperplatymeric	20 (31.75%)	11 (10.78%)	31 (18.79%)	**13.5**	**0.0037**
		Platymeric	25 (39.68%)	45 (44.12%)	70 (42.42%)		
		Eurymeric	18 (28.57%)	42 (41.18%)	60 (36.36%)		
		Stenomeric	0 (0%)	4 (3.92%)	4 (2.42%)		
		Total	63 (38.18%)	102 (61.82%)	165 (100.00%)		
	L	Hyperplatymeric	16 (26.23%)	7 (6.36%)	23 (13.45%)	**14.1**	**0.0028**
		Platymeric	25 (40.98%)	54 (49.09%)	79 (46.20%)		
		Eurymeric	17 (27.87%)	45 (40.91%)	62 (36.26%)		
		Stenomeric	3 (4.92%)	4 (3.64%)	7 (4.09%)		
		Total	61 (35.67%)	110 (64.33%)	171 (100.00%)		
PIL	R	No_Pilaster	34 (52.31%)	32 (31.68%)	66 (39.76%)	**8.8**	**0.0316**
		Light_Pilaster	22 (33.85%)	39 (38.61%)	61 (36.75%)		
		Medium_Pilaster	8 (12.31%)	25 (24.75%)	33 (19.88%)		
		Prominent_Pilaster	1 (1.54%)	5 (4.95%)	6 (3.61%)		
		Total	65 (39.16%)	101 (60.84%)	166 (100.00%)		
	L	No_Pilaster	27 (45.76%)	39 (36.79%)	66 (40.00%)	4.6	0.2056
		Light_Pilaster	26 (44.07%)	42 (39.62%)	68 (41.21%)		
		Medium_Pilaster	5 (8.47%)	21 (19.81%)	26 (15.76%)		
		Prominent_Pilaster	1 (1.69%)	4 (3.77%)	5 (3.03%)		
		Total	59 (35.76%)	106 (64.24%)	165 (100.00%)		
CNEM	R	Mesocnemic	5 (11.63%)	13 (15.29%)	18 (14.06%)	0.1	0.7685
		Eurycnemic	38 (88.37%)	72 (84.71%)	110 (85.94%)		
		Total	43 (33.59%)	85 (66.41%)	128 (100.00%)		
	L	Mesocnemic	4 (8.33%)	15 (18.07%)	19 (14.50%)	1.6	0.2049
		Eurycnemic	44 (91.67%)	68 (81.93%)	112 (85.50%)		
		Total	48 (36.64%)	83 (63.36%)	131 (100.00%)		

bold *= Significance at p<0.05*

5.2.3.1.2 Differences between age groups

The longer a bone is exposed to bending forces, the more likely it is, that it adapts its shape to better withstand those forces. This concept also applies to ageing: the longer a person lives, the longer their bones will be exposed to external bending forces. Therefore, age might also influence bone shape. In order to test whether age did influence the prevalence of certain bone

shapes, differences between the age groups were tested via a Pearson's chi square test. This proved important since the proportions of adult, mature and senile individuals differ slightly among burial location and layers. So, in order to make sure that any differences that might be prevalent among those factors, are not caused by a dominance of one age group, the influence of age on bone shape had to be excluded.

The following analysis demonstrates (Table 29) that none of the three indices showed significant differences in bone shape distribution among the three age groups, which suggests that overall, age did most likely not influence lower limb diaphyseal shape.

However, regarding the platymeric index, there was an unsignificant trend of slightly less flattened shapes among seniles, but no such trend could be observed for the cnemic and pilastric indices.

Table 29 Prevalence of bone diaphyseal shapes among adults, matures and seniles

Index	Side	Shape	Adult	Mature	Senile	Total	X^2	p-value
PLATY	R	Hyperplatymeric	16 (23.19%)	12 (17.65%)	3 (10.71%)	31 (18.45%)	6.8	0.3435
		Platymeric	30 (43.48%)	26 (38.24%)	14 (50.00%)	70 (42.42%)		
		Eurymeric	22 (31.88%)	29 (42.65%)	9 (32.14%)	60 (36.36%)		
		Stenomeric	1 (1.45%)	1 (1.47%)	2 (7.14%)	4 (2.38%)		
		Total	69 (41.82%)	68 (41.21%)	28 (16.97%)	165 (100.00%)		
	L	Hyperplatymeric	12 (17.65%)	8 (10.69%)	3 (10.00%)	23 (13.45%)	5.5	0.4802
		Platymeric	33 (48.53%)	32 (43.84%)	14 (46.67%)	79 (46.20%)		
		Eurymeric	21 (30.88%)	28 (38.36%)	13 (43.33%)	62 (36.26%)		
		Stenomeric	2 (2.94%)	5 (6.85%)	0 (0%)	7 (4.09%)		
		Total	68 (39.77%)	73 (42.69%)	30 (17.54%)	171 (100.00%)		
PIL	R	No_Pilaster	30 (43.48%)	26 (38.24%)	10 (34.48%)	66 (39.76%)	8.3	0.2145
		Light_Pilaster	28 (40.58%)	22 (32.35%)	11 (37.93%)	61 (36.75%)		
		Medium_Pilaster	10 (14.49%)	18 (26.47%)	5 (17.24%)	33 (19.88%)		
		Prominent_Pilaster	1 (1.45%)	2 (2.94%)	3 (10.34%)	6 (3.61%)		
		Total	69 (41.57%)	68 (40.96%)	29 (17.47%)	166 (100.00%)		
	L	No_Pilaster	26 (40.00%)	25 (35.71%)	15 (50.00%)	66 (40.00%)	4.5	0.6071

Index	Side	Shape	Adult	Mature	Senile	Total	X^2	p-value
		Light_Pilaster	30 (46.15%)	28 (40.00%)	10 (21.43%)	68 (41.21%)		
		Medium_Pilaster	7 (10.77%)	15 (21.43%)	4 (13.33%)	26 (15.76%)		
		Prominent_Pilaster	2 (3.08%)	2 (2.86%)	1 (3.33%)	5 (3.03%)		
		Total	65 (39.39%)	70 (42.42%)	30 (18.18%)	165 (100.00%)		
CNEM	R	Mesocnemic	4 (7.41%)	10 (21.28%)	4 (14.81%)	18 (14.06%)	4.0	0.1343
		Eurycnemic	50 (92.59%)	37 (78.72%)	23 (85.19%)	110 (85.94%)		
		Total	54 (42.19%)	47 (36.72%)	27 (21.09%)	128 (100.00%)		
	L	Mesocnemic	4 (7.27%)	10 (20.83%)	5 (17.86%)	19 (14.50%)	4.1	0.1272
		Eurycnemic	51 (92.73%)	38 (79.17%)	23 (82.14%)	112 (85.50%)		
		Total	55 (41.98%)	48 (36.64%)	28 (21.37%)	131 (100.00%)		

bold *= Significance at p<0.05*

5.2.3.1.3 Differences between social classes

Table 30 shows the differences in femoral diaphyseal shape between cemetery and cloister burials. Significant differences in shape patterns could only be detected in the platymeric index but not in the pilastric or cnemic ones. Generally, people buried in the cemetery and in the cloister, both tended to have a platymeric to eurymeric (platy.: ~42-46%; eury.: ~36%) shape. In the cemetery more people tended towards platymery (L: ~50%; R: ~44%) than towards eurymery (L: ~31%; R: ~33%) and a considerable amount also presented with hyperplatymeria (L: ~17%; R: ~23%). However, in the cloister, people showed predominantly a eurymeric shape (L: ~52%; R: ~46%) followed closely by platymery (L: ~36%; R: ~39%). But whilst hyperplatymeria still occurs relatively frequently among people buried in the cemetery (~20%), it is very rare in the among people buried in the cloister (~5%). Stenomery is again a very rare occurrence in both burial sites.

The pilastric index shows no significant differences in femoral diaphyseal shape between cloister and cemetery burials, in both burial locations no pilastric and light pilastric shapes are the most prevalent with people buried in the cemetery showing a tendency towards more no pilastric shapes (cloister: ~28%; cem.: ~46%) and those from the cloister a tendency towards more light pilastric shapes (cloister: ~41%; cem.: ~44%).

No significant difference between cloister and cemetery burials could be detected in the tibial cnemic index, with eurycnemic shapes being vastly more prevalent.

Table 30 Prevalence of bone diaphyseal shapes among cloister and cemetery

Index	Side	Shape	Cemetery	Cloister	Total	X^2	p-value
PLATY	R	Hyperplatymeric	29 (23.39%)	2 (4.88%)	31 (18.79%)	**19.4**	**0.0002**
		Platymeric	54 (43.55%)	16 (39.02%)	70 (42.42%)		
		Eurymeric	41 (33.06%)	19 (46.34%)	60 (36.36%)		
		Stenomeric	0 (0%)	4 (9.76%)	4 (2.42%)		
		Total	124 (75.15%)	41 (24.85%)	165 (100.00%)		
	L	Hyperplatymeric	21 (16.54%)	2 (4.55%)	23 (13.45%)	**10.0**	**0.0186**
		Platymeric	63 (49.61%)	16 (36.36%)	79 (46.20%)		
		Eurymeric	39 (30.71%)	23 (52.27%)	62 (36.26%)		
		Stenomeric	4 (3.15%)	3 (6.82%)	7 (4.09%)		
		Total	127 (74.27%)	44 (25.73%)	171 (100.00%)		
PIL	R	No_Pilaster	55 (44.72%)	11 (25.58%)	66 (39.76%)	6.1	0.1063
		Light_Pilaster	43 (34.96%)	18 (41.86%)	61 (36.75%)		
		Medium_Pilaster	22 (17.89%)	11 (25.58%)	33 (19.88%)		
		Prominent_Pilaster	3 (2.44%)	3 (6.98%)	6 (3.61%)		
		Total	123 (74.10%)	43 (25.90%)	166 (100.00%)		
	L	No_Pilaster	53 (43.44%)	13 (30.23%)	66 (40.00%)	3.7	0.2979
		Light_Pilaster	49 (40.16%)	19 (44.19%)	68 (41.21%)		
		Medium_Pilaster	16 (13.11%)	10 (23.26%)	26 (15.76%)		
		Prominent_Pilaster	4 (3.28%)	1 (2.33%)	5 (3.03%)		
		Total	122 (73.94%)	43 (26.06%)	165 (100.00%)		
CNEM	R	Mesocnemic	12 (12.77%)	6 (17.65%)	18 (14.06%)	0.2	0.6790
		Eurycnemic	82 (87.23%)	28 (82.35%)	110 (85.94%)		
		Total	94 (73.44%)	34 (26.56%)	128 (100.00%)		
	L	Mesocnemic	13 (13.54%)	6 (17.14%)	19 (14.50%)	0.1	0.8122
		Eurycnemic	83 (86.46%)	29 (82.86%)	112 (85.50%)		
		Total	96 (73.28%)	35 (26.72%)	131 (100.00%)		

Bold *= Significance at p<0.05*

5.2.3.1.4 Changes over time

Furthermore, it was tested whether there was a difference in diaphyseal shape between the upper and lower layers in the cemetery. As can be deducted from Table 31, burial layer did not significantly influence the pattern of distribution of bone cross-sectional shapes, this means that bending forces applied to the bone diaphysis did not change significantly over the period analysed. However, it can be observed that people from the upper layer (1) expressed less hyperplatymeria (R:~11%; L:~7%) than those from the lower layer (2) (R:25%; L:~19%).

Concerning the pilastric index, shape distribution is very similar between the layers with the majority of shapes classifying as having no or just a small pilaster. However, a strong pilaster is consistently more prominent in the lower layer (R: LD1: ~0%, LD2: ~7%; L: LD1: ~1, LD2: ~4%). But the sample size of the highly pilastric group is too small for any reliable interpretations. No differences were detected in the cnemic index, with both layers showing vastly more eurycnemic than mesocnemic shapes.

Table 31 Prevalence of bone diaphyseal shapes among the upper and lower layers

Index	Side	Shape	1	2	Total	X^2	p-value
PLATY	R	Hyperplatymeric	8 (10.96%)	23 (25.00%)	31 (18.79%)	6.3	0.0964
		Platymeric	31 (42.47%)	39 (42.39%)	70 (42.42%)		
		Eurymeric	32 (43.84%)	28 (30.43%)	60 (36.36%)		
		Stenomeric	2 (2.74%)	2 (2.17%)	4 (2.42%)		
		Total	73 (44.24%)	92 (55.76%)	165 (100.00%)		
	L	Hyperplatymeric	5 (6.67%)	18 (18.75%)	23 (13.45%)	7.0	0.0707
		Platymeric	36 (48.00%)	43 (44.79%)	79 (46.20%)		
		Eurymeric	29 (38.67%)	33 (34.38%)	62 (36.26%)		
		Stenomeric	5 (6.67%)	2 (2.08%)	7 (4.09%)		
		Total	75 (43.86%)	96 (56.14%)	171 (100.00%)		
PIL	R	No_Pilaster	29 (39.19%)	37 (40.22%)	66 (39.76%)	5.5	0.1373
		Light_Pilaster	28 (37.84%)	33 (35.87%)	61 (36.75%)		
		Medium_Pilaster	17 (22.97%)	16 (17.39%)	33 (19.88%)		
		Prominent_Pilaster	0 (0%)	6 (6.52%)	6 (3.61%)		
		Total	74 (44.58%)	92 (55.42%)	166 (100.00%)		
	L	No_Pilaster	28 (38.36%)	38 (41.30%)	66 (40.00%)	7.3	0.0632
		Light_Pilaster	37 (50.68%)	31 (33.70%)	68 (41.21%)		
		Medium_Pilaster	7 (9.59%)	19 (20.65%)	26 (15.76%)		
		Prominent_Pilaster	1 (1.37%)	4 (4.35%)	5 (3.03%)		
		Total	73 (44.24%)	92 (55.76%)	165 (100.00%)		
CNEM	R	Mesocnemic	9 (15.79%)	9 (12.68%)	18 (14.06%)	0.1	0.8043
		Eurycnemic	48 (84.21%)	62 (87.32%)	110 (85.94%)		
		Total	57 (44.53%)	71 (55.47%)	128 (100.00%)		
	L	Mesocnemic	10 (19.23%)	9 (11.39%)	19 (14.50%)	1.0	0.3207
		Eurycnemic	42 (80.77%)	70 (88.61%)	112 (85.50%)		
		Total	52 (39.69%)	79 (60.31%)	131 (100.00%)		

Bold *= Significance at p<0.05*

5.2.3.2 Differences in bone shape and robusticity

The following part of the study is dedicated to the analysis of bone shape and robusticity based on direct index values. This will allow for more subtle differences in patterns, that were obscured by the broader groupings of the previous analyses, to become apparent. Furthermore,

in the case of femoral robusticity and humeral diaphyseal shape, there are no clear set cut-off values to separate them into shape expressions.

5.2.3.2.1 Differences between men and women

Since the previous analyses on bone shape already showed that most of the differences occurred between men and women, the direct indices were firstly compared between the sexes to assess the influence of sex on bone shape and strength. Table 32 shows that significant differences between the sexes existed for the platymeric and pilastric index, as already shown previously, but also for FMS, HMS, TiROBU, HuL/Th and HuROBU.

The average values of FMS for both women and men centre around 1, which means that the medio-lateral and antero-posterior bending forces applied to the bone were quite balanced, causing the shape of the diaphysis to be rather rounded. Men showed on average slightly higher values than women.

Concerning HMS the values are on average slightly higher than one and are generally higher in females than in males, suggesting that the female humeri were systematically subjected more to repetitive forces applied along the axis of the maximum midshaft diameter. Overall, though, for all bone diaphysis shape indices, the effect size of the p-value was below 0.3, meaning the effect of sex on diaphysis shape, though statistically significant, was only small.

When looking at the robusticity indices standardised by length alone, only those concerning the humerus and tibia show a significant difference between men and women. In all cases, the effect size is higher than 0.3 but lower than 0.5 and would therefore be described as moderate. Whilst tibial robusticity shows significantly higher values in males than in females for right and left bones, the humerus only shows significant differences for the right side and displays the same pattern as the tibia. Finally, when standardizing bone diaphyseal shape by length and body mass, only the femur shows significant differences between the sexes, with females showing greater values then men, although the effect was considered small.

It becomes apparent, as several studies already suggested (Ruff *et al.* 1991; Ruff 2000; Lieberman *et al.* 2001; Wescott 2006; Stock & Shaw 2007; Laffranchi *et al.* 2020), that bone robusticity is well influenced by bone length and by body mass of the individual, and therefore it seems that diaphyseal diameters alone, and by extension also single bone measurements, are not as reliable when assessing bone robusticity then the indices standardised by length and/or body mass.

Table 32 Results of the Mann-Whitney U test for all bone indices comparing men to women on unpaired data.

Index	Side	Sex	max	min	mean	median	sd	W	p-value	n
PLATY	L	F	102.47	66.78	81.44	80.02	8.70	**2,503**	**0.0060**	61
		M	102.23	73.21	84.77	83.56	6.97			110
	R	F	96.01	64.59	80.42	80.27	7.84	**2,234**	**0.0010**	63
		M	107.73	69.89	85.25	84.25	8.29			102
PIL	L	F	120.48	74.69	99.76	100.63	8.88	**2,464**	**0.0243**	59
		M	126.40	82.99	103.47	102.19	8.61			106
	R	F	119.89	77.04	99.53	99.49	8.73	**2,238**	**0.0006**	64
		M	134.31	82.31	105.43	104.54	8.95			102
CNEM	L	F	90.28	67.38	77.18	76.26	5.29	2,327	0.1101	48
		M	93.14	63.58	75.25	75.87	5.29			83
	R	F	89.01	67.34	77.53	77.40	5.45	2,158	0.0959	43
		M	85.72	63.05	75.67	75.76	5.02			85
FMS	L	F	1.20	0.75	1.00	1.01	0.09	**2,464**	**0.0243**	59
		M	1.26	0.83	1.03	1.02	0.09			106
	R	F	1.23	0.77	1.00	1.00	0.09	**2,238**	**0.0006**	65
		M	1.34	0.82	1.05	1.05	0.09			101
HMS	L	F	1.52	1.09	1.28	1.28	0.09	**2,986**	**0.0136**	52
		M	1.43	1.07	1.24	1.24	0.08			92
	R	F	1.44	1.11	1.30	1.30	0.08	**3,389**	**0.0068**	53
		M	1.52	1.06	1.25	1.25	0.09			101
HuL/Th	L	F	24.44	16.99	20.35	20.10	1.60	912.5	0.1582	33
		M	24.61	17.26	20.74	20.72	1.42			67
	R	F	22.87	17.47	20.32	20.34	1.25	**760.5**	**0.0016**	35
		M	24.24	18.56	21.23	21.01	1.25			70
FeL/Th	L	F	23.30	17.75	19.44	19.21	1.18	1,810.5	0.2029	48
		M	22.36	17.51	19.65	19.53	1.13			87
	R	F	24.16	16.74	19.33	19.21	1.21	1,624.5	0.1040	51
		M	21.75	17.15	19.55	19.55	1.04			80
HuROBU	L	F	14.88	10.98	12.35	12.14	0.93	920	0.1751	33
		M	14.69	10.30	12.57	12.45	0.85			67
	R	F	14.17	10.31	12.38	12.27	0.79	**685**	**0.0002**	35
		M	15.11	11.40	12.97	12.83	0.77			70
FeROBU	L	F	15.23	11.05	12.41	12.37	0.81	1,654	0.1515	47
		M	14.24	11.00	12.57	12.50	0.75			83
	R	F	15.57	10.60	12.35	12.32	0.83	1,730	0.2654	50
		M	13.89	10.91	12.46	12.49	0.69			80
TiROBU	L	F	15.17	11.95	13.63	13.77	0.76	**557**	**0.0000**	37
		M	16.41	12.70	14.41	14.35	0.81			62
	R	F	14.82	11.92	13.61	13.74	0.78	**450**	**0.0005**	26
		M	16.51	13.14	14.36	14.31	0.80			65
HMR	L	F	2.30	1.43	1.84	1.79	0.22	697	0.4141	29
		M	2.54	1.46	1.89	1.88	0.25			54

Index	Side	Sex	max	min	mean	median	sd	W	p-value	n
	R	F	2.43	1.58	1.94	1.91	0.23	738	0.4215	29
		M	2.61	1.48	1.98	2.00	0.26			57
FMR	L	F	3.44	2.16	2.73	2.73	0.32	**2,323**	**0.0097**	46
		M	3.31	1.99	2.57	2.57	0.29			79
	R	F	3.36	2.02	2.68	2.65	0.31	**2,302**	**0.0073**	47
		M	3.32	1.94	2.52	2.51	0.27			76

Bold *= Significant at p<0.05*

5.2.3.2.2 Differences between age groups

Whilst age did not seem to have an influence on the diaphyseal shape indices, as already established in the previous section, it did have an influence on the femoral indices standardised by body mass and/or bone length.

For FeL/Th, FeROBU and FMR alike, the significant differences could be observed between the adult and mature and adult and senile groups only. Only the comparison between adults and seniles had a moderate effect size for right and left FeROBU, right and left FMR and left FeL/Th, but only the right FeL/Th showed a moderate effect size between adults and matures as well as between matures and seniles. (Table 33)

Table 33 Results of the Mann-Whitney U test for all bone indices comparing all the age groups on unpaired data

Index	Side	Age	max	min	mean	median	sd	W	p-value	n
PLATY	L	Adult	102.47	69.79	82.46	82.68	7.36	3.3571	0.1866	68
		Mature	102.23	67.56	84.92	84.21	8.21			73
		Senile	97.70	66.78	82.89	82.02	7.34			30
	R	Adult	101.62	66.90	81.75	80.75	7.94	4.3743	0.1122	69
		Mature	100.83	64.59	84.54	84.39	8.62			68
		Senile	107.73	70.51	84.73	84.39	8.76			28
PIL	L	Adult	121.55	80.76	101.54	101.13	7.85	2.0077	0.3665	65
		Mature	126.40	74.69	103.06	102.73	9.48			70
		Senile	126.00	84.47	101.16	99.27	9.45			30
	R	Adult	122.86	82.63	102.16	101.16	7.73	1.5959	0.4503	69
		Mature	121.55	80.76	101.54	101.13	7.85			68
		Senile	126.40	74.69	103.06	102.73	9.48			29
CNEM	L	Adult	93.14	63.58	76.71	76.38	5.41	1.5436	0.4622	55
		Mature	90.28	66.05	75.39	75.55	5.20			48
		Senile	85.15	64.49	75.46	75.15	5.51			28
	R	Adult	89.01	68.60	77.44	77.06	4.97	3.4874	0.1749	54
		Mature	87.01	63.05	75.33	75.74	5.31			47
		Senile	85.18	64.79	75.67	76.32	5.30			27

Index	Side	Age	max	min	mean	median	sd	W	p-value	n
FMS	L	Adult	1.22	0.81	1.02	1.01	0.08	2.0077	0.3665	65
		Mature	1.26	0.75	1.03	1.03	0.09			70
		Senile	1.26	0.84	1.01	0.99	0.09			30
	R	Adult	1.23	0.83	1.02	1.01	0.08	1.5959	0.4503	69
		Mature	1.27	0.77	1.04	1.04	0.10			68
		Senile	1.34	0.88	1.05	1.03	0.11			29
HMS	L	Adult	1.45	1.09	1.25	1.24	0.08	2.5168	0.2841	59
		Mature	1.52	1.07	1.26	1.24	0.10			60
		Senile	1.38	1.15	1.27	1.28	0.06			25
	R	Adult	1.52	1.06	1.26	1.25	0.09	0.6164	0.7348	60
		Mature	1.47	1.08	1.27	1.28	0.10			64
		Senile	1.44	1.12	1.27	1.27	0.09			30
HuL/Th	L	Adult	24.44	18.01	20.36	20.17	1.32	3.0854	0.2138	42
		Mature	24.61	16.99	20.79	20.53	1.71			40
		Senile	22.73	17.26	20.79	20.79	1.28			18
	R	Adult	23.95	17.47	20.72	20.57	1.22	3.0854	0.2138	44
		Mature	24.24	17.86	20.96	20.79	1.46			46
		Senile	22.57	20.00	21.41	21.81	1.00			15
FeL/Th	L	Adult	22.11	17.51	19.15	**19.04*&**	0.97	**14.0092**	**0.0009**	56
		Mature	23.30	17.89	19.80	**19.89***	1.21			56
		Senile	21.58	18.31	20.06	**20.10&**	1.06			23
	R	Adult	21.03	16.74	19.00	**18.98*&**	0.88	**18.7985**	**<0.0000**	59
		Mature	24.16	17.15	19.78	**20.00***	1.24			49
		Senile	21.30	18.22	19.95	**20.09&**	0.91			21
HuROBU	L	Adult	14.88	10.98	12.39	12.33	0.77	1.6874	0.4280	42
		Mature	14.69	11.14	12.58	12.32	1.01			40
		Senile	13.76	10.30	12.56	12.73	0.82			18
	R	Adult	14.52	10.31	12.68	12.59	0.78	1.3164	0.5178	44
		Mature	15.11	11.18	12.81	12.63	0.91			46
		Senile	13.99	12.00	12.94	12.96	0.65			15
FeROBU	L	Adult	14.04	11.00	12.24	**12.15*&**	0.69	**11.8790**	**0.0026**	52
		Mature	15.23	11.37	12.63	**12.69***	0.80			55
		Senile	14.09	11.71	12.85	**12.76&**	0.69			23
	R	Adult	13.56	10.60	12.12	**12.13*&**	0.64	**17.6195**	**0.0001**	58
		Mature	15.57	10.95	12.60	**12.83***	0.81			50
		Senile	13.60	11.82	12.78	**12.87&**	0.57			21
TiROBU	L	Adult	15.76	11.95	13.96	13.97	0.88	3.5584	0.1688	46
		Mature	16.07	12.52	14.31	14.39	0.81			35
		Senile	16.41	12.68	14.16	14.05	0.94			18
	R	Adult	15.77	12.25	14.05	14.06	0.79	1.0992	0.5772	43
		Mature	16.50	11.92	14.25	14.23	0.93			31
		Senile	16.51	13.00	14.18	14.03	0.92			17
HMR	L	Adult	2.34	1.43	1.81	1.79	0.23	4.4738	0.1068	35

Index	Side	Age	max	min	mean	median	sd	W	p-value	n
		Mature	2.54	1.52	1.91	1.89	0.25			35
		Senile	2.30	1.68	1.94	1.88	0.21			13
	R	Adult	2.50	1.48	1.93	1.90	0.25			37
		Mature	2.61	1.60	2.01	2.00	0.26	2.1408	0.3429	37
		Senile	2.30	1.59	1.94	1.98	0.21			12
FMR	L	Adult	3.44	1.99	2.54	**2.50*&**	0.31			52
		Mature	3.17	2.05	2.67	**2.69***	0.29	**10.2049**	**0.0061**	53
		Senile	3.41	2.16	2.75	**2.69&**	0.31			20
	R	Adult	3.32	1.99	2.48	2.44	0.28			58
		Mature	3.23	1.94	2.65	2.63	0.28	**14.0380**	**0.0008**	46
		Senile	3.36	2.21	2.72	2.68	0.29			19

Bold *= Significant at p<0.05*

*, & = Significance in the post-hoc test at p<0.05

5.2.3.2.3 Differences between social classes

Among the people buried in the cloister complex and those buried in the cemetery, only the femoral diaphyseal shape indices, namely FMS, the platymeric and the pilastric indices, show any significant differences. In all cases, people buried in the cloister showed slightly higher values than those from the cemetery, suggesting that the cloister people experienced slightly higher or more frequent external antero-posterior bending forces to the bone shaft. However, whilst the difference was significant, the effect size remained small, which means that the differences between people from the cloister and the cemetery were minimal.

Furthermore, FMS is only slightly higher than 1 in both groups, indicating that the femur was subjected only to moderate or little physical stress. (Table 34)

Table 34 Results of the Mann-Whitney U test for all bone indices comparing cloister to cemetery burials on unpaired data

Index	Side	Location	max	min	mean	median	sd	W	p-value	n
PLATY	L	Cemetery	102.23	66.78	82.39	82.38	7.37	**1,886**	**0.0013**	127
		Cloister	102.47	73.21	87.02	85.98	7.96			44
	R	Cemetery	99.48	64.59	82.03	81.54	7.98	**1,629**	**0.0006**	124
		Cloister	107.73	69.89	87.57	87.88	8.47			41
PIL	L	Cemetery	126.00	74.69	101.14	101.05	8.84	**1,990**	**0.0189**	122
		Cloister	126.40	89.46	105.01	104.33	8.38			43
	R	Cemetery	134.31	77.04	102.19	100.92	9.20	**2,040**	**0.0260**	123
		Cloister	126.78	87.77	105.93	105.48	9.11			43
CNEM	L	Cemetery	93.14	63.58	75.98	75.59	5.37	1,599	0.6754	96
		Cloister	85.58	64.49	75.90	76.71	5.37			35
	R	Cemetery	89.01	63.05	76.17	76.01	4.96	1,460	0.4582	94

Index	Side	Location	max	min	mean	median	sd	W	p-value	n
		Cloister	87.01	64.79	76.64	77.75	5.95			34
FMS	L	Cemetery	1.26	0.75	1.01	1.01	0.09	**1,990**	**0.0189**	122
		Cloister	1.26	0.89	1.05	1.04	0.08			43
	R	Cemetery	1.34	0.77	1.02	1.01	0.09	**2,040**	**0.0260**	123
		Cloister	1.27	0.88	1.06	1.05	0.09			43
HMS	L	Cemetery	1.52	1.07	1.26	1.25	0.09	1,959	0.8122	109
		Cloister	1.47	1.12	1.26	1.25	0.09			35
	R	Cemetery	1.52	1.06	1.27	1.25	0.10	2,257	0.9536	115
		Cloister	1.44	1.10	1.27	1.27	0.08			39
HuL/Th	L	Cemetery	24.61	17.26	20.59	20.42	1.49	917	0.7266	74
		Cloister	23.96	16.99	20.67	20.49	1.51			26
	R	Cemetery	24.24	17.47	20.91	20.74	1.32	1,037	0.6439	76
		Cloister	23.91	17.86	20.97	20.88	1.33			29
FeL/Th	L	Cemetery	23.30	17.51	19.58	19.42	1.18	1,772.50	0.9643	99
		Cloister	21.41	17.93	19.57	19.37	1.06			36
	R	Cemetery	24.16	16.74	19.46	19.48	1.14	1,417	0.9886	103
		Cloister	21.75	18.28	19.48	19.23	1.01			28
HuROBU	L	Cemetery	14.88	10.30	12.50	12.38	0.87	1,002	0.7563	74
		Cloister	14.59	11.14	12.49	12.30	0.90			26
	R	Cemetery	15.11	10.31	12.77	12.59	0.82	1,057	0.7498	76
		Cloister	14.65	11.25	12.80	12.70	0.84			29
FeROBU	L	Cemetery	15.23	11.00	12.52	12.46	0.80	1,677.50	0.9393	95
		Cloister	13.63	11.37	12.49	12.48	0.71			35
	R	Cemetery	15.57	10.60	12.41	12.41	0.77	1,388	0.8842	102
		Cloister	13.89	11.50	12.45	12.27	0.66			28
TiROBU	L	Cemetery	16.07	12.52	14.13	14.16	0.78	878	0.9769	76
		Cloister	16.41	11.95	14.10	14.17	1.15			23
	R	Cemetery	16.50	12.44	14.17	14.06	0.81	819	0.7389	68
		Cloister	16.51	11.92	14.07	14.09	1.01			23
HMR	L	Cemetery	2.40	1.43	1.86	1.86	0.23	609	0.8272	63
		Cloister	2.54	1.52	1.89	1.84	0.26			20
	R	Cemetery	2.61	1.48	1.96	1.93	0.26	693	0.7623	63
		Cloister	2.60	1.61	1.98	1.91	0.24			23
FMR	L	Cemetery	3.44	1.99	2.63	2.63	0.32	1,451	0.8364	93
		Cloister	3.09	2.09	2.63	2.59	0.27			32
	R	Cemetery	3.36	1.94	2.57	2.57	0.30	1,080	0.3638	98
		Cloister	3.19	2.08	2.63	2.64	0.29			25

Bold *= Significant at $p<0.05$*

5.2.3.2.4 Changes over time

Comparisons between the two burial layers revealed that only the right platymeric index and the right humeral length-thickness index show significant differences between the burial layers. However, in both cases, the effect sizes were small, which means that the difference observed was likely not very meaningful. The platymeric index displayed slightly higher values in the upper layer and the humeral length-thickness index presented with higher values in the lower layer. It must be noted that, although absent among the diaphyseal shape indices, an overall trend of slightly higher values in the lower layer can be observed among the indices standardised by body mass and/or length. (Table 35)

Table 35 Results of the Mann-Whitney U test for all bone indices comparing burial from Layer 1 to those from Layer 2 on unpaired data

Index	Side	LD	max	min	mean	median	sd	W	p-value	n
PLATY	L	1	102.47	72.59	84.81	83.57	7.92	4,070	0.1439	75
		2	101.82	66.78	82.62	82.68	7.56			96
	R	1	107.73	67.14	85.17	84.56	8.52	**4,048**	**0.0237**	73
		2	101.62	64.59	82.01	81.68	8.13			92
PIL	L	1	122.65	82.99	101.63	101.53	7.33	3,174	0.5472	74
		2	126.40	74.69	102.56	101.23	9.96			91
	R	1	119.89	82.31	103.10	101.54	7.99	3,320	0.7862	75
		2	134.31	77.04	103.21	101.77	10.29			91
CNEM	L	1	93.14	63.58	75.36	75.57	5.87	1,839	0.3129	52
		2	90.28	66.05	76.35	75.99	4.99			79
	R	1	85.72	64.79	75.76	75.09	5.02	1,795	0.2743	57
		2	89.01	63.05	76.72	76.65	5.37			71
FMS	L	1	1.23	0.83	1.02	1.01	0.07	3,174	0.5472	73
		2	1.26	0.75	1.03	1.01	0.10			92
	R	1	1.20	0.82	1.03	1.01	0.08	3,320	0.7862	74
		2	1.34	0.77	1.03	1.02	0.10			92
HMS	L	1	1.47	1.08	1.27	1.25	0.09	2,736	0.3825	60
		2	1.52	1.07	1.25	1.25	0.09			84
	R	1	1.52	1.12	1.28	1.28	0.09	3,383	0.1140	71
		2	1.47	1.06	1.26	1.25	0.09			83
HuL/Th	L	1	24.44	18.29	20.55	20.33	1.31	1,096	0.6902	36
		2	24.61	16.99	20.65	20.58	1.58			64
	R	1	23.95	17.47	20.64	20.57	1.20	**1,044.50**	**0.0377**	48
		2	24.24	17.86	21.16	21.00	1.36			57
FeL/Th	L	1	21.60	17.54	19.49	19.35	1.13	2,064.50	0.4815	57
		2	23.30	17.51	19.64	19.41	1.16			78
	R	1	21.22	17.15	19.32	19.15	1.03	1,808.50	0.3541	52

Index	Side	LD	max	min	mean	median	sd	W	p-value	n
		2	24.16	16.74	19.56	19.61	1.15			79
HuROBU	L	1	14.88	11.33	12.42	12.33	0.78	1,032	0.3908	36
		2	14.69	10.30	12.54	12.48	0.93			64
	R	1	14.51	10.31	12.62	12.53	0.77	1,104	0.0901	48
		2	15.11	11.18	12.90	12.81	0.85			57
FeROBU	L	1	14.09	11.20	12.49	12.34	0.73	2,021	0.8468	55
		2	15.23	11.00	12.53	12.50	0.81			75
	R	1	13.56	10.91	12.32	12.25	0.67	1,762	0.2502	52
		2	15.57	10.60	12.49	12.51	0.79			78
TiROBU	L	1	16.07	11.95	14.02	14.17	0.89	1,107	0.5626	41
		2	16.41	12.52	14.19	14.12	0.87			58
	R	1	16.45	11.92	13.97	13.94	0.85	825	0.1199	40
		2	16.51	12.55	14.28	14.31	0.85			51
HMR	L	1	2.23	1.46	1.81	1.79	0.19	655	0.1861	30
		2	2.54	1.43	1.90	1.88	0.26			53
	R	1	2.50	1.48	1.94	1.91	0.24	816	0.3876	39
		2	2.61	1.58	1.99	1.96	0.26			47
FMR	L	1	3.31	2.16	2.60	2.56	0.30	1,676	0.2307	54
		2	3.44	1.99	2.65	2.68	0.32			71
	R	1	3.32	1.94	2.54	2.51	0.28	1,506	0.0907	51
		2	3.36	2.02	2.62	2.61	0.30			72

Bold *= Significant at p<0.05*

5.2.3.3 Bilateral asymmetry of bone shape and robusticity

The following section will explore the degree and the direction of lateralization of the indices. When carrying out physical activities, the prominent arm is usually more involved than the other and bears the brunt of the forces applied to it. Therefore, higher degrees of bilateral asymmetry could be indicative of more mechanical loading and the directional asymmetry will inform about preferred arm or leg use.

5.2.3.3.1 Bilateral asymmetry in men and women

As marked in Table 36, a significant degree of bilateral asymmetry was only detected in males, with the right side consistently being more pronounced than the left. In the diaphyseal shape measurements, namely the pilastric index, FMS and HMS, the effect of the p-value is moderate but for the humeral robusticity measurements standardised by length and/or body mass, such as HuROBU and HMR, the effect size was even higher than 0.5 and could therefore be classified as large. This means that the differences between right and left values in men are all meaningful, especially those describing bone strength. Whilst the diaphyseal shape indices

were also significantly different for humeral and femoral measurements, once standardised only the humeral indices showed any significant right-left differences. These results would suggest that overall, men experienced more mechanical loading on the bones than females as the differences between right and left bones are consistently higher than among females. Furthermore, among men, bilateral asymmetry was more prominent in the arm bones than in the leg bones, suggesting that the latter were subjected to more regular external stressors, which would indicate that physical activities were mainly focused on tasks carried out with the arms than relying on frequent locomotion.

Table 36 Results of the Wilcoxon signed ranks test for bone indices

Index	Sex	Side	max	min	mean	median	sd	mean	V	p-value	n
PLATY	F	L	102.47	66.78	81.44	79.31	9.23	-0.55	853	0.3436	58
		R	101.40	66.90	80.86	79.66	7.74				58
	M	L	102.23	73.21	85.09	84.21	7.33	0.26	1,985	0.9446	93
		R	118.40	69.89	85.42	84.22	8.63				93
PIL	F	L	120.48	80.76	100.01	100.31	8.41	-0.15	825	0.6479	59
		R	119.89	77.04	99.90	99.18	8.77				59
	M	L	126.40	82.99	103.47	102.31	8.15	1.70	**1,204**	**0.0027**	91
		R	134.31	82.31	105.32	103.82	9.26				91
CNEM	F	L	90.28	67.38	77.37	76.72	5.19	0.10	362	0.7043	46
		R	89.01	67.34	77.47	77.77	5.55				46
	M	L	93.14	64.49	75.34	75.57	5.19	0.08	1,151	0.3618	81
		R	85.18	63.05	75.40	75.38	5.12				81
FMS	F	L	1.20	0.81	1.00	1.00	0.08	-0.15	825	0.6479	59
		R	1.20	0.77	1.00	0.99	0.09				59
	M	L	1.26	0.83	1.03	1.02	0.08	1.66	**1,226**	**0.0036**	91
		R	1.34	0.82	1.05	1.04	0.09				91
HMS	F	L	1.52	1.09	1.29	1.28	0.09	0.29	448	0.9704	42
		R	1.44	1.11	1.29	1.28	0.09				42
	M	L	1.43	1.07	1.24	1.23	0.08	1.26	**1,021**	**0.0148**	77
		R	1.52	1.08	1.26	1.25	0.10				77
HuL/Th	F	L	23.10	16.99	20.41	20.00	1.60	-1.01	174	0.1289	22
		R	22.87	17.86	20.18	20.17	1.22				22
	M	L	24.61	18.29	20.94	20.74	1.36	1.00	305	0.0679	43
		R	24.24	18.56	21.15	20.93	1.24				43
FeL/Th	F	L	23.30	17.67	19.25	19.12	1.15	-0.11	457	0.5360	42
		R	24.16	17.53	19.23	19.15	1.21				42
	M	L	22.36	17.51	19.61	19.49	1.16	0.00	1,014	0.8646	67
		R	21.75	17.61	19.61	19.48	1.03				67
HuROBU	F	L	14.18	11.05	12.35	12.27	0.91	-0.27	118	0.7990	22
		R	14.17	11.25	12.30	12.18	0.69				22

Index	Sex	Side	max	min	mean	median	sd	mean	V	p-value	n
	M	L	14.69	11.47	12.70	12.53	0.83	2.08	**185**	**0.0003**	43
		R	15.11	11.40	12.97	12.71	0.83				43
FeROBU	F	L	15.23	11.05	12.30	12.29	0.80	0.09	387	0.7648	42
		R	15.57	11.05	12.32	12.30	0.84				42
	M	L	14.24	11.00	12.58	12.48	0.78	-0.46	1,263	0.1368	66
		R	13.89	11.07	12.51	12.49	0.68				66
TiROBU	F	L	15.03	11.95	13.62	13.77	0.77	-0.12	128	0.5457	29
		R	15.04	11.92	13.61	13.56	0.80				29
	M	L	16.41	12.48	14.39	14.32	0.84	0.04	649	0.7226	54
		R	16.51	12.90	14.39	14.36	0.80				54
HMR	F	L	2.30	1.43	1.85	1.79	0.23	1.97	63	0.1231	20
		R	2.30	1.58	1.89	1.90	0.20				20
	M	L	2.54	1.49	1.90	1.88	0.25	4.81	**93**	**0.0000**	37
		R	2.61	1.48	1.99	1.93	0.28				37
FMR	F	L	3.41	2.16	2.68	2.68	0.32	-0.18	377	0.9315	40
		R	3.36	2.02	2.67	2.66	0.33				40
	M	L	3.31	1.99	2.56	2.56	0.29	-1.18	1,203	0.0649	63
		R	3.32	2.02	2.52	2.51	0.26				63

Bold *= Significant at p<0.05*

5.2.3.3.2 Differences in bilateral asymmetry between men and women

In a next step, it was tested whether there were any differences in the direction and in the degree of asymmetry between men and women. The directionality was assessed by comparing %DA scores and the degree of asymmetry was explored through comparisons of %AA scores. For %DA, only three indices showed significant differences between men and women. The pilastric index, FMS and humeral length-thickness index all showed that, while males tended to have a clearly right-biased asymmetry, females either tended towards no asymmetry or a left-biased one. Only one index showed significant differences in the degree of asymmetry between men and women. Bilateral asymmetry was significantly higher in men than in women for the platymeric index. However, except for the differences between men and women for HuL/Th, where the women generally tended to left-biased and then men to right-biased asymmetry, none of the differences were deemed meaning full when considering the effect sizes. (Table 37 & Table 38)

Since in many indices, men were found to display significant degrees of asymmetry and females did not as shown through the Wilcoxon signed ranks tests, and some even showed significant differences between men and women, it was decided to continue the analysis for males and females separately.

Table 37 Indices showing a significant difference in %DA between men and women

Index	Sex	max	min	mean	median	sd	W	p-value	n
PIL	F	12.56	-10.54	-0.15	0.07	5.37	**2,119**	**0.0297**	59
	M	17.35	-21.10	1.66	2.18	5.69			91
FMS	F	12.56	-10.54	-0.15	0.07	5.37	**2,119**	**0.0297**	59
	M	17.35	-21.10	1.66	2.18	5.69			91
HuL/Th	F	5.44	-10.05	-1.01	-1.03	3.54	**296**	**0.0136**	22
	M	6.56	-4.50	1.00	0.32	2.57			43

***B**old = Significance at p<0.05*

Table 38 Indices showing a significant difference in %AA between men and women

Index	Sex	max	min	mean	median	sd	W	p-value	n
PLATY	F	12.15	0.17	5.45	4.61	3.70	**3,310**	**0.0191**	58
	M	15.55	0.01	4.09	3.20	3.60			93

***Bold** = Significance at p<0.05*

5.2.3.3.3 Differences in bilateral asymmetry between age groups

Among the age groups, the Kruskal-Wallis tests revealed that the only statistically relevant difference occurred in the tibial robusticity index in males regarding the absolute degree of asymmetry. Only the difference between adults and matures was significant even though seniles displayed overall the lowest values (Table 39). Significantly higher values in the adults compared to the older groups might suggest that the physical stress the bone was exposed to generally decreased over time, leading also to a decrease in bone robusticity with age and an equaling out of both sides. This however is not supported by the findings from the previous section which strongly hint at a generally increasing robusticity with increasing age. Therefore, and due to the rather small effect size of this difference, this result should not be interpreted as a sign of decreasing physical activities with age.

Table 39 Indices showing a significant difference in %AA between the different age groups

Index	Sex	Age	max	min	mean	median	sd	X^2	p-value	n
TiROBU	F	Adult	5.27	0.06	1.90	1.87	1.55	1.4203	0.4916	11
		Mature	4.95	0.64	2.55	2.24	1.78			8
		Senile	4.75	1.42	2.96	2.50	1.44			5
	M	Adult	6.52	0.40	3.50	3.14*	2.03	**8.8977**	**0.0117**	25
		Mature	4.56	0.19	1.84	1.40*	1.20			15
		Senile	5.06	0.19	1.81	1.03	1.66			9

Bold *= Significance at p<0.05*
***** *= Post-hoc test significant at p<0.05*

5.2.3.3.4 Differences in bilateral asymmetry between social classes

In a next step, differences in the direction and degree of lateralization of the indices were explored. This follows the same train of thought already laid out in the previous section on bilateral asymmetry of bone measurements. Differences between social classes might also be reflected in different kinds of activities carried out. Depending on the kinds, intensity or regularity of the activities, bone shape will adapt to the bending forces put upon it by those activities, and the dominant limb is prone to experience the majority of those forces. The only significant difference in directional asymmetry (Table 40) could be detected in the platymeric index in women, where women from the cloister tended towards a clearly left-biased asymmetry and those from the cemetery did not show much asymmetry in any direction, however this difference was not considered meaningful.

Regarding the degree of asymmetry, only males showed some differences between cloister and cemetery burials and exclusively in the two femoral robusticity indices, with people buried in the cloister displaying significantly higher, albeit not very meaningful degrees of asymmetry than those buried in the cemetery (Table 41).

Table 40 Indices showing a significant difference in %DA between cloister and cemetery burials

Index	Sex	Location	max	min	mean	median	sd	W	p-value	n
PLATY	F	Cemetery	11.98	-12.15	0.41	0.19	6.51	**390**	**0.0280**	46
		Cloister	6.94	-12.01	-4.21	-4.53	5.84			12
	M	Cemetery	15.39	-9.56	0.26	0.22	5.21	782	0.9964	71
		Cloister	10.51	-15.55	0.25	-0.17	6.34			22

Bold *= Significance at p<0.05*

Table 41 Indices showing a significant difference in %AA between cloister and cemetery burials

Index	Sex	Location	max	min	mean	median	sd	W	p-value	n
FeROBU	F	Cemetery	9.05	0.04	2.26	1.64	2.02	188	0.6315	31
		Cloister	5.00	0.00	1.80	1.85	1.31			11
	M	Cemetery	4.94	0.00	1.87	1.43	1.34	**234.5**	**0.0430**	52
		Cloister	4.28	0.21	2.64	2.93	1.25			14
FMR	F	Cemetery	15.33	0.37	4.48	3.37	3.79	188	0.2458	30
		Cloister	9.25	0.01	3.07	2.34	2.66			10
	M	Cemetery	10.50	0.19	3.39	2.67	2.70	**191**	**0.0101**	50
		Cloister	10.17	2.61	5.58	5.05	2.36			14

Bold *= Significance at p<0.05*

When comparing differences not only between the cemetery and cloister, but also between the different burial areas on the cemetery, it becomes clear that only the platymeric index still shows a significant difference in %DA, namely are cloister burials and those close to it predominantly left-biased and those buried midway from the church are predominantly right-biased. However, none of the differences turned out meaningful. (Table 42)

Table 42 Indices showing a significant difference in %DA between individuals buried inside, close and midway to and far from the church complex

Index	Sex	Location	max	min	mean	median	sd	X^2	p-value	n
PLATY	F	Cloister	6.94	-12.01	-4.21	-4.53*	5.84	**13.0303**	**0.0046**	12
		Close	8.81	-11.67	-3.67	-3.88$^{\&}$	6.25			11
		Mid	11.98	-6.55	2.74	2.85*$^{\&}$	5.28			26
		Far	8.91	-12.15	-1.35	-0.63	7.64			9
	M	Cloister	10.51	-15.55	0.25	-0.17	6.34	0.8042	0.8485	22
		Close	6.32	-6.66	0.87	0.74	3.76			14
		Mid	14.46	-9.32	0.08	-0.36	5.01			39
		Far	15.39	-9.56	0.17	-0.33	6.66			18

Bold *= Significance at p<0.05*

** & = Post-hoc test significant at p<0.05*

5.2.3.3.5 Changes in bilateral asymmetry over time

None of the indices displayed any statistically relevant differences in bilateral asymmetry, directional or intensity, over time.

5.2.3.4 Comparison to other Luxembourgish sites

The following Table 43 shows the mean indices for femoral length-thickness, femoral robustness, and the pilastric index between several Luxembourgish sites divided where possible by sex and side and in chronological order. Six of the sites can be considered rural (Givenich, Diekirch, Grevenmacher and Fentingen), whilst the remaining three (St.Esprit, Knuedler and Grund-Wenzelsmauer) can be classified as urban. Furthermore, comparisons between the latter three sites should prove very interesting since they all represent cemeteries from Luxembourg City and are roughly contemporaneous. Regarding femoral diaphyseal shape at midshaft, only comparisons with the older rural sites are possible. Among the four rural sites, Givenich and Fentingen display overall the highest values but generally, differences are low between all the sites. Differences between the sexes are also highest in the two latter sites, although statistical significance cannot be calculated. All values, except for the left female pilastric index in Givenich fall above 100, classifying them as light pilastric with a weak linea aspera. Looking only at those values would suggest that possibly, people from Fentingen and Givenich were engaged in increased physical activities involving the lower limbs, however due to a lack of raw data and data on the upper limbs, no definitive conclusions can be reached. When comparing the individuals from Knuedler to those older rural sites, it immediately becomes apparent, that they fall into the same index range. Especially males fall right in the middle of the range of the values from the rural sites, while females show slightly lower index values than the other females. And whilst the differences between males and females among the Knuedler individuals are more similar to those from Givenich and Fentingen, the right-left differences are very small and rather similar to those displayed in Grevenmacher.

The femoral length-thickness index from Knuedler is very similar to that detected in Grund-Wenzelsmauer, with the only difference that male values are greater than female ones. Greater male values are also found among the Diekirch population but not in Grevenmacher, and both sites display overall slightly higher values than Knuedler. This might suggest that the individuals from Grevenmacher and Diekirch experienced higher antero-posterior bending forces on their lower limbs. The femoral robusticity index does not show any relevant differences between the sites.

Table 43 Comparison of mean index values between older and contemporaneous Luxembourgish sites

			PIL		FeL/Th		FeROBU		Publication
site	**Period**	**sex**	**R**	**L**	**R**	**L**	**R**	**L**	
Givenich	8th-10th C	M	106.8	107.6				12.0	Rehbach et al. (2009), Weidig et al. (2009)
		F	104.2	98.0			13.2	12.6	
Diekirch	11th/12th-15th C	M	107.4	103.4	20.1	20.2	12.7	12.7	From Trautmann (2012)
		F	107.4	100.7	19.0	19.3	11.8	12.2	
Grevenmacher	8th-15th C	M	100.5	102.0	20.2	19.6	12.7	12.5	Trautmann (2012)
		F	100.2	100.0	20.2	19.7	12.9	12.5	
Fentingen	10th-15th C	M	104.4	109.3			12.4	11.9	Rehbach et al. (2005), Nothwang & Rehbach (2006)
		F	109.9	101.1			12.2	12.4	
St. Esprit	12th-17th C	M					12.3		Rehbach & Bis-Worch (2006), Nothwang et al. (2006), Rehbach et al. (2007), Rehbach (2008), Rehbach & Nothwang (2009)
		F					12.3		
Knuedler	14th-18th C	M	105.4	103.5	19.6	19.7	12.5	12.6	Kremmer (hic)
		F	99.5	99.8	19.3	19.4	12.4	12.4	
Grund-Wenzelsmauer	16th-18th C	M			19.1				Trautmann & Trautmann (2011)
		F			19.5				

5.2.4 Discussion and Conclusion

5.2.4.1 Locomotive behaviour

Overall, the bone diaphysis of women tends to be more rounded, and the antero-posterior and medio-lateral diameters are balanced in relation to each other. Regarding men, a similar overall pattern is prevalent, but the antero-posterior diameter is generally more often enlarged. This suggests that at least some individuals in this sample, and mainly males, experienced stronger antero-posterior bending forces on the femoral diaphysis, which is often associated with increased mobility. However, the very rare occurrence or absence of stenomeric, strongly pilastric or hypercnemic values suggests that locomotive behaviour associated to long distance walking, which would lead to increased and repeated antero-posterior bending forces on the bone diaphysis was not prevalent in this population. These results are in accordance with those from other studies (Ruff *et al.* 1984; Stock & Pfeiffer 2004; Marchi 2008; Sparacello & Marchi 2008; Sparacello *et al.* 2011; Macintosh *et al.* 2014, 2017) that show that settled and industrialised populations experienced way less antero-posterior bending forces to the bone diaphysis than pre-industrialised populations such as hunter-gatherers or horticulturalists, which is likely due to the lower mobility rates among recent industrialised populations. The differences observed between men and women, however, are not necessarily due solely to different locomotive behaviour but could also be influenced by genetics, as several studies concluded, that sex alone may also influence bone shape (Tanner 1989; Callewaert *et al.* 2010; Gosman *et al.* 2011). Further differences could be observed among the different age groups, especially between adults and seniles, with seniles generally showing higher index values than

adults suggesting that they were exposed to higher rates of external bending forces on the bone. However, these results do not mean that seniles were generally more mobile than adults, but rather reflect the impact of everyday locomotive behaviour on the bone over the individual's life. The longer a bone is exposed to environmental factors, the more it adapts its shape to the forces that are applied to it. Further differences in lower limb diaphyseal shape could be detected between cloister and cemetery burials, which suggests that people from the cloister were slightly more mobile than those in the cemetery. However, the differences are not meaningful and only concern the diaphyseal shape, whereas none of the robusticity indices are involved. Since unstandardised indices are also considered to be less reliable indicators of bone robusticity and because the effect sizes of the differences are so small, it is very likely that there were no relevant differences in the degree of locomotive behaviours between the two burial locations. The same can be said for the differences between the burial layers.

5.2.4.2 Physical activity

Manual activities would be expected to leave traces on upper limb bones when carried out repeatedly especially if they are sufficiently intense. Therefore, strong differences in humeral diaphyseal shape and robusticity between the different groups should indicate differences in physical activity patterns. The fact that humeral cortical bone properties adapt to physical stresses has been explained in a study by Rhodes and Knüsel (2005). They analysed men from two late medieval populations one weapon-injured and the other consisting of an injured and an uninjured group and compared them to populations with varying activity levels. The comparisons suggested that both medieval groups engaged in strenuous activities probably related to weapon use but displayed different movement patterns (Rhodes & Knüsel 2005). The only meaningful differences in the Knuedler population, however, were detected among men and women. Relating to the differences between the sexes, this might reflect differences in labour division between men and women, an assumption which seems to be supported by higher index values in men compared to women. This suggests that men carried out more strenuous physical activities on a regular basis since their bone were more exposed to external bending forces. However, some studies suggest that generally, men tend to have more robust bones than females even if the bones are subjected to the same kind and intensity of mechanical loading (Jones *et al.* 1977; Haapasalo *et al.* 1996). Since the differences here are rather small, the latter explanation could explain also the differences observed in this sample. The differences detected between the layers are too random and too small to reflect any change in physical activities over time. Furthermore, the HMS values are overall closer to 1, which hints

at a rather low degree of bending forces applied to the humeral diaphysis and therefore does not suggest that the people from this sample carried out very strenuous tasks on an everyday basis.

5.2.4.3 Lateralisation

Only men showed meaningful bilateral asymmetry in several indices, mainly concerning humeral robusticity, which might suggest that their bones were exposed more regularly to higher degrees of bending forces causing differential bone apposition in the right and left body sides. However, when looking at absolute asymmetries, females showed overall a higher degree of asymmetry in the platymeric index, even though that was not deemed significant when examining the paired data. Studies on professional athletes have also shown that generally, bilateral asymmetry was not as high in females as it was in males, although they practised the same activities over the same prolonged time periods. A study by Jones et al. (1977) that measured cortical widths and thickness of humeri from radiographs of the playing and non-playing arms of professional tennis players showed that the playing arm in men, was ~35% thicker than the non-playing arm, whereas the difference in females was just ~28%. He observed the same trend in the antero-posterior diameter, for which the playing arm was 9.9% larger in men but only 7% larger in females (Jones *et al*. 1977). A study by Haapasalo et al. (1996) came to a similar conclusion, although young males and females showed significant side differences in all parameters tested, except for humeral length which was only significant in men, the ranges of asymmetry were overall lower in females than in males (Haapasalo *et al*. 1996). Therefore, it is very plausible that, as established in the previous section, physical stress on bones was generally fairly low in this population, the bone of females simply did not react as strongly to the stimuli as men's bone did. Generally, few indices show differences between the burial locations and age groups and none between the burial layers, and additionally, effect sizes of the significant differences were always small. This absence of clear differences in lateralisation suggests at first glance that locomotive behaviour and physical activities were not too different between the groups. However, the general absence of significant asymmetries among female indices and among the majority of the men's, rather suggests that lateralisation was possibly not as easy to detect in indices, especially in the standardised ones, leading to the conclusion that robusticity indices might not be the best indicators for assessing lateralisation. However, several studies on professional athletes, where regular strenuous activity patterns are known, have come to a different conclusion. For example, professional tennis players display a significant amount of hypertrophy of the distal humeral epiphysis (Jones *et al*. 1977), as well

as increased length in the playing arm (Haapasalo *et al*. 1996). Handball players seem to have significant humeral retrotorsion in their throwing arm (Pieper 1998), and cricketers were found to have higher levels of humeral robusticity, a more circular humeral diaphyseal shape and more humeral and ulnar rigidity in their playing arm (Shaw & Stock 2009).

5.2.4.4 Conclusion

The fact that moderately meaningful differences could be detected between age groups, especially between adults and seniles, as well as between men and women for the standardised and unstandardised indices respectively and especially those of the femur suggest that bone robusticity respectively shape was influenced to some extent by age and sex. This supports the fact that stress on the bone diaphysis, especially antero-posterior bending forces associated closely with locomotion and physical activities, change bone shape significantly over time and more robust bone shapes do not necessarily reflect increased mobility or activity in a certain group but can also reflect only the repeated application of these external stressors on an everyday basis as the person ages. However, this presumes that an individual will keep carrying out the same or similar tasks or movements throughout their life into old age, which is often not the case anymore in modern societies, where the elderly generally engage in less physically exhausting tasks than the young. This decrease in mechanical load on the bones would mean though that the rate of bone loss will eventually outrun that of bone gain (Garn *et al*. 1992; Stirland 1993), a pattern that is not observed in this population, however, which is more in agreement with results obtained by Mazza (2019) on pre-Hispanic horticulturalists, among which bone robusticity shows a clear increase with age (Mazza 2019). This leads to believe that in both populations, horticulturalists and the people from Knuedler, physical activities that outweighed age-induced bone resorption were carried out regularly into old age.

Furthermore, differences between the sexes could be due to several biological factors that might influence the bones reactivity to external stressors. Sex differences in growth patterns (Tanner 1989), and related to that, the sex differences in the secretion and on the receptors of insulin-like growth factors and growth hormones (Callewaert *et al*. 2010), as well as the effects of sex hormones (Gosman *et al*. 2011) might render female bones less susceptible to react to mechanical loading (Macintosh *et al*. 2017). In fact, a study on rats has shown, that exercised male rats showed significantly more geometrical adaptation to the mechanical loading than female rats, which in return developed denser bones. This increase in bone density might have

limited the bone's adaptive response to stress in females (Järvinen *et al*. 2003; Macintosh *et al*. 2017).

Therefore, it cannot be entirely excluded that age or sex might have influenced some of the differences detected between the burial locations since the proportion of men compared to females is higher in the cloister (M: ~69%; F: ~31%) than in the cemetery (M: 59%; F: 41%). And the amount of older people compared to younger ones is higher in the cloister (A: ~27%; M: ~48%; S: ~25%) than in the cemetery (A: ~43%; M: ~39%; S: ~18%) especially since increased mobility would not be expected among people buried in the cloister, who are generally considered to be of higher social status and thus probably not as prone to a lot of daily physical activity that could have contributed to differences in bone shape.

In conclusion, the differences in bone shape and robusticity observed between the social groups and over time are too few, not meaningful enough and likely influenced by other factors such as sex or age. Therefore, it is very likely that locomotive behaviours and intensity of regular physical activity did not differ significantly between the two perceived social classes and did not change much over time. Regarding mobility, these results are not surprising since generally, mobility is not as high anymore in urbanised and sedentary populations and is especially low in industrialised ones and some studies showed, that already medieval populations only showed slightly higher bone cross-sectional properties than modern control groups (Ruff *et al*. 1984; Stock & Pfeiffer 2004; Marchi 2008; Sparacello & Marchi 2008; Sparacello *et al*. 2011; Macintosh *et al*. 2014, 2017). Furthermore, according to historical sources, due to its status as the biggest and main church in Luxembourg city at the time (Bis-Worch 2011), the burial ground at the Franciscan monastery on the "Knuedler", was quite sought after. Therefore, it can be assumed that, although people buried in the cloister were of higher social rank, the ones buried in the cemetery possibly also belonged to a more or less well-situated part of the population. This assumption could also be supported by the fact that HMS and FMS both centred around 1 and the pilastric, platymeric and cnemic indices reflected rather balanced and rounded diaphyseal shapes, suggesting that none the groups engaged in regular strenuous physical activities.

Finally, it has to be pointed out that external measurements of bone diaphyseal shape and robustness might not be suitable to detect more subtle differences in mobility and physical stress between and within populations and groups, as information on the internal bone structure cannot be accounted for and they repeatedly underestimate values of bone shape derived from cross-sectional data (Wescott 2006). Subtle changes in bone apposition or specific patterns of

cortical thickening etc., such as the tendency for female cortical bone to react to stressors predominantly with increase in bone density rather than thickness (Järvinen *et al*. 2003), might not be detectable through external measurements alone, but necessitates the use of cross-sectional data obtained from CT-scanning. Therefore, results obtained from external measurements should never be compared directly to those of cross-sectional data.

5.3 Entheseal changes

5.3.1 Introduction

The area where a ligament, tendon or joint capsule attaches to the bone is called an enthesis. Continuous use of muscles and joints, but also traumatic injuries and arthropathies can cause changes in the bone surface of these attachment sites, altering their surface morphology. These changes in surface morphology, also often referred to as entheseal changes, when caused by use wear or enthesopathies when very pronounced and obviously caused by pathological changes to the area, have often been used in attempts to reconstruct physical activity in past populations (Hawkey & Merbs 1995; al-Oumaoui *et al*. 2004; Mariotti *et al*. 2004, 2007; Villotte 2006, 2008; Villotte *et al*. 2010; Laffranchi *et al*. 2020). Since the 1980s attempts have been made continuously to develop standardised methods for recording entheses but nowadays, still no consensus has been reached as to which method provides the most accurate results (Michopoulou *et al*. 2015; Palmer *et al*. 2019; Perez-Arzak *et al*. 2022), which is the reason why many of them are still in use today.

5.3.2 Methods

This study uses the scoring method developed by Mariotti et al. (2004) and (2007), as it provided clear illustrations and descriptions of changes on the entheses of the majority of long bones as well as guidelines on the statistical analysis of the recorded data. The recording system is also not as detailed as more recently developed methods like the Coimbra method, which would be very time consuming to record for large skeletal series such as this one (Henderson *et al*. 2013, 2016), and is easier to use while the results remain comparable (Palmer *et al*. 2019). Furthermore, the author had already received training in the usage of this method by participating as error tester in a study on entheseal recording methods at the University of Tübingen.

Mariotti et al. (2007) record three traits for all entheses listed in Table 44, the degree of robusticity which ranges from 0, absence of or very weak change to 4 strong surface and/or

border changes at the enthesis, as well as the degrees of osteolytic (OL) and osteophytic (EF) lesions ranging from 0, absent to 3 large osteophytes or osteolytic lesion covering most of the enthesis.

First, the muscle attachment sites were combined into muscle groups used in the movement of a specific joint, namely shoulder, elbow (flexion/extension), forearm (pronation/supination), hip, knee, and foot. The classification for each enthesis can be found in Table 44. The scores of the attachment sites within each of the joints were then added to form a common score, separated by body side and this score was then compared between the sexes, age groups, burial layers and burial location. Since for many individuals, not all attachment sites in a functional area could be recorded, it was decided to still calculate the score, if of all bones involved, at least two attachment sides could be scored. In the end, this procedure only had to be applied to the functional area of the shoulder, in order to maximise sample size in all comparative groups. Finally, the distribution of the combined scores by functional area were classified into three categories:

A	</=2	low-medium
B	</=3	medium-strong
C	</=4	strong-very strong

This was done to represent the proportions of entheseal changes visually in stacked bar charts. As recommended in Mariotti et al. 2007, grouping the low to medium development categories into one, helps to visualise general trends in the data. Only individuals for whom a clear sex and age estimation was possible were included in the analyses. Juveniles as well as adults of unknown age and/or sex were excluded.

Finally, the proportion of entheses with OL and EF lesions was also explored visually, as the presence of the latter, especially at high expression, can be considered indicative of enthesopathy.

Table 44 Muscle attachment sites sorted by functional complex (after Mariotti et al.2007)

FUNCTIONAL COMPLEX	ENTHESIS	ABBR.	BONE
SHOULDER	Costoclavicular ligament	CSLC	Clavicle
	Conoid ligament	COLC	
	Trapezoid ligament	TRLC	
	Musculus pectoralis major	MPMC	
	Musculus deltoideus	MDC	
	Musculus pectoralis major	MPMH	Humerus

FUNCTIONAL COMPLEX	ENTHESIS	ABBR.	BONE
	Musculus latissimus dorsii/teres major	MLH	
	Muscukus deltoides	MDH	
ELBOW	Musculus triceps brachii	MTBS	Scapula
	Musculus brachioradialis	MBRH	Humerus
	Musculus biceps brachii	MBBR	Radius
	Musculus triceps brachii	MTBU	Ulna
	Musculus brachialis	MBU	
FOREARM	Musculus pronator teres	MPTR	Radius
	Interosseous membrane	IMR	
	Musculus supinator	MSU	Ulna
HIP	Musculus gluteus maximus	MGMF	Femur
	Musculus iliopsoas	MIF	
KNEE	Musculus vastus medialis	MVMF	Femur
	Quadriceps tendon	QTT	Tibia
	Quadriceps tendon	QTP	Patella
FOOT	Musculus soleus	MST	Tibia
	Achilles tendon	ATC	Calcaneus

5.3.3 Results

5.3.3.1 Differences in entheseal scores by groups and functional area

Differences between degrees of robusticity were also tested between all the groups for all functional areas. Functional areas are a grouping of entheses sometimes located on several different bones, whose interplay allows the movement of a specific joint, such as the shoulder, the elbow etc.. The calculation of a common score out of all the detailed scores recorded for each enthesis in a specific functional area, allowed for a more detailed evaluation of the use of different joints as compared between the sexes, age groups, burial locations, and layers. The premise of this analysis relies on the assumption, that a joint which has been frequently and intensely in use should show a higher score of entheseal robusticity than that of a joint which has not been used as frequently or as intensely, allowing thus to maybe detect division of labour between the sexes or the social classes and even track changes in habitual physical activities over time.

5.3.3.1.1 Differences between men and women

The Wilcoxon tests revealed significant differences in the degree of entheseal robusticity between men and women in the shoulder, elbow, forearm, and hip on the left body side and in the shoulder, forearm and knee on the right body side. For right and left, the effect size was

moderate for sex comparisons in the shoulder complex and for left only also in the elbow complex, the remaining effect sizes were small and thus biologically not relevant.

This suggests that biological sex had an influence mainly on the expression of the entheses in the shoulder but not so much on the other functional complexes. Overall, men clearly showed greater degrees of robusticity than females, except for the foot where the difference is not as marked (Table 45). This trend also becomes clearly visible when observing Figure 52 contrasting the simplified scores of the left and right body sides between the sexes. At least for the right body side, females and men display a vaguely similar pattern in entheseal developmental degrees, with the forearm and the hip showing the least development. However, in men, the shoulder and elbow then show similar values as the knee and the foot, whereas in women, the lower limbs show overall higher development degrees than the upper limbs. In females and in males, this pattern is even stronger expressed on the left side, with all upper limb values in females showing lesser degrees of development than the lower limbs.

When considering only the joint areas of individuals aged between 20-39 years, there is no significant difference anymore between males and females in the forearm and in the hip on the left and in the forearm and knee on the right body side. This is also visible in the bar charts (Figure 53) where the only clear difference between males and females are the degrees of entheseal development in the shoulder and elbow, which is higher in men. Only in men, a similar pattern as in the analysis with all age classes included, can be observed. Still, also among the younger age categories, men show slightly higher degrees of entheseal development overall.

Table 45 Differences by sex for all functional areas

Joints	Side	Sex	max	min	mean	median	sd	W	p-value	n
shoulder	L	F	3.14	0.38	1.62	1.65	0.75	758.5	0.0005	40
		M	4.00	0.75	2.20	2.15	0.72			64
	R	F	3.00	0.13	1.63	1.63	0.76	709.5	0.0001	36
		M	4.00	0.83	2.30	2.25	0.71			73
elbow	L	F	3.40	0.40	1.60	1.50	1.03	125.5	0.0313	12
		M	3.80	0.80	2.28	2.20	0.77			36
	R	F	3.60	0.60	1.82	1.90	0.96	128.5	0.1731	10
		M	3.60	0.80	2.26	2.30	0.77			36
forearm	L	F	3.33	0.00	1.51	1.33	0.85	1437	0.0335	47
		M	4.00	0.00	1.90	1.67	0.93			79
	R	F	3.33	0.00	1.56	1.67	0.86	1202	0.0208	40
		M	4.00	0.00	1.98	2.00	0.88			81

Joints	Side	Sex	max	min	mean	median	sd	W	p-value	n
hip	L	F	4.00	0.50	1.76	2.00	0.93	2256	0.0113	61
		M	4.00	0.50	2.19	2.00	1.01			97
	R	F	4.00	0.00	1.93	2.00	1.02	2271	0.0810	58
		M	4.00	0.50	2.26	2.00	1.07			94
knee	L	F	3.67	0.00	1.77	1.67	0.91	191.5	0.1585	16
		M	3.67	0.67	2.21	2.33	0.93			32
	R	F	3.00	0.00	1.70	1.67	0.91	250.5	0.0343	21
		M	4.00	0.67	2.31	2.50	0.99			36
foot	L	F	4.00	0.50	2.33	2.00	1.18	312	0.6658	15
		M	4.00	0.50	2.43	2.50	0.95			45
	R	F	4.00	0.50	2.33	2.25	1.12	379	0.6014	18
		M	4.00	1.00	2.50	2.50	0.89			46

***Bold**=significance at p<0.05*

Entheseal changes between men and women

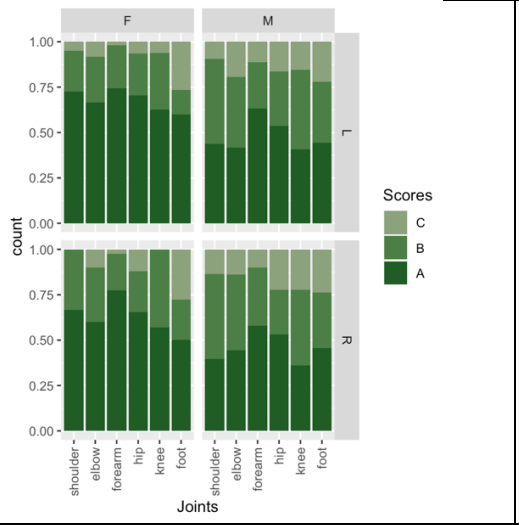

Figure 52 Bar charts illustrating the frequency of low, medium and strong degrees of entheseal development among men and women of all age groups

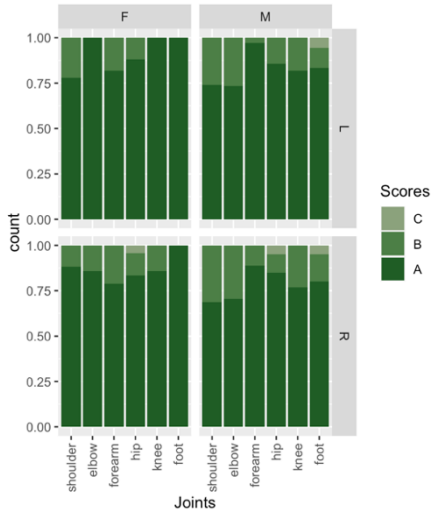

Figure 53 Bar charts illustrating the frequency of low, medium and strong degrees of entheseal development among men and women aged between 20-39y

5.3.3.1.2 Differences between the age groups

For all functional areas examined, significant differences in entheseal robusticity were detected between the different age groups. Pairwise Wilcoxon tests additionally revealed that, except for the left shoulder and knee, as well as for the right knee, where no significance was observed between mature and senile individuals, the significant differences existed between all age groups and effect sizes were considered moderate for comparisons of adults and matures as well as matures and seniles and were considered large between adults and seniles (Table 46). The ANOVA tests yielded the same results as the Kruskal-Wallis tests.

This clear trend of increasing entheseal robusticity with age, observable throughout all functional complexes on the left and right body side, suggests that entheseal robusticity is strongly correlated with age, which might have relevant consequences for the upcoming analyses. The significant increase in entheseal robusticity by age is well illustrated in the bar charts displaying the frequency of the simplified scores by joint. Whereas the highest degree of development (C) is virtually absent in the adults (20-40y) age group and A (low development) is by far the most prominent category in all joint areas, the prevalence of category B (medium development) increases notably and that of category C increases slightly in the mature category (40-60y) and finally, among the seniles (60+), category C occurs as frequently as category B and the presence of A decreases noticeably. (Figure 54)

Table 46 Differences by age for all functional areas

Joints	Side	Age	max	min	mean	median	sd	X^2	p-value	n
shoulder	L	Adult	2.63	0.38	1.59	1.63*&	0.58	21.59	0.0000**	45
		Mature	3.75	0.38	2.19	2.25&	0.76			39
		Senile	4.00	0.88	2.44	2.53*	0.83			20
	R	Adult	2.75	0.38	1.66	1.63*&	0.60	31.46	0.0000**	49
		Mature	3.63	0.13	2.30	2.38&#	0.73			17
		Senile	4.00	0.88	2.73	2.75*#	0.76			21
elbow	L	Adult	2.40	0.40	1.52	1.80*&	0.62	21.38	0.0000**	21
		Mature	3.60	0.80	2.37	2.30&#	0.79			20
		Senile	3.80	2.40	3.11	3.20*#	0.49			7
	R	Adult	2.80	0.6	1.66	1.80*&	0.63	21.48	0.0000**	24
		Mature	3.60	1.40	2.59	2.60&#	0.64			18
		Senile	3.60	2.80	3.25	3.30*#	0.41			4
forearm	L	Adult	3.00	0.00	1.29	1.33*&	0.67	34.21	0.0000**	58
		Mature	3.33	0.33	1.91	2.00&#	0.92			36
		Senile	4.00	1.33	2.56	2.67*#	0.78			25
	R	Adult	2.67	0.00	1.41	1.33*&	0.71	28.10	0.0000**	55
		Mature	3.67	0.33	2.02	2.00&#	0.84			45
		Senile	4.00	0.67	2.60	2.67*#	0.84			21
hip	L	Adult	3.00	0.50	1.39	1.00*&	0.76	52.64	0.0000**	67
		Mature	4.00	0.50	2.33	2.50&#	0.85			65
		Senile	4.00	1.00	2.90	3.00*#	0.89			26
	R	Adult	3.50	0.00	1.48	1.00*&	0.81	53.81	0.0000**	64
		Mature	4.00	0.50	2.34	2.25&#	0.90			60
		Senile	4.00	1.00	3.20	3.50*#	0.82			28
knee	L	Adult	2.67	0.00	1.29	1.33*&	0.74	15.65	0.0004	16
		Mature	3.67	1.00	2.39	2.33&	0.73			23
		Senile	3.67	1.33	2.59	2.67*	0.91			9

Joints	Side	Age	max	min	mean	median	sd	X^2	p-value	n
foot	R	Adult	2.67	0.00	1.27	1.00*&	0.79	20.70	0.0000**	20
		Mature	4.00	1..00	2.51	2.33&	0.69			25
		Senile	4.00	1.00	2.58	2.84*	0.89			12
	L	Adult	3.50	0.50	1.66	2.00*&	0.70	26.98	0.0000**	25
		Mature	4.00	1.00	2.73	2.75&#	0.73			22
		Senile	4.00	1.50	3.31	4.00*#	0.92			13
	R	Adult	3.50	0.50	1.73	2.00*&	0.73	30.83	0.0000**	28
		Mature	3.50	2.00	2.84	3.00&#	0.51			22
		Senile	4.00	1.50	3.29	3.50*#	0.84			14

Bold *= significance at p<0.05*

**/&/# = post-hoc tests significant at p<0.05*

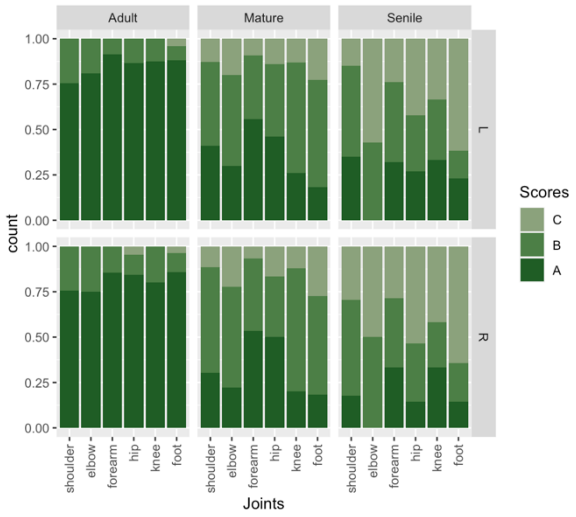

Figure 54 Bar charts illustrating the frequency of low, medium, and strong degrees of entheseal development among all individuals aged 20-40y

5.3.3.1.3 Differences between social classes

Differences between social classes were estimated by comparing people buried inside, to people buried outside the cloister complex.

The Wilcoxon tests revealed significant differences between cloister and cemetery burials in the left forearm and knee and in the right shoulder, forearm, hip and knee. Furthermore, all p-values have to be considered not meaningful as the effect sizes were all small, except that from the right knee, which was moderate. Therefore, the only relevant difference is that observed for the right knee complex, with people from the cloister exhibiting a higher degree of entheseal robusticity than those from the cemetery. As a general trend, the degree of robusticity seems to be higher among the people buried in the cloister than those buried in the cemetery (Table 47). However, as has already been mentioned in the section on postcranial indices, due to the higher number of older males in the cloister compared to the cemetery, these differences might also

have been influenced by age and sex. In fact, when removing all individuals aged >40 from the analysis, no significant differences between cloister and cemetery can be detected in any of the joint areas, which confirms the previous suspicion that the differences detectable in the whole sample are largely due to average age differences between the two groups. However, while the degree of entheseal development was roughly the same across all joint areas among people buried in the cemetery, the upper limbs of the people buried in the cloister showed more entheseal robusticity than their lower limbs and more than the upper limbs of the people from the cemetery. Generally, for both body sides among the younger people, the entheses from the shoulder joint showed the highest degrees of entheseal robusticity (Figure 56), whereas when all age groups were considered, the knee showed the highest degree of entheseal robusticity, followed closely by the shoulder and the elbow (Figure 55).

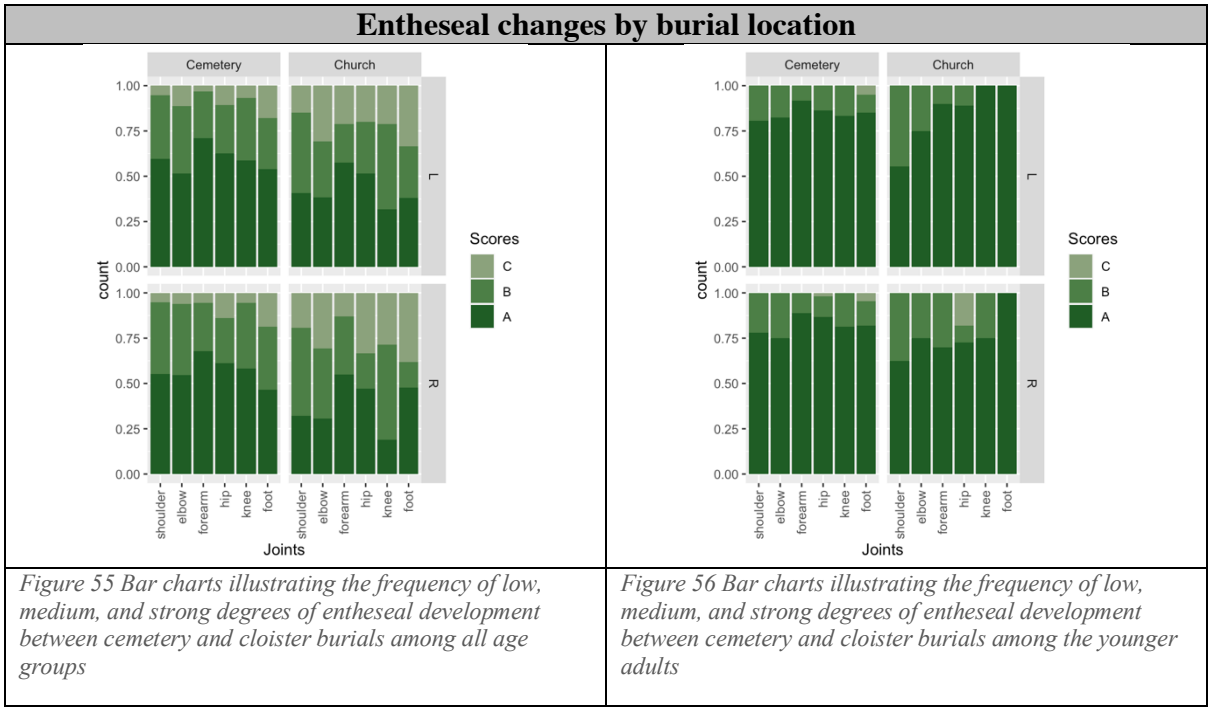

Figure 55 Bar charts illustrating the frequency of low, medium, and strong degrees of entheseal development between cemetery and cloister burials among all age groups

Figure 56 Bar charts illustrating the frequency of low, medium, and strong degrees of entheseal development between cemetery and cloister burials among the younger adults

Table 47 Differences by burial location for all functional areas

Joints	Side	Location	max	min	mean	median	sd	W	p-value	n
shoulder	L	Cemetery	4	0.38	1.92	2	0.73	892	0.2753	77
		Cloister	3.75	0.38	2.14	2.13	0.90			27
	R	Cemetery	4	0.38	1.98	2	0.71	854.5	0.0173	78
		Cloister	4	0.13	2.34	2.63	0.92			31
elbow	L	Cemetery	3.8	0.4	2.05	2	0.85	195	0.4556	35
		Cloister	3.6	0.8	2.28	2.2	0.97			13
	R	Cemetery	3.6	0.6	2.00	2	0.79	135	0.0532	33
		Cloister	3.6	1.4	2.57	2.6	0.80			13
forearm	L	Cemetery	3.33	0	1.63	1.67	0.82	1146	0.0303	93
		Cloister	4	0.33	2.10	2	1.08			33
	R	Cemetery	3.67	0	1.74	1.67	0.86	1040	0.0341	90
		Cloister	4	0	2.15	2	0.94			31
hip	L	Cemetery	4	0.5	1.96	2	0.96	1838	0.1841	123
		Cloister	4	0.5	2.24	2	1.13			35
	R	Cemetery	4	0	2.04	2	1.03	1640	0.0499	116
		Cloister	4	0.5	2.44	2.5	1.11			36
knee	L	Cemetery	3.67	0.33	1.86	1.67	0.83	180	0.0436	29
		Cloister	3.67	0	2.37	2.67	1.02			19
	R	Cemetery	4	0	1.81	1.67	0.93	203	0.0036	36
		Cloister	4	0	2.55	2.67	0.94			21
foot	L	Cemetery	4	0.5	2.28	2	0.88	322	0.1723	39
		Cloister	4	0.5	2.64	3	1.18			21
	R	Cemetery	4	0.5	2.38	2.5	0.85	396.5	0.4294	43
		Cloister	4	0.5	2.60	2.5	1.15			21

***Bold**=significance at p<0.05*

5.3.3.1.4 Changes over time

When comparing the upper to the lower layer, barely any differences in the degree of expression of the entheses that make up the different joints, could be detected. Solely the entheses involved in the movement of the left foot showed a significant and moderately meaningful difference, with the lower layer showing higher values on average than the upper (Table 48). The same trend, albeit non-significant also holds true for the right foot, but no such trend was observed among the other joints. This suggests that entheseal robusticity did not change significantly over time. This is furthermore supported by the results of the evaluation of the scores excluding individuals >40y. The only significant difference observed was in the left hip. The bar charts for left and right body side both illustrate no clear trend in entheseal robusticity levels between the joint areas nor between the burial layers (Figure 57), and a very similar pattern is found among the younger adults (Figure 58).

Entheseal changes by burial layer

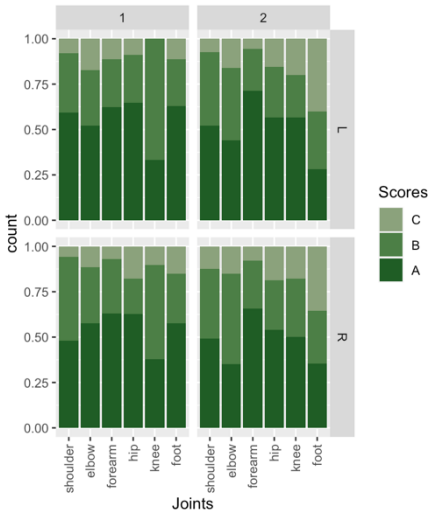

Figure 57 Bar charts illustrating the frequency of low, medium, and strong degrees of entheseal development between burials from the upper layer (Layer 1) and the lower layer (Layer 2) among all age groups

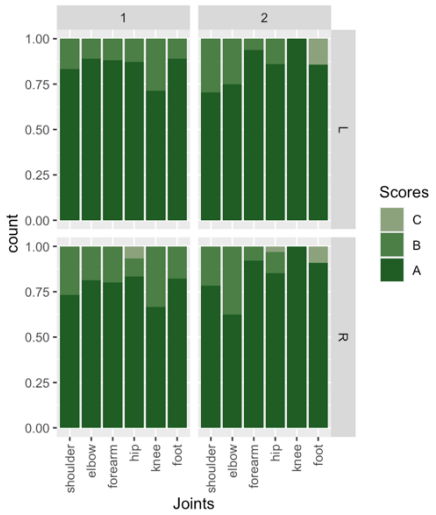

Figure 58 Bar charts illustrating the frequency of low, medium, and strong degrees of entheseal development between burials from the upper layer (Layer 1) and the lower layer (Layer 2) among all age groups

Table 48 Differences by Layer for all functional areas

Joints	Side	Layer	max	min	mean	median	sd	W	p-value	n
shoulder	L	1	3.75	0.38	1.89	1.88	0.80	1100	0.3448	37
		2	4	0.38	2.02	2	0.77			67
	R	1	4	0.4	2.08	2.13	0.71	1452.5	0.8602	52
		2	4	0.13	2.08	2.17	0.86			57
elbow	L	1	3.6	0.6	2.18	2	0.79	304	0.7400	23
		2	3.8	0.4	2.04	2.2	0.97			25
	R	1	3.6	0.6	2.08	2	0.82	218.5	0.9520	26
		2	3.6	0.6	2.26	2.4	0.85			20
forearm	L	1	4	0.33	1.89	1.67	0.92	2193	0.1995	53
		2	3.67	0	1.65	1.67	0.91			73
	R	1	4	0.33	1.87	1.67	0.85	1836	0.9521	57
		2	3.67	0	1.82	2	0.94			64
hip	L	1	4	0.5	2.04	2	0.83	3150	0.7508	68
		2	4	0.5	2.02	2	1.12			90
	R	1	4	0.5	2.12	2	0.99	2826	0-9371	67
		2	4	0	2.15	2	1.12			85
knee	L	1	3	0	2.09	2.33	0.82	283	0.7886	18
		2	3.67	0.33	2.04	1.835	1.01			30
	R	1	3.67	0	2.09	2.33	0.88	397.5	0.8976	29
		2	4	0	2.08	2	1.12			28

Joints	Side	Layer	max	min	mean	median	sd	W	p-value	n
foot	L	1	4	0.5	2.13	2	0.86	265.5	0.0092	35
		2	4	0.5	2.80	3	1.07			25
	R	1	4	0.5	2.27	2	0.88	394.5	0.1125	33
		2	4	0.5	2.65	3	1.00			31

Bold=significance at p<0.05

5.3.3.1.5 Percentage of osteolytic and osteophytic lesions by joints

Overall, enthesophytic (EF) lesions were more common than osteolytic ones and the distribution seems to be similar between the left and right sides. The occurrence of EF and OL lesions, which according to Mariotti et al. (2004) are considered to be signs of enthesopathy, is strongly linked with age, with not only their presence but also their degree of expression increasing with old age, though this is way more marked for EF than for OL, for which the increase also seems to be mostly limited to the shoulder elbow and hips. Again, when comparing the two burial locations, people from the cloister seem to have more marked EF formation than those from the cemetery, which is likely again influenced by the unequal age distribution in the two groups. However, OL lesions seem to appear generally more frequently among the cemetery burials. Furthermore, the presence of both OL and EF, was more marked among people from the lower layer than those from the upper layer, and this especially concerned the enthesis of the muscles used in hip movement.

Finally, there seems to be a general trend that the presence of EF was more marked in the lower limbs whereas OF was slightly more common in the upper limbs. (Figure 59, Figure 60)

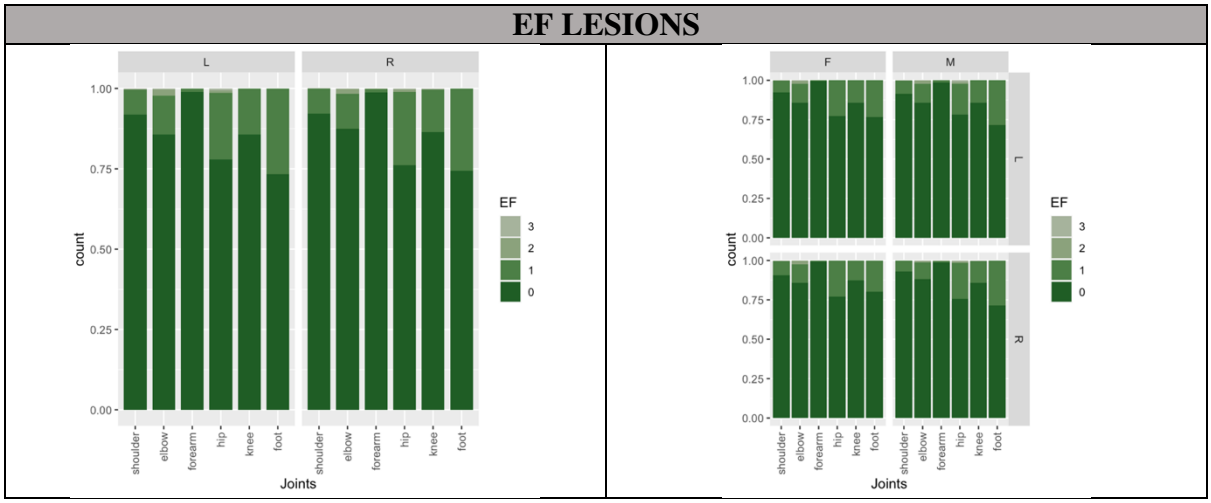

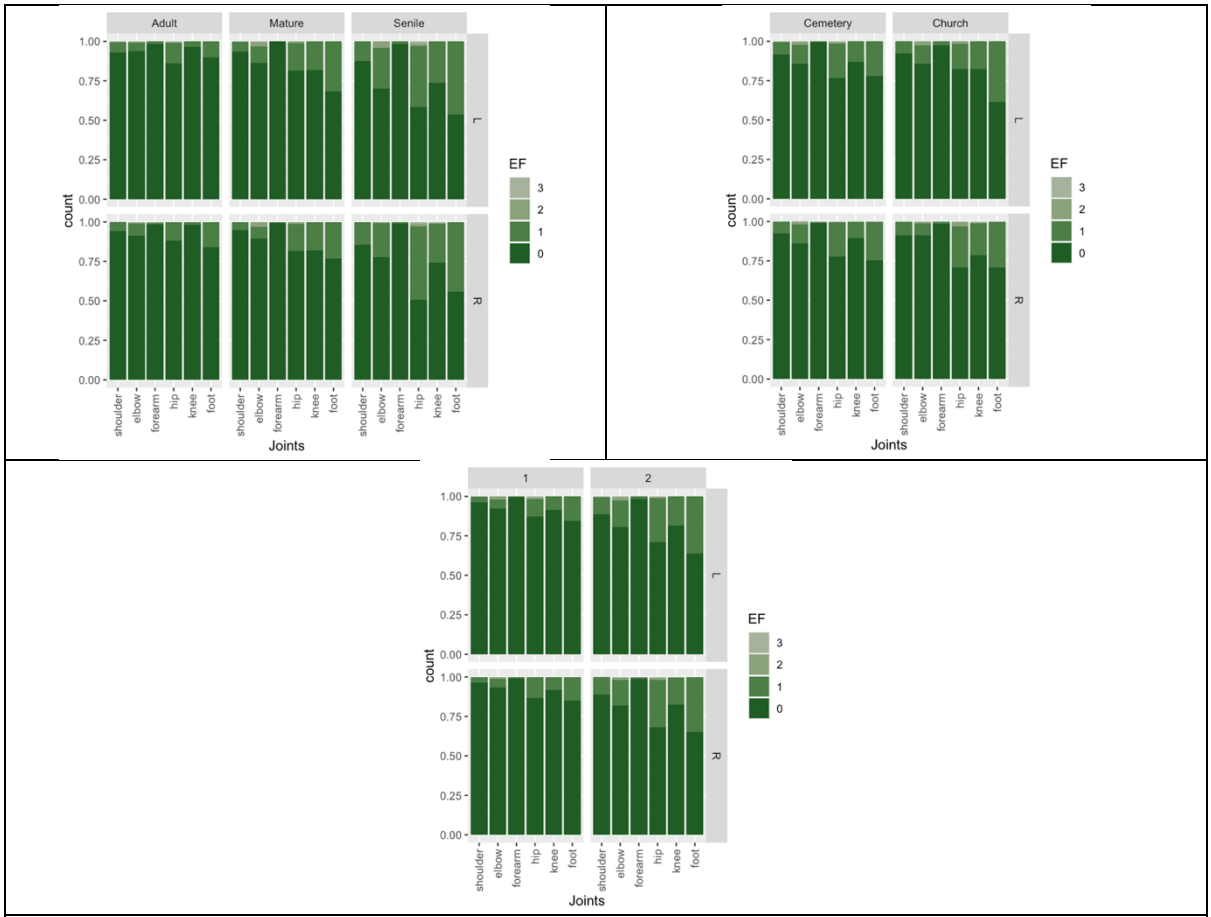

Figure 59 Distribution of all EF lesions of all entheses within one joint area by Side, Sex, Age, Burial Location and Layer

OL - LESIONS

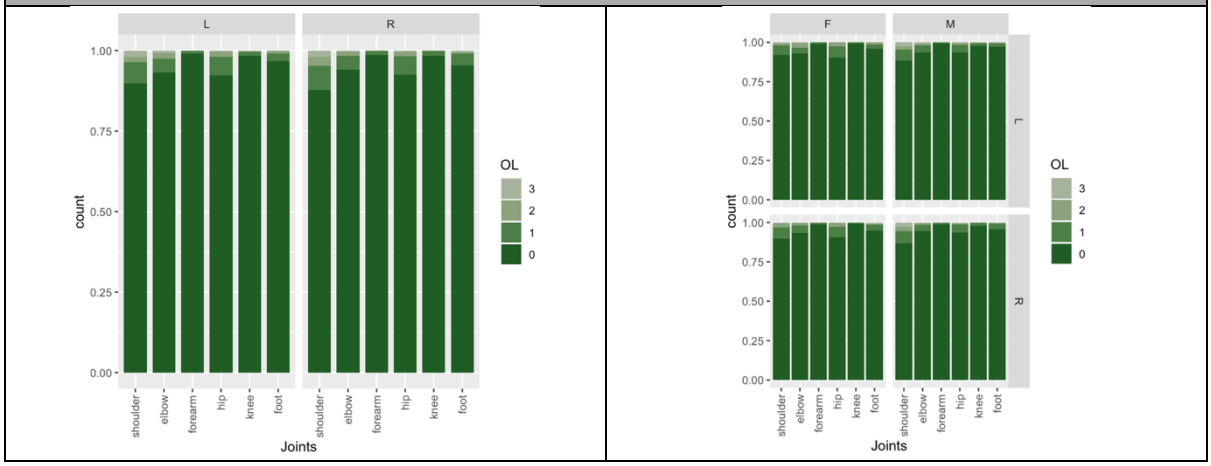

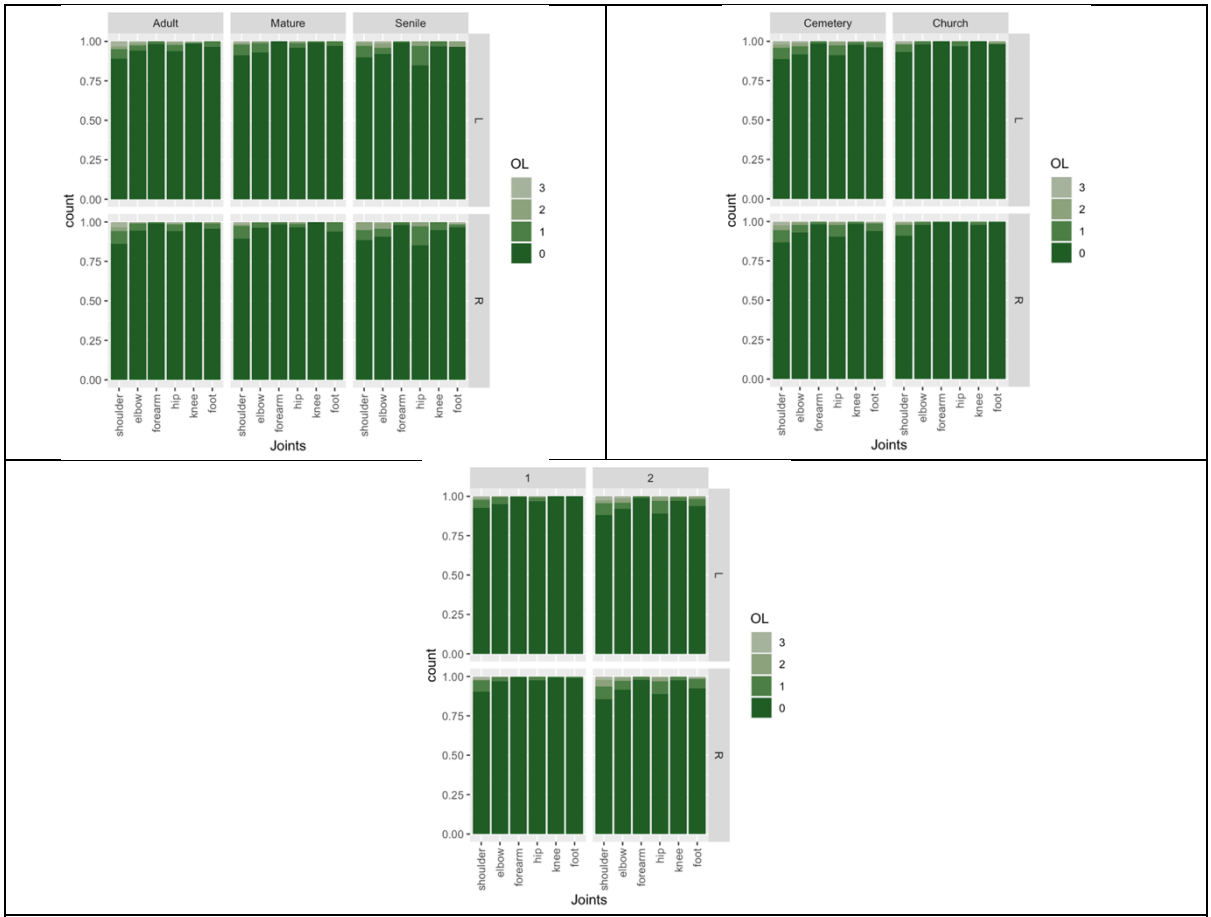

Figure 60 Distribution of all OL lesions of all entheses within one joint area by Side, Sex, Age, Burial Location and Layer

5.3.4 Discussion and Conclusion

5.3.4.1 Differences between men and women

The majority of joint complexes showed a significant difference between men and women in this sample, and the shoulder yielded the highest differences, even when corrected for age. This suggests that at least some kind of labour division was present among males and females buried in this cemetery, with males probably carrying out tasks that made more frequent use of the muscles moving and stabilising the shoulder joint, such as sickle use (Perry 2004), and thus being probably more involved in manual labour than women. Nevertheless, the overall entheseal score of the shoulder complex and all the other joint complexes as well were not particularly high, especially when corrected for age, with the low to medium expression category (0-2 scores) being most prevalent. When considering all age groups, the changes were equally severe in the upper than in the lower limbs in men and worse in the lower limbs for females. However, among the younger age groups, differences were slightly more pronounced in the upper than in the lower limb for both sexes. This pattern has been observed also in a study on an early medieval Great Moravian population (Havelková *et al*. 2011). However, these

analyses are based on the method developed by Villotte (2006), in which some of the muscle insertions scored, differ from those used in this study, although these attachment sites are used in the same joint complexes analysed in the present study. Havelková et al. (2011) describe this pattern, prevalent in males and females, as corresponding to agricultural activities practiced in a rather flat environment, which results in less use of the leg musculature relative to the arm musculature. However, a study by Niinimäki and Bages Sotos (2013) found that activity intensity did not influence lower limb entheses at all.

A similar pattern has also been observed in the sample from Grevenmacher, a medieval rural site from Luxembourg (Trautmann 2012), but to a greater extent than in this sample. This might suggest that the people in Luxembourg City did on average not actually engage in regular strenuous farming activities that would have required extensive use of the upper limbs.

5.3.4.2 Differences between the age groups

Differences between the age groups demonstrated a clear correlation of age with enthesis development in this sample. This trend was corroborated already by numerous studies (Mariotti *et al.* 2007; Cardoso & Henderson 2010; Milella *et al.* 2012; Niinimäki & Baiges Sotos 2013). In fact, several of those state that age, likely due to the prolonged and regular exposure to microtraumas to the entheses sites throughout life, shows the highest correlation with entheseal robusticity. Therefore, all analyses were also run for individuals younger than 40 years of age, which reduced significant differences between groups and prevalence of strong robusticity degrees a lot.

5.3.4.3 Differences between social classes

Differences between the social classes were tested in order to possibly detect any differences in labour division between the two groups. However, the differences detected in the first analyses are mainly influenced by age due to the higher proportion of males buried in the cemetery. When analysing only individuals below 40 years of age, the significant differences between the two burial groups disappear completely. Differences in the degree of entheseal expression in the upper limb have also been tested for in a comparison between people from a castle representing the higher social classes and those from the hinterland, representing the lower social classes, in early medieval Great Moravia. However, contrary to the findings in the present study, Havelková et al. (2011) discovered that in particular males from the hinterland showed higher degrees of entheseal development in the upper limbs in comparison to those from the castle hinting at different activities carried out by the two groups. Furthermore, a study

on Nubian skeletons from Kerma also found higher entheseal robusticity scores among lower social class individuals than upper social class individuals (Schrader 2015). This is further supported by findings by Van Cant (2019) which showed that upper-class males and females from medieval/postmedieval Oosterweel presented only light to moderate entheseal changes compared to their lower class contemporaries from rural Flemish sites. Two other studies on postmedieval Dutch and Belgian populations however, also could not differentiate between social classes based on entheseal development, suggesting that division of labour was not as marked between the social classes (Palmer *et al.* 2016; Palmer & Waters-Rist 2019). Other studies on people with known labour history have also shown that labour intensity did not really affect entheseal change as much as expected (Cardoso & Henderson 2010), with one finding no difference between the different labour categories and other even finding higher degree degrees of entheseal robusticity among light workers such as employees, painters, shoemakers etc. than among hard workers such as manual labourers, farmers or miners (Milella *et al.* 2012). Regarding the lack of differences in lower limb entheseal robusticity, the study by Niinimäki and Bages Sotos (2013) already mentioned before found that entheseal changes of the lower limbs are not affected by activity intensity. This means that the lack of differences in lower limb entheseal robusticity between the burial groups not necessarily indicates no differences in activities concerning the lower limbs between these two groups. However, overall, it seems that the lack of differences in entheseal development between cloister and cemetery burials suggests that division of labour was not extensive between the two groups and due to the high prevalence of little to moderate change, they also likely did not generally engage in very hard and strenuous work, at least not from a young age. These results are similar to those detected in the Dutch and Belgian samples which, like this sample represent largely the postmedieval period (Palmer *et al.* 2016; Palmer & Waters-Rist 2019). It is very likely, also given the urban setting of the cemetery, that none of the people buried at this site engaged in any physical activities that might have been strenuous and repetitive enough to induce entheseal changes, such as intense farming (Havelková *et al.* 2011).

5.3.4.4 Changes over time

No differences could be detected between the two burial layers, which suggests that physical activities did not change over time. No direct studies on enthesial development have so far been performed comparing several time periods. However, some studies have detected differences between enthesial development among social classes, which was significantly different in the medieval period (Havelková *et al*. 2011), but not anymore in the postmedieval period (Palmer

et al. 2016; Palmer & Waters-Rist 2019). Therefore, it might potentially be possible to assess in activity patterns over time by studying entheseal morphology. However, in this case, the period studied was likely also not long enough to have resulted in major differences of occupation and thus physical stress to the bones.

5.3.4.5 Conclusion

To conclude, this study corroborates those that have found a significant relationship between age and degree of entheseal robusticity. Increasing age was the most important factor causing increase in entheseal robusticity. This relationship was so strong that, when comparing individuals of all age groups between cloister and cemetery burials, a significant amount of higher robusticity values was found among cloister burials, which was likely influenced by the higher presence of people over 40, in this group. When correcting for age, no differences between the burial groups could be detected anymore. This suggests that division of labour between the two groups was not marked enough to produce significant differences. This might be due to the nature of activities usually performed by town residents, which are often not as strenuous as those performed by farmers, especially since there are several reasons to suppose that none of the people buried in this cemetery came from very low social classes. However, differences between men and women hint at a labour division between the sexes, with males engaging generally in more strenuous activities than females, especially involving the shoulder and elbow, areas particularly used in weightlifting (Perry 2004). Overall, however, as suggested by Cardoso (2018), there is a trend among researchers to interpret past occupations as unchanging and correlated invariably to a specific socioeconomic status, which was not necessarily true however. Especially among towns people, occupations and the accompanying stresses on bones were diverse, making clear differentiations between socioeconomic groups based solely on reconstruction of physical activities nearly impossible. People from the same socioeconomic status could well express different degrees of entheseal expression depending on their occupation. Shop keepers would not be engaged in as much manual labour perhaps as a blacksmith or a cloth dyer but would also spend a lot of the time standing, whereas a tailor would be rather sitting long periods of time, engaged in skilful handywork (Cardoso 2018; Palmer & Waters-Rist 2019). Therefore, the diversity of occupations within all social groups might obscure any differences in entheseal changes.

5.4 Reconstruction of habitual body posture

5.4.1 Introduction

Next to the analysis of bone robusticity, bilateral asymmetry and entheseal changes, which explore the extent to which a bone has been shaped by external stressors, in order to reconstruct locomotive behaviour or the intensity and regularity of manual physical activities, reconstruction of habitual body posture can also inform about regular physical activities and labour division.

A repetitive and long-held body posture can leave traces on the skeleton, based on which, that posture can be reconstructed. The most commonly analysed features are the squatting facets of the tibia, which are used, as the name already suggests, to determine whether an individual engaged in activities that required regular and prolonged squatting.

The squatting facets are small flattened bony areas on the anterior rim of the distal epiphysis of the tibia and are essentially small upwards curving extensions of the distal articular facet connecting to the talus. While squatting, although the main weight of the body rests on the feet, the ankles and knees are locked in a strongly flexed position. Due to the flexion the talar neck is pushed upward and the distal tibia slides backwards on the talar trochlea, putting both bones into close contact, which in return creates the small facets on the frontal rim of the distal tibial epiphysis (Boulle 2001a, b).

Although activity induced, squatting facets are often listed and recorded as anatomical variants (Finnegan 1978; Grupe *et al.* 2015).

5.4.2 Methods

In a first step, the absence and presence of tibial squatting facets was recorded, and the frequency calculated for each body side against the number of scoreable areas. Next, since in most cases of squatting facets occurred bilaterally, an overall frequency combining right and left occurrences against all areas present was calculated. Only adult individuals were included in the analysis. For comparisons by sex, all individuals with indeterminate sex were excluded and for comparisons by age all individuals with indeterminate age were excluded.

All statistical comparisons were done by chi square tests.

5.4.3 Results

Overall, squatting facets occurred slightly more frequently on the right side than on the left side, in most cases however, both the left and the right tibiae were affected, if both were scoreable. This is a rather unsurprising result since squatting facets usually occur bilaterally.
Generally, men show slightly more squatting facets than women although the difference is not significant. Cloister burials also display a higher frequency of squatting facets than cemetery burials although the difference is only significant when frequencies for both right and left sides are considered together. These differences might be linked to the differences observed between men and women, since the proportion of men is higher among the cloister than among the cemetery burials. Furthermore, squatting facets seem to occur slightly more often in the upper layer than in the lower one, and seem to become more frequent with old age, despite not being statistically relevant. (Table 50)
When considering the total number of individuals affected by squatting facets, the tendencies remain the same as with the by bone comparisons and no differences between the groups are statistically significant. Overall, when considering all individuals, including those of indeterminate sex and age, about 27.27% of all scoreable bones and about 28.75% of all individuals with scoreable bone areas display squatting facets. (Table 49)

Table 49 Frequency of squatting facets by scoreable individual compared by sex, age, burial location, and side

Grouping		n	present	p-value
All		160	46 (28.75%)	
Sex	F	54	15 (27.78%)	0.7536
	M	96	29 (30.21%)	
Age	Adult	55	15 (27.27%)	0.5020
	Mature	53	14 (26.24%)	
	Senile	26	10 (38.46%)	
Location	Cemetery	116	29 (25.00%)	0.0888
	Cloister	44	17 (38.64%)	
Layer	1	70	23 (32.86%)	0.3114
	2	90	23 (25.56%)	

Table 50 Presence of squatting facets by side, sex, age, burial location, and layer, including results of the Pearson's chi square and Fisher's exact tests for each group comparison.

Grouping		Right			Left			TOTAL		
		n	present	p-value	n	present	p-value	n	present	p-value
All		157	44 (28.03%)		151	40 (26.49%)		308	84 (27.27%)	
Sex	F	52	14 (26.92%)	0.7434	51	13 (25.49%)	0.7686	103	27 (26.21%)	0.6583
	M	95	28 (29.47%)		90	25 (27.78%)		185	53 (28.65%)	
Age	Adult	55	15 (27.27%)	0.5191	54	15 (27.78%)	0.6007	109	30 (27.52%)	0.3136
	Mature	51	12 (23.53%)		51	12 (23.53%)		102	24 (23.53%)	
	Senile	25	13 (36.00%)		23	8 (34.78%)		48	17 (35.42%)	
Location	Cemetery	114	28 (24.56%)	0.1156	110	26 (23.64%)	0.1930	224	54 (24.11%)	**0.0416**
	Cloister	43	16 (37.21%)		41	14 (34.15%)		84	30 (35.71%)	
Layer	1	68	21 (30.88%)	0.4860	64	18 (28.12%)	0.6962	132	39 (29.55%)	0.4380
	2	89	23 (25.84%)		87	22 (25.29%)		176	45 (25.57%)	

5.4.4 Discussion and Conclusion

With 28.75% of individuals presenting squatting facets, the values observed in this population are slightly higher than those determined for a French 14-16h century site (26%) and a good deal higher than those estimated for a French 18th century site (18%), but are lower than those from a French medieval site (38%) (Boulle 2001b). And although the results from this study are not entirely comparable to those from the study on French sites by Boulle (2001a), since Boulle (2001a) studied the frequency of talar squatting facets, these results still seem to roughly corroborate those of Boulle 2001a, especially when considering, that tibial talar facets are assumed to occur more frequently than those on the talus (Verna *et al.* 2014). However, another study by Theureau (1985) on the medieval-postmedieval cemetery of Saint-Pierre-le-Puellier in France, found a prevalence of squatting facets of 43.2% in the postmedieval phase, with values increasing considerably from phase A, the oldest phase, to phase C, the youngest phase, and showing a large but non-significant difference between men and women, especially in the youngest occupation phase. Women had a much higher frequency of squatting facets than men (Theureau 1985). Such a stark difference between the sexes, which was also observed by Boulle (2001a), is however not found among the population from Luxembourg City. Here, men have slightly higher values than women but the difference between the sexes is statistically not relevant. One possible explanation for this discrepancy towards the other studies is, that many of the men, and especially the older men, buried in this cemetery and cloister complex, were friars from the Franciscan monastery the cemetery belonged to, which is also supported by the significantly higher amount of squatting facets among cloister burials. Tibial squatting facets are caused by prolonged dorsiflexion of the ankle, a position most often associated with squatting. However, some studies suggest, that prolonged kneeling might cause similar defects (Ubelaker 1979). Since prolonged kneeling is part of the everyday life of a monk during prayer, it could be assumed, that kneeling, rather than squatting might have been the primary cause for the development of the squatting facets in these men. This interpretation would also be supported by the fact that the vast majority of the squatting facets were really small in size and looked more like a small extended lip of the distal articular surface onto the anterior side of the bone, which might indicate a less strong dorsiflexion. Another potential indication to prolonged kneeling is found in individual 2008-78/151 which, next to displaying clear squatting facets on the right and left tibia, also exhibited extension facets on the dorsal side of the second to fourth metatarsals of the right and left foot. The formation of these facets would be best explained

through the same system as the squatting facets, namely a hyper dorsiflexion, of the toes however in this case, which would probably be achieved through prolonged kneeling (Ubelaker 1979). In any case, due to the lack of significant differences between men and women, the squatting facets do not indicate a substantial division of labour between the sexes.

The low percentage of squatting facets in general indicates that squatting was not a position that was frequently employed by the majority of the population. This decline in squatting facets towards the end of the middle-ages and in postmedieval times is often attributed to a change in daily habits mainly due to the introduction of novel furniture. Cooking stoves started to replace open, floor-level hearths in homes and the use of comfort furniture such as chairs replaced the need to crouch on the floor (Boulle 2001b).

Figure 61 Squatting facets in the tibiae of 2016-082/452

6 Palaepathology

6.1 Joint diseases

The human body's ability to move is ensured by a multitude of different types of joints each allowing a different range of movements. Two main categories of joints can be distinguished: synarthrodial joints which are non-moving or partially moving joints such as the cranial sutures (fibrous joints), growth plates (synchondroses) or intervertebral discs (amphiarthroses), and synovial joints, also called diarthroses, which are joints that allow movement (Rössler & Rüther 2005; Larsen 2015; Salva & Merrill 2017). The following section will focus on the synovial joints. Synovial joints are composed of articulating bones whose ends are covered in avascular hyaline cartilage. All synovial joints are enclosed by the fibrous joint capsule which, together with the articulated bones, forms the joint cavity, which separates the two articulating bones. The inner surface of the joint capsule is lined by synovial tissue that secretes synovial fluid into the joint cavity. The synovial fluid then fills the joint cavity and coats the hyaline cartilage of the articulating bones and ensures a smooth movement of the articulating bones within the joint capsule (Varshney 2016). The joint is held in proper articulation by ligaments and next to the joint type, also restricts movement of the joint (Rössler & Rüther 2005). There are three main types of synovial joints: uniaxial joints, which include hinge joints and pivot joints, biaxial joints, which include condyloid and saddle joints and triaxial joints, which encompass plane as well as ball and socket joints (Figure 62). All these joint types allow for different kinds and ranges of movement. They all have in common that usually one joint surface is more stable and serves as a base along which the other joint surface moves. Due to their different degrees of freedom, they are also generally affected by degenerative changes to different degrees (Schiebler *et al.* 1995).

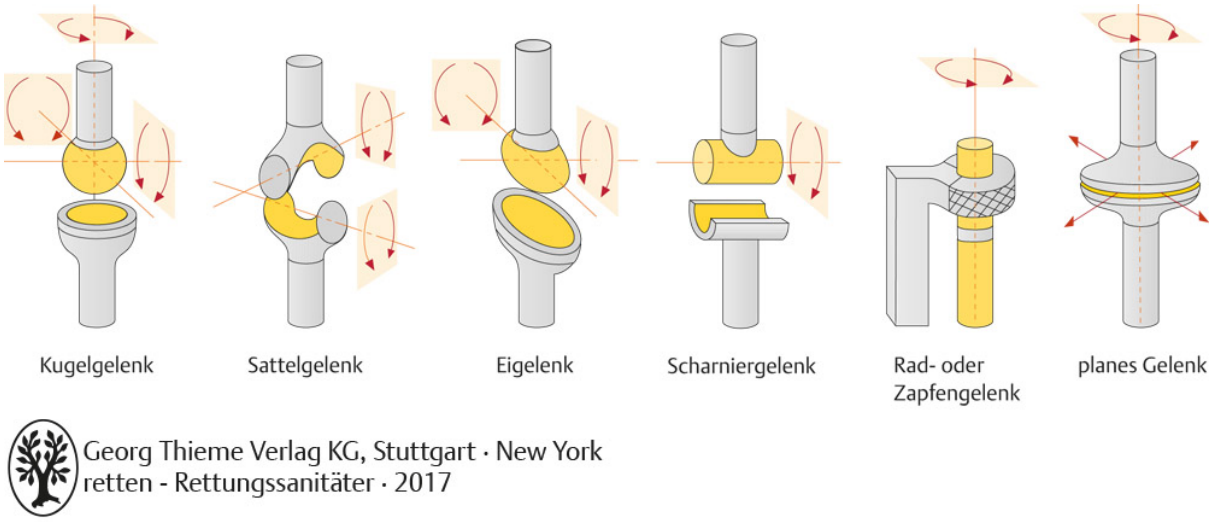

Figure 62 Illustration of the different joint types sourced from (Brand *et al.* 2017)

Over- and misload as well as trauma can lead to damage of the cartilage covering the joint surfaces, which leads to development of degenerative changes visible on joint surfaces of the bones (Adler 2005). Therefore, patterns of degenerative joint disease can reveal information on specific activity patterns that were carried out on a regular basis. However, it is to be kept in mind that degenerative joint disease is influenced by many factors besides activity, and as such, age, sex, differences in bone growth as well as the properties of the studied joint might all influence the frequency and intensity of degenerative joint disease, and these factors must be considered when trying to make inferences about activity patterns based on degenerative changes in the joints (Grupe *et al.* 2015; Larsen 2015). Furthermore, a lack of agreement on the definitions of degenerative joint disease and osteoarthritis among different studies, complicates direct comparisons of frequency and intensity of joint disease across different populations (Larsen 2015).

6.1.1 Degenerative Joint disease and Osteoarthritis

6.1.1.1 Introduction

Next to dental diseases, degenerative joint disease is the most common pathological condition observed in skeletal assemblages and modern populations (Weiss & Jurmain 2007; Waldron 2009; Schrader 2019). Degenerative joint disease usually starts with damage to the tissues that make up the joint, in most cases to the hyaline cartilage, affecting the stability of the joint in question. The first sign of degenerative joint disease observable in the skeleton is usually the formation of osteophytes, bony outgrowths, on the surfaces or margins of the joints, that occur as a response to the stress caused by the damage to the joint. Continued use of the joint after

damage has occurred can eventually lead to destruction and loss of cartilage and thus to bone-on-bone contact during movement of the joint. This bone-on-bone contact then causes eburnation, a polishing of the two articulating joint surfaces. Eventually, fusion of the joint surfaces, called ankylosis, may occur (Waldron 2009; Roberts & Manchester 2010; Schrader 2019). Among palaeopathologists, there is still no common consensus as to when degenerative changes in the joints can be addressed as osteoarthritis (Aufderheide & Rodriguez-Martin 1998; Schrader 2019). Some authors such as Cockburn et al. (1979) state that only the presence of eburnation is characteristic of the disease, whilst others such as Waldron (2009) and Rogers et al (1987) claim that, whilst presence of eburnation is the tell-tale sign of osteoarthritis, the presence of at least two of four types of strong degenerative changes, namely marginal osteophytes, new bone formation and/or pitting on the joint surface and alteration in joint contour, also allows a diagnosis for osteoarthritis (Cockburn *et al.* 1979; Rogers *et al.* 1985; Waldron 2009; Larsen 2015).

A distinction is further made between primary and secondary osteoarthritis. Primary osteoarthritis is usually caused by a metabolic disturbance of the cartilage covering the joint surfaces caused generally by over-or misloading of the joint and is the main cause for age-related degenerative joint changes. Secondary osteoarthritis is usually caused by disturbances to the joint function such as inflammatory processes, traumatic injuries etc. (Adler 2005; Weiss & Jurmain 2007). Since primary and secondary degenerative joint disease usually, but with a few exceptions, cause the same type of bone destruction and formation, a distinction between the two is often not possible in the skeletal material (Stloukal & Vyhnánek 1975). Based on the assumption that over- and misloading can lead to degenerative changes in the joints, several attempts were made to link activity patterns to patterns in degenerative joint disease. However, whilst there is a common consensus that aforementioned over- and misloading can lead to degenerative changes, the results of the studies trying to link specific activities to specific forms of joint disease have yielded ambiguous results (Weiss & Jurmain 2007; Larsen 2015). Whilst several studies showed that manual workers showed degenerative changes in specific joints used in activities at their habitual workplace other studies could not find such direct links between patterns of osteoarthritis and occupation (exhaustive lists of such studies have been compiled in works by Larsen (2015) and Weiss and Jurmain (2007)). Considering all this and the fact that the development of osteoarthritis is not only dependent on environmental or behavioural factors, but is also influenced by sex, age, genetic predisposition, obesity etc. a reconstruction of activities based on patterns of degenerative joint disease always needs to be considered with care (Weiss & Jurmain 2007; Waldron 2009; Larsen 2015). Nonetheless, based

on intensity and frequency of degenerative joint changes, an attempt will be made in the following section, to make inferences about possible habitual activities for the people buried in the Knuedler cemetery. These patterns of degenerative joint disease will then also be compared to other contemporaneous European sites.

6.1.1.2 Methods

In order to detect any differences in the severity and presence of degenerative joint disease, several steps were undertaken.

First the severity of joint disease was scored after Schultz (1988), the coding of which can be found in Table 51:

Table 51 Recording scheme for degenerative joint diseases (after Schultz, 1988)

Stage	Description
0 (here: blank)	The bone is either nor present or could not be scored
1	No visible changes
2	Light sclerotic lesions at margins; no change in joint outline
3	Slight bony outgrowths on the margins and/or erosive lesions on the bone surface
4	Pronounced osteophyte growth and possible joint deformation, and/or polishing of the surface

The degree of severity was scored for each joint surface on every bone.

In a next step, an overall joint score was determined for the left and right body side separately by calculating the average joint score from each joint surface involved in the specific joint. The list of joints with all the bone joint surfaces of which they are composed of can be found in Table 52:

Table 52 List of joints and the joint surfaces that they are composed of

Joint	Bones
acromio-clavicular Joint	Acromial end of clavicula
	Acromion of scapula
shoulder	Proximal end of humerus
	Glenoid cavity of scapula
elbow	Distal end of humerus
	Proximal end of radius
	Proximal end of ulna
hand	Distal end of radius
	Distal end of ulna
	All carpalia, metacarpalia and phalanges
hip	Acetabulum of the os coxae
	Proximal end of the femur
knee	Distal end of the femur
	Patella
	Proximal end of the tibia
foot	Distal end of the tibia
	Distal end of the fibula
	All tarsalia, metatarsalia and phalanges

In most cases, especially for the hands and feet, not all joint surfaces involved could be scored for every individual. In these cases, only the available joint surfaces were included in the determination of the score. An average joint score was then calculated for each joint, by age, sex, burial location and layer in order to visually detect any differences between the groups. In order to facilitate visual comparisons, this specific joint score was then assigned to a broader score again, following the categories already presented in Table 51. The exact composition of each larger joint score can be found in Table 53.

Table 53 Simplified overall joint scores used for representation in the graphs

Old score	New score	Description
1	0	No changes to the joint
>1-2	1	Light changes to the joint either in only one or multiple bones forming the joint
>2-3	2	Moderate changes to the joint either in only one or multiple bones forming the joint
>3-4	3	Severe changes to the joint either in only one or multiple bones forming the joint (OA)

These newly calculated joint scores were then used to design graphs in order to better visualise patterns and differences in the development of degenerative joint disease by joints and groups. Finally, the total absence or presence of degenerative joint disease irrespective of severity or number of joints affected was estimated for all individuals that could be evaluated. This also included individuals where not all joints were present. In order to determine overall absence or presence, the average of all joint scores was taken for each individual. If the average score for the individual was 1, no degenerative joint disease was present. If the score was >1 it meant that at least one joint was affected by degenerative joint disease to some degree.

6.1.1.3 Results

Overall, regarding severity and frequency of degenerative joint disease, the right joints seem to be more affected than the left joints, which could indicate that the majority of the population was right-handed. The dominant arm would be used more intensely in day-to-day activities and manual tasks, causing more degenerative changes to develop on that side.

6.1.1.3.1 By Joint

6.1.1.3.1.1 ACJ:

A total of 118 right and 122 left acromio-clavicular joints could be examined, of which 62 (52.54%) right ones and 55 (45.08%) left ones presented degenerative changes.

Overall, males were more frequently affected than women, but the difference was only statistically significant in the left joint. Females also experienced markedly more frequently degenerative joint disease in the right (41.03%) than in the left (29.27%) acromio-clavicular joint. The trend was the same in men but less pronounced (R: 57.14%; L: 51.90%). A significant difference between burial locations was observed among men, with those from the cloister showing more frequently degenerative changes in the joint than those from the cemetery. The same trend was also present in the left joint but was not significant. The differences observed in the index, were only significant for differences in burial locations including all individuals in the right joint, with individuals from the cloister displaying higher scores than those from the cemetery.

Only males from Layer 2 displayed significantly more severe and more frequent degenerative changes in the right acromio-clavicular joint, however the trend was also present among all individuals and females, although females from Layer 1 displayed more DJD than those from Layer 2 on the right side.

Frequency and severity of degenerative changes in the right and left acromio-clavicular joint showed a clear relation to age, with young adults showing no degenerative changes in the joints and frequency gradually increasing until matures II and seniles, which showed the highest frequency and severity of degenerative changes in both right and left joints. (Table 54, Table 55, Table 56, Table 57, Table 58, Table 59, Table 60, Table 61)

6.1.1.3.1.2 Shoulder joint:

A total of 166 right and 172 left shoulder joints could be examined and of those, 92 (54.44%) right and 85 (49.42%) left were affected by degenerative changes. Regarding both the right and left shoulder joints, degenerative changes occurred more frequently and more severely in males than in females. However, only in the left shoulder, the differences between males and females regarding occurrence and severity of the changes, was statistically significant. The right shoulder joint showed a significantly higher index and more changes among cloister burials than among cemetery burials. Significance was detected also only in males, but females showed the opposite trend albeit non-significant. The same trend was observed also for the left shoulder but was only significant for males. Layer 2 also showed the highest severity and occurrence in both the right and left joint, but the difference was only statistically significant for the index scores overall and for males for the right shoulder. The same trend was also observed in cloister and cemetery burials with cloister burials having a significantly higher frequency and index of DJD overall in the right and for males in the right and left shoulder joints. Both the right and

the left shoulder joints showed a strong correlation with age overall and for males and females, with young adults showing the lowest index scores and frequency and seniles the highest index scores. But frequency of degenerative changes was highest among matures II overall and for males in the right and left joints and was highest in seniles for females in the right and left joints. Therefore, since the cloister complex burials and Layer 2 yield a proportionately higher number of mature and senile individuals, it is possible that the differences observed in those two categories might to some extent be influenced by age. (Table 54, Table 55, Table 56, Table 57, Table 58, Table 59, Table 60, Table 61)

6.1.1.3.1.3 Elbow joint:

A total of 197 right and 195 left elbow joints could be examined, of which 88 (44.67%) right and 82 (42.05%) left joints showed degenerative changes. For both the right and left joints, tendentially more males were affected than females, and severity was also higher in males than in females, but the differences were never statistically significant. Regarding differences between cloister complex and cemetery burials, the same trend as for the shoulder joint could be observed. Individuals buried in the cloister experienced on average more degenerative changes and a higher index score than those buried in the cemetery. The trend reached statistical significance overall and for males in the right and only for males in the left joint. Both the right and left joints showed a significantly higher frequency and severity of degenerative changes in Layer 2 than in Layer 1 among males. In females the trend was the opposite but not statistically significant. Severity and frequency of degenerative changes were both most influenced by age in the right and in the left joints. Both severity and frequency increased significantly with old age. Severity was always highest in seniles but frequency was highest among mature II in males and among seniles in females. Therefore, as already previously mentioned, age might have also had an effect on the differences observed among the burial locations and layers in males. (Table 54, Table 55, Table 56, Table 57, Table 58, Table 59, Table 60, Table 61)

6.1.1.3.1.4 Hand joints:

A total of 231 left and 228 combined hand joints could be analysed and 113 (48.92%) left and 122 (53.51%) showed signs of degenerative joint disease. Overall, males had more severe and more frequent degenerative changes than women, but only the frequency in the left hand joints reached statistical significance. No significant changes were observed in severity. Both severity and frequency were significantly higher overall and among males from the cloister complex than among those from the cemetery, for both the right and left hand joints. The difference was

clearly more marked in the right than in the left hand bones. Females showed the same trend, but it was not statistically relevant. And whilst mainly males showed slightly more frequently changes in the lower layer in the right and left hand joints, this difference was not significant. Age on the other hand showed again a strong correlation with occurrence and severity of degenerative joint disease with both factors increasing with old age in both males and females. (Table 54, Table 55, Table 56, Table 57, Table 58, Table 59, Table 60, Table 61)

6.1.1.3.1.5 Hip joint:

A total of 214 right and 220 left hip joints could be analysed, of which 123 (57.48%) right and 127 (59.35%) left were affected by degenerative changes. Although males were generally more and more severely affected than females, the difference between the sexes was not statistically relevant. Males showed significantly more and more severe degenerative changes among cloister complex burials than among cemetery burials. Both males and females from Layer 2 were more frequently and more severely affected than those from Layer 1 but statistical significance was only detected regarding frequency in the right hip of males and regarding severity in the left hip of males. Occurrence and severity of degenerative joint disease in the hip was strongly correlated with age. Most senile individuals presented degenerative changes in the right and left hip, except for senile males, which only presented 88.89% of changed left joints and had their frequency peak in the mature II group (96%). Young adult males and females showed no degenerative changes in the left hip, and young adult females showed no changes in the right hip but one young adult male did show degenerative changes in the right hip. The changes observed in this young male's (2008-78/1316) hip likely occurred as a consequence to incorrect loading after a well healed and rather well aligned oblique fracture of the right tibia and fibula. (Table 54, Table 55, Table 56, Table 57, Table 58, Table 59, Table 60, Table 61)

6.1.1.3.1.6 Knee joint:

A total of 233 left and 220 right knee joints were examined for degenerative joint disease and 73 (31.33%) left and 69 (31.36%) right knees were affected. Although men tended to be affected more often than women by changes in the joint, this difference was not statistically significant. Both the right and left knee were significantly more affected in individuals buried in the cloister complex than those buried in the cemetery. This trend was also very clear in males and statistically relevant. However, females from both locations showed similar rates of degenerative changes. Generally, males from Layer 2 were more affected in the right knee and

those from Layer 1 in the left knee. However, no significant differences were detected between the burial's layers for men and women.

Again, age was significantly correlated with frequency and intensity of degenerative joint disease. Seniles and matures II showed the highest index values and highest occurrence of degenerative changes in the knee. Generally, young adults were not affected by degenerative joint disease in the knee except for one individual (2008-78/838), a female who had osteomyelitis in the left proximal tibial epiphysis. (Table 54, Table 55, Table 56, Table 57, Table 58, Table 59, Table 60, Table 61)

6.1.1.3.1.7 Foot joints:

A total of 209 combined right and 212 combined left foot joints could be examined. 103 (49.28%) right and 104 (49.06%) left foot joints showed degenerative changes in one or more of the single joints of which the foot joint area is composed. While on both sides, males tended to have more cases of joint disease in the foot than females, the difference was not statistically significant. A significant difference was however detected again between burial locations within males. Cloister complex burials exhibited stronger and more frequent joint disease than cemetery burials. No significant differences were observed between the burial layers.

But age showed a correlation with frequency and severity of joint disease in the foot, with cases increasing in frequency and severity in old age. (Table 54, Table 55, Table 56, Table 57, Table 58, Table 59, Table 60, Table 61)

Table 54 Scores of degenerative joint disease for each joint of the right body side

Scores Right body side			**ACJ**		**shoulder**		**elbow**		**hand**		**hip**		**knee**		**foot**	
			n	score	n	score	n	score	n	score	n	score	n	score	n	score
Sex	F		39	1.77	56	1.39	70	1.34	81	1.28	79	1.61	78	1.33	74	1.19
	M		77	1.97	108	1.59	124	1.49	140	1.35	130	1.75	129	1.28	119	1.27
Age	All	Y.A.	14	1.00	23	1.04	26	1.08	28	1.01	28	1.02	22	1.00	24	1.02
		Adult	33	1.35	46	1.16	49	1.16	59	1.13	53	1.26	51	1.05	48	1.06
		Mature I	23	1.80	30	1.45	30	1.28	43	1.21	42	1.56	38	1.17	33	1.17
		Mature II	23	2.67	37	2.03	41	1.82	45	1.54	43	2.19	41	1.65	37	1.40
		Senile	24	2.75	30	2.20	37	1.86	43	1.67	36	2.46	40	1.70	35	1.50
	F	Y.A.	6	1.00	11	1.00	11	1.00	13	1.02	13	1.00	11	1.00	12	1.01
		Adult	10	1.10	13	1.04	16	1.11	19	1.05	18	1.11	17	1.00	15	1.04
		Mature I	8	1.56	9	1.56	14	1.41	15	1.24	15	1.77	14	1.26	11	1.22
		Mature II	7	2.43	13	1.92	16	1.67	19	1.55	17	2.12	16	1.74	16	1.33
		Senile	7	3.07	10	2.10	11	1.53	12	1.62	13	2.23	12	1.78	12	1.28
	M	Y.A.	8	1.00	12	1.08	15	1.13	15	1.00	15	1.03	11	1.00	12	1.03
		Adult	23	1.46	33	1.21	33	1.18	40	1.17	35	1.34	34	1.08	33	1.07
		Mature I	14	1.79	21	1.41	26	1.21	26	1.21	27	1.44	23	1.12	21	1.15
		Mature II	16	2.78	24	2.08	25	1.92	26	1.53	26	2.23	23	1.56	19	1.47
		Senile	16	2.53	18	2.31	24	2.00	29	1.68	23	2.59	27	1.67	23	1.62
Location	All	Cloister	22	2.23	45	1.62	48	1.65	54	1.56	57	1.80	52	1.54	49	1.43
		Cemetery	96	1.87	127	1.49	149	1.38	174	1.24	157	1.63	168	1.23	160	1.18
	F	Cloister	4	2.25	9	1.28	13	1.21	13	1.33	15	1.30	14	1.46	13	1.24
		Cemetery	35	1.71	47	1.41	57	1.37	68	1.27	64	1.69	64	1.30	61	1.18
	M	Cloister	18	2.22	31	1.79	33	1.83	40	1.63	40	2.04	35	1.56	34	1.50
		Cemetery	59	1.89	77	1.51	91	1.38	100	1.23	90	1.62	94	1.18	85	1.17

Scores Right body side			ACJ		shoulder		elbow		hand		hip		knee		foot	
			n	score	n	score	n	score	n	score	n	score	n	score	n	score
Distance to Church	All	Cloister	22	2.23	45	1.62	48	1.65	54	1.56	57	1.80	52	1.54	49	1.43
		Close	22	2.09	34	1.54	32	1.43	41	1.23	32	1.44	41	1.24	43	1.27
		Mid	51	1.76	64	1.49	81	1.35	96	1.25	85	1.68	86	1.22	80	1.13
		Far	23	1.89	29	1.41	36	1.40	37	1.25	40	1.71	41	1.23	37	1.16
	F	Cloister	4	2.25	9	1.28	13	1.21	13	1.33	15	1.30	14	1.46	13	1.24
		Close	6	2.00	10	1.40	10	1.33	12	1.11	13	1.42	15	1.23	18	1.30
		Mid	22	1.77	27	1.50	34	1.43	41	1.34	36	1.83	36	1.32	30	1.13
		Far	7	1.28	10	1.20	13	1.27	15	1.21	15	1.57	13	1.33	13	1.13
	M	Cloister	18	2.22	31	1.79	33	1.83	40	1.63	40	2.04	35	1.56	34	1.50
		Close	14	1.86	21	1.55	21	1.45	25	1.28	18	1.47	21	1.22	18	1.24
		Mid	29	1.76	37	1.49	47	1.29	53	1.18	47	1.57	46	1.16	45	1.14
		Far	16	2.16	19	1.53	23	1.48	22	1.28	25	1.80	27	1.19	22	1.17
Layer_ dual	All	1	50	1.67	77	1.45	87	1.32	99	1.27	90	1.55	88	1.24	87	1.22
		2	68	2.13	93	1.67	110	1.55	12	1.35	124	1.77	132	1.34	122	1.24
	F	1	13	1.77	21	1.48	26	1.25	28	1.19	27	1.44	24	1.27	21	1.14
		2	26	1.77	37	1.51	44	1.40	53	1.33	52	1.70	54	1.36	53	1.21
	M	1	37	1.64	54	1.44	59	1.37	67	1.31	60	1.63	59	1.21	61	1.26
		2	40	2.28	54	1.77	65	1.64	73	1.37	70	1.85	70	1.35	58	1.27

Notice: Y.A. = Young Adult

Table 55 Kruskal-Wallis and Mann-Whitney U tests for the scores of degenerative joint disease for each joint of the right body side

Scores Right body side			ACJ		shoulder		elbow		hand		hip		knee		foot	
			W/ X^2	p-value	W/ X^2	p-value	W/ X^2	p-value	W/ X^2	p-value	W/ X^2	p-value	W/ X^2	p-value	W/ X^2	p-value
Sex	F		1294.5	0.1962	2815	0.2519	3863	0.1620	5205.5	0.2860	4628	0.2108	4890	0.6823	4033.5	0.2952
	M															
Age	All	Y.A.	49.22	**<0.0000**	91.76	**<0.0000**	65.24	**<0.0000**	86.11	**<0.0000**	113.54	**<0.0000**	63.02	**<0.0000**	51.22	**<0.0000**
		Adult														
		Mature I														
		Mature II														
		Senile														
	F	Y.A.	20.25	**0.0005**	33.54	**<0.0000**	15.11	**0.0045**	32.35	**<0.0000**	45.02	**<0.0000**	22.14	**0.0002**	19.42	**0.0007**
		Adult														
		Mature I														
		Mature II														
		Senile														
	M	Y.A.	29.93	**<0.0000**	59.72	**<0.0000**	52.58	**<0.0000**	51.59	**<0.0000**	71.94	**<0.0000**	38.84	**<0.0000**	33.61	**<0.0000**
		Adult														
		Mature I														
		Mature II														
		Senile														
Location	All	Cloister	782	**0.0438**	2110.5	**0.0445**	2797.5	**0.0127**	3082.5	**<0.0000**	3848.5	0.1007	3138	**0.0002**	2854.5	**0.0021**
		Cemetery														
	F	Cloister	46	0.2192	271.5	0.4860	417	0.4266	399.5	0.5645	609	0.0855	430	0.7739	365.5	0.6368
		Cemetery														
	M	Cloister	403	0.1063	776	**0.0067**	957	**0.0009**	1179	**<0.0000**	1194.5	**0.0015**	1022.5	**<0.0000**	918	**0.0010**
		Cemetery														
Distance to Church	All	Cloister	5.37	0.1468	4.96	0.1749	7.72	0.0521	16.78	**0.0008**	4.88	0.1810	14.06	**0.0028**	12.67	**0.0054**
		Close														
		Mid														
		Far														
	F	Cloister	2.22	0.5279	4.90	0.1794	0.78	0.8538	2.04	0.5635	5.97	0.1130	0.46	0.9268	1.95	0.5831
		Close														
		Mid														
		Far														
	M	Cloister	3.73	0.2918	8.05	**0.0451**	13.01	**0.0046**	17.87	**0.0005**	12.52	**0.0058**	15.79	**0.0012**	12.23	**0.0066**
		Close														
		Mid														
		Far														
Layer_ dual	All	1	1399	0.0805	2939.5	**0.0424**	3969.5	**0.0240**	6013	0.4269	4643.5	**0.0278**	5439.5	0.3327	5398	0.8218
		2														
	F	1	177	0.8008	382.5	0.9226	539	0.6513	760	0.8530	596	0.2431	640	0.9185	551.5	0.9531
		2														
	M	1	523.5	**0.0205**	1056	**0.0090**	1450	**0.0113**	2210	0.3050	1705	0.0558	1807.5	0.1469	1748.5	0.9103
		2														

Notice: Y.A. = Young Adult

Table 56 Scores of degenerative joint disease for each joint of the left body side

Scores Left body side			ACJ		shoulder		elbow		hand		hip		knee		foot	
			n	score	n	score	n	score	n	score	n	score	n	score	n	score
Sex	F		41	1.41	56	1.39	68	1.38	83	1.22	80	1.62	82	1.30	76	1.23
	M		79	1.91	108	1.60	121	1.39	139	1.34	134	1.72	135	1.30	119	1.28
Age	All	Y.A.	18	1.00	21	1.02	24	1.00	28	1.00	25	1.00	23	1.02	19	1.01
		Adult	38	1.32	46	1.15	52	1.09	54	1.06	56	1.31	57	1.13	49	1.08
		Mature I	23	1.76	33	1.47	37	1.28	47	1.25	43	1.55	38	1.15	37	1.27
		Mature II	21	2.41	34	1.90	37	1.72	43	1.42	43	2.15	42	1.65	35	1.45
		Senile	22	2.52	33	2.11	40	1.81	48	1.69	39	2.33	40	1.66	36	1.51
	F	Y.A.	8	1.00	11	1.00	12	1.00	15	1.00	13	1.00	13	1.04	11	1.00

Scores Left body side			ACJ		shoulder		elbow		hand		hip		knee		foot	
			n	score	n	score	n	score	n	score	n	score	n	score	n	score
		Adult	15	1.07	14	1.04	16	1.09	17	1.05	19	1.21	18	1.11	16	1.09
		Mature I	6	1.67	10	1.55	13	1.39	15	1.33	15	1.70	13	1.23	13	1.40
		Mature II	6	1.83	11	1.59	14	1.58	19	1.31	18	2.14	16	1.73	14	1.37
		Senile	6	2.17	10	1.95	13	1.80	14	1.50	12	2.21	13	1.52	13	1.26
		Y.A.	10	1.00	10	1.05	12	1.00	13	1.01	12	1.00	10	1.00	8	1.03
	M	Adult	23	1.48	32	1.20	36	1.08	37	1.06	37	1.37	39	1.14	33	1.07
		Mature I	17	1.79	21	1.43	24	1.23	29	1.22	28	1.46	24	1.11	23	1.20
		Mature II	15	2.63	23	2.04	23	1.80	24	1.52	25	2.16	24	1.58	19	1.52
		Senile	14	2.61	21	2.14	25	1.81	32	1.76	27	2.39	26	1.72	23	1.65
Location	All	Cloister	24	1.85	45	1.63	53	1.42	59	1.46	56	1.75	54	1.46	50	1.43
		Cemetery	98	1.73	128	1.48	142	1.37	173	1.24	164	1.64	179	1.25	162	1.21
	F	Cloister	5	1.20	9	1.28	13	1.29	14	1.23	15	1.33	14	1.43	13	1.38
		Cemetery	36	1.44	47	1.41	55	1.38	69	1.22	65	1.62	68	1.28	63	1.20
	M	Cloister	18	2.03	31	1.80	35	1.50	41	1.57	38	1.97	36	1.48	34	1.47
		Cemetery	61	1.87	77	1.51	86	1.34	98	1.25	96	1.63	99	1.24	85	1.21
Distance to Church	All	Cloister	24	1.85	45	1.63	53	1.42	59	1.46	56	1.75	54	1.46	50	1.43
		Close	24	2.00	34	1.54	34	1.46	43	1.21	37	1.53	46	1.29	44	1.29
		Mid	54	1.66	65	1.48	75	1.30	91	1.22	89	1.69	91	1.23	82	1.18
		Far	20	1.63	29	1.41	33	1.43	39	1.31	38	1.62	42	1.23	36	1.20
	F	Cloister	5	1.20	9	1.28	13	1.29	14	1.23	15	1.33	14	1.43	13	1.38
		Close	8	1.62	10	1.40	12	1.39	14	1.55	15	1.43	18	1.28	18	1.27
		Mid	22	1.50	27	1.50	33	1.42	42	1.26	38	1.86	36	1.31	31	1.20
		Far	6	1.00	10	1.20	10	1.27	13	1.18	12	1.46	14	1.19	14	1.11
	M	Cloister	18	2.03	31	1.80	35	1.50	41	1.57	38	1.97	36	1.48	34	1.47
		Close	15	2.07	21	1.55	21	1.47	24	1.23	21	1.62	22	1.30	19	1.27
		Mid	32	1.77	37	1.49	42	1.20	48	1.19	49	1.59	51	1.20	46	1.17
		Far	14	1.89	19	1.53	23	1.50	26	1.37	26	1.69	26	1.28	20	1.23
Layer_ dual	All	1	50	1.60	75	1.49	82	1.29	102	1.26	93	1.52	95	1.26	83	1.21
		2	72	1.87	97	1.55	113	1.45	130	1.32	127	1.77	138	1.32	129	1.30
	F	1	12	1.33	19	1.42	25	1.35	30	1.19	27	1.48	25	1.28	21	1.10
		2	29	1.45	37	1.38	43	1.38	53	1.25	53	1.69	57	1.31	55	1.28
	M	1	37	1.68	50	1.55	52	1.27	67	1.31	62	1.57	65	1.24	57	1.25
		2	42	2.11	58	1.63	69	1.48	72	1.38	71	1.86	70	1.36	62	1.31

Notice: Y.A. = Young Adult

Table 57 Kruskal-Wallis and Mann-Whitney U tests for the scores of degenerative joint disease for each joint of the left body side

Scores Left body side			ACJ		shoulder		elbow		hand		hip		knee		foot	
			W/ X^2	p-value	W/ X^2	p-value	W/ X^2	p-value	W/ X^2	p-value	W/ X^2	p-value	W/ X^2	p-value	W/ X^2	p-value
Sex	F		1199	**0.0101**	2486	**0.0420**	4043	0.8274	4965	0.0627	4865	0.2383	5383.5	0.6830	3936.5	0.1033
	M															
Age	All	Y.A.	45.36	**<0.0000**	78.95	**<0.0000**	73.24	**<0.0000**	78.39	**<0.0000**	97.46	**<0.0000**	59.00	**<0.0000**	52.32	**<0.0000**
		Adult														
		Mature I														
		Mature II														
		Senile														
	F	Y.A.	18.18	**0.0011**	27.44	**<0.0000**	22.94	**0.0001**	25.19	**<0.0001**	40.41	**<0.0000**	15.06	**0.0046**	16.02	**0.0030**
		Adult														
		Mature I														
		Mature II														
		Senile														
	M	Y.A.	26.31	**<0.0000**	53.62	**<0.0000**	50.62	**<0.0000**	53.06	**<0.0000**	59.06	**<0.0000**	41.83	**<0.0000**	40.85	**<0.0000**
		Adult														
		Mature I														
		Mature II														
		Senile														
Location	All	Cloister	1066	0.4371	2471	0.1416	3370	0.2110	3889.5	**0.0040**	4065.5	0.1797	3830	**0.0049**	3086	**0.0064**
		Cemetery														
	F	Cloister	101	0.5998	234.5	0.5639	358.5	0.9930	473	0.8969	592.5	0.1730	468	0.9084	398	0.8658
		Cemetery														
	M	Cloister	493.5	0.4925	876.5	**0.0210**	1208	0.0560	1336.5	**0.0011**	1291.5	**0.0064**	1263	**0.0020**	947	**0.0021**
		Cemetery														
Distance to Church	All	Cloister	4.22	0.2390	2.58	0.4618	4.18	0.2426	9.16	**0.0272**	2.30	0.5134	8.04	**0.0451**	10.18	**0.0171**
		Close														
		Mid														
		Far														
	F	Cloister	3.46	0.3265	1.98	0.5769	0.43	0.9339	0.41	0.9378	5.70	0.1274	0.49	0.9207	0.9568	0.8117
		Close														
		Mid														
		Far														
	M	Cloister	2.07	0.5581	5.63	0.1310	6.39	0.0940	12.13	**0.0070**	8.14	**0.0432**	9.91	**0.0194**	11.13	**0.0110**
		Close														
		Mid														
		Far														
Layer_ dual	All	1	1643	0.3693	3418	0.4600	4053	0.0957	6336	0.6048	5090.5	0.0670	6448	0.7974	5137	0.5948
		2														
	F	1	164	0.7328	369.5	0.7278	589	0.4656	794	0.9958	676.5	0.6786	750	0.6425	479	0.2048
		2														
	M	1	642	0.1583	1333	0.4409	1390.5	**0.0190**	2262.5	0.5084	1784	**0.0363**	2095	0.3445	1728.5	0.8319
		2														

Notice: Y.A. = Young Adult

Table 58 Frequencies of degenerative joint disease for each joint of the right body side

Frequencies Right body side			ACJ			shoulder			elbow			hand		
			n	freq.	p-value	n	freq.	p-value	n	freq.	p-value	n	freq.	p-value
Sex	F		39	16 (41.03)	0.1008	58	28 (48.28%)	0.2602	70	27 (38.57%)	0.2251	81	41 (50.62%)	0.4639
	M		77	44 (57.14%)		108	62 (57.41%)		124	59 (47.58%)		140	78 (55.71%)	
Age	All	Y.A.	14	0 (0.00%)	**<0.0001**	23	2 (8.70%)	**<0.0001**	26	1 (3.85%)	**<0.0001**	28	2 (7.14%)	**<0.0001**
		Adult	33	9 (27.27%)		46	9 (19.57%)		49	11 (22.45%)		59	18 (30.51%)	
		Mature I	23	11 (47.83%)		30	17 (56.67%)		40	15 (37.50%)		43	21 (48.84%)	
		Mature II	23	22 (95.65%)		37	35 (94.59%)		41	31 (75.61%)		45	41 (91.11%)	
		Senile	24	20 (83.33%)		30	17 (93.33%)		37	29 (45.08%)		43	38 (88.37%)	
	F	Y.A.	6	0 (0.00%)	**0.0002**	11	0 (0.00%)	**<0.0001**	11	0 (0.00%)	**0.0042**	13	1 (7.69%)	**<0.0001**
		Adult	10	1 (10.00%)		13	1 (7.69%)		16	4 (25.00%)		19	5 (26.32%)	
		Mature I	8	3 (37.50%)		9	6 (66.67%)		14	7 (50.00%)		15	7 (46.67%)	
		Mature II	7	6 (85.71%)		13	11 (84.62%)		16	10 (62.50%)		19	17 (89.47%)	
		Senile	7	6 (85.71%)		10	9 (90.00%)		11	6 (54.55%)		12	11 (91.67%)	
	M	Y.A.	8	0 (0.00%)	**<0.0001**	12	2 (16.67%)	**<0.0001**	15	1 (6.67%)	**<0.0001**	15	1 (6.67%)	**<0.0001**
		Adult	23	8 (34.78%)		33	8 (24.24%)		33	7 (21.21%)		40	13 (32.50%)	
		Mature I	14	7 (50.00%)		21	11 (52.38%)		26	8 (30.77%)		26	13 (50.00%)	
		Mature II	16	16 (100%)		24	24 (100%)		25	21 (84.00%)		26	24 (92.31%)	
		Senile	16	13 (81.25%)		18	17 (94.44%)		24	21 (87.50%)		19	25 (86.21%)	
Location	All	Cloister	22	17 (77.27%)	**0.0100**	41	28 (68.29%)	**0.0407**	48	29 (60.42%)	0.2251	54	40 (74.07%)	**0.0005**
		Cemetery	96	45 (46.88%)		128	64 (50.00%)		149	59 (47.58%)		174	82 (47.13%)	
	F	Cloister	4	3 (75.00%)	0.2864	10	4 (40.00%)	0.7316	13	4 (30.77%)	0.5219	13	8 (61.54%)	0.3900
		Cemetery	35	13 (37.14%)		48	24 (50.00%)		57	23 (40.35%)		68	33 (48.53%)	
	M	Cloister	18	14 (77.78%)	**0.0433**	29	23 (79.31%)	**0.0053**	33	24 (72.73%)	**0.0007**	40	31 (77.50%)	**0.0010**
		Cemetery	59	30 (50.85%)		79	39 (49.37%)		91	35 (38.46%)		100	47 (47.00%)	
Distance to Church	All	Cloister	22	17 (77.27%)	0.0590	41	28 (68.29%)	0.1529	48	29 (60.42%)	**0.0269**	54	40 (74.07%)	**0.0057**
		Close	22	12 (54.55%)		30	16 (53.33%)		32	15 (46.88%)		41	20 (48.78%)	
		Mid	51	22 (43.14%)		67	25 (52.24%)		81	27 (33.33%)		96	43 (44.79%)	
		Far	23	11 (47.83%)		31	13 (41.94%)		36	17 (47.22%)		37	19 (51.35%)	
	F	Cloister	4	3 (75.00%)	0.5775	10	4 (40.00%)	0.3689	13	4 (30.77%)	0.7339	13	8 (61.54%)	0.5510
		Close	6	2 (33.33%)		9	5 (55.56%)		10	5 (50.00%)		12	4 (33.33%)	
		Mid	22	9 (40.91%)		28	16 (57.14%)		34	12 (35.29%)		41	21 (51.22%)	
		Far	7	2 (28.57%)		11	3 (27.27%)		13	6 (46.15%)		15	8 (53.33%)	
	M	Cloister	18	14 (77.78%)	0.1769	29	23 (79.31%)	0.0505	33	24 (72.73%)	**0.0043**	40	31 (77.50%)	**0.0064**
		Close	14	8 (57.14%)		20	10 (50.00%)		21	9 (42.86%)		25	14 (56.00%)	
		Mid	29	13 (44.83%)		39	19 (48.27%)		47	15 (31.91%)		53	22 (41.51%)	

Frequencies Right body side			ACJ			shoulder			elbow			hand		
			n	freq.	p-value	n	freq.	p-value	n	freq.	p-value	n	freq.	p-value
		Far	16	9 (56.25%)		20	10 (50.00%)		23	11 (47.83%)		22	11 (50.00%)	
	All	1	50	24 (48.00%)	0.3968	77	37 (48.05%)	0.1273	87	33 (37.93%)	0.0906	99	51 (51.52%)	0.5970
		2	68	38 (55.88%)		92	55 (59.78%)		110	55 (50.00%)		129	71 (55.04%)	
	F	1	13	6 (46.15%)	0.6452	21	10 (47.62%)	0.9399	26	10 (38.46%)	0.9884	28	16 (57.14%)	0.3932
		2	26	10 (38.46%)		37	18 (48.65%)		44	17 (38.64%)		53	25 (47.17%)	
	M	1	37	18 (48.65%)	0.1475	54	26 (48.15%)	0.0517	59	22 (37.29%)	0.0288	67	34 (50.75%)	0.2569
		2	40	26 (65.00%)		54	36 (66.67%)		65	37 (56.92%)		73	44 (60.27%)	

Notice: Y.A. = Young Adult

Table 59 Frequencies of degenerative joint disease for each joint of the right body side (continuation)

Frequencies Right body side			hip			knee			foot		
			n	freq.	p-value	n	freq.	p-value	n	freq.	p-value
Sex	F		79	41 (51.90%)	0.1113	78	22 (28.21%)	0.4411	74	34 (45.95%)	0.4057
	M		130	82 (63.08%)		129	43 (33.33%)		119	62 (52.10%)	
Age	All	Y.A.	28	1 (3.57%)	**<0.0001**	22	0 (0.00%)	**<0.0001**	24	3 (12.50%)	**<0.0001**
		Adult	53	19 (35.85%)		51	5 (9.80%)		48	20 (41.67%)	
		Mature I	42	24 (57.14%)		38	9 (23.68%)		33	12 (36.36%)	
		Mature II	43	41 (95.35%)		41	26 (63.41%)		37	28 (75.68%)	
		Senile	36	36 (100%)		40	26 (65.00%)		35	27 (77.14%)	
	F	Y.A.	13	0 (0.00%)	**<0.0001**	11	0 (0.00%)	**<0.0001**	12	1 (8.33%)	**0.0015**
		Adult	18	3 (16.67%)		17	0 (0.00%)		15	5 (33.33%)	
		Mature I	15	9 (60.00%)		14	5 (35.71%)		11	4 (36.36%)	
		Mature II	17	16 (94.12%)		16	9 (56.25%)		16	12 (75.00%)	
		Senile	13	13 (100%)		12	7 (58.33%)		12	9 (75.00%)	
	M	Y.A.	15	1 (6.67%)	**<0.0001**	11	0 (0.00%)	**<0.0001**	12	2 (16.67%)	**0.0003**
		Adult	35	16 (45.71%)		34	5 (14.71%)		33	15 (45.45%)	
		Mature I	27	15 (55.56%)		23	4 (17.39%)		21	7 (33.33%)	
		Mature II	26	25 (96.15%)		23	15 (65.22%)		19	15 (78.95%)	
		Senile	23	23 (100%)		37	18 (66.67%)		23	18 (78.26%)	
Location	All	Cloister	57	38 (66.67%)	0.1113	52	26 (50.00%)	**0.0009**	49	30 (61.22%)	0.0560
		Cemetery	157	85 (54.14%)		168	43 (25.60%)		160	73 (45.62%)	
	F	Cloister	15	6 (40.00%)	0.3055	14	4 (28.57%)	1.0000	13	6 (46.15%)	0.9868
		Cemetery	64	35 (54.69%)		64	18 (28.12%)		81	28 (45.90%)	
	M	Cloister	40	32 (80.00%)	**0.0077**	35	20 (57.14%)	**0.0005**	34	23 (67.65%)	**0.0318**
		Cemetery	90	50 (55.56%)		94	23 (24.47%)		85	39 (45.88%)	
Distance to	All	Cloister	57	38 (66.67%)	0.2683	52	26 (50.00%)	**0.0115**	49	30 (61.22%)	0.1184

Frequencies Right body side			hip			knee			foot		
			n	freq.	p-value	n	freq.	p-value	n	freq.	p-value
Church		Close	32	15 (46.88%)		41	11 (26.83%)		43	23 (53.49%)	
		Mid	85	46 (54.12%)		86	22 (25.58%)		80	32 (40.00%)	
		Far	40	24 (60.00%)		41	10 (24.39%)		37	18 (48.65%)	
	F	Cloister	15	6 (40.00%)		14	4 (28.57%)		13	6 (46.15%)	
		Close	13	6 (46.15%)	0.4916	15	3 (20.00%)	0.8931	18	10 (55.56%)	0.7778
		Mid	36	22 (61.11%)		36	11 (30.56%)		30	12 (40.00%)	
		Far	15	7 (46.67%)		13	4 (30.77%)		13	6 (46.15%)	
	M	Cloister	40	32 (80.00%)		35	20 (57.14%)		34	23 (67.65%)	
		Close	18	9 (50.00%)		21	6 (28.57%)		18	10 (55.56%)	
		Mid	47	24 (51.06%)	**0.0246**	46	11 (23.91%)	**0.0059**	45	18 (40.00%)	0.1088
		Far	25	17 (68.00%)		27	6 (22.22%)		22	11 (50.00%)	
Layer_ dual	All	1	90	45 (50.00%)	0.0595	88	25 (28.41%)	0.4406	87	45 (51.72%)	0.5510
		2	124	78 (62.90%)		132	44 (33.33%)		122	58 (47.54%)	
	F	1	27	13 (48.15%9	0.6307	24	7 (29.17%)	0.8999	21	10 (47.62)	0.8557
		2	52	28 (53.85%)		54	15 (27.78%)		53	24 (45.28%)	
	M	1	60	32 (53.33%)	**0.0331**	59	16 (27.12%)	0.1692	61	32 (52.46%)	0.9361
		2	70	50 (71.43%)		70	27 (38.57%)		58	30 (51.72%)	

Notice: Y.A. = Young Adult

Table 60 Frequencies of degenerative joint disease for each joint of the left body side

Frequencies Left body side			ACJ			shoulder			elbow			hand		
			n	freq.	p-value	n	freq.	p-value	n	freq.	p-value	n	freq.	p-value
Sex	F		41	12 (29.27%)	**0.0179**	56	22 (39.29%)	**0.0481**	68	28 (41.18%)	0.8102	83	34 (40.96%)	**0.0480**
	M		79	41 (34.17%)		108	60 (55.56%)		121	52 (42.98%)		139	76 (54.68%)	
Age	All	Y.A.	18	0 (0.00%)	**<0.0001**	21	1 (4.76%)	**<0.0001**	24	0 (0.00%)	**<0.0001**	28	2 (7.14%)	**<0.0001**
		Adult	38	9 (23.68%)		46	8 (17.39%)		52	8 (15.38%)		54	14 (25.93%)	
		Mature I	23	11 (47.83%)		33	18 (54.55%)		37	15 (40.54%)		47	21 (44.68%)	
		Mature II	21	17 (80.95%)		34	29 (85.29%)		37	28 (75.68%)		43	33 (76.74%)	
		Senile	22	18 (81.82%)		33	29 (87.88%)		40	31 (77.50%)		48	41 (85.42%)	
	F	Y.A.	8	0 (0.00%)	**0.0002**	11	0 (0.00%)	**<0.0001**	12	0 (0.00%)	**0.0001**	15	1 (6.67 %)	**0.0001**
		Adult	15	1 (6.67%)		14	1 (7.14%)		16	3 (18.75%)		17	3 (17.65%)	
		Mature I	6	2 (33.33%)		10	6 (60.00%)		13	6 (46.15%)		15	7 (46.67%)	
		Mature II	6	5 (83.33%)		11	6 (54.55%)		14	9 (64.29%)		19	11 (57.89%)	
		Senile	6	4 (66.67%)		10	9 (90.00%)		13	10 (76.92%)		14	12 (85.71%)	
	M	Y.A.	10	0 (0.00%)	**<0.0001**	10	1 (10.00%)	**<0.0001**	12	0 (0.00%)	**<0.0001**	13	1 (7.69%)	**<0.0001**
		Adult	23	8 (34.78%)		32	7 (21.88%)		36	5 (13.89%)		37	11 (29.73%)	
		Mature I	17	9 (52.94%)		21	11 (52.38%)		24	9 (37.50%)		29	13 (44.83%)	

Frequencies Left body side			ACJ			shoulder			elbow			hand		
			n	freq.	p-value	n	freq.	p-value	n	freq.	p-value	n	freq.	p-value
		Mature II	15	12 (80.00%)		23	23 (100%)		23	19 (82.61%)		24	22 (91.67%)	
		Senile	14	12 (85.71%)		21	18 (85.71%)		25	19 (76.00%)		32	27 (84.38%)	
Location	All	Cloister	24	13 (54.17%)	0.3183	45	27 (60.00%)	0.0985	53	27 (50.94%)	0.8102	59	36 (61.02%)	**0.0312**
		Cemetery	98	42 (42.86%)		127	58 (45.67%)		142	55 (38.73%)		172	77 (44.77%)	
	F	Cloister	5	1 (20.00%)	1.0000	9	3 (33.33%)	1.0000	13	6 (46.15%)	0.6851	14	6 (42.86%)	0.8745
		Cemetery	36	11 (3058%)		47	19 (40.43%)		55	22 (40.00%)		69	28 (40.58%)	
	M	Cloister	18	11 (30.56%)	0.3733	31	23 (74.19%)	**0.0135**	35	20 (57.14%)	**0.0446**	41	29 (70.73%)	**0.0139**
		Cemetery	61	30 (49.18%)		77	37 (48.05%)		86	32 (37.21%)		98	47 (47.96%)	
Distance to Church	All	Cloister	24	13 (54.17%)	0.1168	45	27 (60.00%)	0.4289	53	27 (50.94%)	0.2204	59	36 (61.02%)	0.1361
		Close	24	14 (58.33%)		34	16 (47.06%)		34	16 (47.06%)		43	19 (44.19%)	
		Mid	54	23 (42.59%)		64	29 (45.31%)		75	27 (33.33%)		90	38 (42.22%)	
		Far	20	5 (25.00%)		29	13 (44.83%)		33	14 (42.42%)		39	20 (51.28%)	
	F	Cloister	5	1 (20.00%)	0.3739	9	3 (33.33%)	0.8819	13	6 (46.15%)	0.8321	14	6 (42.86%)	0.9544
		Close	8	3 (37.50%)		10	4 (40.00%)		12	6 (50.00%)		14	5 (35.71%)	
		Mid	22	8 (36.36%)		27	12 (44.44%)		33	12 (36.36%)		42	17 (40.48%)	
		Far	6	0 (0.00%)		10	3 (30.00%)		10	4 (40.00%)		13	6 (46.15%)	
	M	Cloister	18	11 (61.11%)	0.2939	31	23 (74.19%)	0.0959	35	20 (57.14)	0.1481	41	29 (70.73%)	0.0787
		Close	15	10 (66.67%)		21	10 (47.62%)		21	9 (42.86%)		24	12 (50.00%)	
		Mid	32	15 (46.88%)		37	17 (45.95%)		42	13 (30.95%)		48	21 (43.75%)	
		Far	14	5 (35.71%)		19	10 (52.56%)		23	10 (43.48%)		26	14 (53.85%)	
Layer_ dual	All	1	50	22 (44.00%)	0.8414	75	34 (45.33%)	0.3460	82	30 (36.59%)	0.1878	102	50 (49.02%)	0.9780
		2	72	33 (45.83%)		97	51 (52.58%)		113	52 (46.02%)		129	63 (48.84%)	
	F	1	12	3 (25.00%)	1.0000	19	8 (42.11%)	0.7569	25	13 (52.00%)	0.1667	30	13 (43.33%)	0.7412
		2	29	9 (31.03%)		37	14 (37.84%)		43	15 (34.88%)		53	21 (39.62%)	
	M	1	37	18 (48.65%)	0.5874	50	25 (50.00%)	0.2807	52	16 (30.77%)	0.0185	67	36 (48.20%)	0.8291
		2	42	23 (54.78%)		58	35 (60.34%)		69	36 (52.17%)		72	40 (55.56%)	

Notice: Y.A. = Young Adult

Table 61 Frequencies of degenerative joint disease for each joint of the left body side (continuation)

Frequencies Left body side			hip			knee			foot		
			n	freq.	p-value	n	freq.	p-value	n	freq.	p-value
Sex	F		80	44 (55.00%)	0.3173	82	24 (29.27%)	0.5330	78	32 (42.11%)	0.0882
	M		134	83 (61.94%)		153	45 (33.33%)		119	65 (54.62%)	
Age	All	Y.A.	25	0 (0.00%)	**<0.0001**	23	1 (4.35%)	**<0.0001**	19	1 (5.26%)	**<0.0001**
		Adult	56	23 (41.07%)		57	8 (14.04%)		49	18 (36.73%)	
		Mature I	43	25 (58.14%)		38	8 (21.05%)		37	15 (40.54%)	
		Mature II	43	41 (95.35%)		42	28 (66.67%)		35	28 (80.00%)	
		Senile	39	36 (92.31%)		40	26 (65.00%)		36	28 (77.78%)	
	F	Y.A.	13	0 (0.00%)	**<0.0001**	13	1 (7.68%)	**0.0052**	11	0 (0.00%)	**0.0005**
		Adult	19	6 (31.58%)		18	2 (11.11%)		16	6 (37.50%)	
		Mature I	15	9 (60.00%)		13	4 (30.77%)		13	4 (30.77%)	

Frequencies Left body side			hip			knee			foot		
			n	freq.	p-value	n	freq.	p-value	n	freq.	p-value
		Mature II	18	17 (94.44%)		16	9 (56.25%)		14	11 (78.57%)	
		Senile	12	12 (100%)		13	7 (53.85%)		13	8 (61.54%)	
	M	Y.A.	12	0 (0.00%)		10	0 (0.00%)		8	1 (12.50%)	
		Adult	37	17 (45.95%)		39	6 (15.38%)		33	12 (36.36%)	
		Mature I	28	16 (57.14%)	**<0.0001**	24	4 (16.67%)	**<0.0001**	23	10 (43.48%)	**<0.0001**
		Mature II	25	24 (96.00%)		24	17 (70.83%)		19	16 (84.21%)	
		Senile	27	24 (88.89%)		26	18 (69.23%)		23	20 (86.96%)	
Location	All	Cloister	56	36 (64.29%)	0.3173	54	25 (46.30%)	**0.0068**	50	30 (60.00%)	0.0766
		Cemetery	164	91 (55.49%)		179	48 (26.82%)		162	74 (45.68%)	
	F	Cloister	15	7 (46.67%)	0.4717	14	4 (28.57%)	1.0000	13	5 (38.46%)	0.7701
		Cemetery	65	37 (56.92%)		68	20 (29.41%)		63	27 (42.86%)	
	M	Cloister	38	29 (76.32%)	**0.0311**	36	19 (52.78%)	**0.0039**	34	24 (70.59%)	**0.0269**
		Cemetery	96	54 (56.25%)		99	26 (26.26%)		85	41 (48.24%)	
Distance to Church	All	Cloister	56	36 (64.29%)	0.6588	54	25 (46.30%)	0.0614	50	30 (60.00%)	0.1619
		Close	37	20 (54.05%)		48	12 (26.09%)		44	23 (52.27%)	
		Mid	89	51 (57,30%)		91	25 (27.47%)		82	33 (40.24%)	
		Far	38	20 (52.63%)		42	11 (26.19%)		36	18 (50.00%)	
	F	Cloister	15	7 (46.67%)	0.5084	14	4 (28.57%)	0.8940	13	5 (38.46%)	0.8777
		Close	15	8 (53.33%)		18	4 (22.22%)		18	9 (50.00%)	
		Mid	38	24 (63.16%)		36	12 (33.33%)		31	12 (38.71%)	
		Far	12	5 (41.67%)		14	4 (28.57%)		14	6 (42.86%)	
	M	Cloister	38	29 (76.32%)	0.1945	36	19 (52.78%)	**0.0388**	34	24 (70.59%)	0.1089
		Close	21	12 (57.14%)		22	6 (27.27%)		19	11 (57.89%)	
		Mid	49	27 (55.10%)		51	13 (25.49%)		46	20 (43.48%)	
		Far	26	15 (57.69%)		26	7 (26.92%)		20	10 (50.00%)	
Layer_ dual	All	1	93	51 (54.84%)	0.4580	95	30 (31.58%)	0.9459	83	41 (49.40%)	0.9365
		2	127	76 (59.84%)		138	43 (31.16%)		129	63 (48.84%)	
	F	1	27	16 (59.26%)	0.5847	25	9 (36.00%)	0.3749	21	7 (33.33%)	0.3385
		2	53	28 (52.83%)		57	15 (26.32%)		55	25 (45.45%)	
	M	1	63	35 (55.56%)	0.1516	65	19 (29.23%)	0.3299	57	32 (56.14%)	0.7496
		2	71	48 (67.61%)		70	26 (37.14%)		62	33 (53.23%)	

Notice: Y.A. = Young Adult

6.1.1.3.1.8 Frequency of joint disease by joint

Observation of the graphs essentially reflects the trends already described above. However, the graphs also reveal an overall trend of joints that are most or least affected by degenerative joint disease.

Among the whole sample and within all groups, the knee remains the least affected joint.

Generally, the joints of the upper limbs, especially, elbow, acromio-clavicular joint and shoulder are less affected by degenerative joint disease than the hip or the feet. However, although more commonly affected by degenerative joint disease, feet and hands rarely showed any moderate or severe changes. The most affected joint across all groups was the hip joint, which, together with the acromio-clavicular joint, also showed the most severe stages of degenerative joint disease. Overall, the right body side seems to have been affected slightly more by degenerative joint disease but the difference between the sides seems to have been minimal. (Figure 63, Figure 64, Figure 65)

Degenerative Joint Disease

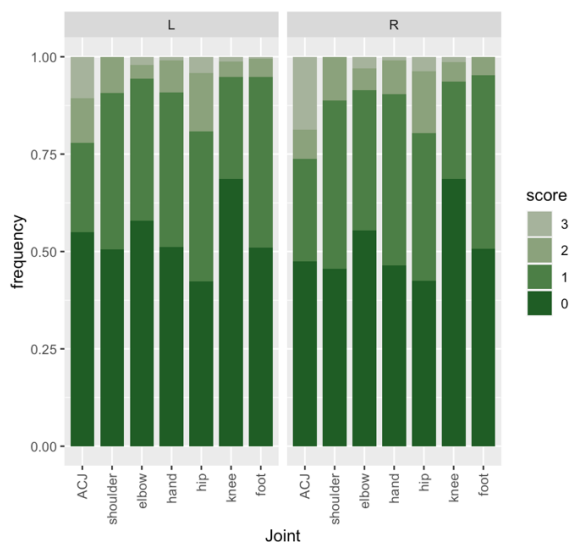

Figure 63 Frequency and severity of degenerative joint disease in the different joints for the right and left sides

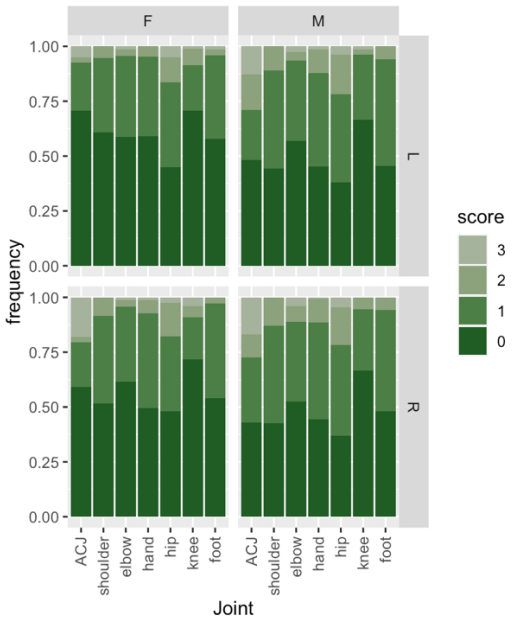

Figure 64 Frequency and severity of degenerative joint disease in the different joints for the right and left sides differentiated by sex

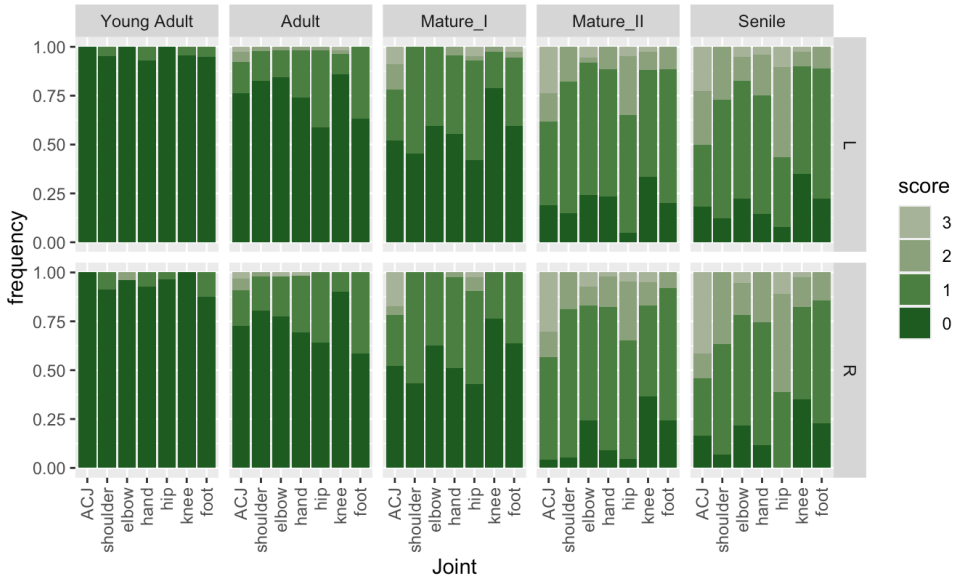

Figure 65 Frequency and severity of degenerative joint disease in the different joints for the right and left sides differentiated by age

6.1.1.3.2 Overall

Of a total of 304 individuals that could be analysed for degenerative changes in any joint in this study, 220 (72.37%) exhibited signs of degenerative joint disease. Since not every joint was available for scoring for the majority of these individuals, this percentage might be underestimated. Overall, males (79.19%) showed significantly more degenerative changes than

women (66.98%). Although insignificant, people buried in the cloister (71.60%) exhibited slightly less degenerative joint disease than those from the cemetery (72.65%). This overall pattern is caused by opposing trends among the sexes. Males displayed more degenerative changes among the cloister (86.27%) burials (cemetery: 76.23%) and females displayed more degenerative changes among the cemetery (71.43%) burials (cloister: 50.00%). But for both sexes, these differences were statistically non-significant. Whilst the frequency of degenerative joint disease in the single joints often showed as significant difference between Layer 1 and 2, the overall frequency of individuals with arthritic changes does not. Only slightly more females showed degenerative changes in any joint in Layer 1 (70.27%) than in Layer 2 (65.2%).

Age showed the strongest correlation with occurrence of degenerative joint disease, with the presence increasing strongly and significantly with age.

When considering only individuals with medium to strong cases of DJD, the frequency of DJD presence drops drastically in all groups, However, significant differences are now apparent among more groupings. Age still shows the same significant trend of increasing DJD presence with old age and males still have more DJD than women. People from Layer 2 now show significantly more cases of DJD than those from Layer 1 and among cloister burials DJD appears to occur more often among cloister then among cemetery burials although the latter difference is not statistically relevant.

This means that, although in cemetery burials and amongst burials from Layer 1, DJD occurred generally a bit more frequently than in Layer 2 or among cloister burials, severe forms of the disease were much more common in Layer 2 and in cloister burials. This trend might be linked, since the majority of the cloister burials actually belong to Layer 2. Furthermore, there are proportionately more mature and senile men buried in the cloister and in Layer 2 than in the cemetery and in Layer 1, which might also contribute to the higher occurrence of moderate-severe changes among these groups. (Table 62)

Table 62 Percentage of individuals affected by any degree of and only moderate and severe DJD by sex, age, burial location, distance to church, and burial layer

Frequencies Arthritis			Arthritis all			Arthritis mod. & sev.		
			n	freq.	p-value	n	freq.	p-value
Sex	F		106	71 (66,98%)	**0.0231**	106	14 (13.21%)	**0.0496**
	M		173	137 (79.19%)		173	35 (20.23%)	
Age	All	Y.A.	32	7 (21.88%)	**<0.0001**	32	0 (0.00%)	**<0.0001**
		Adult	68	44 (64.71%)		68	2 (2.94%)	
		Mature I	53	44 (83.02%)		53	4 (7.55%)	
		Mature II	57	56 (98.25%)		57	20 (35.09%)	
		Senile	52	50 (96.15%)		52	23 (44.23%)	
	F	Y.A.	16	2 (12.50%)	**<0.0001**	16	0 (0.00%)	**<0.0001**
		Adult	23	13 (56.52%)		23	0 (0.00%)	
		Mature I	18	15 (83.33%)		18	3 (16.67%)	

Frequencies Arthritis			Arthritis all			Arthritis mod. & sev.		
			n	freq.	p-value	n	freq.	p-value
		Mature II	23	22 (95.65%)		23	5 (21.75%)	
		Senile	17	15 (88.24%)		17	5 (29.41%)	
	M	Y.A.	16	5 (31.25%)	**<0.0001**	16	0 (0.00%)	**<0.0001**
		Adult	45	31 (68.89%)		45	2 (4.44%)	
		Mature I	32	27 (84.38%)		32	0 (0.00%)	
		Mature II	32	32 (100%)		32	15 (46.88%)	
		Senile	33	33 (100%)		33	17 (51.52%)	
Location	All	Cloister	81	58 (71.60%)	0.8576	81	20 (24.69%)	0.0769
		Cemetery	223	162 (72.65%)		223	32 (14.35%)	
	F	Cloister	22	11 (50.00%)	0.0571	22	3 (13.64%)	0.1318
		Cemetery	84	60 (71.43%)		84	11 (13.19%)	
	M	Cloister	51	44 (86.27%)	0.1378	51	17 (33.33%)	**0.0156**
		Cemetery	122	93 (76.23%)		122	18 (14.75%)	
Distance to Church	All	Cloister	81	58 (71.60%)	0.5664	81	20 (24.69%)	0.2575
		Close	55	39 (70.91%)		55	9 (16.36%)	
		Mid	117	82 (70.09%)		117	14 (11.97%)	
		Far	51	41 (80.39%)		51	9 (17.65%)	
	F	Cloister	22	11 (50.00%)	0.1894	22	3 (13.64%)	0.4885
		Close	19	13 (68.42%)		19	2 (10.53%)	
		Mid	48	33 (68.75%)		48	7 (14.58%)	
		Far	17	14 (82.35%)		17	2 (11 76%)	
	M	Cloister	51	44 (86.27%)	0.4073	51	17 (33.33%)	0.1098
		Close	26	21 (80.77%)		26	4 (15.38%)	
		Mid	64	47 (73.44%)		64	7 (10.94%)	
		Far	32	25 (78.12%)		32	7 (21.88%)	
Layer_ dual	All	1	132	97 (73.48%)	0.7030	132	13 (9.85%)	**0.0060**
		2	172	123 (71.51%)		172	39 (22.67%)	
	F	1	37	26 (70.27%)	0.5980	37	2 (5.41%)	0.1459
		2	69	45 (65.22%)		69	12 (17.39%)	
	M	1	84	66 (78.57%)	0.8454	84	11 (13.10%)	0.0701
		2	89	71 (79.78%)		89	24 (26.97%)	

Notice: Y.A. = Young Adult
Notice: mod. = moderate
Notice: sev. = severe

6.1.1.4 Discussion and Conclusion

Degenerative joint disease is the most common pathological condition observed in skeletal assemblages and modern populations (Weiss & Jurmain 2007; Waldron 2009; Schrader 2019). It is caused by damage to the cartilage covering the joint surfaces, usually due to an over- or misloading of the joint, which constitutes a primary osteoarthritis. Damage to the cartilage leads to differential distribution of load in the joint, which then leads to marginal or joint surface osteophyte formation (Figure 67). Through continued use of the joint, the damaged cartilage can wear off completely and the ensuing bone-on-bone friction during movement can cause eburnation (Waldron 2009; Roberts & Manchester 2010; Schrader 2019) (Figure 66). Generally, occurrence and intensity of degenerative joint disease can be influenced by factors such as genetic predisposition, obesity, age, sex etc. but physical activity is still considered to be a major cause for the development of degenerative joint changes (Adler 2005; Klaus *et al.* 2009; Larsen 2015).

In all joints, males showed significantly more frequent and severe occurrence of degenerative joint disease but in many cases, these differences did not reach statistical significance. Regarding overall occurrence of arthritic changes per individual however, men had

significantly more degenerative changes in the joints than women, even when only considering moderate and severe changes. This pattern was also observed in a majority of studies on contemporaneous populations, and there as well, statistical significance was not reached for male/female differences in many of the joints (Klaus *et al.* 2009; Stech 2009; Timmermann 2009; Trautmann 2012; Roßbach 2015; Kairies 2021) This suggests, as has also been proposed by the aforementioned studies, that men's joints were exposed to heavier and/or more frequent loads, meaning that men carried out more strenuous physical activities than women on a daily or at least regular basis. This is particularly important to note since nowadays, women, especially in old age, tend to be more predisposed to developing osteoarthritis than men, likely due to hormonal changes brought on by menopause etc. (Arden & Nevitt 2006). When looking at differences between men and women, (Figure 64) it also becomes clear that men and women had slightly different patterns of degenerative joint disease. In men, the right and left body sides showed very similar patterns of joint disease distribution and severity. In females, only the right side showed a pattern of distribution similar to that of men, but the left body side showed clearly less changes in the arm, further hinting at differences in habitual activities between the two sexes, with women generally considered to be responsible for the less strenuous tasks of household maintenance, such as weaving, needle work, cooking etc. (Ennen 1993; Opitz 2006).

Age seems to be a major factor for development of degenerative joint disease in the Knuedler population as well. Frequency and intensity of degenerative changes in joints increased significantly with age for each joint examined. The number of individuals affected by any form of degenerative joint disease showed also a stark and statistically significant increase with age. Age-related degenerative joint disease is usually caused by a combination of loss of elasticity of the cartilage covering the joints in old age, increased joint instability due laxity of ligaments, impaired muscle function, prolonged use of the joints etc. (Arden & Nevitt 2006; Stech 2009). In fact, in modern urbanised populations, the occurrence of osteoarthritis is rare before the age of 40 (Arden & Nevitt 2006; Waldron 2009). And indeed, this pattern seems to be reflected as well in the Knuedler population. Although overall occurrence in degenerative joint disease is already pretty high (64.71%) in adults (~30-39years), when following definitions for osteoarthritis after Waldron (2009), which roughly correspond to moderate and severe scores in this study, the overall frequency of osteoarthritis in adults drops to 2.94% and no cases could be detected among young adults (~20-29years). However, in the mature II (35.09%)(50-59years), and senile (44.23%)(60+) age categories, the frequency of osteoarthritis was already much more substantial. Light degenerative joint changes did however also occur in young

adults from the Knuedler cemetery but in at least 2 of 7 cases, the development of degenerative changes in a joint was caused by a fracture and osteomyelitis respectively. Furthermore, it is only in the mature age group that a clear increase in degenerative changes of the shoulder and acromio-clavicular joints becomes apparent. Among adults, the foot and the hip are clearly the most affect joint areas, whereas in the 40+ age groups, the hip, shoulder and ACJ are most affected (Figure 65).

Intensity and frequency of degenerative joint disease are evaluated in an attempt to reconstruct habitual physical activity in the population buried at Knuedler cemetery. In both Layers, although, except for the knee, all joints showed similar frequency and intensity rates, the ACJ, shoulder and the hip showed the highest values for intensity and frequency of degenerative joint disease. The shoulder joint is a triaxial ball-in-socket joint which allows for movement along three axes: outwards and inwards rotation, extension and flexion as well as abduction and adduction (Schiebler *et al.* 1995). Higher frequency and intensity of degenerative changes in the shoulder joint is suggestive of frequent carrying and lifting activities but also of swinging motions that are carried out while cutting with a sickle or processing stone or soil with a pickaxe and might hint at activities where the arms were regularly lifted above the head, such as chopping wood, (Waldron 2009; Roberts & Manchester 2010; Larsen 2015). Higher index values and frequency of degenerative joint disease in the acromio-clavicular joint would also support this theory. However, compared to other contemporary sites, index values and frequency of joint disease were not particularly elevated. In fact, compared to the population from Emden, an upper- to middle class population, shoulder joint disease intensity and frequency is rather low. Stech (2009) argues that, although the individuals probably belonged to an upper to middle class part of the population, the professions they were likely engaged in, such as trade and seafaring, caused them to be exposed to a lot of strenuous carrying and lifting activities in their daily lives, which probably favoured development of degenerative changes in the joint. The comparatively lower values established for the Knuedler population suggest that this was not the case here and that the activities carried out were rather moderate in nature. The index values from the Knuedler cemetery for the shoulder joint most closely resemble those from Ellwangen-Jagst, Ihlow, both German sites and Grund/Wenzelsmauer, a soldiers' cemetery from Luxembourg City. Based on the index values, Kairies (2021) concludes that strenuous activities involving the shoulder such as reaping with a sickle or wood chopping must have been carried out to a greater extent. Since only index values from the older Layer 2 resemble those found by Kairies (2021), this might have also been the case for this group of individuals from the Knuedler cemetery. High index values in the shoulder joints of soldiers

from Grund/Wenzelsmauer were to be expected as the carrying of weapons and regular physical exercise must have put a toll on their joints. It has to be kept in mind however that the majority of people buried and examined in Layer 2 from Knuedler were mature or older and that age showed a strong association to joint disease frequency and intensity in this sample. At Ellwangen, the majority of individuals examined for the late and postmedieval groups were adults, and seniles were especially rare. Therefore, age, rather than strenuous activity might be the cause for the overall elevated arthrosis index values in Layer 2 from the Knuedler cemetery. The index values from Layer 1 resembled closely those from Ihlow, inhabitants of a convent. Timmermann (2009) argues that the low intensity and low frequency of degenerative joint disease, despite the overall higher age of the individuals buried there, is due to the fact that strenuous activities were rather delegated to external workers that were not buried amongst the monks of the convent. This would suggest that the people buried in Layer 1 from the Knuedler cemetery experienced similar living conditions than the inhabitants from the convent in Ihlow. However, at 48.05%, the frequency of joint disease is noticeably higher among the Knuedler population than among the inhabitants of the Ihlow convent (38.3%). Grevenmacher, a rural medieval site from Luxembourg shows consistently higher index and frequency values in the shoulder joint. Trautmann (2012) suggests increased physical activity involving the upper arms, such as the aforementioned sickle cutting or wood chopping, which would be in line with agricultural activities that the population of Grevenmacher likely practiced on a daily or regular basis. Expectedly, the lower values from Luxembourg City suggest, that the urban population was not involved in such activities on a regular basis (Thewes 1994; Ittrich 2004; Opitz 2006; Larsen 2015). (Table 63, Table 64)

Regarding frequency of joint disease in the shoulder, the Knuedler population shows values similar to those from early postmedieval Völklingen, an urban population from the Saarland in Germany. In their study, Rossbach (2015) compared individuals from Völklingen to those from Hettstedt, a mining town in Saxony-Anhalt. She found that individuals from Hettstedt showed degenerative changes in the shoulder and hip joints much more frequently than those from Völklingen and concluded that the mining activities contributed to the higher frequencies among people from Hettstedt and that Völklingen showed frequencies characteristic for an urban population where trade was the main occupation. Therefore, based on the rather low arthrosis intensity and moderate frequency of degenerative joint disease in the shoulder, it is likely that the individuals buried in the Knuedler cemetery practiced activities that were physically not very demanding in the use of the arms. This is further supported by the low index values and lower frequency of values in the elbow joint. It has to be noted though that in

the majority of comparative samples, the elbow joint is after the knee the least affected joint. Generally, activities involving extension and flexion of the forearm and supination and pronation of the hand are thought to affect the elbow joint (Schiebler *et al.* 1995). Studies on modern individuals of known profession indicate that degenerative joint disease in the elbow is particularly frequent in miners, smiths and manual workers (Jansen & Haas 1991; Freyschmidt 2016). Due to the low frequency and intensity of degenerative joint disease in the elbow, it is very unlikely that the people buried in the Knuedler cemetery carried out similar tasks. This pattern is found in most urban comparative samples. However, those where clearly agricultural tasks were carried out, such as Grevenmacher, showed higher index values and frequencies in the elbow joint. The soldiers from Grund/Wenzelsmauer even showed the highest index values in the elbow joint. This is likely related to the recoil shocks (Jansen & Haas 1991; Freyschmidt 2016) they might have experienced while fighting or shooting with weapons. (Table 63, Table 64)

The most affected joint in the Knuedler population is the hip. Degenerative changes in the hip and knee are usually caused by tasks such as walking or running but also standing for long periods of time (Cooper 1995; Cooper *et al.* 1998; Stech 2009). Body weight is also thought to play a major role in the development of arthrosis in the hip and knee joints (Cooper *et al.* 1998; Abbate *et al.* 2006; Melanson 2007; Sowers & Karvonen-Gutierrez 2010; Sellam & Berenbaum 2012). However, the knee joint, due to the presence of the menisci, is much more stable than the hip joint so that degenerative changes take much longer to develop in the knee (Waldron 2009). The hip on the other hand, due to its many degrees of freedom is particularly at risk for developing arthritic changes (Waldron 2009; Roberts & Manchester 2010). Regarding the intensity of degenerative changes in the hip, the individuals from Knuedler cemetery show similar values than the soldiers from Grund/Wenzelsmauer and Ihlow, whilst the other sites all showed higher values. Concerning frequency of degenerative changes in the hip, the individuals from Luxembourg fall into the middle of the spectrum and show frequencies similar to those observed in other urban settings, including upper-middle class populations, such as upper class urban individuals from Rostock (Ittrich 2004) and an urban population from Völklingen (Roßbach 2015). Inhabitants of the Ihlow convent showed lower frequency of hip degenerative joint disease (Timmermann 2009). The comparatively low intensity and average frequency of degenerative joint disease suggests that the tasks affecting the hip joint were not so extensive as to cause severe forms of degenerative joint disease but were practised enough to produce degenerative changes in slightly more than half the population. Therefore, the changes observed are mostly consistent with tasks involving lots of walking and long-time

standing, which are tasks most in line with trading professions (Stech 2009). (Table 63, Table 64)

Compared to other populations such as those from Hettstedt, Emden and Brandenburg (Posselt 1997; Stech 2009; Roßbach 2015), the Knuedler population showed relatively little degenerative joint disease in all joints that could be compared. Hettstedt is known to be a mining town with most inhabitants being involved in this kind of activity (Roßbach 2015), whilst life in Emden, a port city, was likely influenced strongly by seafaring professions that would involve a lot of strenuous manual labour even for the upper class buried inside the cloister (Stech 2009). Life in Brandenburg was marked by poverty and most individuals were involved in agricultural activities (Posselt 1997; Jungklaus 2009, 2011). All these activities account for the overall higher prevalence of degenerative joint disease among these populations.

The overall pattern of degenerative joint disease observed among the individuals from the Knuedler cemetery suggests that they did not practice very strenuous daily activities. The pattern resembles that observed for other urban areas (Ittrich 2004; Roßbach 2015). However, degenerative joint disease frequency is still a bit higher than that of the privileged inhabitants of the Ihlow convent and the upper-class individuals from Rostock. The lower frequency among upper class individuals is explained by the authors of these studies by the fact that the people were most likely able to delegate strenuous tasks to others (Timmermann 2009). Therefore, differences between cloister and cemetery burials were tested among the Knuedler population. Males showed significantly more severe and more frequent degenerative changes in the majority of the examined joints among cloister burials. At first glance this might suggest that individuals buried in the cloister were exposed to more strenuous activities than those from the cemetery. This would reflect the opposite of what was expected since, as previously established, individuals of higher social status, which were usually buried inside or a least close to the cloister, should have lower frequency and intensity of degenerative joint disease. However, the age of the individuals buried in both locations has to be considered as well. Whilst in the cloister, the number of mature and senile males was vastly predominant, the distribution among the age groups was much more balanced in the cemetery. Therefore, since degenerative joint changes seem to get worse and more frequent with age, age might have also influenced the occurrence of degenerative joint diseases in both burial locations. The frequency and intensity of degenerative joint disease of the knee (Figure 66) among the Knuedler population is much higher in cloister than in cemetery burials in men, whereas there is barely any difference between the burial locations in females. Kneeling might lead to degenerative

changes in the knee (Haj-Mirzaian *et al.* 2021). Therefore, the higher index and frequency of degenerative joint disease of the knee in male cloister burials might reflect a lifestyle marked by that posture, which would be consistent with the daily routines of friars, who were bound to pray several times a day (Montford 2002).

6.1.1.4.1 Conclusion

To conclude, the patterns of degenerative joint disease observed in the population buried in the Knuedler cemetery are most consistent with those observed in other urban populations, where no particularly strenuous daily activities such as agricultural practices were carried out on a regular basis. The generally high number of older (40+years) individuals in this population complicates comparisons to other sites as the age distribution skews frequency and intensity of degenerative joint disease. Furthermore, while attention was paid to choose comparative sites where degenerative joint disease was evaluated according to methods similar to those used in this study, direct comparisons are still difficult due the lack of consensus on when to consider degenerative changes as arthritic changes and whether to score only osteoarthritis or all degenerative changes. A general consensus on recording methods for degenerative joint diseases would greatly improve cross-site comparisons for this disease.

Examples of Degenerative Joint Disease

Figure 66 Striated eburnation (osteoarthritis) on left distal femoral epiphysis (2008-78/1154)

Figure 67 DJD without eburnation in Ra +Ul R of 2008-78/215

Table 63 Mean index scores for degenerative joint disease for all major joints compared to other Medieval and Postmedieval European sites

Time period	Site	Country	Type of settlement	Shoulder	Elbow	Hip	Knee	Publication
mid-17th-18th C	Knuedler	Luxembourg	urban	1.46	1.31	1.55	1.24	Kremmer (hic)
14th-mid-17th C	Knuedler	Luxembourg	urban	1.67	1.55	1.77	1.34	Kremmer (hic)
12th-14th C	Grevenmacher	Luxembourg	rural	2.3	2.15	2.15	1.4	Trautmann (2017)*
Late medieval	Ellwangen-Jagst	Germany	urban	1.65	1.8	2.4	1.85	Kairies (2021)&
Early postmedieval	Ellwangen-Jagst	Germany	urban	1.7	2.13	2.47	2	Kairies (2021)&
late 16th-early 18th C	Grund/ Wenzelsmauer	Luxembourg	urban	1.65	1.9	1.65	1.6	Trautmann&Trautmann (2011)*
10th-18th C	Emden	Germany	urban	2.3	1.7	2.5	2.0	Stech (2009)
12th-16th C	Ihlow	Germany	monastic	1.52	1.24	1.71	1.23	Timmermann (2009)

*=the original values were based on scores 0-3, which correspond to the scores 1-4 used in this study. For comparative reasons, the original scores were therefore upped by 1 to correspond to the scoring system used in this and other studies. Furthermore, an average value was calculated from the male and female scores presented in the respective works.
&=an average score was calculated from the average values of the different age groups.

Table 64 Mean frequencies for degenerative joint disease for all major joints compared to other Medieval and Postmedieval European sites

Time period	Site	Country	Type of settlement	Shoulder	Elbow	Hip	Knee	Publication
mid-17th-18th C	Knuedler	Luxembourg	urban	48.05	37.93	50.00	28.41	Kremmer (hic)
14th-mid-17th C	Knuedler	Luxembourg	urban	59.78	50.00	62.90	33.33	Kremmer (hic)
12th-14th C	Grevenmacher	Luxembourg	rural	73.8	66.5	66.2	6.6	Trautmann (2017)
10th-18th C	Emden	Germany	urban	90.3	40.8	86.3	51.3	Stech (2009)
Early post-medieval	Völklingen	Germany	urban	44.8	33.7	46.6	23.3	Rossbach (2015)
12th-16th C	Ihlow	Germany	monastic	38.3	11.7	40.9	9.2	Timmermann (2009)
15th C	Hettstedt Kirche	Germany	urban	72.3	55.9	80.1	44.1	Rossbach (2015)
18th-19th C	Hettstedt Gym.	Germany	urban	82.3	72.3	82.7	76.5	Rossbach (2015)
13th-18th C	Rostock	Germany	urban	27.8	24.5	56.7	37	Ittrich 2004
16th-18th C	Brandenburg	Germany	urban	98.6	83.9	96.4	82.4	Posselt 1997

6.1.2 Ankylosis of joints

6.1.2.1 Introduction

Ankylosis describes the complete or partial fusion of two joint surfaces and is most commonly found in the spine, but any joint can be affected. A reduction in the joint cavity and destruction of cartilage can lead to ossification of ligaments, which can lead to complete fusion of the joint area. Ankylosis usually occurs as a consequence to degenerative joint disease but trauma, infections, genetic defects and metabolic conditions are also known to cause ankylosis (Grupe *et al.* 2015).

6.1.2.2 Results and discussion

A total of 6 cases of ankylosis that do not involve the spine have been observed in the Knuedler cemetery. (Figure 68) In one case (2008-78/1021) ankylosis of the knee joint was likely caused by septic arthritis as a result of severe osteomyelitis. This case will be discussed further in the section on osteomyelitis. The majority of cases concern the hand or foot bones. In two of these cases, ankylosis is accompanied by degenerative changes and in the other two no degenerative changes were observed in the surrounding joints, which is why they were most likely congenital in nature. In one case, the left mandibular condyle was fused to the glenoid cavity on the skull (Table 65). In this case, severe degenerative changes could be observed in the right temporo-mandibular joint. This ankylosis likely caused the individual noticeable problems during food intake as chewing was rendered practically impossible on the left side and movement on the right was also strongly restricted.

Table 65 Cases of Ankylosis with possible aetiology

Ankyloses				
Individual	**Sex**	**Age**	**Fusion area**	**Possible Aetiology**
2008-78/1021	M	Senile	Femur-Patella-Tibia L	Septic arthritis due to osteomyelitis
2008_78/710	M	Young Adult	Proximal – medial phalanx 5 R+L foot	congenital
2016_082/113	M	Senile	MC3 spinous process - capitate	congenital
2016_082/439	M	Senile	Medial – distal phalanx R foot	degenerative
2008_78/666	M	Mature	MT3 – medial cuneiform L	degenerative
2008_78/147	M	Adult	Mandibular condyle – glenoid cavity L	degenerative

Figure 68 Ankylosis of MT3 with lateral cuboid (2008-78/666)

6.1.3 Osteochondritis dissecans

6.1.3.1 Introduction

Osteochondritis dissecans presents as rounded depression on a joint surface (Roberts & Manchester 2010) (Figure 69, Figure 70). The lesion occurs as a result to an osteochondral fracture (Waldron 2009). As a result, the blood supply to the completely or incompletely detached fragment is disrupted and the necrotic piece remains in the joint for a while, during which time it can either grow back into the defect or gets absorbed (Waldron 2009; Roberts &

Manchester 2010). The aetiology of the condition is still not entirely clear but direct trauma or repetitive microtrauma (Waldron 2009) have been put forward as possible causes, along with a genetic predisposition (Mann & Hunt 2005).

Osteochondritis dissecans

Figure 69 Osteochondritis dissecans in the lateral condyle of the right tibia (2008-78/668)

Figure 70 Osteochondritis dissecans at the distal epiphysis of a subadult tibia (2008-78/1424)

6.1.3.2 Results and Discussion

A total of 12 cases of osteochondritis dissecans were discovered among the burials from the Knuedler cemetery. According to Roberts and Manchester 2010, the conditions is more frequent in men than in women, a tendency that was not found among the Knuedler burials, where females and males were nearly equally affected by the condition (M:n=5, F:n=6). Furthermore, juveniles and young adults are thought to be most affected by the condition (Adler 2005), a tendency, which could also not be confirmed for the Knuedler population. Here, only one young adult and one infans II showed a lesion whereas among adults one case and among matures 6 (mature I: 4; mature II: 2) cases were recorded. Three cases were seen in adults whose age could not be further determined. The most commonly affected joint is the knee joint (Adler 2005). This trend proved true for the Knuedler population: in 9 of the 12 cases, changes occurred in either the patella, tibial plateaus, or distal femoral epiphysis (Table 66).

Table 66 Individuals with osteochondritis dissecans lesions

Osteochondritis dissecans					
Individual	**Sex**	**Age**	**Bone**	**Side**	**Area**
2013_015/160	F	Mature	Tibia	L	Lateral condyle
2016_082/452	F	Mature	Talus	R+L	trochlea
2008_78/1043	M	Young Adult	Talus	R+L	Medial condyle
			Patella	R+L	trochlea
2008_78/1283	F	Adultus	Talus	L	head
2008_78/1393	M	Mature	Tibia	L	Medial condyle
			Talus	R+L	trochlea

Osteochondritis dissecans					
2008_78/1424	INDET	Infans II	Tibia	L	Distal epiphysis
2008_78/1453	F	Adultus	Femur	R	Center of distal epiphysis
2008_78/1465	F	Mature	Tibia	L	Lateral condyle
2008_78/152	F	Adult	Humerus	R+L	Between trochlea and capitulum
2008_78/247	M	Mature	Femur	R	Center of distal epiphysis
2008_78/625	M	Adultus	Tibia	R	Distal epiphysis
2008_78/668	M	Mature	Tibia	R+L	Medial condyle

6.1.4 Degenerative joint disease of the spine

6.1.4.1 Introduction

The human spine carries most of the weight of the body and head. The complex system of joints in the spine, in combination with the intervertebral discs, back muscles and ligaments also renders it very flexible but stable at the same time (Menninger & Waibel 1996; Rössler & Rüther 2005). The doubles-shaped curvature in the spine together with the elastic intervertebral discs cushion shocks that occur while walking and running, and therefore renders some parts of the spine, namely those vertebrae at the peak of the curvatures more susceptible to wear and tear (Menninger & Waibel 1996; Roberts & Manchester 2010). Over- and misloading but also age-related processes can lead to the formation of degenerative changes in the spine usually through damage of the cartilaginous intervertebral disc. Reactions in forms of osteophytes then occur in the vertebral bodies and joints in an attempt to stabilise the spine (Menninger & Waibel 1996; Waldron 2009). Spondylosis deformans describes the degenerative changes in the vertebral bodies and Spondylarthrosis deformans those occurring the intervertebral joints. If the intervertebral disc is damaged, it can protrude into the plates of the vertebral bodies and cause Schmorl's nodes. Further elaborations on these pathologies will be given in the relative sections. The formation of degenerative changes in the spine has previously been linked to over- and misloading on the spine and workers who engage in heavy manual labour present more often with strong degenerative spine changes (Liebert *et al.* 1971).
Therefore, the study of degenerative changes in the spine can provide insights into the patterns and intensity of daily activities of a population (Schultz 1982; Larsen 2015).

6.1.4.2 Methods

In order to detect any differences in the severity and presence of degenerative joint disease in the spine, several steps were undertaken.
First, any changes observed on the vertebral body and intervertebral joints were recorded after a simplified scheme based on Schultz (1988) and modified by Trautmann (2012). This system was chosen in order to guarantee comparability to other Luxembourgish sites such as

Grevenmacher, which have been recorded in the same way. At the same time, since the scheme is very similar to that by Brothwell (1981) used in Ellwangen-Jagst by Kairies (2021), for the evaluation, the base scores were raised by 1 in order to obtain values comparable to the Ellwangen-Jagst site. The scoring system for Spondylosis deformans can be found in Table 67 and that for Spondylarthrosis deformans in Table 68:

Table 67 Recording scheme for Spondylosis deformans (after Trautmann 2012 simplified from Schultz 1988)

Stage	Description
0 (blank)	Vertebra is either not present or could not be scored
1	No visible changes
2	Light lipping/ light osteophytes at margins
3	Moderate osteophyte development at margins, outline may be enlarged
4	Pronounced osteophyte growth and possible deformation of the vertebral body. Ankylosis may occur.

Table 68 Recording scheme for Spondylarthrosis deformans (after Trautmann 2012 simplified from Schultz 1988)

Stage	Description
0 (blank)	Vertebral joint is either not present or could not be scored
1	No visible changes
2	Light sclerotic changes on the joint surface and margin, no changes to the outline
3	Moderate osteophyte development at margins, outline may be enlarged, light erosive lesions on the surface are possible
4	Pronounced osteophyte growth and possible joint deformation, and/or eburnation of the surface. Ankylosis may occur.

To quantify the severity of spondylosis deformans, an overall score was determined for the superior and inferior facies, by calculating an average value of the two body sides.

To quantify the severity of spondylarthrosis deformans, an overall score was calculated for all intervertebral joints of each vertebra, by calculating an average value.

These decimal scores were then attributed to a discrete score again, following the conversion system presented in Table 69, in order to visualise trends in severity across the different vertebrae in stacked percentage bar charts.

Next, a combined average score, based on the scores of the vertebral body and intervertebral joints, was calculated for each vertebra. The raw scores for each vertebra were then combined to form an average score for all cervical, thoracic and lumbar vertebrae in order to quantify the overall arthritis intensity of the different spinal segments.

This score was then compared statistically between the sexes, age groups, burial layers and locations.

Finally, a percentage was calculated for all individuals affected by arthritic changes in the cervical, thoracic, and lumbar spine as well as for the spine overall. The distribution of affected

individuals was compared statistically between the sexes, age groups, burial layers and locations.

Schmorl's nodes were recorded as absent or present to calculate the percentage of individuals affected by the lesions for each spinal segment. A differentiation into light Schmorl's nodes and severe Schmorl's nodes was undertaken after Üstündag (2010) with the cut off for size lying at 2mm. Only a visual representation for severity was provided in the stacked bar charts for each vertebra.

Table 69 Simplified overall joint scores used for representation in the graphs

Old score	New score	Description
1	0	No changes to the joint
>1-2	1	Light changes to the intervertebral joints and body
>2-3	2	Moderate changes to the intervertebral joints and body, can also include a mix of light and severe changes
>3-4	3	Severe changes to the intervertebral joints and body, including ankylosis

6.1.4.3 Spondylosis deformans

Spondylosis deformans describes degenerative age- or activity induced changes on the vertebral body. Due to deterioration of the intervertebral disc (*chondrosis intervertebralis*), the intervertebral space is being reduced, which in turn leads to a decrease in the ability of the disc to function as biomechanical buffer (Adler 2005; Rössler & Rüther 2005). The reduction and sometimes loss of the intervertebral disc leads to initial instability in the affected spinal segment, which usually leads to bad posture that is being constantly corrected by extensive use of the back musculature (Rössler & Rüther 2005). The disc degeneration is strongly linked to advancing age, with chemical changes in the composition of the disc, but also the constant daily stress put on the spine, favouring its degeneration (Roberts & Manchester 2010). The further reduction of the intervertebral space usually leads to the formation of marginal osteophytes on the vertebral body (Waldron 2009). Horizontally growing osteophytes are often called spondylophytes whilst vertically growing osteophytes are called syndesmophytes (Grupe *et al.* 2015). Severe cases of spondylosis deformans, can lead to a complete ankylosis of two or more vertebrae if the osteophytes on the vertebral margins fuse together. An ankylosis in the spine leads to stiffening, but also stabilisation of the affected spinal segment (Roberts & Manchester 2010), which is often associated with an easing of painful clinical symptoms in modern-day patients (Rössler & Rüther 2005). The degeneration of the disc can eventually also lead to changes on the surfaces of the affected vertebral bodies, with pitting and erosion and sometimes new bone formation considered to be the tell-tale signs (Roberts & Manchester

2010). Usually, degenerative changes in the spine are more common in men than in women (Adler 2005), and occur foremost in the lumbar and cervical spine (Waldron 2009).

6.1.4.3.1 Results

A total of 704 cervical vertebral bodies could be analysed for spondylosis deformans occurrence and severity. Of those, 237 (33.67%) displayed degenerative changes. Stage 1 degenerative changes were most common at 50.21%, followed by stage 2 changes (31.22%) and stage 3 changes (18.57%). At 36.89% (n=166), males were more affected by degenerative changes than females (30.56%; n=66), but the difference was statistically not significant (p=0.1083). No significant difference in occurrence was detected between the locations (cloister: 33.96%, n=54; cemetery: 34.59%, n=183; p=0.8832) but in Layer 1 (26.71%, n=78), individuals had significantly less spondylosis than in Layer 2 (40.15%; n=159) (p=0.0002). Differences between males and females in the occurrence of spondylosis deformans of the cervical vertebrae are overall not very marked. This also holds true when examining males and females by burial layer and location. However, females seem to experience more stage 2 and 3 changes in the 4th and 5th vertebra (Figure 71).

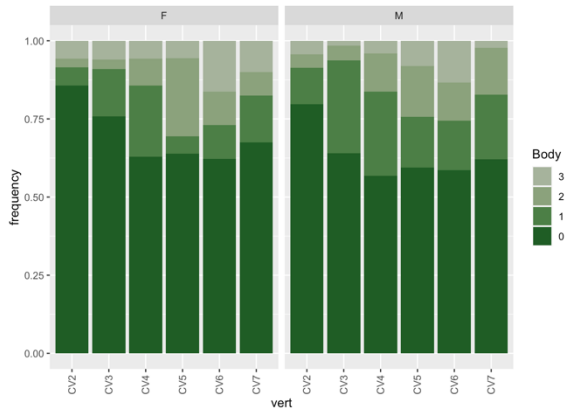

Figure 71 Frequency of spondylosis deformans in the cervical spine differentiated by sex

Overall, vertebrae CV4-CV7 seem to be most affected by spondylosis deformans than CV2 and CV3. The expression of stage 2 and 3 changes peaks at CV5 and CV6 and decreases again at CV7. Increased severity in the middle of the cervical spine, where flexibility is higher and a decrease towards the less flexible thoracic spine was expected. In fact, CV5 is often named as the most affected vertebra of the cervical spine due to its location at the peak of the forwards curve in the cervical area (Adler 2005).

Furthermore, a comparison of spondylosis deformans presence and absence and severity clearly shows a strong correlation with age (Figure 72), which reached statistical significance ($p<0.0001$). Overall, young adults (n=0) did not show any degenerative changes to the cervical vertebral bodies. In adults (16.76%, n=29), the majority of vertebrae were still unaffected but slight changes gained in frequency. Among matures I (26.61%, n=33), light changes to the vertebral bodies increased in frequency as well as moderate and more severe changes. Only in matures II (57.45%, n=81) and in seniles (63.95%, n=94), the majority of vertebrae showed some degree of degenerative change to the vertebral bodies, with moderate and severe changes dominating overall. The overall pattern observed among males and females also only becomes apparent in the matures and senile age groups. Here, the peak at CV4 and CV5 is very clear and a light but distinct decrease in severity can be observed from CV6 to CV7.

Seven individuals presented fusion of bones in the cervical spine, and of those, four concerned the fusion of two vertebrae. In 5 cases, the fusions were found in relation to strong degenerative changes in the surrounding vertebrae. Individual 2008-78/818 and 2008-78/1457, two mature males, showed complete ankylosis of the bodies and arches of the 4th and 4th cervical vertebrae. Individual 2008-78/541, a senile male, had the bodies and arches of the 5th and 6th cervical vertebrae fused and individual 2008-78/1480, a mature male, showed fusion of the bodies and arches of the 6th and 7th cervical vertebrae. Individuals 2008-78/1704 and 2016-082/186, two mature males, had each a pair of cervical ribs fused to the body and transverse processes of the 7th cervical vertebra. Individual 2008-78/1444, a mature male, showed a fused cervical rib on the right body side of the 7th cervical vertebra. An articular facet on the right body side suggests the presence of a right cervical vertebra as well but that one was not found during analysis.

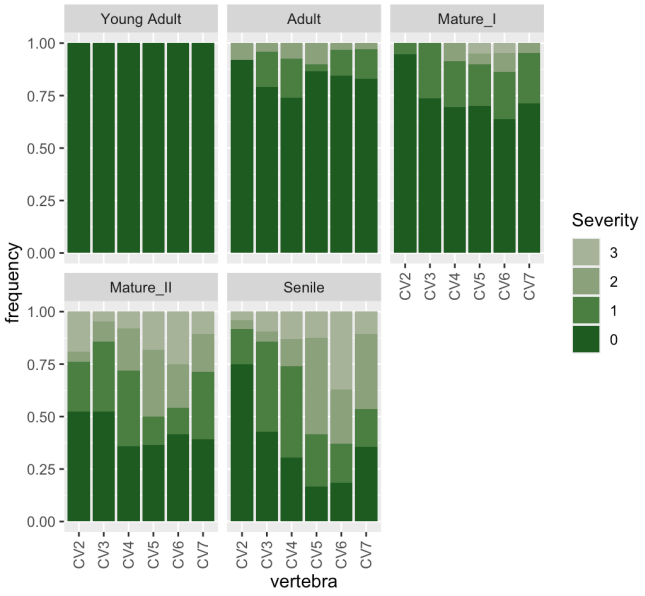

Figure 72 Frequency of spondylosis deformans in the cervical spine differentiated by age

A total of 1873 adult thoracic vertebral bodies could be examined for occurrence of spondylosis deformans, and of those, 47.41% (n=888) were affected by some degree of degenerative change. The majority of degenerative changes (73.65%) were of stage 1, followed by 22.41% of stage 2 and 3.94% of stage 3. For males 1198 bodies were analysed and 588 (49.08%) showed signs of degenerative changes and for females, 648 bodies were examined and 286 (44.14%) had traces of degenerative changes, this difference reached statistical significance (p=0.0422). 27 vertebral bodies belonged to individuals that could not be sexed. Regarding spondylosis deformans distribution in the thoracic spine, differences between males and females are generally not very marked and roughly follow the same trend. However, in women, the peak of affection lies at TV5 and TV6 and that of males between TV6 and TV9 and most specifically TV8. Males experience also more cases of stage 3 severity overall, especially around TV6-TV12 (Figure 73).

This comes as no surprise as some areas of the spine are more mobile than others. With the flexibility being highest in the middle of the thoracic spine, as most of the bending movements occur in this area, naturally use wear will also be highest there. In fact, TV8 is often considered to be the vertebra of the thoracic spine that is most affected by degenerative changes, as it is situated at the peak of the backwards curve of the spine (Roberts & Manchester 2010).

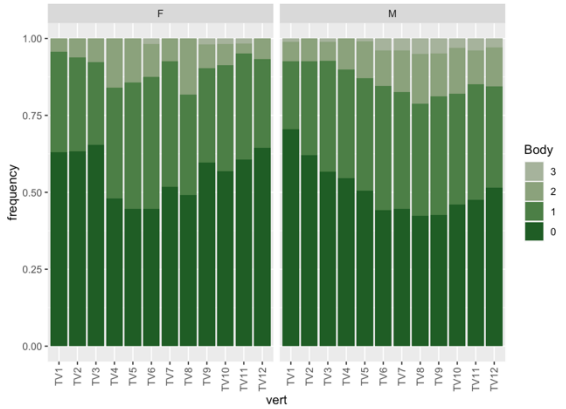

Figure 73 Frequency of spondylosis deformans in the thoracic spine differentiated by sex

As Figure 74 shows, there was a clear correlation between spondylosis deformans occurrence and age ($p<0.0001$). While young adults showed barely any degenerative changes (5.02%, n=13) and only of stage 1, the frequency increased visibly in adults (28.35%, n=148), although predominantly for light changes, in matures I (45.48%, n=166) about half of the vertebrae were affected and in matures II (72.85%, n=279) and seniles (85.45%, n=276) most of the vertebrae were affected, with severity also increasing considerably from the mature to the senile age category.

Furthermore, individuals buried in the cloister complex showed significantly more spondylosis deformans (58.64%, n=224) than those from the cemetery (44.53%, n=664) ($p<0.0001$), although this difference might be influenced by the higher prevalence of matures and seniles in the cloister complex. This is furthermore supported by the fact that the difference is only significant in men (cloister: 61.72%; cemetery: 45.04%; $p<0.0001$) but not in women (cloister: 51.16%; cemetery: 43.06%; $p=0.1588$). Moreover, individuals from Layer 2 had significantly more (52.05%, n=547) vertebrae affected than those from Layer 1 (41.48%, n=341)($p<0.0001$), which might either hint at changing habits concerning the use of the back or could also reflect the higher number of older matures and seniles in Layer 2.

Five cases of ankylosis were observed in the thoracic spine, whereas 3 concerned fusions of two vertebrae. All cases were found in relation to moderate or strong degenerative changes in the surrounding vertebrae. Individual 2008-78/516, a mature male, showed fusion of the bodies of the 11th and 12th thoracic vertebra through a large osteophyte on the right body side. Individual 2008-78/192, an adult female whose age could not be determined precisely, showed fusion of the arch and bodies of the 3rd and 4th thoracic vertebrae. Individual 2008-78/1021, a senile male, showed fusion of the 5th and 6th thoracic vertebral bodies and arches. In this case, both bodies were however collapsed and surrounded by heavy new bone formation. The

individual also presented with advanced osteomyelitis in the left femur and right scapula. The collapse of these vertebrae might therefore likely be the result of osteomyelitis, but in the absence of cloacae, and sequestrum, the diagnosis cannot be securely established.

Individual 2008-78/1065, a female senile, showed fusion of the left 12th rib to the transverse process of the 12th thoracic vertebra. Individual 2008-78/1444, a mature male had the 12th right rib fused to the 12th thoracic vertebra, resembling a lumbar vertebral transverse process on the right side. On the left side of the 12th thoracic vertebra however, no articular facet for the 12th rib was observed and no 12th rib was recovered, suggesting agenesis of the left 12th rib.

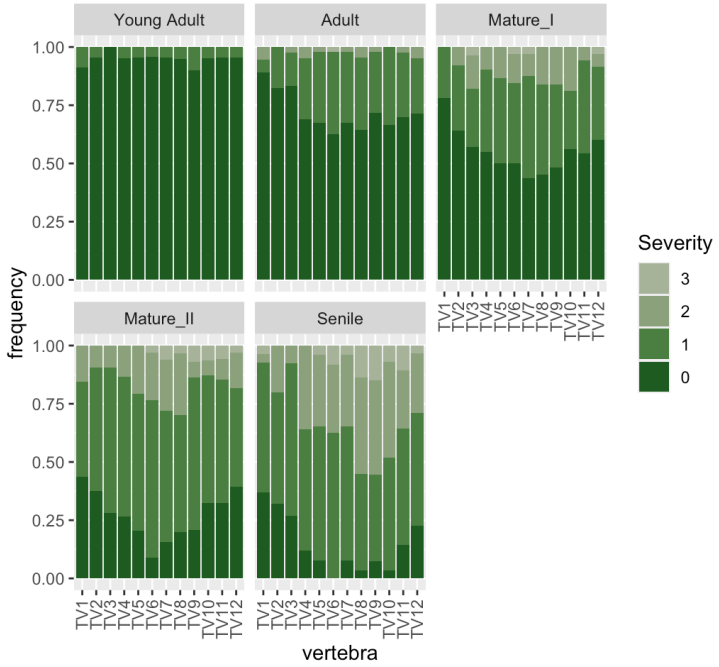

Figure 74 Frequency of spondylosis deformans in the thoracic spine differentiated by age

A total of 953 lumbar vertebral bodies were analysed and of those 406 (43.42%) showed signs of degenerative changes. For males, 578 bodies were examined and of those 257 (44.46%) had degenerative changes and for females, 342 bodies were analysed and of those 139 (40.64%) showed evidence of degenerative change. Although men showed slightly more vertebrae affected by spondylosis deformans than females, this difference was not statistically significant (p=0.2581). Among males and females, differences in the distribution of spondylosis deformans in the lumbar spine were not particularly marked, but females displayed more cases with higher severity than males. Overall, the frequency and degree of degenerative changes increases very slightly towards the caudal end of the lumbar spine (Figure 75). Being at the peak of the forward curve of the lumbar spine, LV4 is often noted as the vertebra most affected

by degenerative changes in the lumbar spine. The lumbar spine bears most of the body weight which makes it highly susceptible to degenerative processes (Roberts & Manchester 2010).

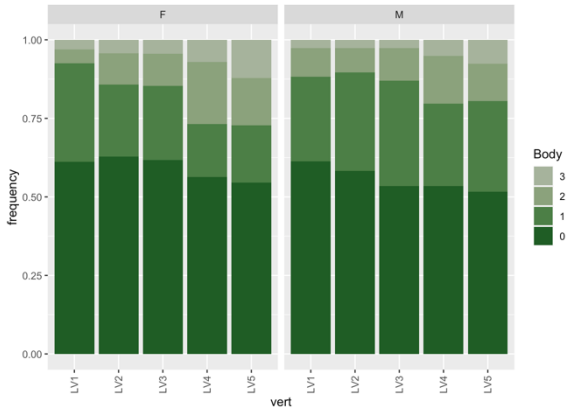

Figure 75 Frequency of spondylosis deformans in the lumbar spine differentiated by sex

Generally, as for all other parts of the spine, age had the highest correlation with spondylosis deformans, increasing in frequency and severity with old age ($p<0.0001$). young adults had barely any vertebrae affected (0.79%) and adults only slightly more (15.29%, n=39), but in matures I, about half of the vertebrae were concerned (49.48%, n=96) and among matures II (72.68%, n=133) and seniles (79.65%, n=137) most of the vertebrae had degenerative changes (Figure 76). Significant differences were also detected among the layers, with 52.06% of vertebrae from Layer 2 (n=278) affected but only 31.92% from Layer 1 (n=128) affected ($p<0.0001$), and between the burial locations, with cloister burials (n=118) showing significantly more (51.08%) affected vertebral bodies than cemetery burials (40.91%, n=288) ($p=0.0068$). Differences between burial locations were significant overall and within Layer 1 but not within Layer 2.

Two cases of ankylosis were observed in the lumbar spine, each time in relation to strong degenerative changes in the surrounding vertebrae. Individual 2008-78/917, a mature female showed fusion of the 2nd and 3rd lumbar vertebrae via a large osteophyte on the right body side. Individual 2008-78/1457, a mature male, next to the fusion in the cervical spine, also showed fusion of bodies and arches of the 4th and 5th lumbar vertebrae.

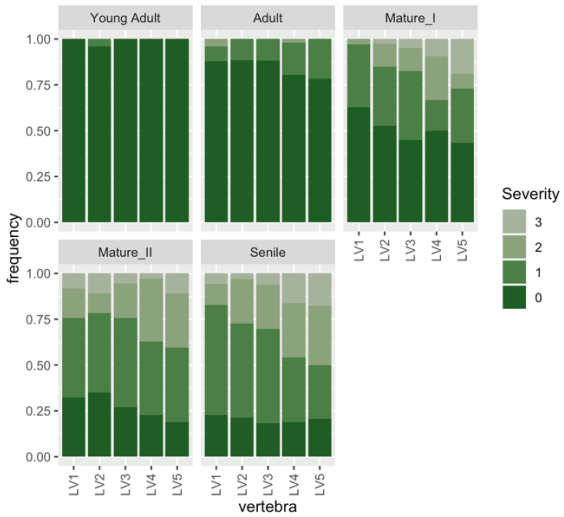

Figure 76 Frequency of spondylosis deformans in the lumbar spine differentiated by age

6.1.4.4 Spondylarthrosis deformans

The term spondylarthrosis deformans designates degenerative age- or activity related changes in the intervertebral joints of the spine (Adler 2005; Roberts & Manchester 2010).

6.1.4.4.1 Results

A total of 838 cervical intervertebral joint areas could be evaluated. Intervertebral joint areas were calculated from a score encompassing as many of the intervertebral joints available for each vertebra and will be referred to as IJA. Of those 838 IJA, 304 (36.28%) showed degenerative changes in at least one of the joints. Males (39.45%, n=217) had more IJA affected than females (29.48%, n=79), and the difference was statistically significant (p=0.0053). Overall, spondylarthrosis in the cervical spine shows similar trends than spondylosis deformans. In females, CV5 is affected the most and in males CV4, which corresponds to the peaks of the forward curvature of the cervical spine, which experiences most physical stresses (Adler 2005). Males seem to have more degenerative changes in the first and second vertebra than females (Figure 77).

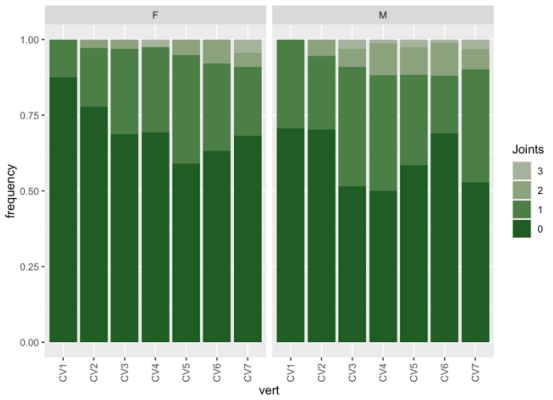

Figure 77 Frequency of spondylarthrosis deformans in the cervical spine differentiated by sex

Again, age showed the strongest correlation with spondylarthrosis, and this was expressed strongest in senile males, which showed the highest amount of and the most severe cases of spondylarthrosis ($p<0.0001$). (young adults: 13.16% (n=15), adults: 23.50% (n=51), matures I: 23.49% (n=35), Matures II: 45.29% (n=77), senile: 69.61% (n=126)) (Figure 78). Another significant difference yielded the comparison between the burial locations, with cloister burials (42.52%, n=91) presenting more vertebrae with spondylarthrosis than cemetery burials (34.13%, n=213) ($p=0.0276$). The difference was significant in males but not in females, although the trend was the same in both sexes. Layer 2 (39.79%, n=189) also presented with more vertebrae with spondylarthrosis than Layer 1 (31.68%, n=115) ($p=0.0156$). As already mentioned before, the differences observed might be due to the higher prevalence of men in the cloister and Layer 2 burials.

Individual 2013-015/191, a senile male buried in the cloister area showed ankylosis of the 5th and 6th cervical vertebrae through the left intervertebral articular facets. The fusion of these two vertebrae occurred in relation to strong degenerative changes in the joints and to a lesser degree also in the bodies of the previous and following vertebrae.

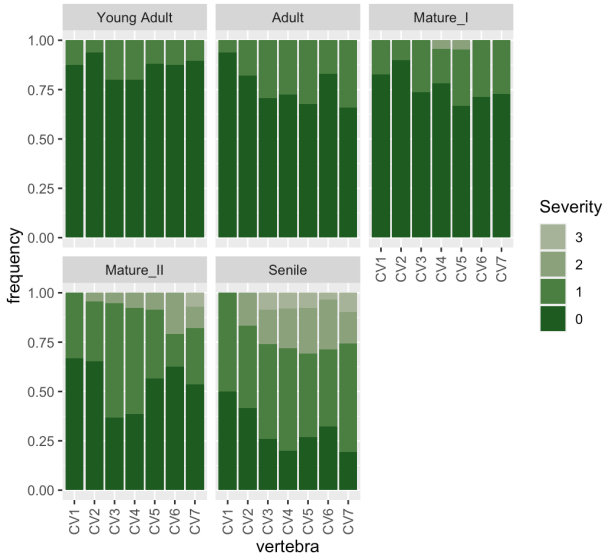

Figure 78 Frequency of spondylarthrosis deformans in the cervical spine differentiated by age

In the thoracic spine, 1973 IJA could be examined for spondylarthrosis and of those, 42.02% (n=829) showed traces of it. The trend of spondylarthrosis is slightly different from that of spondylosis. Whilst in spondylosis, generally the whole midsection of the thoracic spine was most affected, in spondylarthrosis it is mostly the upper midsection from ~TV4-TV6 and then the lower section from ~TV10-TV12, which might also be related to the curvature of the spine. No significant difference (p=0.0532) could be observed between males (43.77%) and females (39.77%) (Figure 79).

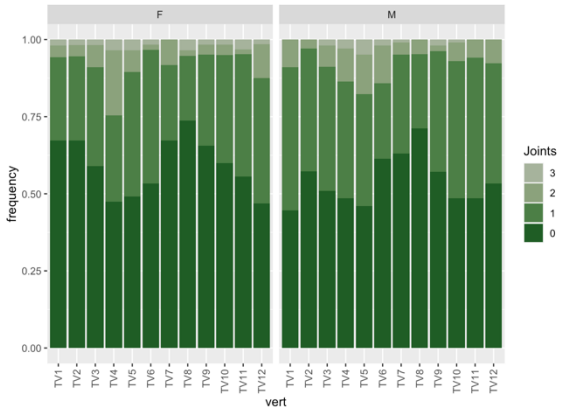

Figure 79 Frequency of spondylarthrosis deformans in the thoracic spine differentiated by sex

However, between the burial locations a significant difference (p<0.0001) was found between cloister complex and cemetery burials, with those buried in the cloister complex exhibiting more (52.85%, n=241) IJA with degenerative changes than those from the cemetery (38.76%, n=588). The difference was only significant in men, however. Vertebrae from Layer 2

displayed significantly more (45.57%, n=483) of degenerative changes on IJA than those from Layer 1 (37.90%, n=346) (p=0.0006) and the difference was only significant additionally in males. The same reasons as already mentioned before, namely the higher prevalence of matures II and seniles, especially males, in Layer 2 and in the cloister burials might have influenced the marked differences. Age also showed a strong correlation with age (p<0.0001). Young adults showed changes in 22.88% (n=62) of IJA and predominantly changes of stage 1, adults had 35.98% (n=190) IJA affected, matures I 37.72% (n=152), matures II 52.59% (n=213) and seniles 58.17% (n=203) (Figure 80).

Individuals 2008-78/670 and 2008-78/1483 showed fusion of the intervertebral joints in relation to strong degenerative changes in the surrounding vertebrae. 2008-78/670, an adult male whose age could not be exactly determined (adultus), presented a fusion of the 5th and 6th thoracic vertebrae through the right intervertebral articular facets. In 2008-78/1483, an adult female, the entire arches of the 4th and 5th thoracic vertebrae were fused via the left and right intervertebral joints.

Individual 2008-78/1457a (273B643), mature male, showed a complete fusion of the entire arches, including the intervertebral joints, rami and spinous process, of the 9th to the 10th thoracic vertebra. The fusion did not occur in relation to strong degenerative changes in the surrounding vertebrae, where changes were only light. Therefore, the fusion of the arches might have been caused by localised trauma, although no fractures or callus formation was observed, or might be congenital in origin.

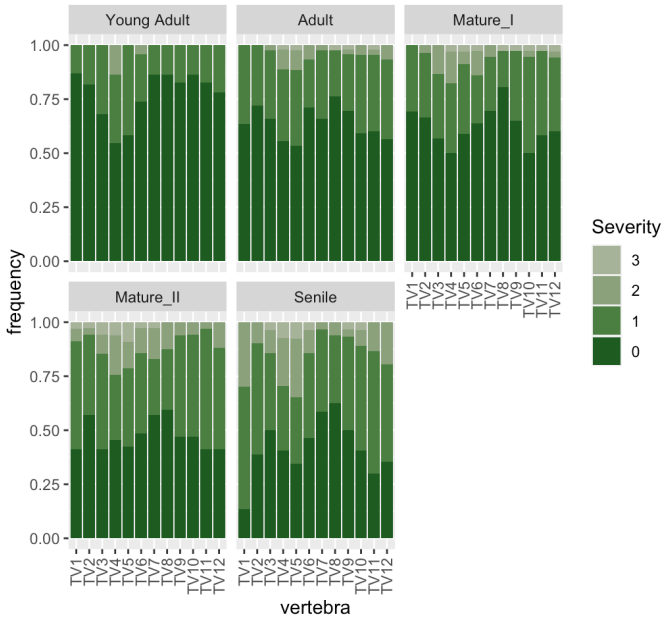

Figure 80 Frequency of spondylarthrosis deformans in the thoracic spine differentiated by age

For the lumbar spine, a total of 957 IJA could be analysed and 531 (55.49%) showed signs of spondylarthrosis. The trend of spondylarthrosis in the lumbar spine follows again that of spondylosis deformans, with cases increasing in frequency towards the caudal end of the spine (L4-L5). Males (56.51%, n=334) and females (53.82%, n=190) (p=0.4210) showed approximately the same amount of spondylarthrosis (Figure 81).

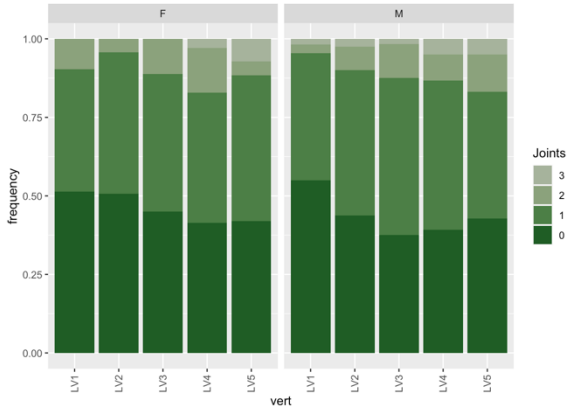

Figure 81 Frequency of spondylarthrosis deformans in the lumbar spine differentiated by sex

As already observed before, significant differences were detected among the burial locations and Layers, with individuals from Layer 2 (60.38%, n=317) and from the cloister (65.57%, n=160) displaying more signs of spondylarthrosis than those from Layer 1 (49.54%, n=214) and those from the cemetery (52.03%, n=371) (Layers: p=0.0008; Location: p=0.0002). In both comparisons, next to the overall trend, differences were only significant among men but not among women. These differences are most likely also due, as previously mentioned, to the higher prevalence of senile and mature men in Layer 2 and among cloister burials. As for the previous spinal segments, spondylarthrosis of the lumbar spine showed a strong correlation with age (p<0.0001). Young adults experienced least changes (10.77%, n=7) and predominantly changes of stage 1. Adults showed 37.36% (n=65) of spondylarthroses in the IJA, also predominantly of stage 1. In matures I, the cases of spondylarthrosis rise to 54.48% (n=68) and the severity increases as well. With 84.07% (n=95) and 85.45% (n=94) of vertebrae affected by spondylarthrosis, matures II and seniles were most affected and showed the most severe cases, but stage 1 was still the dominating expression (Figure 82).

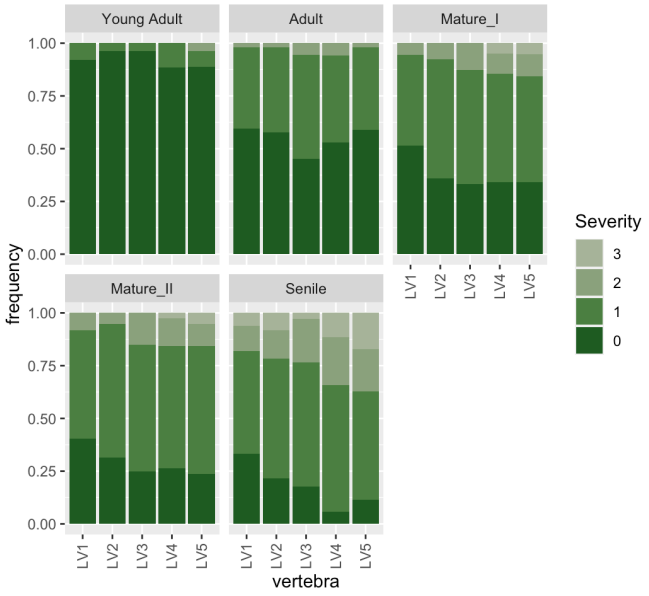

Figure 82 Frequency of spondylarthrosis deformans in the lumbar spine differentiated by age

6.1.4.5 Frequency and severity of degenerative joint disease in the spine

Lastly, to get a better idea of the overall degree of degenerative joint disease in the spine, a combined score for the small joints and body was calculated for all vertebrae present.

This severity code was then also calculated for the whole cervical spine. The following Table 70 illustrates the mean severity codes for the cervical (CV), thoracic (TV) and lumbar (LV) spine and compares them across the different groups. N represents the number of individuals with scoreable spine sections included in the comparison. Score indicates the combined score for all scorable small joints and bodies for all available vertebrae of the respective sections of the spine. Like the occurrence of spondylosis and spondylarthrosis deformans, the overall vertebral severity scores show the strongest correlation with age in all spinal segments, with young adults showing the lowest degree of severity and seniles the highest. In all age categories and overall, arthrosis in the cervical and thoracic spine is less severe than in men but the difference is not statistically significant. The opposite trend was observed for the lumbar spine but also this difference was not statistically relevant. The same trends, concerning differences between burial locations and layers, already observed in frequency of spondylosis and spondylarthrosis of the thoracic and lumbar spine could be observed in regard to severity. Individuals from cloister burials and from Layer 2, especially men in both cases, had significantly more severe arthritis than those from the cemetery and from Layer 1, and females did not show any relevant differences. As previously mentioned, the differences are likely caused by a higher prevalence of matures and seniles, mainly men, in the cloister complex and Layer 2 burials.

Overall, the people buried in the Knuedler cemetery did not suffer from strong degrees of arthrosis in the spine. As 1 represents no degenerative changes, most individuals had only very light degrees of arthritis and/or that not many vertebrae within the respective segments were affected. This might indicate that they were not exposed to a lot of physical stresses related to strenuous activity during life, and that natural degenerative processes through age were the main cause for degenerative joint disease in the spine. (Table 70)

Table 70 Summary and test results for the severity code combining data for spondylarthrosis and spondylosis deformans by spinal section

Groupings			CV			TV			LV		
			n	score	p-value	n	score	p-value	n	score	p-value
All			166	1.37		216	1.43		222	1.57	
Sex	F		54	1.29	0.1262	79	1.40	0.2871	81	1.60	0.7233
	M		107	1.41		131	1.46		136	1.55	
Age	All	Young adult	21	1.04	**<0.0001**	26	1.10	**<0.0001**	29	1.04	**<0.0001**
		Adult	42	1.14		56	1.25		58	1.26	
		Mature I	32	1.20		44	1.37		46	1.60	
		Mature II	36	1.50		46	1.60		45	1.80	
		Senile	34	1.88		40	1.81		42	2.05	
	F	Young adult	10	1.01	**0.0019**	13	1.10	**0.0021**	14	1.02	**<0.0001**
		Adult	11	1.13		18	1.31		19	1.36	
		Mature I	9	1.22		16	1.42		16	1.85	
		Mature II	13	1.37		19	1.53		19	1.75	
		Senile	11	1.68		12	1.67		13	1.98	
	M	Young adult	11	1.06	**<0.0001**	13	1.09	**<0.0001**	15	1.05	**<0.0001**
		Adult	31	1.14		38	1.23		39	1.21	
		Mature I	22	1.20		26	1.35		29	1.49	
		Mature II	22	1.59		27	1.65		25	1.83	
		Senile	21	2.01		26	1.89		27	2.09	
Location	All	Cloister	44	1.46	0.3278	54	1.52	**0.0447**	57	1.74	**0.0140**
		Cemetery	122	1.33		162	1.42		165	1.51	
	F	Cloister	9	1.19	0.8948	15	1.42	0.5163	16	1.67	0.7782
		Cemetery	45	1.32		64	1.40		65	1.57	
	M	Cloister	32	1.56	0.2119	37	1.58	**0.0282**	38	1.78	**0.0046**
		Cemetery	75	1.34		94	1.42		98	1.47	
Layer	All	1	75	1.32	0.4340	96	1.35	**0.0237**	97	1.45	**0.0084**
		2	91	1.40		120	1.52		125	1.66	
	F	1	20	1.21	0.3993	30	1.38	0.3171	31	1.45	0.1370
		2	34	1.34		49	1.41		50	1.68	
	M	1	52	1.37	0.1788	63	1.33	**0.0047**	63	1.44	**0.0163**
		2	55	1.43		68	1.59		73	1.65	

Regarding the prevalence of arthritic changes in the different spinal segments by individual, significant differences were only detected between the age groups for all spinal segments and between burial locations for the lumbar spine. In all spinal segments, prevalence of degenerative joint disease increased strongly with age. However, in young adults changes in the thoracic spine (46.15%) were already noticeably more prevalent than in the cervical spine (28.81%) or in the lumbar spine (13.79%). Moreover, individuals buried in the cloister (84.21%) complex displayed significantly more arthritic changes in the lumbar spine than those

buried in the cemetery (70.30%) (p=0.0394). The differences were significant for the groups in general and for males but not for females. The same trends can be observed in the cervical and thoracic spines, but they do not reach statistical significance. Finally, more than half of the individuals from the Knuedler cemetery show signs of degenerative joint disease in the different spinal segments. This prevalence is not only caused by the high amount of mature and senile individuals in the sample as adults also show a higher prevalence. A high frequency of arthritic changes of the spine usually indicates higher load of physical activity. Past populations in general show more arthritic changes in the spine than modern ones due to their generally more active lifestyles (Roberts & Manchester 2010). The overall low severity grades, which are only more notable in the mature and senile age categories and only quite light in the young adult and adult age groups suggests that physical load was not terribly extensive however, even if most of the people buried on the cemetery were exposed to it. (Table 71)

Table 71 Frequency of Spondylosis and Spondylarthrosis by spinal sections

Groupings			CV			TV			LV		
			n	present	p-value	n	present	p-value	n	present	p-value
All			166	109 (65.66%)		216	170 (78.70%)		222	164 (73.87%)	
Sex	F		54	32 (59.26%)	0.1692	79	59 (74.68%)	0.2275	81	59 (72.84%)	0.7250
	M		107	75 (70.09%)		131	107 (81.68%)		136	102 (75.00%)	
Age	All	Young adult	21	5 (28.81%)	**<0.0001**	26	12 (46.15%)	**<0.0001**	29	4 (13.79%)	**<0.0001**
		Adult	42	25 (59.52%)		56	40 (71.43%)		58	36 (62.07%)	
		Mature I	32	19 (59.38%)		44	37 (84.09%)		46	41 (89.13%)	
		Mature II	36	28 (77.78%)		46	41 (89.13%)		45	41 (91.11%)	
		Senile	34	32 (94.12%)		40	38 (95.00%)		42	41 (97.62%)	
	F	Young adult	10	2 (20.00%)	**0.0263**	13	6 (46.15%)	**0.0429**	14	2 (14.29%)	**<0.0001**
		Adult	11	7 (63.64%)		18	12 (66.67%)		19	14 (73.68%)	
		Mature I	9	4 (44.44%)		16	14 (87.50%)		16	15 (93.75%)	
		Mature II	13	10 (76.92%)		19	17 (89.47%)		19	16 (84.21%)	
		Senile	11	8 (81.82%)		12	10 (83.33%)		13	12 (92.31%)	
	M	Young adult	11	3 (27.27%)	**<0.0001**	13	6 (46.15%)	**0.0005**	15	2 (13.33%)	**<0.0001**
		Adult	31	18 (58.06%)		38	28 (73.68%)		39	22 (56.41%)	
		Mature I	22	15 (68.18%)		26	22 (84.62%)		29	26 (89.66%)	
		Mature II	22	18 (81.82%)		27	24 (88.89%)		25	24 (96.00%)	
		Senile	21	21 (100%)		26	26 (100%)		27	27 (100%)	

Location	All	Cloister	44	30 (68.18%)	0.6814	54	46 (85.19%)	0.1792	57	48 (84.21%)	**0.0394**
		Cemetery	122	79 (64.75%)		162	124 (76.54%)		165	116 (70.30%)	
	F	Cloister	9	6 (66.67%)	0.7230	15	13 (86.67%)	0.3311	16	12 (75.00%)	1.0000
		Cemetery	45	26 (57.78%)		64	46 (71.88%)		65	47 (72.31%)	
	M	Cloister	32	23 (71.88%)	0.7926	37	32 (86.49%)	0.3722	38	34 (89.47%)	**0.0152**
		Cemetery	75	52 (69.33%)		94	75 (79.79%)		98	68 (69.39%)	
Layer	All	1	75	48 (64.00%)	0.6821	96	88 (78.12%)	0.8526	97	69 (71.13%)	0.4130
		2	91	61 (67.03%)		120	95 (79.17%)		125	95 (76.00%)	
	F	1	20	11 (55.00%)	0.6252	30	24 (80.00%)	0.3951	31	22 (70.97%)	0.7655
		2	34	21 (61.71%)		49	35 (71.43%)		50	37 (74.00%)	
	M	1	52	36 (69.23%)	0.8030	63	49 (77.78%)	0.2665	63	45 (71.43%)	0.3716
		2	55	39 (70.91%)		68	59 (85.29%)		73	57 (78.08%)	

6.1.4.6 Schmorl's nodes

The intervertebral disc consists of a central part called nucleus pulposus and the fibrocartilaginous annulus fibrosus, and both structures are separated from the adjacent vertebral end plates by a thin hyaline layer called cartilaginous endplate (Moon *et al.* 2013). When the nucleus pulposus herniates through the often already weakened or ruptured cartilaginous and bony endplates and penetrates into the vertebral body, the resulting lesion is called Schmorl's node (Üstündag 2009; Waldron 2009; Dar *et al.* 2010). Therefore, the presence of Schmorl's nodes is generally associated with the degeneration of the intervertebral disc, and mainly damage to the cartilaginous endplates (Üstündag 2009; Roberts & Manchester 2010), either through trauma, activity- or age-related processes. However, congenital defects, such as Scheuermann's kyphosis, have also been linked to the formation of Schmorl's nodes (Faccia & Williams 2008). They occur most frequently in the lower thoracic and lumbar spine and their aetiology is still under debate, but next to developmental problems in the intervertebral disc area, acute trauma and several pathological conditions, heightened stress on the spine, which is usually activity related ,is often considered as the main cause of their formation (Üstündag 2009; Waldron 2009). Modern medical literature suggests that Schmorl's nodes are mostly painless, but some cases of painful Schmorl's nodes have been described as well (Kyere *et al.* 2012).

6.1.4.6.1 Results

In the cervical spine, Schmorl's nodes are a very rare occurrence, with only a total of (3.87%) cases for the whole cervical area regardless of sex or age. Differences between males (5.19%) and females (2%) are also not very marked. The occurrence of Schmorl's nodes also does not seem to be related strongly to age in this area and the few Schmorl's nodes that were observed were all of very light expression. The absence/presence score for Schmorl's nodes of the complete cervical spine overall did not show any significant differences in distribution between any of the groups. The occurrence of Schmorl's in the cervical area was also not related to age (Table 72, Figure 83, Figure 84).

Schmorl's nodes CV

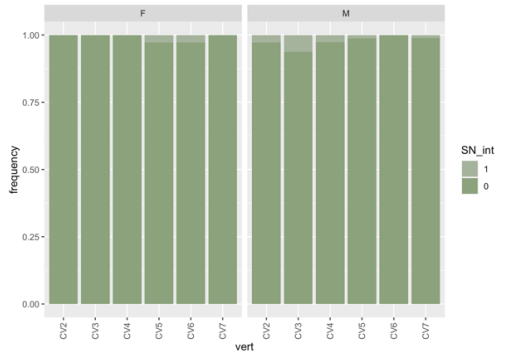

Figure 83 Prevalence of Schmorl's nodes in the cervical spine, differentiated by sex

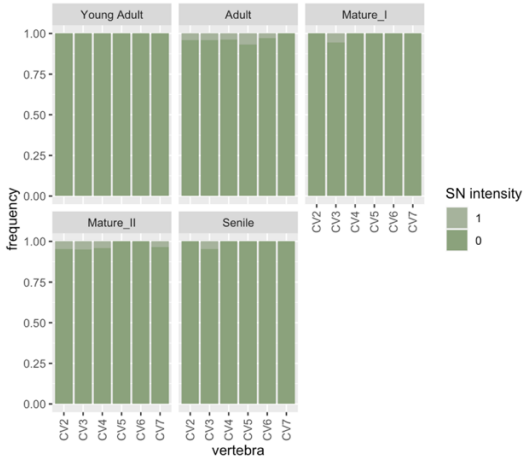

Figure 84 Prevalence of Schmorl's nodes in the cervical spine, differentiated by age

In the thoracic spine however, the amount of Schmorl's nodes increases significantly (60.19%). As can be seen in the graphs, Schmorl's nodes were more frequent and more severe towards the caudal end of the thoracic spine, which also corresponds approximately with the areas of most frequent spondylosis and spondylarthrosis occurrence. Males (68.75%) experienced significantly more frequent and more severe Schmorl's nodes than females (48%), with frequencies being similar among men and women towards the cranial end of the thoracic spine and then increasing rapidly and strongly in men towards the lower end (Table 72, Figure 85). As can be deduced from Figure 86, the severity and occurrence of Schmorl's nodes, in contrast to the degenerative joint disease, does not show a strong relation with age. Of note is however, that males developed Schmorl's nodes already to a higher extent as young adults, which might indicate early differences in labour division between the sexes. No particularly relevant

differences could also be detected among the burial locations, where the occurrence of Schmorl's nodes was only slightly higher in females from the cemetery (50.79%) than those from the cloister (33.33%), or between the burial layers, where occurrence and severity was only slightly higher in Layer 1 (70.49%) than in Layer 2 (67.16%) among males. In Layer 1, cemetery burials (62.32%) were generally more affected than cloister burials (56.52%) and in layer 2 the opposite trend could be observed (cemetery: 60.22%, cloister 57.69%) but the differences were not very marked and statistically not significant (Table 72).

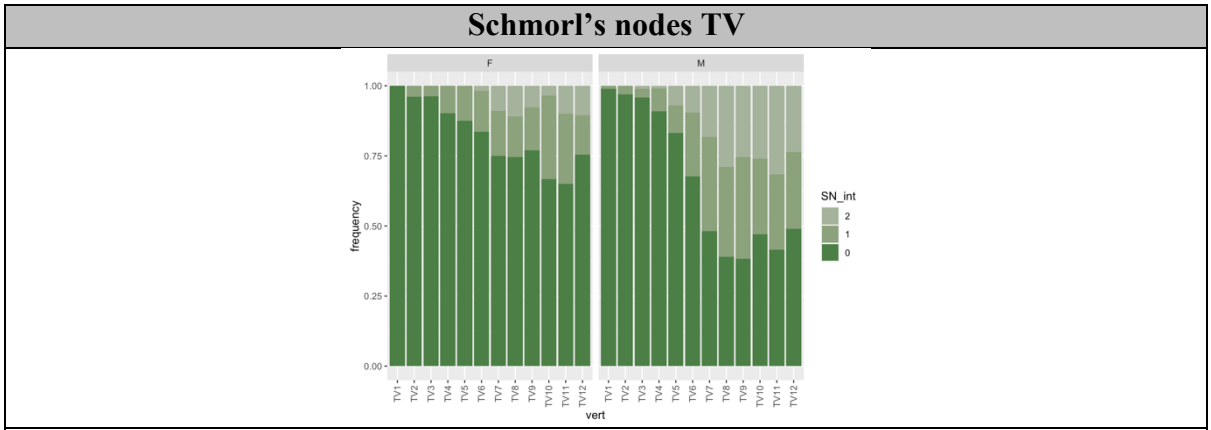

Figure 85 Prevalence of Schmorl's nodes in the thoracic spine, differentiated by sex

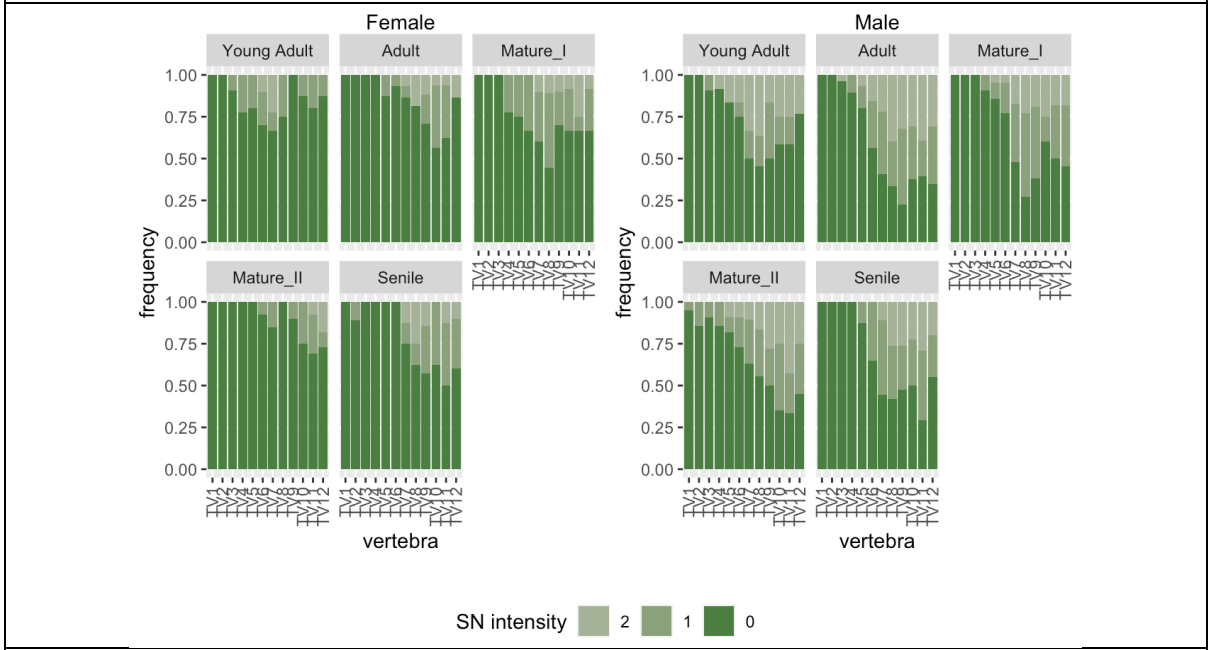

Figure 86 Prevalence of Schmorl's nodes in the thoracic spine, differentiated by sex and age

In the lumbar spine, Schmorl's nodes are more frequent (36.36%) than in the cervical spine but less frequent than in the thoracic spine. They occur significantly more frequently in men (43.85%) than in in women (23.29%) (Table 72, Figure 87). A direct correlation with age could not be observed, but in men, Schmorl's nodes occur more frequently in all age groups (Figure

88). Females showed slightly but insignificantly more severe, and more frequent Schmorl's nodes in Layer 2 (30.43%) than in Layer 1 (11.11%) and in men they occurred slightly more often and were slightly more severe in Layer 2 (46.38%) than in Layer 1 (40.98%). Cemetery burials (39.87%) generally presented with more Schmorl's nodes than cloister burials (25.49%), but the difference was statistically insignificant, except in Layer 1, where significantly more people from the cemetery (37.68%) presented with Schmorl's nodes than those from the church (9.09%) (Table 72).

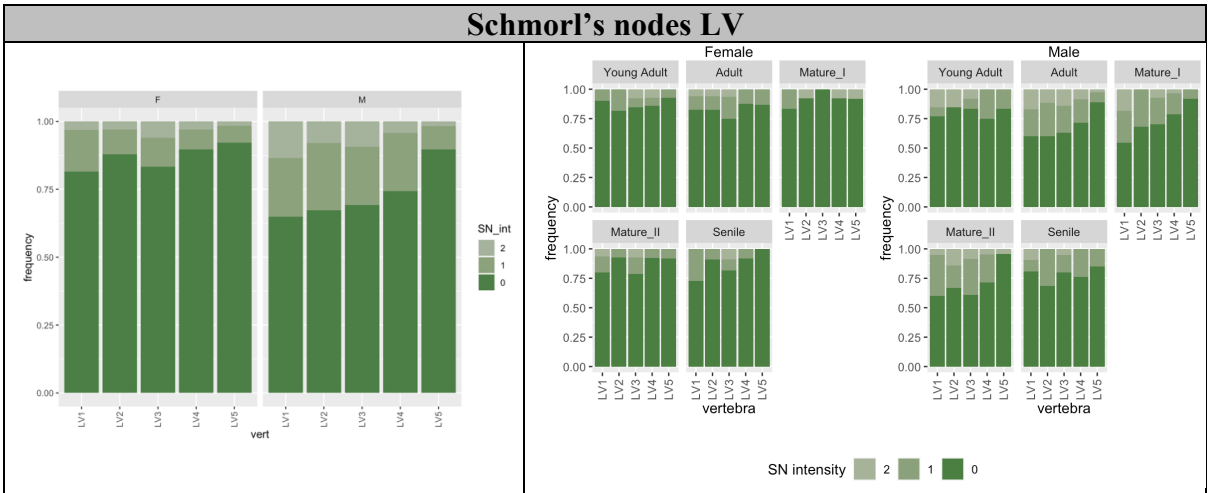

Figure 87 Prevalence of Schmorl's nodes in the lumbar spine, differentiated by sex

Figure 88 Prevalence of Schmorl's nodes in the lumbar spine, differentiated by sex and age

Table 72 Percentage of individuals affected by Schmorl's nodes by spinal section

Groupings		CV-SN			TV-SN			LV-SN		
		n	present	p-value	n	present	p-value	n	present	p-value
Sex	F	50	1 (2.00%)	0.6641	75	36 (48.00%)	**0.0034**	73	17 (23.29%)	**0.0035**
	M	98	5 (5.10%)		128	88 (68.75%)		130	57 (43.85%)	
Location	Cemetery	121	5 (4.13%)	1.0000	162	99 (61.11%)	0.6190	158	63 (39.87%)	0.0634
	Cloister	34	1 (2.94%)		49	28 (57.14%)		51	13 (25.49%)	
Age	Young Adult	21	0 (0.00%)	0.9239	26	12 (46.15%)	0.5132	29	9 (31.03%)	0.8787
	Adult	38	2 (5.26%)		56	36 (64.29%)		56	23 (41.07%)	
	Mature I	28	1 (3.57%)		41	27 (65.85%)		43	14 (32.56%)	
	Mature II	32	2 (6.25%)		42	24 (57.14%)		41	15 (36.59%)	
	Senile	32	1 (3.12%)		39	24 (61.54%)		37	14 (37.84%)	
Layer	1	64	4 (5.88%)	0.6632	92	56 (60.87%)	0.8592	91	28 (30.77%)	0.1398
	2	85	2 (2.30%)		119	71 (59.66%)		118	48 (40.68%)	

6.1.5 DISH

6.1.5.1 Introduction

DISH stands for Diffuse Idiopathic Skeletal Hyperostosis and is also commonly referred to as "Morbus Forestier" (Waldron 2009). As the name already indicates, the aetiology of DISH remains unknown but hormonal disturbances might play a role in its development as a link between dish and obesity and Type II Diabetes could be established in various studies (Rogers & Waldron 2001; Sencan *et al.* 2005; Mader & Lavi 2009; Waldron 2009; Merashli *et al.* 2015). Characteristic for DISH is the ossification of the anterior longitudinal ligament and sometimes also other ligaments of the spine, whereas the posterior longitudinal ligament is often not involved. Usually, the condition spans several vertebrae and may even affect the whole spine. Typically, ethe ossified anterior longitudinal ligament looks like melted candle way flowing down the right side of the vertebral bodies. Characteristic is also that the intervertebral space and joints are not involved. Extra-spinal characteristics include the formation of bone spurs at entheses and ligaments, which occur predominantly on the calcaneus, olecranon of the ulna and the patella (Forestier & Rotes-Querol 1950; Waldron 1985, 2009; Aufderheide & Rodriguez-Martin 1998; Rogers & Waldron 2001).

6.1.5.2 Results and Discussion

One individual with DISH was observed among the individuals buried in the Knuedler cemetery. Individual 2008-78/536, a mature II male presented with the typical right-sided candle wax -like ossification of the anterior longitudinal ligament between the 6th and 10th thoracic vertebrae (Figure 89, Figure 90). Large and smooth right-sided osteophytes were also observed on the 11th and 12th vertebrae but no ankylosis occurred. The intervertebral disc spaces were not involved, and the intervertebral joints were not fused either and only showed light degenerative changes. Furthermore, a large bone spur was observed at triceps muscle insertion of the right ulna and at the interosseous crest of the right radius. The left radius and ulna showed lighter osteophyte formation at the interosseous crest and olecranon respectively, whilst light-moderate osteophytes were recorded around the right and left acetabular rims. All these manifestations correspond to the diagnostic criteria set out in Waldron (2009).

Rogers and Waldron (2001) and Waldron (1985) concluded that DISH was especially prevalent among monks and that this could be related to potential obesity due to the copious amounts of food that were served in monasteries and the rather high standard of living of the monks. This could also have been the case for individual 2008-78/536, as certainly friars from the

Franciscan monastery were also buried in the cemetery belonging to the convent. However, it has to be kept in mind that the Franciscan monks were part of a mendicant order, which generally followed a more ascetic lifestyle (Montford 2002).

Diffuse Idiopathic Skeletal Hyperostosis (DISH)	
Figure 89 DISH in 2008-78/536 with sparing of the intervertebral disc space (anterior view)	*Figure 90 DISH in 2008-78/536 (right lateral view)*

6.1.5.3 Discussion

The spine carries the majority of the human head and body weight and adopts a stabilizing and cushioning function while standing, walking and running. Whilst back muscles and ligaments as well as an elaborate joint system ensure stability and mobility in the spine, the intervertebral disc bears the brunt in cushioning shocks that occur during daily activities. Due to chemical age-related processes through which the intervertebral disc loses its elasticity and through over- or misloading, damage can occur to the intervertebral disc, which in turn reduces the intervertebral space and can eventually lead to osteophyte formation on the margins of the vertebral bodies and cause degenerative changes in the intervertebral joints (Menninger & Waibel 1996; Adler 2005; Rössler & Rüther 2005; Roberts & Manchester 2010). The disc degeneration is strongly linked to advancing age, with chemical changes in the composition of the disc, but the constant daily stress put on the spine can favour and speed up its degeneration (Roberts & Manchester 2010). As such, intensity and frequency of degenerative changes in the spine can provide information on overall workload and intensity of past populations (Liebert *et al*. 1971; Schultz 1982; Stirland & Waldron 1997; Sofaer Derevenski 2000; Larsen 2015).

Overall, the distribution of degenerative changes in the spine follows the expected pattern that many studies have also observed (Caselitz 1983; Knüsel *et al*. 1997; Ittrich 2004; Stech 2009; Kairies 2021). Due to the double-S-curvature of the spine, areas of maximum and minimum stress exist along the spinal column, with those areas at the peak of the curvatures being exposed to the highest load and also being the most mobile areas. Generally, the 5th and 6th cervical, 8th thoracic and 4th lumbar vertebrae are strongest and most commonly affected by degenerative changes (Roberts & Manchester 2010), a pattern that was also clearly discernible in the population from Knuedler. The lumbar and cervical spine, which are considered to be the most mobile spinal segments, are usually most strongly affected by degenerative changes (Figure 91, Figure 92). These areas are mostly responsible for lateral-, dorsal- and ventral flexion as well as for rotational movements. The thoracic spine, especially the area of the upper vertebrae (TV1-TV5), is considered to be the least flexible part (Güntz 1958). In the Knuedler cemetery though, the thoracic spine showed the highest frequency of combined spondylosis and spondylarthrosis deformans, followed by the lumbar and cervical areas. Furthermore, as for the Emden individuals (Stech 2009), in females, the peak frequency of degenerative changes in the thoracic spine was between TV4-5, which are generally considered less mobile. Stech (2009) attributes this pattern to a potential over- or misloading of the spine in females and therefore as a sign for different activities or workloads between men and women. Regarding the similarity of the pattern distribution, this interpretation could also apply for females of the Knuedler sample. Differences between the sexes, in activity intensity at least, have already been suggested by differences in frequency and intensity of joint disease of the large articulations. A statistically significant difference in spondylosis deformans frequency between men and women in the thoracic spine lends further weight to this interpretation. However, a study by Duncan et al. (2012) on recent human data showed that women had a different pattern of degenerative changes in the spine, with higher osteophytosis scores occurring in the midthoracic region (TV6-8) than in men (Duncan *et al*. 2012). This could suggest that females generally show different distribution of degenerative changes in the spine. Overall however, the frequency and intensity of degenerative changes increases caudally for every spinal segment (cervical, thoracic and lumbar), a pattern which is characteristic for degenerative changes of the spine (Caselitz 1983). The same pattern is also observed for Schmorl's nodes which show highest frequency and intensity in the lower thoracic and lumbar spine, a pattern also observed by Dar et al. (2011) and Üstündag (2009) and is likely due to increased load bearing in that area.

Examples of degenerative changes in the spine	
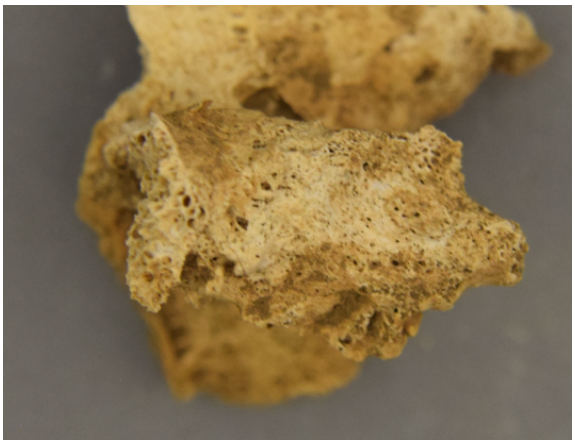	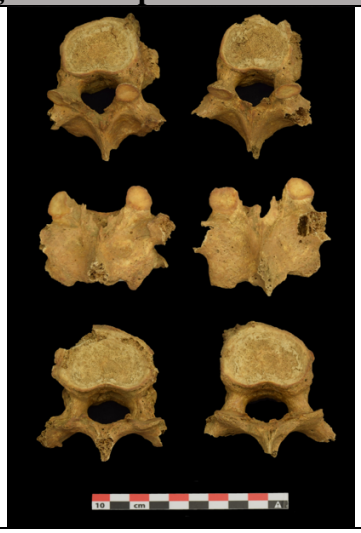
Figure 91 Osteoarthritis in the right inferior intervertebral joint of a lumbar vertebra (2008-78/670)	*Figure 92 Degenerative changes in the lower thoracic vertebrae (spondylophytes) (2008-78/1021)*

Generally, males showed stronger and more frequent degenerative changes in all spinal segments. This concerns spondylosis deformans, spondylarthrosis deformans, as well as their cooccurrence, but only sex differences for spondylosis deformans in the thoracic spine reached statistical significance. This is in line with what other studies on contemporaneous archaeological remains concluded as well (Sofaer Derevenski 2000; Stech 2009; Trautmann 2012; Roßbach 2015; Kairies 2021), and generally suggests that men were engaged in more strenuous activities on a daily basis. This same pattern was also reflected in the intensity and prevalence of degenerative joint disease, which further supports this interpretation. The same trend was also observed for the occurrence of Schmorl's nodes and even reached statistical significance in the thoracic and lumbar spinal segments. This is in agreement with studies by Trautmann (2012) for a medieval rural Luxembourgish site and by Üstündag (2009) for a 16th -18th century Cistercian cemetery from Austria. The aetiology of Schmorl's nodes is still under debate, with trauma, overloading of the vertebrae or congenital weakening being cited as possible causes (Üstündag 2009; Dar *et al*. 2010). However, osteoporosis might also contribute to the development of Schmorl's nodes, as it renders the bone weak and brittle, and the endplates might break easier under the pressure of the protruding disc fragment. Since osteoporosis occurs more frequently in women (Adler 2005; Bonnick 2006), next to differences in daily labour, this condition might also contribute to the higher frequency of Schmorl's nodes in women.

In the Knuedler population, age consistently shows a strong correlation with degenerative changes in the spine, which was to be expected as even today age-related wear and naturally

occurring loss of elasticity of the intervertebral disc is thought to be the main cause for the development of degenerative spinal disease (Menninger & Waibel 1996; Adler 2005; Waldron 2009; Roberts & Manchester 2010). The same pattern was also observed among the contemporaneous comparative samples (Stech 2009; Timmermann 2009; Trautmann 2012; Roßbach 2015; Kairies 2021). The frequency of Schmorl's nodes did not show a significant correlation with age. Only young adults had slightly less often Schmorl's nodes but the frequency in the adult, mature and senile age groups was very similar across all spinal segments. Several studies have also suggested that Schmorl's nodes, unlike other degenerative spinal pathologies, are not age-dependent (Timmermann 2009; Üstündag 2009; Trautmann 2012).

In order to test whether there were any differences between groups of different social status, the frequency and severity of degenerative changes was assessed for individuals buried in the cemetery and those buried inside the cloister complex. Concerning spondylosis deformans and spondylarthrosis deformans, individuals from the cloister were generally more affected than those from the cemetery, but no statistical significance could be reached. In contrast, individuals from the cemetery showed a higher frequency of Schmorl's nodes among all sections of the spine and statistical significance was reached for comparisons by individual affected by at least one Schmorl's node (cloister: 48.10%; cemetery: 56%; p=0.0084). As already noted for the differences in degenerative joint disease of the long bone articulations, the age distribution between the two burial locations has to be considered as well. Therefore, the overall prevalence of mature and senile individuals among the cloister burials might have contributed to the overall higher frequency of degenerative vertebral changes. Knüsel et al. (1997) also tried to assess differences between individuals of different social status by comparing priory burials to cemetery burials from the Gilbertine Priory of St. Andrew, Fishergate, York. No statistically significant differences were found between the burial sites, which led to the conclusion that degenerative changes in the spine (Spondylosis and spondylarthrosis deformans) were no suitable proxies to assess differences in physical activities between groups. However, since Schmorl's nodes are not as strongly age-related, they might be more suitable to assess differences in activity patterns between the two groups, which might suggest then, that individuals buried in the cemetery were exposed to more mechanical stress to the spine than those from the cloister.

Due to differences in scoring methods, direct cross-site comparisons are difficult and need to be considered with care. Nevertheless, an attempt was made in order to put the results obtained

for the Knuedler population into perspective. In all spinal segments, the prevalence of Schmorl's nodes among the Knuedler population was lower than that observed in Grevenmacher (Trautmann 2012), and at 80.9% overall, more individuals were affected in Grevenmacher than in Luxembourg City (60.24%) which might suggest that individuals from the Knuedler cemetery were less exposed to strenuous physical activities that put stress on the spine, such as carrying heavy loads on a daily basis (Sofaer Derevenski 2000). This difference would reflect the fact that urban populations are generally less exposed to strenuous activities than rural populations. For the urban population of Emden (Stech 2009), only overall frequency for Schmorl's nodes as available and the score lay at 46.8% for women and 60.7% for men. In the Knuedler assemblage, the frequencies amounted to 53.33% for women and 64.15% for men and are therefore very similar although slightly higher than those from Emden. This might suggest that the individuals buried in the Knuedler cemetery were exposed to more stress to the vertebral column than the Emden population. Compared to burials from the Cistercian priory of Klostermarienburg in Austria (31.4%) (Üstündag 2009), prevalence in Schmorl's nodes in Luxembourg City was almost double as high, which would suggest that they experienced more mechanical stress to the spine. Regarding frequency of spondylosis and spondylarthrosis, when compared to urban Ellwangen-Jagst, the frequencies observed in the Knuedler cemetery across all spinal segments for the different age groups is fairly similar, suggesting exposure to similar amounts of mechanical stress to the spine. In the Knuedler cemetery, overall frequency for spondylosis deformans and spondylarthrosis deformans combined lies at 80.16%. Compared to Emden (Stech 2009), this value is lower, since there, already 90.4% of women and 94% of men are affected by spondylosis deformans only. Hettstedt, a mining town in northern Germany showed higher frequency of degenerative vertebral changes at 96.2%, which is likely due to the mechanical stresses caused by mining activities. Overall frequency in degenerative vertebral changes from Knuedler is most similar to that observed in early postmedieval Völklingen (80.6%), a town from the Saarland. In her dissertation, Rossbach (2015) argues that this elevated frequency is evidence for regular exposure to mechanical stress throughout life. No significant difference between the age groups were detected in those two locations. However, a significant difference was detected for all spinal segments among the individuals buried in the Knuedler cemetery, suggesting that age was the driving factor also behind the overall high frequency rate, although heightened exposure to mechanical loading to the spine must also be considered. Next to Grevenmacher, the only site from Luxembourg suitable for comparison is the soldier's cemetery from

Grund/Wenzelsmauer (Trautmann & Trautmann 2011). Here, only indices could be compared and like for the joints, the index scores from Grund/Wenzelsmauer had to be modified to match those from the Knuedler cemetery. Overall, index values of males were lower for the individuals from the Knuedler cemetery. (Grund/Wenzelsmauer: CV:M: 1.5; TV:M: 2.1; LV:M: 1.9). The higher index values observed in individuals from Grund/Wenzelsmauer might reflect the more strenuous living conditions of soldiers. However, regarding females, values were only lower in the cervical spine (G/W:F:CV: 1.5; TV: 1.0; LV: 1.0), whereas for the thoracic and lumbar spine, females from Grund/Wenzel Mauer showed no changes at all. However, it has to be kept in mind that sample size of Grund/Wenzelsmauer (n=23) is rather small overall and that females were very rare (n=4) and all young adults and adults (Trautmann & Trautmann 2011).

6.2 Congenital defects

6.2.1 Introduction

Congenital malformations or anomalies are variations of normal anatomical structures that are initiated by pathological changes to normal intrauterine development (Aufderheide & Rodriguez-Martin 1998; Matussek *et al.* 2022). Congenital changes might be caused by genetic defects developing in the foetus or by external environmental factors affecting the mother, such as infections, medications or hormonal imbalances (Aufderheide & Rodriguez-Martin 1998; Roberts & Manchester 2010; Matussek *et al.* 2022). While some congenital defects can remain asymptomatic, others might eventually cause discomfort or even be fatal (Aufderheide & Rodriguez-Martin 1998), which is why their presence or frequency within a population can relate valuable information on their health status.

6.2.2 Results and Discussion

6.2.2.1 Spinal dysraphism/Spina bifida occulta

Spinal dysraphism or spina bifida refers to all congenital anomalies resulting in vertebral and sacral arch defects, mainly incomplete midline closure (Kumar & Tubbs 2011; Venkataramana 2011) (Figure 95). A distinction is made between apert defects which show external protrusion of the spinal cord, nerves, meninges and/or cerebro-spinal fluid and usually cause severe neurological problems, and occult defects which show no external defects and are mostly asymptomatic (Aufderheide & Rodriguez-Martin 1998; Roberts & Manchester 2010; Wahl &

Zink 2013). Spina bifida occulta is the most commonly reported defect in archaeological literature, especially the defects involving the lumbo-sacral area, primarily the sacrum (Aufderheide & Rodriguez-Martin 1998; Roberts & Manchester 2010). Furthermore, spina bifida occulta might have a genetic component as in modern cases it is often reported in several members of the same family (Grupe *et al.* 2015).

A total of 24 cases of spinal dysraphism or spina bifida occulta were observed in the Knuedler sample (Table 73), 22 (91.6%) of those cases concerned the sacrum, which corresponds to 9.13% of all individuals, including subadults, where a sacrum was present. Of all 24 cases, males (70.83%) were more often affected than females (16.67%) and in 3 cases (12.5%), the condition occurred in subadults of indeterminate sex. Distribution across the two burial phases was equal. When looking at age distribution, 1 case was recorded for infans I (4.17%), 3 cases were found among juveniles and young adults respectively (12.5%), and at 45.83%, adults featured the majority of cases, followed then by matures (16.67%) and seniles (8.33%). Partial spina bifida occulta of the sacrum (72.73%) was more common than complete non-fusion (27.27%).

The overall prevalence of spina bifida occulta of the sacrum from the Knuedler cemetery is about twice as high as that observed in a post-medieval Romanian town, which lay at 4% (Groza *et al.* 2016). Individuals from the prehistoric Dakleh oasis however showed a higher prevalence at 15.6% (Molto *et al.* 2019). Furthermore, Groza et al. (2016) and Molto et al. (2019) found a decline in incidence with age, when only comparing adults. The same could be observed in the Knuedler sample, where incidence was highest among adults. However, it was less common in subadults and young adults. Groza et al. (2016) could not detect any relevant differences in occurrence between the sexes, however, in the Knuedler sample, males were clearly more often affected than females, a trend which was also observed in the Dakleh Oasis (Molto *et al.* 2019).

Table 73 List of individuals with partial or complete Spina Bifida Occulta

Spina Bifida Occulta						
ID	**Sex**	**Age**	**Layer**	**Location**	**Segment**	**Stage**
2016_082/44	M	Adult	1	Cloister	sacrum	Partial Lower
2008_78/1145	F	Adult	2	Cemetery		
2008_78/1148	M	Senile	2	Cemetery		
2008_78/1488	M	Adult	2	Cemetery		
2008_78/217	Indet	Juvenile	2	Cloister		
2008_78/226	Indet	Juvenile	2	Cloister		
2008_78/576	F	Adult	2	Cemetery		
2008_78/671	F	Mature	1	Cemetery		
2008_78/674	M	Mature	1	Cemetery		
2008_78/676	M	Mature	1	Cemetery		
2008_78/710	M	Young Adult	1	Cemetery		
2008_78/809	M	Adult	1	Cemetery		

Spina Bifida Occulta						
2008_78/816	M	Adult	1	Cemetery		
2008_78/563	M	Adult	1	Cemetery		Partial Upper
2008_78/1293+517	M	Adult	2	Cemetery		
2008_78/1354	F	Adult	2	Cemetery		
2008_78/603	M	Adult	1	Cemetery		Complete
2016_082/399	M	Young Adult	2	Cloister		
2008_78/1179	Indet	Infans I	2	Cemetery		
2008_78/138	M	Young Adult	1	Cemetery		
2008_78/148	M	Juvenile	1	Cemetery		
2008_78/380	M	Senile	1	Cloister		
2008_78/1444	M	Mature	2	Cemetery	CV 2	Non-fusion
2008_78/1336	M	Adult	2	Cemetery		

6.2.2.2 Sacralisation and Lumbarisation

Vertebrae involved in sacralisation and lumbarisation are also commonly referred to as lumbosacral transitional vertebrae. Sacralisation describes the process when the 5th lumbar vertebra takes on characteristic traits of a first sacral vertebra. Lumbarisation describes the opposite process, namely when the 1st sacral vertebra shows features of a 5th lumbar vertebra. In both cases, the assimilation can be complete or partial (Figure 93, Figure 94). Supernumerary vertebrae are also classed as a transitional vertebra and like the 5th lumbar vertebra an additional 6th lumbar vertebra can also undergo sacralisation. Supernumerary vertebrae, lumbarisation and sacralisation already develop in utero and are already present at birth (Aufderheide & Rodriguez-Martin 1998; Bron *et al*. 2007).

A total of 20 cases of sacralisation and 16 6th single and sacralised lumbar vertebrae were observed in the Knuedler assemblage but no lumbarisation was recorded. Of the 20 sacralisations, 10 involved the 5th and 10 a 6th lumbar vertebra. Nine were partial and 11 were complete fusions. (Table 74)

Men (n=12) were more often affected by sacralisation than women (n=7) and distribution among the age groups was as follows: juvenile: n=1; adult: n=5; mature: n=11 and senile: n=3. Lumbosacral transitional vertebrae are usually asymptomatic and mostly only discovered incidentally, however in some instances they may cause back pain and stiffness (Bron *et al*. 2007).

Table 74 List of Lumbosacral Transitional Vertebrae

Lumbosacral Transitional Vertebrae						
ID	**Sex**	**Age**	**Layer**	**Location**	**Vertebra**	**Stage**
2008_78/1100	F	Mature	2	cemetery	LV5	Partial Sacralisation
2008_78/585	F	Mature	1	cemetery	LV5	
2008_78/200	M	Mature	2	cloister	LV5	
2008_78/93	Indet	Mature	1	cloister	LV5	
2008_78/148	M	Juvenile	1	cemetery	LV5	
2008_78/809	M	Adult	1	cemetery	LV5	
2008_78/1065	F	Senile	2	cemetery	LV5	

Lumbosacral Transitional Vertebrae						
2008_78/279	F	Senile	2	cemetery	LV6	
2008_78/1300	M	Adult	2	cemetery	LV6	
2008_78/347	M	Mature	1	cloister	LV5	Complete Sacralisation
2008_78/1444	M	Mature	2	cemetery	LV5	
2008_78/95	F	Mature	1	cloister	LV5	
2008_78/709	F	Adult	1	cemetery	LV6	
2008_78/1167	M	Mature	2	cemetery	LV6	
2008_78/1393	M	Mature	2	cemetery	LV6	
2013_015/352	M	Mature	2	cloister	LV6	
2008_78/149	M	Adult	1	cemetery	LV6	
2008_78/205	F	Adult	1	cemetery	LV6	
2008_78/345	M	Mature	1	cloister	LV6	
2008_78/799	M	Senile	1	cemetery	LV6	
2016_082/44	M	Adult	1	cloister	LV6	Supernumerary vertebrae (single)
2008_78/1356	F	Senile	2	cemetery	LV6	
2008_78/154	M	Mature	1	cemetery	LV6	
2008_78/676	M	Mature	1	cemetery	LV6	
2008_78/707	F	Senile	1	cemetery	LV6	
2008_78/738	M	Adult	1	cemetery	LV6	

6.2.2.3 Spondylolysis

Spondylolysis describes the partial or complete separation of the vertebral arch from the body. The aetiology of the condition is still under debate today. On one side, cooccurrence with other spinal malformation suggests a congenital origin. However, other studies have observed a link between repeated microtrauma to the lumbosacral area and frequency of spondylolysis, suggesting that it is acquired in life. The main consensus nowadays is that both factors probably contribute to its development and that the separation occurs either through dissolution or after fracture of the pars interarticularis of the vertebral lamina (Aufderheide & Rodriguez-Martin 1998; Mays 2006; Ward *et al.* 2009). In the case of fracture, both acute trauma and fatigue fracture due to constant stress on the area have been discussed (Ward *et al.* 2009; Roberts & Manchester 2010).

A total of 14 cases of spondylolysis have been observed in the Knuedler sample and the vast majority (n=10) occurred in the 5th lumbar vertebra (Figure 96, Figure 97). In fact, the 5th lumbar vertebra is the most commonly affected site (Mays 2006). It occurred twice in a 6th lumbar vertebra, one in a 4th and one in a 4th cervical vertebra, albite unilaterally. Of all cases, the bilateral type (n=11) was the most prevalent. Taking into account only indiviudals that had a complete 5th lumbar vertebra preserved (n=195), the prevalence of 5th lumbar spondylolysis lies at 5.1%. This result is in line with reported prevalence in modern and archaeological samples, where prevalence ranges between 3-6% (Ward *et al.* 2009; Sakai *et al.* 2010). Furthermore, 3.59% of affected individuals were males and 1.02% were females and 1 was of indeterminate sex, compared to the whole population, which confirms a male prevalence of the condition, which had already been established in past studies (Kalichman *et al.* 2009; Sakai *et*

al. 2010). Furthermore, there is a slight prevalence in spondylolysis among seniles. The scarcity of cases among subadults compared to adults might lend support to the theory that stress fractures contribute to the development of spondylolysis. (Table 75)

Table 75 List of spondylolysis cases

Spondylolysis						
ID	**Sex**	**Age**	**Layer**	**Location**	**Segment**	**Stage**
2008_78/1171	M	Senile	2	cemetery	LV4	bilateral
2008_78/670	M	Adultus	1	cemetery	LV5	
2008_78/1481	Indet	Infans II	2	cemetery	LV5	
2008_78/148	M	Juvenile	1	cemetery	LV5	
2008_78/536	M	Mature	2	cemetery	LV5	
2008_78/1148	M	Senile	2	cemetery	LV5	
2008_78/1167	M	Mature	2	cemetery	LV5	
2008_78/1354	F	Adult	2	cemetery	LV5	
2008_78/1390	F	Adult	2	cemetery	LV5	
2008_78/751	M	Senile	1	cemetery	LV5	
2008_78/738	M	Adult	1	cemetery	LV6	
2008_78/1022	M	Senile	2	cemetery	CV4	unilateral
2008_78/1476	M	Senile	2	cemetery	LV5	
2008_78/676	M	Mature	1	cemetery	LV6	

6.2.2.4 Cranial synostoses

Cranial synostosis describes the premature fusion and obliteration of one or several cranial sutures. This process starts already before birth and an estimated 1 in 2000/2500 live births present with the condition, making it overall a rare occurrence. Craniosynostosis can occur spontaneously, be caused by a syndrome or be inherited, whereas the most common case is spontaneous occurrence (Governale 2015). Fusion of one or more cranial sutures prevents normal cranial growth and will lead to deformation of the overall cranial shape (Schaaf & Zschocke 2013). The overall shape is dependent on which suture is fused. Fusion of the sagittal suture prevents growth in breadth, which is then compensated by growth in length creating a shape referred to as scaphocephaly. Fusion of the sagittal suture is also considered to be the most common type of craniosynostosis. A complete ossification of either the coronal or sagittal sutures prevents lengthwise growth of the skull, which then results in compensatory growth in breadth and height. This shorter but higher and broader cranial shape is referred to as brachycephaly. If fusion of the coronal or sagittal sutures occurs only unilaterally, this leads to unbalanced growth on both sides causing plagiocephaly. Complete fusion of both the coronal and lambdoid sutures causes excessive growth in height resulting in turricephaly and premature closure of the frontal suture creates a triangular skull shape through reduced growth in breadth of the frontal bone, called trigonocephaly (Gellrich & Essig 2011; Grupe *et al.* 2015). Only one individual from the Knuedler cemetery presented a craniosynostosis. In individual 2008-78/818, a mature male, the left side of the coronal had completely obliterated prematurely,

leading to a deformation of the overall cranial shape (Figure 102). A complete or partial ossification of the coronal suture prevents lengthwise growth of the skull, which then results in compensatory growth in breadth and height. In the case of the analysed individual, the fusion occurred unilaterally, additionally causing unbalanced growth on the left and right sides and the resulting skull shape is called plagiocephaly. The individual also showed a smaller, slightly rounded and medially bent left mandibular condyle. This deformation was likely caused by the growth differences in the left side caused by the premature closure of the left coronal suture. It cannot be inferred however whether this deformation caused any problems during mastication, but the teeth did not show any abnormal use wear patterns. Untreated craniosynostosis can lead to increased intracranial pressure (Panchal & Uttchin 2003), causing symptoms such as headache, nausea and vomiting in the early phases but may eventually lead to stupor, coma, muscle weakness and even cardiopulmonary arrest if the pressure keeps rising (Freeman 2015). Given the advanced age of individual 2008-78/818, possible complications from craniosynostosis were likely not that severe.

6.2.2.5 Concha bullosa

Concha bullosa is a common anatomical variant and it is estimated that nowadays it occurs in about 9-72% of individuals depending on the population studied (Mays *et al.* 2014; Balikci *et al.* 2016). Concha bullosa describes hypertrophy (enlargement) of the middle nasal conchae, which are inferior projections of the ethmoid bones, through pneumatization of the middle turbinate (Mays *et al.* 2011). The variant can occur unilaterally or bilaterally and is often associated to a deviated septum and might cause infections of the paranasal sinuses (Stallman *et al.* 2004).

Individual 2008-78/194 a male mature buried in the cloister area from Layer 1 presented a strongly enlarged right middle nasal concha with associated deviation of the nasal septum (Figure 98). Small, irregular bone spicules on the concha suggest at the presence of an infection, maybe of the nasal cavity. Unfortunately, it was not possible to assess the inside of the paranasal sinuses. However, on the posterior side of the left side of the maxilla, an area of bone resorption at the wall of the maxillary sinus could be observed, which suggests that an infection of the maxillary sinuses was present as well.

The present case resembles very strongly the lesion described in Mays et al. (2011). Mays et al. (2011) propose fibrous dysplasia or an osteoblastic neoplasm as differential diagnoses and reject both options. Fibrous dysplasia is rejected due to lack of fibre bone and the concha lacks the characteristics of a malignant (destruction of the cortex) and benign (would occur either on

the surface of the concha or would fill the concha with bony deposits) neoplasms (Mays *et al.* 2011).

Although incidence of concha bullosa is quite high in modern populations, it is rarely described in palaeopathological literature. The oldest recorded case of concha bullosa dates back to the Bronze Age and was found in an individual at a site in Spain (Rubio Salvador *et al.* 2019). Only 7 more reports on concha bullosa were found in palaeopathological literature, of which two sites presented 2, respectively 24 cases. This brings the total count of reported cases of concha bullosa to 32, suggesting that the condition was less common in the past than it is today (Derums 1987; Mays *et al.* 2011, 2014; Gawlikowska-Sroka *et al.* 2016; Tonina *et al.* 2018; Rusu *et al.* 2019a; Buzi *et al.* 2020).

6.2.2.6 Os acromiale

If the acromial apophysis does not fuse to the scapular spine, an os acromiale develops (Hunt & Bullen 2007). Mostly the os acromiale remains asymptomatic and is today mostly an incidental finding during radiography. However, it is thought that os acromiale might predispose for rotator cuff disease and shoulder impingement (You *et al.* 2019). The aetiology of os acromiale is still under debate, with genetic predisposition (Angel *et al.* 1987), activity-related stressor in adolescence (Stirland 2000) being brought forward. Nowadays, both genetic and environmental factors are thought to contribute to its formation (Case *et al.* 2006; Hunt & Bullen 2007).

A total of 2 individuals from the Knuedler cemetery presented an os acromiale. In both cases the condition occurred unilaterally, and the presence of the occurrence could only be confirmed through a growth plate at the end of the scapular spine where the acromion was supposed to be attached. The os acromiale itself was not recovered. Individual 2008-78/1312, a senile male from Layer 2 buried in the cemetery showed the condition on the right scapula (Figure 99) and individual 2008-78/1334, a young adult of 20-24 years from Layer 2 buried in the cemetery presented it on the left side. Since the acromion fuses relatively late between 18-25 years, it is possible that in the case of 2008-78/1334, the acromial epiphysis simply has not started fusion yet. Therefore, only one confirmed case can be reported for this site, which accounts for about 0.57% of all adult individuals who had the right scapula preserved (n=177). This percentage is fairly low compared to frequencies from other archaeological sites. A frequency of 7.7% was recorded for a medieval Danish sample (Case *et al.* 2006), it occurred in 19% of the individuals recovered from the Tudor war ship Mary Rose (Stirland 2000; Mays 2008) and in British medieval-postmedieval samples it reaches frequencies between 8-13% (Mays 2008).

6.2.2.7 Anomalous coracoclavicular joint

The coracoclavicular joint is a diarthrotic synovial joint that formed between the conoid tubercle of the clavicle and the superior surface of the horizontal part of the scapular coracoid process (Gumina *et al.* 2002; Paraskevas *et al.* 2009). The coracoclavicular joint is reported with incidences ranging between 0.55-21% depending on the population and geographical area, as it is thought to occur much more frequently in Asians than in Europeans or North Africans. Furthermore, unilateral occurrence is more frequent than bilateral occurrence and males were more commonly affected than females. Usually the joint is completely asymptomatic but in some cases osteoarthritis can develop in the joint or other complications such as humeral head fracture, cervicobrachial syndrome or limited mobility can occur (Gumina *et al.* 2002). The aetiology of the joint is still under debate with some favouring a genetic cause and others suggesting that its development is activity-related due to an increase in cases in old age (Paraskevas *et al.* 2009).

Two cases of a unilateral coracoclavicular joint were observed in the Knuedler cemetery. In both cases the condition occurred on the left body side. Both individuals were males, which is in agreement with the previously mentioned prevalence in males and occurred in an adult-mature I (35-44 years) (Figure 101) and mature II (50-59years) (Figure 100) individual respectively. Both individuals were buried in completely different locations, one on the cemetery and the other in the cloister. Activity-related stress was mentioned as one of the possible causes for the development of the joint and therefore a correlation with degenerative joint disease was checked. The adult-mature I individual (2008-78/885) showed noteworthy degenerative changes in the left elbow, but the mature individual did not show relevant degenerative joint changes. In the case of the adult, an activity-related development might be considered, since degenerative joint disease at a younger age is often associated with increased physical activity.

6.2.2.8 Developmental hip dysplasia

Developmental hip dysplasia is considered to be a spectrum disorder ranging from simple acetabular dysplasia to hip subluxation and dislocation. As the term developmental implies, the condition has its onset already in utero. Acetabular dysplasia describes the mildest form on the spectrum and represents a shallow acetabulum with reduced concavity, but the femoral head remains in articulation within the joint. Subluxation is the intermediate stage and is characterised by lateral displacement of the femur, which articulates with the lateral margin of

the dysplastic acetabulum. The most severe stage is congenital hip dislocation in which the femoral head has lost contact with the articular surface of the acetabulum entirely and often forms a secondary acetabulum on the on the lateral side of the iliac blade (Aufderheide & Rodriguez-Martin 1998; Mitchell & Redfern 2011). In the latter case, aplasia of the lunate surface occurs and results in flattening and elongation of the acetabulum, leading to a characteristic small and triangular shape. The femoral head is also atrophied and flattened and presents a vertical groove formed by the round ligament. Downwards-pointing marginal exostoses on the head are also a common occurrence (Aufderheide & Rodriguez-Martin 1998; Waldron 2009). The condition occurs more frequently in females than in males and the left hip is usually more often affected than the right but bilateral appearance is also frequent. The development of osteoarthritis in the femur and secondary acetabulum usually indicates that the individual was able to walk and probably lived into old age (Waldron 2009). A waddling gait is considered characteristic of developmental dysplasia of the hip if the joint was functional (Waldron 2009; Roberts & Manchester 2010).

Three individuals from the Knuedler cemetery show signs of developmental hip dysplasia.

Individual 2008-78/1342, an adult-mature I (35-44y) female, presents with a triangular dysplastic acetabulum of the right os coxa (Figure 104). Furthermore, a smooth, circular groove on the lateral aspect of the iliac wing suggests the presence of a secondary acetabulum caused by dislocation of the femur. The corresponding femoral head is dysplastic, shows a large central groove and a small downwards-pointing exostosis at the lower margin (Figure 103). The femur also displays coxa vara, meaning the femoral neck angle is smaller than 120º. Apart from some slight areas of pitting, the femoral head did not show any degenerative changes, nor were any found in the smooth circular depression thought to be the secondary acetabulum. The right femur also appeared shortened and thinner compared to its healthy left counterpart, suggesting that it was not used as much as the left one.

Individual 2008-78/1440, a female adult (30-39y), shows a small, triangular, dysplastic acetabulum on both the right and left ossa coxa (Figure 106). While the acetabulum is preserved completely on the right os coxa, on the left it is broken and only the upper rim remains visible. The lateral aspect of the iliac blade is intact and shows no signs of formation of a secondary acetabulum. However, a flattened area between the cranial rim of the triangular acetabulum and the anterior inferior iliac spine suggests that articulation of the femur occurred in that area. Both femora appear thin and relatively short with a lateral bend in the proximal part of the diaphysis (Figure 105). The femoral neck displays coxa vara, and the right femoral head

appears dysplastic and flattened but dome-shaped. The head of the left femur is missing. No degenerative changes were observed in the secondary acetabulum or on the femoral head.

Individual 2008-78/1487, a mature (40-49y) female, presents atrophied and strongly deformed right and left femoral heads (Figure 109). The femoral neck is nearly non-existent. The heads are extremely flattened and possess very large, downwards-pointing marginal exostoses, giving it a "molten" appearance. Severe degenerative changes can be observed on the deformed joint surface of both heads, including severe pitting and eburnation, indicative of osteoarthritis. The left acetabulum appears hypoplastic and shallow and seems slightly elongated towards the iliac wing (Figure 110). It is surrounded by a ridge of bony exostoses. The lunate surface exhibits strong pitting and eburnation. The left femur articulates with the acetabulum suggesting that no dislocation had taken place. The right acetabulum presents a large secondary acetabulum right above the ischium, extending in a triangular shape onto the lower part of the lateral aspect of the iliac wing (Figure 108). The secondary acetabulum does not present as a depression but is raised and its surface strongly pitted with eburnation. The flattened head of the right femur articulates with this secondary acetabulum suggesting that dislocation of the hip occurred. Although heavily remodeled since the secondary acetabulum developed right at its rim, the remnants of a triangular, dysplastic primary acetabulum are visible right at the margins of the secondary one.

Individuals 2008-78/1342 and 1440 represent clear cases of congenital hip dysplasia, more precisely congenital acetabular dysplasia with subsequent dislocation of the hip. 2008-78/1342, represents a unilateral case, with affection of the right limb, which is less common. The little degenerative changes observed in the joint are indicative of reduced mobility.

For 2008-78/1487, due to the strong degenerative changes in the femoral head, a traumatic injury leading to hip dislocation was also considered. A radiograph of the left femur might suggest so (Figure 107). However, the remnants of a dysplastic primary acetabulum on the right os coxa suggest otherwise, although a combination of congenital and traumatic hip dislocation cannot be excluded. The left acetabulum appears hyperplastic and shallow, indicative of acetabular dysplasia without dislocation.

Therefore, congenital hip dysplasia seems to be the most likely diagnosis for all three individuals. Congenital hip dysplasia is also notoriously more common in females and all presented individuals were female. Since it is believed that congenital hip dysplasia might have a familial component (Waldron 2009), the position of all these individuals on the cemetery was checked. Although they were all buried in the cemetery section, individuals 2008-78/1342 and 1487 were buried in the same area on the cemetery in close proximity to each other. They were

lying in the same burial row but separated by 2 individuals. Three burial layers were identified in the cemetery section and 2008-78/1487 was buried in the lowest and 1342 in the middle layer. The close burial proximity might suggest some form of relatedness between these two individuals, however one displayed bilateral and the other unilateral congenital hip dysplasia. 2008-78/1440 however, was buried in a completely different area on the cemetery than the other two.

6.2.2.9 Slipped femoral capital epiphysis and Legg-Calvé-Perthe's disease

Slipped femoral capital epiphysis (SFCE) is characterised by an inferior-posterior displacement of the femoral capital epiphysis during late childhood and adolescence. After displacement, fusion of the neck in the new position occurs. Several factors, such as a genetic predisposition, the adolescent growth spurt or trauma and obesity in childhood have been considered to play a role in its development (Ortner 2003a; Wasterlain & Umbelino 2014). The majority of cases occur unilaterally but in about 25%, bilateral slippage has been noted (Aufderheide & Rodriguez-Martin 1998). In most cases, a stress fracture at the epiphyseal growth plate leads to a medial and downward displacement of the proximal femoral epiphysis. This displacement may cause aseptic necrosis of the bone and can lead to changes in the outline of the femoral head. Once healed, the centre of the head appears displaced towards the axis of the neck and the neck appears strongly shortened overall and can even be non-existent on the superior side (Ortner 2003a; Wasterlain & Umbelino 2014). As a result of the displacement of the head out of the acetabulum, osteoarthritis may occur and, in some cases, a secondary acetabulum is formed on the lateral side of the iliac blade. Typically however, the ligamentum teres stays intact and therefore there is usually no obliteration of the fovea capitis, and often there is nearly no change in the outline of the epiphysis (Ortner 2003a; Grauer 2019). According to Waldron (2009), SFCE often presents cystic lesions in the femoral head on radiographs. Bilateral occurrence is not common but also not a rare occurrence (Grauer 2019).

Legg Calvé-Perthe's disease (LCP) is defined as osteochondrosis of the femoral head in children (Aufderheide & Rodriguez-Martin 1998; Smrcka *et al.* 2009). Avascular necrosis of the femoral head occurs due to obstruction of blood flow to the femoral proximal epiphysis (Aufderheide & Rodriguez-Martin 1998; Ortner 2003a; Smrcka *et al.* 2009; Herrerín & Garralda 2012).

Characteristic features of the condition are a "mushroom-shaped" femoral head, absence of the fovea capitis and positioning of the head that is lower than the great trochanter and the acetabulum is usually wider and flatter and presents an irregular articular surface (Aufderheide

& Rodriguez-Martin 1998; Herrerín & Garralda 2012). Earl onset osteoarthritis might obscure the typical features of LCP. Radiographic features include opacity and flattening of the epiphyseal centre and, in the last stage, radiolucent areas where no bone has been replaced after necrosis (Wasterlain & Umbelino 2014).

The exact aetiology of both conditions is still under debate, with genetic predisposition, trauma, infection, metabolic conditions, environmental factors, haematological disorders and hormonal imbalances being mentioned as possible triggers (Smrcka *et al.* 2009; Herrerín & Garralda 2012; Grauer 2019) The condition occurs rarely bilaterally and onset is generally around 3-10 years (Aufderheide & Rodriguez-Martin 1998; Ortner 2003a).

Both SFCE and LCP have been reported in archaeological literature, but the occurrence is still rare. Furthermore, due to early onset osteoarthritis in both conditions, a clear distinction between the two is often difficult (Wasterlain & Umbelino 2014).

Individual 2008-78/150 (30-39y), an adult male, presents an enlarged, flattened mushroom-shaped head (Figure 111). The centre of the head appears superior-posteriorly displaced. The whole head appears also superior-posteriorly displaced leading to shortening of the neck. No degenerative changes were observed on the head nor on the neck of the femur. Although shallow, the fovea capitis is preserved. The head seems to be placed below the great trochanter but since that one has been damaged taphonomically, its full height remains unknown. A radiograph of the femoral head did not reveal any signs of fracture nor traces of cystic lesions (Figure 113). The acetabulum is enlarged and flattened to accommodate the enlarged femoral head. No degenerative changes were observed in the acetabulum, and it did not extend significantly upwards into the iliac blade.

Individual 2008-78/1471 (40-49y), a mature male, presents a strongly enlarged, flattened and mushroom-shaped head, which is displaced posteriorly on the neck of the femur, leading to significant shortening and thickening of the neck (Figure 112). The superior part the neck seems almost non-existent. The head shows severe osteoarthritic changes such as extensive osteophyte formation on the margins and eburnation and pitting of the joint surface. The head is placed below the greater trochanter and the fovea capitis is entirely obliterated though it is impossible to determine whether that happened as a result of the heavy eburnation or through detachment of the ligamentum teres. Radiographically, no cystic lesions could be determined in the head (Figure 114). However, the structure of the trabecular bone at neck-head junction seems disrupted, which might indicate a healed fracture, however, the large dense osteophytes make interpretation difficult. The acetabulum is enlarged and rimmed by osteophytes. It is deeper than normal and extents slightly upwards into the iliac blade.

Both individuals show characteristics which are consistent with a diagnosis for slipped femoral epiphysis or Legg-Calvé-Perthe's disease and in both cases the opposite leg is not affected. Regarding individual 2008-78/150, the mushroom-shaped enlarged head are more indicative of LCP, as is the absence of cystic lesions on the radiograph. However, the shortened neck, the displaced centre of the head as well as the presence of the fovea capitis are characteristics strongly in favour of SCFE, which is why both conditions need to be considered equally likely. The strong mushroom shape as well as the enlargement of the head and absence of fovea capitis, as well as the thick short neck are indicative of LCP, but the displacement of the head centre would be rather characteristic for SFCE. Additionally, the strong osteoarthritis in the hip might have also led to obliteration of the fovea capitis. Therefore, both LCP and SFCE will be considered equally as differential diagnoses for this individual.

6.2.2.10 Congenital or traumatic radial dislocation

Congenital radial dislocation is a rare congenital disorder in which the radial head loses contact with the capitulum humeri due to dislocation. In most cases the radius is dislocated posteriorly and in most cases occur bilaterally, although bilateral occurrence is not anymore a diagnostic criterion (Agnew & Davis 1993). Congenital radial dislocation is the most common congenital elbow abnormality (Kelly 1981). Radiographic diagnostic criteria for congenital radial dislocation are as follows: 1. Shortening of the ulna or overlength of the radius, 2. Aplasia or hypoplasia of the capitulum humeri, 3. Grooving of the distal radius, 4. Prominent ulnar (medial) epicondyle, 5. Partially defective trochlea humeri, and/or 6. Dome-shaped radial head with an elongated narrow neck (Aufderheide & Rodriguez-Martin 1998; Amin *et al.* 2018). Congenital radial dislocation is usually painless in childhood but leads to restricted movement in the joint, especially limited extension. In adolescence or adulthood, the condition may cause pain in the elbow joint (Langenberg *et al.* 2020).

The right distal humeral epiphysis of individual 2008-78/1080, a young adult male, appeared strongly enlarged (Figure 115). On the posterior side, the fossa olecrani was very shallow and instead the surface of the trochlea humeri was extended slightly proximally and was flattened due to the reduced fossa olecrani. Since the capitulum humeri was broken off, it was not possible to comment on its shape. However, based on the trochlea size, the size of the broken area and the proximity to the lateral epicondyle, it seems as if the capitulum humeri was not as prominently developed as the trochlea humeri. Slight degenerative joint change in the form of a small pitting spot was visible on the anterior side of the enlarged trochlea humeri. The ulnar epicondyle was also slightly enlarged. The ulna was unfortunately missing, but the radius

presented with a slightly enlarged and dome-shaped radial head with a thinned and slightly elongated neck (Figure 117). An eburnated spot was situated on the superior-medial side of the radial head. Additionally, the radial tubercle showed a broad sunken line at its center with a smooth surface, whereas the margins of the tubercle, especially the anterior margin appeared smooth and raised. Since the radius was broken shortly below the midshaft, no observations could be made regarding the full length of the radius or possible changes in the distal epiphysis. No further changes were observed in the remaining skeleton. Radiographs of the affected radius and humerus did not show any structural abnormalities in the respective epiphyses (Figure 116). The right elbow joint appeared completely normal, except for a deep groove at the center of the left radial tuberosity.

Therefore, this individual presents most of the signs of congenital radial dislocation. However, the absence of the ulna, distal radius and capitulum humeri prevent a clear diagnosis. Furthermore, the unilateral character of the lesion, although not a reason for exclusion, is much rarer than bilateral expression in congenital radial dislocation.

Conditions causing a dome-shaped radial head and enlarged humeral trochlea are rare. Nevertheless, 3 differential diagnoses are proposed that may lead to this deformity.

Traumatic radial dislocation may lead to changes in the elbow joint. The most common cause for traumatic radial dislocations is a Monteggia type fracture, i.e. a fracture of the Ulnar and/or Radial neck, followed by fracture of the capitulum humeri (Oka *et al.* 2010; Roberts & Manchester 2010; Langenberg *et al.* 2020). Radiographs showed no evidence of fracture in the humerus or radius. The missing capitulum humeri was clearly caused by excavation damage due to the exposed lighter-colored fracture margins. Since the ulna has not been recovered, it is impossible to determine whether it was fractured or not. Dislocation might also be caused by a pulled elbow in infancy, in which trauma to the joint, such as abrupt and forceful pulling or a fall, leads to a relaxation of the ligaments that wrap around the radial head, which might then lead to subluxation and dislocation of the radial head (Kelly 1981; Kaas & Struijs 2012). Traumatic radial dislocation is mostly differentiated from the congenital form by a concave head shape, as opposed to a convex head shape in the congenital condition. However, if the fracture and subsequent dislocation occurred closely after birth and was never corrected, the prolonged loss of contact of the radial epiphysis with the capitulum humeri during skeletal development may also lead to the formation of a dome-shaped radial head (Oka *et al.* 2010). Therefore, traumatic radial dislocation that occurred shortly after birth must be considered as an equally likely diagnosis to the congenital form. In order to differentiate between both cases, the presence of the ulna and an intact capitulum humeri would be required.

Klinefelter-Syndrome (KS) is a genetic disorder affecting only males. It is mainly characterised by soft tissue abnormalities, but some skeletal deformations may also occur, such as hypertelorism, a deeper palate and mild elbow dysplasia, as well as various other, mainly cranial skeletal deformities. Furthermore, males suffering from KS are on average 2.5cm taller than healthy men (Bird & Hurren 2016). The individual analysed here is male but does not present with hypertelorism or a particularly high palate nor any of the other cranial abnormalities that are often associated with the disorder. However, 2008-78/1080 is rather tall compared to the other men on the cemetery. He reached a height of 174.64cm whereas the average height of males from the cemetery was 167.85cm (after the Formula by Siegmund (2010) on the Femur).

Nail-patella syndrome also presents dislocation of elbow and convex radial head but characteristically presents with hypoplastic patella but in this individual the patellae were normal in size (West & Louis 2015).

Several osteochondrodysplasias may also occasionally cause dislocation of the radial head (Kaas & Struijs 2012).

Congenital Anomalies and Anatomical variants	
Figure 93 Partial sacralisation of LV5 (2008-78/200)	*Figure 94 Partial bilateral sacralisation with pseudoarthroses of 2008-78/1300*

Figure 95 Spina bifida occulta of individual 2008-78/380

Figure 96 Spondylolysis of LV5 and non-fusion of arch of S1 (2008-78/1354)

Figure 97 Spondylolysis of LV5 of 2008-78/1390

Figure 98 Concha Bullosa

Figure 99 Facet for os acromiale on the right scapula of 2008-78/1312

Figure 100 Unilateral coracoclavicular joint on clavicula L of 2013-015/183

Figure 101 Unilateral coracoclavicular joint on clavicula L of 2008-78/885

Figure 102 Craniosynostosis of the left side of the coronal suture causing plagiocephaly (2008-78/818)

Figure 103 Unilateral congenital hip dysplasia in 2008-78/1342 view of right femur with small, flattened head

Figure 104 Unilateral congenital hip dysplasia in 2008-78/1342 view of right os coxa with triangular acetabulum

Figure 105 Bilateral congenital hip dysplasia in 2008-78/1440 view of the femora with dysplastic heads

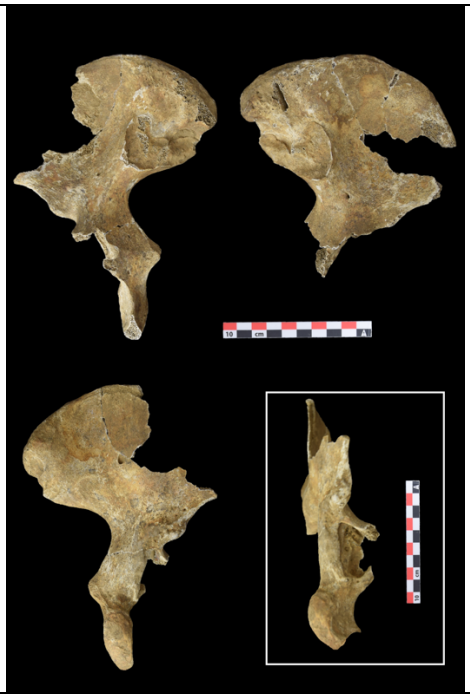

Figure 106 Bilateral congenital hip dysplasia in 2008-78/1440 view of the ossa coxa with dysplastic acetabulum

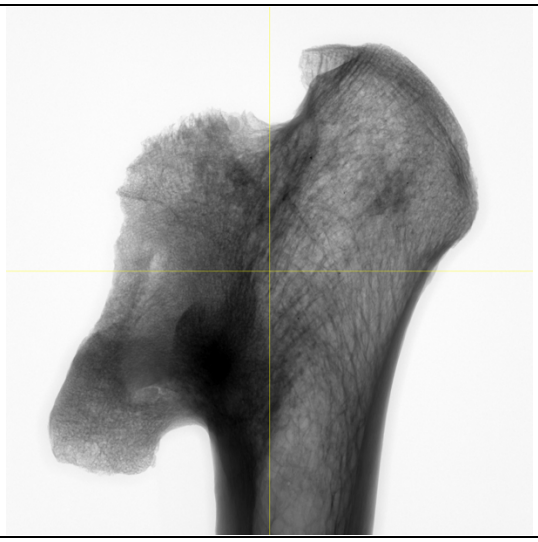

Figure 107 Radiograph of the left femur of 2008-78/1487 (probable congenital hip dysplasia)

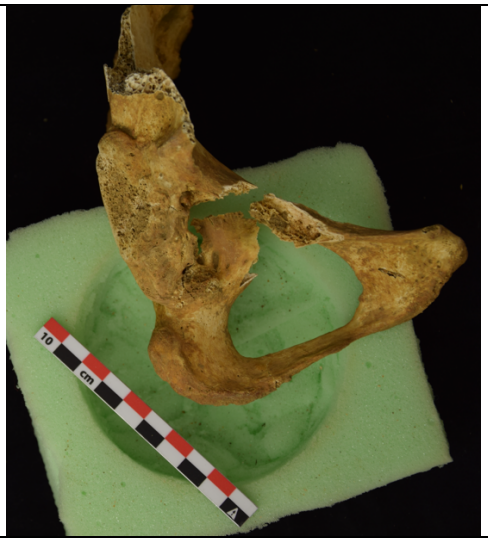

Figure 108 Formation of prominent secondary acetabulum in 2008-78/1487

Figure 109 Bilateral congenital hip dysplasia of 2008-78/1487 view of femurs with flattened, elongated heads

Figure 110 Bilateral congenital hip dysplasia of 2008-78/1487 view of shallow acetabulum left

Figure 111 Epiphysiolysis or Perthe's disease of the left femoral head (slipped femoral epiphysis) of 2008-78/150 showing an enlarged and displaced head with no degenerative changes and osteochondritis dissecans in the distal epiphysis

Figure 112 Modification of the femoral head with osteoarthritis likely from Perthe's disease or SCFE, but trauma cannot be excluded (2008-78/1471)

Figure 113 Radiograph of the epiphysiolysis/Perthe's disease of 2008-78/150, showing no signs of fracture

Figure 114 Radiograph of femur of 2008-78/1471

Figure 115 Enlarged right elbow joint of 2008-78/1080

Figure 116 Radiograph of enlarged humeral distal epiphysis (2008-78/1080)

Figure 117 Comparison of the right and left radius of individual 2008-78/1080 showing the slightly enlarged and domed head and slightly elongated and thinned neck of the right radius. The left radius presents a deep smooth dip in the center of the radial tuberosity but shows no other pathological changes or anatomical variations

6.3 Neoplastic disease

6.3.1 Introduction

Neoplasia is defined as the proliferative and uncontrolled growth of cells, which eventually results in the formation of tumours, an abnormal growth of tissue. Therefore, the term neoplasm simply refers to a tumour (Roberts & Manchester 2010; Marques 2019). Abnormal cell proliferation is triggered by several cumulative genetic and epigenetic mutations caused by the complex interplay of bone microenvironment, biological age, genetic predisposition and exposure to carcinogenic substances over the course of an individual's life (Aufderheide & Rodriguez-Martin 1998; Marques 2019; Siek *et al.* 2021a). A distinction is made between two main types of neoplasms: benign neoplasms and malignant neoplasms.

Benign neoplasms are not cancerous, usually slow-growing, generally do not metastasise into other tissues (Aufderheide & Rodriguez-Martin 1998; Waldron 2009; Marques 2019) and are thought to be more common than malignant tumours (Hakim *et al.* 2015). The majority of benign tumours are clinically asymptomatic and are mostly detected as incidental findings during radiography for other medical conditions but depending on their size and location they may cause secondary effects that might even end up being fatal. In fact, many benign tumours will grow in size continuously if left untreated, with growth often starting already childhood, and can compress nerves, blood vessels or organs (Hesketh 2013; Hakim *et al.* 2015).

Malignant tumours are cancerous and tend to be fast growing, and due to the infiltrative and invasive properties of their cells, they are also very prone to metastasise into other parts and tissues of the body (Marques 2019) and usually interfere with the body's systemic functions, often leading to serious health problems (Waldron 2009).

A further distinction is usually made between primary and secondary neoplasms. Primary neoplasms describe the original tumour in the body. Secondary tumours are essentially metastases, cancer cells that detached from the primary tumour and spread to other tissues in the body via the lymphatic system or the bloodstream (McKinnell 2006; Waldron 2009). All benign tumours are primary tumours and malignant tumours can either be primary or secondary tumours, and all secondary tumours are always malignant (Waldron 2009).

An additional classification is usually undertaken based on the kind of tissue the tumour arose in: those arising from bone, those arising from cartilage, those of haematopoietic origin and those arising from different soft tissues (Waldron 2009; Marques 2019).

6.3.2 Osteomata

6.3.2.1 Introduction

Osteomata are considered benign true primary slow-growing osteogenic and osteoblastic lesions and usually present as rounded overgrowths of well-organised compact bone without surface irregularities (Capasso 1997; Aufderheide & Rodriguez-Martin 1998; Waldron 2009; Marques 2019; Siek *et al.* 2021b). They originate in the periosteum and do not penetrate the bone cortex (Aufderheide & Rodriguez-Martin 1998; Eshed *et al.* 2002; Waldron 2009). The exact aetiology of osteomas is still unclear with some authors classifying them simply as benign neoplasms and others as hamartomas or even as lesions related to focal hyperostosis (Capasso 1997; Aufderheide & Rodriguez-Martin 1998; Eshed *et al.* 2002). Osteomata are usually single occurrences, but accumulations of several osteomata have also been frequently observed. In case of multiple osteomata, they do not overlap and occur as distinct lesions. Osteomata affect predominantly the cranial bones, with the ectocranial side affected more frequently than the endocranial side, followed by osteomata inside the sinuses. However, they can also form in the postcranial skeleton but these occurrences are much more uncommon (Capasso 1997; Siek *et al.* 2021b).

6.3.2.2 Results and Discussion

A total of 14 (12.96%) individuals of 108 presented with one or several osteomata on cranial bones (Table 76). Since lesions were only observed in cranial bones, only individuals that had all major cranial vault bones (frontal, occipital, temporal, parietal right and left) and maxilla preserved, were retained for the frequency calculation. No osteomata were recorded in the postcranial skeleton. This result was expected as cranial bones are most commonly affected by this lesion (Capasso 1997; Aufderheide & Rodriguez-Martin 1998; Waldron 2009; Siek 2020). Five (35.71%) cases were recorded on parietals, 5 (35.71%) cases on frontal bones, 2 (14.29%) on the maxilla and one on a temporal (7.14) and occipital (7.14%) respectively. In 4 (28.57%) cases, the lesions occurred in the sinuses (3x in frontal, 1x in maxillary sinus), in 6 (42.86%) cases they occurred ectocranially, in 3 (21.43%) cases endocranially and once (7.14%) on the lingual side of the maxillary alveolar process. Overall, this follows the expected distribution as according to clinical literature, osteomas occur most frequently on the ectocranial side of frontal and parietal bones, followed by lesions in the sinuses and endocranial lesions (Waldron 2009; Siek *et al.* 2021b). Some authors however record a predominance in the sinuses (Marques 2019), as many sinuses could not be assessed because they were not broken it is impossible to

verify this in the Knuedler assemblage. With 2 (14.29%) young adults and 4 (28.57%) adults presenting osteomata and 8 (57.14%) cases recorded in seniles and matures, the frequency also seems to increase with age. With 8 (57.14%) males and 6 (42.86%) females presenting osteomata, the difference between the sexes is as expected quite balanced. Both these trends have also been observed by Eshed et al. 2002 on modern crania from the Hamann-Todd collection and by Siek et al. 2021 on a polish archaeological collection. The frequency increase with age might be explained by the fact that osteomata are considered slow growing and are thought to start developing already in childhood, thus becoming noticeable only in advanced age (Siek *et al.* 2021b). The majority of recorded osteomata were single occurrences, but individual 2008-78/1182, a young adult presented with 3 grouped osteomata on the left ectocranial parietal, and the osteomata were associated with distinct cribra cranii.

Generally, osteomata are without clinical symptoms and in modern patients are usually just incidental findings on radiographs, which makes it difficult to gauge their true prevalence in modern populations (Giuffra *et al.* 2019). However, depending on their location, osteomata may cause secondary effects. Osteomas occurring the sinuses might grow large enough to block the sinusoidal ducts and may thus lead to nasal discharge, sinusitis, mucocele, headache, facial pain and possibly loss of smell (Greenspan 1993; Marques 2019). If they are located endocranially, they might press against the brain and thus cause neurological complications. Osteomata occurring in the orbits might compress the optic nerve and lead to vision loss (Greenspan 1993). The osteomata observed in the sinuses of the individuals from the Knuedler cemetery were too small and likely did not cause any of the aforementioned problems. However, it cannot be excluded that the ones occurring endocranially, especially the large one observed in individual 2008-78/1368 might have caused some clinical manifestations.

Table 76 List of all individuals with osteomata and their location

	Osteomata					
ID	**Sex**	**Age**	**Layer**	**Burial Location**	**Nb. of Osteomata**	**Location on bone**
2013_015/157	M	Senile	2	Cloister	1	Frontal sinus R
2013_015/164	F	Mature II	1	Cloister	1	Parietal L ectocranial
2013_015/169	F	Senile	2	Cloister	1	Frontal L endocranial
2013_015/181	M	Mature II	2	Cloister	1	Parietal R ectocranial
2008_78/1182	F	Young Adult	2	Cemetery	3	Parietal L ectocranial
2008_78/1289	M	Adult	2	Cemetery	1	Temporal R endocranial
2008_78/1291	F	Senile	2	Cemetery	1	Frontal R ectocranial
2008_78/1310	M	Mature II	2	Cemetery	1	Alveolar process R lingual
2008_78/1361	F	Adult	2	Cemetery	1	Frontal sinus R
2008_78/1368	F	Young Adult	2	Cemetery	1	Occipital R endocranial
2008_78/147	M	Adult	1	Cemetery	1	Parietal R ectocranial
2008_78/153a	M	Mature I	1	Cemetery	1	Parietal L ectocranial
2008_78/380	M	Senile	1	Cloister	1	Frontal sinus R
2008_78/885	M	Adult	1	Cemetery	1	Maxillary sinus R

Photo Table Osteomata	
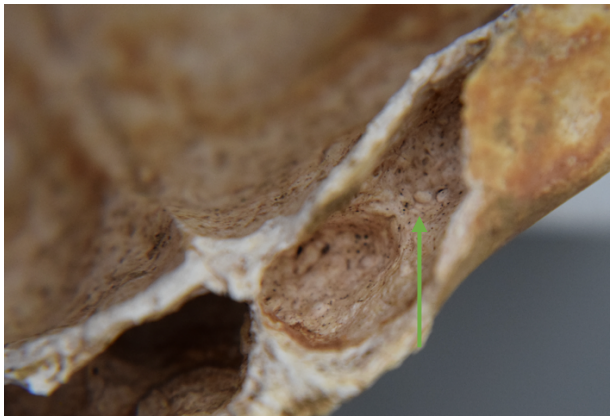	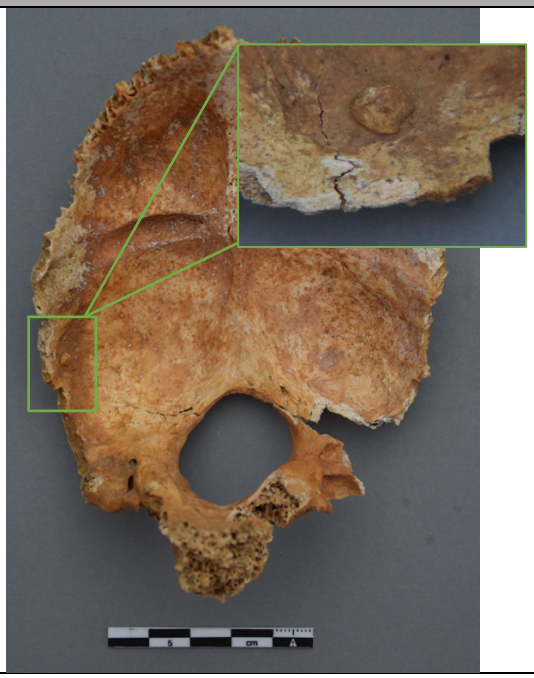
Figure 118 Two small osteomata inside the frontal sinus of individual 2008-78/1361	*Figure 119 Large osteoma on the endocranial side of the occipital next to the lambdoid suture of individual 2008-78/1368*

6.3.3 Intraosseous ganglia

6.3.3.1 Introduction

Intraosseous ganglia are benign non-neoplastic intramedullary osteolytic bone lesions of unknown aetiology (Bonar 2009; Davies *et al.* 2015). Characteristically, in living individuals, they are lined by fibrous tissue and filled with viscous mucous fluid. They occur most commonly in the hip, knee, ankle, shoulder and wrist (Schajowicz *et al.* 1979; Bonar 2009) and are usually located adjacent to a joint (Sakamoto *et al.* 2013). Intraosseous ganglia occur slightly more frequently in males and affect predominantly skeletally mature individuals of middle age, with a peak incidence being observed in individuals in their 40s and 50s (Bonar 2009). Generally, intraosseous ganglia are not associated with osteoarthritis in joints, although some rare cases have been described in literature (Schajowicz *et al.* 1979; Bonar 2009; Sakamoto *et al.* 2013; Davies *et al.* 2015). Juxta-articular cysts associated to osteoarthritis in the joints are referred to as degenerative subchondral cysts (Bonar 2009; Davies *et al.* 2015). However, Adler (2005) uses a reversed terminology, referring to cysts associated with osteoarthritis as interosseous ganglia and those without degenerative joint changes as subchondral bone cysts. In the following section, the former terminology will be used as it is more widespread in clinical literature and studies. Strictly speaking, interosseous ganglia are

not neoplastic diseases, however, in the majority of clinical literature they are listed under benign neoplastic conditions, which is why they are treated under neoplastic diseases in this work as well.

Several other pathological conditions can cause cysts and cyst-like lesions in bones, and among those, the most common ones are the simple bone cyst, aneurysmal bone cyst, subchondral bone cyst, non-ossifying fibroma, chondromyxoid fibroma, fibrous dysplasia and giant cell tumour of bone, chondroma, benign chondroblastoma and eosinophilic granuloma (Lagier *et al.* 1987; Capasso *et al.* 1992; Bonar 2009; Kacki *et al.* 2010; Marques 2019; Siek & Spinek 2021). All types of cysts and pathological conditions causing cystic lesions in bone will be considered for the differential diagnosis of the lesion found in individual 2008-78/665 from the Knuedler cemetery.

6.3.3.2 Results

Individual 2008-78/655, a mature male from Layer 1 buried in the cemetery, presents an osteolytic lesion in the left os coxae and more precisely in the ilium. The lesion is located just below the ventral side of the cortical bone towards the central area of the distal os ilium right superior to the lunate surface of the acetabulum (Figure 121, Figure 122, Figure 123). The lesion was observable with the naked eye since the os coxae was already broken open, having been destroyed during the excavation process, which explains the light-coloured fracture borders. Unfortunately, since the missing parts of the os coxae were either not retrieved or had been completely destroyed, no reconstruction of the bone was possible and therefore, the true size of the lesion cannot be determined. At the widest extensions, the lesion is approximately 2cm wide, 2cm high and 2.3cm deep. The shape is ovoid, but due to the missing parts, it cannot be ascertained that this was also the case for the whole lesion. The walls of the lesion show a clear, rather smooth sclerotic border, separating the cavity from the surrounding trabecular bone (Figure 121, Figure 122). At least in the observable area, the lesion did not cause swelling on the ventral or dorsal sides of the ilium. Since a large part of the acetabular lunate surface is missing as well, it cannot be determined for certain whether the lesion had penetrated through or caused swelling in the acetabulum. However, examination of the associated femur head did not show any evidence of infection or compression through an external mass. No osteoarthritis or degenerative changes were recorded in the acetabulum or femoral head. A radiograph was performed to check whether further lesions were located inside the ilium, but none could be detected, and to define the radiographic appearance of the lesion, as radiographic signs are frequently used to distinguish between different types of cysts and pathological conditions

causing cyst-like lesions. On the radiograph, the lesion appears as a rounded, slightly oblong cavity with a thin sclerotic rim (Figure 120). No periosteal reaction or cortical thickening was observed around the lesion. Some flaking of the bone cortex was observed near the fracture borders, which happened as a result of post-mortem damage to the bone (Figure 121). Since the lesion is incomplete and cannot be reconstructed, it is also impossible to determine whether it consisted of one single or of several cavities. It is possible that, had the bone not been broken, this lytic lesion might have gone unnoticed. No other lesions or bone changes were observed in the remainder of the skeleton after macroscopic examination. It has to be mentioned that the skeleton was nearly complete, with notably the cranium and left humerus missing.

6.3.3.3 Discussion and Conclusion

The absence of multiple lesions and the presence of a smooth sclerotic rim, its well defined character on the radiograph and the size of the lesion suggests that the lesion was slow-growing and was thus most likely benign, excluding thereby aggressive and malignant neoplasms as possible causes for the lesion (Ragsdale *et al.* 2018; Siek & Spinek 2021).

The lesion location in the ilium is rather unusual as the majority of bone cysts and cyst-like lesions occur in long bones (Waldron 2009; Marques 2019; Siek & Spinek 2021), which makes it difficult to narrow the differential diagnoses down to one primary diagnosis.

Based on the lesion's unusual location and its location within the bone, it's appearance on radiograph as well as sex and age of the individual, an *interosseous ganglion* seems to be the most probable diagnosis for the bone cavity observed in the left ilium of individual 2008-78/655. Intraosseous ganglia are juxta-articular lesions that occur most frequently in the hip, ankle wrist and shoulder area (Bonar 2009; Sakamoto *et al.* 2013; Davies *et al.* 2015). The lesion of individual 2008-78/655 occurred in the hip joint area, directly above the acetabulum. Although lesions in the ilium are rarer than those in the long bones, several cases in the ilium have been described in past clinical studies and all those lesions occurred at the distal end of the ilium, close to the acetabulum (Schajowicz *et al.* 1979; Sakamoto *et al.* 2013). Typically, intraosseous ganglia are not associated to osteoarthritic changes in the joint (Bonar 2009; Davies *et al.* 2015), and no such changes were recorded in the hip joint of individual 2008-78/655. The interosseous ganglion is generally a solitary lesion (Crabbe 1966), which seems also to be the case for the lesion in individual 2008-78/655, where no further lesions were detected in the left ilium nor did the remainder of the skeleton show any macroscopically detectable bone changes such as cortical swelling, associated with cystic bone lesions. On radiograph, the interosseous ganglion is defined by a thin sclerotic rim, and location and

generally an eccentric location in or near an epiphysis and can look very similar to a simple bone cyst, an aneurysmal bone cyst, or lesions caused by chondromyxoid fibroma and fibrous dysplasia (Schajowicz *et al.* 1979; Bonar 2009; Sakamoto *et al.* 2013). The lesion of individual 2008-78/655 presents a thin sclerotic rim and is situated eccentrically in very close proximity to the acetabulum. Most importantly though, the intraosseous ganglion has a male preponderance and occurs primarily in middle-aged adults and is relatively rare in children. Individual 2008-78/655 is a male aged 40-49 years (Bonar 2009; Sakamoto *et al.* 2013), which means the individual fulfils all the predilection criteria for the development of interosseous ganglia.

Several other conditions can cause similar bone lesions and they will be discussed as differential diagnoses in the following section.

Subchondral bone cysts are lesions that occur when synovial fluid presses against bone due to cartilage damage, which is why these cysts are usually associated with osteoarthritis. (Guangyi. *et al.* 2013; Xinyun *et al.* 2014)Another origin of these lesions has also been proposed, namely that bone necrosis due to microtrauma might lead to the formation of a fluid-filled cavity (Guangyi. *et al.* 2013). Degenerative subchondral cysts, like interosseous ganglia occur more frequently in middle-aged adults and are located in very close proximity to joints (Bonar 2009). Radiographically they present the same characteristics as intraosseous ganglia, namely eccentric location close to a joint and a sclerotic margin (Adler 2005). The lesion observed in individual 2008-78/655 was most likely no subchondral bone cyst since no osteoarthritis was observed in the acetabulum or femur. However, due to the missing part of the acetabulum, degenerative subchondral cyst cannot be entirely excluded from diagnosis.

Simple bone cysts, fluid filled cavities of unknown aetiology, occur most frequently in long bones, in particular in the metaphyses of long bones but seldomly, the ilium, talus and calcaneus can also be affected in older juveniles and adults (Aufderheide & Rodriguez-Martin 1998; Mascard *et al.* 2015). Lesions in the pelvis remain rare however, accounting for only about 2% of clinically reported cases and might be underdiagnosed because most simple bone cysts in the pelvis remain asymptomatic as the pelvis is not a weight bearing bone (Hammoud *et al.* 2005). The common consensus nowadays is, that they develop during bone growth, and are the result of halted bone formation in the metaphysis. The cavity is then filled with fluid and when bone formation resumes, normal bone is being deposited again between the growth plate and the cyst (Hammoud *et al.* 2005). Furthermore, single bone cysts affect mostly individuals younger than 20 years, but the lesion can persist well into adulthood, and they occur more frequently in males. Periosteal reactions generally do not occur with simple bone cysts.

(Aufderheide & Rodriguez-Martin 1998; Mascard *et al.* 2015; Marques 2019). The simple bone cyst presents as an ovoid lytic lesion located concentrically and consisting of only one well defined round or ovoid cavity, often with a sclerotic rim and accompanied by cortical thinning (Marques 2019; Siek & Spinek 2021). Since simple bone cysts are rare in the ilium and the individual presented here is mature, a simple bone cyst seems unlikely but not impossible for the observed lesion.

Aneurysmal bone cysts are blood-filled cavities and occur most frequently in long bones but up to 9% of cases have been detected in the pelvis. Pelvic lesions occur mostly around the obturator foramen and peripherally to the triradiate cartilage at the centre of the acetabulum (Mascard *et al.* 2015). In the Knuedler case, the lesion is located in the ilium right above the acetabulum, which means that the lesion is located in close proximity to the triradiate cartilage. However, for aneurysmal cysts, the age of predilection is also in individuals younger than 20 years, but they can occur at any age. It has to be noted though that occurrence decreases with age and the condition is especially rare in those over 50 years (Mascard *et al.* 2015). Furthermore, aneurysmal bone cysts tend to be situated closer to the bone cortex and often lead to destruction of the latter and formation of an eggshell like outer layer surrounding the fibrous sack of the cyst. Whilst a lot of the lesion of 2008-78/655 is missing, no eggshell-like layer was observed. Furthermore, aneurysmal bone cysts tend to produce periosteal reactions, which have also not been detected in this case.

On x-ray, the aneurysmal bone cyst usually shows fine-walled cystic cavities, the "soap bubble" sign, and are located eccentrically, cortical bone bulging is also a common feature, and the lesion presents as well defined with or without a sclerotic rim. The x-ray of the lesion of 2008-78/655 showed a well-defined margin with sclerotic rim and presented as a single cavity. According to Ragsdale et al. (2008), this type of margin is referred to as Type IA margin and typically occurs in bone cysts, enchondromas and non-ossifying fibromas. However, as the lesion is partially broken and destroyed, it cannot be determined whether the rest of the lesion was also unicameral or not. Overall, the mature age of the individual as well as the location of the lesion in the ilium and the absence of periosteal reaction suggest that aneurysmal bone cyst is not the best fitting diagnosis for this lesion.

The same can be said for giant cell tumour which also creates large well-defined lytic lesions. *Giant cell tumours* are rare benign bone lesions occurring predominantly in the metaphyses of long bones (Mendenhall *et al.* 2006), but the pelvis has also been mentioned among the commonly affected areas (Marques 2019). Among the benign neoplastic conditions however, they are relatively common (Marques 2019). They can be slow-growing but more often are

locally aggressive and cause a lot of bone destruction (Mendenhall *et al.* 2006; Marques 2019). Giant cell tumour usually does not produce sclerotic margins however, which are clearly present in this case and appears eccentrically on radiographs (Turcotte 2006). But the age of predilection for developing giant cell tumour lies between 20-50 years (Mendenhall *et al.* 2006), which matches the age range of this individual. However, it is generally more frequently observed in women (Mendenhall *et al.* 2006). The presence of sclerotic margins makes the diagnosis of giant cell tumour rather unlikely for the lesion of 2008-78/655.

Enchondromas are slow-growing benign tumours which are already present at birth and develop slowly during childhood and adulthood. They affect primarily bones of cartilaginous origin and account for about 10%-25% of all skeletal tumours (Park 2015). Tubular bones of the hand are most frequently affected, followed by long bones but lesions in the pelvis have also been reported (Waldron 2009; Marques 2019). On the radiograph, the enchondroma presents a well-defined sclerotic and lobulated margin. Enchondromas have no sex predilection and are today detected mostly in individuals in their 2nd-4th decades of life (Waldron 2009; Park 2015; Marques 2019). The lesion described for individual 2008-78/655 would fit the description of enchondroma quite well, which is why enchondroma will be kept as differential diagnosis. However, the lesion does not display a lobulated margin on radiograph, but it has to be kept in mind that the lesion is not complete.

Chondromyxoid fibroma, a tumour originating in cartilage also causes well demarcated lytic lesions in bones and radiographs should show sclerotic margins and, in some cases, also specks of tissue calcification. However, chondromyxoid fibroma is a fairly uncommon benign tumour but pelvic involvement is not too uncommon. Mean age of modern patients with pelvic chondromyxoid fibroma was around 48 years (Marques 2019; Sono *et al.* 2019).

Chondromyxoid fibroma should be kept as differential diagnosis for the lesion observed in 2008-78/655, even in the absence of calcified tissue.

Chondroblastoma are rare cartilaginous tumours that occur predominantly in long bones and more seldom also in other bones (Aufderheide & Rodriguez-Martin 1998; Waldron 2009; Marques 2019) but among those, the ilium and especially the acetabular region are most commonly affected (Marques 2019). They affect primarily children, adolescents and young adults and are very rare after 30 years of age. They are defined as spherical or oval lytic lesions with well-defined and, on radiograph, often sclerotic margins (Waldron 2009) and are often accompanied by periosteal reactions (Marques 2019). The age of predilection of chondroblastoma as well as the likely presence of periosteal reaction makes it a very unlikely

differential diagnosis since the lesion from individual 2008-78/655 shows no periosteal new bone formation and the individual is at 40-49 years considered too old to present such a lesion. *Fibrous dysplasia* should also be considered as differential diagnosis. Fibrous dysplasia occurs due to proliferation of fibrous tissue in bone marrow and is a relatively rare congenital condition (Chapurlat & Meunier 2000). There are two forms of fibrous dysplasia, the non-aggressive monostotic form which usually only affects one bone and occurs most frequently in the femur, tibia and ribs, and the aggressive polyostotic form in which several bones are affected, mainly the pelvis, long bones, ribs and cranium. A "ground-glass" appearance on radiograph is typical for this condition if the degree of fibrous tissue in the lesion is high. Characteristic is also bowing of weight-bearing bones, named shepherd's crook deformity, although this does not occur in all cases (DiCaprio & Enneking 2005; Marques 2019). Pelvic involvement is only noted for the polyostotic form (Marques 2019). However, the remainder of 2008-8/655's skeleton did not show evidence of further lesions, although for absolute clarity, it would be necessary to evaluate radiographs of all other postcranial bones to verify this. Furthermore, there was no "ground glass" appearance on the radiograph and none of the weight-bearing bones showed signs of bowing. The absence of multiple lesions, as well as the mature age of individual 2008-78/655 render fibrous dysplasia a very unlikely diagnosis for this lesion.

Another possible condition that might be considered is *non-ossifying fibroma*, although the condition also occurs predominantly in long bones of children and adolescents and pelvic involvement is very rare. Non-ossifying fibroma is more common in males and mostly located in the bone cortex (Bowers *et al.* 2013). It is demarcated by a sclerotic border which shows scalloped edges on the radiograph (Marques 2019). The radiograph of the lesion of 2008-78/655 did not show scalloped edges and the lesion was clearly located in the trabecular bone. Additionally, cortical thinning is typical for this condition but that could not be observed in this specimen, at least not in the preserved parts. Furthermore, the age of individual 2008-78/655 largely excludes non-ossifying fibroma as possible diagnosis.

In conclusion, due to the fragmentary nature of the lesion observed in the left ilium of individual 2008-78/655, no clear diagnosis was possible. It is clear however, that the lesion was slow-growing and benign. When considering all factors listed before, an intraosseous ganglion seems to be the best fitting diagnosis for this individual although, simple bone cyst, chondromyxoid fibroma, enchondroma and aneurysmal bone cysts should be kept as differential diagnoses. Subchondral bone cyst, fibrous dysplasia, chondroblastoma and non-ossifying fibroma can be largely excluded as possible differential diagnoses. Intraosseous

ganglia are also uncommon findings today, which is likely due to the fact that they are mostly asymptomatic, and the majority are incidental findings on radiographs (Schajowicz *et al.* 1979; Bonar 2009). Only one single intraosseous ganglion has been identified so far in the archaeological record. It is located in the iliac bone of a 15 year old individual from 13th-15th century St. Mary Spital cemetery in London (Walker 2012). Therefore, this case adds to the sparse record of published bone cysts in general and especially intraosseous ganglia in the archaeological record.

Intraosseous Ganglion

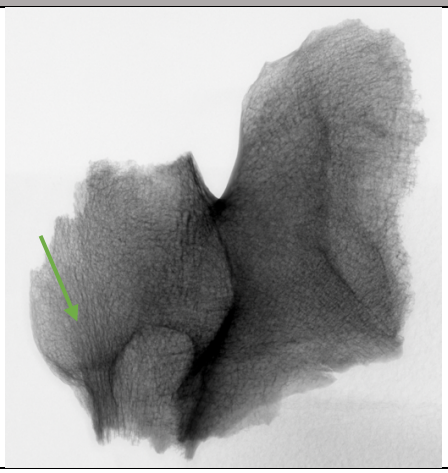

Figure 120 Radiograph of the left ilium with probable intraosseous ganglion above the acetabulum (2008-78/655)

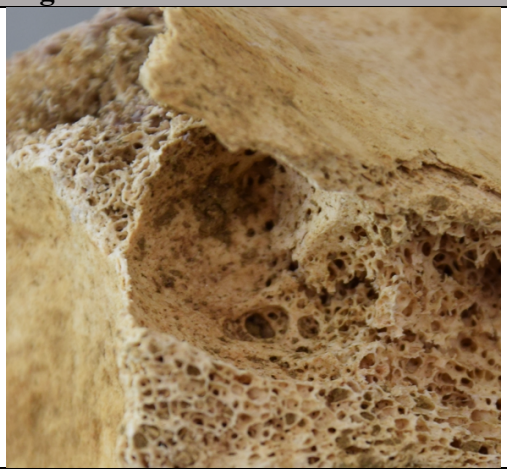

Figure 121 Close-up of the cavity above the acetabulum probably caused by and intraosseous ganglion, showing the smooth borders (2008-78/655)

Figure 122 Ventral view of the cavity probably caused by an intraosseous ganglion (2008-78/655)

Figure 123 Top view of the left ilium with the cavity visible in the lower right corner superior to the acetabulum (2008-78/655)

6.3.4 Malignant neoplasms

6.3.4.1 Introduction

Nowadays, cancer is, after cardiovascular disease, the second most common cause of death globally (David & Zimmerman 2010; Ritchie *et al.* 2018). However, evidence of cancer in the skeletal record seems relatively sparse. Since the 1900, only 272 cases of malignant neoplasm have been reported from the palaeontological and archaeological record, demonstrating the antiquity of cancer (Hunt *et al.* 2018). According to Siek (2019), four principal theories have been established to explain this relative lack of cancerous lesions observable in past populations, compared to the high incidence of cancer in modern populations. He summarised them as "The Age at Risk Argument", "the Early Death Argument ", "the Omission and Preservation Argument", "and the Ancient Environment Argument" (Siek 2019). The Age at Risk Argument mainly postulates that people did not live long enough to reach older age where cancer risk increases (Aufderheide & Rodriguez-Martin 1998; Roberts & Manchester 2010; Siek 2019). The Early Death Argument posits that people did develop neoplasms in the past but that, in absence of medical care, they succumbed to the disease before it could leave traces on the skeleton (Ricci *et al.* 1995; Aufderheide & Rodriguez-Martin 1998; Roberts & Manchester 2010; Siek 2019). The Ancient Environment Argument proposes that the load of environmental carcinogens was too low in the past to cause cancer (Aufderheide & Rodriguez-Martin 1998; David & Zimmerman 2010; Roberts & Manchester 2010; Siek 2019). This argument is support by the fact that the industrialisation brought along environmental pollution due to radiation, harmful chemicals and other potentially carcinogenic particles, that past populations probably never encountered or at least not in such high concentrations (Roberts & Manchester 2010). Finally, the Omission and Preservation Argument surmises that soft tissue tumours decay and secondary bone lesions are quite frail and exposed to a host of taphonomic factors that might alter the bone surface to such an extent that detection of the lesions is rendered impossible. Among such factors are for example soil acidity, rodent or other animal activity, tree root etchings etc. (Aufderheide & Rodriguez-Martin 1998; Capasso 2005; Siek 2019). The argument also addresses possible underdiagnosis of cancer in the past due to limited medical knowledge and lack of diagnostic tools (Ricci *et al.* 1995; Roberts & Manchester 2010; Siek 2019). The Omission and preservation argument remains also pertinent today, as a recent study by Marques et al. (2018) has shown. Several skeletons were sampled from an assemblage where all individuals had a neoplasm as cause of death, and they were then analysed macroscopically without knowledge of the prior tumour. The results showed that macroscopic

analysis was not sufficient to clearly distinguish the lesions associated with the neoplastic process as they were too unspecific (Marques *et al.* 2018). Also, comparisons of archaeological material to modern reference collections might also lead to underdiagnosis of cancer since reference collections usually represent the extreme cases of the disease that could be reached due to modern medicine, whereas it is likely that the majority of cancer lesions in the archaeological record actually only show lighter expression of the conditions, which might then not be as readily recognizable as neoplastic lesions (Ragsdale *et al.* 2018). Therefore, it is important to always consider differential diagnoses when assessing neoplastic lesions in past populations. On one hand, if the lesions are not specific, differential diagnoses cover the whole range of possible pathologies that might cause such lesions, on the other hand, if the patterns of lesion type and distribution are more specific, considering differential diagnoses might help to narrow down the possible underlying diseases responsible for the formation of the lesions.

6.3.4.2 Results

6.3.4.2.1 Individual 2008-78/380

Individual 2008-78/380 was buried in Layer 1 and recovered from within the cloister area. The skeleton was mostly complete and bone surface preservation was good. The skeleton was represented by a fragmented cranium, maxilla, mandible, the left scapula, both clavicles and ossa coxae, all ribs, the majority of the cervical and all of the thoracic and lumbar spine, several right and left hand and foot bones, as well as the right and left upper and lower appendicular skeleton except for the left patella. Ageing and sexing were based on diagnostic features of the skull and pelvis described in detail in the Methods chapter of this thesis. Individual 2008-78/380 was a senile male and numerous beads found among the hand bones suggest that he was buried with a rosary. The sex, age, burial position, and presence of a rosary suggest that 2008-78/380 might have been one of the monks living in the Franciscan monastery. Before the description of the main lesions, it is necessary to address the other pathological lesions observed in the skeleton. These were mainly degenerative changes in the joints of the long bones, ribs, and vertebrae, including osteoarthritis with eburnation on some rib head and neck articular facets, on the left scapular acromion, on the right and left clavicular acromial ends, and on the right distal ulnar and radial epiphyses. Furthermore, moderately strong osteophytes were observed on the distal end, lateral side around the contact area of the fibula on the right and left tibiae. Additionally, there was a small button osteoma inside the frontal sinus. No further lesions were observed in the postcranial skeleton.

The cranium however displayed several osteolytic and mixed lesions. A small erosive spot surrounded by a light spiculated periosteal reaction was observed on the endocranial side of the right temporal close to the sphenosquamous suture. A small round dip with a light periosteal reaction was observed endocranial on the right parietal close to the lambdoid suture. Another larger round dip with periosteal reaction (lamellar and spiculated) was recorded also endocranial on the right parietal but close to the coronal and sagittal sutures and located at the end of a meningeal vessel. Compared to the meningeal vessel on the left parietal, the one on the right was not particularly enlarged. The lesion on the right parietal was perfectly circular and, in its centre, penetrated the tabula externa creating a small circular hole of ~3mm Ø with only slightly jagged margins (Figure 125, Figure 126). On the left parietal, a small lesion, which looked like a deep arachnid granulation at the end of the meningeal vessel, also pierced the tabula externa but the opening measured only ~1mm. No ectocranial lesions were detected. The left zygomatic process of the frontal bone was broken, and the broken-off part was still attached to the frontal process of the left zygomatic bone. The left zygomatic process was enlarged from the outside and inside was a large lytic lesion whose walls were densely covered in new woven bone (spongiosclerosis) (Figure 128). The lesion continued into the top part of the frontal process of the zygomatic bone (Figure 130). Ectocranial, the surface around the lesion was smooth and no periosteal reaction could be observed. This type of lesion, showing both osteolytic and osteoblastic processes is called a mixed lesion. Another smaller lytic lesion also with new bone formation, but to a lesser extent was discovered at the zygomatic tubercle on both the left zygomatic and left maxillary bone (Figure 127). No periosteal reaction was detected on the ectocranial surface either. The remaining skeleton did not present any visible lesions. In a next step it would be advisable to take radiographs of several postcranial elements in order to check for further osteolytic lesions within the bones. The left parietal and the frontal with part of the right parietal as well as the maxilla and zygomatic bones were subjected to radiography. On the radiograph, the lytic lesion in the zygomatic process appears cloudy and not well demarcated, without a clear sclerotic border. Two further translucent areas were discovered on the frontal bone which are related to small thinning lesions on the endocranial surface which seem to rather represent arachnid villi (Figure 129).

6.3.4.2.2 Individual 2008-78/247

Individual 2008-78/247 was buried in Layer 2 in the cloister area. The skeleton was fairly well preserved, with most bone being present and surface preservation being overall good. The

skeleton was represented by a fragmented cranium, maxilla and mandible, all ribs, the majority of vertebrae, sacrum, several hand and foot bones, the right and left scapula and ossa coxae as well as the upper and lower left and right appendices. Age and sex were assessed based on morphological features of the skull and pelvis described in the Methods section. Individual 2008-78/247 was estimated to be a mature male and pieces of a belt buckle were found in the grave.

2008-78/247 showed multiple osteolytic lesions, several accompanied by irregular periosteal reactions, throughout the skeleton. The most prominent lesions were located on the ossa coxae, more precisely on the ilia. The right ilium presented a large area of aggressive periosteal reaction on the posterior side of the iliac blade close to the iliac crest (Figure 135, Figure 133). A large area of the iliac blade was missing along the area with periosteal reaction. The missing area margins were rounded, suggesting that at least part of the missing area might have contained a large lytic lesion. This assumption is supported through the presence of a large osteolytic lesion inside the trabecular bone of the right ilium in a fragment close to the iliac crest and the posterior iliac spine. The walls of the osteolytic cavity showed already very irregular new bone formation (Figure 137). It was not possible to directly fit the fragment to the iliac blade. Several more patches of reactive bone were observed on the right ilium and a smaller lytic lesion was recorded on the lower anterior iliac spine (Figure 135). On the left os coxae, a large lytic cavity was observed on the posterior side of the ilia blade (Figure 136). The walls of the osteolytic cavity were covered in irregular and slightly spiculated new bone and it seems like the cavity had already broken through the cortex as it was only covered by a thin layer of irregular and spiculated new bone (Figure 131, Figure 132). Additional lytic lesions were recorded on the auricular surface of the left ilium (Figure 134). A radiograph revealed further 7 lytic lesions that were not visible macroscopically, in the trabecular section of the left os coxae along the anterior border and the acetabulum (Figure 138).

Osteolytic lesions were also observed in the right scapula (Figure 140), the most prominent lesion being a large hole penetrating through the scapular spine, surrounded by light new bone formation. The lesion presented with an irregular contour but sharp margins giving it a “pinched-out” appearance (Figure 139). Two further osteolytic lesions were discovered on a radiograph in the apex of the right scapula (Figure 141). Macroscopically, none of the long bones showed any osteolytic or osteoblastic lesions. Radiographs of the femora and tibiae did not reveal any lesions either. However, a radiograph of the right humerus revealed the presence of two well defined osteolytic lesions, one in the proximal diaphysis situated rather concentrically and one in the middle of the diaphysis situated eccentrically. Both lesions did

not show a sclerotic border (Figure 142). A radiograph of several cranial fragments revealed several osteolytic lesions that were not visible macroscopically. Three lytic lesions without sclerotic margins and with rather unclear borders were situated in the left parietal. In the occipital, 3 osteolytic lesions with non-sclerotic diffuse margins were discovered in a line along the upper arm of the cruciform eminence and a 4th was situated directly next to it. At least two more lesions were discovered in or next to the right lateral arm of the cruciform eminence (Figure 143). Although macroscopically, no lesions were visible on the inner and outer tables of the cranium, a rounded osteolytic lesion with irregular aggressive new bone formation on the walls, was discovered inside the diploe of a fragment of the left parietal (Figure 144). A small (~3mm long) osteolytic lesion with sharp margins and surrounded by light new bone formation, was situated on the medial side of the left mandibular ramus (Figure 145). A small osteolytic lesion was also found on the ectocranial side of the occipital base (Figure 146) and two lesions with reactive bone were located on the ectocranial side of the sphenoid ala major close to the glenoid cavity of the left temporal (Figure 147). Several vertebrae, mainly the cervical ones, also showed osteolytic lesions of moth-eaten appearance on the vertebral arches (Figure 149). A large round osteolytic lesion of typical "moth-eaten" appearance, surrounded by aggressive periosteal reaction was located on the left side of the body of the sacral S1. Another lesion was located on the upper plate of S1 (Figure 148). Additionally, a few lumbar vertebrae also showed one lytic lesion without reactive bone on the vertebral plates and in the transverse processes, but radiographs of the vertebrae without macroscopically visible lesions did not reveal any further lesions. Radiograph of the ribs revealed a few small lytic foci inside the bodies of some of them, but none were visible with the naked eye.

6.3.4.2.3 Individual 2016-082/418

Individual 2016-082/418 was buried in the cloister area in Layer 2. The skeleton was preserved quite well, but the lower appendices and feet were missing. However, the cranium with maxilla and mandible, both scapulae, claviculae and ossa coxae as well as the majority of the spine and ribs and the right and left upper appendices were preserved. Bone surface preservation was good for the postcranial skeleton and the cranial base and facial bones, but the cranial vault was heavily eroded. Age and sex estimation followed the standard guidelines for morphological features of the skull and pelvis described in the Methods chapter. However, while sex estimation was straight forward, age estimation proved rather challenging. Most of the sutures could not be used reliably due to erosion and the pubis and auricular surface were mostly

destroyed by osteolytic lesions and/or covered by new bone formation. 2008-78/418 was a male individual of adult or even mature age and was included as adult in the demographic analyses. The cranium and all of the post cranial bones with the exception of the hand bones, ulnae and radii, were covered extensively with osteolytic lesions with the majority of lesions exhibiting periosteal reactions. The most prominent lesions were situated on the iliac blades of the right and left ossa coxae. Whilst the left ilium was covered extensively in patches of small lytic lesions of "moth-eaten" appearance and periosteal new bone formation (Figure 151), the right ilium showed a large coalesced lytic lesion on the anterior side of the iliac blade, surrounded by spiculated and irregular new bone formation (Figure 150, Figure 152). The rest of the iliac blade and ischium presented patches of smaller lytic lesions. The left os pubis presented many small osteolytic lesions of "moth-eaten" appearance without periosteal reaction (Figure 153). Both humeri showed extensive osteolytic lesions on the proximal epiphysis, metaphysis and proximal diaphysis (Figure 154). Periosteal reactions were also observed in patches among the lytic lesions, as a close-up shows (Figure 155). The right humerus showed a badly healed fracture of the complete distal epiphysis, which resulted in major destruction of the joint, leading to degenerative changes. A radiograph as well as CT-scans revealed traces of lead shrapnel (white dense dots on the radiograph) inside the fracture, which were not visible from the outside, as well as a few small lead shrapnel fragments inside the olecranon of the right ulna (Figure 156). This indicates that the fracture was likely caused by a gunshot wound to the elbow rather than a consequence of the underlying condition or through a fall. Macroscopically, the right and left clavicle showed increased porosity in the acromial end and on radiographs, osteolytic lesions inside the trabecular bone were revealed (Figure 157). The sternum, body and manubrium, showed increased porosity, with one small but clear lytic lesion at the anterior distal end (Figure 158). The vertebrae showed slight surface porosity, but radiographs did not reveal any osteolytic lesions. Many ribs showed evidence of osteolytic lesions and in some, they were very extensive. Most lesions were located in the middle or towards the sternal end of the ribs, heads were also involved but less frequently and less intensely (Figure 161, Figure 162). All lytic lesions on the ribs were accompanied by strong new bone formation, presenting either as unregular lamellated or unregular spiculated deposits, partially altering the bone contour (Figure 163, Figure 164, Figure 165, Figure 166). Radiographs of the ribs revealed that the lesions were mostly solely lytic with ill-defined margins, however, three ribs showed sclerotic lesions associated to lytic ones (Figure 177). Both scapulae showed many osteolytic lesions with periosteal new bone reaction, mainly along the spine, glenoid and on the coracoid (Figure 159, Figure 160). Although the posterior part of the vault was heavily eroded and a

clear distinction between osteolytic and taphonomic alteration was impossible, a few osteolytic lesions were discovered on the anterior side of the cranial vault (Figure 168, Figure 169). In one case, the lesion was surrounded by increased porosity and a light bony reaction (Figure 168). Further osteolytic lesions were also visible on the ectocranial side of the right and left greater wing of the sphenoid (Figure 167) and the lesions extended internally into the zygomatic bone, which was clearly visible on a CT-scan (Figure 173). A large osteolytic lesion of "moth-eaten" appearance was also observed at the base of the right temporal right next to the glenoid cavity and extending into the sphenoid (Figure 171). The majority of the cranial base showed small lytic lesions and increased porosity (Figure 172). Another larger lytic lesion of "moth-eaten" appearance was situated on the superior medial border of the right orbital roof. Strong and aggressive new bone formation associated to the lytic lesion can be observed across the complete orbital roof (Figure 170). Several small osteolytic foci were observed across the left orbital roof. CT-scans of the cranium revealed several more lytic lesions inside the diploe that were not visible from the outside. The margins of the majority of the lesions were not well defined. (Figure 173, Figure 174). Lastly, the mandibula also presented with a larger lytic lesion in top of the alveolar process of the right body. No periosteal reaction was associated with this lesion. The teeth in this area had already been lost after death and the alveola had already closed completely. However, the lesion does not resemble that of a closing alveola and occurred after loss of teeth or might have contributed to the loss (Figure 175). A small patch of periosteal new bone was found on the lateral side of the left mandibular ramus. A healed oblique fracture was also observed in the left mandibular body at the height of the missing premolars, just posterior to the mental foramen (Figure 176). No signs of infection were observed in the area and the callus was only small. A radiograph of the mandible did not reveal any further osteolytic lesions besides that already observable macroscopically. Therefore, it can be assumed that the fracture did not occur as a consequence of the underlying pathological condition. Only 2 possible pure osteoblastic lesions were observed. One involves the auricular surface of the left ilium, which seems to be covered by a thick smooth layer of bone, with some areas of unorganised bone showing underneath (Figure 178). The other was recorded on the posterior broken border of the left ilium, which exposed the trabeculae. A spot featuring bone formation within the trabecular space, called spongiosclerosis, was observed without an associated osteolytic lesion and was probably associated with the osteoblastic lesion of the auricular surface due to its close proximity (Figure 179).

6.3.4.2.4 Individual 2008-78/669

Individual 2008-78/669 was buried in Layer 1 on the cemetery. The skeleton was fairly complete and the surface rather well preserved, conserving nearly the complete cranium in a fragmented state, the maxilla, the mandible, both scapulae and clavicles, the sternum, both ossa coxae with the exception of the pubis, 11 right and left ribs, with the 12th ribs missing congenitally, the complete spine including the sacrum, a few right and left hand bones as well as right and left sides of the upper and lower appendicular skeleton, with the exception of the right radius and right patella. Only some vertebral bodies had been partially destroyed during excavation, but it was possible to refit all fragments. Ageing and sexing using the standard methods involving the cranium and ossa coxae, described in the Method chapter of this thesis, revealed that individual 2008-78/669 was a mature (40-49y) female.

Only one single lesion was observed for individual 2008-78/669. The 10th thoracic vertebra showed a multitude of lytic lesions in the spinous process (Figure 180, Figure 181) The rest of the vertebral arch was missing. The lesions were quite small in diameter and mostly elongated or oval. The margins of the lesions appear moth-eaten and the trabecular bone inside the spinous process had nearly completely been destroyed, probably due to coalescing lesions. No periosteal reaction was observed around the lesions on the vertebral arch or body nor on the surrounding vertebrae. The body of the 10th vertebra showed no lesions at all, nor did the surrounding vertebrae. The body of the 10th thoracic vertebra had been broken apart during excavation and the trabecular structure was exposed in many areas. No further lesions were detected in the remaining skeleton. However, a light active periosteal reaction was observed along the intertrochanteric line of the right femur and a light healed periosteal reaction was recorded on the medial side of the left femoral midshaft and on both the lateral and medial sides of the left tibial midshaft.

Radiographic analysis of the 9th thoracic vertebra reveals no lesions (Figure 182). However, a rounded radiolucency could be observed in the proximal metaphysis/epiphysis of the right humerus (Figure 183), which might be suggest the presence of further lytic lesions in the skeleton, that are not visible with the naked eye.

6.3.4.3 Discussion and Conclusion

Many of the lesions observed in the different individuals described above share similarities. They are all osteolytic or mixed lesions and, in many cases, but not all, are accompanied by more or less severe periosteal reactions. Purely osteoblastic lesions were not observed.

Altogether, for most individuals the kind of lesion and their distribution is highly indicative of malignant neoplastic disease. The following section will present the most likely differential diagnoses for the lesions presented in the previous section and will discuss the lesion pattern of each individual in regard to the differential diagnosis in order to find the most plausible diagnosis for each individual. The conditions considered in the differential diagnosis are, in the order of likelihood, Metastatic Carcinoma, Leukaemia, Multiple Myeloma, Langerhans Cell Histiocytosis, Mycoses and, in one case, localised infection. These diagnoses were selected and considered because they can all produce multiple osteolytic lesions throughout the whole skeleton.

6.3.4.3.1 Metastatic carcinoma

Cancer metastases represent lesions that arise when cancer cells break away from a primary tumour, most commonly an organ tumour, and spread to other areas of the body and other tissues via direct spread, the bloodstream and/or the lymphatic system (McKinnell 2006). Since the internal structure and composition of bone is composed of a variety of cells, minerals and hormonal growth factors, it is one of the most common sites of predilection for cancer metastases (Coleman 2001; Fournier *et al.* 2014; Macedo *et al.* 2017; Fornetti *et al.* 2018). In fact, metastatic carcinoma is the most common malignant neoplasm and is also more prevalent than benign bone tumours (Marks & Hamilton 2007). Prostate and breast carcinoma are the tumours that spread to bone most frequently, followed by carcinoma of the thyroid, lung and kidney. Other carcinomas such as bladder and renal cell carcinoma can also form bone metastases but do so rather infrequently (Aufderheide & Rodriguez-Martin 1998; Coleman 2001; Coleman *et al.* 2006; Waldron 2009; Macedo *et al.* 2017; Maurizi & Rucci 2018). In rare cases, other tumours such as melanoma, osteosarcoma, gastrointestinal cancers or meningioma etc. can also metastasise to bone (Ather Enam *et al.* 1996; Coleman *et al.* 2006; Portales *et al.* 2015; Macedo *et al.* 2017; Odri *et al.* 2022). Skeletal metastases can be classified as osteoblastic, osteolytic and mixed. Osteoblastic lesions are the result of higher activity of osteoblastic cells leading to excessive bone formation on the bone surface and inside the trabeculae, which is also referred to as spongiosclerosis (Macedo *et al.* 2017; Biehler-Gomez *et al.* 2019). Osteolytic lesions are defined through an increased activity of osteoclasts resulting in bone destruction (Macedo *et al.* 2017). Mixed lesions are characterised by the simultaneous presence of osteolytic and osteoblastic reactions, and usually present as an osteolytic defect with either aggressive periosteal new bone formation on the bone surface and/or with

spongiosclerosis of the exposed trabeculae within the lytic cavity (Macedo *et al.* 2017; Biehler-Gomez *et al.* 2019). The distribution of metastatic lesions follows that of red bone marrow in the skeleton (Morgan *et al.* 1990; Macedo *et al.* 2017). Therefore, areas of predilection for bone metastases are the majority of bone of the axial skeleton, such as ribs, sternum, vertebrae and cranium (Macedo *et al.* 2017; Marques 2019), but the appendicular skeleton is also frequently affected, most commonly the ossa coxae and the proximal epi- and metaphyses of the humerus and femur (Marques 2019). Different carcinomas produce different patterns of metastases throughout the body (Figure 124). Whilst prostate carcinoma produces predominantly osteoblastic lesions, renal carcinoma produces predominantly osteolytic lesions (Coleman 2001; Waldron 2009). However, although breast cancer is listed here as producing mainly osteoblastic lesions, many sources attribute mainly lytic lesions and mixed lesions to this cancer (Aufderheide & Rodriguez-Martin 1998; Ortner 2003b; Marks & Hamilton 2007; Waldron 2009). Lung cancer is generally considered to produce predominantly mixed and osteolytic lesions (Waldron 2009; Wasterlain *et al.* 2011; Wu *et al.* 2021), same as thyroid cancer (Waldron 2009) and renal cancer (Coleman 2001; Waldron 2009). Bladder cancer is listed among the cancers with a predominance of osteolytic lesions, however, Biehler-Gomez et al. (2019) reported skeletal metastases of an individual clinically diagnosed with bladder carcinoma and the dominant lesion type was osteoblastic, followed by mixed lesions, whereas lytic lesions only account for 9% of all defects. Most skeletal metastases occur in older individuals over 40 years of age (Waldron 2009; Marques 2019). Except for 2008-78/669, all individuals presented with predominantly osteolytic or mixed lesions. In individual 2008-78/380, only the cranium was visibly affected, and radiographs revealed one potential lytic lesion in the proximal humerus. Individual 2008-78/669 only showed excessive osteolytic lesions in the spinous process of the 10th thoracic vertebra. Individuals 2008-78/247 and 2016-082/418 displayed a very similar pattern of distribution of the lesions, with the ilium showing most lesions, followed by the scapulae, cranium and humerus. In individual 2016-082/418, the ribs were also strongly affected. Apart from 2008-78/669, all individuals were male and mature or senile. 2016-082/418 might have been slightly younger since accurate age estimation was hindered by the lesions and taphonomy. The combination of osteolytic and mixed lesions and scarcity of purely osteoblastic lesions, together with the sex and age of the individuals puts lung carcinoma as a possible candidate for the primary soft tissue tumor, but other tumors such as thyroid or renal tumors are also plausible. According to Waldron (2009) lung carcinoma is the second most common cause for bone metastases after prostate carcinoma in men and is also overall more frequent in men than in women. Renal carcinomas metastasise to bone less

frequently than lung carcinoma but are also more common in men. Thyroid cancer also metastasises quite frequently into bone but occurs predominantly in women (Coleman 2001; Waldron 2009). Individual 2016-082/418 had likely lead shrapnel embedded into the distal humerus and proximal ulna and considering that hard callus formation around the fracture had already finished, the bone had been remodeled and degenerative changes were already visible in the deformed joint, the lead might have been there for a considerable time already, at least 12 weeks, as this is when remodeling of bone after hard callus formation usually starts (Kalfas 2001; Grupe *et al.* 2015). Lead is classified as a group 2A-carcinogen, which means that it is probably carcinogenic to humans (IARC 2006). This means that due to its daily exposure to lead individual 2016-082/418 might have been at a greater risk of developing cancer, which might also explain the possibly younger age of onset compared to the other individuals. Regarding individual 2008-78/669, who is a mature female, carcinoma of the breast, which produces predominantly osteolytic lesions might be a suitable candidate for the primary soft tissue tumor though thyroid cancer cannot be excluded either. However, it has to be kept in mind that the estimation of the primary tumors is only speculative as they are solely based on occurrence statistics in modern populations.

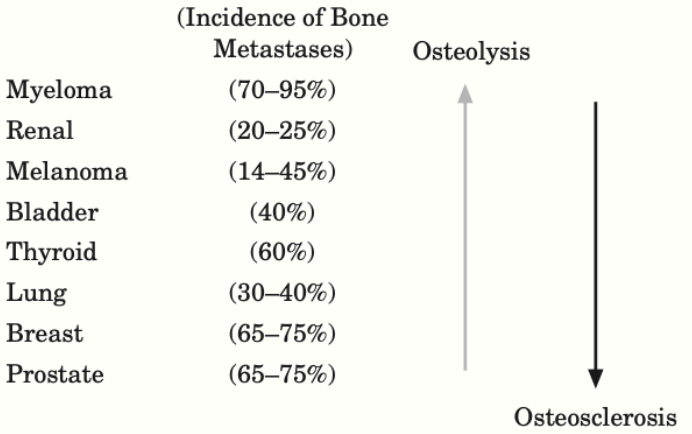

Figure 124 Primary soft tissue carcinomas and the type of metastatic lesions they produce (from Coleman (2001))

6.3.4.3.2 Leukaemia

Descriptions of skeletal changes associated with Leukaemia, especially in adults, are rare in palaeopathological literature. Leukaemia is a malignant condition of the myeloid and lymphoid blood cells. Skeletal involvement includes diffuse osteopenia and marked pitting in the metaphyseal area of the bones (Rothschild *et al.* 1997; Aufderheide & Rodriguez-Martin 1998; Grauer 2019). There are two types of leukaemia, chronic, which occurs only in adults and acute, which is more common in children but also occurs in adults and males are more frequently

affected than females (Waldron 2009). Skeletal lesions in adults differ from those seen in juveniles and children. According to Rothschild et al. (1997) in adults all bones are affected but to a lesser degree than in children, but multiple small lytic foci occurred characteristically in areas of the skull, as well as in the metaphyseal areas of clavicles, on the scapula along the glenoid cavity, scapular spine and apex. The humerus was affected by enlarged vascular channels in the proximal metaphysis, but diaphysis and distal ends were unaffected. Radius, Ulna as well as hand bones did not show any lytic lesions. Larger lytic lesions with minimal periosteal reaction were observed on the proximal femur but not on the diaphysis and distal ends, tibia and fibula were unaffected but lytic lesions with periosteal reactions were detected in some foot bones. In the thoracic area, the sternum and the ribs were heavily perforated by small lytic lesions. The vertebrae were all affected by multiple small lytic lesions in the body and arches with a focus on the cervical and sacral region and displayed slight periosteal reaction. Holes and fronts of resorption were recorded on the ilia especially along the anterior and posterior areas of the iliac crest, but lesions also occurred in the ischium and pubis (Rothschild *et al.* 1997). Rothschild et al. (1997), compared lesions of a subadult suffering from lymphocytic leukaemia to those of an adult suffering from myelocytic leukaemia, and therefore it is unclear whether the lesions described in the adult are reflect adult expression of the disease or are characteristic of myelocytic leukaemia. The distribution and type of the lesions in leukaemia differ from those observed in 2008-78/699, 2008-78/247 and 2008-78/380 and therefore leukaemia can be excluded as differential diagnosis for these individuals. However, considering the lesions observed in individual 2008-78/418, the type of lesions, their number and distribution is highly consistent with the pattern described for adult myelocytic leukaemia by Rothschild et al. 1997. Additionally, especially the pelvic lesions of 2008-78/418 resemble strongly those depicted in Rothschild's et al. (1997) study. The only factor that is not as consistent with leukaemia is the presence of larger lytic foci especially in the cranium such as the one in the right orbit, as well as the periosteal reactions near the lesions on the ilium and cranium and the possibly osteoblastic reaction in the left ilium. These kind of lesion have not been described by Rothschild et al. (1997) or in other palaeopathological literature (Aufderheide & Rodriguez-Martin 1998; Waldron 2009; Grauer 2019). Nevertheless, since skeletal lesions in adult leukaemia have not been described in any other studies in detail so far, it cannot be excluded that such lesions might still occur in other cases of leukaemia. Individual 2016-082/418, has metal, probably lead shrapnel embedded in the distal humerus and proximal ulna. Two case studies, on concerning and adult human (Crosby 1977) and one concerning a juvenile primate (Krugner-Higby *et al.* 2001), have observed a link between ingestion of large

lead quantities and subsequent development of myeloid leukaemia (Whitehead *et al.* 2015). Furthermore, paternal occupational exposure to lead has been associated with acute childhood myeloid leukaemia (Buckley *et al.* 1989). Therefore, it is possible that 2008-78/418 might have developed leukaemia due to constant lead exposure, this is of course only speculative. In conclusion, leukaemia remains a strong possibility in differential diagnosis for the lesions observed in individual 2008-78/418 and a decision between metastatic carcinoma and leukaemia as primary diagnosis cannot be made at this point for individual 2008-78/418.

6.3.4.3.3 Multiple myeloma

Multiple myeloma is a haematological cancer affecting the plasma cells in bone marrow and about 80% of modern patients present with skeletal lesions (Rajkumar & Kumar 2016). Bone lesions are characteristically purely osteolytic in nature, have sharply defined and smooth margins, an appearance which is also referred to as "punched-out" lesions, and completely lack periosteal and osteoblastic reaction (Grauer 2019; Riccomi *et al.* 2019). Most of the lesions are similar in size and rather small (5mm-2cm Ø) and occur predominantly in the cranium, ribs, vertebrae, pelvis and proximal femur (Aufderheide & Rodriguez-Martin 1998; Rothschild *et al.* 1998; Waldron 2009; Grauer 2019). Due to the periosteal and spongiosclerotic reactions observed in individuals 2016-082/418, 2008-78/247 and 2008-78/380, multiple myeloma can be excluded as differential diagnosis. However, the condition must be kept as differential diagnosis for individual 2008-78/669 which displayed multiple small lytic lesions in the spinous process of the 10th thoracic vertebra, without any new bone formation.

6.3.4.3.4 Langerhans Cell Histiocytosis

Langerhans Cell Histiocytosis is characterised by abnormal proliferation of the Langerhans cells found in haematopoietic bone marrow. These abnormal histiocytes are responsible for the removal of abnormal and dead cells. (Abla *et al.* 2010; Grauer 2019). Characteristic skeletal lesions associated to Langerhans Cell Histiocytosis are purely lytic lesions. The presence of sclerotic margins or reactive bone is possible but not always given (Grauer 2019). In modern populations, the incidence of skeletal involvement in Langerhans Cell Histiocytosis is also quite variable ranging from 28-83% for unifocal to 19-28% for multifocal lesions (Satter & High 2008). Three clinical manifestations need to be distinguished within Langerhans Cell Histiocytosis. Whilst the presentation and nature of the skeletal lesions is similar across all three manifestations, their distribution throughout the skeleton varies. Letterer-Siwe disease is

characterised by multiple lesions on the cranial vault and base. Hand-Schüller-Christian disease presents multiple large and coalescing lesions on the cranium, typically without any periosteal reaction. Eosinophilic granuloma is the unifocal expression of Langerhans Cell Histiocytosis and is generally characterised by a single oval or round cranial osteolytic lesion with a sloping margin and which occasionally presents a sequestrum at its center. Eosinophilic granuloma due to its unifocal nature can be excluded from the list of differential diagnoses. In all three conditions, involvement of the long bones is possible and consists of lytic foci primarily in the metaphysis with subperiosteal new bone formation (Aufderheide & Rodriguez-Martin 1998; Grauer 2019). Overall, the disease affects predominantly young individuals as 80% of modern cases were recorded in individuals younger than 30 years and 50% before the age of 10 (Marks & Hamilton 2007). The higher age ranges of the individuals analysed here already render Langerhans Cell Histiocytosis a rather unlikely diagnostic option. Additionally, the majority of cranial lesions observed in the analysed individuals show jagged margins and some also present osteoblastic reactions within the lytic lesions, which is not in agreement with any of the typical cranial lesions described for the different types of Langerhans Cell Histiocytosis.

6.3.4.3.5 Mycoses

Several groups of fungi can cause infections that may cause osteolytic lesions that mimic lesions typically found in metastatic carcinoma (Hershkovitz *et al.* 1998), although generally skeletal involvement is quite rare (Aufderheide & Rodriguez-Martin 1998; Marques *et al.* 2013). Fungal infections spread to bones via the bloodstream (Aufderheide & Rodriguez-Martin 1998). Generally, fungal infections only rarely affect the bone tissue (Grauer & Roberts 2019). Lytic lesions caused by mycoses usually present as fronts of resorption rather than space-occupying lesions. New bone formation occurs rather unfrequently in mycoses (Hershkovitz *et al.* 1998; Assis & Codinha 2010; Grauer & Roberts 2019) though it might be present in form of circumferential periosteal reactions around a lytic lesion. Characteristic for all fungal infections is the presence of blunt spiculae occurring throughout the skeleton (Lieverse *et al.* 2014; Micarelli *et al.* 2019). Of all possible mycoses, only three are endemic to Europe, those are sporotrichosis, histoplasmosis and cryptococcosis (Micarelli *et al.* 2019). Sporotrichosis and histoplasmosis can already be excluded from differential diagnosis as the former affects mainly the forearms (Hershkovitz *et al.* 1998), which show no lesions in any of the analysed individuals, and the latter never affects vertebrae (Buikstra 1976), which are areas of predilection in 3 of the analysed individuals. Cryptococcosis produces generally well

circumscribed lytic lesions and new bone formation is rare (Aufderheide & Rodriguez-Martin 1998; Grauer & Roberts 2019). Furthermore, the lesions can occur throughout the skeleton including the hands and feet and distal portions of long bones (Binder *et al.* 2014). Due to the nature of the lytic lesions (distribution throughout the skeleton, jagged and moth-eaten margins as well as reactive new bone in the trabeculae) observed in all four described individuals, as well as the rarity of bone involvement in the condition itself, cryptococcosis would be a rather unlikely differential diagnosis.

6.3.4.3.6 Infection

Tuberculosis is a chronic bacterial infectious disease caused primarily by the mycobacterium tuberculosis, although other members of the mycobacterium family can also affect humans (Roberts & Buikstra 2019). The infection generally starts in the lung and from there it can spread to bone via lymph nodes (Lieverse *et al.* 2014). Typical skeletal lesions of tuberculosis are osteolytic and osteoblastic lesions, with the spine being most frequently involved. Involvement of the spine is mainly restricted to the vertebral bodies and the vertebral arches and spinous and transverse processes are only very rarely affected. Furthermore, in the majority of cases there is joint involvement (Aufderheide & Rodriguez-Martin 1998; Roberts & Buikstra 2019). The bones most commonly affected after the spine include the ribs, pelvis, femur and small bones and phalanges of hand and feet and the shoulder, and in those areas, joints are most frequently affected. The cranium however is rarely involved (Roberts & Buikstra 2019). On the ribs, the lesions are most commonly osteoblastic while in the skull they are mostly well-circumscribed and purely lytic. On the long bones the lytic foci are typically well-circumscribed and accompanied by light periosteal reaction (Santos & Roberts 2001; Ortner 2003c; Assis & Codinha 2010; Lieverse *et al.* 2014; Roberts & Buikstra 2019).

The lesions observed in the cranium of individual 2008-78/380 and the lack of lesions in the vertebrae do not correspond to the typical pattern of tuberculosis and therefore the condition can be ruled out for this individual. The osteolytic lesion observed in the spinous process of individual 2008-78/669 is also not typical for tuberculosis which affects predominantly the vertebral bodies, whereas those were not affected at all in 2008-78/669. This means that tuberculosis can be ruled out as differential diagnosis for this individual as well. The multitude of lytic lesions observed throughout the skeleton of 2016-082/418 and 2008-78/247 show some similarities to lesions caused by tuberculosis. Especially the strong involvement of the ribs in 2016-082/418 is often observed also in tuberculosis infections. However, even though the

vertebral bodies in both individuals show osteolytic lesions, they have not led to structural instability not ankylosis of the spine (Pott's disease). Furthermore, in both individuals the vertebral arches are affected more often than the bodies, which is rather uncommon in tuberculosis. Additionally, none of the analysed individuals showed involvement of the joints.

6.3.4.3.7 Osteomyelitis

Osteomyelitis, a pyogenic viral infection of the bone marrow (Roberts 2019), was considered as possible cause for the lytic lesions observed in the spinous process of individual 2008-78/669. However, the complete lack of periosteal reaction and bone remodelling exclude osteomyelitis as possible differential diagnosis for this individual.

6.3.4.3.8 Conclusion

In conclusion, metastatic carcinoma seems to be the most likely diagnosis for all described individuals. However, for individual 2008-78/669, multiple myeloma should also be strongly considered even if there is no typical involvement of the cranium. For individual 2016-082/418, leukaemia and metastatic carcinoma have to be considered as equally plausible diagnoses.

Photo Table 2008-78/380

Figure 125 Top view of the frontal bone and part of the right and left parietal with the lytic lesion

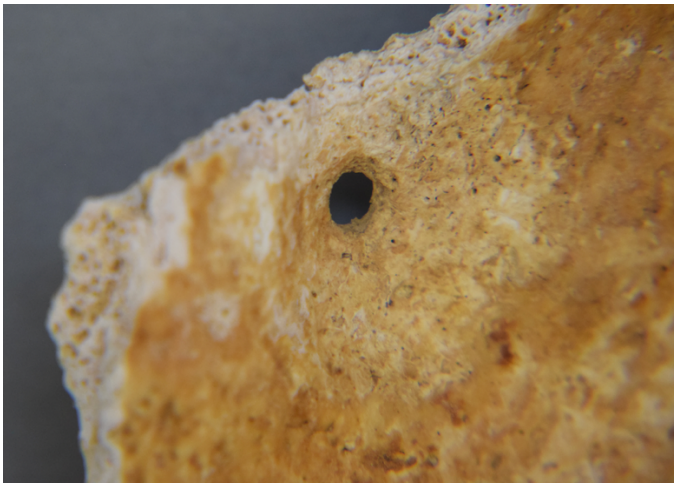

Figure 126 Close-up of the lytic lesion on the endocranial surface of the right parietal bone close to the coronal and sagittal sutures

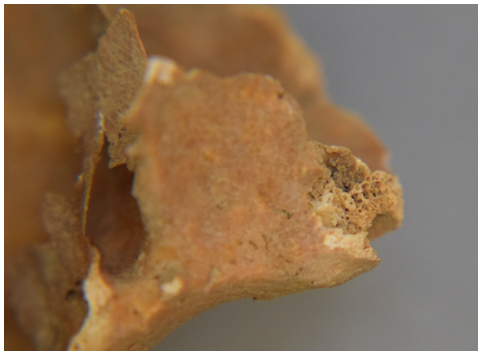

Figure 127 Smaller lytic lesion with bone reaction in maxilla at the zygomaticomaxillary suture

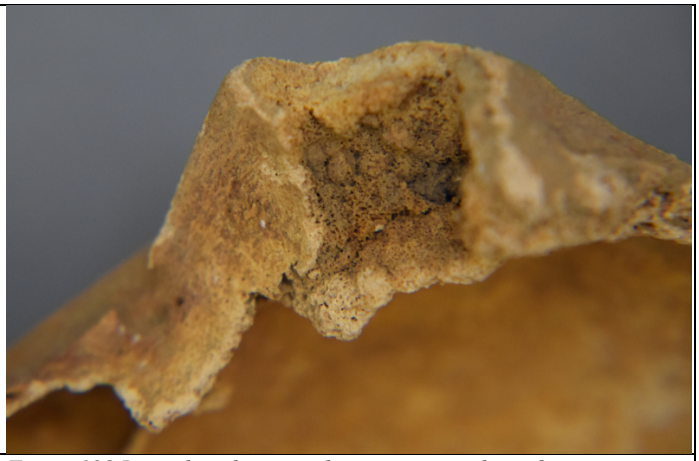

Figure 128 Large lytic lesion with extensive new bone formation inside left zygomatic process of frontal bone

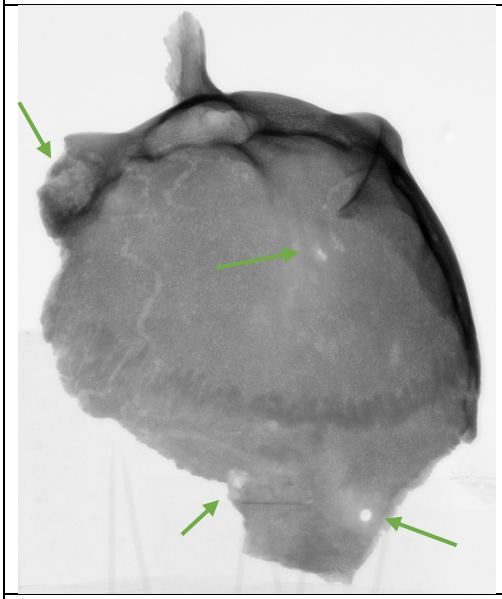

Figure 129 Ectocranial view of radiograph showing lytic lesions and the cloudy undefined lytic lesion in the left frontal process, reflecting the osteoblastic bone growth on the lesion walls

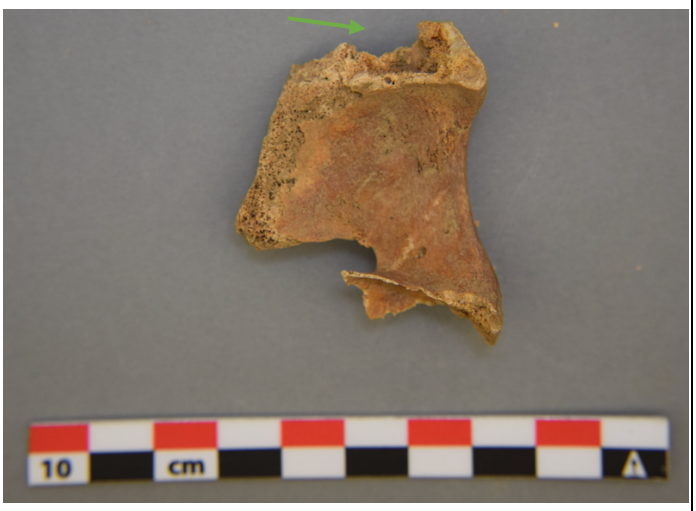

Figure 130 Lytic lesion with bone reaction inside frontal process of left zygomatic bone

Photo Table 2008-78/247	
	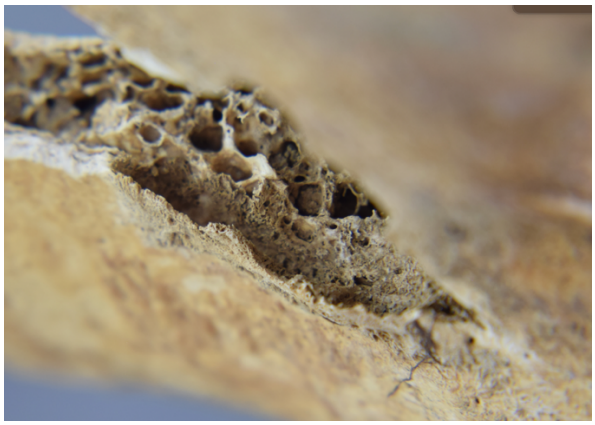
Figure 131 Strong irregular periosteal reaction covering an underlying osteolytic lesion on the lateral side of the left ilium	*Figure 132 View into the osteolytic lesion covered by irregular new bone, showcasing also intense new bone formation inside cavity (left ilium)*
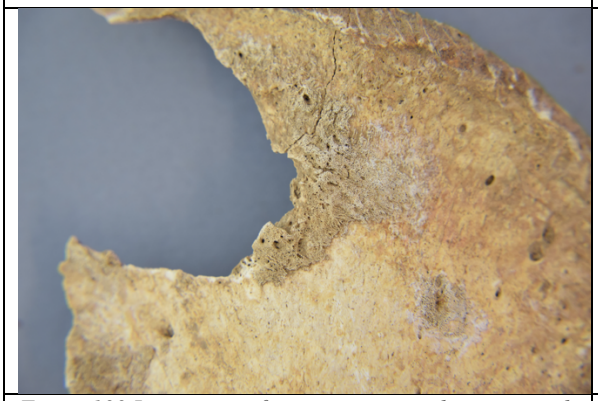	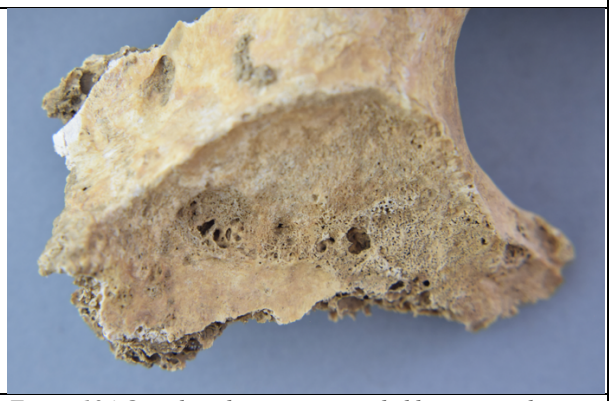
Figure 133 Large area of aggressive irregular periosteal reaction on the lateral side of the right ilium	*Figure 134 Osteolytic lesions surrounded by reactive bone on the auricular surface of the left ilium*

Figure 135 Lateral side of the right ilium with osteolytic lesions and aggressive periosteal reactions

Figure 136 Lateral side of the right ilium with osteolytic lesions and aggressive periosteal reaction

Figure 137 Large osteolytic lesion with aggressive new bone formation inside the trabecular bone at the right iliac crest

Figure 138 Radiograph of the left os coxae showing several osteolytic foci with diffuse margins that were not visible macroscopically

Figure 140 Posterior view of the right scapula with lytic lesions

Figure 139 Close-up of the osteolytic lesion in the scapular spine, surrounded by light reactive bone lesions

Figure 141 Radiograph of the right scapula revealing the presence of further osteolytic lesions in the apex

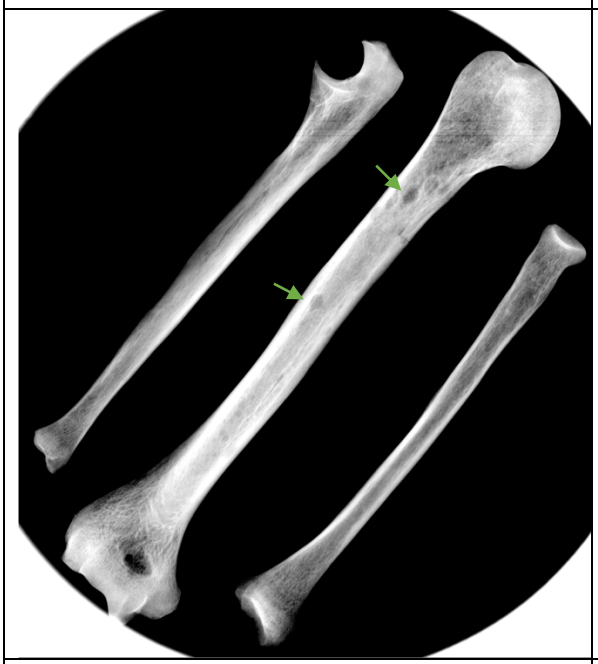

Figure 142 Osteolytic lesions in the right humerus that were not visible macroscopically

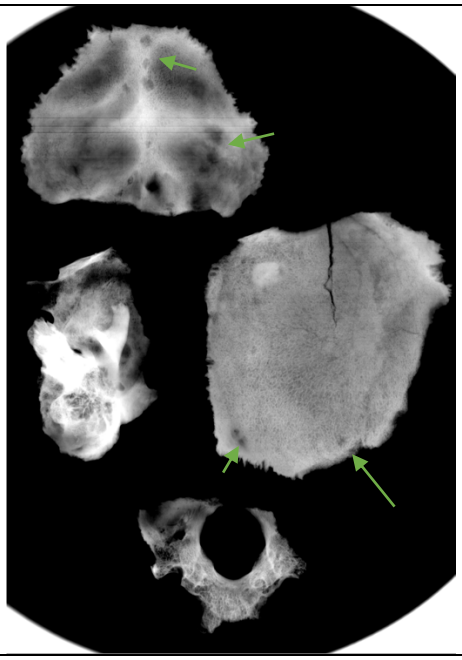

Figure 143 Osteolytic lesions inside the left parietal and occipital that were not visible macroscopically

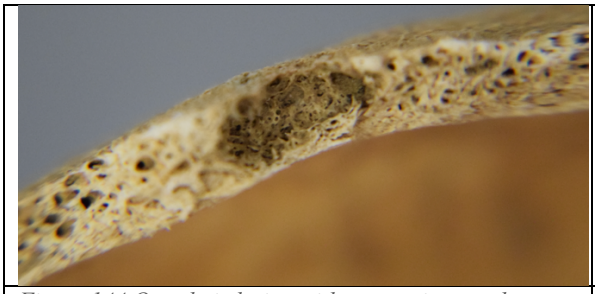

Figure 144 Osteolytic lesion with aggressive new bone formation inside the diploe of the left parietal

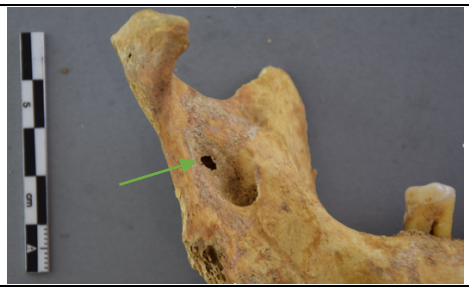

Figure 145 Osteolytic lesion on the inner side of the left mandibular ramus

Figure 146 Osteolytic lesion at the endocranial side of the occipital base

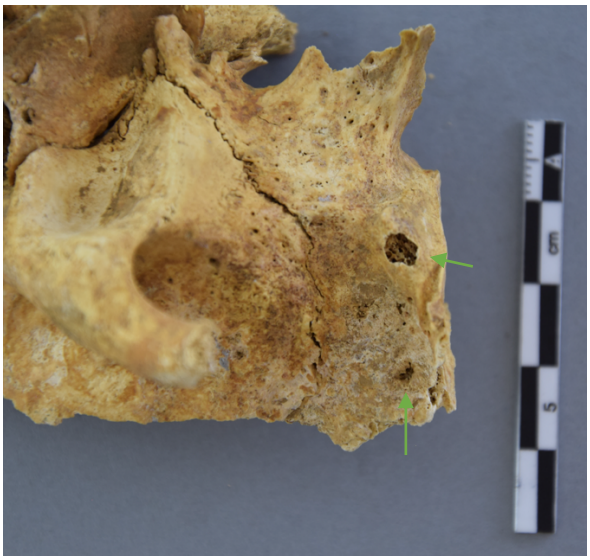

Figure 147 Osteolytic lesion and reactive bone on the ectocranial side of the left greater sphenoid wing

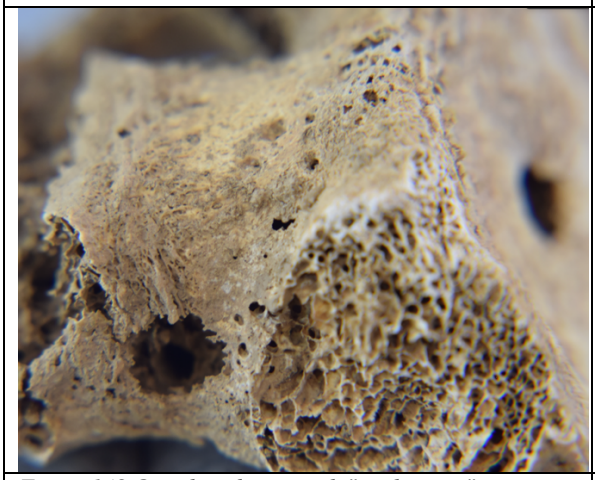

Figure 148 Osteolytic lesion with "moth-eaten" appearance in S1 of the sacrum with aggressive periosteal reaction at the margins (further osteolytic lesion on the S1 vertebral plate)

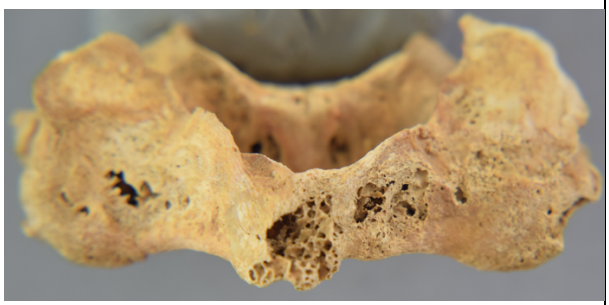

Figure 149 Osteolytic lesions in the vertebral arch of a cervical vertebra

Photo Table 2016-082/418

Figure 150 Right of coxae with osteolytic lesions and aggressive periosteal reaction

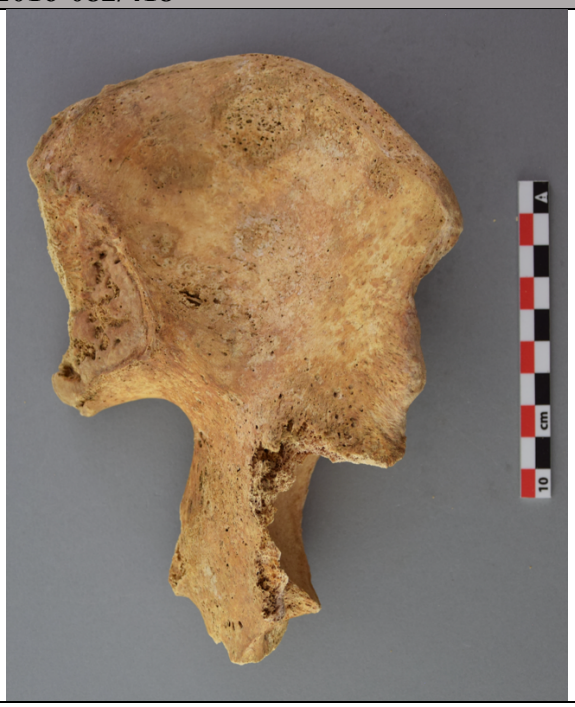

Figure 151 Left of coxae with osteolytic lesions and lihght aggressive periosteal reaction (surface change of the auricular surface)

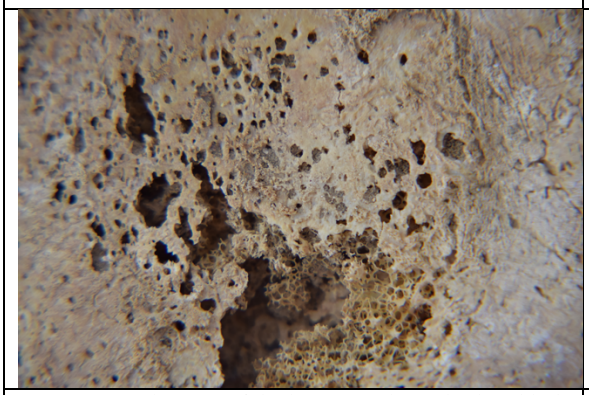

Figure 152 Close-up of the lesion on the right iliac blade showing coalesced lytic lesions with aggressive periosteal reaction

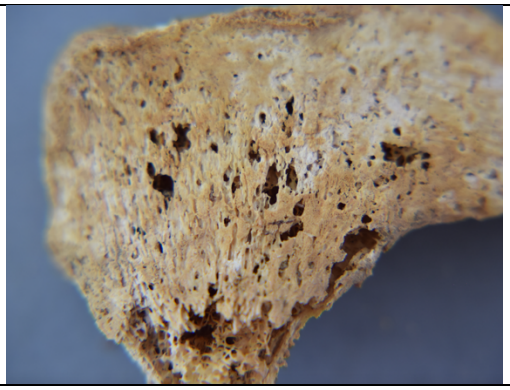

Figure 153 Multiple osteolytic lesions on the left os pubis

Figure 154 Right humerus with osteolytic lesions at the proximal meta- and epiphysis and a healed fracture at the distal epiphysis

Figure 155 Close-up of the osteolytic lesions in the right proximal humeral meta- and epiphysis with light aggressive periosteal reaction

Figure 156 Radiograph of the right Radius, Ulna and Humerus showing lead shrapnel in the distal humeral fracture and inside the ulnar olecranon

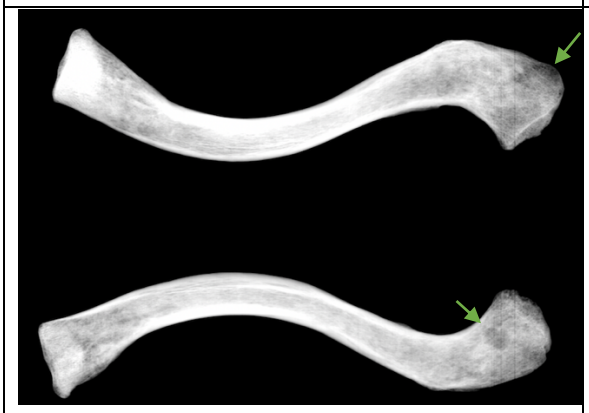

Figure 157 Radiograph showing an osteolytic lesion in the right and left clavicles

Figure 158 Small osteolytic lesions in the sternum

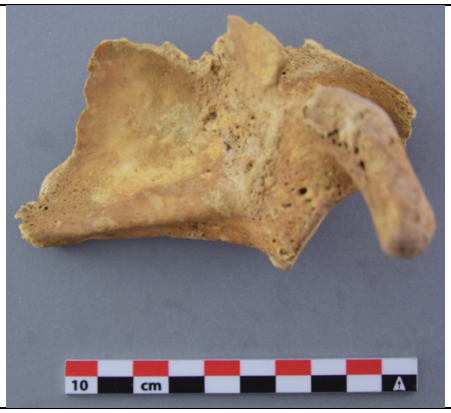

Figure 159 Osteolytic lesions on the left scapula with periosteal reaction

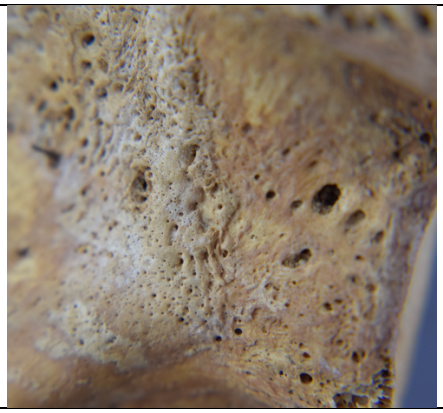

Figure 160 Close-up of one of the osteolytic lesions on the left scapula with thick irregular but smooth periosteal reaction

Figure 161 Right ribs with osteolytic lesions and periosteal reaction

Figure 162 Left ribs with mixed osteolytic lesions and periosteal reaction

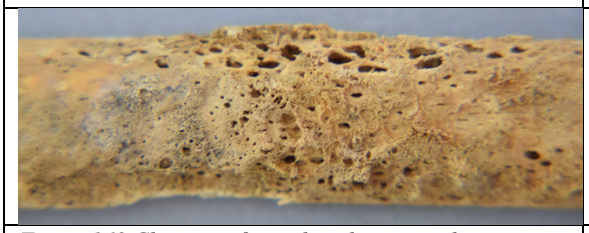

Figure 163 Close-up of osteolytic lesions with extensive aggressive periosteal reaction on left rib ventral side

Figure 164 Close-up of mixed lesions with extensive aggressive periosteal reaction on left rib top view

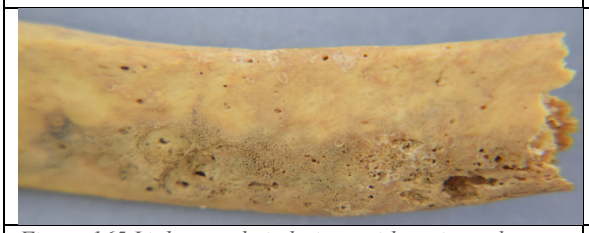

Figure 165 Light osteolytic lesions with periosteal reaction on right rib ventral side

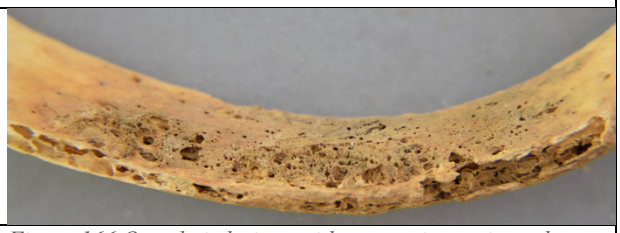

Figure 166 Osteolytic lesions with aggressive periosteal reaction on right rib bottom view

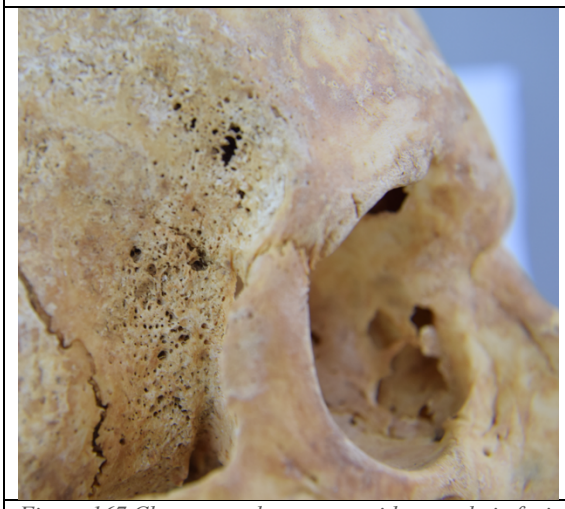

Figure 167 Close-up on large area with many lytic foci on the ectocranial side of the sphenoid

Figure 168 Close-up of an osteolytic lesion on the left parietal next to the sagittal suture

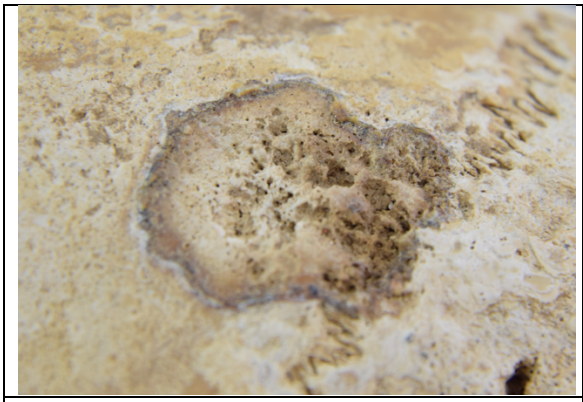

Figure 169 Close-up of an osteolytic lesion at the coronal suture (rather a dense porous spot)

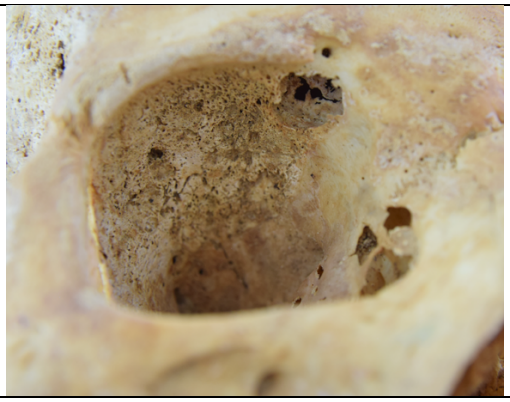

Figure 170 Osteolytic lesion of "moth-eaten" appearance and extensive and aggressive new bone formation throughout the right orbit

Figure 171 Osteolytic lesion of "moth-eaten" appearance at the base of the left temporal and sphenoid

Figure 172 Oblique-basal view of the cranium showcasing several osteolytic lesions and periosteal reactions

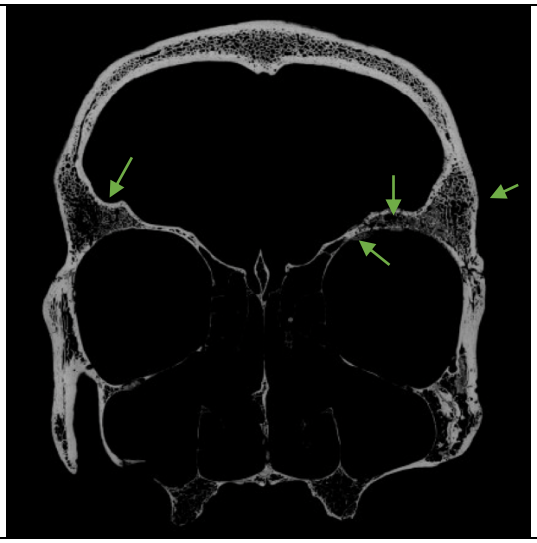

Figure 173 CT-scan of the cranium with large osteolytic lesion in the left sphenoid and a smaller one in the right orbit, and the new bone deposition on the orbital roof

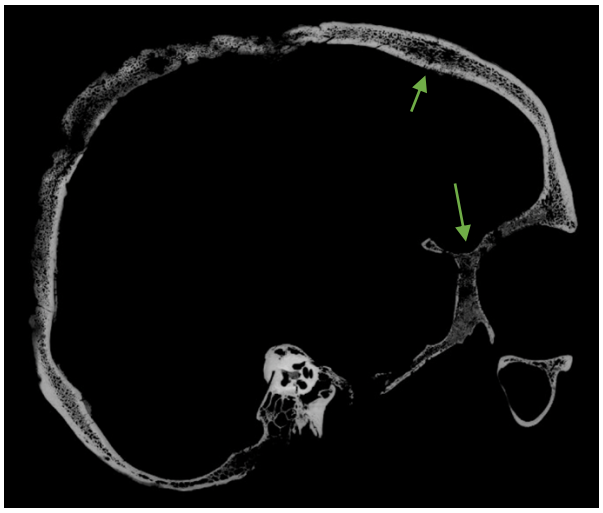

Figure 174 Lateral view of the cranium showing an osteolytic lesion in the diploe of the frontal and inside the sphenoid and orbital roof

Figure 175 Mandible with osteolytic lesion on the right alveolar process and a healed fracture on the left body

Figure 176 Healed fracture of the left mandibular body with patch of periosteal new bone formation on the ramus

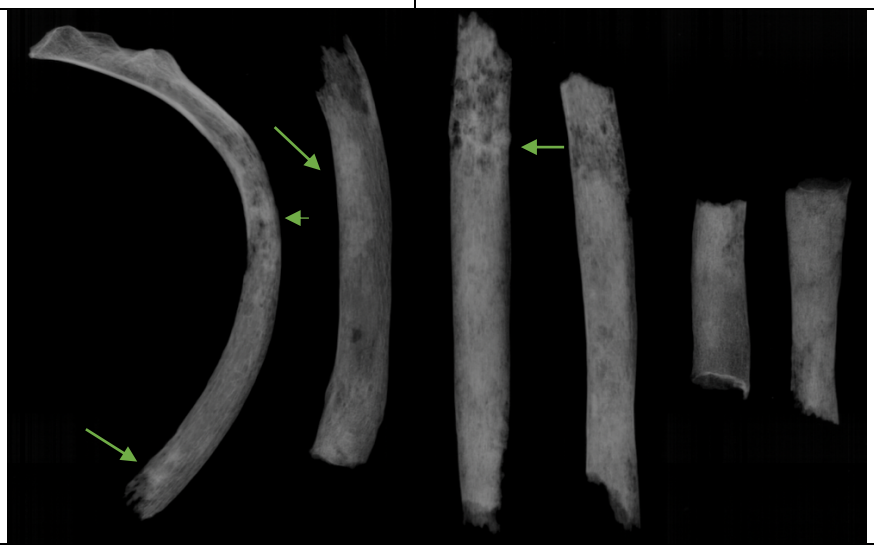

Figure 177 Radiograph of ribs showing osteolytic lesions and sclerotic areas (green arrow) indicative of osteoblastic reaction

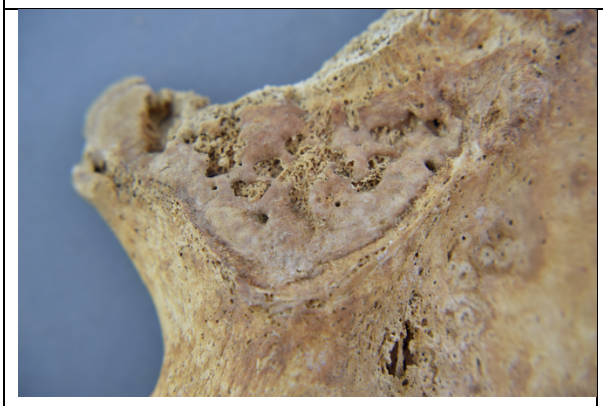

Figure 178 Probable osteoblastic lesion covering the complete auricular surface of the left ilium

Figure 179 Spongiosclerosis indicative of an osteoblastic lesion within the trabeculae of the left os ilium, probably in relation to the lesion in Figure 178

Photo Table 2008-78/699	
	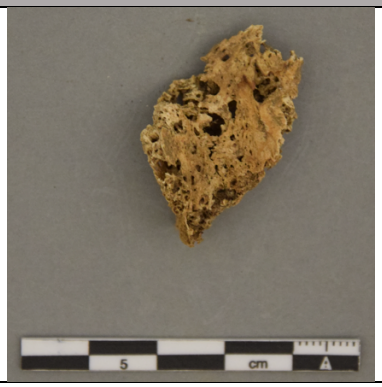
Figure 180 Top view on the lytic lesions of the spinous process of the 10th vertebra	*Figure 181 Bottom view on the lytic lesions of the spinous process of the 10th vertebra*
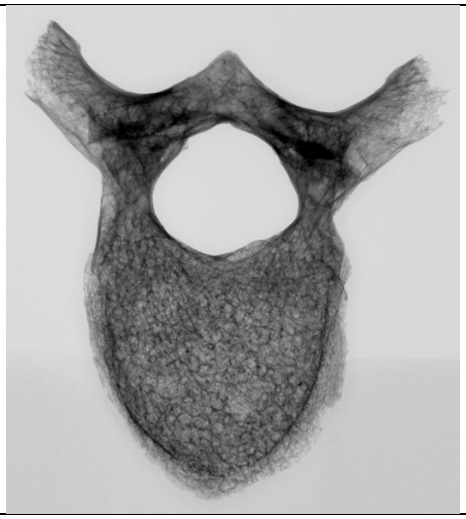	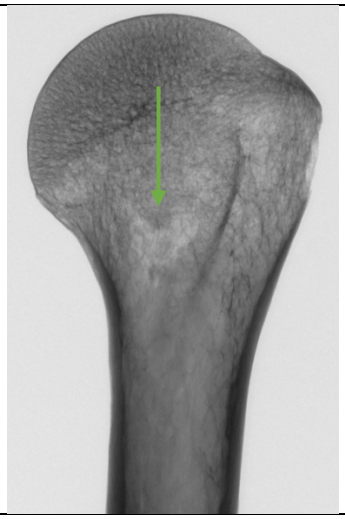
Figure 182 Absence of lytic lesions in the 9th thoracic vertebra	*Figure 183 Possible lytic lesion (ill-defined radiolucency without sclerotic margin) in the metaphysis of the left humerus*

6.4 Miscellaneous Conditions

The following section describes some solitary skeletal lesions observed among individuals of the Knuedler cemetery for which no precise diagnosis could be found so far or where a classification into one of the main chapters of pathological conditions was not possible due to inconclusive and variable differential diagnoses.

Furthermore, it serves as a place to present the analysis on ossified thyroid remnants as this did not fit into any of the other chapters.

6.4.1 2016-082/403

The skull of individual 2016-082/403, a senile female (F??) from Layer 2 and buried in the cloister, was entirely fragmented, exposing the diploe at the fracture margins. This revealed

that the cranial vault bones, especially, primarily the parietals close to the sagittal suture, were slightly thickened. Furthermore, the structure of the diploe appeared looser in the parietals and frontal bone but much denser in the occipital bone, especially around the internal and external cruciform eminence.

In all cranial fragments, parts of strongly enlarged diploic vein channels were observed (Figure 184, Figure 185, Figure 188). The pattern and enlarged state of the diploic veins was especially clear on a radiograph of the frontal bone (Figure 189). One small round dip (~1cm∅) was found endocranially on a small cranial vault fragment (likely parietal, side unknown), which might have been caused by pressure of a soft tissue mass. Finally, osteoblastic bone reactions in the form of irregular and sometimes superimposed bony spicules are located on the frontal bone along enlarged and deep arachnid villi along the midline of the bone and on both parietals in proximity of the sagittal suture and the sagittal end of the meningeal vessel imprints (Figure 186, Figure 187). No lesions were observed on the external cranial vault table.

The investigation into possible causes for the observed pathological lesions is still ongoing but the differential diagnoses that have been reached so far will be presented briefly in the following section.

Paget's disease

A more detailed description of Paget's disease can be found in the chapter on Metabolic disease. In short, regarding the cranial bones only, Paget's disease is characterised by a thickening of the cranial vault bones resulting from a thickening of the diploe through deposition of disorganised and brittle bone. This usually entails that the diploe loses much spongy structure and appears rather dense (Brickley & Ives 2008). A slight thickening can also be observed in the cranial vault fragments of 2006-082/403, however, the diploe does not appear dense but rather lose. However, it is also possible that condition observed here corresponds to the first stage of Paget's disease which is marked by bone resorption and hypervascularisation (Brickley & Ives 2008). However, whilst Paget's disease is often associated to the aforementioned diploic expansion, so far the author of this thesis did not find any studies that mentioned enlargement of the diploic veins in relation to Paget's disease. However, it is entirely possible that both phenomena occurred independently from each other. Furthermore, Paget's disease is not considered to produce endocranial bone deposition, even though this might also have occurred independently of the diploic resorption and diploic vein enlargement.

Hyperostosis frontalis interna

Hyperostosis frontalis interna should be considered as another differential diagnosis for the observed lesions. Hyperostosis frontalis interna is characterised by bilateral nodular bone growths on the endocranial surface of the frontal bone but may also affect the endocranial surface of other bones of the cranial vault (Waldron 2009). Furthermore, depending on the size and frequency of the nodules hyperostosis frontalis interna can be classified into 4 types (A, B, C, D) (Western & Bekvalac 2017). The bone depositions observed on the endocranial side of the frontal and both parietals do not appear nodular but seem to be more pointed and resemble small spicules. However, based solely on comparisons to photographs, in size but not in frequency, they resemble more or less the Type B lesions illustrated in Western and Bekvalac (2017). The author of this thesis could not find any studies mentioning association diploic vein enlargement and hyperostosis frontalis interna, however, the to conditions might have just occurred independently of each other.

Anomaly of the diploic veins

The enlargement of the diploic veins might be due to anomalies of the diploic vein, which are considered rather rare and literature is rather scarce (Iwamuro *et al.* 2016; Tabani *et al.* 2020). Often these anomalies of the diploic veins do not cause any clinical symptoms are often picked up as incidental findings or during cranial surgery (Elsberg & Schwartz 1924; Iwamuro *et al.* 2016). The anomalies described in literature, such as the sinus pericranii (Brix *et al.* 2009), did not match the lesions observed in 2006-082/403. Furthermore, anomalies of the diploic veins are not reported to cause endocranial bone depositions.

Meningioma

So far, the most fitting differential diagnosis that explains all observed pathological lesions of the cranial vault of 2006-082/403 would be a meningioma.

Meningiomas are thought to arise from the arachnoidal cells in the arachnoid villi (Waldron 1998; Marques 2019). In about 22% of the clinically reported cases, they produce osteolytic lesions but in 78% they produce osteoblastic lesions, starting on the endocranial table before eroding through the skull vault and causing lesions on the outer table (Campillo 1991; Marques 2019). In fact, Campillo (1991) states that large ectocranial and endocranial lesions caused by meningioma are rather rare and that the most common form constitutes in small endocranial bone exostoses, which is exactly the type of lesions observed in individual 2006-082/403. Therefore, the endocranial bone depositions observed in 2006-082/403, and especially their

location around the sagittal sulcus, meningeal artery and arachnid villi, are suggestive of meningioma.

Furthermore, several studies have found that meningiomas, and other hypervascular cranial tumors, can cause enlargement of the diploic veins, either due to the tumors high need in blood supply or due to increased cranial pressure (Elsberg & Schwartz 1924; Matsushima *et al.* 2019; Tabani *et al.* 2020).

Therefore, all lesions, the endocranial bone depositions and the enlarged diploic veins can be typical signs of a meningioma. The lack of lesions on the outer table could suggest that the individual had an early form of meningioma, where the condition was not yet advanced enough to infiltrate the bone and pierce though the outer table.

6.4.2 2013-015/161

The case of individual 2013-015/161, will also be mentioned in the chapter on metabolic diseases. The individual presents with a large and thickly lamellated spot of periosteal new bone formation on the proximal third of the right ulnar diaphysis. A taphonomic fracture exposes the inner structure of the lesions and therefore, it can be observed that the lesion only involves the periosteum of the ulna and not the bone cortex. Due to the fracture which dissects also the cortex down to the medullary canal, osteomyelitis as possible cause for the formation of such a lesion can be largely dismissed as no signs of infection inside the canal or the cortex are visible (Aufderheide & Rodriguez-Martin 1998; Rana *et al.* 2009; Waldron 2009). A thin sheet of periosteal new bone also covers part of the mid-diaphysis, and the surrounding are of the lamellated deposit. Periosteal new bone formation is then also observed enveloping all of the right 5th metacarpal diaphysis and part of the right 4th metacarpal diaphysis. Apart from very strong grooved and pitted enamel defects on the erupting permanent teeth, no further lesions were recorded on any of the bones (Figure 239, Figure 240, Figure 191). Several metabolic conditions may cause periosteal reaction and enamel defects, and as such a metabolic condition must be considered as differential diagnosis for this individual (Brickley & Ives 2008; Lewis 2009; Brickley & Mays 2019). However, the distribution of the periosteal reaction does not seem typical for metabolic disease, as it is confined to the right ulna and two metacarpals, whereas periosteal reactions in systemic metabolic disease are usually more wide-spread and occur bilaterally (Brickley & Ives 2008; Rana *et al.* 2009). A slow growing tumour cannot be excluded as differential diagnosis for the lesions present in this individual (Aufderheide & Rodriguez-Martin 1998). Due to the young age of the individual, Ewing's sarcoma was considered as differential diagnosis as hair-on-end and lamellated (onion-skin-

like) periosteal reactions are most common for this tumour. However, the tumour is primarily osteolytic in nature and the periosteal reaction occurs as a result to cortical erosion. Furthermore it occurs most commonly in the lower body such as on the leg bones or pelvis (Waldron 2009). The profile of the lesion however shows no cortical erosion below the periosteal reaction. Other tumours that can produce a lamellated periosteal reaction are Chondroblastoma and the different forms of osteosarcoma, however, for the latter, the sunburst pattern is much more common. Chondroblastomas are often accompanied by lytic lesions (Rana *et al.* 2009; Waldron 2009; Marques 2019). Both lytic lesions and sunburst pattern periosteal reactions are not present in this case. Alternatively, localised infection or trauma might have caused such a strong lamellated and localised periosteal reaction (Rana *et al.* 2009), which is why both latter options should be considered as the most probable causes for this lesion.

6.4.3 Ossified Thyroid

Ossification of the thyroid cartilage starts after the 2nd decade and is generally complete by the 6th decade of life (Golghate *et al.* 2014; Sabnis & Mane 2020), which is why the presence of an ossified cartilage is often seen as indicative of an advanced age for the individual in question (Leggio & Introna 2021). Cartilage ossification occurs in both males and females but in females the cartilage never ossifies completely whereas in males it often does so in old age (Sabnis & Mane 2020).

A total of 27 (6.91%) individuals presented a completely or partially ossified thyroid cartilage. (Figure 190) The majority of individuals was male (81.48%; n=22), 14.82% (n=4) were female and one (3.70%) was of indeterminate sex. Differences of occurrence of ossified thyroid between age groups and sex were explored via Pearson's chi square tests conducted in RStudio. When comparing the absence and presence of ossified thyroid between males and females, men had significantly mor often an ossified thyroid than women. (M:12.02%; F: 3.54%; p=0.0123). All cases occurred in adults. For the analysis by age group, one case was omitted as it was recovered from an individual of indeterminate age. No statistically relevant difference in thyroid ossification frequency could be observed between the age groups (p=0.1898). However, an increasing trend with age was evident, with only one case manifesting in young adults (2.78%), 4 cases were observed in adults (5.71%), 15 cases were seen in matures (12.93%) and 6 cases were recorded in seniles (10.71%).

This study essentially confirms that ossification of the thyroid cartilage is age dependent and that males are more commonly affected than females (Sabnis & Mane 2020). What is

interesting to note, is that individual 2008-78/1106, a male young adult of 20-29 years presents a fully ossified thyroid cartilage, which is exceptionally rare for that age. The individual did not show any other pathological lesions. Causes for such an early ossification of thyroid cartilage might be traumatic compression, benign and malignant thyroid neoplasms or hormonal dysfunctions. In absence of any other pathological lesions, a simple anatomical variation should also be considered (Khoo *et al.* 2002; Leggio & Introna 2021).

Miscellaneous Cases

Figure 184 Enlarged and sclerotised diploic veins (2016_082/403)

Figure 185 Large groove inside cruciform eminence on occipital, likely an enlarged diploic vein (2013-015/403)

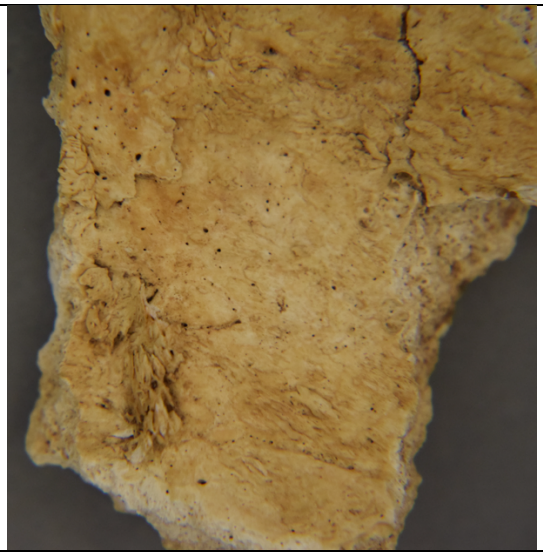

Figure 186 Endocrnial bone deposits on parietal of 2016-082/403

Figure 187 Endocrnial bone deposits on frontal of 2016-082/403

Figure 188 Enlarged and sclerotised diploic vein in the frontal bone (2016_082/403)

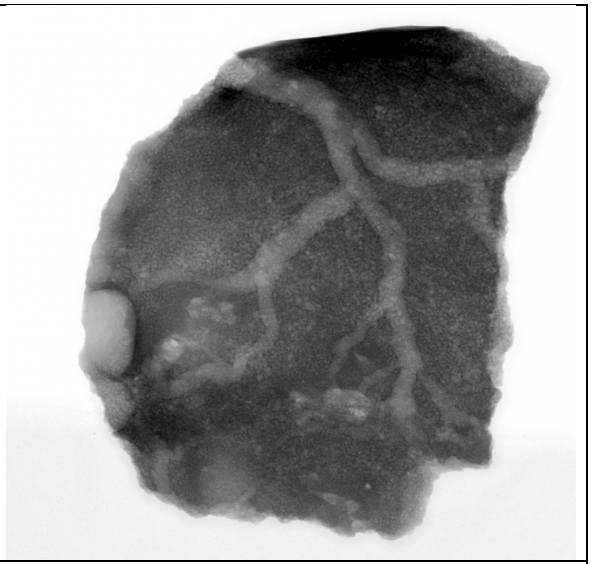

Figure 189 Radiograph revealing enlarged and sclerotised diploic veins in frontal bone R side and central part (2016_082/403)

Figure 190 Partially ossified cartillage of indiviual 2008-78/194

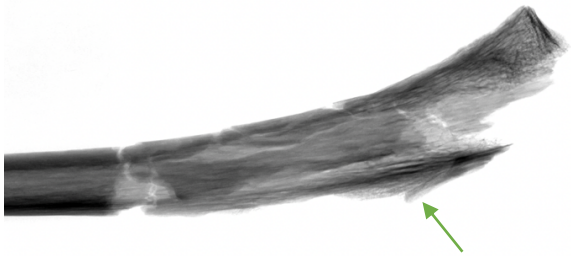

Figure 191 Radiograph of the left ulna displaying clearly the lamellar structure of the periosteal new bone deposit and showing no evidence of lytic lesions inside the bone (2013-15/161)

6.5 Trauma, Peri- and Postmortem procedures

6.5.1 Introduction

Evidence of antemortem trauma is often easily recognised in the archaeological record since the dislocation of bone and the resulting new bone formation during the healing process cause visible changes to the normal anatomical appearance of a bone (Ortner 2003a; Roberts & Manchester 2010). However, differentiation between perimortem trauma and postmortem damage often proves difficult (Waldron 2009). Furthermore, trauma that occurred in childhood might not be detectable anymore in adult remains or even in subadults, since oftentimes fracture

damage and healing processes are being completely remodeled during skeletal growth and maturation (Lewis 2007).

More common than trauma to bone, however, is trauma to soft tissues, which only leaves traces on bones on very rare occasions, which means that this kind of trauma is seldomly picked up on in the archaeological record. All these circumstances might generally lead to an incomplete picture of trauma frequencies in past populations (Lovell 2008; Redfern & Roberts 2019). Nevertheless, the study of trauma in archaeological remains may help to shed light on the living conditions of a population, the risks they were exposed to and the level of medical care they were provided with.

A trauma is generally defined as an injury to living tissue caused by external forces (Lovell 1997). There are four injury mechanisms: direct trauma, indirect trauma, stress induced trauma and pathologically induced trauma, all leading to different fracture types. The fracture types are also caused by different or combinations of different types of stress on the bone, namely tension, compression, twisting, bending and shearing. In between these categories, a differentiation is also made between fractures that pass through the bone, called complete fractures and those that do not penetrate the bone entirely, called infarction or incomplete fractures (Redfern & Roberts 2019). Additionally, the velocity and angle at which the external force is applied as well as the stability and elasticity of the bone can have an effect on the type of fracture that occurs (Rössler & Rüther 2005).

Next to fractures, traumatic injuries to the soft tissues may also be detectable on bones in the form of extra-skeletal ossifications. The most common form is myositis ossificans traumatica, which is the result of an ossifying intramuscular bruise caused by muscle tears or blunt force trauma. It usually takes on the shape of an irregular mass of bone attached to a bone. However, the ossified bruise might also just form a calcified mass within the muscle tissue and damage to ligaments, tendons and joint capsules might also lead to ossification (Aufderheide & Rodriguez-Martin 1998; Lovell 2008).

Traumatic subluxations and dislocations may occur when damage to the ligaments in the joints leads to a partial or complete loss of contact between the two joint surfaces. Without reduction of the dislocation, deformation of the bone and joint surfaces as well as damage, such as ossification of the soft tissue components of the joint, might ensue (Redfern & Roberts 2019).

Whilst fractures and dislocations are primarily thought to be accidental, there are other kinds of trauma that are considered to be mainly the result of interpersonal violence and these all fall under the mechanism of direct trauma, namely blunt force trauma, sharp force trauma and projectile trauma (Roberts & Manchester 2010).

Blunt force trauma is caused by contact of a blunt object to the bone and usually results in either a single linear fracture in the case of a light blow, or comminuted injury with concentric radiating fractures in the case of a heavy blow (Komar & Buikstra 2007; Roberts & Manchester 2010; Wedel & Galloway 2014; Redfern & Roberts 2019). Impact with a blunt object, such as a fall on a hard surface may also produce the typical depressed fracture of a blunt force trauma (Roberts & Manchester 2010; Grupe *et al.* 2015; Redfern & Roberts 2019). Sharp force trauma can be divided into cutting and chopping injuries, whereas chopping injuries can cause both blunt and incised marks on the bone (Komar & Buikstra 2007). Usually a sharp-edged object such as a knife sword or axe blade causes sharp force injuries (Roberts & Manchester 2010). If unhealed, they are characterised by a straight, smooth and sometimes even polished margin, with the opposite margin being uneven with flaking and a roughened appearance. Depending on the weapon, blow angle and velocity, the fracture outline might be just a straight line or be elliptical (Redfern & Roberts 2019). Projectile fractures may leave different kinds of traces on bones depending on the size of the projectile as well as its angle and velocity on impact. As such, gunshot wounds are characterised by a rather small circular entry wound with radiating fractures externally and a beveled margin internally, whereas the exit wound shows beveling on the external surface. If both exit and entry points can be recorded or if the projectile is still stuck in the bone, a reconstruction of the direction and angle at which the shot was fired can be undertaken, and potential tissue damage and its complications can be assessed (Waldron 2009; Roberts & Manchester 2010).

A fracture, be it indirect or direct, may be accompanied by complications such as deformation of the bones, infection, avascular necrosis and eventually even death if vital organs were damaged (Waldron 2009).

Generally, however, soon after the fracture occurs, the healing process begins. The healing process starts with an initial haematoma formation around the fracture area. Subsequently increased fibroblast activity in the area leads to the formation of a soft fibrous callus which unites the two loose bone ends (Aufderheide & Rodriguez-Martin 1998). This process starts approximately 2-3 weeks after the initial fracture occurred and at this stage, the fracture edges are usually blunted and smooth. After about 4-6 weeks replacement of the fibrous callus by woven bone commences, which adheres to the surface of the bone next to the fracture location. This process takes about 8-12 weeks and ends in the formation of a hard callus which unites the two bone halves. After completion of the hard callus, remodeling of bone in the affected area commences during which the woven bone of the hard callus is gradually replaced by

lamellar bone, a process which takes around 8-12 weeks. After that, remodeling of the bone and callus continues constantly by smoothing out the surface etc.
In cases of minor displacement of the bone, bone remodeling might end up obliterating many if not all signs of the fracture over time.
In some cases, however, especially in case of complications, the fracture ends might never unite, creating instead a pseudoarthrosis at the contact area (Aufderheide & Rodriguez-Martin 1998; Lovell 2008; Grupe *et al.* 2015).
For the sake of completion, surgical procedures such as trephination as well as amputation will also be addressed in this chapter and postmortem procedures such as autopsies will be discussed as well.

6.5.2 Methods

Fractures, dislocations/subluxations, stress fractures, myositis ossificans traumatica, sharp force trauma and projectile trauma were evaluated separately. Due to the small number of cases in the other categories, only fractures were evaluated statistically. The separation was undertaken in order to keep the data comparable to that of other sites, where frequency of trauma was calculated based solely on bone fractures, including blunt force trauma.

6.5.3 Results

6.5.3.1 Fractures

A total of 9.97% (n=39) of individuals (n=391) experienced at least one fracture on the head, torso, arms, or legs**.** Considering only juveniles and adults whose sex could be determined, men (14.75% n=27) had overall more frequently traumatic lesions than women (8.85%, n=10), but the trend was not statistically relevant (p=0.1359). A comparison in trauma distribution across all age groups showed an increasing trend of fracture prevalence with age but it was not statistically significant (p=0.3775). Neonates and infans II did not show any traumatic injuries, infans I (4.35%) and juveniles (4.55%) each presented 1 fracture, among adults (11.32%) 12, among matures (12.07%) 14 and among seniles (17.86%) 10 individuals had at least one fracture. Although frequency auf trauma was slightly higher in Layer 2 (11.97%) than in Layer 1 (7.01%), that trend was also not significant (p=0.1087). However, a significant difference in fracture prevalence was detected between the burial locations, with more individuals from the cemetery (12.09%, n=33) than from the cloister (5.08%, n=6) exhibiting at least one bone fracture.

Table 77 List of individuals with bone fractures

Location	Layer	ID	Sex	Age	Side	Bone	Fracture type	Status
Cemetery	2	2008_78/1040	F	Mature I	L	MC5	oblique	Misaligned
Cloister	1	2016_082/400	M	Juvenile	L	Rib 1x	transverse	Aligned
Cloister	2	2016_082/418	M	Adult	R+L	5, 8. Ribs; Mandible	oblique	Aligned
Cemetery	2	2008_78/1001	M	Mature I	L	Ribs 2x	transverse	Aligned
Cloister	2	2008_78/1043	M	Young Adult	R+L	Proc styl. cranium	oblique	Aligned
Cloister	2	2008_78/1083	M	Senile	L	Radius; 11. Rib	Colles; transverse	Aligned; Misaligned
Cemetery	2	2008_78/1091	M	Mature I	/	LV1	Compression	
Cemetery	2	2008_78/1167	M	Mature I	R+L	Proc styl. Cranium, TV12	Oblique, compression	Aligned; Non-fusion
Cemetery	2	2008_78/1289	M	Adult	R	6, 7. Rib	transverse	Misaligned
Cemetery	2	2008_78/1310	M	Mature II	R	4, 5. Rib	transverse	Aligned
Cemetery	2	2008_78/1312	M	Senile	R+L	3, 5, 9, 10, 11. Rib; 10. Rib	transverse	Aligned
Cemetery	2	2008_78/1316	M	Young Adult	R	Tibia, Fibula	oblique	Aligned
Cemetery	2	2008_78/1317	M	Mature I	R+L	Nasale	crush	Aligned
Cemetery	2	2008_78/1340	M	Adult	L	Rib 1x	transverse	Aligned
Cemetery	2	2008_78/1431	F	Senile	R	Tibia	oblique	Misaligned
Cemetery	2	2008_78/1449	M	Mature I	L	10. Rib	transverse	Aligned
Cemetery	2	2008_78/1451	M	Senile	R	Ribs 2x	transverse	Aligned
Cemetery	2	2008_78/1454	M	Senile	R	7. Rib	transverse	Aligned
Cemetery	2	2008_78/1457	M	Mature II	R	Ribs 4x	transverse	Aligned
Cemetery	1	2008_78/146	M	Adult	R	1, 2. Prox. Phal foot	compression	Misaligned
Cemetery	2	2008_78/1476	M	Senile	L	Tibia	Comminuted?	Aligned?
Cemetery	2	2008_78/1478	M	Senile	/	Rib 1x; LV4+5	Transverse, compression	Aligned
Cemetery	2	2008_78/1483	F	Adult	/; R	TV8 proc. Spin.; 12. Rib		Aligned
Cemetery	1	2008_78/153	Indet	Infans I	L	Femur	oblique	Misaligned
Cemetery	2	2008_78/191	M	Young Adult	R	1. Rib, TV8+9	Transverse, compression	Aligned
Cemetery	1	2008_78/204	M	Mature I	L	LV4+5 transv. Proc.	oblique	Aligned
Cemetery	2	2008_78/215	M	Mature II	R	MT5	compression	Misaligned
Cemetery	2	2008_78/247	M	Mature II	R+L	1-12. Ribs	transverse	Aligned
Cloister	1	2008_78/345	M	Mature II	R+L	Nasale	crush	Misaligned
Cemetery	2	2008_78/576	F	Adult	L	Radius	Colles	Aligned
Cloister	1	2008_78/603	M	Adult	/	Cranium	Depressed	
Cloister	1	2008_78/667	F	Mature II	/	Rib 2x	transverse	Aligned
Cloister	1	2008_78/670	M	Adultus	R	11. Rib	transverse	Aligned
Cemetery	1	2008_78/707	F	Senile	R+L	Ulna proc.styl.; MC5	/; oblique	Aligned; misaligned
Cemetery	1	2008_78/793	F	Senile	R	Radius, Ulna	Colles	Aligned
Cemetery	1	2008_78/794	M	Senile	L	12. Rib	transverse	Misaligned
Cemetery	1	2008_78/800	F	Adult	R	Ulna	Oblique	Misaligned
Cemetery	2	2008_78/957	F	Young Adult	L	LV3 transv. Proc.	transverse	Aligned
Cemetery	2	2008_78/976	F	Mature II	L	4, 5, 9, 10, 11 Ribs	transverse	Aligned

transv.=transverse; proc. styl.= processus styloideum

A total of 96 fractures were recorded in the Knuedler sample. The number of fractures is much higher than that of affected people, which means that several individuals must have had two or more factures. Especially the presence of multiple, mostly consecutive rib fractures increases

the number of total fractures in the sample. Indeed, the vast majority (72.92%, n=70) of fractures occurred in the torso, which included the spine, ribs and sacrum/coccyx, followed by fractures in the head area (10.42%, n=10), upper limbs (8.33%, n=8) and lower limbs (8.33%, n=8). In the upper arms, no side prevalence was observed (R: n=4, L; n=4), but in the lower limbs, the right side (n=6) was more often affected than the left (n=2). (Table 77, Figure 200)
Among the upper limb, no fractures were observed in the clavicles, scapulae and humeri. The majority of fractures concerned either the radius or the ulna. Three radius fractures were Colles fractures of the wrist (Figure 192) (2008-78/793, 576, 1083), where the radius is broken at the distal metaphysis and the metaphysis and epiphysis are angled posteriorly. These fractures are thought to be caused when trying to break a fall by extending the hands to land on them first. Therefore, Colles fractures are usually taken as a sign for accidental fracture (Larsen 2015).
One very misaligned right Ulna fracture (2008-78/800) was identified as a likely parry fracture (Figure 193). A parry fracture is considered to result from defense against a blow or hit when raising the arm to protect the head, and is therefore often taken as evidence for interpersonal violence (Larsen 2015). Considering this information, it is particularly interesting that this type of fracture was detected in a women, instead of a man, who, due to warfare for example, were often more prone to be exposed to violence (Larsen 2015).
Among the lower limbs, only one child had a femur fracture (Figure 194), which mimicked long bone bowing of rickets. However, a radiograph (Figure 195) revealed the presence of a fully healed fracture. The bone was visibly shorter than its healthy right counterpart, which likely created problems while walking for the child in question. Most lower limb fractures were of the lower leg or foot. The tibia presented 2 oblique and 1 probably comminuted or crush fracture (Figure 196). One of the oblique fractures was very well aligned (2008-78/1316) and one was slightly displaced (2008-78/1431) (Figure 197). Regarding the tibia with a comminuted fracture (2008-78/1476), the diagnosis remains unsure. The tibia presented a normal size proximal diaphysis but around midshaft, it flattened considerably on the medial side before expanding again to normal size at the height of the distal metaphysis. No thick callus was formed in the depressed area. A radiograph was made, but no clear fracture line could be observed on there either. However, a strong periosteal reaction was discovered on the whole shaft, and especially on the corresponding fibula. The fibula was broken in half due to taphonomic damage and showed thick diffuse bone formation that narrowed the medullary canal considerably. Additionally, the individual showed unilateral spondylolysis on LV5, the complete lower right intervertebral facet joint was broken off and had formed a pseudoarthrosis with the vertebral arch, which might be rather a sign of trauma than of a stress fracture.

Fractures

Figure 192 Healed Colles fracture of the left radius of 2008-78/793

Figure 193 Misaligned Parry fracture in the right Ulna of 2008-78/800

Figure 194 Oblique fracture of the left femur of a subadult (2008-78/153) mimicking rickets

Figure 195 Radiograph of oblique fracture of the left femur of a subadult (2008-78/153) mimicking rickets

Figure 196 Healed comminuted fracture of the right tibia diaphysis with periosteal reactions on the fibula as well (2008-78/1476)

Figure 197 Healed oblique fracture of the right tibia of 2008-78/1431

Figure 198 Healed fracture of both ossa nasalia of 2008-78/1317

Figure 199 Non-fusion of fractures on two consecutive left ribs of 200-78/1001

2016-082/418 presented a rather well aligned and only slightly displaced oblique fracture of the mandible. The individual also suffered from probable metastatic carcinoma, which might have weakened the bone and predisposed for a fracture. However, the individual also presented with a projectile trauma to the elbow, which suggests that the mandibular fracture might have also been acquired through interpersonal violence. (Figure 156, Figure 175, Figure 176)

Except for 2 rib fractures, all fractures had fully healed, and remodeling had already taken place, meaning they occurred at least ~20-30 weeks before death. The rib fractures of 2008-78/1001, however, showed non-union of both bone parts and the callus surface appeared irregular, suggesting an earlier stage of healing, at which the hard callus had not yet fully formed, and bone fusion was not yet complete, probably less than 12-18 weeks after fracture formation (Figure 199).

The majority of the fractures was also well-aligned although some slight displacement was still obvious in all cases (e.g. Figure 198).

Figure 200 Distribution of fractures by body part

6.5.3.2 Subluxation and Dislocation

Three cases of possible traumatic dislocations were already described in the chapter about congenital anomalies as their differential diagnosis includes congenital dislocations which were deemed as equally plausible causes for the lesions observed than traumatic dislocations. Individual 2008-78/1487 suffered from a hip dislocation which shows signs of a congenital but also of a traumatic origin. Individual 2008-78/1080 shows symptoms indicative of a radial dislocation although it remains unclear whether the dislocation was congenital or occurred in early childhood as a result to trauma. 2008-78/1471 shows signs that suggest either slipped

femoral epiphysis or Legg-Calvé-Perthe's disease. However, the enlargement of the acetabulum and slight flattening of it towards the iliac blade might also be suggestive of traumatic subluxation, even though the first two conditions seem more likely. All these conditions are described in detail in the chapter on congenital anomalies.

6.5.3.3 Myositis ossificans traumatica

Two individuals presented signs of myositis ossificans traumatica.

Individual 2008-78/148, a male juvenile (18-20y) showed very strong bone formation on the distal left femur, in particular on the posterior side, where thick bone formation had taken place (Figure 201). Altogether, the ossified area strongly resembled tendons, ligaments or muscle tissue. However, due to the extent of the lesion, other conditions that may cause such large bone formations had to be considered as well, such as pedunculated osteochondroma, bizarre parosteal osteochondromatous proliferation, subungual exostosis, chondroblastoma, enchondroma, osteoblastoma, bone cysts, Ewing's sarcoma, osteosarcoma, parosteal or periosteal sarcoma etc. However, a radiograph of the bone revealed no signs of osteolytic or sclerotic foci inside the bone and together with the shape of the lesion, they both exclude the afore mentioned conditions.

Individual 2008-78/193, a mature male, has a large bone growth spanning from proximal to mid diaphysis on the lateral side of the left femur (Figure 202). The surface of the bone growth is smooth, and the shape resembles that of a tendon or ligament, suggesting that it is most likely an ossified tendon or ligament. This individual also suffered from Osteoarthritis in both wrists and generally displayed moderate degenerative changes in all joints.

Myositis ossificans traumatica usually starts after trauma to a muscle or soft tissue overlying bone, mostly due to a blow or fall.

Myositis Ossificans Traumatica	
Figure 201 Myositis ossificans traumatica left femur of 2008-78/148	*Figure 202 Myositis ossificans traumatica left femur of 2008-78/193*

6.5.3.4 Stress fractures

Since the aetiology of spondylolysis suggests a genetic component to their formation, spondylolyses were already described in detail in the chapter about congenital anomalies.

It must be noted here though, that in one individual, 2008-78/1167, spondylolysis of LV5 occurred together with a compression fracture of the TV12 and a bilateral fracture of the cranial processus styloideum. This might indicate that in this case, the spondylolysis of LV5 was probably caused by the same trauma that caused the other fractures, such as a fall on the back or lower back.

6.5.3.5 Blunt force trauma

Blunt force traumata are injuries caused by direct contact of a solid object with the bone or when bone makes direct contact with the blunt object. As such, a blunt force injury might have been caused by accident like falling on a blunt object or by violence such as through a blow. Therefore, individual 2008-78/603 was added to the statistic on fracture prevalence in the Knuedler cemetery.

2008-78/603, an adult (30-34y) male from layer 1 buried in the cemetery, midway to the cloister and church, presented a large 5cm long and 2.5cm wide, oval shaped depression on the frontal bone (Figure 203, Figure 204). The depression extended from close to bregma towards the left frontal tubercle and did not penetrate the tabula interna of the cranium. The surface was completely smooth, and no signs of infection could be observed, implying that the fracture

healed without complications. The size, location and shape of the fracture suggests that it was inflicted by a blow to the head with a rather broad, long blunt object such as a rod, and that it was most likely inflicted from the top, suggesting that the perpetrator was placed higher up than the victim or that the victim was sitting or kneeling. However, an accidental origin cannot be ruled out.

6.5.3.6 Sharp force trauma

Sharp force trauma describes fractures caused by sharp-edged objects such as knives, swords, axes etc., that leave characteristic fracture patterns on the bones. Since sharp force trauma is almost exclusively caused by direct contact of the sharp-edged blade to bone, a violent interaction is generally assumed to be at the root of its formation. As most comparative studies evaluate sharp force trauma and violence separately from fractures, sharp force trauma was not included in the statistical analysis for fracture frequency of the site.

Individual 2008-78/99, a senile male from Layer 1 buried in the cloister area, displayed a large unhealed sharp force trauma spanning nearly the complete left side of the cranial vault (Figure 205, Figure 206). The full extent of the injury cannot be gauged, since a large part of the anterior side of the cranial vault is missing and was not recovered. The cranium was heavily fragmented, and the lesion could only be reconstructed after gluing it back together. However, moisture and earth pressure caused some of the cranial fragments to bend, which complicated the reconstruction. Furthermore, the typical signs of a sharp force injury are clearly recognizable: a smooth, even polished margin exposing the diploe and penetrating the tabula interna was observed on the right side and an irregular, chipped margin on the left side. The angle of the straight polished margin allows to reconstruct the angle of the blow. The blow was administered by an aggressor positioned on higher ground than the victim or the victim was sitting or kneeling at the time of the blow. The blow likely occurred from the front, which is suggested by the large blown out area close to the sphenoid and frontal bone and the narrower cut towards the posterior side of the parietal. The blade penetrated the skull at a slightly right tilted angle suggesting that the perpetrator was right-handed. No signs of healing were found around the injury margins, implying that the individual died either during or shortly after the sharp force trauma had been inflicted. Likely, serious damage to the brain as well as heavy blood loss caused the almost immediate death of this individual.

2013-015/357, is also briefly mentioned here. The individual presented with either a healed penetrating blunt force trauma or trephination at bregma, a detailed description of that lesion can be found under the surgical procedures section. However, an unhealed, non-penetrating,

oval sharp force injury was located on the right side of the frontal bone. It featured a clear cut at its center and a polished surface. No signs of healing were observed, meaning that the cut occurred shortly before, during or shortly after death. (Figure 212)

For the sake of completeness, another cranium needs to be described here, which was not evaluated in the scope of this study, since it was recovered from grave fill without an associated postcranium, grave or layer. However, cranium number 2008-78/344, an adult male from the cemetery displayed two sharp force traumata on the cranial vault. They were likely related to each other and were situated on the posterior-superior side of the right parietal, close to the sagittal suture. Both cuts, a smaller non penetrating one was situated closer, and a slightly larger penetrating injury was located parallel to the first. Both cuts were healed, showing a smooth surface and fully remodeled and blunted fracture margins. The injury was non-penetrating, sharp edged and displayed a glossy surface, thus not showing any signs of healing. (Figure 207)

6.5.3.7 Projectile trauma

Projectile trauma describes an injury inflicted by a small object hitting bone at high velocity. In the case of a gunshot trauma, the injury is usually characterised by a small circular entry wound with sharp and smooth outer margin and beveled inner margin, and often features an exit hole which is characterised by inner smooth and sharp margins and outer margin beveling. Radiating fractures may occur around the entry and exit wounds (Lovell 2008; Redfern & Roberts 2019).

Two cases of projectile trauma were discovered among the Knuedler sample.

Individual 2013-015/353, an adult male from Layer 2 buried inside the cloister area, presented with an oval projectile stuck in its right orbital roof (Figure 208). The projectile was likely made of lead, which is why radiography and CT-scans produced disturbances in the area around the bullet, so that clear measurements were not feasible. The entry hole was located directly above the right orbital margin. Based on the location of the bullet inside the orbital roof and the location of the entry wound, an approximate reconstruction of the shooting angle was possible. The shooter was in front of the individual and was placed slightly higher than 2013-015/353, alternatively, 2013-015/353 was sitting or kneeling the moment he was shot. The bullet was already being absorbed by the surrounding bone and the entry wound showed signs of healing, namely smooth and blunted margins, indicating that the individual survived for some time after the shot. Additional signs for a longer survival are the smoothed and blunted

chipping margins on the maxillary teeth. Impact from a high velocity object often causes dental chipping as the force of the impact makes the jaws clash together. Smoothed chipping therefore indicates that the individual must have used his teeth for some time after the chipping occurred. However, such a lesion is bound to have caused some complications for 2013-015/353. Although it cannot be determined for certain, it is likely that the right eye was lost or at least dysfunctional after the shot. Furthermore, the bullet penetrated and destroyed part of the brain, more precisely the frontal lobe, between the entry wound and the orbit, which might have caused neurological problems. In fact, damage to the frontal lobe has been associated with the development of inference problems in working memory, difficulty in problem solving and decision making, and changes in social behaviour (Benton 1968; Dimitrov *et al.* 1996; Thompson-Schill *et al.* 2002). Lastly, the bullet, which was likely made of lead, as most bullets from before 1650AD were made of that material (Manton 1994; Hernberg 2000), might have caused lead poisoning into the brain (McQuirter *et al.* 2001). In fact, studies have shown that exposure to high lead concentrations in adults can lead to organ and system dysfunctions, central nervous and cardiovascular disorders, hypertension, decreased cognitive function, memory loss, fatigue, headache, depression, insomnia and even a decreased ability to perform everyday tasks (Miracle 2017). Medical reports from the 18th century describe palsy, pallor, encephalopathy and abdominal cramps as typical symptoms and reported also a high fatality rate for the condition (Hernberg 2000). Lead poisoning in adults generally takes longer to develop (Miracle 2017) and in cases of retained bullets from projectile trauma, ranges of onset between 10-40 years after the injury have been reported (Manton 1994). Without soft tissue evidence however, these theories remain merely speculation.

Evidence of another projectile trauma was found during examination of individual 2016-015/418, an adult or mature male from layer 2 buried in the cloister area, suffering likely from metastatic carcinoma. The individual presented a badly healed fracture of the distal right humerus, leading to deformation in the proximal ulna and radius as well. Radiographs and CT-scans revealed the presence of shrapnel, likely lead, within the distal humerus and a few splinters within the proximal ulna. As was already discussed in more detail in the chapter on Neoplastic disease, the prolonged exposure to lead might have contributed to the development of metastatic carcinoma in this individual. The fracture was fully healed but function of the elbow was severely restricted. No further inferences can be made from the injury.

Traumatic Injuries

Figure 203 Large healed blunt force trauma on frontal 2008-78/603

Figure 204 Close-up of the arge healed blunt force trauma on frontal 2008-78/603

Figure 205 Large unhealed sharp force trauma crossing the left parietal of 2008-78/99

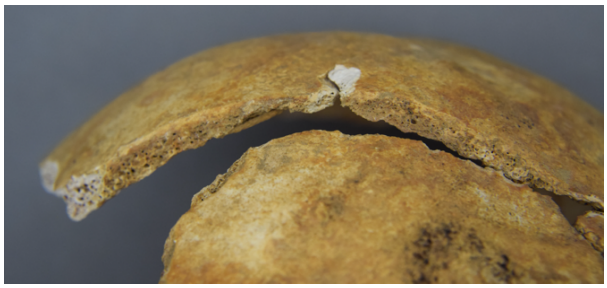

Figure 206 Close-up of unhealed sharp force trauma crossing the left parietal of 2008-78/99

Figure 207 Healed sharp force trauma at posterior right parietal of 2008-78/344 (from grave fill).

Figure 208 Healed gunshot wound with bullet stuck in orbital roof (2013-015/353)

6.5.3.8 Surgical procedures

Two individuals were discovered in the Knuedler sample which showed confirmed evidence of surgical procedures. Amputation is the removal of part of a limb by sharp instruments, and the same definition stands for trephination except that a part of the calvarium is being removed. 2008_78/729 a mature (40-49y) male presented an amputation of the right humerus, just above midshaft. There were no signs of healing, such as new bone formation or smoothing and blunting of the injury margins, which indicates that the individual died during or soon after the procedure. (Figure 209, Figure 210) The individual also showed strong periostitis on the left and right tibiae and fibulae as well as two pipe holes, one on the right and one on the left, and severe dental caries.

2008-78/1040, a mature (40-49y) female, displayed a trephination with cut marks along the margins (Figure 211). The trephination presented as a circular hole with smooth margins and light internal beveling indicative of drilling as technique. The hole was situated on the left parietal right next to the sagittal suture and close to the coronal suture, which is a typical location for trephinations in the past (Wahl & Zink 2013). There are no visible signs of healing, which means that the individual died either during or shortly after the procedure. The cut marks around the hole were probably made to delimitate the area where the hole should be drilled and/or to scalp the area for access. It cannot be excluded that the procedure was conducted postmortem either. Other than the trephination, the individual also presented strong periostitis with exostosis formation on the distal left tibia and fibula.

For the sake of completeness, another cranium needs to be mentioned here that was not incorporated into any statistical tests or analyses conducted for this thesis, as it is only a cranium from a grave fill find with no associated postcranial remains, grave or layer attribution. However, cranium number 2013-015/357 (male adult), which was excavated in the cloister area showed a large depression crossing the bregma of the cranium (Figure 212). The shape of the depression was oval and about 4cm long and 2.5cm wide. At its center, but located slightly towards the posterior end, was an oval hole that penetrated the tabula interna. Nevertheless, the lesion showed signs of healing such as smooth surface of the depression and blunted margins of the hole. The whole lesion was surrounded and covered by light new bone formation, maybe indicative of some sort of infection. The general appearance of the lesion as well as its location might be indicative of a healed trephination, as the left parietal close to the sagittal and coronal sutures was a preferred site for trephination (Wahl & Zink 2013). Furthermore, the smooth depression surface and absence of marginal bone beveling would also suggest scraping of the

bone rather than a blow with a hard object as cause for this injury. However, blunt force trauma must also be considered as a possibility for the formation of the lesion, especially when considering the presence of another, unhealed sharp force trauma on the cranium, which might suggest that the individual was exposed to violent altercations more frequently.

6.5.3.9 Autopsies

Finally, evidence of two autopsies under the form of craniotomies was also recovered from the Knuedler cemetery.

Individual 2008-78/343 a mature male from Layer 1, buried in the cloister area, was represented only by a skull base, a few ribs and a femur, whereas it is unclear whether the femur belongs to the same individual. However, no further bones were found in the grave and metric sexing determined the femur as belonging to a male. Of interest however is mainly the cranial base, which was separated from its missing skull cap by a large circumferential cut, typically performed when opening a skull during autopsy. The cut occurred in two phases, as can be seen by overlapping cut marks and a step in the cut in the occipital (Figure 215).

Individual 2008-78/765, a mature (45-54y) male, was buried in the middle of the cemetery among a row with several other skeletons in Layer 1, and the postcranium was nearly complete. This individual had only its skull cap preserved, which had been separated from the base by a large circumferential cut approximately at the height of the internal occipital eminence. The right side of the frontal and part of the right parietal were missing. This individual also showed steps in the cutting line indicative of several attempts to cut through the bone. The skull cap also showed extensive cut or scratch marks along the sagittal suture on the left parietal as well as arched cut marks starting all at the same point on the temporal just above the zygomatic process and reaching up to the cut marks along the sagittal suture (Figure 213). These marks are probably indicative of fleshing or scalping before skull opening procedure (Crozier *et al.* 2021). A row of short parallel cut marks was also found in the center of the frontal bone, at the obliterated former metopic suture (Figure 214).

Apart from light osteophyte formation at femoral, tibial and fibular ligament attachment sites, no further pathological changes were detected in the postcranium. Furthermore, the sternum and ribs were intact, suggesting that the chest was not opened and only a craniotomy had been performed.

Surgical procedures and Autopsies

Figure 209 Amputation at the right humerus (2008-78/729)

Figure 210 Amputation at the right humerus (2008-78/729) view of the cutting surface

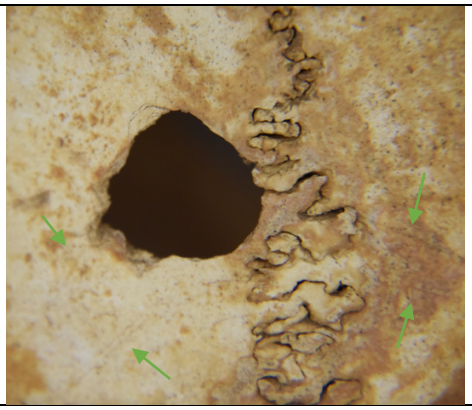

Figure 211 Evidence of trephination with cutmarks (arrows) at the margins of 2008-78/1040

Figure 212 Penetrating blunt force trauma or trephination close to bregma of 2013-015/357 (from grave fill)

Figure 213 Cut marks (probably for fleshing) at the right temporalis muscle attachment of 2008-78/765 an autopsied individual

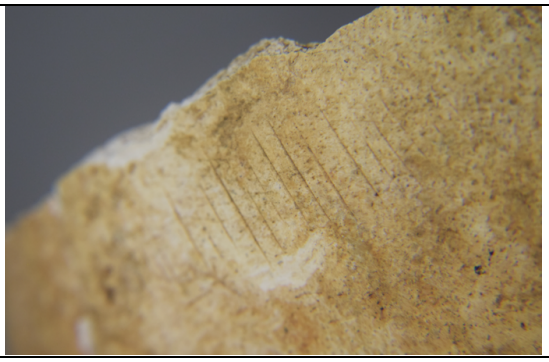

Figure 214 Cutting marks on the frontal of an autopsied individual (2008-78/765)

Figure 215 Autopsy of 2008-78/343

6.5.4 Discussion and Conclusion

Trauma is generally described as an injury to living tissue caused by external forces (Lovell 1997). Understanding the different fracture mechanisms as well as fracture patterns across the human body can help to shed light on living conditions in past populations. As such, a differentiation between fractures that might be accidental in origin, stress fractures that can be indicative of repeated trauma due to specific activities and fractures caused by interpersonal violence is vital in order to better assess past populations' occupational or lifestyle hazards and lifeways as well as exposure to conflict (Larsen 2015; Lovell & Grauer 2018; Dittmar *et al.* 2021; Mant *et al.* 2021).

A study by Dittmar et al. (2021) on a high and a low status cemetery from medieval Cambridge revealed that trauma occurred more frequently in older males and in individuals from a low status cemetery, when compared to a high-status cemetery, thus implying that people of that socioeconomic class were involved in more physical activities that put them at a higher risk of incurring accidents. In fact, within the Knuedler population, males were also more frequently affected by traumatic lesions than females, suggesting that they were engaged, on a daily basis, in activities that increased their risk of fracture. Furthermore, a significant difference in trauma frequency was also observed between the burial locations with individuals buried in the cemetery showing more fractures than those from the cloister area. This distribution pattern might suggest that those buried in the cemetery led more accident-prone lives than those from the cloister, implying that they belonged to different socioeconomic groups. Compared to trauma frequencies from other European sites, the results from the Knuedler cemetery lie for both the older and younger periods in the middle of the spectrum of occurrence. In both periods, the values lie below those estimated for a poor house hospital in Regensburg (Von Heyking 2012), suggesting that the inhabitants of Luxembourg City buried in the Knuedler cemetery were exposed to less every day risk to accidents than those buried in the poor house, implying a different socioeconomic background for the two groups. Rossbach (2015) observed an increase in trauma incidence from the medieval to postmedieval times in both her studied sites but it was much more marked in Hettstedt. In Luxembourg City, a decrease in fracture frequency was observed, even though the decrease was not statistically relevant. Comparisons of trauma frequency to other sites is not without problems. For example, in this study, only fractures and blunt force trauma were included in the evaluation. Rossbach et al. (2015), however, recorded blunt force trauma separately. Grauer & Roberts attained such low frequencies because only long bone trauma was assessed etc. Such differences in recording and

evaluation methods may lead to erroneous conclusions and make inter-site comparisons challenging. (Table 78)

When considering the frequency distribution of trauma across the different body parts, it becomes apparent that most fractures are registered for the torso. This discrepancy is also likely due to the more elevated number of bone elements in this region compared to others and due to the lack in protective tissue such as overlying muscle in that area (Roberts & Manchester 2010). However, ribs are the bone elements that are most commonly fractured. According to Waldron (2009), a strong cough or repeatedly carrying heavy goods might cause rib fractures, but accidents or interpersonal violence are much greater and more likely contributors to rib fractures than the aforementioned possibilities (Larsen 2015). Furthermore, several studies confirmed that rib fractures are very common, if not the most common type of fracture throughout the roman, medieval and postmedieval periods (Roberts & Cox 2003; Brickley 2006). Different types of fractures on long bones might also be highly indicative of either violence or accident. As such, the Colles fracture, which occurred in a total of three individuals in this sample is considered to result from trying to break a fall with the hands (Larsen 2015). The parry fracture, a fracture involving the ulnar shaft is often taken as an indication of an attempt for self-protection against blows to the head (Larsen 2015). One such fracture occurred in the Knuedler sample in a female buried in the cemetery area. Furthermore, even though the fracture had healed with no evidence of infection, it showed a strong degree of displacement.

Regarding fracture healing and alignment, most fractures in the sample were healed and well aligned, only a few, such as the parry fracture or an oblique fracture, showed obvious signs of displacement. Additionally, only two rib fractures were still in a state of healing. None of the fractures showed any signs of active or past infections. This suggests that the fractures were adequately taken care of and that basic knowledge regarding hygiene and fracture reduction and healing was present and accessible to the majority of people buried in that cemetery. This is not uncommon though as most urban areas had professions such as barber surgeons or bonesetters who had experience with fracture reduction, bone manipulation and splinting (Grauer & Roberts 1996; Wahl & Zink 2013). Therefore, it does not come as a surprise that other surgical practices such amputations and trephinations were carried out as well. Indeed, there is also evidence from historical sources about such procedures (Wahl & Zink 2013). However, one of the trephinations and the amputation were not survived by the respective individuals, which is also likely due to the greater risk of blood loss or damage to the brain in these procedures. As evidence for specialist knowledge in wound treatment, individual 2016-082/418 should be listed. This individual survived a gunshot wound to the head where the

bullet got stuck inside the orbital roof. The entry wound was well healed although not closed but did not show any signs of infection. The bullet was already partially absorbed into the bone of the orbital roof, which also showed no signs of past or active infection. Furthermore, the probable loss of the eye and likely neurological problems that ensued must have required greater after-care as well. But this projectile trauma is not only evidence for adequate medical treatment in Luxembourg City, but it is also evidence for interpersonal violence, which is supported by 4 further cases of either projectile, sharp force or blunt force trauma. The individuals were buried in the cemetery but also in the cloister area. In fact, during excavations in the 1970ies, two ornate gravestones belonging to soldiers or military personnel were discovered inside the cloister (Mousset 1999), showing that soldiers were buried on this cemetery together with the rest of the towns people and the monks of the convent. Since Luxembourg City, a garrison town at the time, was subjected to several sieges and due to changing rulers was also involved in several wars (Pauly 2011), it comes as no surprise to find victims of these wars on the cemetery.

Finally, two cases of autopsies were discovered on the cemetery. Whereas in the Middle Ages and early postmedieval times, these procedures were mainly reserved for criminals, as it was believed that opening the human body after death would corrupt its integrity, already in the late 15th century, autopsies became more frequent and historical sources confirm the autopsy of known people at the time. This suggests that autopsies had become more accepted already. And indeed, in the later postmedieval period a distinction was made between autopsies and dissections. Whilst dissections were still carried out on criminals and served the sole purpose of studying human anatomy, autopsies were generally carried out to determine cause of death if wanted or needed. Oftentimes, the cranial vault was not opened during dissections whereas it was frequently done so during autopsies (Burton 2005; Crozier *et al.* 2021). Based on all this evidence, it is safe to suggest, that these two individuals with signs of an autopsy were not necessarily criminals, but an unusual cause of death might have prompted their relatives or authorities at the time to investigate cause of death via an autopsy.

Table 78 Trauma frequencies across medieval and potmedieval Europe

Period	Site	Trauma freq. (%)	Publication	Year
10. - 16. C.	St. Helen	2,9	Grauer & Roberts	1996
11. - 19. C.	Serbien	4,3	Djuric et al.	2006
15. C.	Hettstedt-Kirche	4,9	Roßbach	2015
medieval	Völklingen	5,7	Roßbach	2015
mid-17th - 18th C	**Luxembourg**	**7,01**	**Kremmer**	**hic**
postmedieval	Völklingen	7,9	Roßbach	2015
late 14th – mid-17th C	**Luxembourg**	**11,97**	**Kremmer**	**hic**
12. – 16. C.	Regensburg	13,2	van Heyking	2012
10. – 16. C.	St. Georgen	13,3	Reiche	2010
10- - 12. C.	Rounds Furnells	19,4	Judd & Roberts	1999
15. /19. C.	Hettstedt	22,2	Roßbach	2015
12. – 17. C.	Chichester	23,3	Judd	2008

6.6 Infectious diseases

Infectious diseases are often used to infer information about the general health status of a population. However, the true prevalence of infectious disease burden of a population remains largely underestimated since most infectious diseases primarily affect the soft-tissue and a spread to the bones never occurs in most infections, since most individuals die or the infection resolves before the spread has happened (Waldron 2009; Roberts & Manchester 2010). This section discusses the main pathological lesions on bones associated to non-specific infections. Periostitis, an inflammation of the periosteum can be caused by many factors including viral and bacterial infections, traumatic lesions but also metabolic disease. It's prevalence can inform about the general disease burden and possible signs of malnutrition in a population (Lewis 2007; Waldron 2009; Grupe *et al.* 2015). Osteomyelitis is a usually bacterial infection of the bone marrow cavity which leads to severe changes in bone appearance (Aufderheide & Rodriguez-Martin 1998). Otitis media and Sinusitis are infections of the middle-ear and paranasal sinuses respectively. High incidence in sinusitis might be indicative of higher levels of air pollution and living situations that promote droplet infections, such as shared living spaces (Boocock *et al.* 1995; Lewis *et al.* 1995a; Waldron 2009; Roberts & Manchester 2010). The following section addresses all these pathological changes and puts the results from the Knuedler cemetery into a wider perspective through comparison to other, roughly contemporaneous sites in Europe.

6.6.1 Periostitis

6.6.1.1 Introduction

The periosteum is a fibrous membrane that covers the bone surfaces except for the joints and the endocranial surface of the skull, and that supports the attachment of muscles on the bones (Lewis 2007; Waldron 2009; Grupe *et al.* 2015). It is composed of two distinct layers, and the lower inner layer retains the capacity to form new bone (osteogenic properties) throughout an individual's life (Lewis 2007; Waldron 2009).

Periostitis is an inflammatory process of the periosteum, which is characterised by fine pitting and longitudinal striation, finally leading to new bone formation that is deposited on top of the original bone cortex (Weston 2008; Roberts & Manchester 2010). The inflammation of the periosteum stimulates the osteoblasts of the lower periosteal layer to secrete and deposit osteoid, an unmineralised and organic tissue of the bone matrix, on the cortical surface of the bone. (Lewis 2007; Trammell & Kroman 2013). If the periosteal inflammation becomes chronic, it can lead to a considerable thickening of the bone diaphysis in the long run (Grupe *et al.* 2015). Active periosteal reaction can be easily distinguished from healed lesions based on their appearance. Whilst active lesions are greyish in colour and represent distinct, porous depositions on the bone surface, composed of woven bone, healed lesions are usually made of lamellar bone and these usually bulkier lesions, which can appear completely remodelled into compact bone, can make the bone seem enlarged, and can occasionally even bear marks of blood vessel imprints (Lewis 2007). Periostitis can be caused by a number of factors such as bacterial or viral infections, traumatic injuries and even metabolic conditions such as scurvy (vitamin C deficiency) or rickets (vitamin D deficiency) (Pinhasi & Mays 2007; Weston 2008). In the case of scurvy, periosteal new bone formation is usually caused through subperiosteal hematomas caused by the underlying vitamin C deficiency which causes weakening of the basement membrane of blood vessels (Snoddy *et al.* 2018).

The tibia is generally the bone most affected by periosteal reactions. Most often periosteal lesions on the tibia result from repeated minor trauma, as the bone is not covered by much soft tissue that would diminish any blows or hits. Alternatively, conditions such as varicose veins or ulcers have been put forward as possible explanations for the high frequency of periosteal reactions on that bone (Waldron 2009; Roberts & Manchester 2010).

6.6.1.2 Methods

Periosteal reactions were recorded for long bones, os coxae, ribs, tarsals, carpals, and cranial bones available. The severity and type of the reaction and its location on each bone was described in the database. For long bones, tarsals, carpals, ribs and os coxae, a classification into the categories established by Steckel et al. (2006) was attempted (Table 79, Figure 216). Furthermore, a differentiation into active, healed, and mixed periosteal reactions was undertaken. The following analysis deals only with periosteal reactions of stages 2-5 after Steckel et al. (2006) as well as active lesions. Category 6, which describes osteomyelitis and category 7, which describes callus formation after bone fracture were not included in the following evaluation. Osteomyelitis was excluded because it deals with infections of the bone marrow as opposed to the periosteum and will be dealt with in more detail in the next section. Callus formation was excluded because it forms primarily a reaction to bone fracture. Fractures and other traumatic lesions will be analysed in a separate section. Periosteal reactions of non-specific origin and those related to defined infectious or metabolic conditions are all included in the following analysis.

All statistical analyses rely on the calculation of crude frequencies for periosteal lesions. This was decided because all individuals with periosteal lesions irrespective of their localisation could be included.

The distribution of active, mixed, and healed periosteal lesions by postcranial bone element is presented in the form of a bar chart of true frequencies. Right and left bones were combined under one bone element. The percentage of occurrence of active, mixed, and healed periosteal lesions was calculated relative to all right and left bones of a bone element present. Only one tarsal showed a lesion. No lesions were found on the carpals; therefore, they are not included on the graph. Cranial and costal lesions are not included on the graph either. Presence of lesions was recorded for every bone of the cranium and all available ribs, the data base entry only allowed for a count of absolute values for all ribs and cranial bones by individual. However, in future work it would be possible to separate all entries for single ribs and cranial bones.

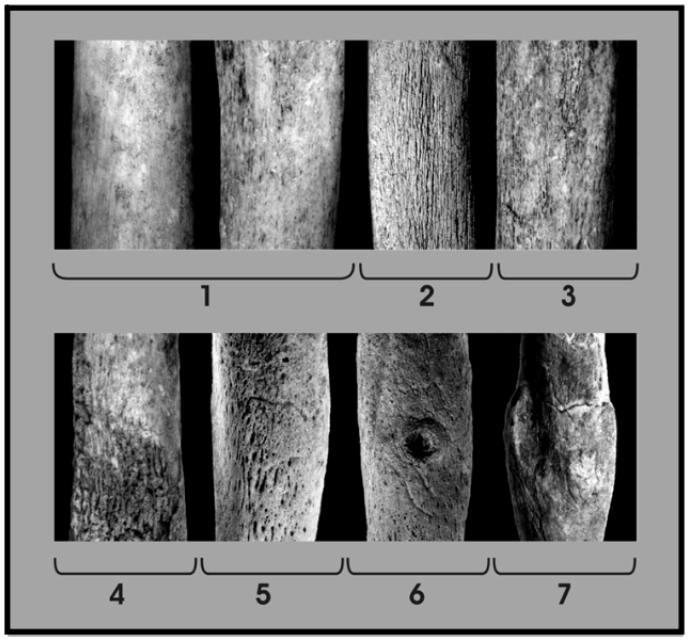

Figure 216 Stages for scoring periosteal reaction (from Steckel et al. (2006))

Table 79 Description of periosteal reaction scores from Steckel et al. (2006) with addition of score for "active" lesion by the author

Score	Description
1	No osteoperiostitis present
2	Markedly accentuated longitudinal striations
3	Slight, discrete patch(es) of reactive bone involving less than one quarter of the long bone surface
4	Moderate involvement of the periosteum, but less than one-half of the long bone surface
5	Extensive periosteal reaction involving over half of the diaphysis, with cortical expansion, pronounced deformation
6	Osteomyelitis (infection involving most of the diaphysis with cloacae
7	Osteoperiostitis associated with a fracture
9	Active lesion

6.6.1.3 Results

Periosteal reactions were recorded for all 391 individuals analysed for the Knuedler site. All crude frequencies presented in the following analysis are referenced to that number. This might have led to an underestimation of prevalence of periosteal reactions since not all individuals were complete.

Overall, 28.64% of individuals presented with either one or several periosteal reactions on any bone. More individuals from the cemetery (30.77%) presented with periosteal lesions than those from the cloister (23.73%) but this difference was not statistically significant. However, significantly more individuals from the younger Layer 1 (35.03%) had periostitis than those from the older Layer 2 (28.64%).

No statistically significant relationship of periostitis to age could be detected among the Knuedler individuals. The very varied frequencies observed within the subadult category are

also likely due to the smaller sample sizes within that age category. Periosteal reactions were most frequently observed in adults (38.57%), matures I (33.33%). Matures II (28.81%), seniles (26.79%) and young adults (27.78%) had a very similar frequency of periostitis. Among the Neonatus, infans I and infans II group, the majority of the cases belonged to individuals with underlying metabolic conditions. When comparing only juvenile and adult individuals of known sex, no statistically relevant differences could be detected between males (32.34%) and females (31.86%).

Generally, postcranial lesions were much more frequent than cranial lesions, as they were recorded only in 22 individuals. In contrast, 100 individuals presented postcranial lesions. 10 individuals had lesions on the cranium and postcranium, 12 only had cranial lesions but for 3 of those, only the cranium could be assessed for periosteal lesions anyway.

Active periostitis was much less frequent than healed periostitis. Mixed lesions, meaning bones that exhibited healed lesions and active ones at the same time, were least frequent. In the scapula and the arm bones, active periostitis was more often observed than healed periostitis. A lot of these cases could however be attributed to individuals with underlying metabolic or infectious disease. In the pelvis and leg bones, healed lesions were much more common. The leg bones also exhibited many more lesions than the arm bones. The majority of lesions was found in the Tibia, which also boasted the majority of severe lesions (Figure 217). Since most periosteal reactions on the tibia, especially the more pronounced reactions also affected the fibula, the fibula presents with the second highest frequency of lesions.

Figure 217 Severe periostitis on the right Tibia and Fibula of 2008-78/1001

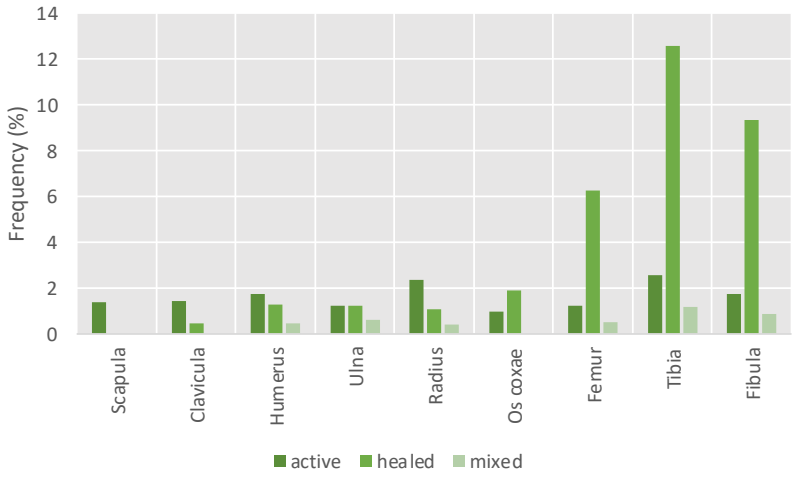

(Scapula: n=425, Clavicula: n=416, Humerus: n=458, Ulna: n=479, Radius: n=469, Os Coxae: n=527, Femur: n=561, Tibia: n=509, Fibula: n=460)

Figure 218 Distribution of active and healed periosteal reactions by bone type

6.6.1.4 Discussion

Periostitis is an inflammatory process of the periosteum causing new bone formation on the surface of bones (Weston 2008; Roberts & Manchester 2010). The causes underlying the new bone formation are manyfold ranging from infections to metabolic conditions and traumatic injuries (Pinhasi & Mays 2007). Therefore, the occurrence of periosteal reactions on bones within a population, can be informative about their general health and exposure to external stressors.

Unfortunately, studies listing frequencies of periosteal reactions are rather rare, which is why the time span of considered sites was slightly widened for this comparison.

When comparing the results from the Knuedler Cemetery to other contemporaneous European sites, the overall frequency of 28.64% individuals with periostitis lies in the middle of the spectrum. Individuals buried in an early medieval cemetery from Bärenthal auf der Scherra (Düring 2014) for example showed a much higher (62%) prevalence of periosteal reactions. For the medieval site of Nova Rača in Croatia, Šlaus (2000) reported a frequency of over 50% periosteal lesions in adults and 60% in subadults, and Novak et al. (2008) reported a total of 48.4% of periosteal lesions for a combined set of 8 Croatian sites dated between 12th-18th century. Individuals buried at Ellwangen-Jagst for example (late medieval: 18.02%; early postmedieval: 13.25%) and in rural Grevenmacher (14.3%) showed considerably lower frequencies of individuals with periostitis (Trautmann 2012; Kairies 2021). Similar values were however observed among individuals buried in 15th century Hettstedt, and in medieval and

postmedieval Völklingen (Roßbach 2015). Although frequencies were calculated separately for active and healed periosteal lesions in that study, the frequencies for active lesions ranged between 36% (Hettstedt Kirche), 44.4% (Hettstedt Gymnasium), 32.1% (medieval Völklingen) and 34.8% (postmedieval Völklingen). Those for active lesions were much lower at less than 10%. Since prevalence calculated for the individuals from Knuedler cemetery includes active and healed lesions, the frequency seems to be also considerably lower than that from those sites. However, like in Hettstedt and in Völklingen, the frequency of lesions increases over time. As the bar chart with active and healed lesions by bone type demonstrates, active lesions were also much less frequent among the Knuedler cemetery burials than healed lesions. In the Grevenmacher burials and in the Hettstedt (Kirche) and Völklingen (late medieval and postmedieval) burials, the lower extremeties, and in particular the tibia, were most affected. Finally, individuals from a cemetery of a 12th -16th century poorhouse in Regensburg yielded a similar frequency of periosteal lesions (26.2%) (Von Heyking 2012). However, other studies on poorhouses in England, namely that in Chichester (Lewis *et al.* 1995b; Ribot & Roberts 1996; Von Heyking 2012), yielded frequencies ranging from 43-64%. At St. Helen-on-the-Walls, a cemetery in York, England, which represents an urban population of rather low social status, frequency of periosteal lesions were around 22.4% (Grauer 1993). This might indicate, that living conditions of the people buried on the Knuedler cemetery might have been similar to those of Minoritenweg or St.Helen-on-the-Walls and therefore more in line with an urban setting of lower status people. Since more individuals from the cemetery lesions than those from the cloister, it could indicate that they were exposed less to the stressors that might be responsible for the formation of such lesions. Unfortunately, no regional urban comparisons were possible. However, it has to be noted that Luxembourg, between the 16th and 18th century, has always been a garrison town. Especially in times of war, a lot of garrisons were stationed in the city and the soldiers and officers were lodged in the living quarters of the regular towns people, which led to severe overcrowding in homes and in the city. Everyone was forced to house soldiers in their homes, except for the clergy. Only affluent people such as the aristocracy, lawyers etc. could afford to pay the fee and avoid the situation (Thewes 2013). Due to the troops stationed in the city and the ongoing wars, even if they did not directly affect the city, food shortages within the city walls were not uncommon (Weis 2004). This situation of overcrowding might have promoted the spread of infectious diseases that led to non-specific periosteal reactions on bones. In at least one case (2016_082/419), the extensive active periosteal reactions can be attributed most likely to a congenital infectious disease or metabolic conditions. Differential diagnoses for this individual include congenital syphilis, congenital

rubella, congenital cytalomegavirus, congenital toxoplasmosis or congenital herpes, but scurvy cannot be excluded either. Since many bones that would be needed to reach a more definitive diagnosis are missing, all differential diagnoses must be considered as possibilities. In a further 6 subadult individuals a scurvy diagnosis seems most plausible, and for two adults, the periosteal lesions also point towards metabolic stress. Further differential diagnoses for these cases are presented in the chapter on metabolic conditions. Individual 2008-78/672, an infans II was also if interest. It presented with very strong periosteal new bone formation on the innerside of several right middle ribs, that was accompanied by deformation of the anterior side of the ribs in close proximity the neck. The ribs had an indent on the anterior side which stretched over several adjacent ribs. No changes were observed on the vertebrae. No specific origin for the deformation of the ribs could be detected. Future plans include the closer investigation of the lesions by radiography, in order to detect any possible internal changes. A localised infection, possibly caused by a fracture currently stands as the preliminary diagnosis. All further periosteal reactions on pelvic- and long bones had to be ascribed to non-specific infections.

6.6.2 Osteomyelitis

6.6.2.1 Introduction

Osteomyelitis is an infection of the bone and bone marrow, mostly caused by bacteria. In 90% of cases, the infection is caused by staphylococcus aureus, but infections by other bacteria such as pneumococcus, meningococcus, mycobacterium etc. and even by fungi, have also been noted (Aufderheide & Rodriguez-Martin 1998; Adler 2005; Grupe *et al.* 2015). The bacteria can either enter the medullary canal through a fracture, by direct spread from a soft-tissue infection surrounding the bone or joint, or via a nutrient foramen through the bloodstream from an infection in another area of the body (haematogenous spread). Haematogenous spread is generally more frequent than traumatic spread and children are usually by much more frequently affected than adults (Aufderheide & Rodriguez-Martin 1998; Waldron 2009). The bacteria that invade the bone marrow cavity are pyogenic. Usually, the infection starts in the sinusoidal veins of a bone through which the bacteria have entered. They cause a subperiosteal abscess at the site of entrance that can spread along the bone. Through enlarged Haversian and Volkmann canals, the bacteria can then spread into the bone marrow cavity. The pus build-up in the marrow cavity leads to restrictions in blood flow, which leads to death of the infected bone. As reaction to the dead bone (sequestrum) the periosteum produces extensive new bone

(involucrum) gradually surrounding all the infected areas. Cloacae, holes reaching from the marrow cavity through the involucrum, form in order to drain the pus that accumulated inside the bone marrow cavity. During the infection process, the bone is extensively remodeled (Aufderheide & Rodriguez-Martin 1998; Waldron 2009; Roberts & Manchester 2010). If the infection reaches the joint, it can cause septic arthritis, in which the whole joint becomes infected and can spread the infection to other adjacent bones in the joint. Most cases of septic arthritis lead to ankylosis of the joint (Waldron 2009).

6.6.2.2 Results

No statistical analyses were performed to analyse frequency of osteomyelitis in the Knuedler cemetery since the number of individuals affected was so small. In total, only 2 individuals could be securely diagnosed with osteomyelitis as all characteristic lesions were present, and one had very likely osteomyelitis. Individual 2008_78/838, a young adult female from Layer 1 buried in the cemetery, presented with flattened but broadened proximal epiphysis and an enlarged diaphysis of the right tibia. The medial condyle presented with a large cloaca approximately at its centre, from which a deep furrow, probably also a drainage canal, leads to the intercondylar area. Furthermore, the medial condyle was enlarged, and the surface was noticeably concave (Figure 219). Closer inspection of the cavity in the medial condyle showed a connection of the cavity to the medullary canal and from the same cavity, cloacae draining out of the lateral and anterior sides of the lateral condyle were noted. A clear point of onset for the lesion cannot be determined but the lesions are most pronounced in the medial condyle and from there, seem to spread to the lateral condyle. The lesions of the proximal part of the diaphysis are not as developed as only enlargement of the bone was observed.

Individual 2008-78/1021, senile male from Layer 2, buried in the cemetery had multiple areas of the skeleton affected by osteomyelitis. The strongest lesion was located in the left femur. The bone was strongly enlarged and presented with a very irregular and strongly remodelled surface (involucrum) and multiple large cloacae. Sequestrae were visible inside the cloacae. The infection reached up until mid-diaphysis and also encompassed the complete distal joint area. The infection had already spread into the joint and the patella had fused to the anterior part of the lateral condyle and the proximal epiphysis of the femur had fused to the posterior area of both femoral condyles at a near 45° angle (Figure 223). Another lesion was observed in the right scapula. The main focus was in the area of the glenoid cavity. The glenoid cavity was completely flattened and eroded, and the surrounding bone thickened by irregular periosteal new bone formation (involucrum). Inside the several cloacae, sequestrate were

visible (Figure 222). The right humerus was not fused to the glenoid cavity and only showed periosteal reactions at the neck and proximal diaphysis. Another area of notice were the 5th and 6th thoracic vertebrae which were fused together and presented with irregular periosteal new bone formation around the bodies. Furthermore, prior to fusion, the body of the 5th thoracic vertebra had partially collapsed, leading to a wedge-shaped appearance of the fused bloc. The arches were largely unchanged. No evidence of cloacae was however detected on the bodies (Figure 221). Both cases stem from different layers but they were both found in individuals from the cemetery, however, due to the small sample size, no statistically relevant conclusions can be drawn from this.

The 4th lumbar vertebra of 2008-78/585 showed strong lytic lesions on the superior body side, with slightly spiculated new bone formation on the anterior body and at the rim of the lytic lesions (Figure 220). The inferior vertebral plate and body did not show any osteolytic lesion nor periosteal reactions. The intervertebral disc must have eroded away or collapsed due to the lytic lesions since there is eburnation on the only intact part of the superior vertebral plate. The same eburnation spot is found on the inferior vertebral plate of the articulating LV3. But except for some surface irregularities and the eburnation spot, LV 3 does not present any major lytic or osteoblastic lesions on the inferior surface. There is a small lesion on the anterior right rim of the inferior vertebral plate, which together with one of the lesions on LV4 forms a sort of tunnel, when stacked. No lesions were observed on LV3's superior vertebral plate, but one large lesion was located on the posterior body side towards the intervertebral canal, which forms a large cavity inside the body. There is mainly bone resorption/erosion on LV4, except for the relatively light spiculed periosteal reaction on the lateral and anterior sides of the body, there is no bone formation inside the lesions. The lesions expose the spongiosa, which has hardened and thickened. It is noteworthy that the lesions on LV 4 and 3 do not affect the arcus, only some new bone formation could be observed on the arcus of LV4 and none on that of LV3. There is some lightly spiculated periosteal new bone formation on the lower anterior and lower right body of LV3, the left body side of LV3 is eroded and cannot be assessed.

Some light degenerative changes were observed in the intervertebral joint of LV3 and LV4 as well. The remaining lumbar vertebrae show no osteolytic lesions or periosteal reactions at all. But all lumbar vertebrae have slightly deformed articular facets causing the whole spine to slightly bend to the right, probably due to the collapse of the right side of LV4.

The 5th lumbar vertebra has a large pseudoarticulation with the right ala of the sacrum, meaning there is partial sacralization of LV5. The articular surface is irregular, with osteophytes around the rims and pitting on the rim and surface. Possibly the articulation is not congenital in origin

but was created after the collapse of LV4 to give strength and support to the spine and prevent it from further collapsing to the right.

Osteomyelitis

Figure 219 Osteomyelitis in the proximal epiphysis of the right tibia of 2008-78/838

Figure 220 Large destructive osteolytic lesion on the superior vertebral plate of TV4 of 2008-78/585

Figure 221 Probably osteomyelitis in thoracic vertebrae of 2008-78/1021

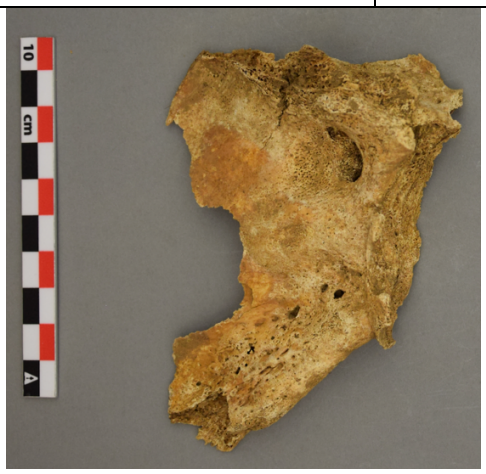

Figure 222 Osteomyelitis in the right scapula of 2008-78/1021

Figure 223 Osteomyelitis in the left femur of 2008-78/1021 with ankylosis of patella and tibia

6.6.2.3 Discussion

Osteomyelitis is a bacterial infection of the bone involving the medullary canal. Pyogenic bacteria can enter the medullary canal either through an infection of an adjacent organ or soft-tissue, through fractures or through the blood stream, and the latter type is more common than the other two (Aufderheide & Rodriguez-Martin 1998; Waldron 2009; Roberts & Manchester 2010). Regarding individual 2008-78/838, no fractures were evident in the bone, which would suggest a haematogenous spread. However, since the origin of the lesion seems to be in the

proximal medial condyle, a micro trauma to the condyle through which bacteria could enter into the bone cannot be excluded entirely. Furthermore, although the lesion drained into the synovial joint, no other bones were affected, as no signs of infection or inflammation were observed in the patella or the distal epiphysis of the femur. Therefore, the infection was probably still contained underneath the cartilage covering the condyle. In the absence of active periosteal reactions, it could also be assumed that the lesion was already healed but bone remodelling had not yet started.

The most common form of osteomyelitis is acute haematogenous osteomyelitis. The most common origin for this kind of osteomyelitis is in the knee (Aufderheide & Rodriguez-Martin 1998). The knee seems to be the primary area of infection in the case of individual 2008-78/1021. However, a slight bend observed in the distal end of the remodelled diaphysis suggests that maybe a fracture is at the origin of the infection. However, due to the extensive remodelling and destruction of the bone, this cannot be determined for certain. According to Waldron (2009) an osteomyelitis infection can also spread into the joint and cause septic arthritis, a condition which ends almost always in ankylosis of the joint. Through the joint, osteomyelitis can also spread to the adjacent bones. Septal arthritis with ankylosis of the knee was also observed in individual 2008-78/1021 however, the infection did not spread to the tibia or the patella. According to Aufderheide and Rodriguez-martin (1998), the knee, together with the hip, make up 70% of septic arthritis cases. However, there was haematogenous spread of the bacteria to the right scapula, which also showed very clear signs of osteomyelitis. What is of note however, is the involvement of the 5^{th} and 6^{th} thoracic vertebrae. Although no clearly diagnostic signs such as cloacae could be observed, the fusion and collapse of the two vertebrae still suggest osteomyelitis as the main cause for the collapse and fusion of the vertebral bodies. The destruction was not severe enough to cause strong kyphosis, which would have been the typical sign of Pott's disease (Pinhasi & Mays 2007). Nevertheless, tuberculous osteomyelitis should be considered as a differential diagnosis for this individual. Tuberculous osteomyelitis is an infection of the bone medullary cavity by mycobacterium tuberculosis. Mostly, the spine is the focal point of these infections. Although the spine also seems to be in volved in individual 2008-78/1021, the primary lesion seems to be located in the knee. Furthermore, the formation of sequestrate and involucrum is rare in tuberculous osteomyelitis (Adler 2005) but they are very present in this individual. Therefore, the most probable cause remains a hematogenous or posttraumatic osteomyelitis, with initial infection starting in the knee and causing septic arthritis of the joint and subsequent spread to other body parts.

The spinal lesions observed in individual 2008-78/585 are highly consistent with those described for spinal tuberculosis, especially since in tuberculosis, the vertebrae are usually the first bony elements to be involved. Furthermore, periosteal reaction though present is rather small in this individual compared to the size of the lesions and apart from trabecular thickening, no boy reactions were observed within the lesions. The large, rather localised lytic lesions and the light spiculated bone reaction surrounding them might also hint at an osteolytic tumor, either primary or secondary (metastases) as the cause for the spinal lesions of 2008-78/585. The tumors that most often spread to bone are prostatic carcinoma (70% metastasise into spine) and breast carcinoma (30-50%), others that metastasise into bone too but less frequently are lung, kidney and thyroid. However prostatic carcinoma usually causes osteoblastic lesions. Breast carcinoma causes mixed lesions and lung, kidney, thyroid and gastrointestinal primary sites usually cause osteolytic lesions (Aufderheide & Rodriguez-Martin 1998; Waldron 2009; Marques 2019). The individual being female and the lesions being lytic, prostate carcinoma can be ruled out. Lesions could be due to carcinoma from any of the above locations or multiple myeloma, which cause very similar lesions. However, multiple myeloma is purely lytic and the lesions usually small (Marks & Hamilton 2007; Marques 2019). These lesions are rather large and there is light bone formation (spicules), so multiple myeloma is not that likely either. Furthermore, metastatic cancer and multiple myeloma mostly affect several bones of the skeleton, which is not the case here. Primary bone tumors that can occur in the spine and cause lytic lesions are spinal hemangioma, osteoblastoma etc., however spinal primary bone tumors are quite rare (Patnaik *et al.* 2016), favoring therefore osteomyelitis and possibly tuberculosis as primary diagnoses.

For the sake of completeness, individual 2008-78/729 also has to be mentioned here. It presented with an amputation of the right humerus and stage 5 periostitis in both tibiae and fibulae. No radiographs of the lower leg bones have been taken yet, but the possibility of an osteomyelitis infection that has not yet created cloacae must also be considered. Often times, the only cure for osteomyelitis was amputation (Waldron 2009). Therefore, regarding the leg lesions, it might be possible that amputation of the arm was carried out in order to remove an osteomyelitis infection, which might have already spread to the legs. However, this theory can of course not be verified.

Compared to Ellwangen-Jagst, especially when only considering the late medieval (n=8) and early postmedieval periods (n=3) (Kairies 2021), the occurrence of osteomyelitis is much lower at 2 individuals. In Grevenmacher, only 1 individual was diagnosed with osteomyelitis (Trautmann 2012).

6.6.3 Sinusitis and Otitis media

6.6.3.1 Introduction

6.6.3.1.1 Sinusitis

Sinusitis designates an inflammation of the paranasal sinuses. The paranasal sinuses are located inside facial bones on the right and left side and are air-filled spaces connected to the nasal cavity. There are four paranasal sinuses, the ethmoid, the sphenoid, the frontal and the maxillary sinus. Usually, it is the maxillary sinus that is most affected by infectious disease (Waldron 2009). There are two forms of maxillary sinus infections, an acute form and the chronic form. In this case, the acute form is irrelevant as only the chronic form is detectable on the bones. An infection of the mucosa inside the sinuses is usually caused by viruses or bacteria that enter the sinus via the respiratory tract. Alternatively, dental abscesses that drain into the maxillary sinuses also frequently lead to chronic sinusitis. Chronic sinusitis leads to periosteal new bone formation inside the sinus, which can range in severity from simple plaque-like spots to spiculated lesions that span the whole cavity (Panhuysen *et al.* 1997). Generally, sinus infections are harmless, but due to their proximity to the brain and orbit, they can cause serious problems when the infection spreads to these areas (Waldron 2009).

6.6.3.1.2 Otitis media

Otitis media describes a viral or bacterial infection of the mucosal membranes of the inner ear. Like for sinusitis, a distinction is made between the acute and chronic form. Due to continuous accumulation of pus within the middle-ear cavity and the subsequent mounting pressure inside the middle-ear, a rupture of the tympanic membrane often ensues. (Aufderheide & Rodriguez-Martin 1998; Roberts & Manchester 2010). Through this rupture, bacteria, viruses and fungi can gain easier access to the middle-ear, causing recurrent infections. Characteristic lesions of chronic otitis media are periostitis inside the middle-ear cavity as well as destructive changes or fusion of the ear ossicles. In very severe cases, the infection can drain into the surrounding bone and cause mastoiditis, an inflammation of the mastoid air cells. In the living, chronic otitis media may eventually cause deafness or tinnitus (Lewis 2007).

6.6.3.2 Results

6.6.3.2.1 Sinusitis

Sinusitis was not recorded in a standardised manner for the Knuedler cemetery. It's presence was only noted when changes were apparent. Therefore, an exact percentage of individuals cannot be calculated at this time, as it has not been recorded how many sinuses were actually broken and allowed assessment of the inside of the maxillary sinuses. Therefore, any attempt to calculate the frequency of sinusitis media in this series would result in an underestimation of the true prevalence since individuals with closed and unscoreable would be included in the analysis as sinusitis absent.

However, the number of detected maxillary sinus infections was also fairly low. A total of 12 individuals had signs of chronic sinusitis infection. In 8 cases the infection was noted only unilaterally and in 4 it was present bilaterally. 8 people with chronic sinusitis were male and 4 female, 7 came from the lower and 5 from the upper layer and 4 were buried in the cloister and 9 were buried in the cemetery. In 6 cases, the lesions were directly associated to a periapical abscess that had drained into the sinus. (Figure 224)

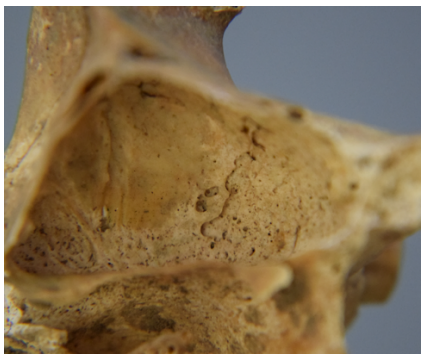

Figure 224 Evidence for chronic sinusitis in right maxillary sinus of 2008-78/1704

6.6.3.2.2 Otitis media

Only two cases of otitis media occurred among the individuals from the Knuedler cemetery. While individual 2008-78/675 only showed exostoses inside and on the rim of the meatus accusticus externus, the lesions of individual 2008-78/1038 were more advanced. On the left glenoid cavity of the skull was a hole that led into the middle-ear canal and within the canal, periosteal new bone formation and the fused ear ossicles were visible. Probably, the pus inside the middle ear drained through a whole into the glenoid cavity causing osteoarthritis in the mandibular condyle.

6.6.3.3 Discussion

Even though direct comparisons to other sites are not possible, it seems that the occurrence of both sinusitis and especially otitis media are very low among individuals from the Knuedler cemetery. At the medieval urban lower class burial ground of St. Mary-on-the-Wall, prevalence of sinusitis was 55% and at Wharram Percy 39% (Lewis *et al.* 1995a). The low occurrence of the disease in the Knuedler sample would definitely not amount to a frequency of 55% since far more than 24 sinuses could be assessed. Prevalence of sinusitis in medieval Maastricht even amounted to 61% (Panhuysen *et al.* 1997). In Emden the prevalence was 10.1%, which seems to be already much closer to the number of cases observed in Luxemburg (Stech 2009). Otitis media was also statistically analysed for Emden, where 16% of the population suffered from middle-ear infections (Stech 2009). Whilst the British sites are representative of urban and rural lower-class individuals, those from Emden date from the 10^{th}-18^{th} century and belong to the upper-class. Judging by the low prevalence of otitis media and sinusitis in the assemblage from the Knuedler cemetery, it could be assumed that both populations experienced a similarly high standard of living. Nowadays, chronic otitis media occurs most often in groups of lower socio-economic status (Adoga *et al.* 2010; Siddartha *et al.* 2011). The few cases discovered in the Knuedler cemetery would thus suggest that the people buried there did not belong to the lower social class which was more susceptible to developing the disease. It is thought that air pollution such as smog in the city can promote chronic sinusitis. In fact, Lewis et al. (1995a), by comparing rural Wharram Percy to urban St. Mary-on-the-Wall, the urban population suffered more frequently from sinusitis than the rural one. Furthermore the tighter living conditions within towns might promote the spread of the disease through droplet infection among residents (Boocock *et al.* 1995).The low number of sinusitis cases might then suggest, that air quality inside Luxembourg City was rather good and the living arrangements of the people buried in the cemetery was not too tight. However, from historical sources it is known that Luxembourg city got very crowded when residents had to host foreign soldiers stationed in the city inside their own homes (Thewes 2013). Higher rates of periosteal reactions did also suggest a higher exposure to pathogens, but the results of the sinusitis and otitis media evaluations seem to contradict this. However, many sinuses were also still intact and could not be assessed, maybe assessment of these individuals as well would help shed more light on this matter.

6.7 Non-specific indicators of stress

Environmental stressors such as malnutrition, famines, infectious diseases but also infestation by internal parasites or extreme climatic conditions can leave traces on bones. To what extent these stressors finally affect the human body is dependent on many factors. The effect of some stressors can be lessened through cultural practices but on the other hand they can also create new stressors (Goodman & Armelagos 1989; Grupe *et al.* 2015). Urbanisation is generally thought to have brought a host of new stressors. High population density in urban areas does not only expose inhabitants to constant social stress, but also promotes the spread of infectious diseases and can emphasise periods of malnutrition or famines (DeWitte & Betsinger 2020; Betsinger & DeWitte 2021). Furthermore, the extent to which these stressors affect an individual is also highly dependent on the individual's immune system (Grupe *et al.* 2015). As such, children, due to their still developing immune system and developing functional properties of their body, are often most affected by external stressors, as they are highly dependent on adequate nutrition and more prone to infectious diseases (Hühne-Osterloh 1989; Jungklaus 2007). Oftentimes, the conditions that might have caused the stress markers in the skeleton would have impacted a child's development and growth and might have led to higher mortality among subadults. Therefore, the stress markers are generally more prevalent in children than in adults (Šlaus 2000; Obertová & Thurzo 2008). Furthermore, during the interpretation of these stress markers, it is important to also take note of their different aetiologies and their relation to the occurrence of certain pathological lesions (Nikiforuk & Fraser 1981; Grupe *et al.* 2015).

6.7.1 Enamel Hypoplasia

6.7.1.1 Introduction

Enamel hypoplasia are defects in the enamel of teeth that primarily describe a reduction in enamel thickness in a specific area of the tooth (Goodman & Rose 1990; King *et al.* 2005). This reduction in enamel thickness is caused by a disruption of ameloblast activity (El-Najjar *et al.* 1978; Hillson & Bond 1997) and can manifest in various forms, ranging from multiple rounded pit defects to linear lines or grooves on teeth that follow the perikymata (Goodman & Armelagos 1985; King *et al.* 2002, 2005). After the formation of the defect, dental enamel does not remodel so that the defect will be preserved on the tooth. Therefore, based on their position on the tooth, it is possible to determine at what age the linear defects have been formed (Goodman *et al.* 1980; Grupe *et al.* 2015). The reasons behind the formation of enamel defects

are considered to be manyfold, with malnutrition, hypocalcaemia and episodes of infectious diseases all being listed as potential causes (Goodman & Rose 1990; Lanphear 1990; Hillson 1996; Schultz *et al.* 1998; King *et al.* 2005). Many studies have also associated the stresses of weaning to linear enamel hypoplasia formation. Especially peaks in enamel hypoplasia occurrence within the possible time frame of weaning across a population have been interpreted as signs of weaning stress rather than more individual factors such as malnutrition or infectious diseases (Corruccini *et al.* 1985; Moggi-Cecchi *et al.* 1994; Wood 1996). Since breast milk provides nutrients such as iron, calcium, zinc and vitamins and strengthens the infants immune system, the weaning process and the introduction of novel food items to the diet decreases the immunological protection and the child is exposed to range of new pathogens (Dittmann & Grupe 2000; Mays *et al.* 2002; Lewis 2007; Quigley *et al.* 2007; Henderson *et al.* 2014; Kaupová *et al.* 2014), which might be severe enough to cause a disruption in enamel formation at the time of weaning. However, it has to be kept in mind that some studies also put this theory into question when they did not find a link between historically reported age of weaning and timing of linear enamel hypoplasia lines on teeth (Blakey *et al.* 1994; Katzenberg *et al.* 1996). Other studies have related the occurrence of Linear enamel hypoplasia to differences in socioeconomic status (Cucina & Işcan 1997; Palubeckaitė *et al.* 2002; King *et al.* 2005; Starling & Stock 2007; Tomczyk, Jacek, Soltysiak Arkadiusz 2007; Miszkiewicz 2015; Nakayama 2016; Minozzi *et al.* 2020) and some also related them to a higher susceptibility to developing caries (Duray 1990) and to earlier mortality (Cook & Buikstra 1979; Cook 1981; Duray 1996; Palubeckaitė *et al.* 2002; Boldsen 2007; Armelagos *et al.* 2009).

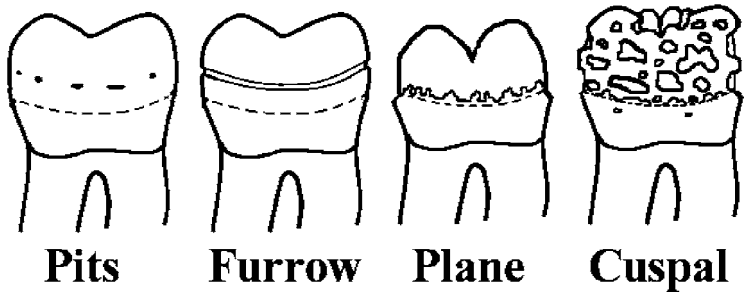

Figure 225 Different types of enamel defects (taken from Pinhasi and Mays, 2007)

6.7.1.2 Methods

Enamel hypoplasia were recorded following the types of expression in Figure 225. However, neither the “plane” type nor the “cuspal” type were detected in the sample and therefore only the coding for the first two types is represented in Table 80. (Figure 228, Figure 229)

Table 80 Scores for recording enamel defects

Score	Description
0	Absence of enamel defects
1	Line defects (LEH)
2	Pit defects

The occurrence of periapical lesions was recorded for every tooth that was sufficiently preserved for scoring. Therefore, teeth destroyed by caries or covered in calculus were not included. Only individuals with scoreable teeth were included in the study. Furthermore, linear enamel defects were scored following the recommendations set out by MoLA (museum of London Archaeology)(Powers 2008). As such, also lines that were very fine and thin and not palpable were recorded as hypoplastic defect. However, lines that were only visible under certain light conditions or discontinuous were omitted.

All analyses were carried out for adults and subadults separately.

For the calculation of crude frequencies, no distinctions were made between individuals with multiple or single lesions nor between the type of the lesion. Both true and crude frequencies were subjected to Pearson's chi square tests in order determine whether there were any statistically significant differences between sex, age, burial layer and location in the occurrence of enamel defects. The frequencies of lesion types were not explored but it was noted that linear enamel hypoplasia made up the majority of cases anyway. With the help of dental growth schemes, it is possible to determine the age at which the defect was formed during tooth maturation. The ageing of the enamel defects was carried out after Reid and Dean (2000) for maxillary and mandibular incisors and following Reid and Dean (2006) for maxillary and mandibular molars. Defects occurring on the premolars were roughly estimated following the dental growth charts of (Smith 1991). If there were multiple lesions on the tooth, all lesions were aged, but, if possible, the strongest line was noted. In a next step, peak enamel hypoplasia age was determined via visual inspection of a line plot. Peak enamel hypoplasia was estimated only for the whole sample. In a first step, all teeth and all defects were included. Next, only linear enamel hypoplasia were included and finally, only teeth with a single defect were entered into a graph. All graphs are based on the whole contingent of permanent dentition including subadults. All hypoplastic defects are represented, so if a tooth presented with several defects of varying degree of expression, all on the tooth were still taken into account in order to represent all possible episodes of stress. No average per individual was calculated, age was

determined for all enamel defects on all teeth except the premolars and deciduous teeth and all age ranges were included in the graph. Only linear defects are represented.

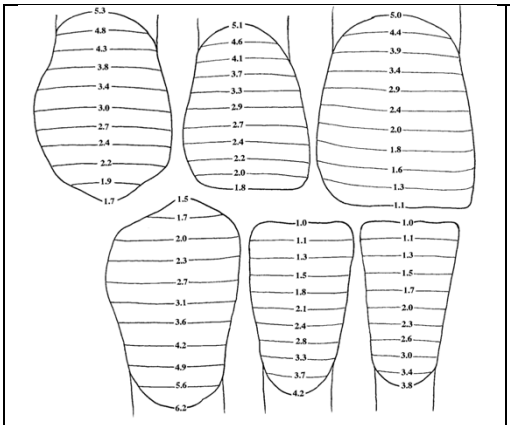

Figure 226 Template for ageing linear enamel defects on front teeth (taken from (Reid & Dean 2000)*)*

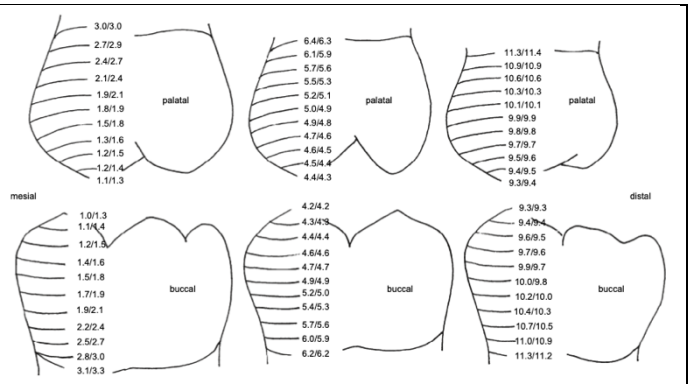

Figure 227 Template for ageing linear enamel defects on molars (taken from (Reid & Dean 2006)*)*

Linear Enamel Hypoplasia (LEH)

Figure 228 Pitted enamel defect on right mandibular M1 of 2008-78/731

Figure 229 Two strong bands of linear enamel hypoplasia across several teeth (2008-78/1342)

6.7.1.3 Results

6.7.1.3.1 Adults

A total of 2756 teeth belonging to 165 individuals were analysed for true, respectively crude prevalence of enamel defects.

6.7.1.3.1.1 True frequency

Of 2756 teeth, 631 (22.90%) had one or more enamel defects. The distribution of enamel hypoplasia by tooth was very balanced between males (23.08%) and females (23.13%). However, when comparing burial locations, significantly more teeth presented with animal defects in the cemetery burials (25.85%) than in the cloister burials (16.38). The exact same

trend could be observed in men and women, but the trend was only significant in males. The same trend can be observed in distance to cloister with those buried in the cloister (16.38%) and close (21.91%) to it showing less affected teeth than those buried in the middle (29.19%) of the cemetery. People buried far away (23.35%) did not differ much from those buried close. Finally, a significant difference could also be detected between the two burial layers, with those buried in the upper layer (25.04%) presenting with significantly more affected teeth than those from the lower layer (21.03%). However, when separating by sexes, although the trend remains the same among both sexes, it becomes statistically insignificant in females. When analysing the distribution of teeth affected by enamel hypoplasia between the burial locations within only Layer 1, no significant difference is initially apparent, unless a further division into males and females is undertaken. Here it becomes apparent that males show significantly more affected teeth among the cemetery burials and females show significantly more affected teeth among the cloister burials. Within Layer 2, differences by location are overall statistically significant with people from the cemetery presenting more affected teeth than those from the cloister. The same trend is also apparent and statistically significant among men and women.

Age also played a significant role in the distribution of enamel defects, with seniles (12.53%) and matures II (18.73%) presenting with significantly less affected teeth than adults (26.91%) or matures I (30.70%). young adults (23.20%) were the second least affected group but the difference to seniles is still statistically relevant. Trends were similar among men and women. This might indicate that people who experiences less stress during childhood also survived longer into old age. It might however also reflect higher rates of caries and ante mortem tooth loss found in this age group. (Table 81)

6.7.1.3.1.2 Crude frequency

The overall crude prevalence of enamel hypoplasia was 49.09%.

Males (56.36%) present with significantly more enamel defects than females (34.62%). There was no statistically significant difference between burial locations (Cemetery: 50.44%; Cloister: 46.15%) nor between distance to church. However, slightly less people buried in the cloister had enamel defects than those from the cemetery. The exact same trend could be observed among males, but in females, enamel defects were more common in the cloister burials than in the cemetery burials. But both within males and within females, differences between burial locations were not statistically significant. There was no significant difference between Layer 1 (52.78%) and Layer 2 (46.24%), but people with enamel defects were more common in Layer 1 than in Layer 2. Within males, the difference between Layer 1 and Layer

2 is negligible but females show clearly more cases of enamel hypoplasia in layer 1 than in layer 2 although the differences remain statistically nonsignificant. No significant correlation with age could be detected, with adults (54.00%) and mature I (60.71%) individuals being most affected and young adults (50.00%), matures II (46.15%) and seniles (34.38%) to a lesser extent. The lower values among seniles might be related to higher caries rates and higher antemortem tooth loss, which might lead to an underscoring of enamel defects in the dentation. It could however also indicate that individuals who experienced no or only light episodes of stress during childhood survived longer into adult hood than those who experienced regular and important episodes of stress as a child. The exact same trend was also found in women and in men, with the exception that in men, young adults had the highest rates of enamel defects, followed by adults and matures. In both cases however, seniles were the least affected by enamel hypoplasia. Within Layer 1 and within Layer 2, no significant differences were detected between burial locations, with differences in Layer 2 being negligible and those in Layer 1 showing that cloister burials were slightly less affected by dental enamel hypoplasia then cemetery burials. (Table 81) Overall, only in 5 individuals, enamel defects, could not be paired across 2 or more teeth. This suggests, that for the majority of cases present here, a systemic origin for the formation of at least some of the hypoplasia lines on the teeth can be assumed.

Table 81 Summary and test result for adult enamel hypoplasia true and crude frequency

Adults	**Enamel hypoplasia**							
Factor		**variable**	**True frequency**			**Crude frequency**		
			n	**presence**	**p-value**	**n**	**presence**	**p-value**
Total			2756	631 (22.90%)		165	81 (49.09%)	
Sex		F	804	186 (23.13%)	0.9741	52	18 (34.62%)	**0.0097**
		M	1924	444 (23.08%)		110	62 (56.36%)	
Age	All	Young Adult	487	113 (23.20%)	**<0.0001**	24	12 (50.00%)	0.2904
		Adult	810	218 (26.91%)		42	23 (54.00%)	
		Mature I	430	132 (30.70%)		28	17 (60.71%)	
		Mature II	630	118 (18.73%)		39	18 (46.15%)	
		Senile	399	50 (12.53%)		32	11 (34.38%)	
	F	Young Adult	216	57 (26.39%)	**0.0206**	13	4 (30.77%)	0.7699
		Adult	213	53 (24.88%)		11	4 (36.36%)	
		Mature I	113	33 (29.20%)		7	4 (57.14%)	
		Mature II	136	19 (13.97%)		11	3 (27.27%)	
		Senile	126	24 (19.05%)		10	3 (30.00%)	
	M	Young Adult	271	56 (20.66%)	**<0.0001**	11	8 (72.73%)	0.2556
		Adult	597	165 (27.64%)		31	19 (61.29%)	
		Mature I	317	99 (31.23%)		21	13 (61.90%)	
		Mature II	481	99 (20.58%)		27	15 (55.56%)	
		Senile	258	25 (9.69%)		20	7 (35.00%)	
Location	All	Cemetery	1853	479 (25.85%)	**<0.0001**	113	57 (50.44%)	0.6087
		Cloister	903	152 (16.83%)		52	24 (46.15%)	

Adults	Enamel hypoplasia							
Factor		variable	True frequency			Crude frequency		
			n	presence	p-value	n	presence	p-value
	F	Cemetery	584	143 (24.40%)	0.1386	41	13 (31.71%)	0.4812
		Cloister	220	43 (19.55%)		11	5 (45.45%)	
	M	Cemetery	1263	335 (26.52%)	**<0.0001**	71	43 (60.56%)	0.2308
		Cloister	661	104 (16.49%)		39	19 (48.72%)	
Distance to Church	All	Cloister	903	152 (16.83%)	**<0.0001**	52	24 (46.15%)	0.9523
		Close	461	101 (21.91%)		29	15 (51.72%)	
		Mid	908	265 (29.19%)		55	27 (49.09%)	
		Far	484	113 (23.35%)		29	15 (51.72%)	
	F	Cloister	220	43 (19.55%)	0.0532	11	5 (45.45%)	0.7130
		Close	119	34 (28.57%)		9	2 (22.22%)	
		Mid	304	80 (26.32%)		22	7 (31.82%)	
		Far	161	29 (18.01%)		10	4 (40.00%)	
	M	Cloister	661	109 (16.49%)	**<0.0001**	39	19 (48.72%)	0.6723
		Close	336	66 (19.64%)		19	12 (63.16%)	
		Mid	604	185 (30.63%)		33	20 (60.61%)	
		Far	323	84 (26.01%)		19	11 (57.89%)	
Layer	All	1	1282	321 (25.04%)	**0.0141**	72	38 (52.78%)	0.4045
		2	1474	310 (21.03%)		93	43 (46.24%)	
	F	1	322	87 (27.02%)	**0.0404**	18	8 (44.44%)	0.2784
		2	482	99 (20.54%)		34	10 (29.41%)	
	M	1	938	234 (24.95%)	0.0584	52	30 (57.69%)	0.7902
		2	986	210 (21.30%)		58	32 (55.17%)	
Layer 1	All	Cemetery	1002	219 (21.86%)	0.2574	46	26 (56.52%)	0.3973
		Cloister	472	91 (19.28%)		26	12 (46.15%)	
	F	Cemetery	378	66 (17.46%)	**0.0014**	12	6 (50.00%)	0.6380
		Cloister	104	33 (31.73%)		6	2 (33.33%)	
	M	Cemetery	618	152 (24.60%)	**0.0010**	34	20 (58.82%)	0.8205
		Cloister	368	58 (15.76%)		18	10 (55.56%)	
Layer 2	All	Cemetery	851	260 (30.55%)	**<0.0001**	67	31 (46.27%)	0.9920
		Cloister	431	61 (14.15%)		26	12 (46.15%)	
	F	Cemetery	206	77 (37.38%)	**<0.0001**	29	7 (24.14%)	0.1380
		Cloister	116	10 (8.62%)		5	3 (60.00%)	
	M	Cemetery	645	183 (28.37%)	**0.0003**	37	23 (62.16%)	0.1554
		Cloister	293	51 (17.41%)		21	9 (42.88%)	

6.7.1.3.2 Subadults

A total of 661 subadult teeth belonging to 42 individuals were eligible for assessment of dental enamel hypoplasia in subadults. The results include hypoplasia lines on permanent and deciduous teeth.

6.7.1.3.2.1 True frequency

About 196 teeth (29.65%) showed one or more enamel defects. Children buried in the cloister (33.82%) had slightly more affected teeth than those buried in the cemetery (27.79%), but the difference was statistically not relevant. Within Layer 1, subadults from the cloister exhibited much more affected teeth than those from the cemetery and within Layer 2 the opposite trend was observed. The distribution of affected teeth between the two burial layers was very

balanced. Age seemed to play an important role in the occurrence of enamel defects. Infans I (2.53%) had the least of teeth affected, whereas the number of teeth affected increased with age, with infans II having 36.13% and juveniles 51.93% of teeth affected. The low number of teeth with enamel defects in the infans I category is likely owed to the fact that the majority only had deciduous teeth, which are generally not affected as much. Deciduous teeth with enamel defects would reflect stresses that occurred already in the mother's womb since that is when most of the deciduous teeth start forming, or shortly after birth, depending on the defect's position on the tooth. They would therefore signal stresses that the mother experienced during pregnancy. All 6 hypoplastic defects detected among infans I, occurred on permanent teeth. 3 were located on freshly erupted first molars, 2 on unerupted incisors and 1 on an unerupted premolar cusp. Among infans II, only 2 deciduous teeth showed a defect. Both deciduous lower canines of individual 2013-015/179, a 7–8-year-old child buried in the cloister, showed a pit defect on the center of the tooth, which might be related to an episode of stress shortly after birth. At 51.93% juveniles showed the highest amount of hypoplastic defects and as such, the number is even higher than that observed among adults, adding weight to the theory that individuals with multiple stress episodes in childhood, died earlier. The differences observed between cemetery and cloister burials are largely due to the distribution of the different age groups between the two burial locations. (Table 82)

6.7.1.3.2.2 Crude frequency

20 (47.62%) subadults presented with one or more enamel defects on their teeth. None of the group comparisons except for age showed any statistically significant differences. However, it can be noted that more subadults from the cloister (53.85%) than from the cemetery (44.83%) had defects. Within Layer 1 and Layer 2 the same trend was observed to different degrees. This differences between burial locations, as previously mentioned, is likely due to the distribution of subadults on the site and within the burial layers. The only significant difference could be detected between the age groups. As already reflected in the true frequencies, the occurrence of enamel defects increased with age. Only 15.79% of infans I had one or more hypoplastic defects, but 81.82% of infans II and 66.67% of juveniles presented defects on their teeth. Both juveniles and infans I have therefore a higher crude frequency of enamel hypoplasia than Adults. While the smaller sample sizes in subadults might contribute to this result, it might also suggest, as already mentioned before, that individuals with enamel hypoplasia, meaning individuals who experienced significant episodes of stress during childhood, did often not survive into adulthood. This would also explain the higher occurrence of individuals with

enamel hypoplasia among the infans II age group. Infans I was expected to show less enamel hypoplasia since deciduous teeth did already form shortly before or shortly after birth, where a child's immune system is still boosted by the antibodies transferred from mother to child through the placenta and through the intake of breastmilk (Hanson *et al.* 2003). (Table 82)

Table 82 Summary and test results for subadult enamel hypoplasia true and crude frequency

Subadults		**Enamel hypoplasia**					
Factor	**variable**	**True frequency**			**Crude frequency**		
		n	**presence**	**p-value**	**n**	**presence**	**p-value**
Total		661	196 (29.65%)		42	20 (47.62%)	
Age	Infans_I	237	6 (2.53%)	**<0.0001**	19	3 (15.79%)	**0.0007**
	Infans_II	191	69 (36.13%)		11	9 (81.82%)	
	Juvenile	233	121 (51.93%)		12	8 (66.67%)	
Location	Cemetery	457	127 (27.79%)	0.1167	29	13 (44.83%)	0.5885
	Cloister	204	69 (33.82%)		13	7 (53.85%)	
Layer	1	241	72 (29.88%)	0.9241	15	9 (60.00%)	0.2311
	2	420	124 (29.52%)		27	11 (40.74%)	
Layer 1	Cemetery	150	33 (22.00%)	**0.0006**	9	6 (60.00%)	1.0000
	Cloister	91	39 (42.86%)		6	4 (66.67%)	
Layer 2	Cemetery	307	94 (30.62%)	0.4174	20	8 (40.00%)	1.0000
	Cloister	113	30 (26.55%)		7	3 (42.86%)	

6.7.1.3.3 Peak age of Enamel hypoplasia

Peak ages of enamel hypoplasia were determined for the complete permanent dentition including that available from subadults.

When considering linear enamel hypoplasia (LEH) on all teeth (Figure 230), it becomes apparent that defects start increasing in frequency rather abruptly in the 2-2.4-year range. From there, the absolute number of lines starts decreasing slightly in the 2.5-2.9-year range and then again over the 3-3.9-year age ranges until they drop more abruptly at around 4 years. The same overall pattern can be observed among the sexes (Figure 231). However, in females the number of lines increases abruptly in the 2-2.4-year age range and then decreases a bit more noticeably in the 2.5-2.9 range and from there, a gradual decrease until the 3.5-3.9 age range can be observed. In the end, a slight increase in LEH can be observed again in the >5 group. In males, lines increase abruptly at 2-2.4 years and peak at 2.5-2.9 years. Then the number of lines drops slightly during the 3-3.4-year range and drops then abruptly during the 3.5-3.9-year range. This difference in pattern between men and women might suggest that they were exposed to stresses at different times during childhood. Differences in weaning age might be one reason for the different patterns observed. The pattern of LEH distribution by age between cloister and cemetery is quite similar. The peak between 2-3 years among cloister burials is not as dramatic

as in the cemetery but both roughly have a peak in LEH around 2-3 years which decreases gradually after that. However, in cemetery burials, a slight increase in lines can be observed after >5 years of age (Figure 232). A comparison between Layer 1 and Layer 2 revealed that the peak in LEH was reached around 2-3 years in both layers, but while it started decreasing slightly but gradually after that until the 3.5-3.9 years age range in Layer 2 before dropping more abruptly, in Layer 1 the peak extended to the age range between 2.5-2.9 years before dropping gradually but more intensely after that. In both Layers, a slight increase in LEH was noted for the group >5 years.

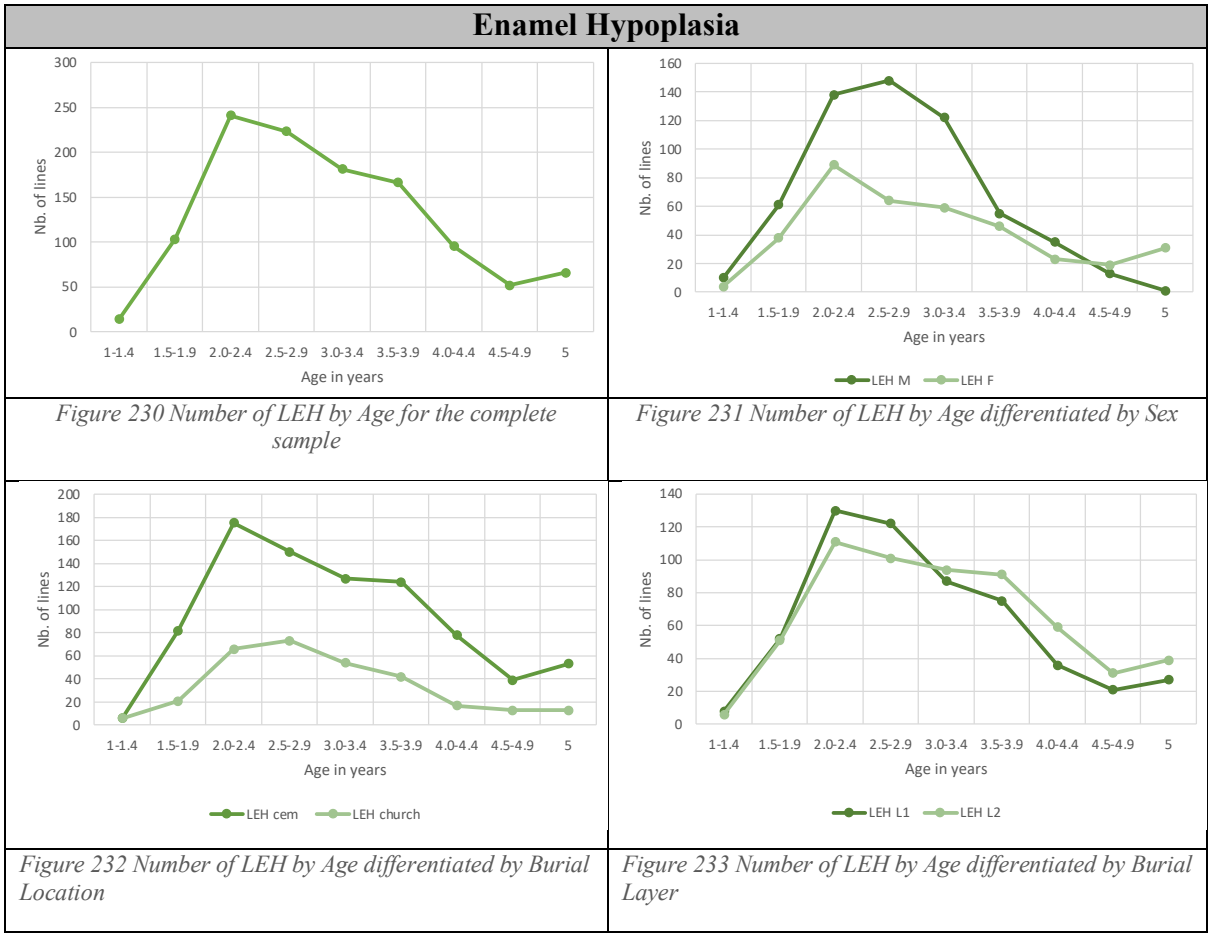

Figure 230 Number of LEH by Age for the complete sample

Figure 231 Number of LEH by Age differentiated by Sex

Figure 232 Number of LEH by Age differentiated by Burial Location

Figure 233 Number of LEH by Age differentiated by Burial Layer

6.7.1.4 Discussion and Conclusion

Enamel hypoplasia are defects expressed most commonly as grooves on teeth, caused by a disruption of ameloblast activity (El-Najjar *et al.* 1978; Goodman & Armelagos 1985; Hillson & Bond 1997; King *et al.* 2002, 2005). This disruption has been linked by various studies to malnutrition, infections, weaning etc. and can thus be generally considered as non-specific indicator of childhood stress (Corruccini *et al.* 1985; Goodman & Rose 1990; Lanphear 1990; Moggi-Cecchi *et al.* 1994; Hillson 1996; Wood 1996; Schultz *et al.* 1998).

When considering the sample from Luxembourg in light of other roughly contemporaneous sites, it becomes apparent that the frequency of individuals with enamel hypoplasia (49.09%) lies in the middle of the possible spectrum of occurrence (Table 81, Table 83). Similar frequencies have been found at sites in Belgium where people from Slijpe, Zottegem and Oosterweel showed very similar frequencies in enamel hypoplasia (Van Cant 2019). Compared to late medieval and early postmedieval Ellwangen in Germany (Kairies 2021), the Knuedler sample exhibited slightly more enamel hypoplasia. However, a similar development over time was noted for both sites, with frequencies increasing, albeit for the Knuedler sample statistically insignificantly so, from the late medieval to the postmedieval period. A similar trend, even if insignificant (Roßbach 2015), was also discovered between medieval and postmedieval burials from Hettstedt in Germany. But many more people from these sites displayed enamel hypoplasia than those from the Knuedler cemetery. For all sites examined, the frequency of enamel hypoplasia is higher than 10%, which Goodman and Rose (1991) considered as representative of recently developed populations with good living conditions (Goodman & Rose 1991). An increase of hypoplasia frequency over time might be related to a development of urbanization as living conditions in urban areas were often associated with a higher prevalence of infectious diseases and higher risk of malnutrition (Garcin *et al.* 2010). Compared to Luxembourgish sites, enamel hypoplasia frequency from the Knuedler cemetery is very similar to that found in burials from Givenich and St. Esprit. Givenich dates from the 12th to 15th century and represents an upper-class population. Especially the older layer from Luxembourg city shows very similar frequencies to those from Givenich. With 69.8% of people affected by enamel hypoplasia, the frequency from St. Esprit cemetery is slightly higher than that from either Layer from the Knuedler. What is striking however, is the stark difference in enamel hypoplasia occurrence between rural Grevenmacher (14%) and all other sites from Luxembourg City (40.09%/69.8%). (Table 83) One explanation might be that the differences observed are due to differences in living conditions between rural and urban sites. In fact, an urban population would be much more at risk of infectious diseases for example as the environment promotes a faster spread (Garcin *et al.* 2010). Garcin et al. (2010) examined 4 early medieval Frankish and Moravian subadult samples representing urban and rural but also coastal and inland populations. They discovered a higher prevalence in the two urban Frankish sites and attributed the results to a heightened exposure to disease and malnutrition in an urban environment (Garcin *et al.* 2010). Primeau et al. 2018 examined linear enamel hypoplasia, middle ear infections and Harris lines between a rural and urban sample and found out that all three lesions, albeit not statistically significant, occurred more often in the urban sample. They

explained this with the "osteological paradox": The higher-class urban citizens must have had better health than the rural population because they survived all the childhood diseases into adult hood. A majority of individuals with no lesions would indicate that those who got them, died before reaching adulthood (Wood *et al.* 1992; Primeau *et al.* 2018) However, also compared to Givenich, a rural site from Luxembourg, the frequency in Grevenmacher remains very low. This difference might be explained by a potential difference in social status of both groups, with Givenich representing upper-class individuals and Grevenmacher reflecting an average rural population. But in this case, values from Grevenmacher should have been higher than those from Givenich. Enamel frequency of Grevenmacher is also really low compared to other European contemporaneous sites with Emden at 24.6% showing the closest values. These differences between sites, that do not seem to be explained easily by differences in social status or living environment, seem to hint at a more complex system guiding enamel hypoplasia formation. (Table 83) Regional and probably also genetic factors might well play a role in the formation of enamel defects (Hillson 1996; Garcin *et al.* 2010). Different geographical areas might pose different problems that people had to cope with, such as different dietary resources, and therefore, differences between social groups etc. might be only observable between regionally close populations (Méndez Collí *et al.* 2009; Garcin *et al.* 2010). In fact, Garcin et al. (2010) found that enamel hypoplasia occurrence in subadults was much more influenced by geographical origin than by social status. Another factor might be differences in scoring enamel hypoplasia in general, with many studies following different recommendations for scoring and evaluating the defects.

Furthermore, as previously mentioned, social status might also influence the formation of enamel hypoplasia. This is based on the fact that children from lower social classes are exposed to more health risks such as malnutrition or disease during childhood (Cucina & Işcan 1997; Palubeckaitė *et al.* 2002; Miszkiewicz 2015; Nakayama 2016). For example, Palubeckaitė et al. (2002) analysed working-class burials from 18th century Spitalfields and upper-class burials from 19th century St. Brides' church crypt and concluded that, although both groups showed equally high crude enamel hypoplasia frequency, the number of lines was much higher among the working-class people, suggesting that they lived through more episodes of childhood stress than their upper-class counterparts. A study by Miszkiewicz (2015) compared linear enamel hypoplasia frequency between priory and cemetery burials from 11th – 16th century Canterbury, UK and found that crude linear enamel hypoplasia was more frequent in cemetery (93.3%) than in priory (78.9%) burials. This study on the Knuedler population also looked at differences between church/cloister and cemetery burials and found that linear enamel

hypoplasia was slightly more frequent among cemetery (50.44%) than among cloister (46.15%) burials, but that difference was not statistically significant. However, cemetery burials (25.85%) had significantly more teeth affected than cloister burials (16.83%). This would suggest that people buried in the cloister complex generally experienced less stress in childhood then those from the cemetery, hinting at differences in social status between people buried in the two burial locations. (Table 83)

Additionally, a significant difference was detected in enamel hypoplasia frequency between the sexes, with males (56.36%) experiencing the defects more often than females (34.62%). (Table 81) This finding does not reflect most trends where females show more enamel hypoplastic defects than men. (Table 83) These studies usually argue that this is due to females being neglected in favour of boys during childhood or that boys' immune system was more frail than that of females and they died earlier than females when subjected to the same stresses (King *et al.* 2005). However, some studies have also found the opposite trend. Here the main reason for men being more affected than women is listed as men being less biologically buffered than females, as female sex hormones cause them to live longer on average and generally females are better protected against infectious diseases (O'Donnell & Moes 2021).

Furthermore, several studies also investigated the link between mortality and occurrence of linear enamel hypoplasia and came to the conclusion that generally groups with more enamel hypoplasia tended to die at a younger age (O'Donnell & Moes 2021). A similar conclusion could potentially be reached for the Knuedler cemetery. Here, infans II showed the highest number of individuals with enamel defects (81.82%), followed by juveniles at 66.67%. Adults on the other hand only showed an overall of 49.09% with young adults at 50.00%, adults at 54.00%, matures I at 60.71%, matures II at 46.15% and seniles at 34.38%. Therefore, individuals who died in childhood had overall more defects than those who survived into adulthood. But once adulthood was reached, enamel hypoplasia did not seem to have an effect on mortality anymore. Maybe the low number of enamel hypoplasia in seniles suggests that mainly people without enamel defects survived into old age, however the difference is more likely caused by the higher degree of caries and antemortem tooth loss, as well as more severe attrition, preventing adequate scoring of defects for this age group. Linear enamel hypoplasia is often associated to higher mortality rates because it is assumed that people who experienced a lot of stress in childhood, have a weakened immune system and were therefore susceptible to die earlier than those without defects (Cook & Buikstra 1979; Duray 1996; Palubeckaitė *et al.* 2002; Boldsen 2007; Armelagos *et al.* 2009).

Lastly, the peak age at formation for linear enamel hypoplastic defects on the Knuedler cemetery lies between 2-3 years and then starts gradually decreasing over the 3–4-year age span until it suddenly drops in the 4–5-year age span (Figure 230). This lies within the normal peak range for most populations studied (Palubeckaitė *et al.* 2002; King *et al.* 2005; Stech 2009; Timmermann 2009; Miszkiewicz 2015). Whilst stresses such as infectious disease or malnutrition cannot be entirely excluded as causes for all or most enamel defects, this peak range falls within the age range during which weaning usually takes place. In fact, several studies on medieval and postmedieval remains suggest a weaning age at around 2-3 years (Nitsch *et al.* 2011; Burt 2013; Haydock *et al.* 2013; Britton *et al.* 2018). Furthermore, breastmilk contains many nutrients and antibodies that boost a child's immune system. Exposure to foreign food items and the possible ways in which they might have been contaminated, and especially the cessation of lactation, which puts a sudden end at the protection afforded by breastmilk, might put a lot of stress on a child's immune system and cause the formation of enamel defects (Dittmann & Grupe 2000). For the peak age at formation, this explanation was adopted as well, and it was assumed that this represented possibly the age at cessation of lactation. However, further discussions on weaning age estimation will be mentioned in the relevant chapter on weaning age reconstruction using a combination of anthropological and biogeochemical methods. It has to be noted here though that differences in the distribution of linear enamel hypoplasia over the different age ranges were observed between the different groups tested. As such, linear enamel hypoplasia peaked clearly at 2-2.4 years in females and dropped more considerably right afterwards and from there decreased gradually until the lowest point at 4.5-4.9 years, while the absolute peak in males was at 2.5-2.9 years but values remained quite high between 2-3.5 years, after which they dropped considerably (Figure 231). This might indicate differential treatment between men and women in childhood or higher susceptibility of males to environmental factors. If peak enamel hypoplasia age is considered representative of weaning age, this might indicate that women were weaned earlier and faster than men, while weaning age ranges in men were longer. However, since the sample size of females was much smaller than that of men, it is also possible that the differences observed were due to smaller sample size. The pattern of linear enamel hypoplasia distribution by age was similar between cloister and cemetery burials. But peak age of formation was clearly 2-2.4 years in the cemetery and was less pronounced between 2-2.9 years in the cloister (Figure 232). In Layer 2 peak age of formation was 2-2.4 years but the number of lines remained quite high until 4 years after which they started dropping clearly. In Layer 1, peak age of formation was at 2-2.4 but remained also high at 2.5-2.9 years after which

the number of lines started decreasing noticeably (Figure 233). What is common to all group comparisons and the overall curve is that linear enamel hypoplasia numbers increase strongly and abruptly between 1-1.9 years and reach their lowest number at around 4.5-4.9 years. This might either suggest that peak age formation is truly related to cessation of lactation and that before that, children were mostly protected from stressors by the immune boost that breast milk offers. This strong increase might however also be caused by the fact that due to abrasion, the lines forming around 1-1.9 years are not scoreable anymore on many teeth as they would be located at the very top of the crown. The only tooth where such early lines could be recorded without major influence of dental attrition was the first molar. However, there are much more front teeth in the dental arcade than first molars, which might then generally lead to an underscoring of defects in that age range.

Table 83 Overview of Enamel Hypoplasia prevalence in medieval-postmedieval European sites

Enamel hypoplasia frequency in Europe						
Time period	**Site**	**Country**	**Type of settlement**	**Socio-economic status**	**EH frequency %**	**Publication**
11th-16th C	Canterbury	England	urban	cementery	93.30*	Miszkiewicz (2015)
15th C	Hettstedt Kirche	Germany	urban		92.10	Rossbach (2015)
Early post-medieval	Völklingen	Germany			92.10	Rossbach (2015)
15th-17th C	Holy Trinity church	Latvia	urban	upper class	84.85*	Pētersone-Gordina et al. (2012)
11th-16th C	Canterbury	England	urban	Priory	78.90*	Miszkiewicz (2015)
1812 AD	Napoleonic mass grave	Lithuania	urban	soldiers	78.50	Palubeckaitė (2006)
12th-17th C	St. Esprit	Luxembourg	urban	mixed	72.20	Rehbach u. Bis-Worch (2006), Nothwang et al. (2006) Rehbach et al. (2007) Rehbach u. Nothwang (2007) Rehbach (2008) Rehbach u. Notwang (2009)
12th-18th C	Slijpe	Belgium	rural coastel		60.80	Van Cant (2019)
12th-17th C	Ihlow	Germany	urban		60.00	Timmermann (2009)
15th-19th C	Oosterweel	Belgium	rural polder	upper class	58.30	Van Cant (2019)
18th C	Hettstedt Gym.	Germany			54.00	Rossbach (2015)
mid-17th-18th C	Knuedler	Luxembourg	urban		52.78	Kremmer (hic)
14th-mid-17th C	Knuedler	Luxembourg	urban		46.24	Kremmer (hic)
14th-19th C	Zottegem	Belgium	rural		42.10	Van Cant (2019)
11th-15th C	Givenich	Luxembourg	rural	upper class	40.70	Rehbach et al. (2009) Weidig et al. (2009)
12th-15th C	Deinze	Belgium	urban		38.30	Van Cant (2019)
12th-16th C	Minoritenweg Regensburg	Germany	urban	Hospital/lower class	36.90	Heyking (2012)
19th C	Viichte	Belgium	rural		36.40	Van Cant (2019)

Enamel hypoplasia frequency in Europe						
Time period	**Site**	**Country**	**Type of settlement**	**Socio-economic status**	**EH frequency %**	**Publication**
Early postmedieval	Ellwangen-Jagst	Germany			35.14	Kairies (2021)
Late medieval	Ellwangen-Jagst	Germany			30.10	Kairies (2021)
10th-18th C	Emden	Germany	urban	upper/middle Class	24.60	Stech (2009)
12th-14th C	Grevenmacher	Luxembourg	rural		14.00	Trautmann (2017)

* = average

6.7.2 Cribra orbitalia and cribra cranii

6.7.2.1 Introduction

Cribra orbitalia describes porous, sometimes even sieve-like lesions on the orbital roof (Wapler *et al.* 2004; Lewis 2009). Cribra cranii, also often referred to as porotic hyperostosis, are porous lesions that occur on the ectocranial surface of the cranial vault bones, most commonly the parietal bone (Brickley 2018). Together with linear enamel hypoplasia, they are one of the most recorded indicators for stress in archaeological populations (Grupe *et al.* 2015). However, the aetiology of the lesion is still debated in literature (Stuart-Macadam 1985, 1992; Wapler *et al.* 2004; Walker *et al.* 2009; Oxenham & Cavill 2011; Rivera & Mirazón Lahr 2017; Brickley 2018; Cole & Waldron 2019; Rothschild *et al.* 2021). Generally, the lesions are considered to be caused by an expansion of the diploë and a thinning of the outer table, resulting eventually in an "hair on end" appearance on radiographs (Lewis 2009; Brickley 2018). Since the diploic bone contains haematopoietic bone marrow, the expansion of the diploë is caused by an increased production of red blood cells, which leads to bone marrow hypertrophy. Increased production of red blood cells is mostly related to anaemia (Brickley 2018). In past research (Stuart-Macadam 1985, 1992; Oxenham & Cavill 2011), cribra orbitalia has most often been linked to iron deficiency anaemia, which makes up the majority of anaemia cases today. Children, neonates and young women are particularly susceptible to iron deficiency anaemia. Next to an iron deficient diet, internal haemorrhages and infestation of intestinal parasites have also been listed often as causes for iron deficiency anaemia, and therefore, the lesions might also be indirectly an indicator for pathogen load from the environment. (Stuart-Macadam 1992; Hesham *et al.* 2004; Grupe *et al.* 2015)

More recently, megaloblastic anaemias, that are most often the result of folic acid- , thiamine- and especially B12 deficiency have been put forward as possible cause for cribra orbitalia and porotic hyperostosis in general (Walker *et al.* 2009). B12 deficiency can be caused by many

factors, for example chronic gastritis and diarrhoea (Long *et al.* 2007), a lack of or insufficient meat consumption (Walker *et al.* 2009) and long-term parasitic infestations (Corcino *et al.* 1970; Olivares *et al.* 2002) can eventually lead to B12 deficiency. However, a study by Wapler et al. (2004) has found that in more than half of the cases, at least cribra orbitalia did not show any histological features related to changes caused by anaemia.

Rivera and Mirazón Lahr (2017) have studied the thickness of the compact and diploic bone in individuals with cribra orbitalia and suggest a different origin for both these conditions. Their study showed that especially individuals with cribra orbitalia presented with thickened compact bone and thinner diploic bone. Therefore, they suggest that cribra orbitalia would be rather associated to anaemias that cause bone hypocellularity and hypoplasia, for example anaemias caused by chronic disease, anaemia of renal failure, aplastic anaemia, anaemia related to endocrine disorders or protein deficiency, whereas porotic hyperostosis would be rather related to anaemias causing expansion of the diploë, such as iron deficiency anaemia.

Rothschild et al. 2021 determined that cribra orbitalia is vascular in nature and the study could not determine any link of the lesion to anaemia or porotic hyperostosis.

Furthermore, Vitamin C deficiency has also been related to the formation of cribra orbitalia as this can cause subperiosteal haemorrhaging, leading to subperiosteal inflammation. The healing of these orbital haemorrhages can cause porotic new bone deposits on the orbital roof which mimic the lesions caused by diploic expansion. Such lesions would be found for example in metabolic conditions such as rickets or scurvy, but could also be caused by traumatic injuries to the eye and in particular the orbit or even by tumours (Lewis 2009; Grupe *et al.* 2015).

Lately, infectious respiratory diseases have also been brought forward as possible causes for cribra orbitalia and cribra cranii (O'Donnell *et al.* 2020).

In short, cribra orbitalia and cribra cranii should be rather considered as an indicator of unspecified stress and can be caused by a variety of conditions such as anaemias, vitamin deficiencies or infestation of intestinal parasites which might be related to nutritional deficiencies, but other causes such as infectious diseases cannot be excluded either. An interaction of several of the afore mentioned factors must also always be considered.

6.7.2.2 Cribra orbitalia

6.7.2.2.1 Methods

Cribra orbitalia or was recorded after the system presented by Steckel et al. (2006) (Table 84; Figure 234). If there was no orbit to score, the entry was left blank in order to facilitate statistical analysis. Lesions were only scored if at least one orbit was present. Therefore, 0 represents an individual with no porotic lesions in at least one orbit, 1 describes restricted light pitting and 2 extensive pitting. Crude frequencies for the lesions were calculated for the sample overall, by burial location, burial layer, age groups and by sex.

Table 84 Scoring system for cribra orbitalia (adapted from (Steckel *et al.* 2006)*)*

Score	Description
0	No cribra orbitalia
1	Cluster of fine foramina covering ≤ 1cm^2
2	>1cm^2 covered in small and/or large foramina with a tendency to cluster together

Figure 234 Illustration of the scoring system for cribra orbitalia after (Steckel *et al.* 2006)

6.7.2.2.2 Results

A total of 173 individuals presented with at least one scoreable orbit and of those, 21 (12.14%) presented with a porotic lesion inside one or both orbits. Slightly more individuals from the cemetery (14.04%) experienced cribra orbitalia than those from the cloister (8.47%) but the difference was statistically non-significant. Cribra orbitalia also occurred slightly more often in Layer 2 (12.75%) than in Layer 1 (11.27%) but this difference was also statistically irrelevant. A significant difference in the distribution of cribra orbitalia was detected among the age groups and concerned only infans I and seniles, infans II and matures and seniles, and adults and seniles. The significant differences detected might be highly influenced however by the small sample sizes in the subadult groups. Among adults and juveniles that could be sexed, females (8.33%) showed slightly less cases than men (9.78%) but the difference was not statistically significant. (Table 86)

Regarding the distribution of severity of the lesions, overall, slightly more individuals experienced a light lesion (52.38%, n=11) than a light one (47.62%, n=10). Adults (young adult-seniles) had 6 (46.15%) light lesions and 7 (53.85%) severe lesions, subadults including juveniles had 5 (62.5%) light lesions and 3 (37.5%) severe lesions.

However, it has to be noted that several cases of cribra orbitalia listed here have been found in combination with other pathological lesions and not as single occurrences. In 3 subadults for instance, the lesion is associated with periosteal reactions and porosities on all or the majority of bones. These individuals express symptoms that are indicative of metabolic or infectious disease and will be discussed in more detail in the section on metabolic diseases. A male mature individual (2008_78/1310) also presents with several lesions that might suggest an underlying metabolic condition. Two more individuals show light periosteal new bone formation on one long bone. A male adult (2008_78/675) presents with signs suggesting an infection of the inner ear. And finally, individual (2016_082/418) presents lesions that are very much in accordance with those produced by metastatic carcinoma, which will be discussed further in the section on neoplastic diseases. Furthermore, in 5 individuals cribra orbitalia cooccurred with cribra cranii, and 2 of these cases could be attributed to the subadults suffering from metabolic or infectious disease. Of the 21 individuals with cribra orbitalia, teeth could only be scored for 20 individuals. Of those 20 individuals, only 12 (60%) also had enamel hypoplasia, 4 of them belonged to children with signs of an underlying metabolic condition. Most of the individuals with cribra orbitalia showed several light bands on the teeth, hinting at several episodes of stress during childhood. However, in the remaining 8 cases, no enamel defects could be detected.

6.7.2.3 Porotic hyperostosis

6.7.2.3.1 Methods

Cribra cranii or porotic hyperostosis was recorded after the system presented by Steckel et al. (2006) (Table 85; Figure 235). If there was no parietal to score, the entry was left blank in order to facilitate statistical analysis. Lesions were only scored if at least one parietal was present. Therefore, 0 represents an individual with no porotic lesions on the parietals, 1 describes light pitting or severe porosity and 2 a gross parietal lesion. Crude frequencies for the lesions were calculated for the sample overall, by burial location, burial layer, age groups and by sex.

Table 85 Scoring system for cribra cranii (adapted from (Steckel *et al.* 2006)*)*

Score	Description
0	No porotic hyperostosis
1	Light pitting or severe parietal porosity
2	Gross parietal lesion with excessive enlargement of bone

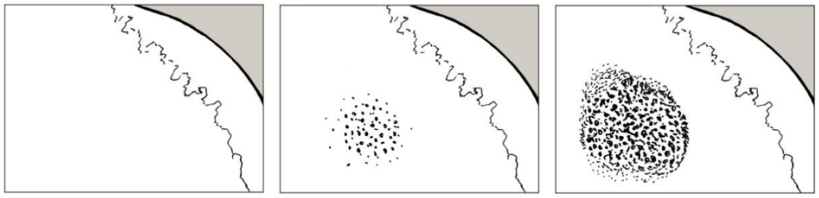

Figure 235 Illustration of the scoring system for cribra cranii after (Steckel *et al.* 2006)

6.7.2.3.2 Results

A total of 215 individuals presented with at least one scoreable parietal and of those, 21 (9.77%) presented with a porotic lesion on one or both parietals. Significantly more individuals from the cemetery (13.87%) experienced cribra orbitalia than those from the cloister (2.56%). Additionally, the lesion was also slightly more frequent in the upper Layer 1 (12.90%) than in the lower Layer 2 (7.38%). Among adults and juveniles, males (10.91%) were also slightly more often affected than females (6.78%). But none of these tendencies reached statistical significance. A significant difference in occurrence of cribra cranii was however detected among the age groups, but this only concerned differences between young adults and seniles. (Table 85) Fine pitting or very extensive pitting could be observed, which after Steckel et al. (2006) all classify under severity score 1. Gross lesions with large foramina and extensive thickening of the vault were not observed. However, within severity score 1, the intensity of the lesion varies from light localised porosity to extensive pitting all over the vault. Four individuals with underlying metabolic conditions displayed extensive porosity and the lesion covered all or a majority of the bone, but in two cases this concerned mainly the temporal bone. However, the foramina were not gross, and no thickening of the vault was observed.

As was the case for cribra orbitalia, many of the cribra cranii lesions were occurred in conjunction with other pathological lesions. As such, 6 individuals, with lesions indicative of metabolic stress or infectious disease presented with porosities all over the cranial vault. They make up most cases within the Neonate, infans I and II age categories. 14 out of 21 individuals with cribra cranii also exhibited enamel hypoplasia but of varying degrees and expression. Moderate to strong enamel hypoplasia was detected in a 6.5-8.5-year-old child (2008-78/728) presenting also with cribra cranii and orbitalia and other signs of metabolic disease. A female

young adult between 20-24 years (2008_78/1334) and 2008_78/1001, a 40–49-year-old male, also expressed strong enamel defects. For the remaining 11 individuals, enamel hypoplasia was either classified as light or moderate.

Table 86 Summary and test results for cribra cranii and cribra orbitalia

Cribra								
Factor		**variable**	**Cribra cranii**			**Cribra orbitalia**		
			n	**presence**	**p-value**	**n**	**presence**	**p-value**
Total			215	21 (9.77%)		173	21 (12.64%)	
Sex		F	59	4 (6.78%)	0.3821	48	4 (8.33)	1.0000
		M	110	12 (10.91%)		92	9 (9.78%)	
Age	All	Neonatus	2	2 (100%)	**0.0008**	-	-	**0.0402**
		Infans I	19	2 (10.53%)		14	3 (21.43%)	
		Infans II	10	1 (10.00%)		10	4 (40.00%)	
		Juvenile	11	0 (0%)		7	1 (14.29%)	
		Young Adult	25	5 (20.00%)		21	2 (9.52%)	
		Adult	39	4 (10.26%)		37	6 (16.22%)	
		Mature I	34	3 (8.82%)		24	2 (8.33%)	
		Mature II	39	4 (10.26%)		32	3 (9.38%)	
		Senile	36	0 (0.00%)		28	0 (0.00%)	
		Adultus	2	0 (0.00%)		-	-	
Location	All	Cemetery	137	19 (13.87%)	**0.0073**	114	16 (14.04%)	0.2884
		Cloister	78	2 (2.56%)		59	5 (8.47%)	
Layer	All	1	93	12 (12.90%)	0.1763	71	8 (11.27%)	0.7697
		2	122	9 (7.38%)		102	13 (12.75%)	

6.7.2.4 Discussion and Conclusion

Environmental stress can impact the body in such a way that lesions can manifest on the bones as a response. The most commonly assessed markers of unspecific stress are cribra orbitalia, porotic hyperostosis (cribra cranii) and linear enamel hypoplasia. The markers are defined as non-specific as generally no clear aetiology for these lesions could be established. Generally, however, they have most often been related to some sort of nutritional stress (Stuart-Macadam 1985, 1992; Wapler *et al.* 2004; Walker *et al.* 2009; Oxenham & Cavill 2011; Rivera & Mirazón Lahr 2017; Brickley 2018; Cole & Waldron 2019; Rothschild *et al.* 2021). As the results of the evaluation of linear enamel hypoplasia have already been discussed extensively in the chapter on dental pathologies, the focus of this section lies strongly on cribra orbitalia and porotic hyperostosis. In order to put the results obtained from the Knuedler cemetery into a wider perspective, they will be compared in the following section to some roughly contemporaneous sites across Europe. Unfortunately, a systematic comparison to other Luxembourgish sites besides Grevenmacher was not possible due to a lack of data. In the following, mainly results for cribra orbitalia will be discussed, as most studies did not record

porotic hyperostosis, however, comparison to four Dutch sites and Ellwangen-Jagst was possible for the latter condition.

Cribra Orbitalia	Porotic Hyperostosis
	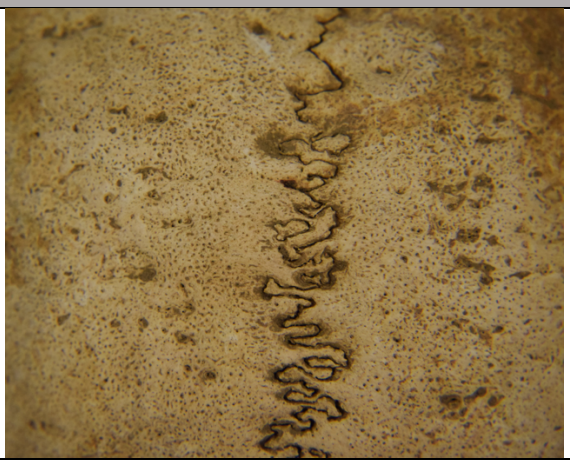
Figure 236 Close-up of cribra orbitalia in leftt orbit of 2008-78/818	*Figure 237 Close-up of porotic hyperostosis along sagittal suture of 2008-78/809*

Compared to other contemporaneous sites, the frequency of cribra orbitalia from the Knuedler cemetery (12.64%) is rather low. In 10th – 18th century Emden for example, the overall occurrence of cribra orbitalia was 26% (Stech 2009). In other towns from the north of Germany, even higher frequencies of cribra orbitalia were recorded, 69.2% for 12th to 16th century Brandenburg (Jungklaus 2009) and 87.8% for 12th to 13th century Schleswig (Hühne-Osterloh & Vogel 1997). Regarding the burials from Emden, which represent a middle-upper class population, frequency of cribra orbitalia was similar to that of linear enamel hypoplasia (Stech 2009). Similarly high frequency in cribra orbitalia (20%) was also detected among the burials from Minoritenweg in Regensburg, a hospice cemetery harbouring mostly burials from lower class individuals. But here, enamel hypoplasia frequency was slightly higher at 36.90% (Von Heyking 2012). Also compared to Ellwangen-Jagst (late medieval: 29.58%; postmedieval: 43.27%) the frequency of cribra orbitalia amongst the Knuedler burials is rather low. At Ellwangen, the frequency of linear enamel hypoplasia mirrors that of cribra orbitalia. Among the Knuedler burials however, the frequency of enamel hypoplasia was considerably higher (49.09%) than that of cribra orbitalia. This and the fact that the frequency of enamel hypoplasia among individuals with cribra orbitalia (52.38%) was very similar to that of the overall population, might suggest that they were of different aetiology. In fact, literature regarding association of cribra orbitalia and linear enamel hypoplasia yielded conflicting results, with some studies not finding a positive correlation between the two lesions (Kozak &

Krenz-Niedbała 2002; Novak *et al.* 2010; Liebe-Harkort 2012) and other demonstrating the opposite (see publications listed in Novak et al. 2010). Linear enamel hypoplasias reflect stress that occurred in childhood only, whilst cribra orbitalia reflects stress that occurred right before death. A similar, but more pronounced pattern was observed among the burials from Hettstedt Kirche (cribra orbitalia: 16.7%; LEH: 92.10%) and Völklingen (cribra orbitalia: 17.5%; LEH: 92.10%) (Roßbach 2015). Cribra orbitalia was exceptionally rare in Ihlow (5%), and it is argued that this might be a sign for better living conditions, meaning good nutrition, low risk of catching infectious disease etc. among the population (Timmermann 2009). For Grevenmacher, frequency of cribra orbitalia was calculated separately for children (17.5%) and adults (9.7%), but generally, the frequency was similarely low as in the Knuedler cemetery, which Trautmann (2012) also associates with an overall good nutritional status of the population.

On the Knuedler cemetery, more individuals from the churchyard experienced cribra orbitalia than those from the cloister complex, although the difference was not significant. The same pattern, also not significant was discovered for porotic hyperostosis and enamel defects This might suggest that those buried in the cloister did not experience as much stress as those from the cemetery. Lower prevalence rates of linear enamel hypoplasia and cribra orbitalia have also been noted as previously mentioned for the convent of Ihlow, where also mainly high-status individuals were buried. A correlation between socioeconomic status and cribra orbitalia was established in a study on 4 medieval/postmedieval Dutch sites. However, against the study author's expectations, the site where most individuals of higher social status were buried, showed the highest frequency of cribra orbitalia (33.3%). They explain these results through the lens of the osteological paradox, namely the higher social status individuals had the means and resources to survive hardship and therefore the chance to develop cribriotic lesions, whereas those of lower status died before the lesions could develop. However, their sample size was quite small, and this might have also skewed the results of their analyses. Overall, lower status individuals showed higher prevalence of stress markers than the middle-upper class individuals (Casna & Schrader 2022). Porotic hyperostosis prevalence can only be compared to Ellwangen-Jagst and the four Dutch sites of Arnhem, Zwolle, Eindhoven church and churchyard. In the four Dutch sites, the prevalence of porotic hyperostosis is overall higher than that observed in the Knuedler cemetery (9.77%). Only Eindhoven outside church, a mix of middle-low status burials, shows the lowest frequency (~15%). The highest frequencies (>25%) were observed in the low status burials of Arnhem and the high-status burials of Eindhoven, however the latter site had a very small sample size (Casna & Schrader 2022). At

8.16% for the late medieval and 6.67% for the postmedieval period, the Ellwangen-Jagst individuals showed very similar frequency of cribra cranii than those from the Knuedler. Ellwangen-Jast was at the height of its power in the 14th century where it could be considered a rather well-situated city. However later on, wars, famines and epidemics also plagued the city, which has been brought up as a possible explanation for the increase in cribra orbitalia frequency over time (Kairies 2021). In Luxembourg city, no significant differences could be detected in cribra orbitalia between the different burial periods. Overall, cribra cranii and orbitalia frequencies are quite low compared to other European sites and are most similar to sites associated with individuals of high social status. The higher prevalence of linear enamel hypoplasia might be explained by the fact that these stress markers are thought to be of different aetiology. On the Knuedler cemetery, considering the peak time of formation, most cases of linear enamel hypoplasia also seem to be associated with weaning stress, although it has to be pointed out that the majority of individuals displayed more than one band on a tooth, hinting at several stressful events in childhood. The fact that of all porous cranial lesions detected, the majority was found among the subadult group, would also suggest that most stressful episodes for the people buried in the Knuedler cemetery occurred during childhood rather than adulthood. However, as previously mentioned, children tend to be more susceptible anyway to developing lesions in response to external stress due to their still developing immune system and organism. This is supported by the fact that the same trend was also found in most other studies on skeletal stress markers (Stech 2009; Trautmann 2012; Roßbach 2015; Kairies 2021). Overall, these results from the Knuedler cemetery suggest that the people buried there, and this includes cloister as well as cemetery burials, might also have rather belonged to a middle to upper social class, which experienced rather good nutritional stability and rather little exposure to infectious diseases.

However, of a total of 391 individuals, only 68 were subadults. This noticeable deficit in children in this sample might also explain the relatively low frequency of cribra orbitalia and porotic hyperostosis in the sample as both lesions tend to occur more often in children than in adults. Furthermore, cribra orbitalia may heal over time if it is not active anymore (Rinaldo *et al.* 2019) and the possibility should be entertained that any childhood lesions might already have healed over among the large groups of mature and senile individuals. Therefore, the results obtained from this study should be considered with care and will be discussed further in the light of other anthropological findings and the historical setting of Luxembourg City between the 14th-18th century in the Discussion chapter at the end.

As with linear enamel hypoplasia, cribra orbitalia frequency might not only be dependent on socioeconomic status or urbanisation, but might also be dependent on local environmental factors (Van Cant 2019). As Van Cant (2019) discovered in their study on 4 Belgian sites, the coastal site of Slijpe seemed to be most affected by cribra orbitalia compared to the other sites analysed. It's situation in marshlands and the presence of malaria in these regions might have promoted the high frequency observed for that site (Van Cant 2019). Also, differences in scoring systems for porous cranial lesions in general might create some of the differences in prevalence (Ulrich-Bochsler 2008) observed across these European sites.

6.8 Metabolic and endocrine disorders

6.8.1 Introduction

Metabolic diseases are conditions caused by hormonal or nutritional deficiencies, such as Vitamin D or C deficiency etc. (Waldron 2009; Roberts & Manchester 2010; Grupe *et al.* 2015; Brickley & Mays 2019). Nutritional deficiencies are usually the result of malabsorption within the gut or low dietary diversity, which can either be caused by a general dependence on staple foods that are lacking in micronutrients or cultural practices like differential allocation of food resources between groups of different socio-economic status. Starvation and famine can also cause malnutrition and lead to the development of metabolic diseases (Schattmann *et al.* 2016; Snoddy *et al.* 2018). But oftentimes, it is a complicated interplay of different factors that leads to the formation of metabolic disease (Brickley & Ives 2008; Kozlowski & Witas 2012) (Figure 238).

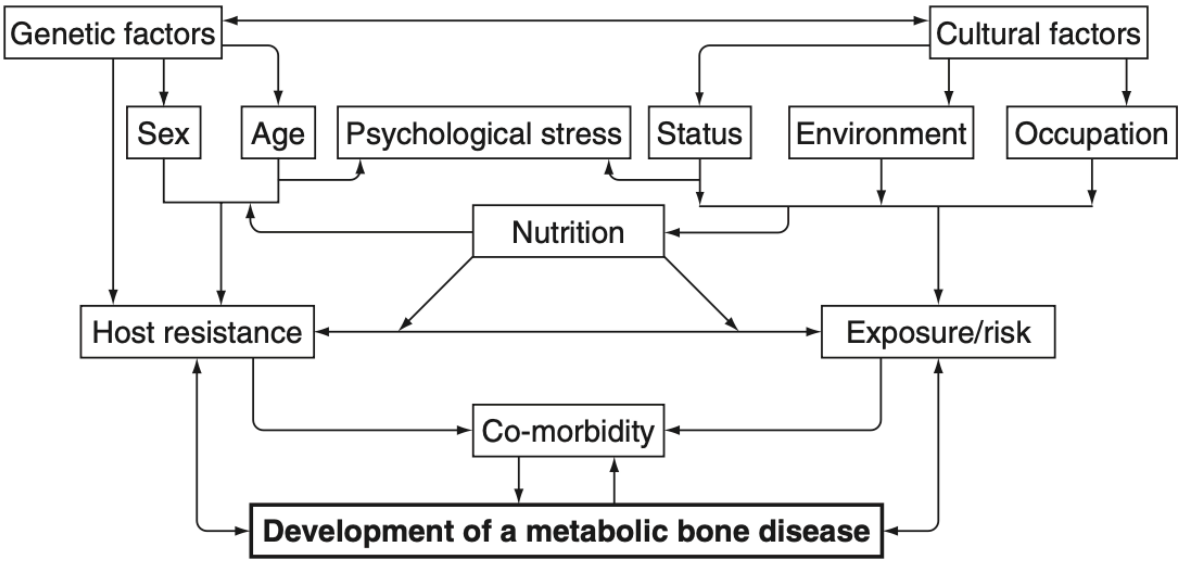

Figure 238 Factors that may have an impact on the development of metabolic disease (from (Brickley & Ives 2008)*)*

Metabolic diseases are many times difficult to assess in the skeleton because most conditions either do not leave any traces on bones at all or the traces that they cause are not pathognomonic (Kozlowski & Witas 2012; Snoddy *et al.* 2018).

Generally, the assessment of unspecific stress markers such as linear enamel hypoplasia, Harris lines etc. is still being used to address questions about the nutritional status and nutritional stress of past populations. However, these unspecific markers of stress cannot reveal information on intake of micronutrients. Therefore, identifying lesions associated clearly with specific nutritional deficiencies can help to shed light on human health and environment interactions in past populations. But associating specific lesions or sets of lesions to a specific micronutrient deficiency is still problematic as many of the lesions can occur in several types of deficiencies and cooccurrence of different conditions needs to be considered as well (Brickley & Ives 2006, 2008; Schattmann *et al.* 2016; Snoddy *et al.* 2018; Brickley & Mays 2019), Often times, several diagnostic areas might be missing in human remains recovered from archaeological sites. Therefore, most of the time, it is not possible to clearly infer the underlying micronutrient deficiency and several differential diagnoses must be considered.

6.8.2 Methods

In this study, all individuals which showed signs of underlying metabolic conditions, which were mostly individuals displaying unusual patterns of new bone formation in a first instance, were assessed for metabolic disease. A focus was put on the two most found metabolic conditions in skeletal remains: scurvy and rickets, but commonly listed differential diagnoses of these two conditions were also considered. The list of diagnostic and suggestive criteria for scurvy used in this study (Table 87) is based on the criteria established by Snoddy et al. (2018). Snoddy et al. (2018) sourced the criteria from several publications and assessed them for usefulness in identifying scorbutic individuals in past populations. All lesions are consequences of the defective collagen synthesis and are mostly reflected by abnormal porosities and periosteal new bone formation in areas where muscle attaches to bone an in joint areas since those areas are most susceptible to the development of subperiosteal haemorrhages (Snoddy *et al.* 2018). In fact, even light muscular actions such as masticatory movements can cause damage to the already weakened blood vessels at attachment sites, which in return produce subperiosteal haemorrhages in these areas. Therefore, lesions on the sphenoid and temporal bones are considered to be particularly diagnostic for scurvy (Ortner & Ericksen 1997; Ortner *et al.* 1999, 2001; Brickley & Ives 2006; Brickley & Mays 2019).

All individuals that showed signs of metabolic disease, meaning abnormal porosity and periosteal reactions, were assessed for the following criteria, and the criteria were marked as either present, absent, or not scoreable. It must be noted though that the criteria were expressed to different extents in the individuals analysed but the degree of expression was not considered in this study since that is not a criterium in the scoring system presented by Snoddy et al. (2018).

Table 87 Criteria for diagnosis of scurvy from human remains (taken from and accumulated by Snoddy et al. (2018))

Anatomical region	Bone	Lesion location	Lesion type	Diagnostic strength
Cranium	calvarium	ectocranial (parietal and/or squamous temporal)	abnormal cortical porosity, SPNB*	diagnostic
		endocranial	Islands of abnormal cortical porosity and/or SPNB	suggestive
	sphenoid	greater wing	abnormal cortical porosity, bilateral SPNB	diagnostic
		Foramen rotundum	SPNB	diagnostic
		lesser wing	abnormal cortical porosity	suggestive
		pterygoid fossae/plates	abnormal cortical porosity, SPNB	diagnostic
	frontal	orbital roof	abnormal cortical porosity, SPNB	diagnostic
	occipital	inferior surface of pars basilaris	abnormal cortical porosity, SPNB	suggestive
	zygomatic	lateral aspect	abnormal cortical porosity, SPNB	suggestive
		internal (posterior) aspect	abnormal cordial porosity	suggestive
	maxilla	anterior surface/infraorbital foramina	abnormal cortical porosity, SPNB	diagnostic
		posterior surface	abnormal cortical porosity, SPNB	diagnostic
		palatal surface	abnormal porosity	diagnostic
	mandible	medial surface/coronoid process	abnormal cortical porosity, SPNB	diagnostic
		mylohyoid line	bilateral SPNB	suggestive
Postcranium	scapula	supraspinous fossa	abnormal cortical porosity	diagnostic
		infraspinous fossa	abnormal cortical porosity, SPNB	diagnostic
	ilium	visceral surface	abnormal porosity, SPNB, Vis	suggestive
	femur	linea aspera and surrounding area	SPNB	suggestive
	ribs	costochondral junction	swelling/flaring	suggestive
		antero-lateral shaft	SPNB	suggestive
	vertebrae	bodies	biconcavity, osteopenia	suggestive
	appendicular skeleton	diaphyses/metaphyses	SPNB (diffuse)	Diagnostic
	appendicular skeleton	diaphyses	ossified hematomas: bilateral	suggestive
	appendicular skeleton	metaphyses	Metaphyseal cupping/flaring	Suggestive

- SPNB = subperiosteal new bone

The lesions observed in scurvy can also be indicative of other metabolic or infectious conditions, especially if many of the diagnostic areas are missing or not affected. Rickets is frequently named as differential diagnosis for scurvy as both conditions share many of the skeletal symptoms (Aufderheide & Rodriguez-Martin 1998; Klaus 2014; Schattmann *et al.* 2016; Morrone *et al.* 2021), and is also one of the most commonly described metabolic conditions especially in postmedieval assemblages (Mays *et al.* 2006; Giuffra *et al.* 2015; Mays & Brickley 2018), which is why all observed lesions, if applicable, were also scored for rickets. A clear identification for rickets was only made however in presence of long bone bowing and widening of the metaphyses as those are widely considered to be the most diagnostic traits (Table 88).

A list of criteria for differential diagnoses of porotic lesions and periosteal new bone formation was taken from Morrone et al. (2021) (Table 89), who sourced the criteria for each differential diagnosis from multiple sources. All criteria are applicable primarily to infantile expression of the conditions. The differential diagnoses comprise other metabolic (rickets, anaemia, osteogenesis imperfecta, infantile cortical hyperostosis) as well as infectious (congenital syphilis, meningitis, rubella, tuberculosis) and neoplastic (leukaemia) conditions as especially porous lesions and periosteal reactions are both common features of these conditions as well. All individuals with lesions were assessed for scurvy and all differential diagnoses. The disease for which most criteria were fulfilled was taken as main diagnosis, but all other possible diseases were kept as differential diagnoses.

Table 88 Suggestive and diagnostic criteria for rickets (taken from and accumulated by Brickley and Ives (2008))

Anatomical region	Lesion	Diagnostic strength
Cranium	Delayed closure of fontanelles	Suggestive
	Thinning of cranial bone	Suggestive
	Bossing of frontal and parietal	Suggestive
	Craniotabes	Suggestive
	Large, square-shaped head	Suggestive
	Ectocranial PNB	Diagnostic
Mandible and Dentition	Delayed deciduous and permanent dentition eruption	Suggestive
	Enamel hypoplastic defects	Suggestive
	Dental caries	Suggestive
	Medial angulation of mandibular ramus	Diagnostic
Vertebrae	Kyphosis or Scoliosis	Diagnostic
Ribs and Sternum	**Alteration of rib neck angle**	Diagnostic
	Lateral straightening of shaft	Diagnostic

	Rachitic rosary	Diagnostic
	Protrusion of sternum with rib angulation	Diagnostic
Pelvis and Sacrum	Exaggerated curvature of ilium	Diagnostic
	Protrusio acetabulae	Diagnostic
	Retarded growth of pelvis/plump ilia	Suggestive
	Flaring, fraying and swelling of distal metaphyses	Diagnostic
	Fraying of margins of growth plate	Diagnostic
	Porosity on growth plate	Diagnostic
	Cupping deformities of growth plates and metaphyses	Diagnostic
	Bowing of upper limbs	Diagnostic
	Bowing of lower limbs	Diagnostic
	Coxa vara (angulation of femoral neck)	Diagnostic
	Knock-knees (angulation of knees)	Suggestive
	Shortening with gross deformity and growth stunting	Suggestive
	Fractures	Suggestive
	Thickening (in healed rickets)	Diagnostic
	Periosteal porosity and PNB	Suggestive
Bold = traits visible also in osteomalacia and residual rickets PNB = periosteal new bone		

Table 89 List of differential diagnoses and their criteria for porous lesions and SPNB (sourced from Morrone et al. 2021, Brickley and Ives (2008, Mays and Brickley (2022) and Brickley and Mays (2019))

Anemia	Congenital Syphilis	Tuberculosis	Rubella	Meningitis	Osteogenesis imperfecta	Leukemia	Infantile Cortical Hyperostosis
cribra orbitalia	Lack of development of nasal bridge (saddle nose)	small granulomas (cortical foci)	enlargement of anterior fontanel and poor mineralization	endocranial lesions, often around sinus drainage areas	beaded ribs	active widespread SPNB formation on long bones	cortical hyperostosis of the ribs, scapulae and clavicles
porotic hyperostosis	Dental stigmata: Moon's molars, Hutchinson's incisors, mulberry molars, enamel hypoplasia	osteomyelitis of the mandible	ribs: poor mineralization and coarsening of trabecular pattern		barrel-shaped rib cage	lytic lesions around the vascular foramina and long bone metaphysis	irregular shape of the ribs
zygomatic bone hypertrophy (thalassemia)	endocranial lesions	ribs: new bone formation and lytic lesions on visceral surfaces	vertebrae: poor mineralization and coarsening of he trabecular pattern		bowing of all long bones		cortical hyperostosis of the pelvic bones
fan-like trabecular organisation of the pelvis, cortical thinning	inflammation of the joints	abscess in the vertebral bodies. Perforation and collapse of the	axial: poor mineralization and thinning of the metaphyseal trabeculae in		fractures of the long bones		bowing of the limbs (mostly femora and humeri)

		affected elements	distal femur, proximal tibia and upper limb				
rib hypertrophy and lesions: hypertrophic and apparently fractured ribs	osteomyelitis, saber shin tibia	ankylosis of spinal elements			thick, shortened, squared long bones		
osteopenia and pitted diaphyseal shafts	axial skeleton: SPNB	Pott's disease			thin, twisted tubular bones		
		axial: active widespread SPNB on long bones			hyperplastic calluses		
					forearm: calcification of the interosseous membrane		

6.8.3 Results

A total of 27 individuals showed bone lesions that might be associated to metabolic disease, in the form of either abnormal porosities, new bone formation or bowing of long bones. Of these, 13 showed signs characteristic for rickets and the majority (12) was found in the form of long bone bowing in adults. In adults, no further lesions apart from long bone bowing were detected, suggesting that they are all cases of residual rickets (Brickley *et al.* 2010). Several differential diagnoses regarding bowing of long bones in adults need to be considered, however. Congenital bowing deformities happen already in the womb but are overall rare occurrences and often they even out during growth so that they are not visible anymore in the adult skeleton (Aufderheide & Rodriguez-Martin 1998). Paget's disease may result in bowing of long bones in adults but none of the other changes associated with the disease such as thickening of the bones and cranial vault could be observed (Aufderheide & Rodriguez-Martin 1998; Brickley & Ives 2008). APBD stands for acute plastic bowing deformities in response to incomplete fractures. APBD can be excluded as differential diagnosis for individual 2008-78/1038 as a radiograph showed absence of fracture in this bone. Whilst APBD is a possible explanation for the deformities observed in the other adult cases, its occurrence is considered rare, and deformities often resolve during growth. At least for individual 2008-78/752, normal variation needs to be considered as well as the medial bending of both tibiae is only light (Brickley *et al.* 2010). Residual rickets and osteomalacia are difficult to differentiate in the archaeological record,

which is why both conditions will be considered equally likely as the cause for the bowing deformities observed.

Individual 2008-78/1141 is an infans I of 1-1.5 years presenting with multiple diagnostic (8) and suggestive signs (4) of subadult rickets described in Table 90. The diagnostic signs that are not listed were not observed. Diagnostic regions that were missing and could therefore not be scored are: all features pertaining to the cranium and sternum. As such this remains the only securely identified case of rickets in the sample. Scurvy was listed as potential differential diagnosis due to slight PNB formation on the ilium and tibial diaphysis, but most of the diagnostic criteria for scurvy were not present. However, cooccurrence of rickets and scurvy is quite common and one condition might obscure the presence of the other, (Schattmann *et al.* 2016) which is why this needs to be taken into consideration as well, although it is rather unlikely in this case. Example photos of rickets cases from the Knuedler cemetery can be found in (Figure 260-Figure 265) in the discussion section of this chapter.

Table 90 Diagnostic lesions and differential diagnosis for individuals with potential rickets

Rickets, Residual Rickets and Osteomalacia								
ID	**Sex**	**Age**	**Location**	**Layer**	**Nb. of diagnostic criteria**	**Diagnostic lesions**	**Suggestive lesions**	**Differential diagnosis**
2008_78/1038	F	Senile	Cemetery	2	1	Strong anterior and lateral bowing of Fe R		congenital bowing deformities; Paget's disease
2016_082/540	F	Mature	Cloister	1	1	Strong anterior bowing of Fe R+L		congenital bowing deformities; Paget's disease; APBD
2008_78/1471	M	Mature	Cemetery	2	1	Strong bowing of Ulna R+L; twist of Ra R+L diaphysis		congenital bowing deformities; Paget's disease; APBD
2008_78/539	F	Adultus	Cemetery	2	1	Lateral bowing of Fe R+L		congenital bowing deformities; Paget's disease; APBD
2008_78/734	M	Senile	Cemetery	1	1	Anterior and lateral bowing of Fe R+L	active and healed PNB on Fe, Ti, Fi	congenital bowing deformities; Paget's disease; APBD
2008_78/738	M	Adult	Cemetery	1	2	Anterior bowing of Fe R+L;	healed periostitis on	congenital bowing deformities;

Rickets, Residual Rickets and Osteomalacia								
ID	**Sex**	**Age**	**Location**	**Layer**	**Nb. of diagnostic criteria**	**Diagnostic lesions**	**Suggestive lesions**	**Differential diagnosis**
						Medial bowing of Ti R+L	Tibiae; light cribra cranii	Paget's disease; APBD; Blout's disease
2008_78/751	M	Senile	Cemetery	1	1	Lateral bowing of Fe L		congenital bowing deformities; Paget's disease; APBD
2008_78/752	M	Adult	Cemetery	1	1	Light medial bowing of Ti R		congenital bowing deformities; Paget's disease; APBD; Blout's disease; normal variation
2008_78/794	M	Senile	Cemetery	1	2	Anterior bowing of Fe R+L; Medial bowing of Ti R+L		congenital bowing deformities; Paget's disease; APBD; Blout's disease
2008_78/820	M	Young Adult	Cemetery	1	1	Medial bowing of Ti R		congenital bowing deformities; Paget's disease; APBD; Blout's disease; normal variation
2008_78/350	M	Adultus	Cloister	1	1	Anteroposterior flattening of the Fi L		congenital bowing deformities; Paget's disease; APBD; reaction to pathological lesion on tibia L
2008_78/991	F	Juvenile	Cemetery	2	1	Strong anterior bowing of Fe L		congenital bowing deformities; Paget's disease; APBD
2008_78/1141	I	Infans I	Cemetery	2	8	• Medial angulation of mandible (condyles) • Rachitic rosary	• Light knock-knees • Cortical thinning and porosity	scurvy

Rickets, Residual Rickets and Osteomalacia								
ID	**Sex**	**Age**	**Location**	**Layer**	**Nb. of diagnostic criteria**	**Diagnostic lesions**	**Suggestive lesions**	**Differential diagnosis**
						• Widening, cupping, fraying of the metaphyses • Light bowing of the long bones upper and lower extremities • Coxa vara	• Small ilium but not plump • Enamel plane defects on unerupted M2	

Table 91 lists all subadult individuals that showed signs of metabolic disease. A diagnosis of probable scurvy was made in the presence of at least 2 diagnostic features and multiple suggestive features and a diagnosis for possible scurvy was made in the presence of 1 diagnostic feature and multiple suggestive features as proposed by Snoddy et al. 2018 and Brickley and Ives (2008). Following this method of interpretation, 9 of 14 individuals with multiple areas of porous lesions and/or periosteal new bone formation could be classified as probably scorbutic as they all present with more than two diagnostic criteria and several suggestive criteria. However, cranial porous lesions and periosteal new bone formation, and especially lesions on the maxilla, mandible and sphenoids are considered diagnostic features as they are associated with mastication, especially porous lesions on the greater wing of the sphenoid are considered pathognomonic (Ortner & Ericksen 1997). Individual 2013-015/355, a neonate did not have any cranial elements preserved and neonate 2016-082/419 was missing the sphenoid, mandible and maxilla and had very severe widespread periosteal reactions also in areas and bones not included in the definition of scurvy. Therefore, it would be safer to consider those rather as possible cases of scurvy, as the remaining features that they express also frequently occur in other metabolic or infectious conditions. Based on the number of diagnostic and suggestive criteria, a diagnosis for scurvy seems most likely for individuals 2008-78/673, 2008-78/728, 2008-78/248 and 2008-78/522. For all other cases, too many features are missing or could not be recorded, or too many diagnostic features were explicitly absent, for a secure diagnosis of scurvy. All individuals were also assessed for the features presented in Table 89 as differential diagnoses (Brickley & Ives 2008; Morrone *et al*. 2021). For individuals 2008-78/1099, 2008-78/728, 2008-78/248 and maybe 2013-015/179, the cranial lesions, specifically cribra orbitalia, might be indicative of anaemia (Oxenham & Cavill 2011). The widespread periosteal new bone formation on the long bones and ilia observed in

individuals 2013-015/355, 2008-78/1099, 2008-78/728, 2016-082/419 and 2008-78/522 is also found in tuberculosis, congenital syphilis and leukaemia, however in all cases, the majority of diagnostic criteria for these conditions are not present. None of the individuals presented with dental stigmata characteristic of congenital syphilis (Hillson *et al*. 1998) nor did they display any vertebral changes or osteomyelitis associated with tuberculosis (Dawson & Robson Brown 2012), and no lytic lesions were found on the long bone diaphysis as would be the case in leukaemia (Morrone *et al*. 2021). It has to be noted though that dental stigmata usually only affect the permanent dentition and as such cannot be used to identify congenital syphilis in neonates and children where permanent teeth have not yet erupted or formed (Rothschild & Rothschild 1997; Hillson *et al*. 1998). Caffey's disease, also called infantile cortical hyperostosis, is a rare disorder of unknown aetiology causing periosteal reaction, with involvement of the mandible considered to be the most diagnostic factor of the disease. Periosteal reactions on the long bones, clavicle or scapula can lead to a thickening of the bone and usually the epiphyses and metaphyses are spared (Aufderheide & Rodriguez-Martin 1998; Lewis 2009; Rusu *et al*. 2019b). Due to the extensive periosteal reaction on the long bones, giving them a thickened appearance and the extensive periosteal reactions on the mandible, Caffey's disease should be considered as differential diagnosis for individual 2008-78/419. Additionally, for individual 2008-78/419, considerable thinning of the cranial vault was observed together with ecto- and endocranial sheet-like periosteal new bone formation and the same spiculated but sheet-like periosteal new bone deposits covered all the long bone surfaces, parts of the clavicles, scapula, pelvis, ribs and vertebrae and strong flaring at the costochondral junction was observed. Therefore, rickets but also diffuse infectious disease, Caffey's disease or even congenital syphilis must be considered as equally possible differential diagnoses to scurvy for this individual. Some illustrations of the lesions can be found in the scurvy photo table in the discussion section. It has to be noted as well that most lesions recorded were only light in expression, except those recorded for the 4 probable scurvy cases where the majority of lesions was moderate or severe. Some of the typical signs of scurvy are illustrated in (Figure 243-Figure 259) in the discussion section of this chapter.

Table 91 Cases of probable and possible scurvy with diagnostic and suggestive criteria

Scurvy										
Location	**Diagnostic criteria**	**2013_015/179**	**2013_015/355**	**2008_78/1099**	**2008_78/153**	**2008_78/673**	**2008_78/728**	**2016_082/419**	**2008_78/248**	**2008_78/522**
Age		Infans II	Neonatus	Infans II	Infans I	Infans I	Infans II	Neonatus	Infans I	Neonatus
Layer		1	2	2	1	1	1	2	1	1
Location		Cloister	Cloister	Cemetery	Cemetery	Cemetery	Cemetery	Cloister	Cemetery	Cemetery
calvarium	*ectocranial (parietal and/or squamous temporal)*	no	/	/	no	yes	yes	yes	yes	yes
	endocranial	no	/	yes	no	yes	yes	yes	yes	yes
sphenoid	*greater wing*	yes	/	yes	yes	yes	yes	/	yes	yes
	Foramen rotundum	/	/	/	no	yes	yes	/	yes	/
	lesser wing	/	/	/	no	/	yes	/	yes	/
	pterygoid fossae/plates	/	/	/	yes	/	yes	/	yes	/
frontal	*orbital roof*	yes	/	yes	no	/	yes	/	yes	/
occipital	inferior surface of pars basilaris	no	/	/	yes	yes	yes	yes	no	yes
zygomatic	lateral aspect	no	/	no	no	yes	yes	/	yes	no
	internal (posterior) aspect	no	/	yes	yes	yes	yes	/	yes	no
maxilla	*anterior surface/infraorbital foramina*	yes	/	yes	no	yes	yes	/	yes	yes
	posterior surface	yes	/	/	yes	yes	yes	/	yes	yes
	palatal surface	yes	/	no	yes	yes	yes	/	yes	yes
mandible	*medial surface/coronoid process*	yes	yes	/	yes	/	yes	/	no	yes
	mylohyoid line	yes	yes	yes	no	/	no	/	no	yes
scapula	*supraspinous fossa*	no	yes	yes	no	yes	/	yes	yes	yes
	infraspinous fossa	no	yes	/	no	yes	/	yes	yes	yes
ilium	visceral surface	no	/	/	yes	/	yes	yes	no	yes
femur	linea aspera and surrounding area	no	/	yes	no	/	/	/	no	no
ribs	costochondral junction flaring	no	yes	no	no	no	no	yes	no	no
	antero-lateral shaft	no	yes	no	yes	no	yes	yes	no	no
vertebrae	biconcave bodies	no	no	no	no	no	no	no	no	no
appendicular skeleton	*diaphyses/metaphyses*	no	yes	yes	no	/	yes	yes	no	yes
appendicular skeleton	Diaphysis ossified haematomas	no	no	maybe	no	/	maybe	maybe	no	no
appendicular skeleton	Metaphyses cupping	no	no	no	no	/	yes	yes	no	no
Total diagnostic criteria		6	4	5	5	8	10	4	10	9
Total suggestive criteria		1	3	4	4	4	8	6	4	4
Where not otherwise specified, the nature of lesions is abnormal porosity and/or PNB; PNB = periosteal new bone*Italics* = diagnostic criteria										

Furthermore, 5 individuals showed signs of an underlying metabolic condition, expressed as areas of abnormal porosity and/or periosteal new bone formation. The lesions were so few that it was not possible to pinpoint any cause for them, and therefore these three individuals will only be considered as possibly suffering from an unknown metabolic or infectious condition. In the case of individual 2013-015/161, a slow growing tumour or a periosteal reaction to infection such as osteomyelitis (Aufderheide & Rodriguez-Martin 1998) cannot be excluded as differential diagnosis which will be further explored in the section on neoplastic disease. The individual presents with a large and thickly lamellated spot of periosteal new bone formation on the proximal third of the right ulnar diaphysis. A thin sheet of periosteal new bone also covers part of the mid-diaphysis, and the surrounding are of the lamellated deposit. Periosteal new bone formation is then also observed enveloping all of the right 5th metacarpal diaphysis and part of the right 4th metacarpal diaphysis. Apart from very strong grooved and pitted enamel defects on the erupting permanent teeth, no further lesions were recorded on any of the bones (Figure 239, Figure 240).

Individual 2008-78/190 presented with a strong backwards bent in the sacral S1. The sacrum and vertebrae showed a very porous surface and were overall very light, hinting at an underlying metabolic condition. Due to the strong bend in the S1-S2 junction of the sacrum, rickets was considered as possible differential diagnosis but no other diagnostic signs of rickets, such as cortical thinning, bowing of long bones or flaring of the metaphyses could be observed in the rest of the skeleton. Only the femora presented with very light periosteal deposits at the anterior aspect of the distal metaphysis (Figure 241, Figure 242). Photos of the lesions of individuals 2008-78/190 and 2013-015/161 can be found in (Figure 239-Figure 242). All individuals displaying possible metabolic disease can be found in Table 92 together with their lesion descriptions.

Table 92 List of individuals with lesions suggestive of metabolic disease, with absence of diagnostic criteria qualifying for a final diagnosis

Diffuse metabolic or infectious disease					
ID	**Sex**	**Age**	**Location**	**Layer**	**Lesion description**
2013-015/161	I	Infans II	Cloister	1	Thick lamellated PNB spot on proximal 3rd of right Ulna diaphysis; PNB on the right MC5 and MC4
2008-78/1310	M	Mature	Cemetery	2	Cribra cranii; cribra orbitalia, light porosity on sphenoid (ala major and inside pterygoid fossa); porosity and PNB on maxilla posterior surface and palate; large osteophyte on auricular surface margin
2008-78/667	F	Mature	Cemetery	1	Light porosity on maxillary palate; extensive PNB on ribs; extensive PNB on margins of long bone entheses
2008-78/190	M	Juvenile	Cloister	2	PNB on distal and proximal femur metaphyses; sacrum S1 is strongly bent backwards creating a near 90° angle with the lumbar vertebrae (looks in appearance like Unterkreuz Syndrome) and the

					sacrum and vertebral bodies are very porous; light porosity on the ilia close to the acetabulum and above the auricular surface.
2008-78/1124	I	Infans I	Cemetery	2	Abnormal porosity on ectocranial side of the sphenoidal ala major; abnormal porosity on posterior maxilla

2013-015/161

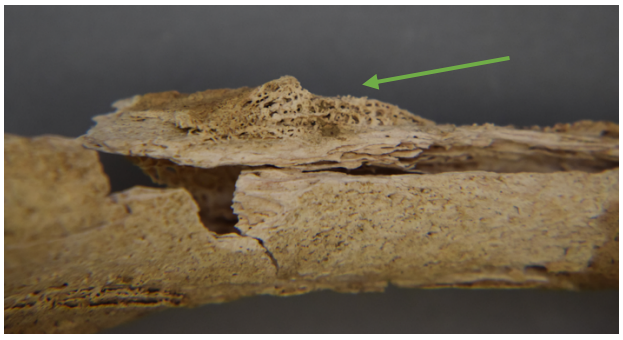

Figure 239 Thick lamellated periosteal new bone deposition on proximal ulna of individual 2016-082/161

Figure 240 Strong enamel defect on left permanent P3 of individual 2016-082/161

2008-78/190

Figure 241 Sacrum with strong bend at the S1-S2 junction of individual 2008-78/190

Figure 242 Light periosteal new bone formation on the distal metaphysis of the right femur of individual 2008-78/190

6.8.4 Discussion

6.8.4.1 Scurvy

Scurvy, also known as Möller-Barlow's disease, is a metabolic condition caused by severe and prolonged vitamin C (ascorbic acid) deficiency (Kozlowski & Witas 2012; Snoddy *et al.* 2018). Vitamin C is provided mainly through the intake of fresh fruit and vegetables but smaller amounts are also found in fish and dairy (Brickley & Mays 2019). Since the human body is unable to synthesise and store vitamin C, humans are dependent on constantly supplying it through regular intake of fruits and vegetables (Brickley & Ives 2008; Waldron 2009). The

lack of vitamin C results in defective collagen synthesis, which leads to skeletal growth retardation and subperiosteal haemorrhaging though weakening of connective tissues such as vascular walls (Aufderheide & Rodriguez-Martin 1998; Schattmann *et al.* 2016). This is usually reflected in the form of abnormal porosities on the endo- and ectocranial surfaces, on the zygomatic, on the sphenoid, especially on the ala major and around the foramen rotundum, in the infra- and supra spinous fossa of the scapula and on long bone diaphyses and metaphyses (Brickley & Ives 2006; Snoddy *et al.* 2018). Abnormal porosity is considered to be the result of an inflammatory angiogenic response to subperiosteal haemorrhaging, with capillaries proliferating and penetrating the bone cortex to remove the remains of the extravasated blood (Browder *et al.* 2000; Ortner *et al.* 2001; Ortner 2003a; Klaus 2017; Snoddy *et al.* 2018). Another feature often associated with scurvy is periosteal new bone formation at the sites of subperiosteal haemorrhaging, which represents a resumption of osteoid production after to vitamin C supplementation. However, as many researchers argue, these deposits of new bone should not be considered as an indication of healing scurvy as very little amounts of vitamin C have already proven to elicit such a reaction (Ortner *et al.* 1999; Stark 2014; Klaus 2017; Snoddy *et al.* 2018; Brickley & Mays 2019). Although technically, the same processes and criteria for diagnosing scurvy apply also to adults, infantile scurvy is usually easier to diagnose than adult scurvy, since expression of the symptoms is not as marked in adults as it is in children (Snoddy *et al.* 2018). In children, the most common age span where scurvy occurs lies between 3 months and 5 years (Schattmann *et al.* 2016; Brickley & Mays 2019), with most common occurrence at 5-24 months, and cases peaking between 8-11 months (Brickley & Ives 2006). This age of onset is usually related to inadequate weaning practices, because normally, breastmilk provides the infant with an adequate amount of vitamin C. The cessation of lactation and switch to foods that are vitamin C deficient, are therefore a major cause for infantile scurvy. Scurvy associated with bad weaning practices has been observed in the nineteenth century among the middle- and upper-class populations and shows that infantile scurvy is thus not only a disease of the poor (Brickley & Ives 2008; Lewis 2009; Waldron 2009). However, cases of neonatal scurvy have also been reported and in that case, the vitamin C deficiency in the neonate is usually due to an intrauterine lack of provision with the vitamin and might indicate that the mother was scorbutic as well (Brickley & Ives 2008). If left untreated, scurvy usually ends up being fatal. Nonetheless, recovery after vitamin C supplementation is generally very fast and remodelling of the bony changes almost immediate, which is why healed infantile scurvy is usually not detectable anymore in skeletal assemblages (Waldron 2009; Snoddy *et al.* 2018).

Since vitamin C deficiency is usually associated with low dietary diversity such as a high dependence on vitamin C deficient foods like cereal crops, or with general famine (Cheung *et al.* 2003; Snoddy *et al.* 2018), identifying scorbutic individuals within a population can help to shed light on living conditions in the past, especially on subsistence strategies and food availability, but also on cultural practices such as food allocations and therefore social inequality (Buckley *et al.* 2014; Crandall 2014; Snoddy *et al.* 2017, 2018).

Out of all individuals recovered from the Knuedler cemetery (n=391), 2.30% (n=9) of individuals showed diagnostic and suggestive signs of scurvy, and only for 4 of them, a diagnosis as probable scurvy was possible. All probable and possible scurvy cases were subadults and make up 13.24% of all subadults (n=68) buried in the cemetery and cloister areas. 12.76% (n=6) of individuals from the cemetery and 14.29% (n=3) of individuals from the cloister were affected by scorbutic lesions.

Furthermore, 3 of the possible scurvy cases were observed in neonates, suggesting that the mothers had been scorbutic as well (Brickley & Ives 2008).

Among three polish postmedieval sites that were not implicated in any major political crises and whose inhabitants led lives mostly reliant on fishing and agriculture, frequencies of subadult scurvy only range between 2.6-4.5% (Krenz-Niedbała 2016).

A frequency of 4% subadult scurvy was recorded among burials from St. Martin's church in Birmingham (Brickley & Ives 2006) and at 3% at St. Marylebone Church in London (see Mays, 2014).

A study on subadults from Castel Tirolo revealed a frequency of 37.5% of subadults with lesions that are suggestive of scurvy and 8.33% that showed several diagnostic features (Paladin *et al.* 2018)

The postmedieval upper-class German cemetery of Jelgava church in Latvia, where a frequency of 21.43% was reached (frequency calculated from raw data provided in the publication of (Pētersone-Gordina *et al.* 2013) Pētersone-Gordina et al. (2013) argue that harsh Latvian winters affected fruit harvests, which led to development of scurvy even among upper-class populations.

That famine was a major cause for the development of subadult scurvy, has been established in a study on individuals from a Kilkenny (Ireland) workhouse, who suffered through the Great Irish famine. In that sample, prevalence of subadult scurvy lay at 67% and that of adults at 41% when all lesions are considered (possible scurvy), and at 22% among subadults and at 9% among adults when only diagnostic features are included (probable scurvy) (Geber 2014).

At 13.24%, the frequency of scurvy, at first glance, seems to be considerably higher than that from the contemporaneous Polish and British sites. However, it is not entirely clear whether those studies reported only probable or also all possible cases of scurvy. If the former was the case, then the frequency of scurvy in the Knuedler cemetery was actually quite similar to these sites at 5.88%, suggesting that the individuals buried in the Knuedler cemetery did not experience living conditions that were particularly harsher than those from postmedieval rural Poland or London. As the study by Paladin et al. (2020) shows, it is possible that a rather high discrepancy between possible and probable scurvy exists within a site. In that case, the authors chose to only retain the number of probable cases for further comparisons.

However, when considering the number of all possible scurvy cases (13.24%) from Luxembourg City, an explanation for this slightly elevated frequency should be explored, and one very prevalent cause for elevated scurvy frequency within a population is considered to be famine. Since Luxembourg is situated in a rather temperate climatic zone, harsh winters, as they occur in Latvia, are, and likely were not a common occurrence, and therefore likely did not ruin fruit harvests leading to food shortages in the city.

However, considering Luxembourg City's rather turbulent history during the period of use of the Knuedler cemetery, the famines and food shortages caused by foreign occupations and during wars and epidemics, which have also been partially historically documented (Weis 2004) (Pauly 2020), should be considered as possible causes for the slightly elevated frequency of scurvy among subadults in Luxembourg City. Contrary though to the victims of the Great Irish famine, food shortages in Luxembourg City were never of long duration (Weis 2004; Pauly 2020), and the cemetery reflects an occupation time of ~400 years, which is why the observed cases of scurvy might possibly only represent victims of these short-time famine events as opposed to being a reflection of the health status of the population as a whole.

Overall, comparative data on adult and subadult scurvy among medieval and postmedieval European sites are rare. According to historical sources, scurvy was more prevalent in the past than what the small frequencies discovered in the archaeological record let assume. This is likely because once Vitamin C is supplied again to the body, recovery from the condition is very fast and bone changes remodel completely in most cases. Alternatively, scurvy weakens the immune system and predisposes for a range of other pathological conditions, which is why it cannot be excluded that individuals died from other pathological conditions before any bony changes could develop. Furthermore, differences in scoring criteria used within the respective studies make direct comparisons of frequencies difficult (Waldron 2009; Mays 2014; Snoddy *et al.* 2018; Brickley & Mays 2019)

Photo Table Possible Scurvy

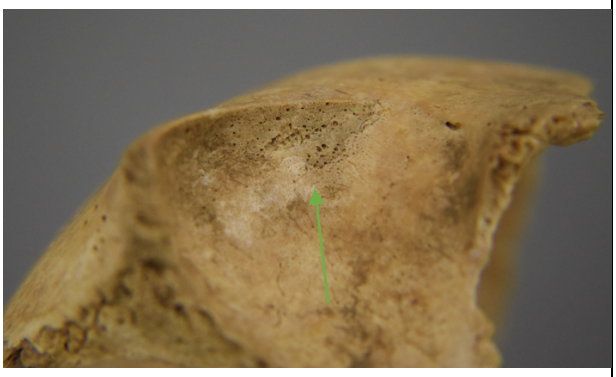

Figure 243 Cribra orbitalia in right orbit of individual 2008-78/248

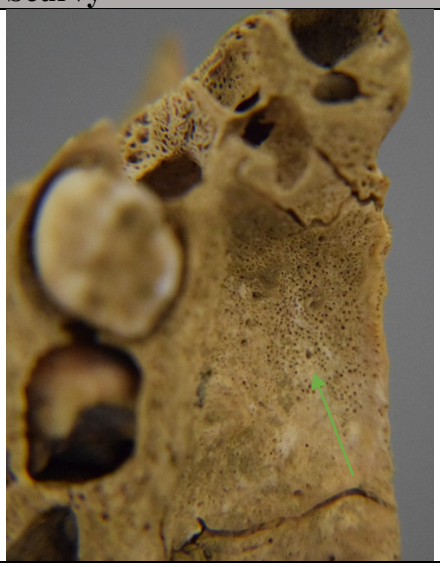

Figure 244 Porous lesion on maxillary palate of individual 2008-78/248

Figure 245 Strong porous lesion on occipital base of individual 2008-78/522

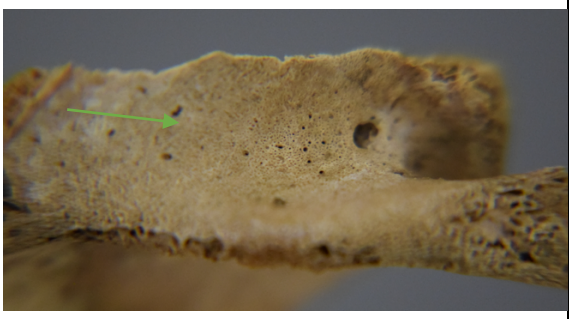

Figure 246 Porous lesion in the supraspinous fossa of the right scapula of individual 2008-78/522

Figure 247 Porous new bone formation above the mandibular foramen in individual 2008-78/673

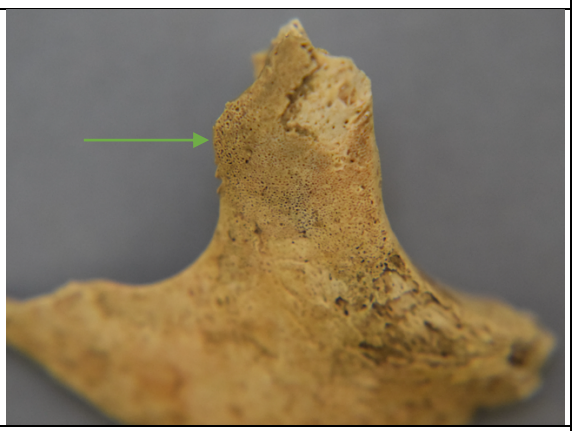

Figure 248 Porous new bone formation on the lateral aspect of the right zygomatic bone of individual 2008-78/728

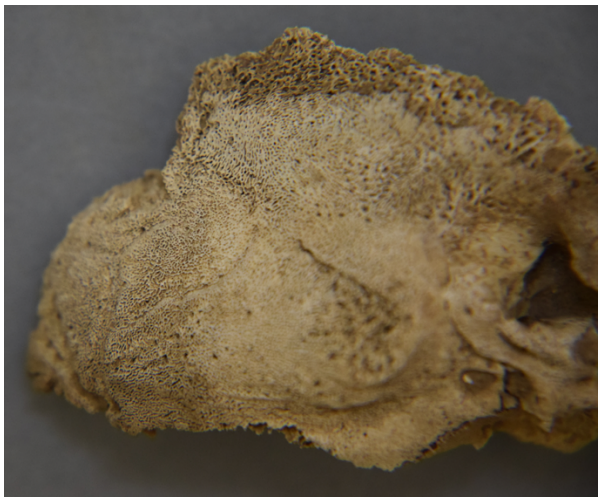

Figure 249 Extensive porous new bone formation on right temporal of individual 2016-082/419

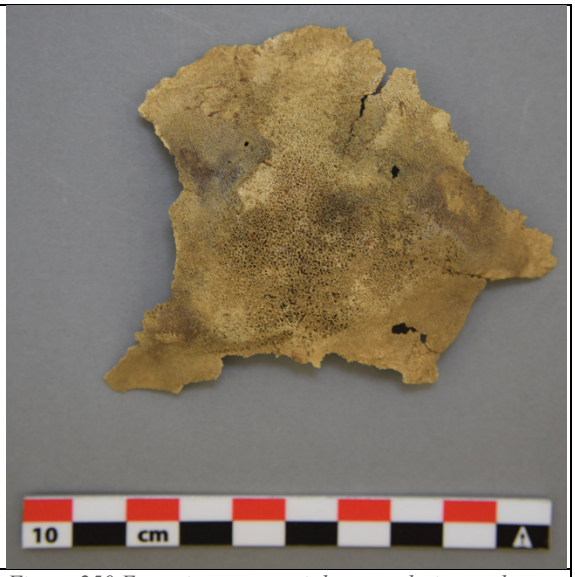

Figure 250 Extensive ectocranial porous lesion and new bone formation on the left parietal of individual 2016-082/419

Figure 251 Extensive porous new bone formation on posterior side of distal right humerus of individual 2008-78/728

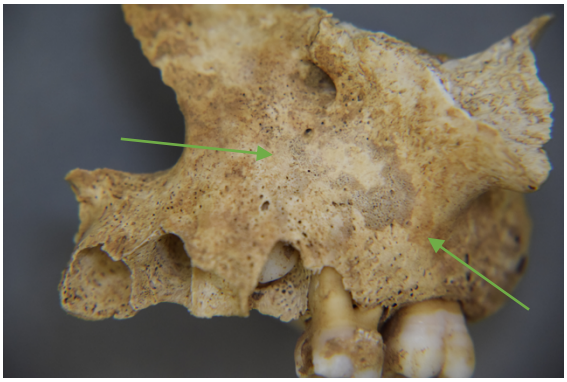

Figure 252 Periosteal new bone formation on anterior side of maxilla and around infraorbital foramen of individual 2013-015/179

Figure 253 Extensive porous new bone formation the proximal metaphysis and diaphysis of the right Ulna of individual 2008-78/728

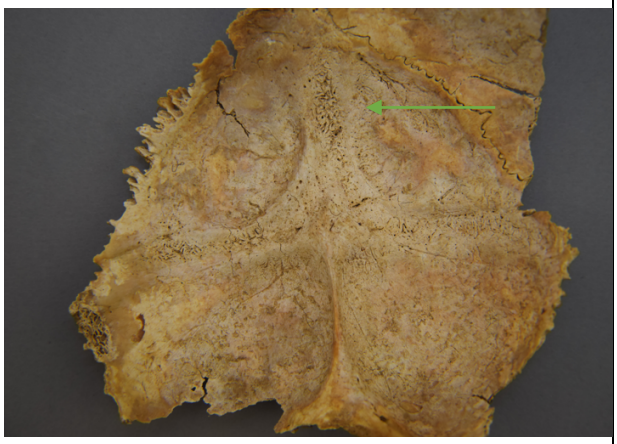

Figure 254 Vascular impressions inside occipital of individual 2008-78/1099

Figure 255 Periosteal new bone formation on left scapular blade anterior side of individual 2016-082/419

Figure 256 Extensive periosteal new bone formation along all of diaphysis and metaphysis of the left and right humerus of individual 2016-082/419

Figure 257 Flaring of the chobn^ndral rib end with exostosis at margin and very porous surfaces of individual 2016-082/419

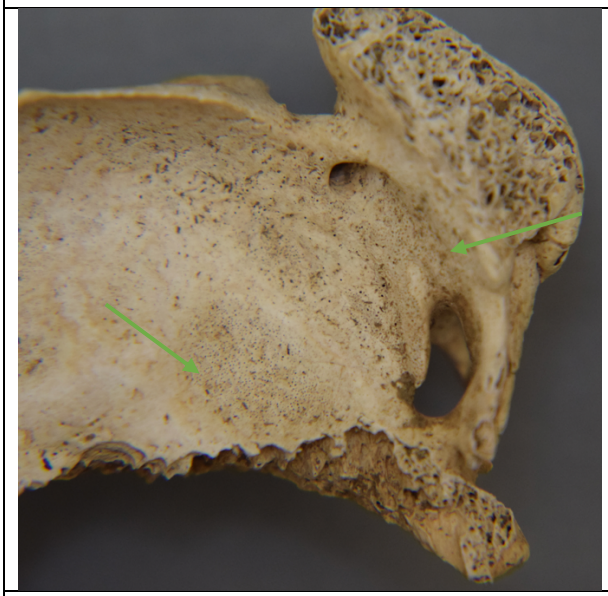

Figure 258 Porous lesions around foramen rotundum on sphenoid of individual 2008-78/728

Figure 259 Porous lesions on ectocranial side of the ala major of the sphenoid from individual 2008-78/728

6.8.4.2 Rickets and Osteomalacia

Rickets in subadults, also referred to as osteomalacia in adults, is a metabolic disease caused by vitamin D and/or calcium deficiency. Next to several forms of acquired rickets, there are also 3 hereditary forms (Brickley & Ives 2008; Waldron 2009). However, a recent study that assessed numerous modern clinical publications on cases of rickets, has shown that calcium deficiency very rarely plays a role in the development of rickets and that nutritional vitamin D deficiency was the cause for the majority of modern rickets cases (Mays & Brickley 2022). Vitamin D is normally absorbed through food intake whereas most foods contain at least some vitamin D. Oily fish, eggs, fortified milk and liver are considered to be major sources of vitamin D. The vitamin is then synthesised through ultraviolet sunlight on the skin. Therefore, next to malabsorption problems of the vitamin in the gut, which is usually caused by rather rare conditions, insufficient exposure to sunlight is the most common cause for the development of rickets (Brickley & Mays 2019). Since vitamin D is essential for maintaining the balance of calcium and phosphorous levels in the blood serum, a lack thereof leads to an imbalance of both minerals, which in return leads to bone resorption and deposition of patches of unmineralised osteoid. The most common skeletal manifestations of rickets, namely bowing of long bones and periosteal new bone deposition, are a result of deposition of unmineralised osteoid, which renders the bones soft and therefore bendy under stress (Ortner & Mays 1998; Mays *et al.* 2006; Brickley & Ives 2008; Waldron 2009; Brickley & Mays 2019). The typical diagnostic criteria for rickets are bowing of long bones of upper and lower extremities, diffuse periosteal new bone formation, thinning of the skull, swelling at the costochondral junction also called the rachitic rosary and cupped, enlarged, fraying and/or porous metaphyses (Waldron 2009). Several additional suggestive criteria have been listed in Brickley and Mays (2019), Brickley and Ives (2008), Ortner and Mays (1998) and Morrone et al. (2021). In itself, rickets is not fatal and supplementation of vitamin D generally stops the condition and the deformed bone starts remodelling (Brickley & Ives 2008; Waldron 2009). However, rickets might predispose to other illnesses such as pneumonia and in case of rickets caused by malabsorption, the malabsorption in itself might cause deadly secondary effects (Waldron 2009). Several studies have found an increase in rickets cases in urban industrialised areas, and as such the condition became more common in postmedieval times (Mays *et al.* 2006; Giuffra *et al.* 2015; Mays & Brickley 2018).

In the Knuedler sample, a total of 13 cases of potential rickets were observed, which corresponds to a total of 3.32% of all individuals buried on the premises of the Knuedler

monastery. This very low percentage suggests that overall provision of Vitamin D rich foods as well as exposure to sunlight were sufficient for the citizens of Luxembourg City that were buried in the Knuedler cemetery, hinting at overall good living conditions. However, it must be kept in mind that rickets can remodel completely over an individual's life and that for most individuals not all bones were preserved for assessment, which might lead to an underestimation of the condition. The vast majority was found in adults and the only indications were bowing of the long bones. Since bowing of long bones can occur in several other conditions as well, these need to be considered as differential diagnoses. The only confirmed case of rickets was observed in a 1-1.5-year-old infant buried in the cloister. Most cases (n=8) were observed in individuals buried after mid 17th century and only 5 were discovered among burials dating from before mid-17th century. This represents a slight increase in cases over time. Indeed, the frequency of rickets increased in the postmedieval period due to expanding urbanisation and the ensuing social and environmental changes such as shifts in infant feeding practices, food availability and air pollution (Mays *et al.* 2006; Giuffra *et al.* 2015; Mays & Brickley 2018). Most of the affected individuals (n=11) were buried in the cemetery and only 2 in the cloister area. If cemetery burials are considered to harbour individuals of lower socioeconomic standing than those buried in the cloister, this result would suggest that rickets was more common in individuals from lower social standing. Oftentimes rickets is coined as a disease of the poor, however, its presence in the middle class has also been attested (Giuffra *et al.* 2015). Compared to 19th century burials from St. Martin's church in Birmingham, where rickets was present among 12.3% of the burials, the values obtained from the Knuedler cemetery are very low and resemble rather those from Wharram Percy (2%) (Mays *et al.* 2006). Mays et al. (2006) explain this difference between the two sites by Birmingham citizen's limited exposure to sunlight due to dark and narrow alleys and air pollution and Wharram Percy's outdoorsy agricultural lifestyle. Therefore, it can be argued that the citizens of Luxembourg City that were buried in the Knuedler cemetery had generally good exposure to sunlight and good access to Vitamin D rich foods. The number of individuals (n=14) with potential rickets was similar to that found in Elwangen-Jagst for the late medieval (n=8) and early postmedieval (n=14) periods (Kairies 2021), suggesting that living conditions in both urban centres were similar in regards to Vitamin D provision.

Photo Table Rickets and Osteomalacia	
Figure 260 Anterior bowing in right Femur of Individual 2008-78/1038 indicative of possible residual rickets or osteomalacia	*Figure 261 Lateral bowing of Tibia R of individual 2008-78/820 indicative of possible residual rickets or osteomalacia*
Figure 262 Anteroposterior flattening of fibula R of individual 2008-78/350	*Figure 263 Medial angulation of the mandibular condyles in Individual 2008-78/1141 with rickets*
Figure 264 Plane enamel defect on unerupted M2 of Individual 2008-78/1141	*Figure 265 Flaring of distal metaphysis and coxa vara of the left femur and metaphyseal cortical thinning in Individual 2008-78/1141*

6.8.5 Paget's disease

6.8.5.1 Introduction

Paget's disease, also called Osteodystrophia deformans is a chronic and slow-progressing bone disorder that mainly affects older individuals (Aufderheide & Rodriguez-Martin 1998; Roberts & Manchester 2010) and remains largely asymptomatic (Aufderheide & Rodriguez-Martin 1998; Tuck *et al.* 2017). Modern clinical surveys have shown that Paget's disease is, after osteoporosis the second most common bone disorder among the elderly (Waldron 2009), especially among men (Mays 2010; Wade *et al.* 2011), although it seems rather rare in the archaeological record (Roberts & Manchester 2010). The exact aetiology of Paget's disease is still not known although some studies suggest that slow viral infections and/or genetic defects might lie at the root of the condition (Aufderheide & Rodriguez-Martin 1998; Roches *et al.* 2002; Brickley & Ives 2008; Mays 2010; Roberts & Manchester 2010). The disease process of Paget's disease can be divided into three phases: the osteolytic phase, the mixed phase and the sclerotic phase. In a first step, the condition leads to an increase of osteoclastic activity, which causes bone resorption and leads to hypervascularisation. The second phase, also called mixed phase, is marked by both bone formation and resorption. Bone formation and resorption are generally balanced but occur at a faster rate and at a more disorganised way than normal, leading to poorer bone quality. Towards the end of the mixed phase, bone production often surpasses resorption causing thickening of the bone structures. Finally, in the sclerotic phase, it comes to a complete cessation of osteoclastic activity with very minimal osteoblastic activity, leading to the formation of sclerotic bone and hypo vascularisation (Aufderheide & Rodriguez-Martin 1998; Brickley & Ives 2008). Clinically Paget's disease is divided into two forms, a mono- and a polyostotic form. The monostotic form affects only a single bone whereas the polyostotic form affects several bones or even the whole skeleton and the afore-described phases result in thickened and often rather brittle bones (Brickley & Ives 2008; Waldron 2009; Roberts & Manchester 2010).

6.8.5.2 Results and Discussion

A possible case of Paget's disease was also found in the Knuedler cemetery. Individual 2008-78/447, a mature (50-59y) male from Layer 2 buried in the cloister area was represented only by a cranium with mandible and the 7 cervical vertebrae. The rest of the postcranial skeleton remained in profile. The cervical vertebrae showed strong degenerative changes of the body (spondylosis deformans and pitting of the vertebral plates) between the 4th and 7th

vertebrae. The body and ramus of the mandible as well as the facial bones did not show any pathological changes. However, the individual suffered from strong periodontal disease throughout the maxilla and mandible. Additionally, the mandibula showed one small periapical lesion (granuloma) on the right and left sides and the maxilla presented 3 large coalesced periapical lesions (cysts) on the right and 2 large coalesced periapical lesions (cysts) on the left side. The individual suffered from significant antemortem tooth loss in both the mandible and maxilla. Except for one tooth with a profound caries lesion, none of the remaining teeth showed evidence of caries. Furthermore, several of the teeth were loose and showed evidence of root hypercementosis.

The skull vault of 2008-78/447 was broken into several larger fragments and was noticeably enlarged. The diploe appeared thickened, sclerotised and dense across the majority of the fragments, losing much of its sponge-like texture. However, the exposed bone appeared rather brittle and disorganised. Even though the bones were thickened, they were rather light in weight. No bone depositions were detected on the endo-or ectocranial side, but small vascular impressions could be seen endocranially (Figure 266, Figure 267). Altogether, the disorganised bone deposition and thickening of the cranial vault bones correspond well to the bone deposition processes described for Paget's disease. In the absence of postcranial bones, and since the facial bones and mandibula do not show obvious enlargement, it is impossible to determine whether the nature of the condition was mono- or polyostotic. Additionally, several studies have detected a link between hypercementosis of teeth and Paget's disease (Rao & Karasick 1982). All remaining loose teeth of this individual showed evidence of hypercementosis. Although Paget's disease remains asymptomatic in most cases (Tuck *et al.* 2017), complications such as bone fractures and deformities, bone and joint pain, deafness, tinnitus , hydrocephalus, malocclusion, tooth migration, tooth loss and severe periodontitis may occur (Falchetti *et al.* 2010; Seton *et al.* 2011; Michou & Orcel 2016). The majority of maxillary and mandibular teeth of individual 2016-082/447 had been lost antemortem and he suffered from severe periodontal disease. Even though all these factors correspond very well to the symptoms and complications of Paget's disease of bone, several differential diagnoses were considered that might have led to cranial thickening. Due to the age of the individual, all lesions affecting primarily children or younger adults were omitted from differential diagnosis. Fibrous dysplasia, Acromegaly, Hyperostosis frontalis interna and Familial expansile osteolysis were retained as possible differential diagnoses.

Fibrous dysplasia is a developmental disorder in which fibrous tissue replaces bone formed by mature osteoblasts (Chapurlat & Meunier 2000; Waldron 2009), which can lead to

disfiguring lesions on bones. However, on the skull, these lesions often affect only one bone instead of the whole vault (Cai *et al.* 2012), which is not the pattern found in the skull of 2016-082/447. Furthermore, fibrous dysplasia is rare in people over 40 years.

Acromegaly is characterised by a deformed and enlarged mental and occipital protuberance as well as supraorbital tori. These deformations are the result of excessive enchondral bone deposition after skeletal maturity due to excess growth hormone caused by a pituitary tumour (Bartelink *et al.* 2014). This pattern of enlargement was not observed in the analysed individual.

Hyperostosis frontalis interna is characterised by bilateral nodular bone growths on the endocranial surface of the frontal bone but may also affect the endocranial surface of other bones of the cranial vault (Waldron 2009). No bone growths were observed on the endocranial side of the frontal bone or any other cranial vault bones in this individual and bone thickening was also not restricted to the frontal bone but affected also the parietals and occipital. Furthermore, the condition is much more common in females (Brickley & Ives 2008; Waldron 2009).

Familial expansile osteolysis is a rare genetic condition resulting in the production of coarse trabecular bone with a thin cortex. However, the disorder is characterised by asymmetric lytic lesions as well, whose remodelling results in the deposition of the coarse trabecular bone (Osterberg *et al.* 1988; Kesterke & Judd 2019). Onset of the condition is usually already in childhood with first clinical symptoms also manifesting by then. In teeth the condition leads to resorption of roots and pulpitis (Osterberg *et al.* 1988), which was not present in the teeth of the analysed individuals.

6.8.5.2.1 Conclusion

After reviewing several possible differential diagnoses for the lesions observed in the skull of 2016-082/447 and considering especially the age and sex of the individual, a diagnosis of Paget's disease seems the most likely diagnosis.

Paget's disease	
	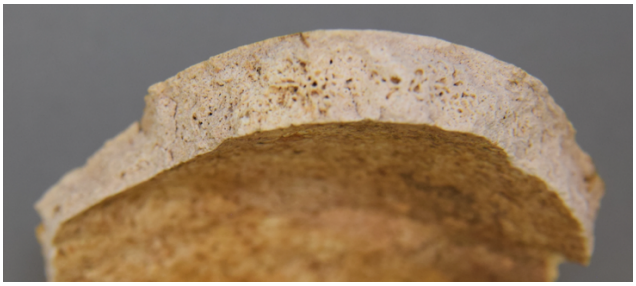
Figure 266 Endocranial view of thickened parietal bones (posterior part of left and right parietal with endocranially obliterated sagittal suture in the center)	*Figure 267 Close-up of thickened skull vault on parietal R showcasing loss of sponge-like structure of the diploe*

6.9 Dental disease

Since the tooth crown is the hardest substance of the human body, teeth are usually among the best-preserved parts in archaeological contexts (Roberts & Manchester 2010). Since they are directly associated with food intake, they can provide a wealth of information on the foods consumed and their preparation. Furthermore, they can also inform about cultural or dentistry practices and oral hygiene, as well as general episodes of stress that the body has been subjected to during the course of life (Waldron 2009; Roberts & Manchester 2010; Grupe *et al.* 2015). In the following chapter, dental diseases of the Knuedler population were examined in order to make inferences about their nutritional status and oral hygiene practices. Furthermore, the results obtained were compared to contemporaneous sites.

6.9.1 Dental calculus

6.9.1.1 Introduction

In absence of oral hygiene, a gelatinous film containing food debris, salivary proteins as well as secretions from a number of bacteria, starts building up on the tooth surfaces, primarily in protected areas such gingival crevices, the interdental space and in dental fissures (Hillson 1996; Caselitz 1998). This film, called plaque, is considered to be at the origin of several dental diseases. If not properly removed, dental plaque starts mineralising at the layer closest to the tooth surface, forming a hard grey-brownish layer on the tooth surface called dental calculus (Hillson 1996; Caselitz 1998; Waldron 2009; Roberts & Manchester 2010). The deposition and build-up of plaque and therefore the formation of calculus is favoured in an alkaline

environment, which is oftentimes associated with a diet rich in proteins. In fact, the consumption of high protein products increases urea levels in blood and thus also in oral fluids such as saliva. Bacteria in the plaque metabolise the urea that they source from the oral fluids into ammonia, which leads to calculus mineralization (Hillson 1979, 1996; Lieverse 1999). Since the minerals deposited during calculus formation are partially derived from plaque fluid, but mostly from saliva, calculus is found more frequently in areas closest to the salivary glands, which means at the buccal side of maxillary molars and on the lingual side of mandibular incisors (Hillson 1996; Roberts & Manchester 2010). However, the causes of calculus formation remain under debate. While protein consumption definitely promotes calculus formation, other dietary patterns such as a diet rich in carbohydrates, or an increased mineral content in drinking water etc., but also different cultural practices and the individual composition of the oral fauna can contribute to or facilitate the formation of calculus (Lieverse 1999). Two different kinds of calculus can be distinguished on the tooth, which vary in their respective degrees of mineralisation (Hillson 1996). Supra-gingival calculus is attached to the tooth crown and usually of a grey-whitish-brown colour, sub-gingival calculus only occurs after recession of the gums on the root surface of teeth and is usually greenish or blackish in colour (Hillson 1996; Roberts & Manchester 2010).

6.9.1.2 Methods

Dental calculus was recorded for all teeth in the dentition, including loose teeth and teeth in sockets. Erupting teeth were excluded from the analysis. Analyses were carried out separately for adults and subadults. No distinction was made within the subadult category between the permanent and the deciduous dentition.

For both adult and subadult individuals, the same three-point recording system based on Brothwell (1981) was used (Table 93 and Figure 268).

True frequencies (by teeth) and crude frequencies (by individuals) of calculus occurrence were calculated for the whole sample but also differentiated by sex, age, burial location and burial layer.

Table 93 Scoring system for dental calculus based on (Brothwell 1981)

Score	Description
0	No calculus visible on tooth
1	Small rim of calculus mainly at the cemento-enamel junction
2	Calculus covers <50% of the tooth surface
3	Calculus covers >50% of the tooth surface

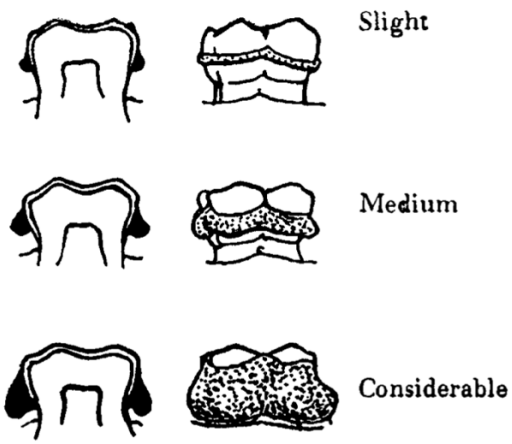

Figure 268 Illustration of the scoring system for calculus intensity after Brothwell 1981 (taken from Hillson 1996 reproduced from Brothwell 1981)

6.9.1.3 Results

6.9.1.3.1 Adults

A total of 2641 teeth were eligible for examination belonging to a total of 164 individuals. 395 anterior teeth (I1-C) and 179 posterior teeth (P3-M3) were lost post-mortem.

6.9.1.3.1.1 True frequency

The calculus true frequency rates describe the presence of calculus relative to all teeth that could be scored. Overall, with 88.87% of all adult teeth showing traces of calculus formation, calculus frequency is very high in this population from Luxembourg City. A significant difference in calculus occurrence could be detected among the sexes with males (91.48%) showing significantly more teeth with calculus than females (82.06%). Both males and females also showed significant differences between burial locations, with those buried in the cloister (84.51%) showing less affected teeth than those buried in the cemetery (91.09%). The same trend, with cemetery burials showing more calculus covered teeth than cloister burials and males suffering from more calculus covered teeth than women, was also observed within Layer 1 and 2, but in females of Layer 1 it was not significant. Overall and in males and females, the

younger Layer 1 (86.43%) also shows significantly less than those from Layer 2 (90.95%). A further correlation with age could also be detected overall and for males and females. Young adults (79.95%) had generally less teeth affected by dental calculus than adults (93.08%) matures I (95.33%) and matures II (93.40%), and among seniles (77.98¨%) the cases drop again. This might be related to the fact that seniles often suffered also from other dental diseases which might have led to a complete destruction or loss of many teeth and therefore loss of calculus as well. (Table 94)

6.9.1.3.1.2 Crude frequency

Calculus crude frequency rates describe the percentage of individuals affected by dental calculus relative to all individuals examined. The Knuedler population had a crude calculus frequency 98.78%, with males (99.09%) being slightly more affected than females (98.04%). None of the group comparisons for crude frequencies showed any significant differences but they follow roughly the same trends as the true frequencies. Overall, it must be noted that calculus frequencies, true and crude are very high in this sample. Nearly all individuals regardless of age showed dental calculus residue on several teeth. Importantly though, calculus severity was generally really low, and the majority of the calculus remnants were just small traces in the interdental spaces or directly at the cemento-enamel junction. Very rarely a complete rim of calculus was observable. Two possible explanations for this must be considered: either calculus formation was generally rather low but widespread, or most of the deposits were lost post-mortem. Figure 269 and Figure 270 show the distribution of calculus severity scores by age group overall and differentiated for males and females. It can be clearly noticed that mild calculus makes up most of the cases, but the proportion of moderate calculus deposits is also fairly prominent. However, really strong deposits occur only very rarely, and more often so in males. However, while overall calculus rates seem to first slightly increase and then decrease again in old age, calculus severity shows a slight but steady increase with age. No noteworthy differences in severity were observed between the sexes, burial locations, and burial layers. (Table 94)

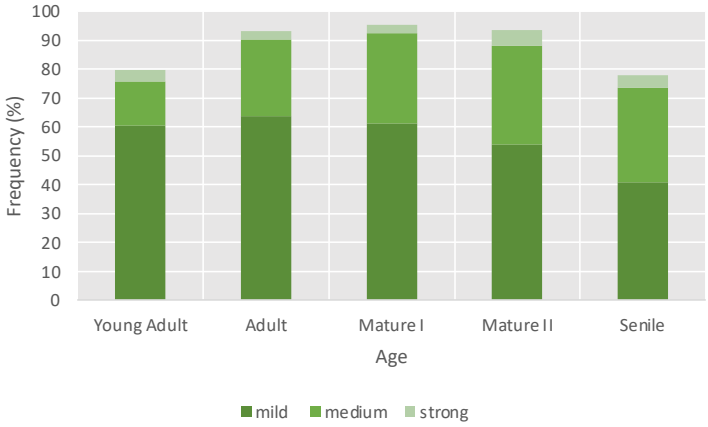

Figure 269 Distribution of dental calculus infestation by age

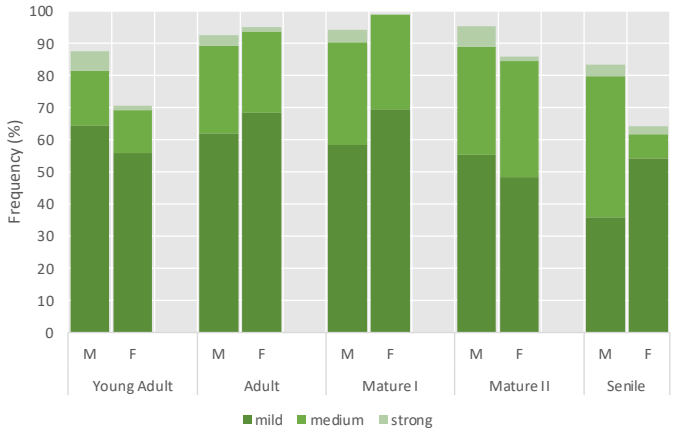

Figure 270 Distribution of dental calculus infestation by age for males and females

Table 94 Summary and test results for adult calculus true and crude frequency

Adults			**Calculus**					
Factor		**variable**	**True frequency**			**Crude frequency**		
			n	**pres.**	**p-value**	n	pres.	p-value
Total			2641	2347 (88.87%)		164	162 (98.78)	
Sex		F	758	622 (82.06)	**<0.0001**	51	50 (98.04%)	0.5345
		M	1855	1697 (91.48%)		110	109 (99.09%)	
Age	All	Young Adult	479	382 (79.75%)	**<0.0001**	24	24 (100%)	0.3762
		Adult	795	740 (93.03%)		42	42 (100%)	
		Mature I	407	388 (95.33%)		28	27 (96.43%)	
		Mature II	576	538 (93.40%)		38	38 (100%)	
		Senile	386	301 (77.98%)		31	30 (96.77%)	
	F	Young Adult	217	153 (70.51%)	<**0.0001**	13	13 (100%)	0.3137
		Adult	203	193 (95.07%)		11	11 (100%)	
		Mature I	98	97 (98.98%)		7	7 (100%)	
		Mature II	128	110 (85.94%)		11	11 (100%)	
		Senile	120	77 (64.17%)		9	8 (88.89%)	
	M	Young Adult	262	229 (87.40%)	**<0.0001**	11	11 (100%)	0.4771
		Adult	592	547 (92.40%)		31	31 (100%)	
		Mature I	309	291 (94.17%)		21	20 (95.24%)	
		Mature II	435	415 (95.40%)		26	26 (100%)	
		Senile	251	209 (83.27%)		20	20 (100%)	

Adults		Calculus						
Factor		variable	True frequency			Crude frequency		
			n	pres.	p-value	n	pres.	p-value
Location	All	Cemetery	1750	1594 (91.09%)	**<0.0001**	112	110 (98.21%)	1.0000
		Cloister	891	753 (84.51%)		52	52 (100%)	
	F	Cemetery	538	455 (84.57%)	**0.0048**	40	39 (97.50)	1.0000
		Cloister	220	167 (75.91%)		11	11 (100%)	
	M	Cemetery	1206	1133 (93.95%)	**<0.0001**	71	70 (98.59%)	1.0000
		Cloister	649	564 (86.90%)		39	39 (100%)	
Distance to Church	All	Cloister	891	753 (84.51%)	**<0.0001**	52	52 (100%)	0.0608
		Close	434	411 (94.70%)		29	27 (93.10%)	
		Mid	851	762 (89.54%)		54	54 (100%)	
		Far	465	421 (90.54%)		29	29 (100%)	
	F	Cloister	220	167 (75.91%)	**0.0008**	11	11 (100%)	0.1765
		Close	116	102 (87.93%)		9	8 (88.89%)	
		Mid	266	212 (79.70%)		21	21 (100%)	
		Far	156	141 (90.38%)		10	10 (100%)	
	M	Cloister	649	564 (86.90%)	**<0.0001**	39	39 (100%)	0.3455
		Close	312	303 (97.12%)		19	18 (94.74%)	
		Mid	585	550 (94.02%)		33	33 (100%)	
		Far	309	280 (90.61%)		19	19 (100%)	
Layer	All	1	1216	1051 (86.43%)	**0.0002**	71	70 (98.59%)	1.0000
		2	1425	1296 (90.95%)		93	92 (98.92%)	
	F	1	301	235 (78.07%)	**0.0203**	18	18 (100%)	1.0000
		2	457	387 (84.68%)		33	32 (96.97%)	
	M	1	893	794 (88.91%)	**0.0001**	51	50 (98.04%)	0.4636
		2	962	903 (93.87%)		59	59 (100%)	
Layer 1	All	Cemetery	791	706 (89.25%)	**0.0001**	45	44 (97.78%)	1.0000
		Cloister	425	345 (81.18%)		26	26 (100%)	
	F	Cemetery	187	147 (78.61%)	0.7732	12	12 (100%)	1.0000
		Cloister	114	88 (77.19%)		6	6 (100%)	
	M	Cemetery	604	559 (92.5559	**<0.0001**	33	32 (96.97%)	1-0000
		Cloister	289	235 (81.31%)		18	18 (100%)	
Layer 2	All	Cemetery	959	888 (92.60%)	**0.0019**	67	66 (98.51)	1.0000
		Cloister	466	408 (87.55%)		26	26 (100%)	
	F	Cemetery	351	308 (87.75%)	**0.0009**	28	27 (96.43%)	1.0000
		Cloister	106	79 (74.53%)		5	5 (100%)	
	M	Cemetery	602	574 (95.35%)	**0.0132**	38	38 (100%)	1.0000
		Cloister	360	329 (91.39%)		21	21 (100%)	

6.9.1.3.1.3 Calculus infestation by tooth

Figure 271 represents calculus intensity for each tooth of the left and right mandible (Lower) and maxilla (Upper). As expected, calculus is most severe on the molars in the maxilla and on the incisors and canines in the mandible. These regions are generally most affected by dental calculus due to their close proximity to the salivary glands, which are situated under the tongue and thus close to the lingual side of the front teeth and in the upper area of the cheek, at the hight of the buccal side of the upper molars (Hillson 1996; Roberts & Manchester 2010). The same pattern was also detected by Trautmann (2012) on the skeletal remains from Grevenmacher, a medieval rural town in Luxembourg.

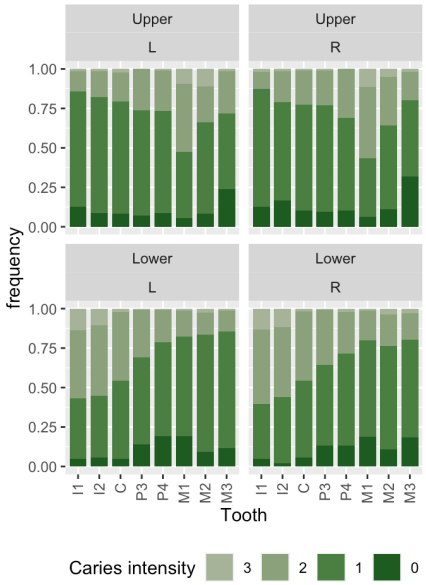

Figure 271 Distribution of dental calculus infestation for the upper and lower jaw as well as right and left body side

6.9.1.3.2 Subadults

Regarding subadults, a total of 44 individuals or 642 permanent and deciduous teeth were eligible for analysis of calculus occurrence. 17 deciduous (DI1-DC) and 51 permanent anterior teeth (I1-C), as well as 7 deciduous (DP3-4) and 9 permanent posterior teeth (P3-M3) were lost post-mortem.

6.9.1.3.2.1 True frequency

Among subadults, caries rates were also fairly high at 52.96%. A clear and significant correlation with age in calculus formation could be observed, with infans I at 16.44% showing by far the lowest percentage of teeth affected by dental calculus, followed by infans II with 53.40% of cases and finally juveniles at 88.94% of affected teeth. Thus, juveniles already experienced about the same levels of calculus infestation as adults. Children from Layer 2 (55.17%) had slightly more calculus covered teeth than those from Layer 1 (49.15%) but the difference was not statistically relevant. However, the difference observed between the burial locations, namely children from the cemetery (49.15%) showing lower calculus rates than those from the cloister (63.55%), was of statistical significance. When investigating differences between burial locations separately for the two layers however, in Layer 2, children from the cloister also had more calculus infested teeth than children from the cemetery but the opposite trend was observed in Layer 1. Overall, caries intensity was rather low in children, with 89.92% (n=348) of the cases being classified as light, 8.27% (n=32) as medium and only 1.81% (n=7)

as severe. Six of the severe cases of dental calculus could be attributed to two juveniles from the cloister and one to a juvenile from the cemetery. (Table 95)

6.9.1.3.2.2 Crude frequency

Crude calculus frequencies among children are actually similar to the true frequency rates and follow the same trends. The overall percentage of individuals with dental calculus amounts to 61.36%. The remaining distributions mirror the trends already observed in the true frequencies but the differences between the groups are not statistically significant, with the exception of age. Infans I (26.32%) were significantly less affected by dental calculus than infans II (81.82%) and juveniles (92.86%). (Table 95)

Table 95 Summary and test results for subadult calculus true and crude frequency

Subadults		**Calculus**					
Factor	**variable**	**True frequency**			**Crude frequency**		
		n	**presence**	**p-value**	**n**	**presence**	**p-value**
Total		642	340 (52.96%)		44	27(61.36%)	
Age	Infans_I	225	37 (16.44%)	**<0.0001**	19	5 (26.32%)	**0.0001**
	Infans_II	191	102 (53.40%)		11	9 (81.82%)	
	Juvenile	226	201 (88.94%)		14	13 (92.86%)	
Location	Cemetery	439	211 (48.06%)	**0.0003**	30	16 (53.33%)	0.1093
	Cloister	203	129 (63.55%)		14	11 (78.57%)	
Layer	1	236	116 (49.15%)	0.1406	15	8 (53.33%)	0.4314
	2	406	224 (55.17%)		29	19 (65.52%)	
Layer 1	Cemetery	146	61 (41.78%)	**0.0039**	9	4 (44.44%)	0.6084
	Cloister	90	55 (38.14%)		6	4 (66.67%)	
Layer 2	Cemetery	293	150 (51.19%)	**0.0095**	21	12 (57.14%)	0.2008
	Cloister	113	74 (65.49%)		8	7 (87.50%)	

6.9.1.4 Discussion and Conclusion

Calculus forms as a result of mineralisation of dental plaque in an oral environment with low pH-levels. Protein rich foods can cause pH-levels in the oral cavity drop. This is beneficial in so far that demineralisation processes of the tooth enamel started during phases of high pH-levels will be halted and reversed, thus reducing the risk for developing dental caries lesions. However, the higher mineral content in the saliva also promotes the mineralisation of the dental plaque leading to calculus formation (Hillson 1996; Caselitz 1998; Lieverse 1999). As such, a diet rich in protein and dairy products are often linked to high calculus rates and should reduce risk of caries infection. However, caries and calculus often occur at the same time in human populations, meaning that the process described is not as straightforward (Hillson 1996).

Calculus true and crude frequency were quite high in the Knuedler sample, which might be suggestive of a high protein diet however, caries rates were equally high. But this pattern was

not only observed for the Knuedler cemetery. Many European sites also showed cooccurrence of caries and calculus at fairly high frequencies (Whittaker & Molleson 1996; Pētersone-Gordina & Gerhards 2012; Trautmann 2012; Miliauskiene & Jankauskas 2015; Roßbach 2015). Trautmann (2012) suggests that this pattern could indicate a diet both high in carbohydrates and proteins, paired with bad oral hygiene. Indeed, calculus build-up could be easily prevented by regularly removing plaque deposits before the mineralisation process begins. Once plaque has started to mineralise, it sticks very firmly to the teeth and removal becomes very difficult without professional dentistry equipment (Hillson 1996). Although many teeth and individuals were affected by calculus deposits, the deposits were predominantly very small and restricted to slight spots mainly close to the gingival line or in interdental spaces. In fact, medium and strong caries deposits only occurred in 31.77% of teeth. However, 71.95% of adult individuals had one or more teeth affected by moderate and strong calculus deposits. This indicates that either not all teeth are affected equally by calculus build-up but could also be indicative of the fact that calculus deposits are often lost during the preparation and recovery of human remains (Hillson 1996). Subadult calculus frequency (61.63%) is lower than that of adults in the Knuedler cemetery. Like the lower caries rates, this was expected since children's teeth have not been exposed to the alkaline environment as long as adults teeth have (Kairies 2021). Compared to other European and Luxembourgish sites, calculus rates of subadults in Luxembourg City were at the higher end of the spectrum, suggesting either a protein-rich diet already in childhood or bad oral hygiene practices already among children. However, calculus rates were still very similar to other contemporary sites and by no means out of the normal range. Children from 18th century Spitalfields cemetery in London for instance had a calculus frequency of 52%, those from Ellwangen-Jagst one between 22.60% and 44.19% and those from Grevenmacher 49.1% (Table 96). In both Grevenmacher and the Knuedler cemetery, infans I was least affected, and the frequency of calculus increased with age, with juvenile calculus frequency already mirroring that of adults.

Table 96 Calculus distribution across late medieval and postmedieval Europe

Calculus frequency in Europe							
Time period	**Site**	**Country**	**Type of settlement**	**Socio-economic status**	**Calculus true frequency %**	**Calculus crude frequency %**	**Publication**
1812 AD	Napoleonic mass grave	Lithuania	urban	soldiers		100.00	Palubeckaitė (2006)
5th-18th C	St Armual Kreuzgang Saarbrücken	Germany		mixed	89.10	100.00	Geber (2006)

Calculus frequency in Europe							
Time period	**Site**	**Country**	**Type of settlement**	**Socio-economic status**	**Calculus true frequency %**	**Calculus crude frequency %**	**Publication**
mid-17th-18th C	Knuedler	Luxembourg	urban		90.95	98.92	Kremmer (hic)
14th-mid-17th C	Knuedler	Luxembourg	urban		86.43	98.59	Kremmer (hic)
12th-17th C	St. Esprit	Luxembourg	urban	mixed		98.40	Rehbach u. Bis-Worch (2006), Nothwang et al. (2006) Rehbach et al. (2007) Rehbach u. Nothwang (2007) Rehbach (2008) Rehbach u. Notwang (2009)
12th-14th C	Grevenmacher	Luxembourg	rural		86.70	96.85*	Trautmann (2017)
11th-15th C	Givenich	Luxembourg	rural	upper class		96.30	Rehbach et al. (2009) Weidig et al. (2009)
17th-18th C	Jelgava Church	Lativia	urban	upper class		96.00*	Pētersone-Gordina et al. (2012)
18th C	Spitalfields	England	urban	Hospital		90.50	Whittaker & Molleson (1996)
Late medieval	Ellwangen-Jagst	Germany	urban			86.97*	Kairies (2021)
Early postmedieval	Ellwangen-Jagst	Germany	urban			82.85*	Kairies (2021)
late 16th-early 18th C	Grund/ Wenzelsmauer	Luxembourg	urban	soldiers		78.30	Trautmann u. Trautmann (2011)
10th-18th C	Emden	Germany	urban	upper/middle class		63.90	Stech (2009)
14th-16th C	Several orthodox churches	Serbia	rural			> 50.00	Srejić (2001)
17th-19th C	Gothenburg, Nya Lödöse	Finland	urban			49.00	Vilkama et al. (2016)
16th-18th C	Koprivno	Croatia	urban		94.60		Šlaus and Artamić (2017)
16th-17th C	Trakai churchyard	Lithuania	urban		85.70		Miliauskienė and Jankauskas (2015)
16th-17th C	Trakai church	Lithuania	urban	upper class	87.10		Miliauskienė and Jankauskas (2015)
12th-17th C	Ihlow	Germany	rural	monastic	93.10		Timmermann (2009)

* = average

6.9.2 Caries

6.9.2.1 Introduction

Together with periodontal diseases, caries is one of the most common infectious diseases of the oral cavity (Touger-Decker & van Loveren 2003). Caries is a progressive and irreversible bacterial infection, that starts in the dental plaque and works its way further into the tooth, through the enamel and dentin until the pulp chamber, if left untreated (Hillson 1996; Caselitz

1998). Bacteria in the dental plaque are responsible for the formation of carious lesions (Caselitz 1998; Roberts & Manchester 2010). The bacteria in the plaque metabolise food debris that gets stuck in between and on teeth and, depending on the nature of the food items, either produce alkaline waste products or lactic acids (Caselitz 1998). This way, the pH-level of the oral cavity and of the fluid of the dental plaque rises and falls during the day. The metabolization of carbohydrates causes the production of lactic acids, which then start demineralising the enamel of the tooth crown or the cementum. If this process overweighs the production episodes of alkaline waste products which raise pH-levels, it will lead to a prolonged decrease in pH-levels in the oral cavity, and the demineralised tissue cannot recover anymore (Hillson 2008). Once the demineralisation process has started, it is usually helped along by a host of bacteria of the oral cavity (Caselitz 1998). Certain areas of the tooth are more predisposed to developing caries than others. As such the interdental spaces and dental fissures are preferred locations for caries formation since food often gets stuck there. Dental caries, if left untreated, can eventually lead to other pathologies of the oral cavity such as periodontal disease, periapical abscesses and even tooth loss (Hillson 1996, 2008; Waldron 2009). The role of sugar in the formation of dental caries has been well established in a study by Gustafsson et al. (1954). Three groups of children were fed different amounts of sugars at different frequencies throughout the day. The results of that study showed that not only the quantity but also the frequency of sugar consumption increased caries formation (Gustafsson *et al.* 1954; Hillson 1996). The involvement of starches in the formation of caries has also been considered but its relation is less clear. (Hillson 1996; Roberts & Manchester 2010) In themselves, starchy products do not seem to be cariogenic but in combination with sugars they are highly so. Proteins and fats, especially milk and dairy products on the other hand are thought to rather protect against caries formation by coating the teeth and due to their high calcium and phosphorous content (Hillson 1996). In prehistoric times, the most common sources of carbohydrates in the diet were cereals and their processed products such as flour and bread. Although sugar was already available in Europe since the high middle-ages and its production and distribution increased vastly during the 16th century, it was still a luxury product reserved for the rich. It is only in the 18th century where sugar production became cheaper and thus sugar became more affordable and widely available (Smith 2015; Eggleston 2019), which led to a stark increase in caries and related dental disease during the 18th century (Corbett & Moore 1976; Palubeckaitė *et al.* 2006). Before the widespread use of sugar, foods were generally sweetened with honey (Kairies 2021). But sugars and grains are not the only sources of carbohydrates in the diet, as some vegetables, especially legumes also contain certain amounts

of it (Slavin 2013). Therefore, high prevalence rates in dental caries do not necessarily indicate a diet high in sugar but can also hint at a diet high in grains and/or vegetables.

6.9.2.2 Methods

Although small localised staining can be the first indication of caries development (Hillson 1996), these stains are difficult to distinguish from regular tooth staining due to other environmental factors. Therefore, stains were recorded separately in this study but only lesions which showed already clear surface modifications were included in the analysis. The recording system follows that established by Trautmann (2012) presented in Table 97.

Table 97 Scoring system for dental caries severity after Trautmann 2012

Score	Description
0	Tooth present but no caries visible
1	superficialis: small cavity on the surface only concerning the dental enamel
2	media: the cavity reaches the dentine
3	profunda: the cavity captures over 2/3 of the dentine layer and extends in direction of the pulpa

In a first step, the distribution of caries frequency by tooth was analysed visually via percentage stacked bar charts. Next, Pearson's chi squared tests were conducted to determine statistically significant differences between the sexes, age groups, burial layers and locations for both true and crude caries frequencies. True caries frequencies are also referred to as caries infestation and crude frequencies as frequency. The exact position of caries lesions on a tooth were also recorded. An evaluation was only conducted for teeth with a single caries lesion. Only fully erupted or erupting teeth that already penetrated into the oral cavity were used in the evaluations.

Finally, significant differences in caries infestation were graphically illustrated using bar charts and including also true frequencies of caries intensity. Adults and subadults were analysed separately but among subadults, no distinction was made between the permanent and deciduous dentition nor between males and females.

6.9.2.3 Results

6.9.2.3.1 Adults

Of all 323 adult individuals, 165 had teeth preserved for the analysis. Therefore, a total of 2766 teeth were analysed. 395 anterior teeth (I1-C) and 179 posterior teeth (P3-M3) were lost post-mortem.

6.9.2.3.1.1 True frequency

True frequency of dental caries expresses the percentage of all teeth affected by caries lesions against all scoreable teeth in the sample. Overall, 25.02% of teeth were affected by carious lesions. Whilst males displayed slightly less carious teeth (24.40%) than females (26.24%) the difference between the sexes was not statistically significant. However, within the different burial locations and layers, different patterns of dental caries distribution could be observed. Overall, people buried in the cloister (20.57%) displayed significantly less caries affected teeth than those buried in the cemetery (27.21%) (Figure 272). This trend was observable in both sexes and more pronounced in females. When looking at differences between burial layers, overall people from the younger Layer 1 (23.36%), had slightly less caries infected teeth than those from the older Layer 2 (26.45%) but the difference is not statistically relevant. When comparing the sexes though, women did show a significant difference in true caries frequencies (L1: 22.22%; L2: 28.93%) but men did not (L1: 23.35%; L2: 25.40%) although the same trend is observable.

Since there were significant differences between the layers at least in women, differences in true frequencies by burial location and by sex were also checked for Layer 1 and 2 separately. Indeed, overall, within Layer 2, no statistically significant differences could be observed between cloister and cemetery burials but the same trend with cloister burials having less teeth affected was evident. And whilst no relevant differences were detected between burial locations among men from Layer 2 (cemetery: 24.76%; cloister: 26.47%), females showed highly significant differences (cemetery: 32.36%; cloister: 16.82%). Within Layer 1 however, the pattern was reversed, with men showing highly significant differences between cloister (13.56%) and cemetery (27.84%) burials but not females, although the same trend was still evident (cemetery: 24.04%; cloister: 18.97%) Since burial location seems to have played overall a significant role in caries true frequency distribution, it was also tested whether distance to church indicated any relevant differences in caries distribution on the cemetery relative to the church. While the overall comparison showed a significance in distributions,

post-hoc tests revealed that, while in females all caries true frequency distributions were significantly different from each other, with people buried inside and close to the cloister complex showing the lowest caries infection rates, males only displayed a significant difference between people buried in the cloister and those buried in the middle of the cemetery. In both males and females, people buried in the cemetery displayed the highest caries infestation rates. Since the separation into zones on the cemetery was only undertaken by the author and is therefore rather arbitrary, these results will not be taken into consideration for further interpretation.

The strongest correlation in dental caries true frequency distribution however was detected between the different age groups, with caries true frequency increasing steadily and strongly with old age until the category of mature I individuals and declining again over mature II and further in seniles. The same trend was visible in men and in women, but statistical significance was only achieved in women. The decline in dental caries in seniles might at first glance seem surprising, however, actual dental caries rates mighty be obscured by antemortem tooth loss, which is often caused by advanced caries lesions (Figure 273, Figure 274). Seniles being the oldest age group might have less detectable caries lesions on their teeth because the majority of their affected teeth has already been lost in life. Furthermore, it becomes apparent that in both males and females, caries severity also starkly increases with age. Overall, caries lesions in this sample were also rather strong, with the combined category of medium and profound lesions being nearly as frequent as superficial ones. All results for group comparisons of caries true frequency can be found in Table 98.

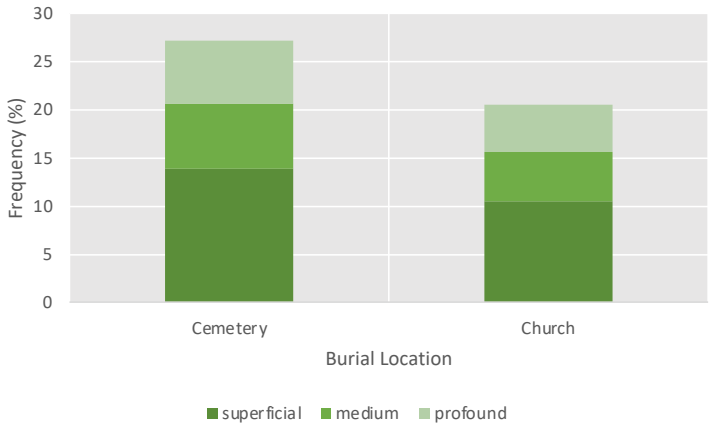

Figure 272 Distribution of caries infestation by burial location

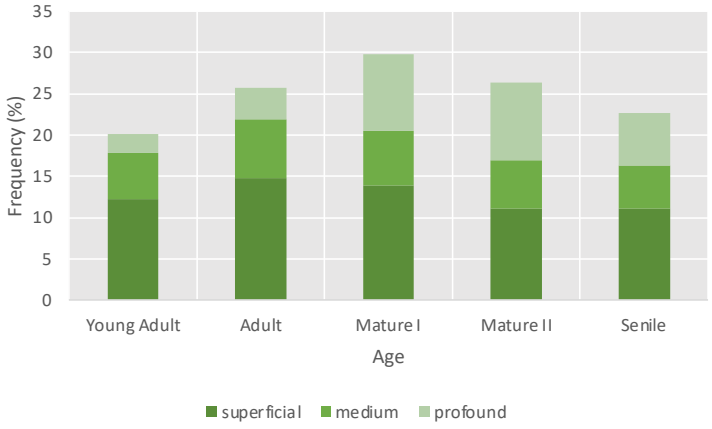

Figure 273 Distribution of caries infestation by age

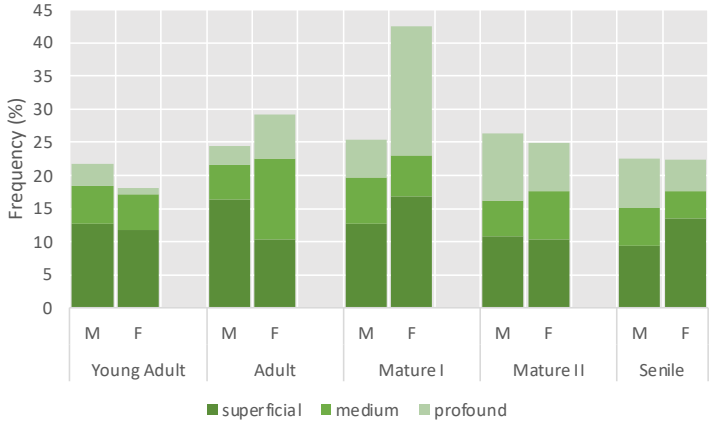

Figure 274 Distribution of caries infestation for males and females by age

6.9.2.3.1.2 Crude frequency

Crude frequency rates compare the number of individuals infected with any amount of caries lesions to all individuals in the sample that could be analysed for caries occurrence. A total of 83.03% individuals were affected by dental caries. 84.68% of males and 80.39% of females had dental caries. Although the difference between the sexes shows no statistical significance, it is evident that males were more often affected by the disease than women. This finding is contrary to that of true frequencies, meaning that, while more males were affected, females had on average more carious lesions per individual. No significant differences could be detected between the burial locations and layers anymore, although overall trends remain the same as in true frequency distributions. More people buried in the cemetery (84.07%) showed dental caries than people buried in the cloister (80.77%) and overall people from Layer 1 (79.91%) were less affected by caries than those from Layer 2 (86.02%). This overall trend was however only caused by males. Males from Layer 1 (76.92%) were significantly less affected by caries than males from layer 2 (91.53%), but in females the trend was reversed (L1: 83.33%; L2:

78.79%) and not relevant. Within Layer 2, men and women buried in the cloister showed higher cases of caries infection than those buried in the cemetery and within Layer 1 this trend was reversed. However, none of these differences reached any statistical significance. A significant relation to age was not detected in crude frequency rates but the trend of caries infections increasing with age is still apparent in both men and women. (Table 98) When considering only medium and profound caries lesions, crude frequency remains fairly high at 67.27%. 73.08% of people buried in the cloister experienced medium and strong caries lesions and 64.6% of people from the cemetery had strong and medium caries lesions. At 65.27% crude caries frequency of strong and medium lesions was slightly lower in Layer 1 than in Layer 2 (68.62%). When considering only strong and medium caries lesions, at 70.27%, men were clearly more affected than women at 60.78%.

Table 98 Summary and test results for adult caries true and crude frequency

Adults			**Caries**					
Factor		**variable**	**True frequency**			**Crude frequency**		
			n	**pres.**	**p-value**	n	pres.	p-value
Total			2766	692 (25.02%)		165	137 (83.03)	
Sex		F	808	212 (26.24%)	0.3119	51	41 (80.39%)	0.4959
		M	1930	471 (24.40%)		111	94 (84.68%)	
Age	All	Young Adult	487	98 (20.12%)	**0.0095**	24	20 (83.33%)	0.2824
		Adult	813	209 (25.71%)		42	37 (88.10%)	
		Mature I	433	129 (29.79%)		28	23 (82.14%)	
		Mature II	631	166 (26,31%)		39	35 (89.74%)	
		Senile	397	90 (22.67%)		31	22 (70.97%)	
	F	Young Adult	221	40 (18.10%)	**0.0001**	13	11 (84.62%)	0.6942
		Adult	213	62 (29.11%)		11	8 (72.73%)	
		Mature I	113	48 (42.48%)		7	6 (85.71%)	
		Mature II	136	34 (25.00%)		11	10 (90.91%)	
		Senile	125	28 (22.4%)		9	6 (66.67%)	
	M	Young Adult	266	58 (21.80%)	0.6323	11	9 (81.82%)	0.3427
		Adult	600	147 (24.50%)		31	29 (93.55%)	
		Mature I	320	81 (25.31%)		21	17 (80.95%)	
		Mature II	482	127 (26.35%)		27	24 (88.89%)	
		Senile	257	58 (22.57%)		20	15 (75.00%)	
Location	All	Cemetery	1852	504 (27.21%)	**0.0001**	113	95 (84.07%)	0.5997
		Cloister	914	188 (20.57%)		52	42 (80.77%)	
	F	Cemetery	585	172 (29.40%)	0.0009	40	32 (80.00%)	1.0000
		Cloister	223	40 (17.94%)		11	9 (81.82%)	
	M	Cemetery	1261	332 (26.33%)	**0.0069**	72	63 (87.59%)	0.2631
		Cloister	669	139 (20.78%)		39	31 (79.49%)	
Distance to Church	All	Cloister	914	188 (20.57%)	**<0.0001**	52	42 (80.77%)	**0.0071**
		Close	466	100 (21.46%)		30	19 (63.33%)	
		Mid	905	287 (31.71%)		54	50 (92.59%)	
		Far	481	117 (24.32%)		29	26 (89.66%)	
	F	Cloister	223	40 (17.94%)	**<0.0001**	11	9 (81.82%)	**0.0127**
		Close	119	16 (13.45%)		9	4 (44.44%)	
		Mid	305	116 (38.03%)		21	20 (95.24%)	
		Far	161	40 (24.84%)		10	8 (80.00%)	

Adults		Caries						
Factor		variable	True frequency			Crude frequency		
			n	pres.	p-value	n	pres.	p-value
	M	Cloister	669	139 (20.78%)	**0.0165**	39	31 (79.49%)	0.2097
		Close	341	84 (24.63%)		20	15 (75.00%)	
		Mid	600	171 (28.50%)		33	30 (90.91%)	
		Far	320	77 (24.06%)		19	18 (94.74%)	
Layer	All	1	1284	300 (23.36%)	0.0616	72	57 (79.17%)	0.2447
		2	1482	392 (26.45%)		93	80 (86.02%)	
	F	1	324	72 (22.22%)	0.0338	18	15 (83.33%)	1.0000
		2	484	140 (28.93%)		33	26 (78.79%)	
	M	1	938	219 (23.35%)	0.2933	52	40 (76.92%)	**0.0330**
		2	992	252 (25.40%)		59	54 (91.53%)	
Layer 1	All	Cemetery	851	229 (26.91%)	**<0.0001**	46	39 (84.78%)	0.1186
		Cloister	433	71 (16.40%)		26	18 (69.23%)	
	F	Cemetery	208	50 (24.04%)	0.2923	12	10 (83.33%)	1.0000
		Cloister	116	22 (18.97%)		6	5 (83.33%)	
	M	Cemetery	643	179 (27.84%)	**<0.0001**	34	29 (85.29%)	0.0819
		Cloister	295	40 (13.56%)		18	11 (61.11%)	
Layer 2	All	Cemetery	1001	275 (27.47%)	0.1983	67	56 (83.58%)	0.3400
		Cloister	481	117 (24.32%)		26	24 (92.31%)	
	F	Cemetery	377	122 (32.36%)	**0.0018**	28	22 (78.57%)	1.0000
		Cloister	107	18 (16.82%)		5	4 (80.00%)	
	M	Cemetery	618	153 (24.76%)	0.5480	38	34 (89.47%)	0.6461
		Cloister	374	99 (26.47%)		21	20 (95.24%)	

6.9.2.3.1.3 Caries infestation by tooth

Figure 275 illustrates the distribution of caries absence and severity by tooth, differentiated for the left and right side of the mandible and maxilla. The distribution is quite similar across the sides and the jaws, with molars being far more affected than incisors and canines. The same trend was also observed among the sexes and age classes. Usually, molars are most prone to dental caries formation as the fissures on their occlusal surface are difficult to clean and during mastication, food debris tends to get stuck in areas with uneven surfaces (Hillson 1996). This also becomes evident when looking at the localisation of caries lesions on the teeth. For this analysis, only teeth with just one single caries lesion were considered (n=504). As shown in Table 99, the vast majority (55.56%) of lesions was recorded on occlusal surfaces of teeth, followed by the interdental space. Due to their smooth walls, lingual and buccal or labial faces of teeth were very rarely affected. Pure apical lesions were also fairly rare in this sample, probably because lesions that originated at the cemento-enamel junction were not recorded under apical lesions.

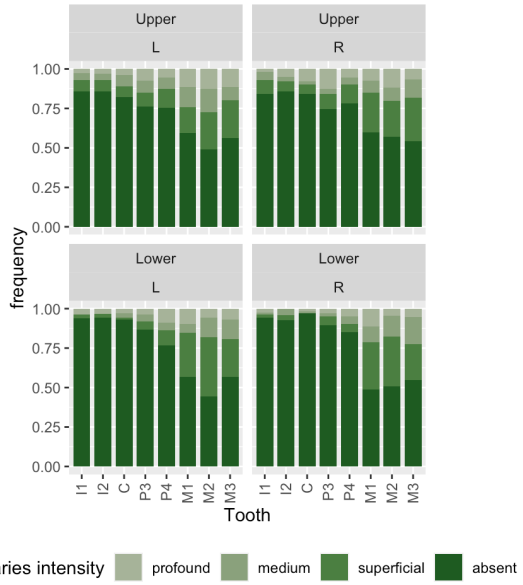

Figure 275 Distribution of caries infestation by tooth for the upper and lower jaw as well as right and left body side

Table 99 Distribution of caries direction in the adult permanent dentition

	occlusal	apical	mesial	distal	labial/buccal	lingual	Total N
All	55.56%	10.12%	15.87%	13.49%	4.56%	0.40%	504

6.9.2.3.2 Subadults

For subadults, a total 44 individuals and 643 could be analysed for caries occurrence. 19 individuals were infans I and comprised 225 teeth, 9 individuals belonged to the infans II group and encompassed 191 teeth and 14 individuals were classified as juvenile and offered 227 teeth for analysis. 17 deciduous (DI1-DC) and 51 permanent anterior teeth (I1-C), as well as 7 deciduous (DP3-4) and 9 permanent posterior teeth (P3-M3) were lost post-mortem.

6.9.2.3.2.1 True frequency

The overall frequency of caries affected teeth of subadults was 16.17%, infans I had 17.33% of their teeth infected, infans II 18.32% and juveniles 13.33%. These values are fairly balanced between the age groups so that no increase in caries with age could be observed. Infans II show the highest caries rates in the sample, which was to be expected since their deciduous teeth have been exposed longer to external cariogenic factors than those of infans I and longer than the permanent teeth of most juveniles. Subadults buried inside the cloister (21.67%) experienced significantly higher caries rates than those buried in the cemetery (13.64%). This overall trend was also observed among children from Layer 1 and 2, but it was only significant for individuals from Layer 2. Generally, however, no significant differences were observed between the two burial layers. (Table 100)

6.9.2.3.2.2 Crude frequency

A total of 59.09% of scoreable children suffered from caries infections. While this rate is very similar for infans I and juveniles, infans II (81.82%) exhibited markedly more infected individuals although the proportions are not statistically different from the other two groups. This mirrors the trend already observed in the true frequencies and the same reasons already mentioned in that section apply here. None of the group comparisons yielded any significant differences but, in all cases, the crude frequency mirrors the trends observed already in the true frequencies. However, the small sample size limits the meaningfulness of the results.

It is worth to mention that the first caries occurred in three individuals aged between 1-2 y, which hints at a diet incorporating carbohydrate-rich foods already at an early age. This would suggest that the weaning period started around that time and, together with a neglected oral hygiene would also explain the rather high caries rates in subadults. This idea will be further explored in the chapter on weaning reconstruction. It has to be noted though that the children analysed are those that died at an early age, which means that the high caries frequency might also have been a result of a compromised immune system of the child. (Table 100)

Table 100 Summary and test results for subadult caries true and crude frequency

Subadults		**Caries**					
Factor	**variable**	**True frequency**			**Crude frequency**		
		n	**presence**	**p-value**	**n**	**presence**	**p-value**
Total		643	104 (16.17%)		44	26 (59.09%)	
Age	Infans_I	225	39(17.33%)	0.3104	19	10 (52.63%)	0.2467
	Infans_II	191	35 (18.32%)		11	9 (81.82%)	
	Juvenile	227	30 (13.33%)		14	7 (50.00%)	
Location	Cemetery	440	60 (13.64%)	**0.0101**	30	15 (50.00%)	0.0726
	Cloister	203	44 (21.67%)		14	11 (78.57%)	
Layer	1	238	37 (15.55%)	0.7403	15	9 (60.00%)	0.9297
	2	405	67 (16.54%)		29	29 (65.91%)	
Layer 1	Cemetery	148	21 (14.19%)	0.4587	9	5 (55.56%)	1.0000
	Cloister	90	16 (17.78%)		6	4 (66.67%)	
Layer 2	Cemetery	292	39 (13.36%)	**0.0055**	21	10 (47.62%)	0.0926
	Cloister	113	28 (24.78%)		8	7 (87.50%)	

6.9.2.4 Discussion and Conclusion

Oral health offers a good basis for the interpretation of past dietary habits. Under the influence mostly of undiligent oral hygiene, food particles that get stuck on and between teeth get metabolised by bacteria in the dental plaque and depending on the chemical composition of these food items, the metabolic waste products of these bacteria either raise or increase pH-levels in the oral cavity (Hillson 1996; Caselitz 1998). Usually pH-levels rise and fall in a balanced manner throughout the day. During more acidic phases, a demineralisation of the

tooth enamel starts and during more alkaline phases, the lost mineral deposits are being replenished (Hillson 1996). If acidic pH-levels persist for a long time however, the demineralization of the enamel continues until a hole is created through which oral bacteria can infect the dental tissue, and this marks the start of a carious lesion (Waldron 2009). Therefore, the formation of caries lesions is promoted by long periods of oral acidity (Hillson 1996). Foods rich in carbohydrates such as cereals and its processed products or sugar are the main reasons for prolonged oral acidity and they are therefore considered to be cariogenic food items (Hillson 1996, 2008; Selwitz *et al.* 2007). Therefore, high levels of caries in a population are usually indicators of firstly bad oral hygiene and secondly of a diet rich in carbohydrates and/or sugar (Selwitz *et al.* 2007). However, it needs to be kept in mind that other factors might also influence caries formation. For example, due to its mineralising properties, a high content of fluor in water might reduce the risk of caries infections (Knappwost 1951; Hillson 1996; Selwitz *et al.* 2007). A stressed immune system might also predispose for increased caries formation. Low social status, poverty but also bad mental health and work stress have shown an association with caries formation risk (Sutton 1990; Segura Marcenes & Sheiham 1992; Selwitz *et al.* 2007). Some studies also found that the presence of enamel defects and hypocalcifications promotes caries formation in teeth (Duray 1990; Hillson 1996; Targino *et al.* 2011). Furthermore, fluctuating hormone levels, genetic factors, and individual salivary flow have also been associated with caries formation (Hillson 1996; Salvolini *et al.* 1998; Lukacs & Largaespada 2006; Selwitz *et al.* 2007). As such, women are generally more prone to developing caries than men, since altered salivary mineral composition and a weakened immune system during pregnancy and even during menopause facilitate the development of carious lesions (Guidozzi *et al.* 1992; Salvolini *et al.* 1998; Streckfus *et al.* 1998; Lukacs & Largaespada 2006). Such a pattern has also been observed in the distribution of caries frequency for many prehistorical and historical populations (Larsen *et al.* 1991; Lukacs 1996; Lukacs & Thompson 2008). However, among the people buried on the Knuedler cemetery, this pattern was only visible to a certain extent. Overall, women had more teeth affected by dental caries, but men were more affected by dental caries than women but the differences between the sexes were only very small and not statistically relevant. The same result was found for the St. Brides Lower cemetery in London, dating between 18th and 19th century, where females displayed higher true caries frequency rates (M: 25.1%; F: 28.1%) but males were overall more affected by caries (M: 82.2%; F: 75.6%) and the difference between the sexes did not turn out significant (Mant & Roberts 2015). No significant differences between men and women in caries rates could also be detected in the high medieval St. Mary Graces and East Smithfield

cemeteries in London (Houston & Upton 2021). This might indicate that among the population buried in the Knuedler cemetery, women's diet, regarding the amount of carbohydrates consumed, was not much different than that of men, if at all, carbohydrate consumption might have been slightly lower when considering the predisposing factors for caries development in women. Occlusal surface caries was most prevalent in the Knuedler cemetery. This type of caries lesion is most often associated with reduced dental wear and therefore the consumption of soft and refined food products (Corbett & Moore 1976; Whittaker & Molleson 1996; Hillson 2008; Malčić *et al.* 2011).

In order to place the cemetery into a wider regional context, a comparison to other roughly contemporaneous Luxembourgish sites was undertaken. Layer 2 from Luxembourg City dating from the late 14th to the mid 17th century could be well compared to the sites of Givenich, Grevenmacher and Luxembourg-St. Esprit. Layer 1 from Luxembourg corresponded chronologically most closely to the sites of Luxembourg-St. Esprit and Grund/Wenzelsmauer. Some of these sites are rural (Givenich, Grevenmacher) and others are urban and most importantly are cemeteries of Luxembourg City. All comparative samples from Luxembourg city are, like the one studied in the present work, associated to a convent. Caries crude frequency rates from Layer 2 (86.02%) and 1(79.17%) in Luxembourg are very similar to those from contemporaneous sites such as Givenich (Rehbach *et al.* 2009; Weidig *et al.* 2009), St. Esprit (Rehbach & Bis-Worch 2006; Rehbach 2008) and Grund-Wenzelsmauer (Trautmann & Trautmann 2011). Both Givenich and St. Esprit have been ascribed to rather higher social class burials. In Givenich all burials were associated with a manor house and in St. Esprit, Rehbach et al. (2005) described several anthropological features, such as a high average age at death or good nutritional status, as being evidence for people of a higher social class. The Knuedler also shows similar crude caries rates than members of a military detachment buried in Grund/Wenzelsmauer, but true frequency rates are considerably higher in the Knuedler cemetery. When comparing Layer 2 to Grevenmacher (Trautmann 2012), a rural site, caries crude prevalence in Luxembourg city seems to be noticeably higher while true frequency is quite similar. This, together with the higher caries rates in the other urban and upper-class burials might indicate a differential access of citizens of Luxembourg City and of higher social rank, to more cariogenic food. But the high prevalence of dental caries also demonstrates fairly bad oral hygiene in all these sites. When looking at sex differences, St. Esprit, Grevenmacher and Givenich all showed the same pattern in crude frequency than Luxembourg City, namely caries being more frequent in men than in women. In Grevenmacher and St. Esprit, caries true frequency was higher in women than in men, which was also observed in the Knuedler

population. When considering the subadult dentition, the caries rates determined for the Knuedler cemetery at 59.09% are higher than those from Grevenmacher at 35.8%, but the caries frequency distribution across those age groups follows the same pattern.

In a next step, the Knuedler cemetery and the other Luxembourgish sites were put into a wider regional context. A total of two sites could be identified that were chronologically and regionally close to the Luxembourgish sites: Völklingen (early postmedieval) (Roßbach 2015) and St. Arnual Kreuzgang (5th – 18th century) from Saarbrücken (Geber 2006). For St. Arnual, only true caries rates were available and those were considerably lower than those from most Luxembourgish sites and only similar to that of the soldiers from Grund/Wenzelsmauer. However, Völklingen showed very similar true and crude caries frequencies. With 79.7% crude caries frequency, early postmedieval Völklingen was especially close to the contemporaneous Layer 1 from Knuedler, but true caries frequency was noticeably higher. It can therefore be observed, that Luxembourgish caries rates are also very similar to sites in close geographical proximity, which might have to do with similar availability and access to food in the larger area.

When putting the Luxembourgish sites in a wider European context, it becomes apparent that overall, caries rates are still within the range of other contemporaneous sites but are rather on the higher end of the spectrum. Sites from Germany that show similarly high rates are Hettstedt Kirche (15th century) and Hettstedt Gymnasium (18th – 19th century) (Roßbach 2015), lower class burials from a hospital in Minoritenweg Regensburg (Von Heyking 2012) and an urban population from Esslingen ((Lehnert 1993) sourced from Roßbach (2015)). Across Europe, caries rates from Luxembourgish sites were most similar to those from a cemetery on Östergötland in Sweden, individuals from the Prozega crypt in Croatia attributed to the upper-class, Spitalfields (London) a hospital cemetery (Whittaker & Molleson 1996), and individuals from the churchyard in Trakai (Miliauskiene & Jankauskas 2015). (Table 101) The latter study also found a strong difference in caries frequency between church and cemetery burials (Table 101); however, it was much more pronounced than that discovered in the Knuedler cemetery (Table 98). Since all afore-mentioned sites are from mixed social backgrounds, high caries frequencies cannot be solely attributed to lower class individuals consuming a carbohydrate intensive diet. Considering also all the sites where dental caries was lower, a more complex picture of caries frequency becomes apparent, which suggests that regional variations in access to certain foods, as well the challenges that different geographical areas pose, but probably also differences in scoring techniques between different sites as well as the number and position of

teeth lost post-mortem may account for the vast discrepancy in caries frequencies throughout Europe.

Table 101 Caries true and crude frequencies across Europe (compiled partially from (Müller & Hussein 2017; Bertilsson *et al.* 2022)*)*

Caries frequency in Europe							
Time period	**Site**	**Country**	**Type of settlement**	**Socio-economic status**	**Caries true frequency %**	**Caries crude frequency %**	**Publication**
18th C	Spitalfields	England	urban	Hospital		89.00	Whittaker& Molleson (1996)
18th-19th C	Hettstedt Gym.	Germany	urban		32.60	88.90	Rossbach (2015)
1100-1810 AD	Linköping Östergötland	Sweden	urban			88.05	Bramstång and Nordin 2017*
12th-17th C	St. Esprit	Luxembourg	urban	mixed	23.70	87.10	Rehbach u. Bis-Worch (2006), Nothwang et al. (2006) Rehbach et al. (2007) Rehbach u. Nothwang (2007) Rehbach (2008) Rehbach u. Notwang (2009)
1570-1740	New Churchyard	England	urban	working class	14.30	87.00	Smith (2019)
14th-mid-17h C	Knuedler	Luxembourg	urban		26.45	86.02	Kremmer (hic)
late 16th-early 18th C	Grund/ Wenzelsmauer	Luxembourg	urban	soldiers	15.30	83.30	Trautmann u. Trautmann (2011)
Early post-medieval	Ellwangen-Jagst	Germany	urban			82.50*	Kairies (2021)
11th-15th C	Givenich	Luxembourg	rural	upper class	21.00	81.50	Rehbach et al. (2009) Weidig et al. (2009)
16th-17th C	Trakai churchyard	Lithuania	urban		25.60	80.00	Miliauskienė and Jankauskas (2015)
Early post-medieval	Völklingen	Germany	urban		36.10	79.70	Rossbach (2015)
18th-19th C	Chelsea Church	Old England	urban	middle class	21.50	79.50	Mant& Roberts (2015)
Mid-17th-18th C	Knuedler	Luxembourg	urban		23.36	79.10	Kremmer (hic)
15th C	Hettstedt Kirche	Germany	urban		20.70	79.00	Rossbach (2015)
18th-19th C	St.Brides	England	urban	working class	26.50	78.90	Mant& Roberts (2015)
13th-19th C	Esslingen	Germany	urban		23.80	78.70	Lehnert (1993)
Late-medieval	Ellwangen-Jagst	Germany	urban			76.39*	Kairies (2021)
17th-18th C	Jelgava Church	Latvia	urban	upper-class		76	Pētersone-Gordina et al. (2012)
12th-14th C	Grevenmacher	Luxembourg	rural		20.60	75.90	Trautmann (2017)

Caries frequency in Europe							
Time period	**Site**	**Country**	**Type of settlement**	**Socio-economic status**	**Caries true frequency %**	**Caries crude frequency %**	**Publication**
18th C	Pozega crypt	Croatia	urban	upper class	18.40	74.40	Malčić et al.(2011)
11th-19th C	Wiebelskirchen	Germany			32.10	73.20	Weimar (1984)
12th-16th C	Minoritenweg Regensburg	Germany	urban	Hospital/lower class	18.40	72.60	Heyking (2012)
1812 AD	Napoleonic mass grave	Lithuania	urban	soldiers	11.50	68.60	Palubeckaitė et al. (2006)
1500-1620	Gothenburg, Nya Lödöse	Sweden	urban		13.00	68.00	Bertilsson et al. (2021)
16th-17th C	Trakai church	Lithuania	urban	upper class	15.20	64.00	Miliauskienė and Jankauskas (2015)
17th C	Gothenburg	Sweden	urban		11.63	60.00	Lingström& Borrmann (1999)
18th-19th C	Capuchin catacombs	Italy, Sicily	urban	upper/middle class		58.50	Seiler et al. (2017)
1500		England			8.10	55.50	Bonsall and Pickard (2015)
15th-17th C	St. Gertrude church	Lativia	urban		6.40	55.2*	Pētersone-Gordina et al. (2018)
15th-16th C	Turku	Finnland	urban	lower class	13.10	54.10	Varrela (1991)
11th-19th C	Wiebelskirchen	Germany			18.60	52.80	Raddaz (1986)
1583	Alghero	Italy	urban	Plague cemetery	5.20	50.70	Giuffra et al. (2020)
17th-19th C	Oulu	Finland	urban		23.20	43.00	Vilkama et al. (2016)
11th-19th C	Wiebelskirchen	Germany			14.10	38.80	Sahner (1984)
14th-18th C	Villingen	Germany	urban	middle class ?	16.00	38.00	Knedeisen (1983)
17th-19th C	Gothenburg	Sweden	urban	lower class soldiers		37.00	Ancini et al. (2020)
10th-18th C	Emden	Germany	urban	upper/middle class	5.30	34.50	Stech (2009)
12th-16th C	Ihlow	Germany	rural	monastic	4.30	32.40	Timmermann (2009)
1400-1700	Zumberak, Virje, Torčec	Croatia	rural		14.00		Šlaus et al. (2018)
5th-18th C	St.Arnual Kreuzgang Saarbrücken	Germany		mixed	15.1		Gerber (2006)
17th-19th C	Norwich	England			17.40		Wells (1968)
16th-17h C	Notre-Dame-du-Bourg	France	urban		19.00		Chazel et al. (2005)
15th-18th C	Koprivno	Croatia			6.30		Adamić and Šlaus (2017)
14th-17th C	Nova Raca	Croatia	rural		9.00		Šlaus et al. (1997)
14th-16th C	Orthodox churches	Serbia	rural		9.00		Srejić(2001)
12th-15th C	Deinze	Belgium	urban		11.70		Van Cant (2019)
12th-18th C	Slijpe	Belgium	rural coastal		10.30		Van Cant (2019)
17th C	Viichte	Belgium	rural		9.70		Van Cant (2019)

Caries frequency in Europe							
Time period	**Site**	**Country**	**Type of settlement**	**Socio-economic status**	**Caries true frequency %**	**Caries crude frequency %**	**Publication**
14th-19th C	Zottegem	Belgium	rural		7.90		Van Cant (2019)
15th-19th C	Oosterweel	Belgium	rural polder	upper class	12.20		Van Cant (2019)
12th-19th C	Moorsel	Belgium	rural		12.60		Van Cant (2019)

* = average

6.9.3 Periodontal disease

6.9.3.1 Introduction

Periodontal disease describes the deterioration of the alveolar bone preceded usually by a recession of gingival tissue (Ogden 2007; Waldron 2009). It is one of the most common oral diseases, and in its mildest form, which is gingivitis, an inflammation of the gingival tissue, is thought to affect between 50-90% of the modern day population (Waldron 2009).

The formation of periodontal disease is strongly linked to the formation and severity of calculus deposits (Aufderheide & Rodriguez-Martin 1998; Waldron 2009; Roberts & Manchester 2010). Strong calculus deposits can cause bleeding of the gums and through these wounds, bacteria of the dental plaque, which in living individuals covers the surface of dental calculus, can enter the gingival tissues and cause inflammation (Hillson 1996; Kinane 2000; Waldron 2009). If the inflammation and irritation of the gums continues, the gingival tissue starts receding and the inflammation can spread to the adjacent alveolar bone and periodontal ligaments causing destruction of the alveolar bone mainly around and inside the tooth socket. Therefore, severe periodontitis often leads to antemortem tooth loss and can even cause periapical abscesses if left untreated (Hillson 1979; Ortner 2003a; Waldron 2009; Roberts & Manchester 2010). There are two types of bone loss associated with periodontal disease. Horizontal bone loss is characterised through the simultaneous reduction in height of all walls of a tooth socket and usually involves several adjoining teeth or even the whole dental arcade. Vertical bone loss is usually concentrated around individual teeth and their direct neighbours and is characteristically surrounded by unaffected bone, although vertical bone loss can occur at the same time as horizontal bone loss. The lesions are distinctly different from periapical lesions and can even lead to a complete loss of the approximal tooth socket wall without much affecting the buccal and lingual walls (Hillson 1996).

6.9.3.2 Methods

Periodontal disease was recorded for every tooth socket and immediate surrounding area of the alveolar bone. In the following study, no difference was made between vertical and horizontal bone loss. Since alveolar disease was not recorded for the entirety of the dental arcade but for each tooth socket, a differentiation into vertical and horizontal bone loss will however be possible if required for future studies. For this evaluation, a composite score was calculated for each individual based on the individual scores of the tooth sockets. These scores were then attributed to the following categories:

Table 102 Scores for the evaluation of periodontal disease based on (Brothwell 1981)

Old score	New score	Description
0	0	No alveolar disease
>0-1	1	Light resorption, <1/3 of tooth root visible
>1-2	2	Moderate resorption, <2/3 of tooth root visible
>2-3	3	Severe resorption, >2/3 of tooth root visible

A score was also given to resorbed or resorbing alveolae with signs of inflammation, which probably contributes to a generally high incidence of alveolar disease in this sample. Subadults and adults were evaluated separately. Differences between groups in absence and presence as well as severity of the periodontal lesions were analysed, and stacked percentage bar charts were chosen to illustrate occurrence and severity of periodontal disease.

6.9.3.3 Results

6.9.3.3.1 Adults

6.9.3.3.1.1 Crude frequency

Overall, 160 individuals could be assessed for periodontal disease and in 138 (86.08%) it was present. A general trend can be observed that people buried in the cloister (90.20%) were slightly more affected by periodontal disease than those buried in the cemetery (84.40%) and more people from Layer 1 (91.18%) experienced periodontal disease than those from Layer 2 (82.61%). However, the only statistically significant differences were observed between men and women and the age groups. Males (89.81%) were significantly more affected by periodontal disease than females (78.00%). These results might be directly related to the afore described caries rates. Overall periodontitis rates in this sample are rather high since often periodontitis occurs as a consequence to severe caries infections, which can be clearly observed

in this sample. However, as opposed to caries rates, which are overall higher among cemetery burials than among cloister burials, periodontal disease is more frequent among cloister burials. One possible explanation for this might be that, since people buried in the cloister were on average older than those from the cemetery, the higher periodontitis rates might reflect just that. Therefore, it was also examined whether age played a role in the development of periodontitis and indeed, a strong correlation of occurrence of periodontal disease with age could be established. Young adults had significantly less (45.83%) and less severe periodontitis than adults (85.71%), matures I (92.59%), matures II (100%) and seniles (97.83%). Severity of periodontal disease also increased strongly with age (Figure 276). Another possible explanation for the discrepancy between caries and periodontitis frequencies by burial locations might be that caries rates in the cloister are underestimated due to antemortem tooth loss, which will be explored in the next sections. This underestimation due to tooth loss is actually supported by the fact that caries frequency seems to peak in matures and decreases again in the senile age cohort.

Overall, it also has to be noted that the generally very high rates of periodontal disease slightly overestimate the actual degree of affection, and this is due to the scoring system used and the way scores were converted for analyses. Even individuals with only one or two localised periodontal infections ("vertical" lesions) that were likely due to infections such as caries or associated to antemortem tooth loss were counted as having periodontal disease, even if the rest of the dental arcade was not affected. If only horizontal lesion had been scored, overall periodontitis rates might have been lower. (Table 103)

Table 103 Summary and results of periodontal disease crude frequency

Adults	**Peridontal disease**				
Factor		**variable**	**Crude frequency**		
			n	**pres.**	**p-value**
Total			160	138 (86.08%)	
Sex		F	50	39 (78.00%	**0.0460**
		M	108	97 (89.81%)	
Age	All	Young Adult	24	11 (45.83%)	**<0.0001**
		Adult	42	36 (85.71%)	
		Mature I	27	25 (92.59%)	
		Mature II	37	37 (100%)	
		Senile	29	28 (96.55%)	
	F	Young Adult	13	5 (38.46%)	**0.0018**
		Adult	11	9 (81.82%)	
		Mature I	7	7 (100%)	
		Mature II	10	10 (100%)	
		Senile	9	8 (88.89%)	
	M	Young Adult	11	6 (54.55%)	**0.0008**
		Adult	31	27 (87.10%)	

Adults		Peridontal disease			
Factor		variable	Crude frequency		
			n	pres.	p-value
		Mature I	20	18 (90.00%)	
		Mature II	26	26 (100%)	
		Senile	19	19 (100%)	
Location	All	Cemetery	109	92 (84.40%)	0.3215
		Cloister	51	46 (90.20)	
	F	Cemetery	39	30 (76.92%)	1.0000
		Cloister	11	9 (81.82%)	
	M	Cemetery	69	61 (88.41%)	0.7428
		Cloister	39	36 (92.31%)	
Distance to Church	All	Cloister	51	46 (90.20%)	0.4116
		Close	26	24 (92.31%)	
		Mid	54	45 (83.33%)	
		Far	29	23 (79.13%)	
	F	Cloister	11	9 (81.82%)	0.8921
		Close	7	6 (86.71%)	
		Mid	22	17 (85.71%)	
		Far	10	7 (70.00%)	
	M	Cloister	39	36 (92.31%)	0.7068
		Close	18	17 (94.44)	
		Mid	32	28 (87.50)	
		Far	19	16 (84.21%)	
Layer	All	1	68	62 (91.18%)	0.1198
		2	92	76 (82.61%)	
	F	1	17	16 (94.12%)	0.0725
		2	33	23 (69.70%)	
	M	1	50	45 (90.00%(	0.9529
		2	58	52 (89.66%)	
Layer 1	All	Cemetery	44	40 (90.91%)	1.0000
		Cloister	24	22 (91.67%)	
	F	Cemetery	12	11 (91.67%)	1.0000
		Cloister	5	5 (100%)	
	M	Cemetery	32	29 (90.62%)	1.0000
		Cloister	18	16 (88.89%)	
Layer 2	All	Cemetery	65	52 (80.00%)	0.3786
		Cloister	27	24 (88.89%)	
	F	Cemetery	27	19 (70.37%)	1.0000
		Cloister	6	4 (66.67%)	
	M	Cemetery	37	32 (63.79%)	0.4020
		Cloister	21	20 (95.24%)	

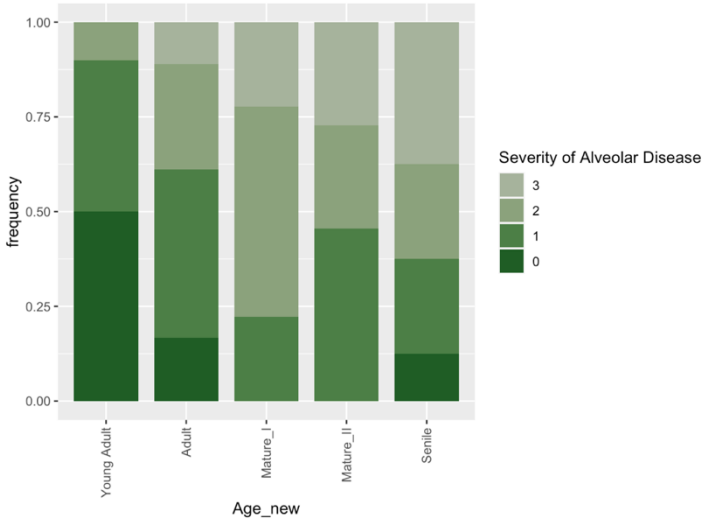

Figure 276 Distribution of severity of alveolar disease by age

6.9.3.3.2 Subadults

6.9.3.3.2.1 Crude frequency

For a total of 38 children, tooth sockets were well preserved enough for analysis.

Overall, only 13.16% (n=5) of all children displayed periodontal disease. None of the group comparisons yielded any significant differences. But a slight correlation with age could be observed, with periodontal disease being more frequent (30.00%) in juveniles than in infans I (5.88%) and in infans II (9.09%). However, sample sizes are simply too small to make out any real trends. In both Infant I and II for instance, only one individual displayed periodontal disease and in juveniles it was also only 3 Individuals. Most of the subadults showed vertical bone loss associated with severe caries infections, except for 2008_78/148, a juvenile buried in the cemetery who experienced slight bone loss affecting the whole dental arcade and only one superficial dental caries. Generally, since most of the lesions were associated to dental caries, they were also rather severe. (Table 104)

Table 104 Summary and test results for subadult periodontal disease crude frequency

Subadults	**Peridontal disease**			
Factor	**variable**	**Crude frequency**		
		n	**presence**	**p-value**
Total		38	5 (13.16%)	
Age	Infans_I	17	1 (5.88&)	0.1931
	Infans_II	11	1 (9.09%)	
	Juvenile	10	3 (30.00%)	
Location	Cemetery	27	3 (11.11%)	0.6154
	Cloister	11	2 (18.18%)	
Layer	1	14	3 (21.43%)	0.3367
	2	24	2 (8.33%)	

Subadults	Peridontal disease			
Factor	variable	Crude frequency		
		n	presence	p-value
Layer 1	Cemetery	9	2 (22.22%)	1.0000
	Cloister	5	1 (20.00%)	
Layer 2	Cemetery	18	1 (5.56%)	0.4457
	Cloister	6	1 (16.67%)	

6.9.3.4 Discussion and Conclusion

Periodontal disease describes a destruction of the alveolar bone related to gingival tissue inflammation. Extensive calculus is considered to be a major contributor to periodontal disease formation (Aufderheide & Rodriguez-Martin 1998; Kinane 2000; Ogden 2007; Waldron 2009). As inflammation of the gingival tissue is most often caused by bacteria from the plaque that enter the gingival tissue, bad oral hygiene which does not prevent the excessive build-up of plaque and calculus has been associated with the formation of periodontal disease (Hillson 1996). But recent studies have shown that periodontal disease can also result from illnesses such as immunodeficiency diseases, diabetes or scurvy. Generalised malnutrition such as Vitamin D and C deficiency and occlusal trauma have all been noted for their possible involvement in periodontal disease formation (Clarke *et al.* 1986; Garcia *et al.* 2001; Tada & Miura 2019; Isola *et al.* 2020) For prehistoric populations, mainly heavy attrition, caries and pulp infections and mineral balance have been listed as probable causes for observed periodontal disease but in return, calculus and bacterial plaque were not found to as heavily involved in periodontal disease occurrence (Clarke *et al.* 1986). Also, many studies have found that men are more affected by periodontal disease (Stech 2009; Shiau & Reynolds 2010a, b; Haytac *et al.* 2013), a pattern that was also observed in the Knuedler cemetery (F: 78%; M: 89.81%). In the Knuedler cemetery, prevalence of periodontal disease was fairly high but still in the upper bounds of the normal range of occurrence in Europe. Similarly high rates of the disease for found in Ihlow (Timmermann 2009), Hettstedt Kirche, Hettstedt Gymnasium, Völklingen (Roßbach 2015) and St. Arnual Kreuzgang (Geber 2006) in Germany. In wider Europe, similar rates were also observed in individuals associated to rural orthodox churches (Srejic 2001) and in upper-class individuals from Jelgava Holy Trinity church in Latvia (Pētersone-Gordina & Gerhards 2012). The majority of these sites belong to urban settlements. Compared to Luxembourgish sites, periodontal disease in the city was higher than that in older rural areas (Grevenmacher) (Trautmann 2012). (Table 105) Like with caries rates, the stronger differences in periodontal disease frequency might also be owed to differences in scoring methods, definitions and analyses. While some studies only consider the clearly inflammatory

periodontitis, others consider all types of alveolar resorption (Stech 2009). For Luxembourg city, the latter inclusion model was chosen, which might explain the relatively high crude prevalence rates. However, periodontal disease, next to bad oral hygiene, is also influenced by individual caries rates and is more prevalent in populations with low attrition rates consuming softer foods (Larsen 2015). Therefore, a combination of poor oral hygiene, consumption of soft foods and high caries rates but also high calculus rates might lie at the root of high periodontal disease occurrence in Luxembourg City.

Table 105 Overview of Periodontal disease prevalence in medieval-postmedieval European sites

Periodontal disease frequency in Europe						
Time period	**Site**	**Country**	**Type of settle ment**	**Socio-economic status**	**Periodontal disease frequency %**	**Publication**
5th-18th C	St Armual Kreuzgang Saarbrücken	Germany		mixed	94.10	Geber (2006)
15th C	Hettstedt Kirche	Germany	urban		93.40	Rossbach (2015)
18th-19th C	Hettstedt Gym	Germany			92.20	Rossbach (2015)
mid-17th-18th C	Knuedler	Luxembourg	urban		91.18	Kremmer (hic)
12th-17th C	Ihlow	Germany	rural	monastic	90.00	Timmermann (2009)
17th-18th C	Jelgava Trinity church	Latvia	urban	upper class	88.13 *	Pētersone-Gordina et al. (2012)
Early postmedieval	Völklingen	Germany	urban		87.30	Rossbach (2015)
14th-16th C	Several orthodox churches	Serbia	rural		83.00	Srejić (2001)
14th-mid-17th C	Knuedler	Luxembourg	urban		82.61	Kremmer (hic)
12th-18th C	Slijpe	Belgium	rural coastal		76.90	Van Cant (2019)
10th-18th C	Emden	Germany	urban	upper/middle class	61.50	Stech (2009)
12th-14th C	Grevenmacher	Luxembourg	rural		50.25	Trautmann (2017)
Early postmedieval	Ellwangen-Jagst	Germany	urban		48.70	Kairies (2021)
15th-19th C	Oosterweel	Belgium	rural polder	upper class	45.50	Van Cant (2019)
15th-17th C	St. Gertrude church	urban	urban		41.27*	Pētersone-Gordina et al. (2018)
19th C	Viichte	Belgium	rural		37.00	Van Cant (2019)
12th-19th C	Moorsel	Belgium	rural		26.70	Van Cant (2019)
14th-19th C	Zottegem	Belgium	rural		22.20	Van Cant (2019)
12th-15th C	Deinze	Belgium	urban		18.30	Van Cant (2019)
Late medieval	Ellwangen-Jagst	Germany	urban		16.18	Kairies (2021)

* = average

6.9.4 Periapical Lesions

6.9.4.1 Introduction

Dental caries, trauma to teeth or strong attrition but also periodontal pockets formed by extensive calculus deposition, can enable oral bacteria to enter into the pulp chamber of the tooth and can lead to infection of the dental pulp, a condition referred to as pulpitis (Hillson 1996; Dias & Tayles 1997; Roberts & Manchester 2010). This then leads to an inflammatory response and in many cases, the infection can be contained and will resolve. However, if the infection persists and becomes chronic, a periapical granuloma starts forming at the apex of the tooth root, which stimulates osteoclastic activity and allows the granuloma to grow. Over time, the granuloma can develop into a periodontal cyst, where the granulomatous tissue is being replaced by fluid and the cyst continues to increase in size. Usually, granulomata are considered to be smaller than 2-3mm in diameter whereas larger lesions are addressed as cysts (Figure 277). Cysts as well as granulomas can cause break-down of the outer walls of the jaws if they grow large enough and close enough to the surface. If the infection of the pulp is highly virulent, pus starts forming in the bone cavity created by a periapical granuloma and an acute periapical abscess can form. They are characterised by the lack of formation of a smooth walled cavity due to their rapid growth owing to the increasing pressure the pus causes inside the bone cavity. If the abscess becomes chronic, it can lead to the formation of a fistula in the jawbone through which the pus can drain into the oral cavity (Hillson 1996; Dias & Tayles 1997; Dias *et al.* 2007; Ogden 2007; Waldron 2009; Grupe *et al.* 2015). In dry bone, due to the rapid growth of the abscess, most of the time it cannot be differentiated from a granuloma or cyst (Ogden 2007). Therefore, the recording of periapical lesions is usually limited to a classification of the lesion into granulomas or cysts.

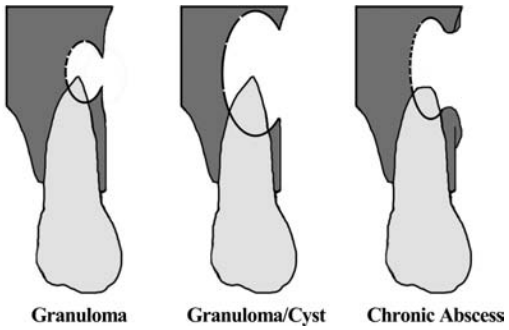

Figure 277 Illustration of the different types of periapical lesions (taken from Pinhasi and Mays, 2007)

6.9.4.2 Methods

The occurrence of periapical lesions was recorded for every tooth socket that was sufficiently preserved for scoring. On an individual level, only individuals with scoreable sockets were included in the study.

Periapical lesions were recorded following the recommendations laid out by Dias and Tayles (1997), the classifications are explained in Table 106.

All analyses were carried out for adults and subadults separately.

For the calculation of crude frequencies, no distinctions were made between individuals with multiple or single lesions nor between the type of the lesion. Both true and crude frequencies were subjected to Pearson's chi square tests in order determine whether there were any statistically significant differences between sex, age, burial layer and location in the occurrence of periapical lesions. The frequencies of lesion type were not subjected to statistical testing but were only illustrated in a bar chart.

Table 106 Scores for recording periapical lesions after (Dias & Tayles 1997)

Score	Description
0	Absence of periapical lesion
1	Granuloma: cavity <2-3mm
2	Cyst: cavity >2-3mm

6.9.4.3 Results

6.9.4.3.1 Adults

6.9.4.3.1.1 True frequency

True frequency was calculated for 3999 tooth positions. The much higher number of sockets available for evaluation as compared to teeth was due to the high number of teeth lost post-mortem in the jaws. Of all recordable tooth sockets, 225 (4.84%) had periapical lesions. Overall, no significant differences could be detected between the sexes and indeed the distribution of periapical lesions is very balanced (M: 5.59%; F: 5.84%). No difference could be detected among burial locations when all individuals and men were considered, but females from the cemetery (6.81%) showed significantly more lesions than those from the cloister (1.98%). They also showed no cases of periapical lesions in cloister burials within Layer 1. Overall and in both sexes, a significant correlation with age could be established, with the frequency of periapical lesions increasing with old age but dropping again among seniles. This

is probably directly related to the increase of caries lesions by age, which can cause periapical abscess when bacteria enter the exposed pulp chamber and cause inflammation at the root apex. The drop in seniles might be explained by healed lesions after the infected tooth had been lost or alternatively, the seniles buried in this cemetery had predominantly better oral hygiene than those that did not reach this age. Overall, granulomas were more prevalent than cysts and the number of cysts increased significantly with age but dropped again in the senile age cohort (Figure 278). (Table 107)

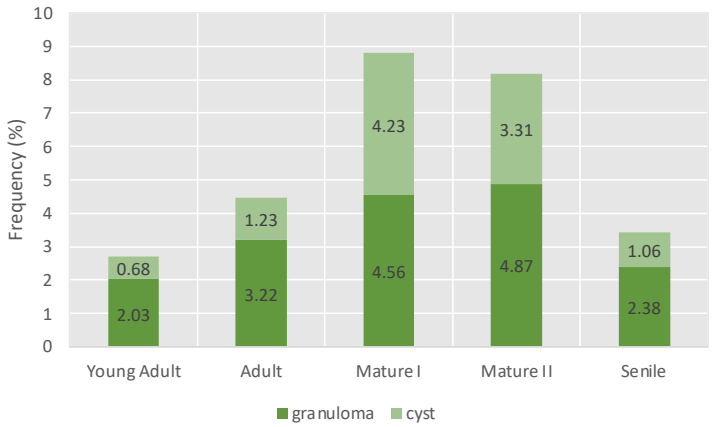

Figure 278 Percentage of granulomas and cysts by age

6.9.4.3.1.2 Crude frequency

A total of 164 individuals could be analysed for periapical lesions and of those 71 individuals had at least one or more such lesions, which corresponds to a frequency of 43.29%. No relevant differences could be observed between the sexes, burial layers and locations. However, statistically insignificant trends could be observed. As such, people buried in the cemetery (47.32%) displayed more periapical lesions then those buried in the cloister (34.62%) and the trend was the same for men and women. Furthermore, overall individuals from Layer 1 (40.00%) exhibited less lesions than those from Layer 2 (45.74%) but while the trend was the same in males, it was balanced in females. When separating by Layers, the trends observed in females cannot be considered since the sample size for this group is simply too small. But in males it becomes clear that in Layer 2, more individuals buried in the cemetery (55.26%) had periapical lesions than those buried in the cloister (38.19%) but in Layer 1 the occurrence was more balanced (cemetery: 58.33%; cloister: 50.00%). The only significant difference was observed between the age groups and the same trend as for the true frequency was prevalent. (Table 107)

Table 107 Summary and test results for adult periapical lesions crude frequency

Adults			**Periapical lesions**					
Factor		**variable**	**True frequency**			**Crude frequency**		
			n	**pres.**	**p-value**	**n**	**pres.**	**p-value**
Total			3999	225 (4.84)		164	71 (43.29%)	
Sex		F	1250	73 (5.84%)	0.7520	51	21 (41.18%)	0.6449
		M	2719	152 (5.59%)		111	50 (45.05%)	
Age	All	Young Adult	590	16 (2.71%)	**<0.0001**	24	7 (29.17%)	**0.0096**
		Adult	1057	47 (4.45%)		42	17 (40.48%)	
		Mature I	614	54 (8.79%)		27	14 (51.85%9	
		Mature II	966	79 (8.18%)		38	24 (63.16%)	
		Senile	756	26 (3.44%)		32	8 (25.00%)	
	F	Young Adult	289	7 (2.42%)	**<0.0001**	13	4 (30.77%)	0.2564
		Adult	279	21 (7.53%)		11	5 (45.45%)	
		Mature I	193	28 (14.51%)		7	5 (71.43%)	
		Mature II	250	11 (4.40%)		10	5 (50.00%)	
		Senile	239	6 (2.51%)		10	2 (20.00%)	
	M	Young Adult	301	9 (2.99%)	**0.0001**	11	3 (27.27%)	**0.0255**
		Adult	778	26 (3.34%)		31	12 (38.71%)	
		Mature I	421	26 (6.18%)		20	9 (45.00%)	
		Mature II	700	68 (9.71%)		27	19 (70.37%)	
		Senile	503	20 (3.98%)		21	6 (28.57%)	
Location	All	Cemetery	2781	166 (5.97%)	0.1553	112	53 (47.32%)	0.1265
		Cloister	1218	59 (4.84%)		52	18 (34.62%)	
	F	Cemetery	998	68 (6.81%)	**0.0035**	40	18 (45.00&)	0.4905
		Cloister	252	5 (1.98 %)		11	3 (27.27%)	
	M	Cemetery	1769	98 (5.54%)	0.8759	71	35 (49.30%)	0.2304
		Cloister	950	54 (5.68)%)		40	15 (37.50%)	
Distance to Church	All	Cloister	1218	59 (4.84%)	0.1284	52	18 (34.62%)	0.4249
		Close	669	30 (4.48%)		28	12 (42.86%)	
		Mid	1400	90 (6.43%)		55	26 (47.27%)	
		Far	712	46 (6.46%)		29	15 (51.72%)	
	F	Cloister	252	5 (1.98%)	**0.0002**	11	3 (27.27%)	0.2785
		Close	164	5 (3.05%)		7	2 (28.57%)	
		Mid	592	52 (8.78%)		23	13 (56.52%)	
		Far	242	11 (4.55%)		10	3 (30.00%)	
	M	Cloister	950	54 (5.68%)	0.2103	40	15 (37.50%)	0.2737
		Close	491	25 (5.09%)		20	10 (50.00%)	
		Mid	808	38 (4.70%)		32	13 (40.62%)	
		Far	470	35 (7.45%)		19	12 (63.16%)	
Layer	All	1	1749	84 (4.80 %)	**0.0498**	70	28 (40.00%)	0.4627
		2	2250	141 (6.27%)		94	43 (45.74%)	
	F	1	434	18 (4.15%)	0.0627	17	7 (41.18%)	1.0000
		2	816	55 (6.74%)		34	14 (41.18%)	
	M	1	1299	66 (5.08%)	0.2687	52	21 (40.38%)	0.3542
		2	1420	86 (6.06%)		59	29 (49.15%)	
Layer 1	All	Cemetery	1116	58 (5.00%)	0.5959	45	21 (46.67%)	0.1266
		Cloister	588	26 (4.42%)		25	7 (28.00%)	
	F	Cemetery	316	18 (5.70%)	**0.0050**	12	7 (58.33%)	**0.0441**
		Cloister	118	0 (0.00%)		5	0 (00.00%)	
	M	Cemetery	845	40 (4.73%)	0.4371	33	14 (42.42%)	0.6928
		Cloister	454	26 (5.73%)		19	7 (36.84%)	
Layer 2	All	Cemetery	1620	108 (6.67%)	0.2093	67	32 (47.76%)	0.5364
		Cloister	630	33 (5.24%)		27	11 (40.74%)	
	F	Cemetery	682	50 (7.33%)	0.1286	12	7 (58.33%)	0.6722
		Cloister	134	5 (3.73%)		6	3 (50.00%)	
	M	Cemetery	924	58 (6.28%)	0.6341	38	21 (55.26%)	0.2066

Adults		Periapical lesions						
Factor		variable	True frequency			Crude frequency		
			n	pres.	p-value	n	pres.	p-value
		Cloister	496	28 (5.65%)		21	8 (38.19%)	

6.9.4.3.2 Subadults

6.9.4.3.2.1 Crude frequency

For subadults, due to the very small number of cases, only crude frequency was calculated. Of 38 children, 7 (18.42%) presented with a periapical lesion. Most lesions were found in in juveniles (40.00%), followed by infans I (11.76%) and infans II (9.09%). No statistically significant difference between the age groups could be detected though, which is largely due to the very small sample sizes. In fact, in infans I, only 2 individuals presented with a lesion and in infants II it was only 1, whereas only 4 juveniles ha lesions. The small sample sizes cause the relatively high percentage values of periapical lesion occurrence. Therefore, none of the groups showed any significant differences in periapical lesion frequency and hardly any trends can be distinguished. (Table 108)

Table 108 Summary and test results for subadult periapical lesions crude frequency

Subadults	Periapical lesions			
Factor	variable	Crude frequency		
		n	presence	p-value
Total		38	7 (18.42%)	
Age	Infans_I	17	2 (11.76%)	0.1842
	Infans_II	11	1 (9.09)	
	Juvenile	10	4 (40.00%)	
Location	Cemetery	27	4 (14.81%)	0.3902
	Cloister	11	3 (27.27%)	
Layer	1	14	2 (14.29%)	1.00009
	2	24	5 (20.83%)	
Layer 1	Cemetery	9	1 (11.11%)	1.0000
	Cloister	5	1 (20.00%)	
Layer 2	Cemetery	18	3 (16.67%)	0.5680
	Cloister	6	2 (33.33%)	

6.9.4.4 Discussion and Conclusion

Periapical lesions are infections at the apex of tooth roots that are mostly caused by bacteria that enter the tooth tissue through an exposed pulpal cavity. Heavy attrition but most commonly severe caries lesions are major causes for pulp chamber exposure and therefore are strongly associated with the formation of periapical abscesses (Scott & Turner 1988; Schroeder 1997; Alt *et al.* 1998; Dias *et al.* 2007). If left untreated, these lesions can do serious damage to an

individual's health, as in its further course, the local infection might spread and eventually lead to an often deadly sepsis (Alt *et al.* 2008).

As already expected, due to the caries rates, especially the high rates of medium and profound caries, the frequency of periapical lesions is quite high in the Knuedler cemetery. The frequency of periapical lesions follows that of caries in that there is a decrease in lesion frequency between the older and the younger Layers. Other sites from Luxembourg and Germany that show equally high caries rates also present with high periapical frequency, such as Hettstedt Kirche, Hettstedt Gymnasium, Völklingen (Roßbach 2015), St. Esprit (Rehbach 2008) and Givenich (Rehbach *et al.* 2009), all urban sites. This suggests that caries is the leading cause for high periapical lesion frequency. However, the high frequency rates also suggest bad oral hygiene among all those urban populations listed above. (Table 109)

Table 109 Overview of Periapical lesion prevalence in medieval-postmedieval European sites

Periapical lesions frequency in Europe						
Time period	**Site**	**Country**	**Type of settlement**	**Socio-economic status**	**Periapical lesions frequency %**	**Publication**
11th-15th C	Givenich	Luxembourg	rural	upper class	55.60	Rehbach et al. (2009) Weidig et al. (2009)
18th C	Hettstedt Gym.	Germany	urban		54.00	Rossbach (2015)
15th C	Hettstedt Kirche	Germany	urban		52.90	Rossbach (2015)
12th-17th C	St. Esprit	Luxembourg	urban	mixed	50.80	Rehbach u. Bis-Worch (2006), Nothwang et al. (2006) Rehbach et al. (2007) Rehbach u. Nothwang (2007) Rehbach (2008) Rehbach u. Notwang (2009)
Early post-medieval	Völklingen	Germany			47.60	Rossbach (2015)
14th-mid-17th C	Knuedler	Luxembourg	urban		45.74	Kremmer (hic)
15th-17th C	St. Gertrude church	Lativia	urban		44.33*	Pētersone-Gordina et al. (2018)
mid-17th-18th C	Knuedler	Luxembourg	urban		40.00	Kremmer (hic)
17th-18th C	Jelgava Church	Latvia	urban	Upper class	35.94*	Pētersone-Gordina et al. (2012)
5th-18th C	St Armual Kreuzgang Saarbrücken	Germany		mixed	33.30	Geber (2006)
Early post-medieval	Lübeck	Germany	urban		31.00	Boenisch & Breuer (1996)
12th-14th C	Grevenmacher	Luxembourg	rural		28.80	Trautmann (2017)
12th-18th C	Slijpe	Belgium	rural coastel		26.90	Van Cant (2019)
late 16th-early 18th C	Grund/ Wenzelsmauer	Luxembourg	urban	soldiers	26.10	Trautmann u. Trautmann (2011)
Late medieval	Ellwangen-Jagst	Germany	urban		20.00	Kairies (2021)
14th-16th C	Several orthodox churches	Serbia	rural		20.00	Srejić (2001)

Periapical lesions frequency in Europe						
Time period	**Site**	**Country**	**Type of settlement**	**Socio-economic status**	**Periapical lesions frequency %**	**Publication**
1812 AD	Napoleonic mass grave	Lithuania	urban	soldiers	18.40	Palubeckaitė (2006)
18th C	Spitalfields	England	urban	Hospital	17.50	Whittaker & Molleson (1996)
10th-18th C	Emden	Germany	urban	upper/middle Class	13.50	Stech (2009)
Early post-medieval	St. Hedwigs Friedhof Berlin	Germany	urban		13.30	Timmermann (2005)
12th-15th C	Deinze	Belgium	urban		11.70	Van Cant (2019)
19th C	Viichte	Belgium	rural		7.70	Van Cant (2019)
Early post-medieval	Spandau	Germany	urban		6.70	Jungklaus (1996)
14th-19th C	Zottegem	Belgium	rural		5.30	Van Cant (2019)
Early postmedieval	Ellwangen-Jagst	Germany	urban		5.15	Kairies (2021)
12th-16th C	Minoritenweg Regensburg	Germany	urban	Hospital/lower class	2.20	Heyking (2012)
12th-17th C	Ihlow	Germany	urban	monastic	0.90	Timmermann (2009)

* = average

6.9.5 Ante-mortem Tooth loss

6.9.5.1 Introduction

Periodontal disease, caries, periapical abscesses, traumata and intentional tooth extraction can all be possible causes for ante-mortem tooth loss, with the first factor accounting for the majority of tooth loss cases in the past as well as in present day (Brothwell 1981; Waldron 2009; Roberts & Manchester 2010). Bone remodelling up to a complete closure of the alveola is indicative of intra-vital tooth loss (Waldron 2009). Remodelling of the alveola starts immediately after the tooth loss and complete closure of the alveola generally occurs between 3-4 months but the exact timing is very variable and can depend on a number of causes (Trombelli *et al.* 2008; Grupe *et al.* 2015). Therefore, it is possible to determine the approximate time of tooth loss before death. If a complete edentulation occurs, which most frequently happens in old age, this can lead to a considerable loss of bone bulk in the affected jaw (Pietrokovski *et al.* 2007; Waldron 2009).

6.9.5.2 Methods

Tooth loss was only systemically recorded as either absent or present for all scoreable tooth sockets in the dental arcade. Notes were made on stage of remodelling of the alveolus in question but those were not used in the following evaluation.

Antemortem tooth loss true and crude frequencies were compared between the sexes, age groups, burial layers and locations.

Finally, the relationship of antemortem tooth loss to caries was explored through visual inspection of bar charts.

6.9.5.3 Results

6.9.5.3.1 Adults

6.9.5.3.1.1 True frequency

Of 3976 scoreable sockets, 751 (18.89%) showed clear signs of antemortem tooth loss. Statistically significant differences in the distribution of ante mortem tooth loss could be detected between all groupings except for overall differences between the two Layers and cemetery and cloister burials of males from Layer 2. Overall, females (21.89%) had lost significantly more teeth than males (17.63%). Overall, people buried in the cemetery seemed to be more affected by tooth loss (19.74%) than those from the cloister (16.95%). However, when separating by males and females it becomes clear that the heavy discrepancy in distributions of female tooth loss brought about the pattern observed in the overall population. Females from the cemetery experienced 25.63% of tooth loss and those from the cloister only 7.14%. In males the trend was the opposite with more tooth loss occurring among cloister burials (19.94%) than among cemetery burials (16.38%). Regarding distance to church, the same pattern already detected in caries occurrence can be observed, namely that people buried in the middle of the cemetery (22.08%) experienced much more tooth loss than the rest. Females reflect this same pattern, but in males those buried far from the church (21.38%) experience most tooth loss. Overall and for males and females, people buried in Layer 1 (15.41%) showed significantly less tooth loss than those from Layer 2 (21.58%). When considering only Layer 1, males and females show the exact opposite trend in differences between burial locations, with men showing more tooth loss in the cloister (21.33%) than in the cemetery (12.20%) and women showing more tooth loss in the cemetery (20.19%) than in the cloister (5.08%). In fact, the results for women in Layer 1 are very similar to those detected in periapical lesions. No periapical lesions occurred in women from Layer 1 buried in the cloister and only 6 teeth were lost after death.

Within Layer 2, a general trend of people buried in the cemetery (23.51%) showing more tooth loss than those from the cloister (16.59%) can be observed overall and for both men and women.

Age showed a very clear correlation with ante mortem tooth loss. Ante mortem tooth loss increased significantly with age; mirroring trends already observed in caries lesions (Figure 279, Figure 280).

Figure 279 also shows that whilst caries rates drop in the mature II and senile age cohorts, antemortem tooth loss is increasing. This adds weight to the theory that caries is in fact underrepresented in seniles because many carious teeth had already been lost by then. It also establishes caries as one of the major causes of tooth loss. (Table 110)

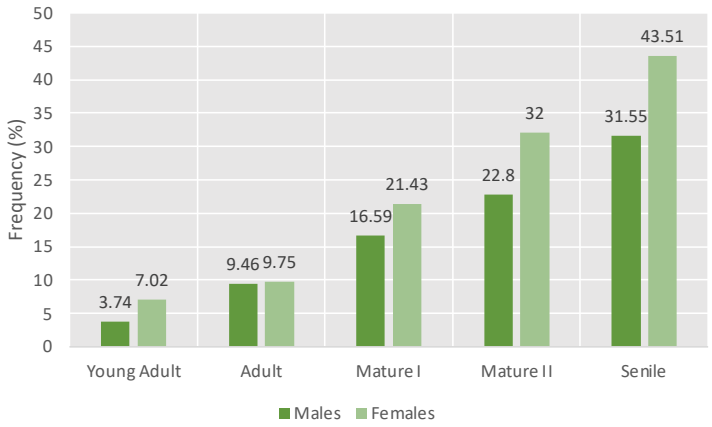

Figure 279 Rates of Antemortem Tooth loss calculated on all tooth sockets for males and females by age

Figure 280 Comparison of true caries and antemortem tooth loss rates for males and females by age

6.9.5.3.1.2 Crude frequency

Of 170 individuals that were eligible for scoring, 107 showed one or more cases of ante mortem tooth loss, which corresponds to a frequency of 62.94%. Approximately the same number of men than women experienced ante mortem tooth loss, which means that, when comparing the results to the true frequency, women lost on average more teeth than men. Overall, more people buried in the cemetery (68.10%) experienced tooth loss than those from the cloister (51.85%),

and the same trend, while insignificant can also be observed among men and women. Distance to church reflects the same pattern as true frequency but the differences between the groups are not significant and the same goes for differences between the Layers, where tooth loss was less prevalent in Layer 1 (57.53%) than in Layer 2 (67.01%). Significant differences could be detected only within Layer 2 in overall and male differences between burial locations where in both instances, cemetery burials (75.71%) contained more individuals with tooth loss than cloister burials (44.44%). The same trend was also prevalent in Layer 1 but not statistically relevant. Age also showed a correlation with ante mortem tooth loss on the individual level, with the number of individuals with tooth loss increasing with age. This trend was clear in the whole sample as well as in men and women but was not statistically significant for the latter. (Table 110)

Table 110 Summary and test results for adult antemortem tooth loss true and crude frequency

Adults			**Ante mortem tooth loss**					
Factor		**variable**	**True frequency**			**Crude frequency**		
			n	**present**	**p-value**	**n**	**present**	**p-value**
Total			3976	751 (18.89%)		170	107 (62.94%)	
Sex		F	1247	273 (21.89%)	**0.0015**	54	34 (62.96)	0.9246
		M	2695	475 (17.63%)		113	72 (63.72	
Age	All	Young Adult	579	31 (5.35%)	**<0.0001**	24	10 (41.67%)	**0.0028**
		Adult	1049	100 (9.53%)		43	20 (46.51%)	
		Mature I	612	111 (18.14%)		28	20 (71.43%)	
		Mature II	959	238 (24.82%)		39	28 (71.79%)	
		Senile	761	266 (34.95%)		35	28 (80.00%)	
	F	Young Adult	285	20 (7.02%)	**<0.0001**	13	6 (46.15%)	0.4833
		Adult	277	27 (9.75%)		12	7 (58.33%)	
		Mature I	196	42 (21.43%)		7	6 (85.71%)	
		Mature II	250	80 (32.00%)		11	7 (63.64%)	
		Senile	239	104 (43.51%)		11	8 (72.73%)	
	M	Young Adult	294	11 (3.74%)	**<0.0001**	11	4 (36.36%)	**0.0016**
		Adult	772	73 (9.46%)		31	13 (41.94%)	
		Mature I	416	69 (16.59%)		21	14 (66.67%)	
		Mature II	693	158 (22.80%)		27	21 (77.78%)	
		Senile	504	159 (31.55%)		22	19 (86.36%)	
Location	All	Cemetery	2761	545 (19.74%)	**0.0388**	116	79 (68.10%)	**0.0411**
		Cloister	1215	206 (16.95%)		54	28 (51.85%)	
	F	Cemetery	995	255 (25.63%)	**<0.0001**	42	29 (77.78%)	0.1014
		Cloister	252	18 (7.14%)		12	5 (41.67%)	
	M	Cemetery	1752	287 (16.38%)	**0.0209**	73	49 (67.12%)	0.3090
		Cloister	943	188 (19.94%)		40	23 (57.50%)	
Distance to Church	All	Cloister	1215	206 (16.95%)	**0.0008**	54	28 (51.85%)	0.1580
		Close	652	102 (15.64%)		30	20 (66.67%)	
		Mid	1404	310 (22.08%)		57	37 (64.91%)	
		Far	705	133 (18.87%)		29	22 (75.86%)	
	F	Cloister	252	18 (7.14%)	**<0.0001**	12	5 (41.67%)	0.3158
		Close	159	24 (15.09%)		9	6 (66.67%)	
		Mid	594	197 (33.16%)		23	17 (73.91%)	
		Far	242	34 (14.05%)		10	6 (60.00%)	

Adults		Ante mortem tooth loss						
Factor		variable	True frequency			Crude frequency		
			n	present	p-value	n	present	p-value
	M	Cloister	943	188 (19.94%)	**0.0008**	40	23 (57.50)	0.2135
		Close	479	75 (15.66%)		20	13 (65.00%)	
		Mid	810	113 (13.95%)		34	20 (58.82%)	
		Far	463	99 (21.38%)		19	16 (84.21%)	
Layer	All	1	1733	267 (15.41%)	**<0.0001**	73	42 (57.53%)	0.2043
		2	2243	484 (21.58%)		97	65 (67.01%)	
	F	1	435	70 (16.09%)	**0.0003**	18	9 (50.00%)	0.1631
		2	812	203 (25.00%)		36	25 (69.44%)	
	M	1	1278	197 (15.41%)	**0.0042**	53	33 (62.26%)	0.7628
		2	1417	278 (19.62%)		60	39 (65.00%)	
Layer 1	All	Cemetery	1145	165 (14.41%)	0.1089	46	26 (56.52%)	0.8193
		Cloister	588	102 (17.35%)		27	16 (59.26%)	
	F	Cemetery	317	64 (20.19%)	**0.0001**	12	7 (58.33%)	0.6199
		Cloister	118	6 (5.08%)		6	2 (33.33%)	
	M	Cemetery	828	101 (12.20%)	**<0.0001**	34	19 (55.88%)	0.1998
		Cloister	450	96 (21.33%)		19	14 (73.68%)	
Layer 2	All	Cemetery	1616	380 (23.51%)	**0.0003**	70	53 (75.71%)	**0.0033**
		Cloister	627	104 (16.59%)		27	12 (44.44%)	
	F	Cemetery	678	191 (28.17%)	**<0.0001**	30	22 (73.33%)	0.3428
		Cloister	134	12 (8.96%)		6	3 (50.00%)	
	M	Cemetery	924	186 (20.13%)	0.5073	39	30 (76.92%)	**0.0083**
		Cloister	493	92 (18.66%)		21	9 (42.86%)	

6.9.5.3.2 Subadults

6.9.5.3.2.1 True frequency

In subadults, a total of 784 tooth sockets could be analysed and 12 (1.53%) showed antemortem tooth loss. Therefore, as expected, ante mortem tooth loss was really low in children. infans I and infans I each had one tooth lost before death and juveniles had lost a total of 10 (3.82%) teeth, thus age played a significant role in the occurrence of tooth loss in children as well. No significant differences could be observed between burial locations and layers but tendentially, children buried in the cemetery had lost more teeth than those buried in the cloister. (Table 111)

6.9.5.3.2.2 Crude frequency

Of 40 children, 7 (17.50%) had experienced tooth loss in life. No significant correlation with age could be observed here, but generally juveniles (36.36%) had more cases of tooth loss than the younger age groups. As already reflected in the true frequencies, most individuals with tooth loss were buried in the cemetery but sample sizes were so small that it would not be advisable to talk about a general trend. (Table 111)

Table 111 Summary and test results for subadult antemortem tooth loss true and crude frequency

Subadults		Ante mortem tooth loss					
Factor	variable	True frequency			Crude frequency		
		n	presence	p-value	n	presence	p-value
Total		784	12 (1.53%)		40	7 (17.50)	
Age	Infans_I	289	1 (0.35%)	**0.011**	18	2 (11.11%)	0.3056
	Infans_II	233	1 (0.43%)		11	1 (9.09)	
	Juvenile	262	10 (3.82%)		11	4 (36.36%)	
Location	Cemetery	546	10 (1.83%)	0.3642	27	5 (18.52%)	1.0000
	Cloister	238	2 (0.84%)		13	2 (15.38%)	
Layer	1	280	6 (2.14%)	0.3648	15	3 (20.00%)	1.0000
	2	504	6 (1.19%)		25	4 (16.00%)	
Layer 1	Cemetery	177	5 (2.82%)	0.4192	9	2 (22.22%)	1.0000
	Cloister	103	1 (0.97%)		6	1 (16.67%)	
Layer 2	Cemetery	369	5 (1.36%)	1.0000	18	3 (16.67%)	1.0000
	Cloister	135	1 (0.74%)		7	1 (14.29%)	

6.9.5.4 Discussion and Conclusion

One of the leading causes for antemortem tooth loss is dental caries but other oral pathologies such as periodontal disease or periapical abscesses are also major causes (Hillson 1996, 2001). Therefore, antemortem tooth loss should always be considered when analysing dental caries. Often times, tooth loss is used to correct dental caries rates in order to provide more accurate results on the actual caries frequency since caries frequency based solely on scoreable lesions tends to underestimate the actual frequency in the population (Lukacs 1995; Hillson 1996; Caselitz 1998; Mant & Roberts 2015). Eventually, antemortem tooth loss can lead to complete edentulation, a phenomenon which occurs predominantly in the elderly.

In the Knuedler Cemetery, antemortem tooth loss was correlated with caries frequency. Both showed a stark increase with age. However, antemortem tooth loss frequency kept rising into the senile age group, whilst the increase in caries frequency peaked at the mature I age group and dropped again in the mature II and senile groups. The most likely explanation for this trend would be that lower caries rates in seniles are caused by the higher tooth loss rate in the same age group. Which would ensue, that at least on the Knuedler Cemetery, caries was the major contributor to antemortem tooth loss.

Like caries frequency, the overall antemortem tooth loss rate was quite high. Tooth loss true and crude frequencies were also slightly higher in the older Layer (L2: 67.01%; L1: 57.53%). This was also reflected in the reduction of caries frequency between Layer 1 and Layer 2, suggesting improved oral health in the younger period, with reduced caries formation and therefore also less tooth loss.

Like caries frequencies, rates of antemortem tooth loss appear to be quite variable across contemporary European sites. True frequencies range from 2% to ~40% and crude frequencies

from ~8%-~90%. Generally, sites that showed low caries rates also showed relatively low levels of antemortem tooth loss. As such, the values for crude frequencies that have been calculated for Luxembourg City are on the higher end of the spectrum of antemortem tooth loss prevalence, which is also reflected in the caries rates. However, true frequency seems to be right in the middle of the spectrum.

Compared to contemporary Luxembourgish sites, antemortem tooth loss rates were rather low among the Knuedler population, with Givenich showing 81.4% tooth loss by individual, St. Esprit individuals suffering from 86.4% and Grevenmacher from 77.2% tooth loss. This might indicate better oral hygiene practices among people buried In the Knuedler cemetery than those from other places in town. However, it has to be kept in mind that the individuals from St. Esprit were also partially patients under the care of the nuns of the St. Esprit convent. A weakened immune system due to illness might have therefore influenced the high caries and antemortem tooth loss rates (Åkesson *et al.* 2016). (Table 112)

Table 112 Overview of Ante mortem Tooth Loss (AMTL) prevalence in medieval-postmedieval European sites (compiled partially from (Müller & Hussein 2017; Bertilsson *et al.* 2022)*)*

Ante mortem tooth loss frequency in Europe							
Time period	**Site**	**Country**	**Type of settle ment**	**Socio-economic status**	**AM tooth loss true frequency %**	**AM tooth loss crude frequency %**	**Publication**
12th-17th C	St. Esprit	Luxembourg	urban	mixed		86.40	Rehbach u. Bis-Worch (2006), Nothwang et al. (2006) Rehbach et al. (2007) Rehbach u. Nothwang (2007) Rehbach (2008) Rehbach u. Notwang (2009)
11th-15th C	Givenich	Luxembourg	rural	upper class		81.40	Rehbach et al. (2009) Weidig et al. (2009)
1100-1810 AD	Linköping Östergötland	Sweden	urban			81.153	Bramstång and Nordin (2017)
12th-14th C	Grevenmacher	Luxembourg	rural		19.00	78.50*	Trautmann (2017)
17th-18th C	Jelgava Church	Latvia	urban	upper class		77.42*	Pētersone-Gordina et al. (2012)
12th-19th C	Moorsel	Belguim	rural		34.30	76.50	Van Cant (2019)
15th-19th C	Oosterweel	Belguim	rural polder	upper class	18.70	75.00	Van Cant (2019)
12th-15th C	Deinze	Belguim	urban		30.07	71.70	Van Cant (2019)
19th C	Viichte	Belguim	rural		45.50	71.40	Van Cant (2019)
14th-16th C	Orthodox churches	Serbia	rural		10.00	70.00	Srejić (2001)
14th-19th C	Zottegem	Belguim	rural		23.30	65.00	Van Cant (2019)

Ante mortem tooth loss frequency in Europe							
Time period	**Site**	**Country**	**Type of settlement**	**Socio-economic status**	**AM tooth loss true frequency %**	**AM tooth loss crude frequency %**	**Publication**
12th-18th C	Slijpe	Belguim	rural coastal		16.50	61.50	Van Cant (2019)
17th C	Gothenburg	Swedwn	urban		3.00	60.00	Lingström & Borman (1999)
14th-mid-17th C	Knuedler	Luxembourg	urban		17.35	59.26	Kremmer (hic)
15th-17th C	St. Gertrude church	Lativia	urban			56.73*	Pētersone-Gordina et al. (2018)
mid-17th-18th C	Knuedler	Luxembourg	urban		14.41	56.52	Kremmer (hic)
18th C	Spitalfields	England	urban	Hospital	8.50	53.80	Whittaker & Molleson (1996)
17th-19th C	Gothenburg	Sweden	urban	lower class soldiers		34.35*	Arcini et al. (2020)
1812 AD	Napoleonic mass grave	Lithuania	urban	soldiers	2.70	33.10	Palubeckaitė (2006)
Late medieval	Ellwangen-Jagst	Germany	urban			22.61	Kairies (2021)
12th-16th C	Minoritenweg Regensburg	Germany	urban	Hospital/lower class		20.20	Heyking (2012)
15th-16th C	Turku	Finland	urban	lower class		13.62*	Varrela (1991)
10th-18th C	Emden	Germany	urban	upper/moiddle class		8.60	Stech (2009)
Early postmedieval	Ellwangen-Jagst	Germany	urban			7.35	Kairies (2021)
18th-19th C	St. Brides	England	urban	lower class	41.50		Mant & Roberts (2015)
18th-19th C	Chelsea church	England	urban	middle class	40.2		Mant & Roberts (2015)
15th-18th C	Koprivno	Croatia	urban		8.10		Adamić and Šlaus (2017)
5th-18th C	St Armual Kreuzgang Saarbrücken	Germany		mixed	26.1		Geber (2006)
16th-17th C	Trakai churchyard	Lithuania	urban		12.1		Miliauskienė and Jankauskas (2015)
16th-17th C	Trakai church	Lithuania	urban	upper class	4.1		Miliauskienė and Jankauskas (2015)
16th-17th C	Notre-Dame-du-Bourg	France	urban		40.96		Chazel et al. (2005)
1560-1620	Gothenburg, Nya Lödöse	Sweden	urban		2.00		Bertilson et al. (2021)

* = average

6.9.6 Dental attrition

6.9.6.1 Introduction

In dentistry and by extension also in anthropology, it is important to distinguish between two types of dental wear: Attrition and Abrasion. However, the definitions for both terms vary slightly in literature. According to Grupe et al. (2015), dental abrasion refers to the mechanical

wear of teeth due to contact with objects such as food items or other foreign substances and the degree to which dental abrasion is expressed is not only dependent on the food items consumed but also on individual factors such as size of the tooth, thickness of enamel or force of mastication. Attrition on the other hand would refer only to wear caused strictly by tooth-on-tooth contact and is mainly related to conditions such as bruxism or diverse malocclusions. Hillson 1996 however proposes a slightly different definition of the terms. Abrasion refers here also to any kind of loss of tooth substance that is not caused by tooth-on-tooth contact. However, tooth-on-tooth contact includes chewing in Hillson's (1996) definition, which means that dental wear caused by food consumption would also be addressed as attrition. For the purpose of this study, the definition of Hillson (1996) was adopted and any reference to dental abrasion will refer to tooth substance loss caused by foreign objects or use of teeth as "tools", attrition will refer to the general tooth wear caused by chewing and influenced by food intake. After the latter definition, dental attrition does not only worsen with age but is also highly dependent on the kind of foods consumed by an individual. Soft and processed foods generally do not cause much or any dental abrasion whereas hard foods such as grains cause stronger dental wear. Especially in the past, foods made from processed grains were highly abrasive since oftentimes, grains were ground to flour on stone mortars, incorporating fine stone flakes and powder into the food items, which acted highly abrasive on teeth (Roberts & Manchester 2010; Grupe *et al.* 2015). Therefore, dental abrasion was generally more severe in the past, especially in agricultural societies, than it is today (Grupe *et al.* 2015). Although dental wear is not a dental pathology but a mechanical process, especially in its later stages, when the tooth pulp gets exposed, it can predispose for a multitude of other dental diseases, most importantly dental caries (Ortner 2003a).

6.9.6.2 Methods

Dental attrition was recorded for all scoreable teeth in the dental arcade. Teeth that were completely destroyed by caries lesions were considered unscoreable but if the occlusal or incisal surfaces were still clearly recognisable, an attrition score was given. Although the statistical analyses were carried out for adults and non-adults separately, they were both recorded with the same 6-point recording system based on the work of Trautmann (2012). Although this system is not as widely used as the one established by Smith (1984), it was nonetheless applied in this study in order to keep the results comparable to those from Grevenmacher, where the former scoring method was also employed. A detailed description of the six stages of dental abrasion can be found in Table 113.

The severity of dental attrition was compared between sex, age, burial layer and location. Comparisons and mean attrition scores were based on all teeth available and not on mean scores calculated by individual. Graphical illustrations for attrition scores by tooth as well as visual comparisons of individual composite attrition scores by sex, age and location were created and described.

Dental abrasion was analysed statistically, and the detected cases have been discussed and described. However, the statistical analysis has to be considered with care since sample sizes are small and data was ordinal. Therefore, only mean scores for visual comparison have been reported in the tables.

Table 113 Scores for dental attrition based on Trautmann (2012)

Score	Description
0	Tooth present without traces of attrition
1	Polish facets on the cusps and enamel
2	Exposure of single spots of dentine, usually accompanied by flattening of cusps
3	Dentine visible on <50% of the tooth surface
4	Dentine visible on >50% of the tooth surface
5	>50% of the tooth crown has been removed

6.9.6.3 Results

6.9.6.3.1 Adults

Overall and within the two burial layers, females (2.04) showed less attrition than males (2.37). The Mann Whitney U test turned out highly significant ($p<0.0000$) when in reality, the difference, at 0.33 was not terribly marked. Within Layer 1 the difference between attrition scores in males and females was 0.31 which was quite similar to that within Layer 2 at 0.36. In the cemetery, males and females had very similar attrition scores (diff: 0.27) but in the cloister the difference in scores was 0.5. Overall, cemetery burials have stronger attrition degrees than cloister burials (diff.: 0.17) ($p=0.0004$). The difference is slightly more marked in women (0.33) ($p=0.0007$) than in men (0.10) ($p=0.0568$). Generally, tooth wear seems to increase with growing distance to cloister but the differences between the burial zones are too small to infer an actual trend. Within Layer 1 the overall sample shows barely any difference in attrition scores between burial locations, but the differences are slightly more marked in men (0.27) and women (0.31) even though they show the opposite trend, with cemetery burials showing higher scores than cloister burials in women and cloister burials showing more attrition than cemetery

burials in men. Within Layer 2, all groups show higher attrition scores in the cemetery than in the cloister, but the difference is most marked in men (0.45). Individuals from Layer 2 showed higher attrition scores than individuals in Layer 1 (0.13). The Mann Whitney U tests showed that the difference was significant (p=0.0065), even though the actual difference is not marked. In the overall sample as well as in males and females, age seems to be the most important factor for increasing attrition scores. Young adults had the lowest score at 1.55, and from there the scores increased steadily until the senile age cohort which displayed the highest scores at 2.75. Senile males even reached an average attrition score of 2.85, while in females the senile mean was 2.63. This indicates that men's teeth wore down stronger with age and this could hint at a different diet between men and women, only leaving a traceable impact on the teeth in the long run. The Kruskal-Wallis test for age also turned out highly significant (p<0.0000). (Table 114) Figure 281 illustrates the distribution of attrition scores by tooth for the upper and lower jaw left and right side. Interestingly, front teeth such as the first and second incisors (I1 and I2) as well as the canines (C) showed the highest degrees of attrition. It would have been expected that the highest degrees would be found in molars since they are primarily involved in mastication. However, many molars could not be scored due to medium or severe occlusal caries lesions, and on some occasions because of calculus deposits on the crown surface. This underscoring of molars, especially in the older age categories where attrition was on average strongest, might explain the patterns observed in this sample.

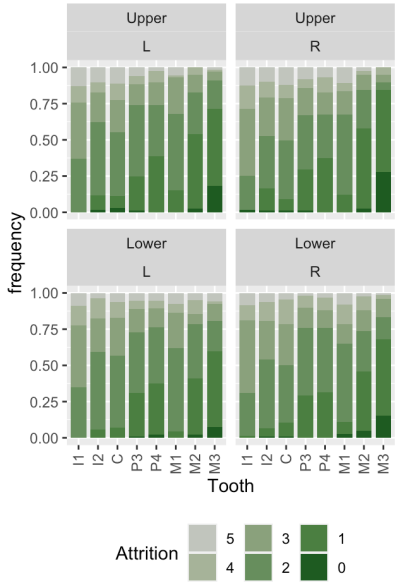

Figure 281 Dental attrition severity by tooth for the upper and lower jaw of the left and right body side of the adult permanent dentition

Table 114 Mean attrition scores for adults by sex, age, burial location and layer

Adults		Attrition		
Factor		**variable**	**by tooth**	
			n	score
Sex		F	766	2.05
		M	1834	2.37
Age	All	Young Adult	477	1.55
		Adult	788	2.02
		Mature I	401	2.57
		Mature II	578	2.70
		Senile	379	2.75
	F	Young Adult	218	1.51
		Adult	202	1.95
		Mature I	96	2.34
		Mature II	130	2.33
		Senile	120	2.63
	M	Young Adult	259	1.58
		Adult	586	2.04
		Mature I	305	2.64
		Mature II	435	2.84
		Senile	244	2.85
Location	All	Cemetery	1759	2.33
		Cloister	869	2.16
	F	Cemetery	548	2.14
		Cloister	218	1.81
	M	Cemetery	1205	2.41
		Cloister	629	2.31
Distance to Church	All	Cloister	869	2.16
		Close	452	2.13
		Mid	845	2.26
		Far	462	2.64
	F	Cloister	218	1.81
		Close	118	1.75
		Mid	273	2.32
		Far	157	2.13
	M	Cloister	629	2.31
		Close	328	2.26
		Mid	572	2.23
		Far	305	2.91
Layer	All	1	1218	2.20
		2	1410	2.33
	F	1	306	1.98
		2	460	2.09
	M	1	890	2.29
		2	944	2.45
Layer 1	All	Cemetery	808	2.18
		Cloister	410	2.23
	F	Cemetery	193	2.10
		Cloister	113	1.79
	M	Cemetery	615	2.21
		Cloister	275	2.48
Layer 2	All	Cemetery	951	2.45
		Cloister	459	2.09
	F	Cemetery	355	2.16
		Cloister	105	1.83
	M	Cemetery	590	2.62
		Cloister	354	2.17

6.9.6.3.2 Subadults

6.9.6.3.2.1 Deciduous dentition

A total of 296 deciduous teeth could be scored for dental attrition belonging to 30 children, of these 220 belonged to infans I and 76 to infans II. A significant difference was observed between the two age classes with the older group (infans II) having a significantly higher mean degree of attrition (2.13) than those from the younger age group (1.01) ($p=0.0014$). This was to be expected as abrasion intensifies with age as already demonstrated for the adults. Furthermore, significant differences in attrition scores were detected among the burial locations with those buried in the cloister (1.91) exhibiting more attrition than those buried in the cemetery (1.10) ($p<0.0000$), a trend which is also true when examining the Layers separately. The difference between Layer 1 (1.42) and Layer 2 (1.04) was not considered significant however ($p=0.0812$). (Table 115)

Figure 282 shows the distribution of dental attrition severity by tooth for the deciduous dentition differentiated by body side. Whilst the canine was least affected by attrition, the incisors and molars were affected to a similar extent. The first deciduous molar (DP3) was the tooth with most attrition, but the first incisor (DI1) showed the most severe degrees. Overall, none of the teeth reached the highest attrition severity degrees.

6.9.6.3.2.2 Permanent dentition

For the permanent dentition, a total of 125 teeth could be scored for attrition and 12 belonged to infans I, 113 belonged to infans II and 228 to juveniles. A clear increase with age in attrition scores could be observed as expected with infans I showing no attrition, infans II had a score of 0.50. and juveniles a score of 1.40 ($p<0.0000$). Since the 12 scoreable teeth of infans I were all erupting M1, no attrition was expected on these. The permanent teeth of infans I are all also either just erupted or erupting and thus attrition scores were expected to be low here as well. The scores of juveniles are higher since their permanent teeth have been in use for longer already and they were by then probably also consuming a diet similar to that of adults. A significant difference ($p<0.0000$) was observed between burial locations with cemetery burials overall and within each Layer displaying higher attrition scores (1.19) than cloister burials (0.85). This means that the permanent dentition shows an opposing trend to the deciduous one. For the deciduous dentition, this is best explained by the age class distribution in the site, since the vast majority of infans I was buried in the cemetery and infans II were distributed rather evenly, overall cemetery values will be lower since infans II have higher attrition scores. For

the permanent dentition the same principle applies to a certain extent. Just over half of juveniles are buried inside the cloister whereas just less than half of infans II are buried inside the cloister. Finally, the difference observed between Layer 1 (1.01) and Layer 2 (1.10) was not deemed statistically significant. (Table 115)

Figure 283 illustrates the distribution of attrition by tooth for the subadult permanent dentition. Here, as expected, the third molar (M3) was least affected by attrition since in most individuals it had likely erupted not too long ago. Interestingly however, the subadult dentition mirrors the pattern of the adult dentition with front teeth most affected by attrition, followed by the first molar. Overall, none of the teeth reached the highest attrition severity degrees.

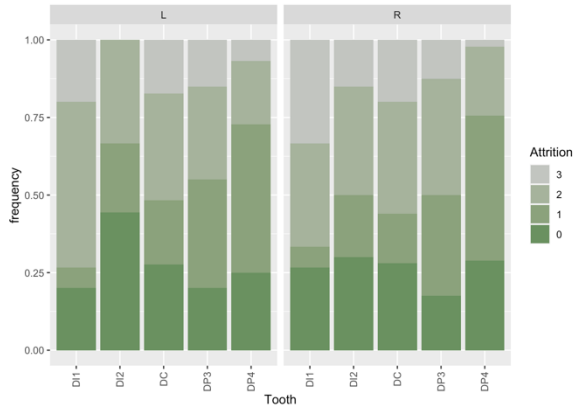

Figure 282 Distribution of dental attrition severity by tooth for the subadult permanent dentition differentiated for right and left body side

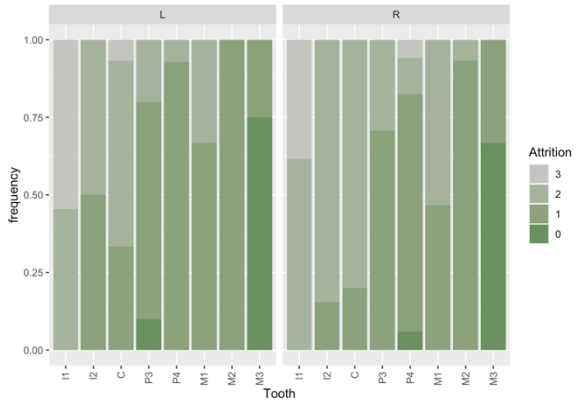

Figure 283 Distribution of dental attrition severity by tooth for the adult permanent dentition, differentiated for right and left body side

Table 115 Mean attrition scores for subadults by sex, age, burial location and layer

Subadults		**Attrition**			
Factor	**variable**	**permanent dentition**		**deciduous dentition**	
		n	**score**	**n**	**score**
Age	Infans_I	12	0.00	220	1.01
	Infans_II	113	0.50	76	2.13
	Juvenile	228	1.40	---	---
Location	Cemetery	226	1.19	222	1.10
	Cloister	127	0.85	74	1.91
Layer	1	125	1.01	112	1.42
	2	228	1.10	184	1.23
Layer 1	Cemetery	73	1.19	77	1.04
	Cloister	52	0.75	35	2.26
Layer 2	Cemetery	153	1.19	145	1.13
	Cloister	75	0.92	39	1.59

6.9.6.3.3 Dental abrasion

Often, deviations from normal horizontal attrition, such as for example the occurrence of grooves on occlusal, incisal or interproximal surfaces or polishing facets on teeth can be indications for a use of teeth as tools (Molnar 2008; Willman *et al.* 2020; Lozano *et al.* 2021). Different activities can leave different traces on the teeth. Specific tooth wear patterns are most commonly seen in professions such as basketing or weaving, where chord or thread is held between the teeth, often resulting in clear grooves on or between teeth (Willman *et al.* 2020; Lozano *et al.* 2021). Other foreign objects can also cause use wear on teeth. A very iconic example would be clay pipe smoking. The abrasive surface of the pipe stem gradually wears off teeth at the location where the pipe is being held, creating pipe stem-sized holes that are well visible when teeth from the lower and upper dental arcade are in occlusion (Kvaal & Derry 1996). In a total of 13 individuals, the distinct traces of clay pipe smoking could be detected (Figure 284). All of the 13 individuals were male, and all age categories were similarly represented. One older male even presented with two very distinct pipe holes on the right and left. In one individual (2008-78/729) the calculus on the teeth was additionally stained completely black, which might be an indication of tobacco use but taphonomic reasons cannot be excluded. Additionally, this mature individual presented with a pipe hole on the right and left side. Evidence of a profound caries lesion on the side of the large pipe hole suggests that the lesion led the individual to start carrying the pipe on the other side. Individual 2008-78/752 also showed evidence of a pipe hole on the right and left sides of the dental arcade but showed no evidence of caries.

Furthermore, 4 cases of potential use wear could be identified. Individual 2008-78/1449, a mature male buried in the cemetery, presented with a deep and narrow furrow which ran across the incisal edge of the canine down the lingual side and across P3 and was then visible again as a deep narrow groove on the occlusal surface of M1 and M2 with wear on M2 additionally sloping down distally. P4 had a large polishing facet on the distal side.

Individual 2008-78/1065 presented with a strongly v-shaped use wear between the right and left I1-C with a large polishing facet on the labial side of the canines.

The lingual side of the upper right canine of individual 2008-78/1482a was slightly hollowed with a deep striation at the base going from the center of the lingual face to the cemento-enamel junction. Finally, individual 2008-78/1457 presented with a distinctly scooped out wear on both upper M1.

In a further 3 individuals it was not entirely clear whether the wear observed was due to pipes or other dental use wear. Two of these individuals were female and one was male.

Figure 284 Example of a pipe hole from the Knuedler cemetery

6.9.6.4 Discussion and Conclusion

Dental attrition is strongly influenced by the quality and texture of the food ingested. In fact, different kinds of food can leave different traces on the surface of teeth. Through microscopic analyses of these traces, it is sometimes even possible to reconstruct more detailed dietary patterns of past populations (El-Zaatari 2010). Hard foods, such as grains, nuts, brittle plants or even raw meat are considered to have a strongly abrasive effect on teeth (Šlaus *et al.* 2011) and continued consumption of such food items during life is the leading cause for increased attrition in old age. Therefore, populations with overall strongly abraded teeth are often considered to consume a diet based on hard abrasive foods. Some studies associate high caries rates with strong tooth abrasion as the wear down of the enamel facilitates access into the tooth tissues for oral bacteria. In heavy dental wear however, the interproximal tooth areas are most often affected by caries lesions since the wear made the occlusal surfaces smooth, causing food to get stuck primarily between the teeth. Occlusal or fissure caries is however most often associated with low dental abrasion as food items get stuck in the fissures (Hillson 1996). Therefore, high occurrence of caries with low dental attrition is not an uncommon finding. Mainly soft but carbohydrate rich diets would cause such a pattern. And this is the exact pattern observed in the population from the Knuedler cemetery. Average dental attrition in Luxembourg City is rather moderate and amounts to 2.2 in the upper and 2.3 in the lower layer, furthermore males show a higher amount of dental attrition than women and cemetery burials a higher degree of attrition than cloister burials. Furthermore, the average abrasion degree is also influenced by the prevalence of old individuals in the cemetery, young adult and adult individuals had average dental wear scores of 1.55 and 2.02 respectively. Unfortunately, due

to the vast array of scoring methods used in different studies on dental abrasion, direct comparisons to most other sites were not possible. However, Trautmann 2012 used the same scoring system in their evaluation of the Grevenmacher sample and found an average degree of attrition of 2.5. This degree is slightly higher than that from Knuedler and might suggest either a shift in dietary patterns or quality of foods from the medieval to postmedieval times or might reflect differences in dietary habits between rural and urban populations. In fact, as milling techniques improved, small inclusions of sand or stone from stone mortars, that were often included in the flower and bread, were eliminated, and rendered these food items less abrasive (Roberts & Manchester 2010). Furthermore, the dehulling of grain used in bread baking made the resulting "white bread" less abrasive on teeth (Schultz 1988). Furthermore, in urban areas, access to fresh produce was much easier than in the countryside, where for example bread was baked or bought once a weak and then stored, making it much harder and more abrasive during consumption (Rösener 2001; Timmermann 2009). The site from Notre-Dame-du-Bourg in France also showed rather low degrees of dental abrasion (Chazel *et al.* 2005), however, the results were not directly comparable as they were based on a five point scale. A study on church and churchyard burials from Trakai, Lithuania showed higher attrition values among churchyard people than church burials (Miliauskiene & Jankauskas 2015), a pattern, albeit rather small, also observable at the Knuedler cemetery. A study on 12th-16th century remains from a convent in Ihlow also found higher dental abrasion degrees in men (Timmermann 2009) and the pattern was also reflected in people from late medieval and early postmedieval Ellwangen-Jagst (Kairies 2021) and medieval rural Luxembourg (Trautmann 2012). Furthermore, front teeth were most affected by dental wear in this sample and this was also found in Grevenmacher, Ihlow and Koprivno in Croatia (Adamić & Šlaus 2017). This wear pattern suggests stronger use of the front teeth. This could be related to the fact that front teeth, due to their early eruption timing, are in use longer than posterior teeth and thus attrition starts earlier (Timmermann 2009). Adamić and Šlaus (2017) suggest that the higher attrition in front teeth might be related to non-dietary factors such as use of teeth as tools. In fact, several potential traces of use wear could be detected in the form of deep grooves on the teeth of 3 individuals, but a conclusive reconstruction of activities that led to these traces could not be reached. However activities such as basket weaving could be good contenders. A further 13 individuals showed distinct traces of clay pipe smoking. This corresponds to a total of 6.34% of individuals that could be examined for the trait, all of them were male. This percentage was rather low when compared to others. 19% of individuals from a plague cemetery from 1710 from Holje showed traces of clay pipe use, in the cathedral of Linköping in Gothenburg it was

found in 28% of individuals and among East End Londoners from the early 19th century the frequency was even 39.6% (Walker & Henderson 2010). 2 cases were also found among the burials from Holy Trinity church in Jelgava Latvia (Pētersone-Gordina & Gerhards 2012) among a Garrison burial from Gothenburg (Arcini *et al.* 2020), among Napoleonic soldiers from a mass grave in Vilnius (Palubeckaitė *et al.* 2006), and in Hettstedt Gymnasium and Völklingen (Roßbach 2015) among others. Clay pipes were first brought to England in Elizabethan times but were still considered luxury goods by then. However, they soon spread to the Netherlands and by the 15th century the use of clay pipes was transported all over Europe, where it became a popular practice among all social classes from the mid-15th century onwards (Kvaal & Derry 1996).

7 Stable Isotope Analysis

7.1 Introduction

Stable isotope analysis of carbon and nitrogen can be used to make inferences about aspects of the dietary composition found in past populations, mainly about the protein content of the diet (DeNiro & Epstein 1978; Deniro & Epstein 1981; Ambrose & Norr 1993). In healthy individuals, the carbon and nitrogen isotopic values of bone collagen broadly reflect the dietary protein intake up to 10-30 years prior to death, depending on the collagen turnover rate of the bone sampled (Libby *et al*. 1964; Hedges *et al*. 2007).

Stable carbon isotope analysis can be used to distinguish between the consumption of C^3 and C^4 plants. During photosynthesis, all plants incorporate less ^{13}C than ^{12}C, however, C^4 and C^3 plants follow a different metabolic pathway wherein C^4 plants absorb less ^{13}C than C^3 plants, resulting in different isotopic signatures (Katzenberg, M. A., & Waters-Rist 2019).

In fact, C^3 plants such as oats, barley , wheat, nuts, legumes and vegetables, which thrive in temperate climates yield $\delta^{13}C$ values of ~ -24‰ to- 35‰, whereas C^4 plants, such as maize, millet, sorghum and sugar cane, which grow predominantly in arid and hot climates, yield $\delta^{13}C$ values between -9‰ and -15‰ (Deines 1980; Katzenberg, M. A., & Waters-Rist 2019).

Several studies have placed the diet-tissue spacing between plants and the bone collagen of the consumer at around 5‰ in terrestrial environments (Krueger & Sullivan 1984; Ambrose &

Norr 1993). This spacing was confirmed experimentally by Ambrose and Norr (1993) in a study on rats, however they concluded that this was only the case when carbohydrates, protein and fats came from the similar sources, namely either from C^3 plants and herbivores consuming C^3 plants or from C^4 plants and herbivores consuming C^4 plants. If one of these components was derived from another source, the diet to collagen spacing was more variable, which is why they recommend that the 5‰ spacing factor should only be considered as a guide. The tissue-tissue spacing between herbivore and carnivore bone collagen is estimated to fall around 0‰ to 2‰ (Bocherens & Drucker 2003). Following these recommendations, a consumer of a purely terrestrial C^3 protein diet should exhibit $\delta^{13}C$ values of bone collagen around -22‰, whereas the consumer of an entirely C4 based diet would exhibit $\delta^{13}C$ values of -8‰ (Kellner & Schoeninger 2007).

Stable carbon isotope analysis is also used to differentiate between terrestrial and marine diets. This is due to the fact that dissolved carbonate is the main source of carbon for marine organisms, whereas in terrestrial organisms CO^2 is the primary source of carbonate. Dissolved carbonate is enriched by -7‰ relative to atmospheric CO^2. Therefore, marine flora and fauna, and all organisms that feed on them display elevated $\delta^{13}C$ values compared to terrestrial plants and organisms (Tauber 1981; Chisholm *et al*. 1982; Schwarcz & Schoeninger 2012; Katzenberg, M. A., & Waters-Rist 2019). However, if the terrestrial component of the diet was dominated by C4 plants, the isotopic differentiation between a purely terrestrial diet and one with a marine component might be obscured (Tauber 1981). The influence of freshwater fish consumption on $\delta^{13}C$ values, is much more variable due to the greater variability of carbon sources in their environment. As such, studies have shown that $\delta^{13}C$ values did not only vary greatly between different species of fish but also within the same species of fish from different lakes and even within the same lake (France 1995; Dufour *et al*. 1999; Katzenberg & Weber 1999; Yoder 2012).

Through nitrogen stable isotope analysis the trophic level of the individuals under study can be determined (Deniro & Epstein 1981; Schoeninger & DeNiro 1984). This is due to step-wise fractionation of ^{14}N along the food chain, which results in an enrichment of $\delta^{15}N$ values of 3-5‰ from the primary source to its consumer (Bocherens & Drucker 2003). The largest difference in $\delta^{15}N$ values is found between marine and terrestrial organisms at about 15‰. These higher $\delta^{15}N$ values are due to the longer food chains in marine ecosystems and because the marine plants, that marine animals consume, have on average higher $\delta^{15}N$ values than terrestrial plants (Schoeninger *et al*. 1983). Therefore, $\delta^{15}N$ together with $\delta^{13}C$ values can also

be used to estimate the proportion of terrestrial vs marine protein component in the diet. Furthermore, freshwater fish, due to longer food chains generally in aquatic ecosystems, generally also exhibits higher $\delta^{15}N$ than terrestrial animals but lower $\delta^{13}C$ values than marine organisms. However, both values can be very variable between and within species as they are highly dependent on the local isotopic signatures (Dufour *et al*. 1999). It has to be noted as well that metabolic and nutritional stress can also lead to elevated $\delta^{15}N$ levels (Fuller *et al*. 2005; Reitsema 2013; Hertz *et al*. 2015; Doi *et al*. 2017; Redfern *et al*. 2019; Nicholls *et al*. 2020) as well as environmental factors such as cattle grazing in saline marshlands (Britton *et al*. 2008), climatic conditions such as aridity or temperature (Heaton *et al*. 1986), the possible presence of several distinct intraregional iso-zones (Stevens *et al*. 2013) or manuring of fields (Bogaard *et al*. 2007; Fraser *et al*. 2011).

7.2 Methods

7.2.1 Sampling strategy

7.2.1.1 Subadults

The most commonly used method to reconstruct weaning age is to investigate Nitrogen-15 isotope ratios ($\delta^{15}N$ values) in bone collagen or dentin, which mainly reflect dietary protein isotope ratios. Because of the trophic level effect, children who are exclusively breastfed will have 2-3‰ higher $\delta^{15}N$ values than their mothers. After introduction of supplementary foods and cessation of lactation, their $\delta^{15}N$ values decrease and start reflecting those found in adult bone collagen (Tsutaya and Yoneda, 2013, 2015). As children's bones grow in length and in width, new bone gets deposited and old bone resorbed (Scheuer & Black 2000). Generally, bone growth at the metaphyses is faster than appositional growth of the diaphysis, due to the increased presence of osteoclasts and osteoblasts in this area (Scheuer & Black 2000; Waters-Rist & Katzenberg 2010), which leads to the newer bone collagen reflecting the $\delta^{15}N$ and $\delta^{13}C$ values of the most recently consumed diet. As bone collagen turnover rate is faster in adolescents than in adults (Hedges *et al.* 2007), and within subadults there is also a decline in bone turnover rates from neonates to juveniles (Frost 1961, 1969), the stable isotope values detected in young children, reflect the diet consumed shortly before death. Furthermore, bone collagen turn-over rate is faster in trabecular bone than in compact bone (Parfitt 2002; Buenzli *et al.* 2018). Following these considerations, it was assumed that, during breastfeeding and after successful weaning completion, the differences between $\delta^{15}N$ values in the diaphysis and

metaphysis should be low as both areas of the bone would either reflect the high $\delta^{15}N$ values of breastfeeding or the lower values of a solid food diet. In early infancy, during exclusive breastfeeding, $\delta^{15}N$ values from the diaphysis could even be considerably lower than those from the metaphyses as the collagen from the midshaft would still reflect the lower $\delta^{15}N$ values from before breastfeeding, since in utero and right after birth, infants tend to have the same or similar $\delta^{15}N$ values as their mother (Katzenberg *et al.* 1996). However, during the weaning process, differences in $\delta^{15}N$ values should be greater between the two bone areas as the compact bone of the midshaft, due to its lower bone collagen turnover rate, still holds the much higher $\delta^{15}N$ values provided by the consumption of breast milk and the trabecular bone of the distal metaphysis, due to the faster turnover rate, reflects the cessation of breast milk feeding. A study on nursing behaviour of neolithic populations from the cis-Baikal region employed this exact method comparing $\delta^{15}N$ values from the midshaft to those of bone metaphyses and was able to successfully determine feeding status of the majority of infant remains included in the study (Waters-Rist *et al.* 2011).

Therefore, samples for stable isotope analysis of 0.2-0.3g were taken at the centre of the diaphysis and at the distal metaphysis of the femur or humerus of 15 children aged between 1-6 years and buried across all layers found at the site, bringing total sample size to 30 (midshaft: n=15; distal metaphysis: n=15). The humerus was only selected, when the femur was not available or either the metaphysis or diaphysis could not be sampled. Even though different long bones have different bone turnover rates and the humerus has a faster bone turnover rate than the femur, intra-skeletal measurements of stable isotopic variation did not detect any significant differences in $\delta^{15}N$ and $\delta^{13}C$ values between different bone types in adults and adolescents (Waters-Rist & Katzenberg 2010; Olsen *et al.* 2014).

7.2.1.2 Adults

All bone samples were taken from femora at the proximal 3rd of the diaphysis on the anterior side and depending on bone surface preservation, either the right or left femur was chosen. The samples were taken so that each area of the cemetery, i.e. far from the church, mid-way to the church, close to the church and inside the cloister area were represented. Furthermore, it was made sure that all adult age groups, all sexes and both Layers were also represented. It was therefore not possible to reach equal sample sizes in all groups. The sample strategy was laid out in this way in order to be able to detect differences in $\delta^{13}C$ and $\delta^{15}N$ ratios between the sexes, age groups, burial locations and layers. Therefore, a total of 58 samples was selected for

analysis. Another 2 samples that had already been analysed for $\delta^{15}N$ an $\delta^{13}C$ by Beta Analytics in the frame of δ14C dating were added to the sample to maximise sample size. These samples were taken from the femur (BETA 1) and from the humerus (BETA 2) respectively. 29 samples belonged to females and 31 belonged to males. 31 samples were from adults (young adults: n=9; adults n=22), 15 from mature and 14 from senile individuals. 14 samples were from individuals buried in the cloister area, and 46 were from individuals buried in the cemetery. From the cemetery group, 9 were from individuals buried close to the church, 25 were from individuals buried midway to church and 12 belonged to individuals buried far from the church. 17 samples belonged to individuals from Layer 1 and 43 samples to individuals from Layer 2.

7.2.2 Sample preparation, collagen extraction and isotope ratio measurements

All bone samples from adults and subadults were prepared in the same way and run under the lab code KNU.

A Saeshin Forte 200 alpha micro-circular saw was used to cut the bone samples. Sample weight for adults ranged between 0.5-1g and sample weight for subadult bone ranged between 0.35-0.36g. The samples were then successively cleaned in Millipore water and acetone and subsequently ground to powder manually to a grain size of less than 0.7mm. Only the adult bone samples were sent for CN elemental analysis to measure collagen content, as advised in Bocherens et al. (2005). Subadult sample size was too small to spare the material and therefore they were run directly for collagen extraction. CN elemental analysis was performed using a Vario EL elemental analyser at the Hydrogeochemistry working group at the University of Tübingen. The results of the CN analysis indicate the percentage of nitrogen in the bone powder ($\%N_{bone}$). All values smaller than $0.4\%N_{bone}$ were considered below the detection limit and should be discarded, however, among the KNU-samples, all values lay well above the threshold and therefore, all samples were retained for collagen extraction.

Collagen extraction followed the protocol of Bocherens et al. (1997) and was performed at the Biogeology working group at the University of Tübingen.

The weight (in mg) needed for each sample for the collagen extraction was calculated based on the results of the CN analysis. For subadults, the entire sample of weighted bone powder (between 350-360mg) was used in the collagen extraction and for adults the weight of bone powder used in collagen extraction ranged from 120mg ($4.0\text{-}4.5\%N_{bone}$)- 450mg ($0.4\text{-}1.0\%N_{bone}$). In a first step, the weighted bone powder was decalcified in 30-40ml 1M HCl for 20 minutes and then filtered through a 5 μm filter. To eliminate the lipids and humic acids, the

residual bone powder was then soaked in 0.125 M NaOH for 20h at ~20°. In a next step, the residue was rinsed and heated at 100° in HCl (pH = 2) for 17h to gelatinise the collagen, which was then filtered (5 μm filter) and the filtrate was subsequently freeze-dried.

Elemental analyses (N_{coll}, C_{coll}) and isotopic measurements for KNU1-40 were conducted at the Institute of Environmental Science and Technology of the Universitat Autònoma de Barcelona (ICTA-UAB) using a Thermo Flash 1112 (Thermo ScientificVC) elemental analyzer coupled to a Thermo Delta V Advantage mass spectrometer with a Conflo III interface. The international laboratory standard IAEA 600 (caffeine) was used together with two in-house reference materials consisting of modern collagen of camel and elk. The analytical error was determined as less than ±0.2‰ (1σ) for $\delta^{13}C$ and $\delta^{15}N$ in the repeated analyses and the reproducibility error for the amounts of C and N was lower than 2%.

Elemental analyses for KNU41-88 were conducted at the Geochemical department of the University of Tübingen, using and elemental analyser NC 2500 connected to Thermo Quest Delta+XL mass spectrometer. The samples were calibrated to an international standard (USGS-40 and UDGD-41) and two in-house reference materials (modern collagen of camel and elk). Based on multiple measurements of matrix matched in-house reference materials, the reproducibility was ±0.19‰ for $\delta^{13}C$ and ±0.24‰ for $\delta^{15}N$ values, and the reproducibility error for the amounts of C and N was lower than 4%.

Samples Beta 1 and Beta 2 were sent for radiocarbon (^{14}C) dating to Beta Analytic Inc. who also did the pretreatment and collagen extraction. $\delta^{13}C$ and $\delta^{15}N$ were also determined. The elemental analysis and isotopic measurements were carried out in a Thermo-Finnegan Delta mass spectrometer, no more specifics were given on the report. The samples were calibrated to 95% the ^{14}C signature of the international standard NIST SRM-4990C (oxalic acid) for ^{14}C values, no calibration standards were reported for $\delta^{13}C$ and $\delta^{15}N$, and quoted errors were reported as 1σ counting statistics.

The ratio of $^{13}C/^{12}C$ was measured relative to the Vienna PeeDee Belemnite standard (V-PDB). The isotopic ratios for carbon are expressed using the δ (delta) value according to the following folmula:

$$\delta^{13}C = [(^{13}C/^{12}C)_{sample}/(^{13}C/^{12}C)_{reference} - 1] \times 1000 \text{ (‰)}$$

The ratio of $^{15}N/^{14}N$ was measured relative to atmospheric nitrogen (AIR).

The isotopic ratios for carbon are expressed using the δ (delta) value according to the following folmula:

$$\delta^{15}N = [(^{15}N/^{14}N)_{sample}/(^{15}N/^{14}N)_{reference} - 1] \times 1000\ (‰)$$

The quality of the collagen was assessed by checking the chemical composition of the bone (%C, %N) and the carbon-to-nitrogen-ratio in collagen ($C:N_{coll}$).
Only collagen samples with a nitrogen percentage in collagen ($\%N_{coll}$) above 5% (Ambrose 1990) and $C:N_{coll}$ between 2.9 and 3.6 (DeNiro 1985) were considered to have well-preserved collagen. Based on these criteria, all samples (KNU1-88) could be included in the analyses. Another criterium often used to assess collagen quality is the collagen yield in the bone sample. It is calculated by dividing collagen weight (mg) after freeze-drying by the weight (g) of the powdered bone sample before collagen extraction. A sample with collagen yield of less than 1wt% is considered too badly preserved for analysis (Van Klinken 1999).

7.3 Weaning Age Reconstruction

7.3.1 Introduction

The impact of infant feeding practices on maternal and infant health as well as on population dynamics is well acknowledged and therefore plays an integral part in the study of past populations (Katzenberg *et al*. 1996). Especially the period of weaning, which includes exclusive breastfeeding, the introduction of solid foods to the diet as well as the cessation of lactation, has immediate and long-term effects on an infant's health, mortality risk, growth and development (Stuart-Macadam & Dettwyler 1995; Van Esterik 2002; Haines & Kintner 2008; Humphrey 2014; Miszkiewicz 2015). In fact, breast milk provides nutrients such as iron, calcium, zinc and vitamins and strengthens the infants immune system, thus with the weaning process and the introduction of novel food items to the diet, the immunological protection decreases and the child is exposed to range of new pathogens (Dittmann & Grupe 2000; Mays *et al*. 2002; Lewis 2007; Quigley *et al*. 2007; Henderson *et al*. 2014; Kaupová *et al*. 2014). Weaning also impacts population growth, as longer lactation periods delay fertility rates and increase birth spacing in the mothers (Huffman 1984; Mays *et al*. 2002; McDade 2005; Demmelmair *et al*. 2006; Haines & Kintner 2008; Kramer & Kakuma 2009; Mays 2010; Lamberti *et al*. 2011; Tsutaya & Yoneda 2013a; Herrscher 2013; Henderson *et al*. 2014;

Humphrey 2014; Kaupová *et al*. 2014). Nowadays, the recommended nursing time is set at 6 months (WHO, 2019) (Fewtrell *et al*. 2007; Kramer & Kakuma 2009) although some studies suggest that a weaning age of 2 years would be more beneficial (Lamberti *et al*. 2011; Kaupová *et al*. 2014)(WHO 2019) However, the duration and timing of breastfeeding and weaning are often influenced by cultural, environmental and economic circumstances (Huffman 1984; Fildes 1995; Stuart-Macadam & Dettwyler 1995; Sellen 2001; Dettwyler 2004; Henderson *et al*. 2014; Kaupová *et al*. 2014; Britton *et al*. 2018). In modern, non-industrialised populations for example, weaning typically occurs around 2-3 years of age (Sellen 2001; Dettwyler 2004), but environmental risks such as famines, diseases or wars might affect the parental decision on when to stop lactation (Quinlan 2007; Kaupová *et al*. 2014). This variability in weaning patterns and its consequences for population growth and development have sparked an interest among bioanthropologists to investigate this process further in past populations.

So far, a number of factors, such as infant mortality (Clarke 1977; Hühne-Osterloh & Grupe 1989; Katzenberg *et al*. 1996; Schurr 1997; Dittmann & Grupe 2000; Lewis 2002; Beaumont *et al*. 2015; Newman & Gowland 2017), non-specific osteological indicators of physiological stress (Hillson 1979; Clarke 1980; Goodman A H *et al*. 1984; Corruccini *et al*. 1985; Hühne-Osterloh & Grupe 1989; Goodman & Rose 1991; Dittmann & Grupe 2000; Miszkiewicz 2015; Newman & Gowland 2017), chemical palaeodietary reconstruction (Sillen & Smith 1984; Hühne-Osterloh & Grupe 1989; Katzenberg *et al*. 1993; Dittmann & Grupe 2000; Tsutaya & Yoneda 2013a, 2015; Tacail *et al*. 2017) and historical records have been used to investigate weaning patterns in past societies.

Since historical records concerning nursing behaviour are scarce and often biased towards the upper social classes (Humphrey 2014; Britton *et al*. 2018), most studies have focused rather on direct analysis of human remains. However, since the possibility exists that the demography of a skeletal sample might not accurately represent that of the actual population, studies based on mortality rates should not be used alone to investigate nursing behaviour (Schurr 1997). Non-specific indicators of physiological stress, such as Harris lines or enamel hypoplasias have also proven to be rather unreliable. For example, whilst some researchers

suggest that age-specific peaks in enamel hypoplasia frequencies coincide with weaning (Hillson 1979; Clarke 1980; Corruccini *et al*. 1985), others argue that peaks in enamel hypoplasia frequency rather reflect exposure to environmental stress or pathogens (Cook 1981; Hillson 1996), or that specific tooth segments are more prone to growth disturbances (Goodman & Rose 1991). Therefore, for over 20 years, dietary reconstruction through stable

isotope analysis has been the method of choice to investigate weaning patterns in prehistoric populations. The most commonly used method is to investigate Nitrogen isotope ratios ($\delta^{15}N$ values) in bone collagen or dentin, which mainly reflect dietary protein isotope ratios. The $\delta^{15}N$ values of infants are the same as those of their mother before and immediately after birth. Because of the trophic level effect, children who are exclusively breastfed, will have 2-3‰ higher $\delta^{15}N$ values than their mothers. After introduction of supplementary foods and cessation of lactation, their $\delta^{15}N$ values decrease and start reflecting those found in adult bone collagen (Tsutaya & Yoneda 2013a, b, 2015). Hence, by combining $\delta^{15}N$ values with age of death of the subadults studied, it is possible to reconstruct nursing behaviour in past societies.

7.3.2 Methods

7.3.2.1 Anthropological methods

The age of all children in this study was determined based on dental eruption after Ubelaker (1978), Schour and Massler (1941) and AlQahtani (2010) if possible and additionally by long bone length measurements after Stloukal and Hanáková (1978).

7.3.2.1.1 Caries:

Of all 26 children (Neonatus: n=3; infans I: n=23), dental caries could be recorded for 21 children between 0-6 years, as an indicator for first introduction of solid foods into the diet. This follows the thought that infant diet, which probably mainly consisted of cereal pap (Fildes 1986; Orme 2003), was the first increased contact with carbohydrates and sugars, especially since, in contrast to milk, the pap tends to stick on and between the teeth without proper and diligent oral hygene. Hillson (1996) states that breastmilk in itself is not considered to be cariogenic. Other studies have also used caries prevalence in conjunction with stable isotope analysis to assess weaning age and foods (Prowse *et al.* 2008; Schmidt *et al.* 2016).
Several modern studies, however, report an increased risk for caries in prolonged breastfeeding, mostly when breastfeeding lasts longer than 12 months, whereas breastfeeding protects against caries when carried out between 6-12 months (Tham *et al.* 2015; Victora *et al.* 2016; Cui *et al.* 2017; Peres *et al.* 2018; Van Meijeren-Van Lunteren *et al.* 2021). However, in their review on literature addressing caries risk and breastfeeding, Peres et al. (2018) also found some studies that only saw an increased caries risk after 18, respectively after 24 months and some that did not find an association between caries risk and breastfeeding duration.

Therefore, the possibility of early-onset caries being a result of prolonged breastfeeding must be taken into account during interpretation of the results. All graphs were designed in Excel.

7.3.2.1.2 Attrition:

Dental attrition was scored after Trautmann (2012) on teeth of 21 individuals aged 0-6 years, but only absence or presence of attrition was evaluated in this study. Attrition was present when any facets of any teeth showed distinct flattening and polishing of the crown and or dentin exposure.

Dental abrasion was used in this study as a proxy for introduction of solid foods as this would result in the first regular contact of abrasive substances on the teeth (Hillson 1996), since breastmilk would not cause any dental abrasion. All graphs were designed in Excel.

7.3.2.1.3 LEH:

Linear enamel hypoplasia (LEH) was recorded for all permanent teeth in the sample (n=2756) since, contrary to deciduous teeth which develop primarily in utero or shortly after birth, the majority develops during early childhood (Hillson 1996). For each tooth, every LEH line on each tooth was scored as absent or present. Additionally, for every LEH line, the age range of its location on the tooth, and subsequently the age range of its creation was recorded.

LEH is most likely caused by stress in childhood, which could be due to famine, chronic or acute illness, malnutrition etc but is also often associated with weaning stress (Corruccini *et al.* 1985; Goodman & Rose 1990; Lanphear 1990; Moggi-Cecchi *et al.* 1994; Hillson 1996; Wood 1996; Schultz *et al.* 1998; King *et al.* 2005). Especially peaks in enamel hypoplasia occurrence within the possible time frame of weaning across a population have been interpreted as signs of weaning stress rather than more individual factors such as malnutrition or infectious diseases (Corruccini *et al.* 1985; Moggi-Cecchi *et al.* 1994; Wood 1996). The increased exposure to pathogens through novel food items and the decrease in immunological protection provided by the mother's breastmilk during weaning (Dittmann & Grupe 2000; Mays *et al.* 2002; Lewis 2007; Quigley *et al.* 2007; Henderson *et al.* 2014; Kaupová *et al.* 2014) might have caused enough stress that led to the formation of enamel defects in the developing teeth. For this study it was assumed, especially since the adults stem all from different time periods, that an accumulation of LEHs in a specific age range could be an indicator for cessation of lactation or weaning stress through contact with novel food items during this age bracket. Three scenarios were tested to control for as many variables as possible. First, all linear defects of all

teeth except premolars were plotted against their age of formation. Next, all linear defects of only incisors and canines were plotted against their age of formation since only incisors and canines cover the whole possible age range in which weaning, and cessation of lactation might occur. Finally, in order to exclude all enamel hypoplastic defects that might have been caused by recurring events such as chronic malnutrition etc., only incisors and canines with a single enamel defect were plotted against age of formation. In the latter case, single hypoplastic defects might also have been caused by acute illness and recurring enamel defects that might reflect continued stress during the weaning period leading up to cessation of lactation are not represented in the latter diagram. Excluded from all analyses were also lines that occurred on just one tooth as they are more likely to represent localised trauma to the tooth (Hillson 1996).

7.3.2.2 Stable isotope methods

For all statistical calculations and for visualisation in scatterplots, the midpoint of the age ranges of subadults was taken as age entered into the analysis. For example, a subadult aged 1-1.5 years was entered as 1.25 years etc.

7.3.2.2.1 Isotope ratio midshaft vs. distal shaft

This method is based on the principles already described in the section on sampling strategies for subadult bone and roughly follows the method tested in Waters-Rist et al. (2011) and (2022).

In a first step, the $\delta^{15}N$ and $\delta^{13}C$ values obtained from the midshaft and distal metaphysis of the femur or humerus were plotted against age. Since women in the Knuedler cemetery have been analysed already for the next study on adult diet, their mean $\delta^{15}N$ and $\delta^{13}C$ values and standard deviation were also calculated and plotted in the diagram. Polynomial regression was performed to characterise the relationship of $\delta^{15}N$ and $\delta^{13}C$ values with age and indicate an overall trend in the data.

Mann-Whitney-U/Wilcoxon tests were used to test the significance of differences between the women from the cemetery and the children as well as between the women and children that were probably breastfeeding or weaning and those that were possibly already weaned. Significance was set at $p<0.05$.

In a next step, the differences in $\delta^{15}N$ and $\delta^{13}C$ values between midshaft and distal metaphysis were calculated for each individual.

Through a polynomial regression, a trend curve was fitted to the data.

As already described in the section on sampling strategy, stable isotope values from the midshaft are thought to represent diet from an earlier phase of the child's life whereas those from the metaphysis are thought to represent diet consumed shortly before death. A difference between midshaft and distal metaphysis stable isotope values could therefore be indicative of a dietary shift, and depending on the direction of the difference, would be either indicative of the start of breastfeeding (midshaft < metaphysis) or could reflect the process of weaning and cessation of lactation (midshaft > metaphysis). As Waters-Rist et al. (2011) and (2022) pointed out, it is necessary to establish a cut-off value based on which a difference between metaphysis and diaphysis is considered to be biologically relevant. They argue that the difference should be at least higher than the analytical error of the isotopic measurements, which lies around ±0.2‰. Furthermore, factors such as influence of different bone turnover and metabolic rates within different parts of a growing bone should be considered, even though a study that measured $\delta^{15}N$ and $\delta^{13}C$ values of metaphyses and diaphysis of children and juveniles older than 7 years established no significant differences in those values between the different bone parts, but some small differences were still noted (overall for all metaphysis/diaphysis differences of all bone types: ±0.1‰-0.2‰ in $\delta^{15}N$ values) (Waters-Rist & Katzenberg 2010). Further studies analysing stable isotope variation in different bone parts found that $\delta^{15}N$ and $\delta^{13}C$ values can vary between ±0.1‰-±0.3‰ within a single bone of the same healthy individual (Chisholm 1989; Katzenberg & Lovell 1999). Waters-Rist et al. (2011) and (2022) therefore suggest using the standard deviation of the mother's mean $\delta^{15}N$ and $\delta^{13}C$ values as cut-off value for the difference between diaphysis and metaphysis, meaning that a difference between diaphysis and metaphysis that is greater than the standard deviation of the mother's mean is considered as indicative of weaning or early breastfeeding and that values below the standard deviation might be attributed as well to a combination of analytical error and natural isotope variation within bone. Based on this premise, they came up with three isotopic patterns in subadult bones.

1. Metaphysis > Diaphysis → breastfeeding
2. Metaphysis < Diaphysis → weaning
3. Metaphysis = Diaphysis → indeterminate (either breastfeeding or weaned)

Then they proceeded to attribute a final classification into breastfeeding, weaning, weaned or indeterminate based on the difference between stable isotope values of midshaft and

metaphysis and difference of isotope values of the subadult bones compared to the mother's mean. Therefore, children following pattern (1.) need to show δ15N values higher than the women's mean + 1SD in at least the distal or midshaft or both bone parts to be considered breastfeeding. If the values all fall below the women's mean + 1SD, they are classified as indeterminate. For pattern (2.) to be finally classified as weaning, the $\delta^{15}N$ values from the midshaft need to be higher than the women's mean + 1SD, otherwise the individual will be classified as indeterminate. For pattern (3.), if both midshaft and metaphysis $\delta^{15}N$ values are higher than the mother's mean + 1SD, this is indicative of breastfeeding, if both fall below that cut-off it suggests a weaned or not breastfed pattern. Waters-Rist et al. (2011) tested their model using a logistic regression to find out whether it would be possible to correctly classify the majority of individuals into breastfeeding and weaning/weaned categories based on $\delta^{15}N$ values, which turned out significant, therefore validating the choice of standard deviation of the mother's mean as a reasonable cut off value.

The same procedure was therefore adapted in this study. Due to the scarcity of individuals in the sample and lack of comparative data from older juveniles as was the case in the study from Waters-Rist et al. (2011), the validity of the cut-off value was not additionally tested by logistic regression for this study.

Since standard variation of females was ±0.2 for $\delta^{13}C$ values, which as about the same as the analytical error and intra-bone isotopic variation, the method was not applied to the $\delta^{13}C$ values.

In a final step, since caries and attrition data are available for several of the individuals sampled, they will be cross-checked with the previously established categories of breastfeeding, weaning, weaned and indeterminate, in order to possibly reach a more conclusive decision on their actual feeding status.

7.3.2.2.2 WARN model

WARN stands for "Weaning Age Reconstruction by Nitrogen-15 isotopes" and is a formula in R, based on a Bayesian model, developed by Tsutaya and Yoneda (2013). Approximate Bayesian computation models are considered to be a robust approach towards dealing with small sample sizes (Tsutaya & Yoneda 2013b). Furthermore, as Bayesian models are based on probability estimations, they are better suited to address analyses of data that involve multiple uncertainties in the input parameters such as natural variation within the data itself and, specifically in the case of isotopic analysis, variation in trophic discrimination factors that could not be adequately accounted for in frequentist statistics (Layman *et al*. 2012). Therefore,

Bayesian statistics is often used in studies on dietary reconstruction (Moore & Semmens 2008; Layman *et al*. 2012; Fernandes *et al*. 2014) and in particular weaning studies on archaeological material (Tsutaya & Yoneda 2013a; De Armas *et al*. 2017; Britton *et al*. 2018; Chinique De Armas & Pestle 2018; Stantis *et al*. 2020; Chinique *et al*. 2022).

The WARN model calculates the beginning and completion of the weaning period, gives an estimate of the enrichment of $\delta^{15}N$ values between mothers and infants and calculates the average $\delta^{15}N$ of the weaning foods, based on the $\delta^{15}N$ data and associated age in years of children under 10 years of age and the mean of their hypothetical mothers. Generally, and also in this study, the mean of the mothers is substituted by the mean of the women buried in the cemetery. This follows the assumption that the women buried in the cemetery were the mothers of the children buried there as well. Furthermore, all calculations and mathematical formulas within the model already factor in, that bone collagen turnover rate slows down with age. The bone collagen turnover rate and the rate at which it slows down with age have been determined by Tsutaya and Yoneda (2013) for subadult ribs, which is why the model is most suitable for $\delta^{15}N$ from subadult rib samples.

Therefore, the WARN model requires three data input points:

1. All the $\delta^{15}N$ values obtained from the sampled subadults (called from dataset)
2. The age of the sampled subadults (called from dataset, ranges were converted to midpoints)
3. The mean of the women and the standard deviation of that mean (manual entry)

The final outputs described above and called maximum density estimates (MDE) are informed by prior probability distributions for the start of weaning (first introduction of solid foods) (t_1) and the end of weaning (cessation of lactation) (t_2), as well as the intra-population variability in $\delta^{15}N$ values of weaning foods (E).

In this study, all parameters and assumptions for the priors were kept at the default setting defined by Tsutaya and Yoneda (2013).

The default assumptions for the priors are:

1. t_1 will occur at 0.5 years ±3 years
2. t_2 will occur at 3 years ±3 years
3. E will be 1.99‰±0.9‰

4. $\delta^{15}N$ of weaning foods will be the average of d15N values from female bone collagen ±3.0‰

Although it would have been possible to customise the priors to this data set, the decision was made to keep the original priors. Current WHO (2009) health guidelines suggest first introduction of solid foods at 6 months after birth, which corresponds to the prior assumption for t1. Based on the previous observations in this study, the assumption that weaning ended at around 3 years was also kept. However, the standard deviation of ±3 years seems really high for both t_1 and t_2, as it would imply for t_1 that solid food intake might have happened before birth already or as late only as 3.5 years. For t_2 the SD implies that cessation of lactation might have started right after birth, which, though unlikely, remains a possibility, and that breastmilk could have been consumed as late as 6 years, which also seems quite unlikely. However, as the results of this study will be compared to those of Britton et al. (2018), in order to keep the analyses comparable across all these datasets, the priors and parameters of the WARN function had to be kept the same as for the comparative datasets, which were the default settings by Tsutaya and Yoneda (2013). Nevertheless, a second model with adapted parameters was calculated as well for the $\delta^{15}N$ values of the metaphysis only. Here, all means were kept as in the original parameters, but SD was informed by the results from the previous analysis on midshaft-metaphysis differences. Therefore, the SD of the first (t_1) and second prior (t_2) was changed to 1.

Additionally, the WARN function calculates the posterior probabilities and the range within a 95% confidence interval (CI) for t_1, t_2, E and the $\delta^{15}N$ values for collagen synthesised from weaning foods. The methods for how to enter the standard priors as well as the input parameters into the WARN model are provided in the description leaflet of the WARN package R (Tsutaya 2019).

7.3.3 Results

7.3.3.1 Anthropological methods

7.3.3.1.1 Caries:

Of the 21 children that had teeth for assessment, just over half (52.38%, n=11) presented with carious lesions of varying intensity (Figure 285). The earliest evidence of caries was recorded in 3 children between 1-2 years of age (50%), suggesting that this age range also roughly

corresponds to the first introduction of solid foods (Figure 286). Individual 2008-78/706 had a medium occlusal caries lesion on the mandibular right DP3. Individual 2008-78/1181 had two superficial approximal lesions on the mesial side of the maxillary right and left DI1 respectively. Individual 2008-78/1140 had a superficial approximal caries lesion on the mesial side of the left maxillary DI2 (DI1 was missing). (Table 116)

Distribution of Dental Caries in Neonatus and Infans I

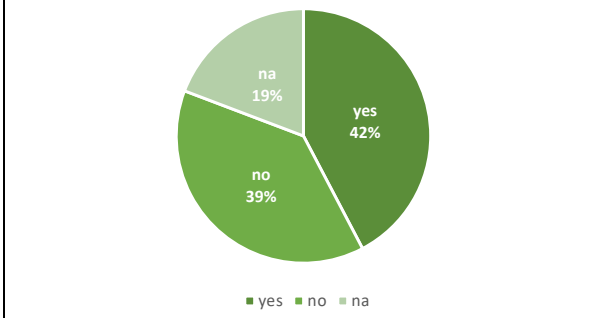

Figure 285 Amount of children aged 0-6y with caries lesions

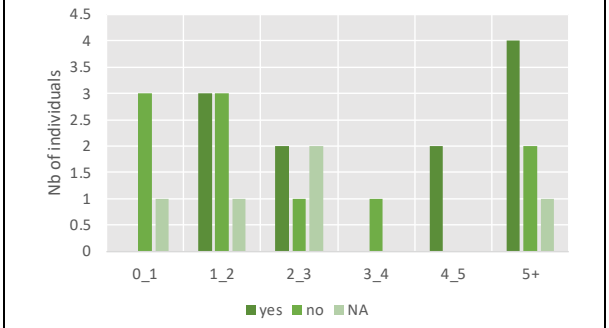

Figure 286 Nb of children aged 0-6y with or without caries lesions by age

Yes = caries present
No = caries absent
NA = no teeth could be scored

7.3.3.1.2 Attrition

A similar pattern can be observed for attrition. Over half of the individuals (71.43%, n=15) had signs of attrition of varying degrees on at least one tooth, and the earliest recorded dental wear occurred in 3 children aged 1-2 years (50%) (Figure 287), which aligns with first caries onset. (Table 116**Error! Reference source not found.**) Furthermore, the severity of dental attrition increases with age, suggesting a longer exposure to abrasive foods in the older age categories starting around 4-5 years (Figure 288).

Distribution of Dental Attrition in Neonatus and Infans I

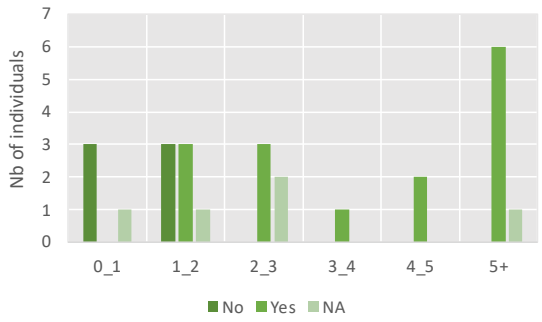

Figure 287 Number of children aged 0-6y with and without dental attrition by age

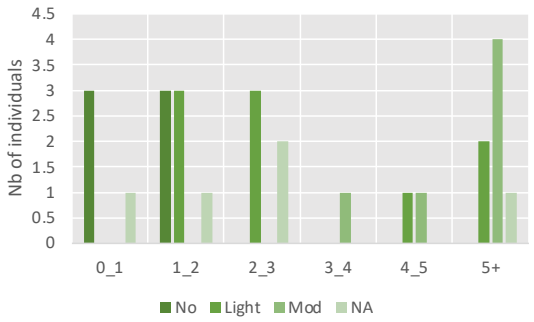

Figure 288 Number of children aged 0-6y with light and moderate attrition by age

Yes = attrition present

No = attrition absent
Light = light attrition (pinpoint dentine exposure)
Mod = moderate attrition (larger area of dentin exposed maybe coalescing of pinpoint exposure)
NA = no teeth could be scored

Table 116 Earliest onset of caries and attrition in subadults

ID	Age	Caries	Attrition
2013_015/355	0	N/A	N/A
2008_78/522	0.1-0.2	No	No
2016_082/419	0.25-0.5	No	No
2008_78/886	0.75-1.5	No	No
2008_78/1195	1	N/A	N/A
2008_78/248	1_1.5	No	No
2008_78/1141	1-1.5	No	No
2008_78/706	1-1.5	Yes	Light
2008_78/1181	1-2	Yes	Light
2008_78/1140	1.5-2	Yes	No
2008_78/1180	1.5-2	No	Light
2016_082/168	1-3	N/A	N/A
2008_78/1465	2-3	N/A	N/A
2008_78/532	2-3	No	Light
2016_082/401	2-3	Yes	Light
2008_78/960	2-3	Yes	Light
2008_78/1462	3-4	No	Mod
2008_78/1179	4	Yes	Mod
2008_78/1090	4-5	Yes	Light
2008_78/296	4-6	No	Mod
2008_78/1362	5-6	N/A	N/A
2013_015/177	5-6	No	Mod
2008_78/153	5-6	Yes	Light
2008_78/987	5-6	Yes	Mod
2008_78/1124	6	Yes	Light
2008_78/673	5.5-6.5	Yes	Mod

7.3.3.1.3 Linear Enamel Hypoplasia (LEH)

As can be seen in the graphs, LEH intensity is higher in the 2–3-year age range when all teeth are considered (Figure 289). This trend however decreases when eliminating those teeth that do not reflect the whole time when weaning could have taken place, namely M1 which does not reflect the older age ranges above 3 years, and P3, P4 and M2, which do not reflect the lower age ranges (Figure 290).

In order to reduce the risk of analysing defects potentially caused by recurring events such chronic illnesses or chronic malnutrition etc. only teeth with one clearly visible LEH line were analysed. And there, the first trend becomes very clear with lines suddenly appearing very frequently at around 2-3 years and declining rapidly afterwards (Figure 291).

Linear Enamel Hypoplasia

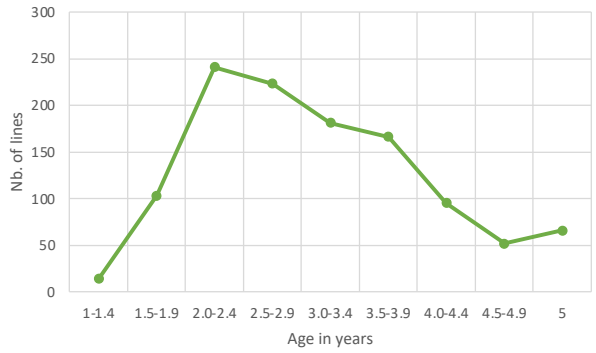

Figure 289 Number of LEH by Age for all teeth except premolars. When considering all teeth, enamel hypoplasia peaks abruptly at 2-2.4 years and slightly less around 2.5-2.9 years and frequency then drops gradually with age.

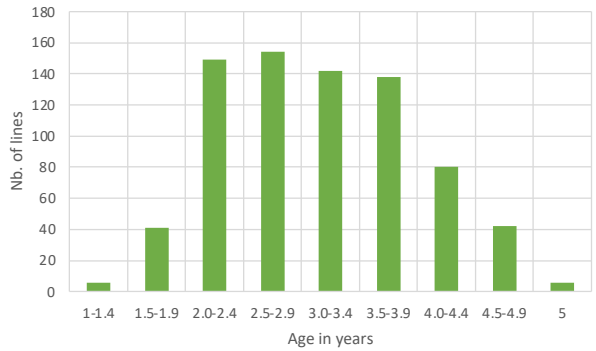

Figure 290 Number of LEH lines by Age for incisors and canines only. When considering only incisors and canines, the peak age of enamel defect formation lies between 2-2.9 years, followed closely by a peak at 3-3.4 years, after which frequency drops quickly with increasing age.

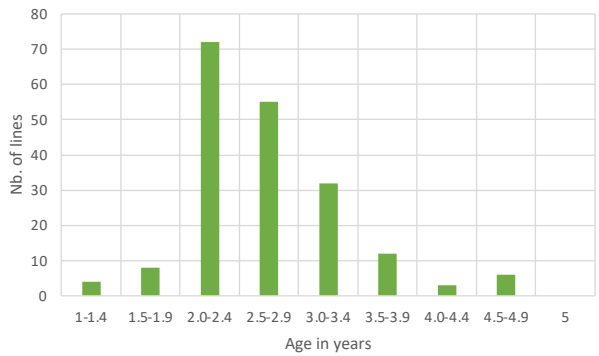

Figure 291 Number of single LEH lines by Age for incisors and canines. LEH peaks abruptly between 2-2.4 years and decreases gradually but strongly with increasing age.

LEH = Linear enamel hypoplasia
Nb. = Number

7.3.3.2 Stable Isotope results

7.3.3.2.1 Collagen preservation and sample quality

The mean collagen yield in the complete sample amounts to 156.36mg/g (n=30, SD=55.52), which corresponds to 15.636wt%. The range of collagen yield in the whole sample was

5.23wt% - 21.93wt%, showing that all values were higher than 1%, indicating adequate preservation of the collagen (Van Klinken 1999). The nitrogen percent in bone for the whole sample was on average 14.98%. Therefore, all bone samples were suitable for analysis and collagen could be extracted successfully from all of them.

The atomic C/N ratios for the whole sample ranged from 3.2 to 3.3 and %N in collagen was higher than 12.5%, suggesting that the extracted collagen was well preserved.

The $\delta^{13}C$ values ranged from -19.0‰ to -20.0‰, with the mean lying around -19.58‰ (n=30; SD=0.26). The $\delta^{15}N$ values ranged from 9.2‰ to 15.5‰ and the average was 11.97‰ (n=30; SD=1.84).

For the midshaft samples only, the $\delta^{13}C$ values ranged from -19.0‰ to -19.8‰, with the mean lying around -19.49‰ (n=15; SD=0.26) and the $\delta^{15}N$ values ranged from 9.7‰ to 15.3‰ and the average was 12.25‰ (n=15; SD=1.86).

For the samples from the distal metaphysis, the $\delta^{13}C$ values ranged from -19.1‰ to -20.0‰, with the mean lying around -19.67‰ (n=15; SD=0.24) and the $\delta^{15}N$ values ranged from 9.2‰ to 15.5‰ and the average was 11.68‰ (n=15; SD=1.84).

7.3.3.2.2 Isotope ratio in the midshaft vs. distal shaft

7.3.3.2.2.1 $\delta^{15}N$, $\delta^{13}C$ and $\delta^{15}N_{diff}$ data trends

Neither the $\delta^{15}N$ values from midshaft nor those from the distal metaphysis showed a linear relationship with age. Therefore, for the midshaft samples, a 2nd order polynomial regression line was fitted to the data as it showed best fit without the p-value becoming insignificant., which is likely due to the wide range between data points and the small sample size (R^2=0.4302; adjusted R2=0.3352; p=0.0342).

Regarding the samples of the distal metaphysis, a 3rd order polynomial regression was fitted to the data, which explained ~51% of the data (R^2=0.5139; p=0.0409)

Even though neither curve fits the data very well, it is evident that $\delta^{15}N$ values from the midshaft and metaphysis decrease with age and that $\delta^{15}N$ values from the midshaft decrease at a slower rate than those from the distal shaft. The lines indicate that values of the midshaft fall within 1σ of the women's mean around the age of 4 years, whereas the values from the metaphysis will fall within 1σ of the mother's mean only at around 2.5 years. However, due to the poor fit of the curves to the data and due to the small and unequal sample size, this can only be taken as a rough indication. Since cancellous bone tends to have a faster bone turnover

rate than cortical bone (Parfitt 2002; Buenzli *et al.* 2018), samples from the distal metaphysis most likely reflect $\delta^{15}N$ values of foods consumed shortly before death, which means that generally, around the age of 2.5y, the majority of children were already consuming a diet similar to that of the adults but a few values from the midshaft at that age still carry the trophic signal of breastmilk, suggesting that at 2.5 years these children were either still weaning or barely weaned. (Figure 293)

Regarding $\delta^{13}C$ values from the midshaft and distal metaphysis, the majority of the values lay within the standard deviation of the mother's mean. For both the midshaft and metaphyseal samples, a 4th order polynomial curve was fitted to detect trends in the data. The 4th order polynomial curve was only a good fit for values of the midshaft however (R^2=0.615, p=0.0345), but the curve still the only best fit for values of the metaphysis (R^2=0.2787, p=0.4674). Some $\delta^{13}C$ values are fairly high around 1-1.5 years but mostly, all values fall within the SD of the mother's mean. (Figure 292)

Trend Lines for $\delta^{15}N$ and $\delta^{13}C$ from midshaft and metaphysis samples

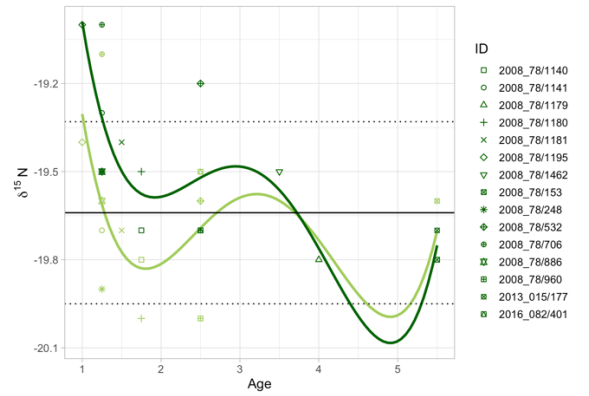

Figure 292 Fitted 4th order polynomial trend lines for $\delta^{13}C$ of midshaft and metaphysis showing different decreasing trends by age in children 1-6 years

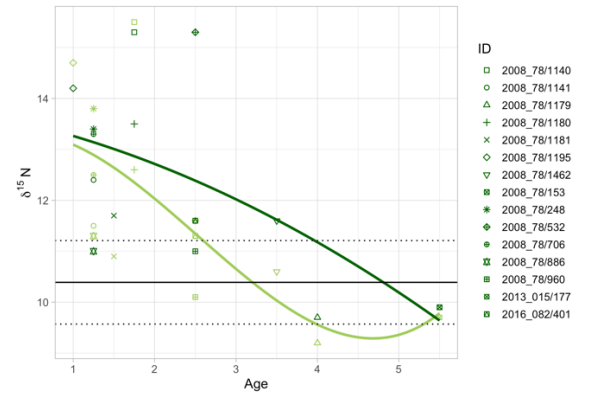

Figure 293 Fitted 2nd and 3rd order polynomial trend lines for $\delta^{15}N$ of midshaft and metaphysis respectively showing different decreasing trends by age in children 1-6 years

Dark green = midshaft $\delta^{15}N$ values and fitted trend line
Light green = distal metaphysis $\delta^{15}N$ values and fitted trend line
Black horizontal line = female $\delta^{15}N$ mean
Dotted horizontal lines = ± 1 Standard deviation (±1σ) from female $\delta^{15}N$ and $\delta^{13}C$ mean
δ15N(‰AIR)

Regarding the distribution of the differences in $\delta^{15}N$ between midshaft and metaphysis, it becomes apparent that in all age groups younger than 4 years, there are some noticeable differences between values of the midshaft and metaphysis, suggesting that between the ages of 1-4y some children in Luxembourg city were already weaning and others still breastfeeding or maybe already finished with breastfeeding. The smallest differences are observed between 1-3 years of age. In order to separate possibly breastfeeding individuals from weaned ones, the

difference of their $\delta^{15}N$ values to the adult women's mean should be considered and children that show $\delta^{15}N$ values that are higher than the mother's mean +1SD should be considered to still be weaning and those that fall within the range of the adult women should be considered weaned. Appropriate cut-off values for biologically meaningful differences between $\delta^{15}N$ values of the midshaft and metaphysis have been discussed in the methods section and should be used to distinguish between weaning or weaned/breastfed individuals. A 4th order polynomial curve was fitted in order to possibly detect a trend in the data, but the curve did not fit well (R^2=0.3561, p=0.3078), probably due to the wide and irregular data spread coupled to a small sample size. Nevertheless, the curve peaks around 2.5-3.0 years, which is influenced by the really pronounced midshaft-metaphysis difference of one individual. This individual displayed a difference of 3.6‰ between midshaft and distal shaft, which constitutes more than one trophic level difference. (Figure 294)

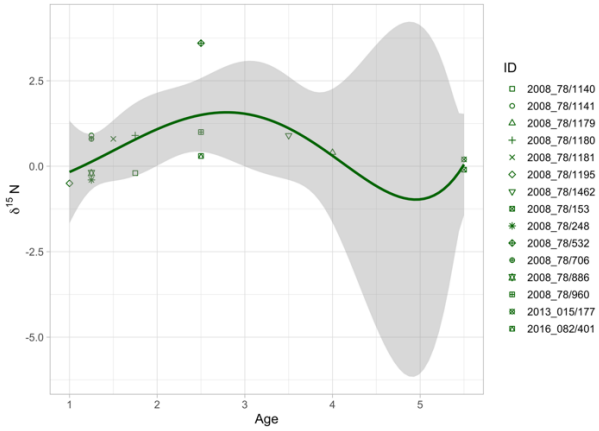

Figure 294 Data spread and fitted 4th order polynomial curve for the d15N differences between midshaft and metaphysis of children aged 1-6 years

7.3.3.2.2.2 Attribution of feeding status by individual

7.3.3.2.2.2.1 Stable isotope data only

The methods that led to the assignment of feeding status have been described in detail in the methods section and the results of this study are shown in Table 117. The results show that 2 of 15 individuals could not be classified as breastfeeding, weaning or weaned based on their $\delta^{15}N$ values. On the previous graphs, it was clear that the spread within the δ15N values in both the midshaft and metaphysis was quite high. And even though weaning and breastfeeding children were detected in all age groups ranging from 1-3/4 years of age, a trend was still recognizable despite the small sample size. Between 1-2 years, 2 individuals were weaning and 2 still breastfeeding whilst one remained indetermined. Breastfeeding decreased then over the

1.5-1.9-year group (n=1) to the 2–3-year group (n=1) and after 3 years, no child showed evidence of breastfeeding anymore. Weaning remained constant over the 1.5-1.9-year group (n=2) and decreased over the 2–3-year group (n=1) to the 3–4-year group (n=1) and after 4 years of age, no child showed evidence of weaning anymore. After 4 years, all children were successfully weaned. (Figure 295)

Table 117 Stable isotope values from midshaft and metaphysis from subadults with inferred weaning status

ID	Age	$\delta_{13Cmidshaft}$	$\delta^{13}C_{metaphyis}$	$\delta^{13}C_{diff}$	$\delta^{15}N_{midshaft}$	$\delta^{15}N_{metaphysis}$	$\delta^{15}N_{diff}$	Feeding Status
2008_78/1195	1	-19	-19.4	0.4	14.2	14.7	-0.5	breastfeeding
2008_78/886	1.25	-19.5	-19.6	0.1	11	11.3	-0.2	indeterminate
2008_78/1141	1.25	-19.3	-19.7	0.4	12.4	11.5	0.9	weaning
2008_78/706	1.25	-19	-19.1	0.1	13.3	12.5	0.8	weaning
2008_78/248	1.25	-19.5	-19.9	0.4	13.4	13.8	-0.4	breastfeeding
2008_78/1181	1.5	-19.4	-19.7	0.3	11.7	10.9	0.8	weaning
2008_78/1140	1.75	-19.7	-19.8	0.1	15.3	15.5	-0.2	breastfeeding
2008_78/1180	1.75	-19.5	-20	0.5	13.5	12.6	0.9	weaning
2008_78/532	2.5	-19.2	-19.6	0.4	15.3	11.6	3.6	weaning
2016_082/401	2.5	-19.7	-19.5	-0.2	11.6	11.3	0.3	breastfeeding
2008_78/960	2.5	-19.7	-20	0.3	11	10.1	1*	indeterminate
2008_78/1462	3.5	-19.5	-19.5	0	11.6	10.6	0.9*	weaning
2008_78/1179	4	-19.8	-19.8	0	9.7	9.2	0.4	weaned
2013_015/177	5.5	-19.7	-19.6	-0.1	9.9	9.7	0.2	weaned
2008_78/153	5.5	-19.8	-19.8	0	9.9	9.9	-0.1*	weaned
MEAN		-19.5	-19.7	0.2	12.3	11.7	0.6	
SD		0.3	0.2	0.2	1.9	1.8	1.0	
Women's mean		10.39						
Women's SD		0.8						

*The differences were calculated on raw data with multiple decimal places. By reporting the values only with one decimal place, the rounding of the values let to slight discrepancies between the midshaft and metaphysis values and the difference between them

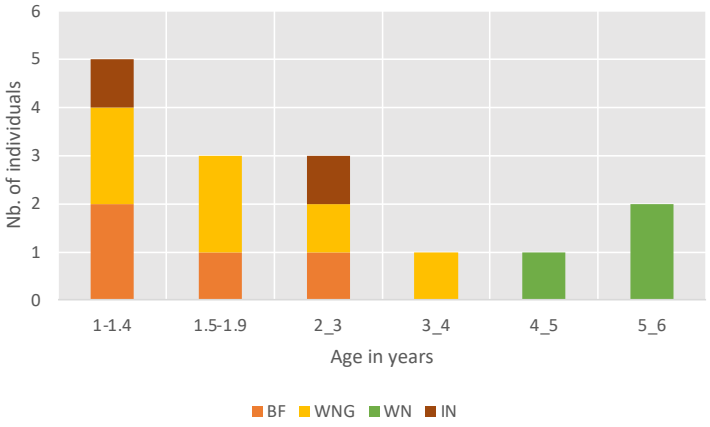

Figure 295 Stacked bar chart showing the number of individuals of different feeding status based on d15N differences between midshaft and metaphysis (BF=breastfeeding, WNG=weaning, WN=weaned, IN=indeterminate)

In an attempt to validate the results from the previous analysis, Mann-Whitney-U tests were performed to establish whether breastfeeding and weaning children had significantly higher

$\delta^{15}N$ values than the women and whether children above 4y did not show any significant differences in $\delta^{15}N$ values compared to the adult women. A Mann-Whitney-U test comparing the $\delta^{15}N$ values from the metaphysis of subadults (11.68‰, n=15) to that of the women (10.39‰, n=29) from the Knuedler cemetery turned out to be statistically significant (W: 315, p=0.0162), suggesting that overall, children had a diet richer in animal protein than the adult females. As this difference is likely influenced by the high number of breastfeeding and weaning children, the age groups were separated into mostly breastfeeding and weaning and into weaned individuals based on the results of the previous analysis. As such, a Mann-Whitney-U test comparing $\delta^{15}N$ values of children below the age of 4 (weaning and breastfeeding group) to those of the adult women and another one was conducted comparing children older than 4 years to the women. The same procedure was also applied to the $\delta^{13}C$ values in order to find out whether $\delta^{13}C$ values did also change with feeding status, a trend that was not clearly recognizable in the scatterplots. Children below 4 years (12.2‰, n=12) had on average significantly higher $\delta^{15}N$ values of the metaphysis (W: 299, p=0.0004) than the adult women, however children older than 4 years (9.6‰, n=3) did not (W: 16, p=0.0803). The same trend can be observed between $\delta^{15}N$ values from the midshaft of children. They were significantly higher in children overall (12.25‰) than in adult women (W: 352.5, p=0.0009), but the trend was only prevalent in children younger than 4 years (12.86‰, W: 329, p=0.0000)) and not between women and children older than 4 years (9.83‰, W: 23.5, p=0.2066). Regarding $\delta^{13}C$ values from the metaphysis, no significant difference could be detected between children overall (-19.66‰, W: 254, p=0.3676) as well as of any of the two age groups (<4: -19.65‰, W: 210.5, p=0.2972; >4: -19.73‰, W: 43.5, p=1) between the adult females (-19.74‰). However, $\delta^{13}C$ values were significantly higher in subadult samples from the midshaft (-19.48‰) compared to those of adult women (W: 332.5, p=0.0041). This trend is also present in children below 4 years (-19.42‰, W:294.5, p=0.0005), but not between women and children older than 4 years (-19.77‰, W:38, p=0.7434). Overall, these results seem to validate the results obtained in the previous study and show that children below 4 years were still weaning or breastfeeding due to their significantly higher $\delta^{15}N$ values compared to adult women and that those above 4 were already fully weaned and consuming the same foods as adults. However, the sample sizes are small and very unequal, which might bias the results of the statistical analysis.

7.3.3.2.2.2.2 Combined stable isotope data and dental status

Therefore, in an effort to verify the results of the midshaft vs. metaphysis method, the established feeding status was checked against the available dental status. As premise, no caries and no attrition were considered indicative of breastfeeding and this combination only matched once with breastfeeding status established before. In one other case of breastfeeding status, no teeth were available for evaluation. For two individuals, breastfeeding status did not match with dental status (marked in red). In the case of 2016-082/401, a 2–3-year-old child, both the midshaft and metaphysis values are higher than the women's average +SD and show no difference between the two bone parts, indicative of breastfeeding. However, the dental status shows presence of caries and attrition on the teeth. Whilst caries might develop as a consequence of prolonged breastfeeding (>12 months) (Tham *et al.* 2015; Victora *et al.* 2016; Peres *et al.* 2018), attrition requires regular contact to abrasive foods to develop. Therefore, since the values of this individual still lie within the female adult $\delta^{15}N$ range, it is possible that the individual was already weaned and was consuming a diet high in animal protein, such as meat or dairy. This hypothesis is further strengthened by the fact that the child was buried inside the cloister, where adults showed higher $\delta^{15}N$ values (11.24‰) than in the cemetery (10.22‰).

Another individual aged 1.5-2 years showed up as breastfeeding due to a very small difference in $\delta^{15}N$ values of the midshaft and metaphysis and really elevated $\delta^{15}N$ values (15.3‰/15.6‰). Compared to the female mean, the values are higher than the expected 3‰ trophic enrichment between breastfeeding infant and mother. A study on scorbutic infant remains also found very elevated $\delta^{15}N$ values. The authors attributed the elevated $\delta^{15}N$ values to starvation underlying the scurvy, rather than to breastfeeding (Nicholls *et al.* 2020). Indeed, several studies have confirmed that starvation can lead to increase in $\delta^{15}N$ (Hertz *et al.* 2015; Beaumont & Montgomery 2016; Doi *et al.* 2017). Therefore, it is possible, that this individual, although not presenting with any skeletal pathological lesions, might have suffered from starvation.

Table 118 Results of dental status with feeding status based on $\delta^{15}N$ values

ID	Age	Caries	Attrition	Feeding Status
2013_015/355	0	N/A	N/A	
2008_78/522	0.1-0.2	No	No	
2016_082/419	0.25-0.5	No	No	
2008_78/886	0.75-1.5	No	No	indeterminate
2008_78/1195	1	N/A	N/A	breastfeeding

2008_78/248	1_1.5	No	No	breastfeeding
2008_78/1141	1-1.5	No	No	weaning
2008_78/706	1-1.5	Yes	Light	weaning
2008_78/1181	1-2	Yes	Light	weaning
2008_78/1140	1.5-2	Yes	No	breastfeeding
2008_78/1180	1.5-2	No	Light	weaning
2016_082/168	1-3	N/A	N/A	
2008_78/1465	2-3	N/A	N/A	
2008_78/532	2-3	No	Light	weaning
2016_082/401	2-3	Yes	Light	breastfeeding
2008_78/960	2-3	Yes	Light	indeterminate
2008_78/1462	3-4	No	Mod	weaning
2008_78/1179	4	Yes	Mod	weaned
2008_78/1090	4-5	Yes	Light	
2008_78/296	4-6	No	Mod	
2008_78/1362	5-6	N/A	N/A	
2013_015/177	5-6	No	Mod	weaned
2008_78/153	5-6	Yes	Light	weaned
2008_78/987	5-6	Yes	Mod	
2008_78/1124	6	Yes	Light	
2008_78/673	5.5-6.5	Yes	Mod	

7.3.3.2.3 WARN model

The WARN model MDEs (maximum density estimators) gave a start date of 1.6y (≥95% CI: 0.2-2.9y) for introduction of solid foods (t_1) and puts cessation of lactation (t_2) at around 3.3 years (≥95% CI: 2.6-4.2y) when considering $\delta^{15}N$ values of the midshaft samples. For the distal metaphysis sample, the first introduction of solid foods (t_1) falls around 1.6 years (≥95% CI: 0.2-2.1y) and 2.2 years (≥95% CI: 1.8-3.0y) for cessation of lactation (t_2). At around 4 years, the midshaft values all fall within the standard deviation (SD) of the mother's mean even though two younger individuals also fall within the SD of the mean (Figure 296). For the distal shaft samples, most of the individuals already fall within the SD of the mother's mean at around 2-3 years old (Figure 297). These differences likely reflect the different bone turnover rate in the two bone parts. As expected, bone collagen turnover is slower in the midshaft than in the metaphysis, which is why midshaft samples may reflect the trophic level signal of breastmilk for longer than samples from the metaphysis. Therefore, only the MDEs calculated from the $\delta^{15}N$ values from the metaphysis will be considered as possible end and start dates for the weaning process and only those results will be used for any further comparisons with other

European datasets analysed by the WARN method. The probabilities of t_1 and t_2 are really small for samples from both bone parts (metaphysis: t_1: 0.0919; t_2: 0.1677; diaphysis: t_1: 0.0594; t_2: 0.1055), which is likely due to the small and unequal sample size and the wide spread of the $\delta^{15}N$ values within the younger age groups. The joint probability, meaning the likelihood that both t_1 and t_2 occurred at the estimated ages is also rather low at 0.0178 for the metaphysis and 0.0064 for the diaphysis. Nevertheless, both joint probability and posterior probability of t_1 and t_2 are above the recommended thresholds of 0.05 for posterior probability and 0.0025 for joint probability (Tsutaya & Yoneda 2013b), which means that the models are valid.

According to the model based on metaphysis samples, the average enrichment between breastfeeding children and their mothers lay around 2.4‰ (≥95% CI: 1.7-3.0‰) and weaning foods had $\delta^{15}N$ values of around 9.7‰ (≥95% CI: 9.0-10.3‰).

A rerun of the WARN model for the metaphysis samples with adjusted priors did not produce significantly different results. Introduction of solid foods (t_1) was estimated to have started around 1.5y and cessation of lactation (t_2) was estimated to have occurred around 2.2y and enrichment between breastfeeding infants and mothers as well as $\delta^{15}N$ values of the weaning foods were estimated at the same values as in the model run with the default parameters. The remaining results such as ≥95%CI ranges of the MDEs, as well as the plots for the distribution of the posterior probabilities of t_1 and t_2, the maternal-infant-enrichment as well as the enrichment of weaning foods can be found in Appendix IV.

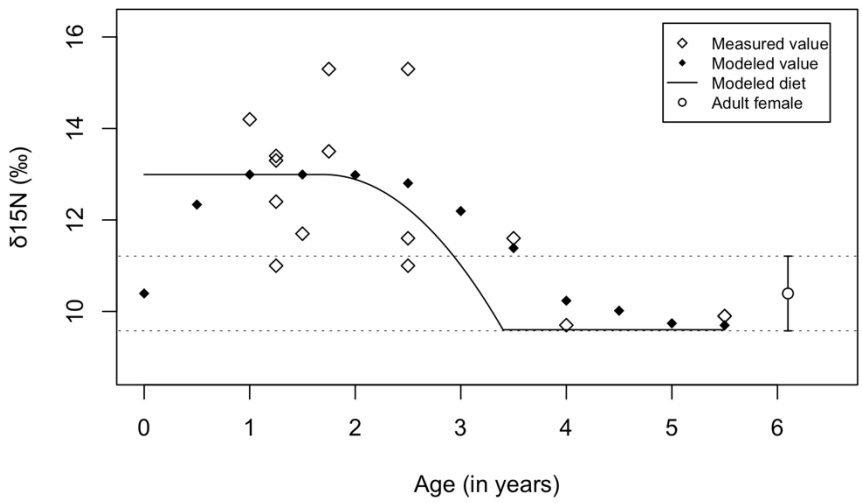

Figure 296 Transverse comparison of $\delta^{15}N$ (‰ Air) values by nonadult age calculated from reconstructed maximum density estimators (MDEs). Mean and SD range for adult females is indicated with an open circle. Results are shown for samples from the mid-shaft of subadults from Luxembourg city

Table 119 Results of the WARN model for the midshaft samples

Results of the WARN model for the midshaft samples					
	MDE	**probability**	**≥95% CI**	**≥95% CI probability**	**Weaning duration**
t_1	1.6	0.05936890	0.2-2.9	0.9520684	1.7
t_2	3.3	0.10553894	2.6-4.2	0.9520684	
E	2.6	0.14125186	2.1-3.2	0.9614725	
$\delta^{15}N_{weaningfoods}$	9.6	0.07757777	8.6-10.6	0.9571692	
Joint probability for t_1 and t_2	0.0064				

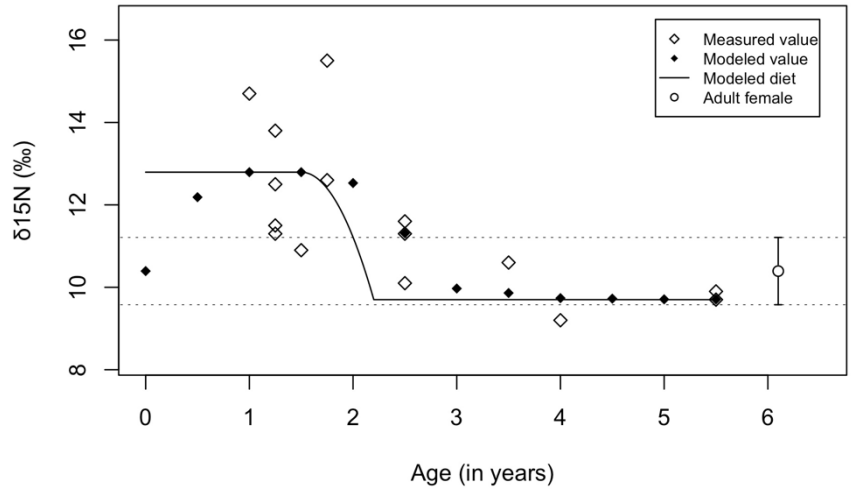

Figure 297 Transverse comparison of $\delta^{15}N$ (‰ Air) values by nonadult age calculated from reconstructed maximum density estimators (MDEs). Mean and SD range for adult females is indicated with an open circle. Results are shown for samples from the distal metaphysis of subadults from Luxembourg City

Table 120 Results of the WARN model for the metaphysis samples

Results of the WARN model for the metaphysis samples					
	MDE	**probability**	**≥95% CI**	**≥95% CI probability**	**Weaning duration**
t_1	1.6	0.0919131	0.2-2.1	0.950836	0.6
t_2	2.2	0.1677381	1.8-3.0	0.950836	
E	2.4	0.1198998	1.7-3.0	0.9601912	
$\delta^{15}N_{weaningfoods}$	9.7	0.1062433	9.0-10.3	0.9568457	
Joint probability for t_1 and t_2	0.0178				

For comparative purposes, the $\delta^{15}N$ values of the femoral metaphysis of 9 children from Grevenmacher, that were sampled, prepared, and extracted by Dr. Chirstoph Wissing and Dr. Bernd Trautmann, who also provided the data, were also entered into the WARN model with default parameters. The results of this analysis can be found in full detail in the Appendix IV. According to the MDEs, solid foods were first introduced into the diet at 1.3y (≥95% CI: 0.3-2.0y) and weaning ended around 2.4y (≥95%CI: 2.1-2.7y), resulting in a weaning duration of 1.1y. These start and end dates for the weaning period are very similar to those found for the children from the Knuedler cemetery in Luxembourg City. In Grevenmacher, breastfeeding infants were about 2.4‰ enriched in δ15N in regard to their mothers (≥96% CI: 1.9-3.0‰) and

the δ15N of weaning foods was around 7.55‰ (≥95% CI: 7.3-7.8‰). As all posterior probabilities were higher than 0.05 and the joint probability higher than 0.0025, the model was considered to be a valid fit for the data.

7.3.4 Discussion

Whilst nursing behaviour has been investigated for prehistoric populations all over the world (Sillen & Smith 1984; Katzenberg *et al*. 1993, 1996; Schurr 1997, 1998; Wright & Schwarcz 1998; Mays *et al*. 2002, 2017; Privat *et al*. 2002; Richards *et al*. 2002; Fuller *et al*. 2006, 2003; Williams *et al*. 2005; Dupras & Tocheri 2007; Jay *et al*. 2008; Prowse *et al*. 2008; Audouze *et al*. 2009; Pearson *et al*. 2010; Gardner *et al*. 2011; Nitsch *et al*. 2011; Waters-Rist *et al*. 2011, 2022; Howcroft *et al*. 2012, 2014; Beaumont *et al*. 2013a; Giuffra & Fornaciari 2013; Haydock *et al*. 2013; Herrscher 2013; Beaumont *et al*. 2015; Tsutaya & Yoneda 2013a, 2015; Burt 2013; Henderson *et al*. 2014; Kwok & Keenleyside 2015; Britton *et al*. 2015; Tessone *et al*. 2015; Britton *et al*. 2018; Schmidt *et al*. 2016; Tsutaya *et al*. 2016; Tacail *et al*. 2017; Tsutaya 2017; De Armas *et al*. 2017; Stantis *et al*. 2020; Chinique *et al*. 2022), studies concerning infant feeding practices in the late middle-ages and postmedieval times in continental Europe are scarce. Apart from one study on children from 9th-10th century sites in the Czech republic (Kaupová *et al*. 2014), one on children from the 5th-7th century Wenigumstadt in Germany (Dittmann & Grupe 2000), and one on 19th century rural Beemster in the Netherlands (Waters-Rist *et al*. 2022) the vast majority of research has been undertaken on skeletal series from the United Kingdom (Mays *et al*. 2002; Richards *et al*. 2002; Burt 2013; Haydock *et al*. 2013; Britton *et al*. 2015, 2018) and the results have shown that, besides weaning ages being different from those in modern and early modern populations, they also show a range of variation in infant feeding practices among different medieval communities, which are likely due to cultural and societal differences (Burt 2013; Haydock *et al*. 2013; Britton *et al*. 2018).

This study sought to offer new insights into weaning practices in late medieval-postmedieval Luxembourg City through a combination of stable isotope analysis and anthropological methods. Since the sample size of subadults was so small on the Knuedler cemetery, it was the aim to use as many methods as possible to narrow down possible age ranges for introduction of solid foods and cessation of lactation in order to understand weaning practices in this region. Up to date, no study has investigated weaning practices from that time period in that region and historical sources concerning childhood care are, to the best of my knowledge, also not available for Luxembourg City or the duchy of Luxembourg. The first study examined

differences in $\delta^{15}N$ values from the midshaft and metaphysis in attempt to discover patterns of breastfeeding, weaning, or weaned status. The method was adapted from Waters-Rist et al. (2011) and (2022) and a further step was added by the author, namely comparison of feeding status to dental status. Based solely on the method by Waters-Rist et al. (2011), the feeding status of 13 out of 15 individuals could be identified. However, comparison to dental status revealed that the classification of 2 individuals might have been influenced by external factors. One individual (2016-082/401) aged 2-3 years was classified as exclusively breastfeeding but had clear evidence of dental attrition and caries lesions, suggesting regular contact with abrasive and possibly cariogenic foods. A closer inspection of the δ15N values and burial location of the individual revealed that, even though the values of both midshaft and metaphysis fell just outside the women's mean +1SD, they were well within the range of women's δ15N values and well within that of women buried in the cloister. Therefore, since individuals from the cloister had overall higher δ15N values than those from the cemetery, it is possible that 2016-082/401 had in fact already been weaned and was consuming a diet high in animal protein, such as meat or dairy.

Another outlier was 2008-78/1140 aged 1.5-2 years which came up as breastfeeding but showed evidence of caries. Caries can result from prolonged breastfeeding (Tham *et al*. 2015; Victora *et al*. 2016; Peres *et al*. 2018; Van Meijeren-Van Lunteren *et al*. 2021) but the $\delta^{15}N$ values of both midshaft and distal shaft were very highly enriched compared to the other children and adult females, namely ~5‰ from the women's mean and ~4.2‰ from the women's mean +1SD, which constitutes more than the expected trophic enrichment between mother and child. Either the child was breastfed by a woman with elevated $\delta^{15}N$ values herself or pathological processes that influenced bone metabolism and $\delta^{15}N$ fractionation might have led to the elevated values observed in 2008-78/1140. In fact, pathological processes and starvation have been shown to lead to elevated $\delta^{15}N$ values in human bone (Katzenberg & Lovell 1999; Geber 2014; Olsen *et al*. 2014; Hertz *et al*. 2015; Beaumont & Montgomery 2016; Doi *et al*. 2017; Curto *et al*. 2020; Nicholls *et al*. 2020). Individual 2008-78/532 aged 2-3 years, showed the highest difference in $\delta^{15}N$ values between midshaft and metaphysis, at 3.6‰. This constitutes a shift of more than one trophic level within the same bone. Bone is being remodelled also in the midshaft during bone growth. In order for the medullary canal to widen, new bone is not only deposited at the outer bone cortex but is also resorbed at the endosteum (Carter *et al*. 1996; Scheuer & Black 2000; Waters-Rist & Katzenberg 2010). Therefore, one would not necessarily expect such a strong difference in $\delta^{15}N$ values during a gradual weaning

process, which means that the difference observed in 2007-78/532 might either reflect a very abrupt cessation of lactation where the midshaft still reflects the full isotopic signal of breastmilk and the metaphysis already that of the adult diet. However, the metaphysis $\delta^{15}N$ value (11.6‰) is still falling above the women's mean +1SD suggesting that breastmilk was possibly still administered alongside solid foods. Furthermore, the $\delta^{15}N$ value of the midshaft (15.3‰) lies well above that of the adult women. As for individual 2008-78/1140, the very elevated $\delta^{15}N$ values might have been the result of pathological or metabolic processes that took place during bone formation in that area, whereas the newer bone of the metaphysis does not reflect these changes anymore. However, too little is known about the actual effects of pathological and metabolic processes on $\delta^{15}N$ fractionation in bone and the interplay of bone growth to reach a conclusive explanation for the values observed in 2008-78/532. 2008-78/532 also did not show any pathological lesions on the bone sampled.

Furthermore, due to the limited availability of subadult bones, invariably children with pathological conditions were also sampled. Individuals 2008-78/153 (5.5-6.5y) and 2008-78/248 (1-1.5y) were suffering from possible scurvy, as explained in more detail in the chapter on metabolic diseases. A study by Nicholls et al. (2020) examined intraskeletal variability in a young infant with scurvy that presented with unusually enriched $\delta^{15}N$ values and concluded that the strong enrichment of $\delta^{15}N$ was likely due to the possible starvation underlying scurvy rather than caused by the pathological processes of scurvy. Since it was already demonstrated that woven new bone presents $\delta^{15}N$ values that are higher than in healthy bone tissues (Katzenberg & Lovell 1999; Olsen *et al*. 2014; Curto *et al*. 2020), an effort was made for both individuals to sample bones that did not show the new bone formation observed in other bone elements and that contributed to the diagnosis of scurvy. Contrary to expectation however, the $\delta^{15}N$ results of both these individuals did not fall out of range for their respective age groups and instead suggest that scurvy or whatever pathological process that might have contributed to new bone formation in other skeletal elements did not influence their $\delta^{15}N$ values. The same holds true for individual 2008-78/1181 (1.5-2y) which suffered from rickets. However, a study by Olsen et al (2014) already suggested that rickets and osteomalacia did possibly not influence $\delta^{15}N$ fractionation or that the complete skeleton was concerned as they did not record any differences in $\delta^{15}N$ between the bones of a single individual. What has to be kept in mind however is, that the $\delta^{15}N$ values of all these individuals possibly reflect a diet that caused their

respective metabolic conditions and which might therefore be different to that of those that did not develop such conditions (Olsen *et al*. 2014).

Overall, the midshaft-metaphysis study showed, that start and end dates for the weaning period in Luxembourg City were very variable with weaning starting as early as 1-1.5 years and lasting up to the age of 3-4 years.

Next, based on the women's mean $\delta^{15}N$ values and the data from the children aged 1-6 years, a general age at introduction of solid foods and an age at cessation of lactation should be determined for the whole population through the application of the Bayesian model WARN. Even though both midshaft and metaphyseal $\delta^{15}N$ values were used in the models, the model based on metaphyseal values is to be preferred over the other since the Tsutaya and Yoneda (2013) based all their mathematical formulas in the model on bone collagen turnover rates of ribs, which have a faster turnover rate than cortical bone. Therefore, the bone turnover rate of the trabecular bone of the metaphysis is most comparable to that of ribs. The model suggested a start of weaning of around 1.6 years and an end of weaning at around 2.2 years. Whilst the start date corresponds roughly to the estimates from the previous method, the end date of weaning seems to be earlier in the WARN model. This shows that, in order to reflect the true variability of the weaning process within a general trend for the whole population, both methods should be used in conjunction.

The results of the LEH formation suggest elevated stress leading to LEH formation around the ages of 2-3 years, followed closely by 3-4 years. These age brackets correspond to the estimated time frame during which weaning was completed in Luxembourg City, suggesting that for most individuals, cessation of lactation occurred around 2-3 years but that in many cases the stresses associated with this process continued well into the 3–4-year age range and that in several cases, weaning might have also just ended in the 3-4 year age group, a fact that seems to be confirmed by the midshaft/metaphysis study.

Using the general start and end dates for the weaning period estimated by the WARN model, the results from Luxembourg City were compared to other contemporaneous European and British sites. Firstly, a comparison can be made to medieval rural Grevenmacher. According to the WARN model, weaning in Grevenmacher occurred around the same time as in Luxembourg City (t_1: 1.3y, t_2: 2.4y), which would suggest that there was no major difference in infant feeding practices between the Middle Ages and the postmedieval period, nor between urban and rural environments in this region. Furthermore, the model suggests that weaning foods in Grevenmacher were less enriched in $\delta^{15}N$ than those in Luxembourg City, which is

also reflected already in the much lower $\delta^{15}N$ values of adults from Grevenmacher compared to those from Luxembourg City, suggesting either regional differences in environmental isotopic signatures or actual differences in diet and therefore in weaning foods. In absence of a local baseline for both sites, no conclusions can be reached on this topic. The Anglo-Saxon site of Raunds Furnells (Haydock *et al.* 2013; Britton *et al.* 2018), the medieval Wharram Percy site (Richards *et al.* 2002; Britton *et al.* 2015), the medieval St. Nicholas Kirk cemetery in Aberdeen (Britton *et al.* 2018), two medieval Czech urban and rural sites (Kaupová *et al.* 2014) and a postmedieval cemetery belonging to the Medici family in Italy (Giuffra & Fornaciari 2013) also suggest cessation of lactation took place between 2-3y. At medieval Fishergate House (Burt 2013; Britton *et al.* 2018), and at the cemetery of postmedieval Spitalfields in London (Nitsch *et al.* 2011; Britton *et al.* 2018) and postmedieval St. Nicholas Kirk in Aberdeen (Britton *et al.* 2018) however, weaning had already ended before or around 2 years. The sites of Raunds Furnells, Wharram Percy, Fishergate House, Spitalfields and St. Nicholas Kirk have also been analysed by the WARN method so that ages at solid food introduction were determined for these sites as well (Britton *et al.* 2018). Additionally, the WARN method suggested an age of cessation of lactation for infants from Wharram Percy, that is earlier than that determined in previous studies and would have occurred rather before the age of 2 years (Britton *et al.* 2018). In all medieval and postmedieval sites analysed by Britton et al. (2018) the age at introduction of solid foods was earlier (t_1 0.3-0.5y) than that determined for Luxembourg City (t_1:1.6y) or Grevenmacher (t_1: 1.3y), except for medieval St. Nicholas Kirk, where t_1 occurred around 1.8 years. In fact, in the case of Aberdeen, historical records even confirmed a breastfeeding age of up to 1.5 years for that time period (Dennison, E. P., DesBrisay, G., & Diack 2002), however, no such records could be found for Luxembourg City. A further comparison could be made with 19th century rural Beemster, where the majority of children were either not or only very shortly breastfed, which was attributed to the working conditions and social expectations of local women at that time (Waters-Rist *et al.* 2022). As breastfeeding lasted quite some time after birth in the Luxembourgish site, women from Luxembourg City were likely not experiencing those social constraints such as work obligations or religious restrictions that would have forced them to cut breastfeeding and weaning time short.

Therefore, the results from Luxembourg City are overall similar to those from medieval and postmedieval European and medieval UK sites. Whilst some studies suggest that there was a diachronic shift in weaning practices over time (Haydock *et al.* 2013; Fulminante 2015; Britton

et al. 2018), this could not be observed in the case of Luxembourg City as weaning ages are very similar to those generated for Grevenmacher, which is regionally very close but dates predominantly to the 14th – 15th century (Trautmann *et al.* 2017).

7.3.4.1 Limitations

This study has of course its limitations starting already with the small sample size of subadults, with some age groups only represented by 1 or 2 individuals and a lack of individuals in the 0-1 years age group, those most likely to have been exclusively breastfed. These factors might have influenced the calculations from the WARN method. Furthermore, the analysis was performed on children that died before, during or just after the weaning process, with some of them also suffering from metabolic conditions, which means we might rather witness weaning practices of diseased children or of children who died because of unsuccessful weaning practices.

The large ranges in $\delta^{15}N$ values in the younger groups might also be influenced by a range of external factors such as differential quality of weaning foods, illness, stress or temporary diet of the mother etc. (Beaumont *et al*. 2015).

Finally, the cause for LEH formation remains debatable and although an effort was made to eliminate as many factors as possible, it is still not sure whether all LEHs counted actually represent weaning stress.

7.3.4.2 Conclusion

In conclusion, the combination of all the methods helps to establish a rough age range for introduction of solid foods and cessation of lactation and the methods corroborate each other. However, the wide range of $\delta^{15}N$ values across the younger age groups hints at a more complex picture of weaning practices, with some children probably being weaned earlier or even later than the suggested age range of 2-3 years. The midshaft/metaphysis method might be particularly useful in case of limited numbers of subadults to at least estimate whether the child was weaning or breastfeeding/weaned. A further differentiation between breastfeeding and weaned can only be made if the $\delta^{15}N$ values of the adult population are approximately known. Waters-Rist et al. (2011) and (2022) recommend using the SD of the adult women as cut off value for differences between metaphysis and midshaft values, in order to avoid differences produced by bone growth mechanisms and analytical error. Following these suggestions, the author of this study proposes that, in the absence of the women's SD, a cut off value of 1‰

could be used to define a biologically meaningful difference in $\delta^{15}N$ values between midshaft and distal shaft, as this would correspond to the lower bounds of the possible range of trophic enrichment between breastmilk consumption and a solid food diet (1-3‰).

The large spread of $\delta^{15}N$ values over several age groups suggests that weaning practices in Luxembourg City were rather heterogenous with some starting the weaning process earlier than others and ending the process earlier than others too. However, since the subadults sampled here were sourced from all Layers in order to maximise sample size, they also reflect weaning practices spanning from the late medieval ages to well into the postmedieval period (~mid 14th-end 18th century). A shift in weaning practices, namely a reduction of the weaning period from medieval to postmedieval times has been noted in several studies already (Haydock *et al*. 2013; Fulminante 2015; Britton *et al*. 2018), which is why it is entirely possible, that the large variation observed in this study might reflect a change in weaning practices over time.

7.4 Diet in late medieval and postmedieval Luxembourg City

7.4.1 Introduction

In the late medieval and postmedieval period, Luxembourg City had established itself as the political and religious capital of the duchy of Luxembourg (Schmitt 1994). With this urbanization and the presence of garrisons in town, the social divide among the citizens of Luxembourg also started to widen (Beck-Baldauff 1986; Thewes 1994). During the 30 years' war the garrison occupation in town intensified, which put a toll on the citizens who were obliged to house the soldiers within their own homes (Thewes 2013). Affluent, often aristocratic families held most of the power in the city but a considerable group of merchants started making a fortune off selling products to the military personnel (Thewes 1994). Little is known however so far about who was buried on which cemetery in town. Regarding the Franciscan monastery and cemetery on the "Knuedler", accounts are scarce and slightly contradictory. Whilst some argue that the cemetery was mainly used for the burial of the less affluent citizens and the church and cloister areas reserved for the wealthy donors and friars (Beck & Beck 2000), archaeological evidence, namely ornate pearls and crosses from cemetery graves, suggest that even those buried in the cemetery of the Franciscan monastery were wealthier citizens (Bis-Worch 2011). The latter hypothesis would not be very surprising as often times, monasteries charged fees for burial on their precincts (De Groote *et al*. 2011; Quintelier *et al*. 2014), which likely some citizens could not afford. However, no such

information is known for the Franciscan monastery analysed here. Therefore, this study on $\delta^{15}N$ and $\delta^{13}C$ data, the first of its kind on skeletal material from Luxembourg City, should help to shed light on possible age- and sex-related, as well as socioeconomic differences within the population buried on the cemetery and inside the cloister area through their dietary habits. By comparing the different dateable Layers, possible dietary shifts over time will also be investigated. The results of the isotopic data will then also be discussed in light of the previously established anthropological results. Altogether, this study should help to shed light on the social stratification of at least a part of Luxembourg City's population in late medieval and postmedieval times.

7.4.2 Methods

The sampling strategy as well as sample preparation and collagen extraction have already been described in the general methods section.

Data acquisition, and statistical evaluation of the anthropological data have already been described in their respective chapters. For the mortality tables and for all analyses involving age groups, the age group 25-34y was added into the young adult category, age group 35-44y was added to adults and age group 45-54y was added to mature I.

Statistical analyses were carried out according to the process described in the Materials and Methods chapter and comprised comparisons between the sexes, age groups, burial layers and locations. Group sizes, values and statistical test results for the anthropological analyses can be found in the respective chapters.

7.4.3 Results

This section primarily reports the results from the isotopic analysis in more detail. For the detailed results of the anthropological analysis, the respective chapters should be consulted. Here, only a short recapitulation of the main results will be provided.

The $\delta^{13}C$ and $\delta^{15}N$ values from terrestrial animal bone collagen used as comparative material in this study, have been sourced from the IsoARCH database (database.isoarch.eu) and stem from the early medieval sites of Klettham, Eching-Kleiststrasse, Aschheim-Bajuwarenring, Germany (Hakenbeck *et al*. 2010), the migration period sites of Eulau, Schönburg, Obermöllern, Rathewitz and Naumburg, Germany (Knipper *et al*. 2013), the early medieval site of Kaldus in Poland (Reitsema *et al*. 2013) and from the 13th-15th century AD site of Saint-Laurent in Grenoble, France (Herrscher *et al*. 2001). Faunal remains from 16th-18th century AD

Aalst in Belgium (Quintelier *et al*. 2014) were also added to the comparative faunal sample set. The selection criteria for the sites within the IsoARCH database and literature were that the sites knew a temperate climate and were located inland. At the start, only medieval and postmedieval sites were selected but to increase sample size, earlier sites were also included. The data for marine and freshwater fish was sourced from Müldner and Richards (2005) and are originally from the 14th-15th century AD deposits of the Dominican Priory at Beverly, Yorkshire, England. The calculated means and standard deviations for all animal groups will only be used as rough guideline to estimate dietary composition of the people buried on the Knuedler cemetery. Since $\delta^{13}C$ and $\delta^{15}N$ values are not only influenced by dietary protein intake but can also be influenced by external environmental conditions such as rainfall, aridity, temperature or manuring of fields (Bogaard *et al*. 2007; Casey & Post 2011; Goude & Fontugne 2016), for more detailed dietary reconstructions a local animal baseline would be needed, which was not available in the present case, as the animal bones from the site have not been analysed yet.

7.4.3.1 Isotopes

7.4.3.1.1 Complete sample

The mean collagen yield in the complete sample amounts to 91.61mg/g (n=60, SD=48.99), which corresponds to 9.161wt%. The range of collagen yield in the whole sample was 2.39wt% -23.23wt%, showing that all values were higher than 1%, indicating adequate preservation of the collagen (Van Klinken 1999). The nitrogen percent in bone for the whole sample was on average 13.63%. Therefore, all bone samples were suitable for analysis and collagen could be extracted successfully from all of them.

The atomic C/N ratios for the whole sample ranged from 3.0 to 3.4 and %N in collagen was higher than 9.3%, suggesting that the extracted collagen was well preserved.

The $\delta^{13}C$ values ranged from -18.5‰ to -20.2‰, with the mean lying around -19.64‰ (n=60; SD=0.31). The $\delta^{15}N$ values ranged from 8.3‰ to 13.3‰ and the average was 10.46‰ (n=60; SD=1.11). (Table 121)

7.4.3.1.2 By Sex

The mean collagen yield for females amounts to 90.70mg/g (n=29, SD=51.34), which corresponds to 9.07wt% and mean collagen yield for males amounts to 92.521mg/g (n=31, SD=47.41), which corresponds to 9.252wt%. Mann-Whitney-U tests did not show any significant differences between the two samples (W=391; p=0.6520) The nitrogen percent in bone of females was on average 13.53% and in males 13.73%, which did not represent a statistically significant difference between the two groups (W=403, p=0.49589), meaning that collagen preservation was similar between bones of males and females. Therefore, differences in bone preservations likely did not influence any differences in $\delta^{13}C$ and $\delta^{15}N$ observed between the sexes.

The $\delta^{13}C$ values of males ranged from -18.5‰ to -20.1‰, with the mean lying around -19.54‰ (n=31; SD=0.35), and those of females ranged between -19.2‰ to -20.2‰ with an average of -19.74‰ (n=29; SD=0.22). (Figure 298, Figure 300)

The $\delta^{15}N$ values of males ranged from 8.3‰ to 13.3‰ and the average was 10.53‰ (n=31; SD=1.34) and those of females ranged from 8.9‰ to 12.3‰ with a mean of 10.39‰ (n=29; SD=0.82). (Figure 298, Figure 299)

Wilcoxonn/Mann-Whitney-U tests revealed that there was no statistically relevant difference in $\delta^{15}N$ values between men and women (W=445; p=0.9528) but showed that males had overall significantly lower $\delta^{13}C$ values than females (W=285; p=0.0141). (Table 121)

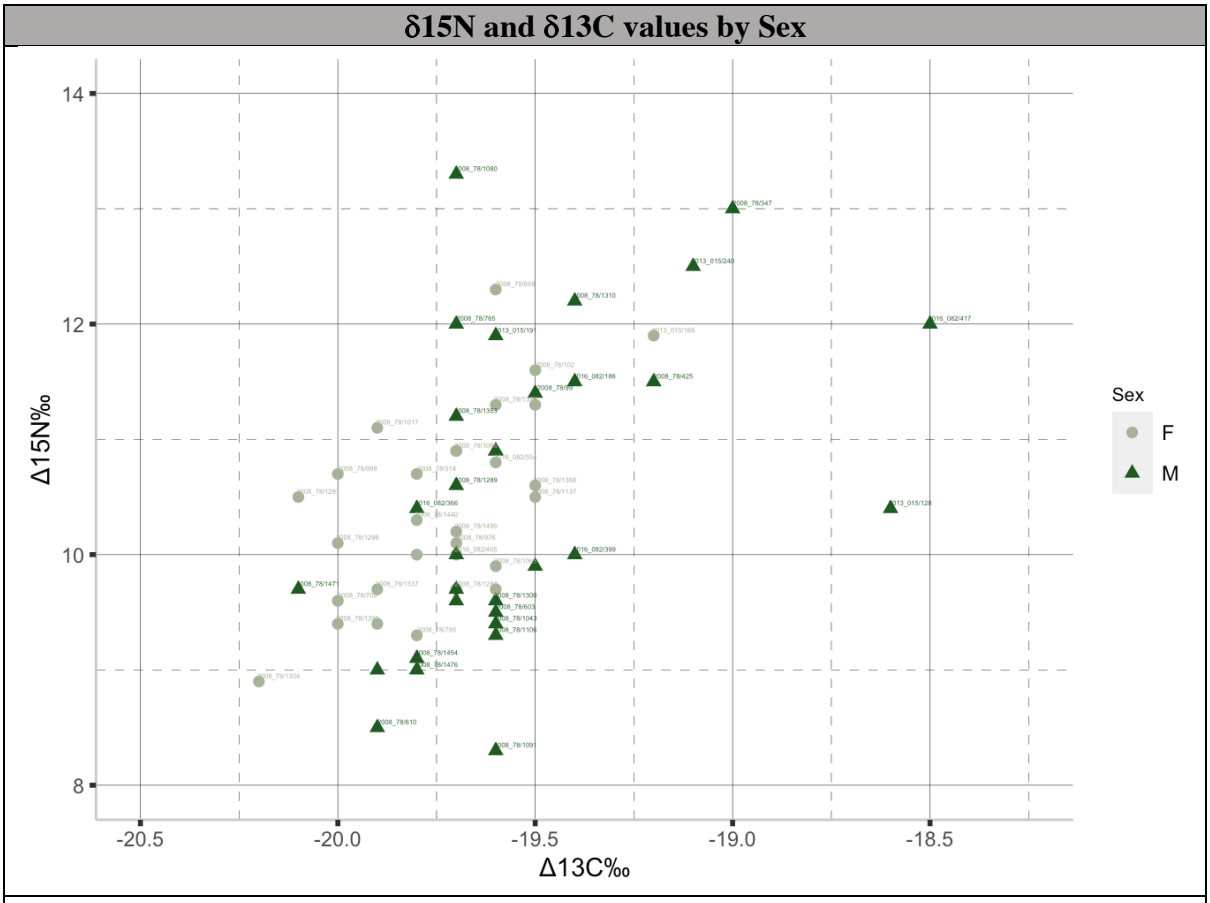

Figure 298 Scatterplot of δ13C and δ15N values of males and females

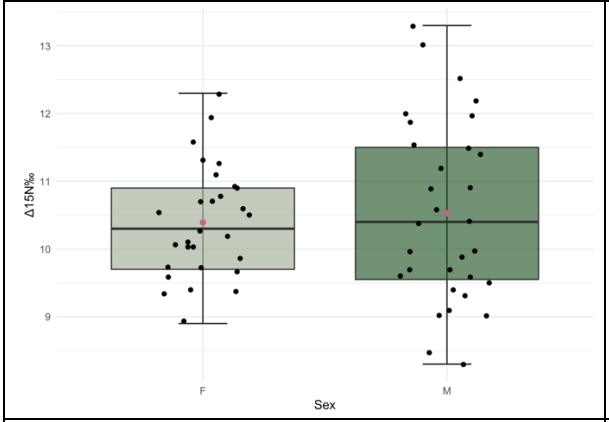

Figure 299 Boxplot of δ15N values of males and females showing the narrower range of female values compared to men's

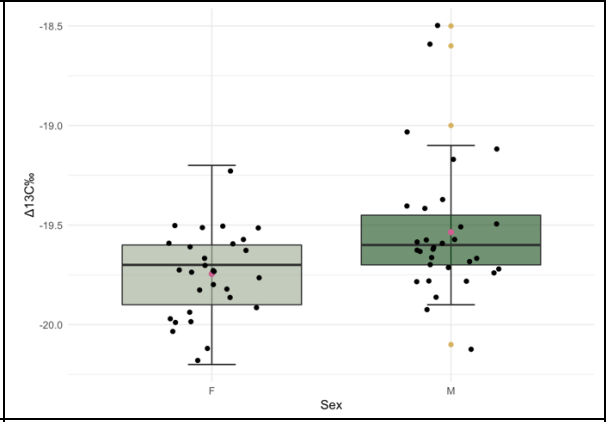

Figure 300 Boxplot of δ13C values of men and women showing the overall higher values δ13C of men

F=Female
M=Male

7.4.3.1.3 By Age

The mean collagen yield for adults amounts to 89.94mg/g (n=29, SD=47.89), which corresponds to 8.994wt%, the mean collagen yield for mature individuals amounts to 86.49mg/g (n=17, SD=48.92), which corresponds to 8.649wt% and the mean collagen yield for senile individuals amounts to 100.55mg/g (n=14, SD=53.68), which corresponds to

10.055wt%. A Kruskal-Wallis test showed that the difference in collagen preservation was not statistically different between all these groups (X^2=1.4490.; p=0.4846). The nitrogen percent in bone of adults was on average 13.55%, in matures 13.51% and in seniles 13.97% which did not represent a statistically significant difference between the two groups (X^2=1.2546, p=0.5340). Therefore, collagen preservation was similar between all groups tested and should not have an influence on the results of the group comparisons of $\delta^{13}C$ and $\delta^{15}N$ values.

The $\delta^{13}C$ values for adults ranged from -18.5‰ to -20.2‰ with a mean of -19.67‰ (n=29; SD=0.29), those of matures ranged from -18.6‰ to -20.1‰ with a mean of -19.58‰ (n=19; SD=0.38) and those of seniles spanned from -19.2‰ to -20.1‰ with a mean of -19.64‰ (n=12; SD=0.22). (Figure 301, Figure 303)

The $\delta^{15}N$ values for adults ranged from 8.5‰ to 13.3‰ with a mean of 10.16‰ (n=29; SD=1.03), those of matures ranged from 8.3‰ to 13.0‰ with a mean of 10.86‰ (n=19; SD=1.21) and those of seniles spanned from 9.0‰ to 11.9‰ with a mean of 10.56‰ (n=12; SD=0.98). (Figure 301, Figure 302)

Kruskal-Wallis tests showed that there was no significant difference between the groups regrading $\delta^{13}C$ (X^2: 0.6028; p=0.7398) and $\delta^{15}N$ values (X^2:5.7205; p=0.0573). (Table 121)

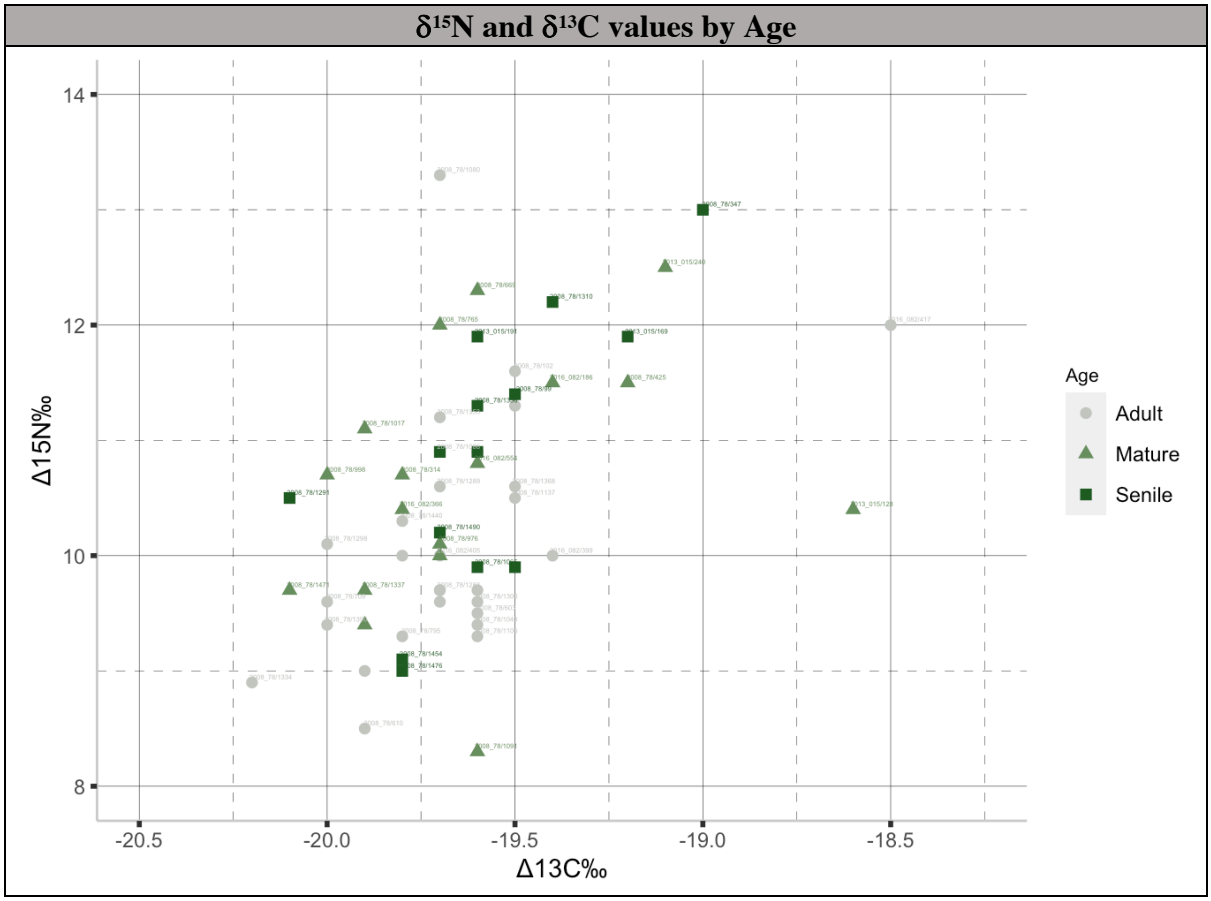

Figure 301 Scatterplot of δ13C and δ15N values by Age

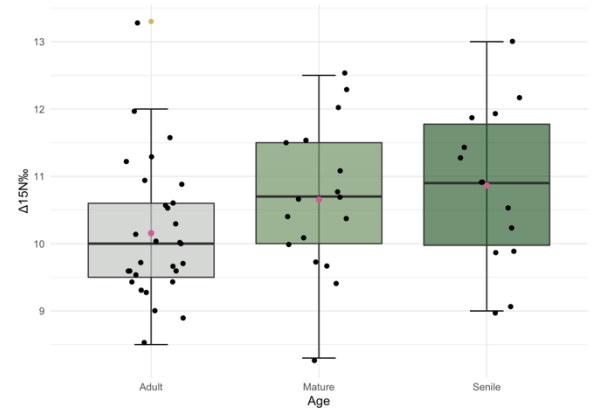

Figure 302 Boxplot of δ15N values of adults, matures and seniles showing slightly but not significantly lower values in adults

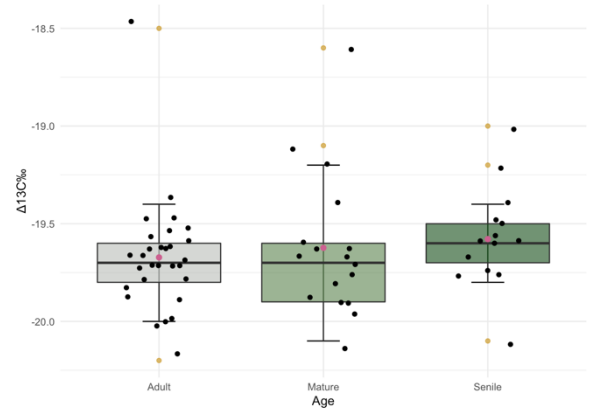

Figure 303 Boxplot of δ13C values of males and females showing no difference between the age groups

7.4.3.1.4 By Layer

The mean collagen yield for Layer 1, which amounts to 75.16mg/g (n=17, SD=53.03), corresponding to 7.516wt% is lower than mean collagen yield for Layer 2, which amounts to 98.43mg/g (n=43, SD=46.17), corresponding to 9.843wt%. This difference was statistically significant (W=202; p=0.0126). The percentage of nitrogen in bone was on average 13.59% for bones from Layer 1 and 13.65% for bone from Layer 2, a difference which was not statistically relevant (W=335; p=0.6223). Since all atomic C/N values were within the accepted range and collagen was extracted successfully from all samples, it is unlikely that the differences in collagen yield would have had a major influence on the $\delta^{13}C$ and $\delta^{15}N$ values of both groups.

The $\delta^{13}C$ values for individuals from Layer 1 ranged from -19.0‰ to -20.0‰ with a mean of -19.61‰ (n=17; SD=0.24) whereas those of individuals from Layer 2 ranged from -18.5‰ to -20.2‰ with a mean of -19.65‰ (n=43; SD=0.33). (Figure 304, Figure 306)

The $\delta^{15}N$ values for individuals from Layer 1 ranged from 8.5‰ to 13.0‰ with a mean of 10.78‰ (n=17; SD=1.24), and those of individuals from Layer 2 spanned from 8.3‰ to 13.3‰ with a mean of 10.34‰ (n=43; SD=1.04). (Figure 304, Figure 305)

Mann-Whitney-U tests showed that there was no significant difference between the two groups regarding $\delta^{13}C$ (W= 430; p=0.2880) as well as $\delta^{15}N$ values (W=445.5; p=0.1918). (Table 121)

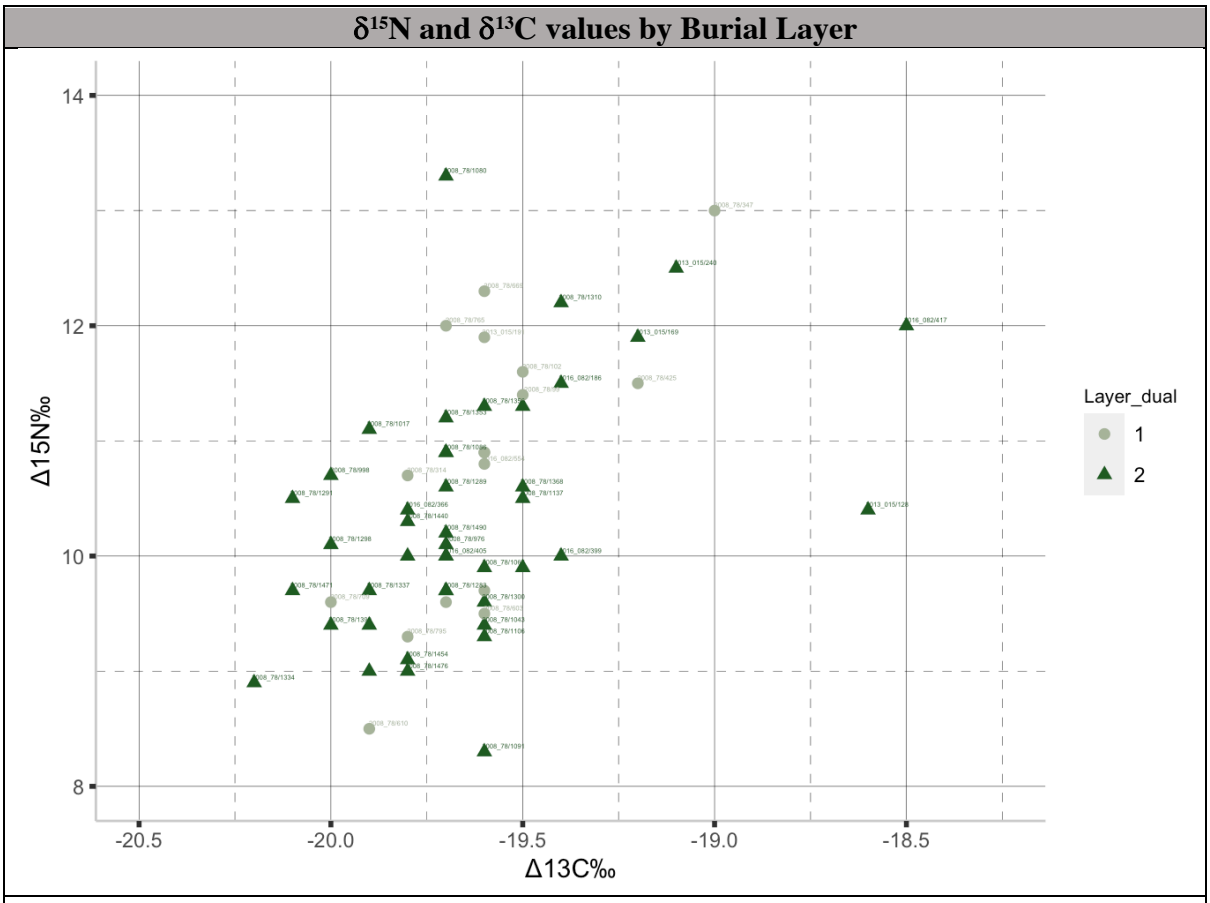

Figure 304 Scatterplot of δ13C and δ15N values by Layer

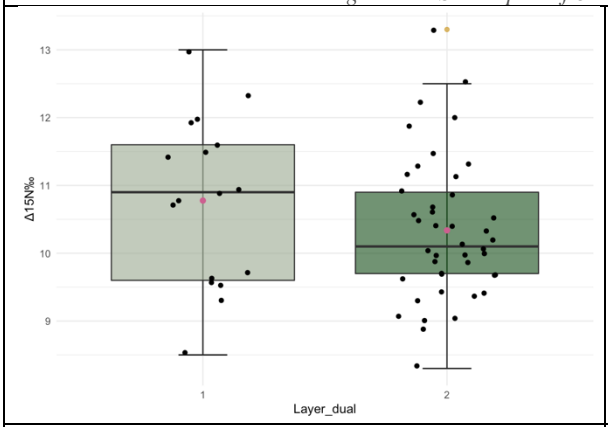

Figure 305 Boxplot of δ15N values of males and females showing no significant difference between the Layers

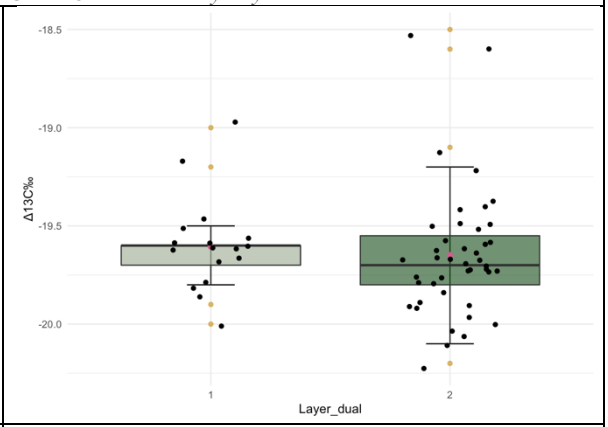

Figure 306 Boxplot of δ13C values of males and females showing no significant difference between the Layers

F=Female
M=Male

7.4.3.1.5 By Location

The mean collagen yield for cloister burials, which amounts to 125.83mg/g (n=14, SD=78.84), corresponding to 12.583wt% is higher than mean collagen yield for cemetery burials, which amounts to 82.69mg/g (n=46, SD=33.56), corresponding to 8.269wt%. This difference was however not statistically significant (W= 205; p=0.1760). The nitrogen percentage in bone lay at an average of 14.44% for cloister burials and 13.39% for cemetery burials. A Mann-Whitney-U test showed that this difference was statistically relevant (W=172, p=0.0089).
However, in bones from both burial locations, the percentage of nitrogen in bone and the mean collagen yield were well above the threshold, and atomic CN values were also all within the acceptable range, indicating good collagen preservation, which is why the differences observed in nitrogen percentage in bone did likely not affect the values of $\delta^{13}C$ and $\delta^{15}N$ in bone collagen and likely had no effect on the differences observed between the two groups.
The $\delta^{13}C$ values for individuals buried in the cloister area ranged from -18.5‰ to -19.8‰ with a mean of -19.34‰ (n=14; SD=0.41) whereas those of individuals buried in the cemetery ranged from -19.2‰ to -20.2‰ with a mean of -19.73‰ (n=46; SD=0.20). (Figure 307, Figure 309)
The $\delta^{15}N$ values for individuals buried in the cloister area ranged from 10.0‰ to 13.0‰ with a mean of 11.24‰ (n=14; SD=0.98), whereas those of individuals buried in the cemetery spanned a range of 8.3‰ to 13.3‰ with a mean of 10.22‰ (n=46; SD=1.04). (Figure 307, Figure 308)
Wilcoxon/Mann-Whitney-U tests showed that there was a significant difference between the two groups regrading $\delta^{13}C$ (W= 120.5; p=0.0004) as well as $\delta^{15}N$ values (W=148.5; p=0.0025), with cloister area burials displaying on average higher $\delta^{15}N$ values and higher $\delta^{13}C$ values than those from the cemetery. (Table 121)

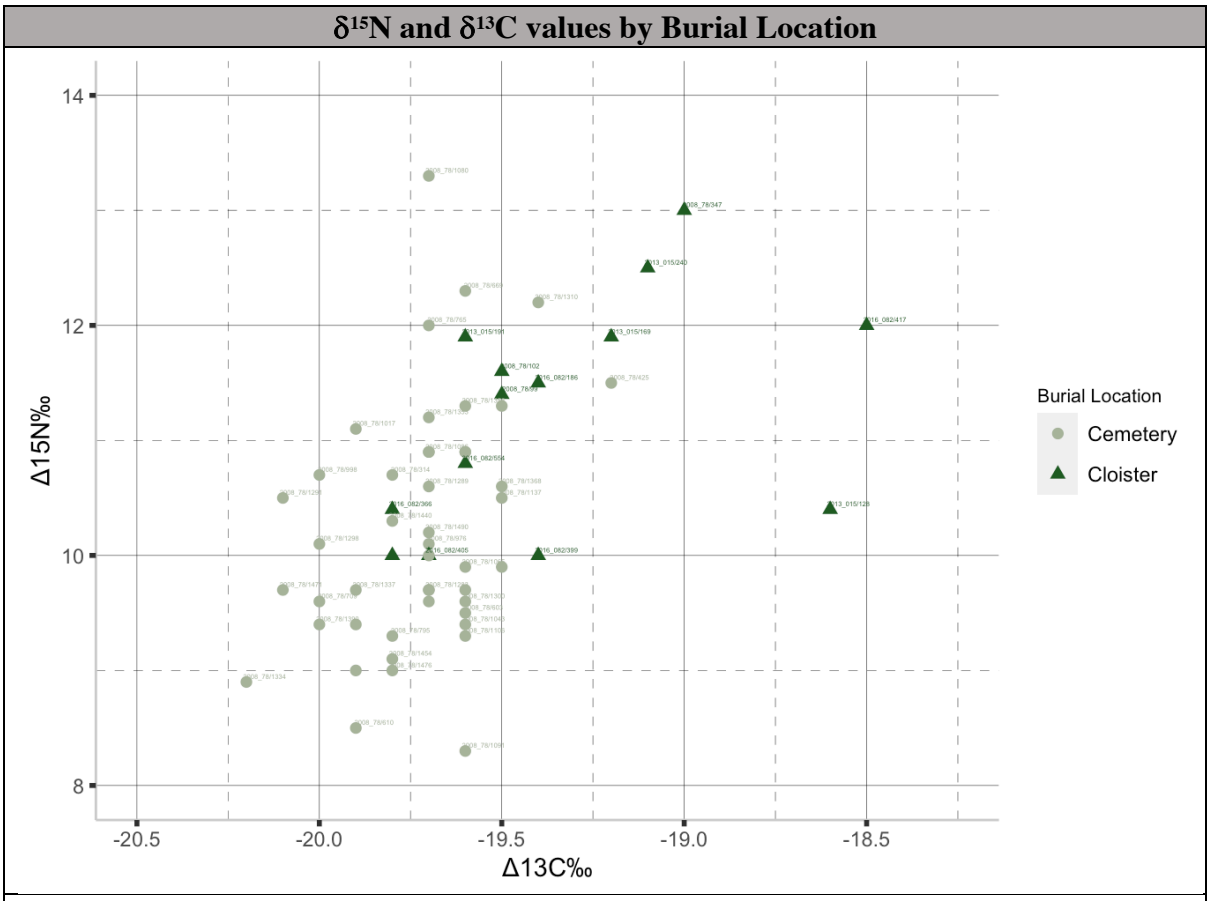

Figure 307 Scatterplot of δ13C and δ15N values by Burial Location

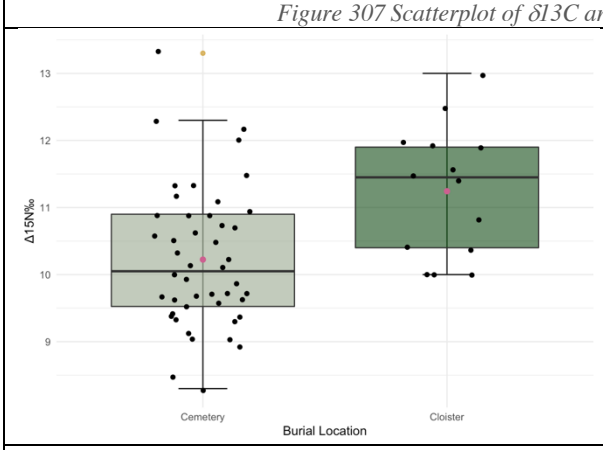

Figure 308 Boxplot of δ15N values showing the significant difference between cloister and cemetery burials

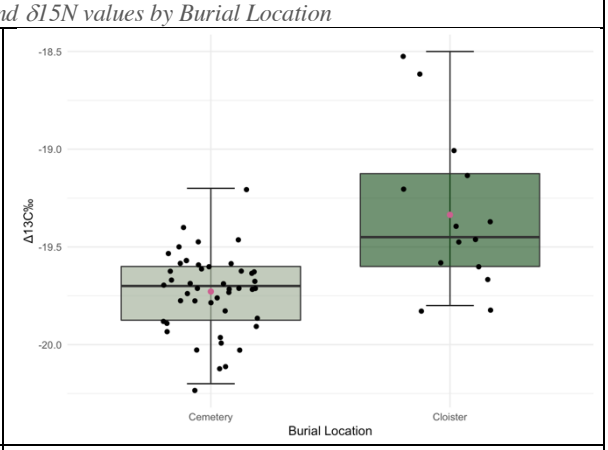

Figure 309 Boxplot of δ13C values showing the significant difference between cloister and cemetery burials

7.4.3.1.6 By Distance to church

The mean collagen yield for cloister burials amounts to 125.83mg/g (n=14, SD=78.84), corresponding to 12.583wt%, the mean collagen yield for burials close to the church amounts to 86.74mg/g (n=9, SD=41.98), which corresponds to 8.674wt%, the mean collagen yield for burials midway to the church amounts to 76.00mg/g (n=25, SD=29.48), which corresponds to 7.600wt% and the mean collagen yield for burials far from the church amounts to 93.57mg/g (n=12, SD=34.44), which corresponds to 9.357wt%. Kruskal-Wallis tests showed no significant difference between any of the groups (X^2=0.6354, p=0.3036). The nitrogen percentage in bone was 14.44% in cloister burials, 13.73% in burials close to church, 13.08% in burials midway to church and 13.78% in burials far from church. This difference was statistically significant at p=0.01819 (X^2=10.0443). Pairwise Wilcoxon tests with Bonferroni correction revealed that only the difference between $\%N_{coll}$ in bones from cloister burials and that in bones from people buried midway to church was statistically significant. However, it is unlikely that this difference in percentage nitrogen in bone between the two groups had an effect on the $\delta^{13}C$ and $\delta^{15}N$ values since overall preservation was good and collagen was successfully extracted from all bones in the sample and atomic C/N levels were all within the acceptable range of 2.9-3.6.

The $\delta^{13}C$ values for individuals buried in the cloister area ranged from -18.5‰ to -19.8‰ with a mean of -19.34‰ (n=14; SD=0.41), those of individuals buried close to the church ranged from -19.2‰ to -19.9‰ with a mean of -19.62‰ (n=9; SD=0.19), those of individuals buried midway to the church ranged from -19.5‰ to -20.1‰ with a mean of -19.72‰ (n=25; SD=0.18) and those of individuals buried far from the church ranged from -19.4‰ to -20.2‰ with a mean of -19.83‰ (n=12; SD=0.21). (Figure 310, Figure 312)

The $\delta^{15}N$ values for individuals buried in the cloister area ranged from 10.0‰ to 13.0‰ with a mean of 11.24‰ (n=14; SD=0.98), those of individuals buried close to the church spanned a range of 9.6‰ to 11.5‰ with a mean of 10.60‰ (n=9; SD=0.62), those of individuals buried midway to the church spanned from 8.3‰ to 13.3‰ with a mean of 10.26‰ (n=25; SD=1.16) whereas those of individuals buried far from the church ranged from 8.9‰ to 12.2‰ with a mean of 9.86‰ (n=12; SD=0.97). (Figure 310, Figure 311)

Kruskal-Wallis tests showed that there was a significant difference within distance to church regarding $\delta^{13}C$ (X^2=17.056; p=0.0007) as well as $\delta^{15}N$ values (X^2=13.0659; p=0.0045). Pairwise Wilcoxon tests with Bonferroni correction revealed that for both $\delta^{15}N$ and $\delta^{13}C$ values,

only the difference between cloister burials and burials midway to and far from the church were statistically relevant, with cloister area burials displaying on average higher $\delta^{15}N$ values and higher $\delta^{13}C$ values than those buried in the middle and at the far end of the cemetery. (Table 121)

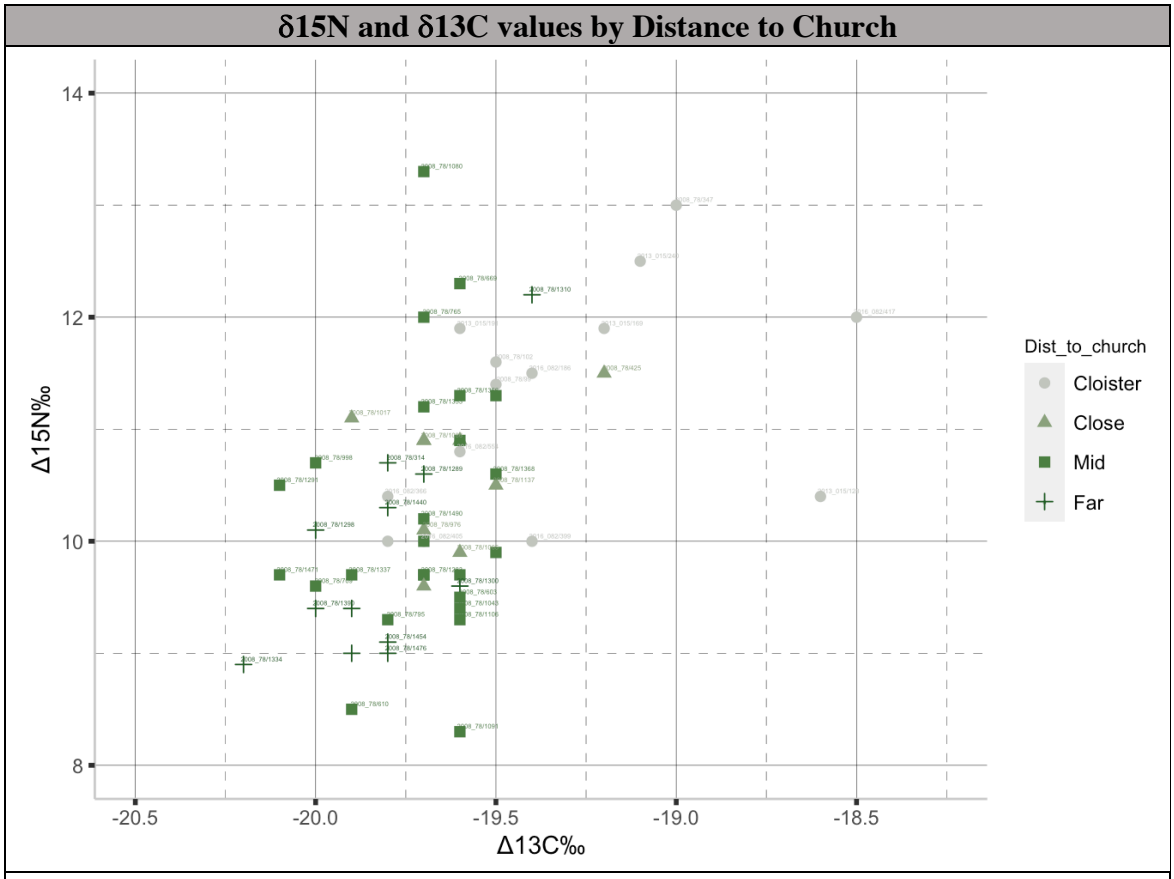

Figure 310 Scatterplot of δ13C and δ15N values by Distance to the church

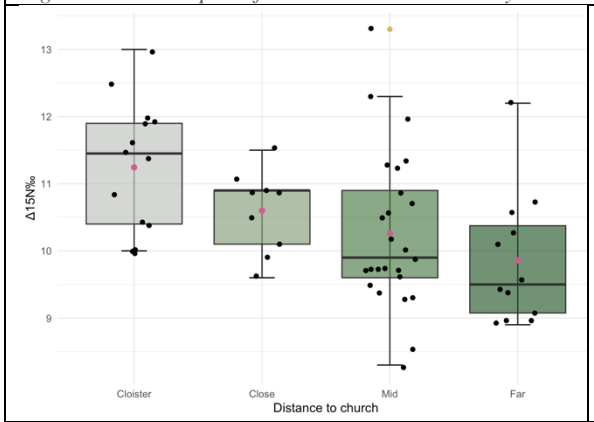

Figure 311 Boxplot of δ15N values showing the gradual decrease in δ15N from cloister burials to burials far away from church

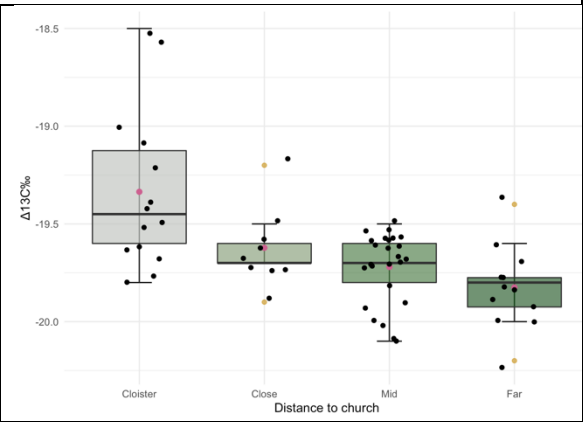

Figure 312 Boxplot of δ13C values showing the gradual decrease in δ13C 15N from cloister burials to burials far away from church

Table 121 Results for the group comparisons of $\delta^{15}N$ and $\delta^{13}C$

			$\delta^{15}N$					$\delta^{13}C$					p-value	
		n	max	min	mean	SD	median	max	min	mean	SD	median	$\delta^{15}N$	$\delta^{13}C$
ALL		60	13.1	8.3	10.46	1.11	10.35	-18.5	-20.2	-19.64	0.31	-19.7		
Sex	F	29	12.3	8.9	10.39	0.82	10.3	-19.2	-20.2	-19.74	0.22	-19.7	0.9528	**0.0141**
	M	31	13.3	8.3	10.53	1.34	10.4	-18.5	-20.1	-19.54	0.35	-19.6		
Age	Adult	29	13.3	8.5	10.16	1.03	10.0	-18.5	-20.2	-19.67	0.29	-19.7	0.0573	0.7398
	Mature	19	13.0	8.3	10.86	1.21	10.7	-18.6	-20.1	-19.58	0.38	-19.7		
	Senile	12	11.9	9.0	10.58	0.98	10.7	-19.2	-20.1	-19.64	0.22	-19.6		
Burial Location	Cemetery	46	13.3	8.3	10.22	1.04	10.05	-19.2	-20.2	-19.73	0.20	-19.70	**0.0025**	**0.0004**
	Cloister	14	13.0	10.0	11.24	0.98	11.45	-18.5	-19.8	-19.34	0.41	-19.45		
Distance to Church	Cloister	14	13.0	10.0	11.24	0.98	11.45*&	-18.5	-19.8	-19.34	0.41	-19.45*&	**0.0045**	**0.0007**
	Close	9	11.5	9.6	10.60	0.62	10.90	-19.2	-19.9	-19.62	0.19	-19.70		
	Mid	25	13.3	8.3	10.26	1.16	9.90&	-19.5	-20.1	-19.72	0.18	-19.70&		
	Far	12	12.2	8.9	9.86	0.97	9.50*	-19.4	-20.2	-19.83	0.21	-19.80*		
Layer-new	1	17	13.0	8.5	10.78	1.24	10.9	-19.0	-20.0	-19.61	0.24	-19.6	0.3368	0.5622
	2	40	13.3	8.3	10.32	1.07	10.1	-18.5	-20.2	-19.65	0.34	-19.7		
	3	3	11.5	10.0	10.63	0.78	10.4	-19.4	-19.8	-19.67	0.23	-19.8		
Layer-dual	1	17	13.0	8.5	10.78	1.24	10.9	-19.0	-20.0	-19.61	0.24	-19.6	0.1918	0.2880
	2	43	13.3	8.3	10.34	1.04	10.1	-18.5	-20.2	-19.65	0.33	-19.7		

7.4.4 Discussion

7.4.4.1 Diet in late medieval and postmedieval Europe

The majority of sources describing diet in medieval and postmedieval times comes from England. However, due to the availability of similar or the same food sources throughout Europe, the general character of the diet can be derived from these sources, even if regional variations in food item availability and quantity probably also led to regional variations in diet

(Yoder 2012). Generally however, the most important resource in medieval diet was cereal grains (Dyer 1983). Grains were mostly consumed in the form of pottages, porridges and bread by the less affluent population. Whilst crops such as barley, oats or rye were primarily consumed by the peasants, bread made of wheat was largely only available to the more affluent individuals. In upper-class households, the cuisine was usually also more sophisticated: pies, tarts, cakes, mushes and fritters were also cooked using finely ground wheat. As a result of the Arab expansion into Europe in the early medieval period, rice was traded as a luxury food item across Europe already in the 13th century and by the 15th century, due to being grown en masse in northern Italy, had become a staple food in late-medieval cookbooks, where it was used in stuffings, as flour in sauces and as a side dish. When cooked with milk, it was also often served to the convalescent and sick (Adamson 2004). Whereas grains were the staple food in medieval diet, meat, dairy products and fresh fruit and vegetables were only available in lesser quantities to the majority of the population (Dyer 1983). Legumes such as broad beans constituted a major source of protein especially among the poorer population (Adamson 2004). To most of the population, access to fruits and vegetables was readily available through gardens that were kept not only in rural areas but also by townspeople and could be bought on markets as well. In England, it is recorded that even the very poor that did not own a garden were granted access to fields to pick greens and beans for consumption. The sole consumption of vegetables however was strongly associated with the poor and among the middle- and upper-classes, a diet heavily reliant on grains and meat was most sought after, especially because garden produce was generally thought to be difficult to digest and recommendations for the culinary preparation different fruits and vegetables to cancel out their negative effects were circulating widely (Adamson 2004; Dyer 2006). Not only the quantity but also the type and quality of meat consumed varied between the social classes. Archaeozoological evidence from Belgium suggests that peasants consumed predominantly meat products from sheep or cattle. Excavations in castles from Belgium confirmed the presence of large and small game, but the main source of meat were still domesticated animals. Contrary to the peasant diet where cattle and sheep were the predominant sources of meat, pig consumption seems to have been predominant in all castle sites (Ervynck 2004). Archaeozoological remains from Luxembourg City were analysed from an excavation inside a townhouse and from the "Bock" castle, as well as from the St. Esprit monastery. Both the sites of the "Bock" castle and the townhouse (11, rue de la Boucherie) date considerably earlier than the Knuedler cemetery, however. During the 10th-12th century, pig remains were the most abundant species found at the "Bock" castle.

Bovid remains were largely predominant during the 8th-11th century in the townhouse but this shifted during the 11th-13th century when pig remains became more abundant, suggestive of more affluent inhabitants (Clavel 2002).

Regarding monastic diet, archaeozoological evidence from Belgium suggests that meat consumption was generally only scarce and restricted to domesticated animals. However, fish remains were found very frequently in monastic contexts, suggesting that their diet was dominated by fish, likely as a result of religious food rules and practices (Ervynck 2004). Several stable isotope studies on monastic samples from England and Belgium suggest that fish was indeed an important source of protein for monks in medieval times (Mays 1997; Polet & Katzenberg 2003). However, at the monastery of St. Esprit in Luxembourg City, which was in use from 1230AD to 1678AD and run by the Order of Saint Clare, no fish remains have been excavated, but pig remains were the most frequently found, followed by caprids and bovids (Rehbach 2008). While other religious orders were bound to strict dietary rules such as the prohibition to consume meat from four-legged animals among Cistercian monks (Yoder 2012), the Franciscan Friars were not subjected to dietary restrictions (Berg & Lehmann 2009), so that a diet relying predominantly on fish, is not necessarily expected for the friars buried on the Knuedler cemetery. Overall, ale was the most important source of drink for all social classes, with middle- and upper classes also frequently consuming wine in varying quantities and lower-class people also often consuming cider, which was cheaper than ale or wine (Dyer 2006). In fact, wine consumption was also fairly important in Luxembourg City. Records from 1444-1500 AD documented locations of wine sellers around the town and the number of wine barrels sold in the city. Based on these data, it was estimated that on average every adult resident consumed 0.6 liters of wine per day (Pauly 1994), notwithstanding any social differences in consumption.

However, as towns started to develop, a clear separation of dietary habits into those of peasants, nobles and clerics was obscured by the emergence of market networks that supplied the inhabitants of the towns and cities with a larger wealth of food items and many urban citizens who had become more affluent through trade were also able to afford more luxury food products (Adamson 2004). Several studies have noted a shift in dietary patterns after the 14th to 15th century, where generally an increase of meat consumption could be observed (Herrscher *et al*. 2001; Müldner & Richards 2007b). This shift in dietary patterns has mostly ben ascribed to urbanization and the subsequent development of market networks in towns (Herrscher *et al*. 2001). Several studies also suggest that there was an increase in marine and/or freshwater fish

consumption from the early to late medieval times likely related to religious food rules (Polet & Katzenberg 2003; Müldner & Richards 2005, 2007b; Müldner 2016) and facilitated by an expansion of fisheries and a refinement of conservation methods that allowed for the transport of Atlantic fish to inland communities (Van Neer & Ervynck 2004; Salamon *et al*. 2008). In fact, written records attest the import of fish from the Atlantic ocean to Rome by the late 14th century (Salamon *et al*. 2008). Even today, one of the marketplaces in Luxembourg City bears the name of "Fëschmaart", meaning fish market. This market was referred to in medieval times as Old market but the name "Fëschmaart" was first reported in a document from the late 17th century (Yegles-Becker 2002), asserting to the trade and therefore consumption of fish in postmedieval Luxembourg City. Earlier evidence for possible fish consumption comes from medieval trading records between 1350-1500 AD. Luxembourgish wine sellers traded their wines as far as Antwerp and brought from there salt, leather buckets and herring back to the city (Pauly 1994).

Records on diet in postmedieval Europe are scarce but they are more abundant for England. In postmedieval England, the diet did not change much between the late medieval and early postmedieval times (Wilson 1973; Stone 2006). However, as towns grew larger and trade widened across Europe and the world, more exotic goods such as exotic fruits or sugar became available, mainly to the upper-classes but gradually also the emerging middle-classes such as merchants, craftsmen etc. in urban centers. Fish consumption has also been attested for postmedieval England with more affluent people having access to more varieties of fresh fish, whereas the lower classes were relying on the widely available and cheaper pickled herring. For much of the postmedieval period though, the diet divide between poor and rich or middle-class individuals remained the same as in late medieval times, with upper- and middle classes able to consume white bread and a variety of meats, while the lower-class diet was restricted to cheaper meats such as mutton, coarse breads and cereal pottages (Sykes 2006; Thirsk 2007; Clayton & Rowbotham 2009). It is very likely, that these broad trends can also be applied to the emerging urban centers in Europe.

7.4.4.2 Diet of the individuals buried in the Knuedler cemetery

In order to be able to make some tentative and preliminary inferences about diet composition in Luxembourg City, the mean $\delta^{13}C$ and $\delta^{15}N$ values of the human remains were compared to those of herbivores (cattle: n=26; caprids: n=23), cervids (n=4), equids (n=15), omnivores (n=29), freshwater fish (n=3), eels (n=6) and marine fish (n=19). In the absence of a local

baseline, a general baseline was constructed from data of various late roman, early medieval, medieval and postmedieval sites across continental Europe. Of course, such a baseline cannot be used to make a detailed dietary reconstruction of the individuals sampled for this study as regional differences in isotopic signatures, such as those caused by different aridity, temperatures etc. (Heaton *et al*. 1986; Britton *et al*. 2008), cannot be accounted for. Therefore, no statistical mixing models for the reconstruction of the percentage of protein sources in the diet was attempted. Instead, the baseline was used as a general guideline to compare the values from Luxembourg City to and make inferences about the overall character of the diet consumed by looking at differences between mean $\delta^{13}C$ and $\delta^{15}N$ values of source proteins and the mean $\delta^{13}C$ and $\delta^{15}N$ values of the human samples.

According to the $\delta^{13}C$ and $\delta^{15}N$ values, the diet in Luxembourg City seems to have been primarily reliant on terrestrial C^3 products. Mean $\delta^{15}N$ values of humans (10.46‰) show a difference of 4.12‰ to the mean of herbivores (6.34‰), which lies within the acceptable 3-5‰ difference between protein source and consumer (Bocherens & Drucker 2003). The same applies to the mean $\delta^{13}C$ values of the humans (-19.64‰) buried on the Knuedler cemetery, which is enriched by 1.74‰ in regard to the herbivore mean (-21.38‰), lying therefore in the 0-2‰ enrichment range of $\delta^{13}C$ between consumer and source (Bocherens & Drucker 2003). Therefore, overall, there is no clear evidence for inclusion of marine or freshwater fish in the diet of the people buried on the Knuedler cemetery.

Nevertheless, inclusion of marine or freshwater fish in the diet should not be dismissed completely in the absence of a local baseline to compare the human $\delta^{13}C$ and $\delta^{15}N$ values to, especially since both $\delta^{13}C$ and $\delta^{15}N$ values are on the upper end of the accepted range of enrichment between source and consumer. (Figure 313)

However, the range of $\delta^{13}C$ and $\delta^{15}N$ values within the Knuedler sample is rather large, namely 1.7‰ for $\delta^{13}C$ and 5‰ for $\delta^{15}N$ values, which constitutes about one trophic level, suggesting that maybe some individuals were either consuming more terrestrial animal protein than others or that some were consuming small amounts of fish, either freshwater or marine alongside a predominantly terrestrial diet. This might especially hold true for those individuals with $\delta^{15}N$ values above 10‰. $\delta^{15}N$ values from collagen of humans consuming only terrestrial protein sources would be expected to range between 4-10‰, whilst the values of those consuming only marine food would range between 10-22‰. However, in the latter case, $\delta^{13}C$ values should also be considerably lower. A purely terrestrial diet is postulated to result in ~-20‰ and that

of a purely marine diet is thought to lie around -12‰ (Schoeninger *et al*. 1983; Richards & Hedges 1999), and the $\delta^{13}C$ values from the Knuedler cemetery all lie much closer to the hypothetical purely terrestrial mean than to the purely marine mean. Therefore, either an increased consumption of terrestrial protein, in particular pig meat, due to their often higher $\delta^{15}N$ values resulting from an omnivorous diet (Dhaliwal *et al*. 2020), or of freshwater fish, which would result in increased $\delta^{15}N$ but not necessarily increased $\delta^{13}C$ values (Dufour *et al*. 1999; Richards *et al*. 2001), seem plausible explanations for the higher $\delta^{15}N$ values observed in some individuals. Indeed, the $\delta^{13}C$ and $\delta^{15}N$ values observed for the Knuedler cemetery are very similar to those from individuals from the St. Callixtus catacomb (mid 3rd – early 5th century AD) in Rome ($\delta^{13}C$: range = -18.9‰ to -20.8‰, mean = -19.8±‰; $\delta^{15}N$: range = 9.7‰ to 11.‰, mean = 10.6‰), for which a freshwater fish consumption of about 18%-43% was estimated using a linear mixing model (Rutgers *et al*. 2009).

Luxembourg City being the religious center of the region and the whole Duchy (Schmitt 1994) at the time likely adhered to the fasting rules set out by the catholic church. Especially the Fransiscan friars that were likely buried as well on the cemetery had to keep these fasting rules, even though they were, as stated above, different from those of the general population. The general population, under catholic fasting rules, was not allowed to eat meat for about a third of the days of the year, which generally meant no meat consumption on two weekdays throughout the year, on religious holidays and during the 40-day Lenten fasting period (Benedictow 2003; Schäuble 2007; Trautmann 2012; Yoder 2012). Therefore, it is very likely that meat was substituted by fish and/or legumes and dairy products during these days. Although no fish remains have so far been excavated in Luxembourg City, the evidence of the growing fish trade in Europe in the late medieval ages (Van Neer & Ervynck 2004; Barrett *et al*. 2011), as well as the records of traded herring against wine from 14th to 15th century documents (Pauly 1994), suggest that fish was sold in Luxembourg City during late medieval times and the presence of the "Fëschmaart", first mentioned as such in a document from 1692AD (Yegles-Becker 2002), as well as historical records from 1388-1500 mentioning fishers and referencing fishing rights in the river Alzette which flows through the lower town (Pauly 2022c) attest to fish consumption during the postmedieval times.

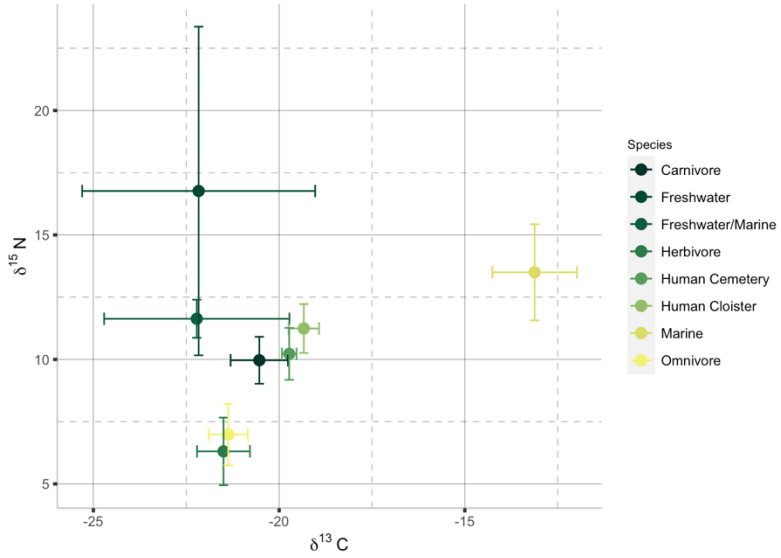

Figure 313 Scatterplot of mean $\delta^{13}C$ and $\delta^{15}N$ values with SD of the Knuedler sample separated by burial location compared to faunal remains from continental Europe

7.4.4.3 Differences in isotopic values between men and women

Even though males (10.53‰) had slightly more elevated $\delta^{15}N$ values than females (10.39‰), that difference was not statistically significant. However, the range of the $\delta^{15}N$ values was considerably greater in men (5‰) than in females (3.4‰). Regarding $\delta^{13}C$ values, men had significantly higher values (-19.54‰) than females (-19.3‰). Furthermore, the range of the values was also noticeably greater in males (1.6‰) than in females (1‰). However, the range of $\delta^{13}C$ values among men is strongly influenced by two prominent outliers (2016-082/417: -18.5‰; 2013-015/128: -18.6‰). When those are removed the range of values drops to 1.1‰, which is very similar to that of women. This suggests that, while overall men's and women's diet was very similar regarding the general composition, the diet of men was more heterogenous than that of women regarding animal protein intake, which implies that some men had more and better access to a variety of protein-rich foods than women. The wider range of $\delta^{15}N$ values and the overall higher $\delta^{13}C$ values of men could indicate that at least some of them had access to aquatic resources and/or consumed small amounts of C^4 plants, such as millet.

Several studies found differences in stable isotope ratios between men and women (Richards *et al*. 2006; Müldner & Richards 2007a; Kjellström *et al*. 2009; Reitsema *et al*. 2010; Reitsema & Vercellotti 2012; Quintelier *et al*. 2014), while others did not (Schäuble 2007; Olsen *et al*. 2018; Dhaliwal *et al*. 2020). In early medieval Giecz (Poland), men had significantly higher $\delta^{15}N$ values than females, which suggests that they ate less meat than the males. No relevant differences were observed between the sexes regarding $\delta^{13}C$ values. Several explanations for

this divide, ranging from different religious fasting rules for women, a belief that heavy foods such as meats were not as digestible to women to consumption of different foods due to different labour division have been brought forward by the authors (Reitsema *et al*. 2010). Since in the Luxembourgish sample, $\delta^{15}N$ values are not statistically different between men and women, the explanations offered by Reitsema et al. (2010) to explain the sex-based differences in Giecz likely do not apply here. A difference in $\delta^{13}C$ values between men and women, albeit the opposite trend than in the Knuedler sample, has been reported from a medieval Italian site, however no specific causes for this difference have been addressed, but it is suggested that the differences between males and females could be caused by contact of males with different foods, due to their work away from home, while women were eating more consistently the same things at home (Reitsema & Vercellotti 2012). A similar pattern was observed at the Iron Age-Late Medieval site of Newark Bay on Orkney where, according to stable isotope values, males had a significantly higher input of marine protein in their diet, which was likely related to either status differences in men and women or differential food access due to sex-based differences in labour division (Richards *et al*. 2006). At the postmedieval site of Aalst, males also display significantly higher $\delta^{13}C$ and $\delta^{15}N$ values than females, suggesting higher component of terrestrial and marine animal protein in their diet. Another similarity to the Knuedler sample is that female stable isotope values from Aalst are more tightly clustered than male values, which according to the authors of the study indicates a less varied diet among females, reflecting again the different gender roles in medieval and postmedieval societies (Quintelier *et al*. 2014). The same findings and conclusions were also reached upon examination of stable isotope values of males and females from the late medieval to early postmedieval priory of Fishergate in England (Müldner & Richards 2007a).

Therefore, it is possible that the significantly lower $\delta^{13}C$ values as well as the more clustered $\delta^{15}N$ values of females reflect dietary differences between males and females, with females having a generally less varied diet than males. The reasons for these differences are manyfold and cannot be pinned down to one cause for the Knuedler sample but, differences in diet due to different observance of religious fasting rules (Bynum 1987) and differences due to sex-based division of labour and the subsequent differential access to food items (Richards *et al*. 2006; Müldner & Richards 2007a; Reitsema & Vercellotti 2012; Quintelier *et al*. 2014) can be regarded as plausible reasons for the sex differences observed in the Knuedler sample.

7.4.4.4 Differences between age groups

In order to test whether later childhood diet was different from that of adult individuals, samples from adult individuals were compared to samples from matures and seniles. Based on the bone collagen turnover rate of 10-30 years in adult individuals (Hedges *et al*. 2007), adults (20-39y), and in particular young adults (20-29y), probably still reflect a residual $\delta^{13}C$ and $\delta^{15}N$ signal of their childhood diet of around 10-19 years, whereas the bone collagen of seniles and matures should reflect only adult diet.

No significant differences were detected among the age groups regarding $\delta^{13}C$ and $\delta^{15}N$ values, suggesting that there were no differences between later childhood/early adult diet and adult diet. At Anglo-Saxon Berinsfield however, a significant difference between diet of young adults and adults could be observed in males, which the authors relate to differences in social status of juveniles and young adults compared to adults, which in that case seems to be supported by the archaeological data as well (Privat *et al*. 2002).

The lack of such data suggests that this was not the case in Luxembourg City, however, a more thorough investigation into childhood diet based on bone samples from subadults would be needed to clarify the nature of children's and juvenile's diets.

7.4.4.5 Differences in isotopic values between socio-economic classes

When comparing the $\delta^{13}C$ and $\delta^{15}N$ values between cloister and cemetery burials it becomes clear that both the $\delta^{13}C$ and $\delta^{15}N$ values from the cloister burials are significantly enriched compared to those of the cemetery burials. The difference between the means of the two groups is 0.39‰ for $\delta^{13}C$ values (cemetery: -19.73‰; cloister: -19.34‰) and 1.02‰ for $\delta^{15}N$ values (cemetery: 10.22‰; cloister: 11.24‰). Regarding $\delta^{13}C$ values, cemetery burials had a smaller range of values (1‰) than cloister burials (1.3‰). However, when removing the two extreme outliers, the range of $\delta^{13}C$ values within cloister burials falls to 0.8‰. But cemetery burials (5‰) had a greater range of $\delta^{15}N$ values than cloister burials (3‰). It also must be noted that in cloister burials, $\delta^{15}N$ values do not fall below 10‰ whereas in cemetery burials 47.83% (n=22) of values fall below 10‰. This suggests that people buried in the cemetery had a more heterogenous and in many cases also a fairly different diet to that of people buried in the cloister. Even though the $\delta^{13}C$ and $\delta^{15}N$ values of the cloister burials still fall marginally within the range of a predominantly terrestrial C^3-based diet ($\delta^{13}C$ -2.04‰ enriched to the herbivore mean; $\delta^{15}N$ 4.9‰ enriched to the herbivore mean) it is very likely that, due to both the enriched

$\delta^{13}C$ and $\delta^{15}N$ values, these individuals consumed either more omnivore protein or more marine or freshwater resources than the people buried in the cemetery. However, the contribution of these sources was not high enough to leave a clear marine signal in the stable isotope values. Marine resources would lead to enriched $\delta^{13}C$ and $\delta^{15}N$ values due to having enriched $\delta^{13}C$ and $\delta^{15}N$ values themselves (Chisholm *et al*. 1982; Schoeninger *et al*. 1983; Katzenberg, M. A., & Waters-Rist 2019). Freshwater resources would predominantly increase $\delta^{15}N$ values but whether an increase in $\delta^{13}C$ values would occur is highly dependent on the geographical region where the fish was caught, as the $\delta^{13}C$ values of freshwater fish are highly dependent on local $\delta^{13}C$ environmental isotopic signatures (Dufour *et al*. 1999). Omnivore protein would have been predominantly sourced from pig in medieval and postmedieval times, as pigs were often also kept in town and close to homes, where they were regularly also fed on leftover scraps from the kitchen (Müldner & Richards 2005).

Since cemetery burials displayed a rather large range in $\delta^{15}N$ values, it was also tested whether there were differences in stable isotope ratios between areas close, midway and far from the church, within the cemetery and the cloister. It has to be mentioned here though, that the separation into the three groups was done arbitrarily by the author and is not based on any documented separations between these areas. Indeed, both $\delta^{13}C$ and $\delta^{15}N$ showed a gradual decline from cloister burials to burials at the far end of the cemetery. Kruskal-Wallis tests also confirmed this trend as statistically significant, but the significant difference existed only between cloister burials and burials midway to and far from church, with burials midway to church showing the largest range in $\delta^{15}N$ values (8.3‰-13.3‰). This trend however suggests that possibly there was not only a social stratification between cloister and church burials but also within the cemetery, which is reflected in the overall isotopic signature of the sampled individuals.

The differences observed between $\delta^{13}C$ and $\delta^{15}N$ of cloister and cemetery burials are further supported by the results of the anthropological analyses described in the previous chapters. In short, individuals from the cloister experienced less caries, less calculus per tooth, less antemortem tooth loss, less periapical lesions and less dental attrition, which are all indicators of a better diet (less cariogenic and abrasive food etc.) as already discussed previously. Furthermore, they also had less enamel hypoplasia suggestive of less stress during childhood. Overall, people buried in the cloister also had a different mortality profile than those from the cemetery, namely cloister burials had a later death peak than cemetery burials, which is usually seen as an indicator of good health as it suggests an overall longer survival rate for this group.

Differences in $\delta^{13}C$ and $\delta^{15}N$ values that have been attributed to differences in diet related to social status have been observed on archaeological sites between burial locations, different cemeteries, different burial types and burials with or without grave goods ranging from the Iron Age to Postmedieval times and across various geographical regions (Schutkowski *et al*. 1999; Privat *et al*. 2002; Le Huray & Schutkowski 2005; Trickett 2006; Müldner & Richards 2007a; Yoder 2012; Reitsema & Vercellotti 2012; Beaumont *et al*. 2013b; Quintelier *et al*. 2014; Trautmann *et al*. 2017; Bleasdale *et al*. 2019; Toso *et al*. 2019; Dhaliwal *et al*. 2020; Paladin *et al*. 2020). The results from the Knuedler cemetery are particularly comparable to those of the burials at the Gilbertine St.Andrew's priory in Fishergate, (Müldner & Richards 2007a), York, to the burials at the Carmelite friary in Aalst (Quintelier *et al*. 2014), to those of the Cistercian Øm Kloster in Denmark (Yoder 2012), those buried at San Michele church in Trino Vercellese, Italy (Reitsema & Vercellotti 2012) and those from Grevenmacher, Luxembourg (Trautmann *et al*. 2017). All these studies have shown that individuals buried within a church or monastery exhibited higher $\delta^{13}C$ and $\delta^{15}N$ values than those buried on the associated cemeteries or, in the case of Aalst, inside the cloister garth. In the cases of the monasteries, the greater prevalence of men buried within the monastery suggests the presence of the residential monks or friars and in all those cases, except at Fishergate, where one solely monastic burial ground was found, it was not possible to distinguish them from the affluent lay population by burial location or position alone (Müldner & Richards 2007a; Yoder 2012; Quintelier *et al*. 2014). In all cases, and this was also the case for the Knuedler cemetery, it was not possible either to distinguish monastic burials from affluent layfolk burials based on $\delta^{13}C$ and $\delta^{15}N$, suggesting that overall diet was similar within the two groups, which is not surprising as monasteries were usually well funded and did not lack food (Mays 1997, 2009; Yoder 2012). Furthermore, according to their religious rules, the Franciscan monks did not have any specific dietary restrictions and oftentimes, during fasting times, meat was replaced by other protein sources such as fish or dairy products. In all monastic samples, people buried outside the monastic complex showed lower $\delta^{13}C$ and $\delta^{15}N$ values compared to those of cloister burials, consistent with a diet not as rich in proteins. Figure 314 illustrates the differences between cloister/church burials and cemetery burials in the Knuedler site, at the contemporaneous monastic site of Aalst and at medieval Grevenmacher. The plot clearly shows the same pattern of enriched $\delta^{13}C$ and $\delta^{15}N$ values in the cloister/church compared to the cemetery, even though overall isotopic signature varies from site to site. A comparison to Grevenmacher would prove particularly interesting as both sites are situated in close proximity and belonged to the Duchy

of Luxembourg, with Grevenmacher displaying many rural characteristics despite officially being a town (Trautmann 2012) and Luxembourg exhibiting typical features of an urban center (Schmitt 1994). The scatterplot shows that Grevenmacher exhibits overall lower $\delta^{13}C$ and $\delta^{15}N$ values than Luxembourg City. It would be interesting to investigate whether this pattern reflects differences in rural and urban diet or, since Grevenmacher dates from the 10th to 14th century and thus earlier than the Knuedler cemetery, between medieval and postmedieval diets. However, to gain clarity on this matter, a local animal baseline of both sites would be needed in order to rule out the possibility of different regional isotopic signatures (Stevens *et al*. 2013).

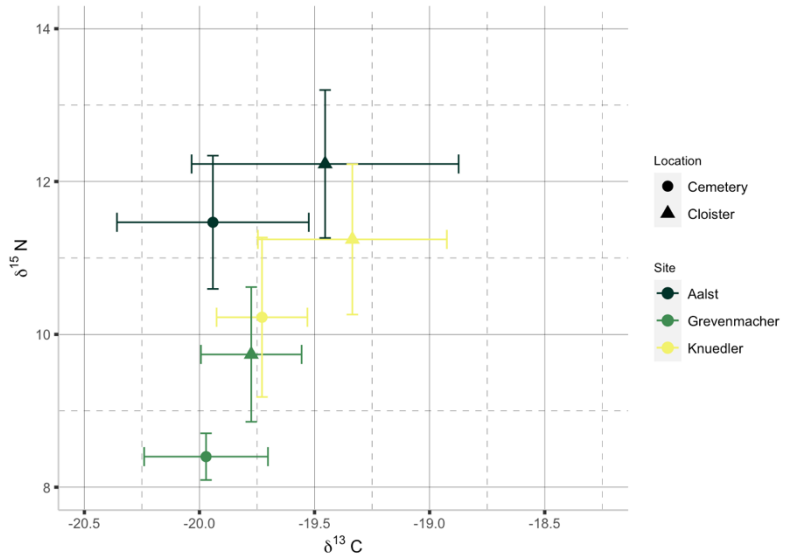

Figure 314 Scatterplot illustrating the differences in $\delta^{13}C$ and $\delta^{15}N$ values between cemetery and cloister/church burials at the Knuedler site (Luxembourg), at Aalst (Belgium) and at Grevenmacher (Luxembourg)

7.4.4.5.1 Special cases

Within the group of individuals buried far from the church and midway to church, there are two outliers which display fairly high $\delta^{15}N$ values. Those belong to individual 2008-78/1080 (midway to church), a young adult which at 13.3‰ also displays the highest $\delta^{15}N$ value of the whole sample and to 2008-78/1310 a mature male which shows signs of an undetermined underlying metabolic condition (see chapter on Metabolic diseases). For the former case, apart from an enlarged and deformed right elbow joint which has been attributed to either congenital or early childhood dislocation (see chapters on congenital and traumatic conditions), no indications neither archaeological nor anthropological were found that might explain the enriched $\delta^{15}N$ value. In the latter case however, there are two possibilities for the enriched $\delta^{15}N$ values. In fact, the $\delta^{13}C$ values of 2008-78/1310 are also enriched compared to the rest of the individuals buried in the far from church group. The first possibility is that, since the individual

likely suffers from a metabolic disease, the physiological processes underlying stable isotope fractionation and distribution throughout the body are compromised, which might lead to increased or decreased stable isotope values that do not directly reflect food intake anymore (Reitsema 2013). Whilst this phenomenon has been confirmed for starvation and during pregnancy (Reitsema 2013), it could neither be confirmed nor refuted for rickets and osteomalacia (Olsen *et al*. 2014). Whilst intraskeletal sampling of areas affected by pathological lesions such as osteomyelitis, calluses or joint disease showed increased $\delta^{13}C$ and $\delta^{15}N$ values in the areas close to and of the pathological lesions as compared to unaffected areas (Olsen *et al*. 2014; Curto *et al*. 2020), in the case of rickets and osteomalacia, all bones showed the same isotopic signatures. The authors argue that this however does not necessarily mean that these conditions do not change isotopic signatures of the bones. As they are systemic diseases, it is possible that simply all bones of the affected individual reflect the increased or decreased isotopic signature caused by the disease (Olsen *et al*. 2014). However, a study examining $\delta^{13}C$ and $\delta^{15}N$ values between skeletons without pathological lesions and those with signs of leprosy, which is also a systemic disease, did not find particularly elevated or depleted $\delta^{13}C$ and $\delta^{15}N$ values in individuals with leprosy compared to those without (Linderholm & Kjellström 2011). In their study on stable isotope ratios in dentine and bone collagen of an infant with probable scurvy and heavily enriched $\delta^{13}C$ and $\delta^{15}N$ values, Nicholls et al. (2020) argue that vitamin C deficiency alone does not disrupt the fractionation processes of stable isotopes in the body and therefore likely won't lead to increased $\delta^{15}N$ values, but that comorbidities that often accompany the disease such as starvation or infection could do so (Nicholls *et al*. 2020). Another study however did not find any elevated stable isotope ratios in infectious diseases, but only in cancer metastases (Drtikolová Kaupová *et al*. 2021). Therefore, it cannot be concluded for certain, whether the elevated stable isotope values observed in 2008-78/1310 are due to physiological disturbance caused by a disease process. The other possibility is, that the individual had a different social status than the others buried in the same area. 2008-78/1310 was buried facing west, whereas all others are facing east. An east facing burial position is considered to be the standard orientation on Christian burial grounds as it follows the belief that Jesus would return in the east. Thus, Christians were usually buried with their head in the west and facing east so that they could witness his return during the resurrection (Pearson 1999; Augenti & Gilchrist 2011; Nater 2018). Priests on the other hand were often buried with the head in the east facing west as they were required to watch over their commune (Effros 1997; Pearson 1999; Nater 2018). Three further burials from the Knuedler cemetery

exhibit an east-west orientation of the body, like 2008-78/1310, they are all male or probably male but of varying ages, with the youngest being 18-20 years old. While their sex would make a case for them being priests or clerics, the lack of characteristic grave goods does not. Only in one burial, remnants of a rosary were found, but the characteristic chalice and paten, which are often mentioned in literature to be typical features of priest burials (Gilchrist 2009, 2011; Augenti & Gilchrist 2011), are missing[1]. However, their absence in the archaeological record must not exclude that they had once been placed in the grave. Individual 2008-78/1091 which is also a mature male and buried facing west, however displayed the lowest $\delta^{15}N$ values (8.3‰) of the whole sample, which means that high $\delta^{15}N$ values, and therefore a likely higher animal protein content in the diet, are not a common feature of west facing graves. Therefore, the reasons behind 2008-78/1310's elevated $\delta^{13}C$ and $\delta^{15}N$ values remain only speculative.

Two further considerable outliers were noticed among the cloister burials. Individuals 2016-082/417 and 2013-015/128, two males, one young adult and the other mature, exhibited the highest $\delta^{13}C$ values of the entire sample (2016-082/417: -18.5±‰;2013-015/128: -18.6‰). At 12‰ (2016-082/417) and 10.4‰ (2013-015/128) their $\delta^{15}N$ values are also rather elevated. If considering the mean of the herbivores sourced from different European archaeological sites as baseline for this site, the $\delta^{13}C$ of both individuals is enriched more than the expected one trophic level enrichment of 0-2‰ between source and consumer (2016-082/417: 2.88±‰; 2013-015/128: 2.78‰) (Bocherens & Drucker 2003). While 2013-015/128 (4.06‰) is still within the range of one trophic level enrichment between consumer and source of 3-5‰ (Bocherens & Drucker 2003), 2016-085/417 (5.66‰) falls just outside of that range. These values suggest that both these individuals had a diet that was different from that of the rest of the people buried on the Knuedler cemetery, likely high in terrestrial animal protein and/or supplemented by marine or freshwater fish to a slightly greater extent. Since better access to animal protein and to fish is considered to have been privy to individuals of higher social status that were affluent enough to pay for such expenses it is possible that they both possessed a higher social status than the rest of the people buried there. However, within the cloister area,

[1] The archaeological evidence, including grave finds, has not been analysed yet. However, in the find books kindly provided by Mme. Bis-Worch from the INRA in Luxembourg, no objects are listed from these graves that would be immediately identifiable as chalice or paten. However, detailed analysis of all the archaeological finds (metal and some ceramic fragments) would be required in order to be certain that the objects are actually absent from the graves.

they are not buried in a separate area that might indicate a privileged burial but are buried in line with other individuals with lower $\delta^{13}C$ and $\delta^{15}N$ values. Another possibility would be that the individuals were not part of the local population. In fact, Franciscan friars, due to belonging to a mendicant order, were not bound to a specific monastery. They were allowed to travel from town to town (Montford 2002). Therefore, it is possible that some of the friars, which, due to the elevated frequency of males, were probably buried inside the cloister, were not native to Luxembourg City and grew up and lived somewhere else, where different environmental conditions and/or dependence on a different kind of diet might have defined their $\delta^{13}C$ and $\delta^{15}N$ values. Furthermore, the presence of men with gunshot wounds inside the cloister as well as the grave slab of a soldier indicate that military personnel was also buried on this cemetery and even inside the cloister. As most soldiers and officers that were stationed in Luxembourg City came from abroad (Weis 2004; Thewes 2011, 2013), it is possible that they might present $\delta^{13}C$ and $\delta^{15}N$ values that are different from those of the local population. Therefore, it is possible that individuals 2016-085/417 and 2013-015/128 were foreigners, possibly soldiers/officers or friars. However, to test this hypothesis, further analyses such as strontium ($^{87}Sr/^{86}Sr$) and oxygen ($\delta^{18}O_{carbVSMOW}$) isotope analyses of teeth and bones would be needed to investigate whether they grew up somewhere else than where they were buried.

7.4.4.6 Differences in isotopic values between the late-medieval and postmedieval times

No significant differences in $\delta^{13}C$ and $\delta^{15}N$ values were detected. Many studies have however noted an increase in $\delta^{13}C$ and $\delta^{15}N$ over time from the early medieval to the late medieval times, which likely reflects a change in diet, probably the inclusion of larger amounts of marine and freshwater fish in the diet (Müldner & Richards 2005; Salamon *et al*. 2008). Although direct comparisons without being able to control for regional variations in isotopic signatures through baselines, are not optimal, it is still evident that the majority of early medieval sites cluster together and the majority of later medieval and postmedieval sites cluster together. This suggests that, while there was a shift in diet between early medieval to late medieval times, diet did not change significantly between the late medieval and postmedieval times. This likely also holds true then for Luxembourg City. A continuity in diet between late medieval and early postmedieval times has been documented in British literature (Wilson 1973; Stone 2006). Access to different food items, also those that would have been imported only became more prevalent in the late postmedieval times and was concentrated mainly around urban centers (Thirsk 2007). Therefore, it is possible that a temporal change in diet had simply not yet taken

place in Luxembourg City or that the possible scarcity of samples from the later postmedieval period obscures any potential secular changes in diet.

7.4.4.7 Conclusion

To conclude, the citizens buried on the Knuedler cemetery and inside the cloister had a diet that was predominantly based on terrestrial animal protein and C^3 plants. Differences in $\delta^{13}C$ values and $\delta^{15}N$ ranges between the sexes suggest that males had a more varied and heterogenous diet than females, which might be due to several factors such as observance of fasting rules or related to gender-based labour division. No significant differences between the age groups suggest that there was no age-based social stratification in the city. The lack of difference in $\delta^{13}C$ and $\delta^{15}N$ values between the two layers suggests that there was no major dietary change between the late medieval and postmedieval period in Luxembourg City, a hypothesis which is also supported by the anthropological data. Significantly higher $\delta^{13}C$ and $\delta^{15}N$ among cloister burials compared to cemetery burials reflects the different social status of these two groups, which was therefore not only defined by their burial position but also characterised by a different diet, in which more affluent layfolk and friars had better access to animal protein, and possibly also marine or freshwater fish, a trend which has been observed in numerous stable isotope studies on medieval and postmedieval sites. Differences between cloister and cemetery burials are furthermore also supported by the anthropological data. Within the cloister area, two individuals showed more depleted $\delta^{13}C$ values than the others, suggesting that they ingested a different diet, possibly richer in marine foods. This might also indicate that they did not grow up locally, a hypothesis that would need to be verified through strontium ($^{87}Sr/^{86}Sr$) and oxygen ($\delta^{18}O_{carbVSMOW}$) isotope analyses.

8 Conclusion

This final chapter will summarise the results from the different chapters of the thesis and bring them together to reach an overarching conclusion on living conditions in Luxembourg City based on the three main pillars: Physical activity, Health and medical care and Diet and Nutrition.

8.1 Physicial activity

According to Wolff's law, bones adapt their shape to the external mechanical forces they are subjected to (Wolff 1892b). Therefore, manual activities would be expected to leave traces on bones when carried out repeatedly, especially if they are sufficiently intense. Hence, strong differences in diaphyseal shape and robusticity, bilateral asymmetry, entheseal changes as well as patterns and intensity of joint diseases between the different groups should indicate differences in physical activity patterns.

Overall, robusticity and joint disease indices as well as enthesial changes were not very pronounced among all the burials from the Knuedler burial complex, suggesting that these individuals did not engage in very strenuous occupations. These findings are not surprising among town residents, where the everyday work load was not as physically demanding and more diverse within a social group than was the farming way of life of rural societies (Cardoso 2018; Van Cant 2019; Palmer & Waters-Rist 2019).

The higher number of bilaterally asymmetrical measurements in men and women in the upper limbs suggests that both sexes, but especially males did engage in manual labour either regular and/or intense enough to cause differential appositional bone growth in the left and right body sides, causing bone growth to be more prominent in the dominant arm. The same tendency was also observed in bone robusticity, with males showing higher humeral robusticity indices than women. Furthermore, males showed higher combined joint entheseal scores than females, especially in the entheses involved in shoulder movement, which was the only area that also showed significant differences between the sexes among younger individuals aged 20-39 years. Males overall showed higher indices of joint disease than women. Altogether, this suggests that there was a division of labour present in the population, with men engaging overall in more strenuous tasks than women, especially related to heavy lifting (Perry 2004). However, it has to be kept in mind that biological factors might be responsible for or might have at least emphasised the differences in robusticity and entheseal changes between the sexes (Jones *et al*. 1977; Haapasalo *et al*. 1996). In fact, differences between men and women in body size, in bone responses to biomechanical stress, as well as in hormonal factors influencing bone and muscle mass growth, might have contributed to the discrepancies observed between the sexes. Some differences could be observed in intensity and frequency of joint disease, entheseal changes and bone robusticity between the burial locations, with individuals from the cloister surprisingly showing higher degrees of expression in all three traits, despite them supposedly belonging to a higher social class than those buried in the cemetery. However, all these traits

also showed a significant correlation with age, with frequency and intensity of expression increasing in old age. The majority of individuals buried in the cloister were mature men, which suggests that the differences detected between the burial locations might have been influenced by age and partially by sex distribution. This is supported by the fact that, after correcting for age, no significant differences could be detected anymore between the two perceived social groups. Overall, this suggests that both social groups engaged in physical activities that put a similar amount of mechanical load on their bones. Interestingly though, differences in bone robusticity between burial locations were strongly focussed on femoral diaphyseal shape, with those from the cemetery showing a generally more elongated shape with a more pronounced linea aspera. Additionally, cloister burials presented significantly more squatting facets on the tibia than cemetery burials. Together with the more robust femoral shape, this might be indicative of prolonged squatting or even kneeling in this group. With the high surplus in men and the older average age at death among cloister burials, this might hint at the presence of friars among the cloister burials.

Regarding changes over time, no differences could be detected between the two burial layers regarding entheseal changes and no clear changes in patterns of robusticity and bilateral asymmetry could be detected. However, men of the older Layer 2 showed an overall higher index of degenerative joint disease, in particular regarding the shoulder, hip and elbow joints, which might be either indicative of a slight shift in everyday physical activity over time or might be influenced by the slight difference in age distribution between the two layers.

8.2 Health and medical care

Throughout the medieval and postmedieval times, the crowded living conditions in urban centres provided fruitful grounds for the spread of diseases (Betsinger & DeWitte 2021), as can be witnessed most notably by the numerous plague epidemics that ravaged European cities from the 14th century onwards (Pauly 2020). According to historical sources, Luxembourg City was not exempt from these problems. The obligation of ordinary townspeople to host garrison personnel and their families within their own homes led to overcrowded living conditions not only within the city but also within the citizens' own homes (Thewes 2013). These crowded living conditions likely facilitated the spread of infectious diseases which is also reflected in the numerous accounts of epidemics that plagued the city during medieval and postmedieval times (Pauly 2020).

Considering these historical accounts, living conditions in Luxembourg City posed a high potential for infectious diseases to spread among the inhabitants. Therefore, it is all the more surprising that not many individuals suffered from chronic infectious diseases such as otitis media or sinusitis or showed signs of chronic bone infections such as periostitis, which is suggestive of a rather good health status.

Furthermore, there was evidence for treatment and attempted treatment for certain medical conditions as well as evidence of care for those suffering from conditions that likely made them dependent on another person. As such, one young woman presented with a healed osteomyelitis lesion in the knee joint. As osteomyelitis rarely heals without proper care and cleaning of the wounds (Lucia *et al*. 2014), this suggests that this young woman was provided with the necessary care to allow the infection to heal.

Three individuals presented congenital hip dysplasia, which likely caused some major locomotive obstacles for them during life. However, one of them reached a mature age, suggesting that this person was cared for into old age.

An unsuccessful arm amputation, an unsuccessful and possibly a successful trephination are evidence for attempts at surgical procedures and medical interventions in case of likely more serious illness. Furthermore, the largely well aligned and well healed fractures, which also did not show any evidence of healed or active infections, suggest that the level of medical care the people buried in the Knuedler cemetery had access to was quite high. The most notable case is that of individual 2013-015/353 who presented a fully healed gunshot wound to the head. The wound of this 35–44-year-old male did not show major signs of infection and showed advanced stages of healing, with the bullet still stuck in the orbit but already partially grown into the orbital roof. The bullet had passed through the brain, which might have caused some brain damage and might have rendered the individual dependent on others.

Additionally, people in the Knuedler cemetery had their average age at death in the adult-mature I age category, which corresponds to the average recorded for medieval and postmedieval cities. However, it is mainly the women from the older Layer 2 and the males from the younger Layer 1 that push the average age at death down. The young age at death of females from Layer 2 might be related to complications during childbirth, whilst the older age at death in the younger layer is possibly indicative of improved care during childbirth or might indicate a shift in burial practices, possibly towards a prevalence of women that were less at risk of dying in childbirth, such as nuns. The adult peak age at death among men from the cemetery in Layer 1 might be attributed tentatively to the sieges and assaults on Luxembourg

City by the French in 1683/84 AD. But except for these two occurrences, the individuals reached a high age at death in the mature II age category and compared to other urban sites, there were quite a lot of seniles buried in the Knuedler friary as well.
All in all, the evidence suggests that the individuals buried in the Knuedler cemetery were generally of good health and had efficient access to medical care.

8.3 Diet and Nutrition

The epidemics that Luxembourg City was subjected to on multiple occasions, but also the few sieges and the turmoils of the wars, mainly the Dutch revolt, the Thirty Years' War and the subsequent conflicts opposing the French and the Habsburg Netherlands, led to temporary food shortages within Luxembourg City and occasionally to episodes of famine (Trausch 1993; Weis 2004; Pauly 2020).
Taking into account this historical context, it is noteworthy that the frequency of non-specific indicators of stress, such as cribra orbitalia, cribra cranii, linear enamel hypoplasia and periostitis are quite low, especially compared to other contemporaneous rural and urban sites. As an increased presence of those indicators is often associated to poor nutritional status or exposure to pathogens, it can be assumed that the individuals buried at the Knuedler friary did not experience much nutritional stress or stress related to illness, neither in child- nor adulthood. This is supported by the low number of children showing distinct signs of scurvy or rickets, two diseases caused by nutritional deficiencies. This suggests that the individuals buried in the Knuedler friary did not suffer from prolonged famines. The few individuals with signs of metabolic disease might reflect those few that did not survive the temporary hardships of the epidemics and sieges. A 1.5-2-year-old child showed very elevated $\delta^{15}N$ values, which is likely the result of breastfeeding, but compared to the mean $\delta^{15}N$ of women in the sample, could also be indicative of starvation. A further indicator of nutritional status in childhood is growth, as nutritional stress or infectious diseases etc. can also stunt or delay growth. Since the individuals from Luxembourg City fell right into the average height of men and women from other medieval and postmedieval towns, it can be assumed that normal growth took place. The growth curves from the subadults also show a normal growth pattern and do not indicate episodes of stunting or delayed growth.
Regarding weaning times, most children were weaned between the ages of 1.5 to 3 years, with first introduction of solid foods starting around 1.5 years of age and cessation of lactation starting around 2.5-3 years of age. The majority of enamel hypoplasia lines on teeth, which are

non-specific indicators of childhood stress, also fall within this range, suggesting that most of them formed as a result of weaning stress. With only about 49% of adults presenting enamel hypoplasia lines, it can be concluded that just under half of the individuals suffered from severe childhood stress such as nutrient deficiencies from inadequate weaning diets or infectious diseases. These values fell right into the middle of the spectrum observed for other European medieval and postmedieval sites and resembled most those from upper social class individuals from Givenich, Luxembourg (Rehbach *et al*. 2009) and Oosterweel, Belgium (Van Cant 2019). Systematic differences in the occurrence of indicators of nutritional stress could be observed between the burial locations, which likely confirms that those buried in the cloister were of higher social standing than those buried in the cemetery. Those buried in the cloister exhibited significantly more enamel hypoplasia, cribra orbitalia and cribra cranii than those from the cemetery.

Furthermore, the nutritional status seems to have worsened from Layer 2 to Layer 1, with all indicators of stress increasing in frequency over time, which might be related to the growing urbanisation of the town at that time.

The results of the stable isotope analysis suggest a primarily terrestrial diet that was possibly supplemented occasionally by marine or freshwater resources, but without a local baseline a more detailed statement is not possible. The cooccurrence of high calculus and caries rates together with good nutritional status and low indicators of stress could be indicative of a balanced diet including a fair amount of protein and carbohydrates and maybe also access to cariogenic foods such as honey, fruits and later sugar, all in combination though with bad oral hygiene, which was not uncommon for the time. The low attrition scores suggest a lack of abrasive substances in the diet, but also mean that teeth are not being self-cleaned as efficiently anymore, which is linked to an increase in caries, but also means that processed foods were probably rather the norm.

The lack of difference in $\delta^{13}C$ and $\delta^{15}N$ values between the two layers suggests that there was no major dietary change between the late medieval and postmedieval period in Luxembourg City, even though the significant decrease in attrition scores over time suggests that the texture of the diet had softened. Nevertheless, the non-significant decrease of caries and calculus over time suggests a slight improvement in oral hygiene.

The significantly higher $\delta^{13}C$ and $\delta^{15}N$ values among cloister burials compared to cemetery burials probably reflect the different social status of these two groups, which was therefore not only defined by their burial position but also characterised by a different diet, in which more

affluent citizens and the friars had better access to animal protein, and possibly also to marine or freshwater fish. These differences in dietary patterns are furthermore also reflected in the dental status, where individuals from the cloister showed significantly less caries lesions and calculus as well as lower attrition scores than those from the cemetery. Whilst among the cloister burials, individuals with caries were also less common than in the cemetery, the number of individuals with calculus was very similar between the two groups, suggesting that there was no major difference in dental hygiene practices between the two social groups.

8.4 Living Conditions

To conclude, the low to moderate exposure to physical activities as well as the good health and nutritional status of the people buried in the Knuedler cemetery suggests that they experienced rather good living conditions, especially compared to other contemporaneous European and Luxembourgish sites. This does not necessarily allow us to conclude that life in Luxembourg City was particularly agreeable, as historical documentation on overcrowding, food shortages and epidemics suggests otherwise. But it rather suggests that the people buried in the Knuedler friary belonged to a group of citizens that were not subjected to all the hardships that life in a city entails, which is also supported by the richly decorated grave goods recovered from cemetery and cloister burials alike (Bis-Worch 2011). Generally, burials in monasteries were more sought after and often also more expensive than regular parish burials and therefore often reserved only to those individuals that could afford them (Ulrich-Bochsler 1997).

The biogeochemical and anthropological data further suggests that living conditions did not change considerably over time in the city.

However, the differences in health and nutritional status observed between cemetery and cloister burials indicate that the latter were of higher social standing than the former. This theory is further strengthened by historical sources that claim that church burials in parish churches and monasteries alike were reserved for the clergy and for affluent benefactors and their families (Ulrich-Bochsler 1997).

Overall, the living conditions reconstructed for the individuals buried in the Knuedler friary are not representative of those of the whole city of Luxembourg in late medieval and postmedieval times but rather reflect those of a more privileged part of Luxembourg City's society.

9 Abstract

Since its first mention in 963AD, the city and especially the fortress of Luxembourg had been growing steadily throughout the medieval times under the rule of the counts of Luxembourg. However, it is only in 1443AD, after the conquest by Philip the Good, duke of Burgundy, that the city of Luxembourg, which by then had become one of the strongest fortresses in western Europe, was finally caught between the fronts of the major political forces of the time. From then on until the demolition of the fortress in the mid-19th century, life in Luxembourg City had been dominated by foreign occupations as well as several sieges and wars.

In order to assess the impact these times of political unrest had on the population of the city, 391 individuals buried inside the cloister and on the cemetery grounds of a Franciscan friary which was in use from ~1255AD until 1778AD, were analysed. The cemetery, located beneath a town square nowadays called "Knuedler", was excavated in 3 campaigns between 2008 and 2018. ^{14}C analyses and evaluation of archaeological data allowed to identify two main burial phases: an older one dating from the mid-14th to the mid-17th century and a younger one dating from the mid-17th century to the cemetery's dissolution in 1778AD. The aim of this study is to investigate whether there are detectable changes in physical activity, health, and diet, and thus in living conditions over time and amongst different socioeconomic groups, represented by the cloister and cemetery burials. These questions were addressed by examining palaeodemographic parameters, stature and growth, markers of physical activity, diseases and indicators of diet and nutritional status and by comparing the results to contemporaneous rural, urban and monastic sites.

The excess of males in the Knuedler sample, especially among cloister burials, suggests that at least the latter did not represent a biologically grown population. Likely, the resident friars were also buried within the monastic precinct. The high life expectancy, low child mortality and mean age at death can also be taken as indicators of good health and nutritional status, as they suggest that the majority of individuals survived well into adulthood. The stature of the individuals under study reached that of average medieval and postmedieval urban centres and no stunting or delayed growth could be detected during childhood. Furthermore, the low incidence of infectious and metabolic diseases and non-specific stress markers indicate that the individuals buried in the Knuedler friary generally did not experience significant nutritional deficiencies. Altogether, this suggests that, despite the historically documented overcrowding of the city and regular food shortages caused by sieges, wars and epidemics, the inhabitants of

Luxembourg City buried in the Knuedler friary were mostly exempt of those hardships. Furthermore, no relevant changes in these health indicators over time could be noted, but discrepancies between the burial locations suggest that those buried within the cloister area were less exposed to infectious diseases and nutritional stress than those buried in the cemetery. Healed infectious diseases, well-aligned fractures and traumatic lesions as well as successful and unsuccessful surgical procedures can be seen as evidence for efficient medical care. The few sharp force and gunshot traumata are evidence of the impact of the wars and sieges on the population of Luxembourg City.

The relatively high proportion of carious lesions and dental calculus could be indicative of a carbohydrate-rich diet with a high protein content, whereas the relatively low dental abrasion suggests that the diet was primarily composed of softer foods with few abrasive components. The results of the stable isotope analyses suggest a diet based primarily on terrestrial C^3 plants and animals that fed on them. Differences between the burial locations suggest that individuals from the cloister had less abrasive and cariogenic substances in their diet and consumed either more meat or supplemented their diet periodically with marine or freshwater resources. No noteworthy shift in dietary patterns could be detected between the burial phases regarding the stable isotope results but a decrease in attrition intensity suggests that the texture of the diet softened over time, likely due to improved food production methods. The generally high frequency of dental pathologies such as caries, calculus and periodontopathies are indicative of a general lack of oral hygiene, a pattern observed also in the majority of the archaeological comparative populations. The study of enamel hypoplasia formation ages, first onset of caries and attrition as well as the combination of two stable isotope methods made it possible to narrow down the weaning age period to 1.5-3 years.

As mechanical loading can leave traces on bones, the examination of bilateral asymmetry, bone robusticity, entheseal changes and degenerative joint disease can inform about the intensity of physical activity a population is subjected to. These markers of physical activity showed only light to moderate degrees of expression and their intensity was correlated with age and sex and not with burial location or phases. This suggests that in both socioeconomic groups and in the late medieval and postmedieval times alike, these individuals were engaged in occupations that were not very strenuous. This is in line with findings of other contemporaneous urban sites and shows that their lifestyle was not as physically demanding as that of rural societies.

Altogether, the results of this study paint the picture of individuals that had rather good living conditions despite the historically documented hardships, therefore likely representing a more

privileged part of Luxembourg City's society. Thus, this interdisciplinary study offers the first detailed insights into the living conditions inside one Europe's strongest fortresses and can serve as a solid basis for further anthropological investigations.

10 Zusammenfassung

Seit ihrer ersten Erwähnung im Jahr 963 n. Chr. dehnten sich die Stadt und insbesondere die Festung Luxemburg im Mittelalter unter der Herrschaft der Grafen von Luxemburg stetig aus. Doch erst 1443 n. Chr., nach der Eroberung durch Philipp den Guten, Herzog von Burgund, geriet die Stadt Luxemburg, die inzwischen zu einer der stärksten Festungen Westeuropas herangewachsen war, endgültig zwischen die Fronten der großen politischen Kräfte der damaligen Zeit. Von da an bis zur Zerstörung der Festung in der Mitte des 19. Jahrhunderts war das Leben in Luxemburg-Stadt von Fremdbesatzungen sowie von mehreren Belagerungen und Kriegen geprägt.

Um die Auswirkungen dieser Zeiten politischer Unruhen auf die Bevölkerung der Stadt zu beurteilen, wurden 391 Individuen untersucht, die im Kreuzgang und auf dem Friedhof eines Franziskanerklosters bestattet wurden, das von ~1255 n. Chr. bis 1795 n. Chr. genutzt wurde. Der Friedhof, welcher sich unter dem heutigen Stadtplatz namens "Knuedler" befindet, wurde in 3 Kampagnen zwischen 2008 und 2018 teilweise ausgegraben. ^{14}C-Analysen und die Auswertung archäologischer Daten ermöglichten die Identifizierung zweier Hauptbestattungsphasen: eine ältere, die von der Mitte des 14. bis zur Mitte des 17. Jahrhunderts datiert, und eine jüngere, die von der Mitte des 17. Jahrhunderts bis zur Auflösung des Friedhofs im Jahr 1778 n. Chr. reicht. Ziel der vorliegenden Studie ist es, zu untersuchen, ob es im Laufe der Zeit und zwischen den zwei Gruppen unterschiedlichen sozialen Status, die jeweils durch die Bestattungen im Klosterinneren und auf dem Friedhof repräsentiert werden, nachweisbare Veränderungen in Bezug auf körperliche Aktivität, Gesundheit und Ernährung, und somit in den Lebensbedingungen gibt. Um diese Fragen zu beantworten, wurden paläodemographische Parameter, Statur und Wachstum, Indikatoren für körperliche Aktivität, Krankheiten und Indikatoren für die Ernährung und den Ernährungszustand untersucht und die Ergebnisse mit denen zeitgenössischer ländlicher, städtischer und klösterlicher Stätten verglichen.

Der Überschuss an Männern in der Knuedler Stichprobe, insbesondere bei den Klostergräbern, deutet darauf hin, dass zumindest letztere keine biologisch gewachsene Bevölkerung darstellten, da die ansässigen Mönche wahrscheinlich auch innerhalb des Klosterbezirks

bestattet wurden. Die hohe Lebenserwartung, die niedrige Kindersterblichkeit und das mittlere Sterbealter können ebenfalls als Indikatoren für einen guten Gesundheits- und Ernährungszustand gewertet werden, da sie darauf hindeuten, dass die Mehrheit der Bevölkerung bis ins Erwachsenenalter überlebte. Die Körpergröße der untersuchten Individuen entsprach dem Durchschnitt mittelalterlicher und früh neuzeitlicher Städte, und es traten keine nachweisbaren Wachstumsverzögerungen während der Kindheit auf. Das geringe Auftreten von Infektions- und Stoffwechselerkrankungen sowie von unspezifischen Stressmarkern deutet außerdem darauf hin, dass die im Knuedler-Kloster bestatteten Personen im Allgemeinen keine signifikanten Ernährungsmängel aufwiesen. Insgesamt deutet dies darauf hin, dass die im Knuedler-Kloster bestatteten Einwohner von Luxemburg-Stadt trotz der historisch belegten Übervölkerung der Stadt und der regelmäßigen Nahrungsmittelknappheit durch Belagerungen, Kriege und Epidemien, weitgehend von diesen Entbehrungen verschont blieben. Darüber hinaus konnten keine relevanten Veränderungen dieser Gesundheitsindikatoren im Laufe der Zeit festgestellt werden, aber die Unterschiede zwischen den Bestattungsorten deuten darauf hin, dass die im Klosterbereich Bestatteten weniger ansteckenden Krankheiten und Ernährungsstress ausgesetzt waren als die auf dem Friedhof Bestatteten. Ausgeheilte Infektionskrankheiten, gut verheilte Frakturen und traumatische Verletzungen sowie erfolgreiche und erfolglose chirurgische Eingriffe können als Beleg für eine effiziente medizinische Versorgung gewertet werden. Die wenigen Verletzungen durch scharfe Gewalteinwirkung und Schussverletzungen zeugen von den Auswirkungen der Kriege und Belagerungen auf die Bevölkerung von Luxemburg-Stadt.

Der relativ hohe Anteil an kariösen Läsionen und Zahnstein könnte auf eine kohlenhydratreiche Ernährung mit hohem Proteingehalt hindeuten, während der relativ geringe Zahnabrieb darauf schließen lässt, dass die Ernährung hauptsächlich aus weicherer Nahrung mit wenigen abrasiven Bestandteilen bestand. Die Ergebnisse der Analyse der Stabilen Isotope deuten auf eine Ernährung hin, die vor allem auf terrestrischen C^3-Pflanzen und Tieren, die sich davon ernährten, basierte. Die Unterschiede zwischen den Bestattungsorten deuten darauf hin, dass die Individuen aus dem Kloster weniger abrasive und kariogene Substanzen in ihrer Ernährung hatten und entweder mehr Fleisch verzehrten oder ihre Ernährung periodisch mit Meeres- oder Süßwasserressourcen ergänzten. Anhand der Ergebnisse der stabilen Isotope konnte keine nennenswerte Verschiebung der Ernährungsmuster zwischen den Bestattungsphasen festgestellt werden, aber eine Abnahme der Zahnabnutzungsintensität deutet darauf hin, dass die Beschaffenheit der Nahrung im Laufe der Zeit weicher wurde, was wahrscheinlich auf

verbesserte Methoden der Nahrungsmittelproduktion zurückzuführen ist. Das allgemein hohe Auftreten von Zahnerkrankungen wie Karies, Zahnstein und Parodontopathien deutet auf einen allgemeinen Mangel an Mundhygiene hin, ein Muster, das auch bei der Mehrzahl der archäologischen Vergleichspopulationen zu beobachten ist. Die Untersuchung des Entstehungsalters der Schmelzhypoplasien, des ersten Auftretens von Karies und Zahnabrasion sowie die Kombination von zwei Methoden basierend auf der Analyse Stabiler Isotope, ermöglichten es, das Abstillalter auf 1,5 bis 3 Jahre einzugrenzen.

Da mechanische Belastungen Spuren am Knochen hinterlassen können, kann die Untersuchung der bilateralen Asymmetrie, der Robustizität des Knochens, der degenerativen Veränderung der Muskelansatzstellen (Enthesien) und der degenerativen Gelenkerkrankungen Aufschluss über die Intensität der körperlichen Arbeit geben. Diese Indikatoren für körperliche Aktivität waren nur leicht bis mäßig ausgeprägt, und ihre Intensität korrelierte mit Alter und Geschlecht, nicht aber mit dem Bestattungsort oder den Bestattungsphasen. Dies deutet darauf hin, dass diese Personen in beiden Gruppen von unterschiedlichem sozialen Status, und sowohl im Spätmittelalter als auch in der frühen Neuzeit keine allzu anstrengenden Tätigkeit ausübten. Dies steht im Einklang mit den Ergebnissen anderer zeitgenössischer städtischer Fundstellen und zeigt, dass der Lebensstil der Stadtbewohner nicht so körperlich anstrengend war wie jener ländlicher Populationen.

Insgesamt zeichnen die Ergebnisse dieser Studie das Bild von Individuen, die trotz der historisch belegten Entbehrungen recht gute Lebensbedingungen hatten und daher wahrscheinlich einen privilegierteren Teil der Gesellschaft von Luxemburg-Stadt repräsentieren. Damit bietet diese interdisziplinäre Studie erstmals detaillierte Einblicke in die Lebensbedingungen innerhalb einer der stärksten Festungen Europas und kann als solide Grundlage für weitere anthropologische Untersuchungen dienen.

11 Bibliography

Abbate LM, Stevens J, Schwartz TA, Renner JB, Helmick CG & Jordan JM 2006 Anthropometric measures, body composition, body fat distribution, and knee osteoarthritis in women. *Obesity* **14** 1274–1281. (doi:10.1038/oby.2006.145)

Abdel Fatah EE, Shirley NR, Mahfouz MR & Auerbach BM 2012 A three-dimensional analysis of bilateral directional asymmetry in the human clavicle. *American Journal of Physical Anthropology* **149** 547–559. (doi:10.1002/ajpa.22156)

Abla O, Egeler RM & Weitzman S 2010 Langerhans cell histiocytosis: Current concepts and treatments. *Cancer Treatment Reviews* **36** 354–359. (doi:10.1016/j.ctrv.2010.02.012)

Acsádi G & Nemeskéri J 1970 *History of Human Life Span and Mortality.*

Adamić A & Šlaus M 2017 Comparative analysis of dental health in two archaeological populations from Croatia: The late medieval Dugopolje and early modern Vlach population from Koprivno. *Bulletin of the International Association for Paleodontology* **11** 11–22.

Adamson MW 2004 *Food in Medieval Times*. Westport Connecticut: Greenwood Press.

Adler C-P 2005 *Knochenkrankheiten*. Springer.

Adoga A, Nimkur T & Silas O 2010 Chronic suppurative otitis media: Socio-economic implication in a tertiary hospital in Northern Nigeria. *PanAfrican Medical Journal*.

Agnew KD & Davis RJ 1993 Congenital Unilateral Dislocation of the Radial Head. *Journal of Pediatric Orthopaedics* **13** 526–528.

Åkesson ML, Wärnberg Gerdin E, Söderström U, Lindahl B & Johansson I 2016 Health-related quality of life and prospective caries development. *BMC Oral Health* **16** 1–9. (doi:10.1186/s12903-016-0166-3)

al-Oumaoui I, Jiménez-Brobeil S & du Souich P 2004 Markers of activity patterns in some populations of the Iberian Peninsula. *International Journal of Osteoarchaeology* **14** 343–359. (doi:10.1002/oa.719)

AlQahtani SJ, Hector MP & Liversidge HM 2010 Brief communication: The London atlas of human tooth development and eruption. *American Journal of Physical Anthropology* **142** 481–490. (doi:10.1002/ajpa.21258)

AlQahtani SJ, Hector MP & Liversidge HM 2014 Accuracy of dental age estimation charts: Schour and Massler, Ubelaker and the London Atlas. *American Journal of Physical Anthropology* **154** 70–78. (doi:10.1002/ajpa.22473)

Alt KW, Türp JC & Wächter R 1998 Periapical Lesions - Clinical and Anthropological Aspects. In *Dental Anthropology Fundamentals, Limits Ad Prospects*. Ed KW Alt. Wien: Springer Verlag.

Alt KW, Nicklisch N, Held P, Meyer C, Rossbach A & Burwinkel M 2008 Zähne als Gesundheits- und Mortalitätsrisiko. In *Traumatologische Und Pathologische Veränderungen an Prähistorischen Und Historischen Skelttresten – Diagnose, Ursachen Und Kontext*, pp 25–42. Eds J Piek & T Terberger. Rahden/westfalen: Verlag Marie Leidorf.

Alter G 2004 Stature in Transition: A Micro-Level Study from Nineteenth-Century Belgium. *Social Science History* **28** 231–247. (doi:10.1215/01455532-28-2-231)

Alter G, Neven M & Michel O 2004 Height, wealth and longevity in xixth century east belgium. *Annales de Demographie Historique* **108** 19–27. (doi:10.3917/adh.108.0019)

Ambrose SH 1990 Preparation and characterization of bone and tooth collagen for isotopic

analysis. *Journal of Archaeological Science* **17** 431–451. (doi:10.1016/0305-4403(90)90007-R)
Ambrose SH & Norr L 1993 Experimental Evidence for the Relationship of the Carbon Isotope Ratios of Whole Diet and Dietary Protein to Those of Bone Collagen and Carbonate. In *Prehistoric Human Bone*, pp 1–37. Eds JB Lambert & G Grupe. Berlin, Heidelberg: Springer.
Amin A, Fisher M & Mazur L 2018 Congenital posterior dislocation of the radial head. In *Consultant for Pediatricians*.
Anderson JY & Trinkaus E 1998 Patterns of sexual, bilateral and interpopulational variation in human femoral neck-shaft angles. *Journal of Anatomy* **192** 279–285. (doi:10.1046/j.1469-7580.1998.19220279.x)
Anderson DL, Thompson GW & Popovich F 1976 Age attainment of mineralization stages of the dentition. *Journal of Forensic Sciences* **21** 191–200.
Angel JL, Kelley JO, Parrington M & Pinter S 1987 Life stresses of the free Black community as represented by the First African Baptist Church, Philadelphia, 1823–1841. *American Journal of Physical Anthropology* **74** 213–229. (doi:10.1002/ajpa.1330740209)
Arcini C, Ahlström T & Tagesson G 2014 Variations in Diet and Stature: Are They Linked? Bioarchaeology and Paleodietary Bayesian Mixing Models from Linköping, Sweden. *International Journal of Osteoarchaeology* **24** 543–556. (doi:10.1002/oa.2247)
Arcini C, Plura CB & Nordin P 2020 A Garrison Cemetery. *International Journal of Historical Archaeology* **24** 203–217. (doi:10.1007/s10761-019-00513-y)
Arden N & Nevitt MC 2006 Osteoarthritis: Epidemiology. *Best Practice and Research: Clinical Rheumatology* **20** 3–25. (doi:10.1016/j.berh.2005.09.007)
De Armas YC, Roksandic M, Nikitović D, Suárez RR, Smith D, Kanik N, Jordá DG & Buhay WM 2017 Isotopic reconstruction of the weaning process in the archaeological population of Canímar Abajo, Cuba: A Bayesian probability mixing model approach. *PLoS ONE* **12** 1–23. (doi:10.1371/journal.pone.0175959)
Armelagos GJ, Brown PJ & Turner B 2005 Evolutionary, historical and political economic perspectives on health and disease. *Social Science and Medicine* **61** 755–765. (doi:10.1016/j.socscimed.2004.08.066)
Armelagos GJ, Goodman AH, Harper KN & Blakey ML 2009 Enamel hypoplasia and early mortality: Bioarcheological support for the Barker hypothesis. *Evolutionary Anthropology* **18** 261–271. (doi:10.1002/evan.20239)
Asma MA, El Fadil EB & El Tinay AH 2006 Development of weaning food from sorghum supplemented with legumes and oil seeds. *Food and Nutrition Bulletin* **27** 26–34. (doi:10.1177/156482650602700104)
Assis S & Codinha S 2010 Metastatic carcinoma in a 14th-19th century skeleton from Constância (Portugal). *International Journal of Osteoarchaeology* **20** 603–620. (doi:10.1002/oa.1084)
Ather Enam S, Abdulrauf S, Mehta B, Malik GM & Mahmood A 1996 Metastasis in meningioma. *Acta Neurochirurgica* **138** 1172–1178. (doi:10.1007/BF01809747)
Audouze F, Drucker DG & Valentin F 2009 Nouvelles données chronologiques, biologiques et alimentaires sur l'enfant mésolithique de Verberie - Le Buisson Campin (Oise). *Bulletins et Mémoires de La Société d'Anthropologie de Paris* **21** 5–18.
Auerbach BM & Raxter MH 2008 Patterns of clavicular bilateral asymmetry in relation to the humerus: variation among humans. *Journal of Human Evolution* **54** 663–674. (doi:10.1016/j.jhevol.2007.10.002)
Auerbach BM & Ruff CB 2004 Human body mass estimation: A comparison of 'morphometric' and 'mechanical' methods. *American Journal of Physical Anthropology*

125 331–342. (doi:10.1002/ajpa.20032)
Auerbach BM & Ruff CB 2006 Limb bone bilateral asymmetry: Variability and commonality among modern humans. *Journal of Human Evolution* **50** 203–218. (doi:10.1016/j.jhevol.2005.09.004)
Aufderheide C & Rodriguez-Martin C 1998 *The Cambridge Encyclopedia of Human Paleopathology*. Cambridge University Press.
Augenti A & Gilchrist R 2011 Life , death and memory. In *The Archaeology of Medieval Europe Vol 2, 12th to 16th Centuries*, pp 494–515. Eds M Carver & J Klapste. Aarhus University Press.
Bach H 1965 Zur Berechnung der Körperhöhe aus den langen Gliedmaßenknochen weiblicher Skelette. *Anthropologischer Anzeiger* **29** 12–21.
Baetsen S 2001 *Graven in de Grote Kerk*. Alkmaar: Rapporten over de Alkmaarse Monumentenzorg en Archeologie.
Balikci HH, Mustafa Gurdal M, Celebi S, Ozbay I & Karakas M 2016 Relationships among concha bullosa, nasal septal deviation, and sinusitis: Retrospective analysis of 296 cases. *Ear, Nose and Throat Journal* **95** 487–491. (doi:10.1177/014556131609501209)
Barrett JH, Orton D, Johnstone C, Harland J, Van Neer W, Ervynck A, Roberts C, Locker A, Amundsen C, Enghoff IB *et al.* 2011 Interpreting the expansion of sea fishing in medieval Europe using stable isotope analysis of archaeological cod bones. *Journal of Archaeological Science* **38** 1516–1524. (doi:10.1016/j.jas.2011.02.017)
Bartelink EJ, Willits NA & Chelotti KL 2014 A probable case of acromegaly from the Windmiller culture of prehistoric Central California. *International Journal of Paleopathology* **4** 37–46. (doi:10.1016/j.ijpp.2013.11.003)
Battles HT 2009 Long bone bilateral asymmetry in the nineteenth-century Stirrup Court Cemetery collection from London, Ontario. *Nexus: The Canadian Student Journal of Anthropology* **21** 1–15.
Beaumont J & Montgomery J 2016 The Great Irish Famine : Identifying Starvation in the Tissues of Victims Using Stable Isotope Analysis of Bone and Incremental Dentine Collagen. 1–21. (doi:10.1371/journal.pone.0160065)
Beaumont J, Gledhill A, Lee-Thorp J & Montgomery J 2013a Childhood diet: A closer examination of the evidence from dental tissues using stable isotope analysis of incremental human dentine*. *Archaeometry* **55** 277–295. (doi:10.1111/j.1475-4754.2012.00682.x)
Beaumont J, Geber J, Powers N, Wilson A, Lee-thorp J & Montgomery J 2013b Victims and Survivors : Stable Isotopes Used to Identify Migrants From the Great Irish Famine to 19th Century London. **98** 87–98. (doi:10.1002/ajpa.22179)
Beaumont J, Montgomery J, Buckberry J & Jay M 2015 Infant mortality and isotopic complexity: New approaches to stress, maternal health, and weaning. *American Journal of Physical Anthropology* **157** 441–457. (doi:10.1002/ajpa.22736)
Beck-Baldauff S 1986 Von den Krämern zu den Freimaurern. Das bewegte Schicksal des Logenhauses. *Ons Staadt* 12–13.
Beck H & Beck F 2000 Les Cordeliers et leur église. *Ons Staadt* 6–11.
Benedictow OJ 2003 Demographic Conditions. In *The Cambridge History of Scandinavia*, pp 237–249. Ed K Helle. Cambridge: Cambridge University Press.
Benton AL 1968 Differential behavioral effects in frontal lobe disease. *Neuropsychologia* **6** 53–60. (doi:10.1016/0028-3932(68)90038-9)
Berg D & Lehmann L 2009 https://franziskaner.net/bullierte-regel/#:~:text=Im%20Namen%20des%20Herrn%20!,ohne%20Eigentum%20und%20in%20Keuschheit. In *FRANZISKUS-QUELLEN*, p 1797.
Berszin C 2009 Kloster, Dorf und Vorstadt Petershausen. Anthropologische Untersuchungen.

In *Kloster, Dorf Und Vorstadt Petershausen. Archäologische, Historische Und Anthropologische Untersuchungen. Forschungen Und Berichte Der Archäologie Des Mittelalters in Baden-Württemberg 30*, pp 119–190. Ed R Röber.

Bertilsson C, Borg E, Sten S, Hessman E, Sjöblom H & Lingström P 2022 Prevalence of Dental Caries in Past European Populations: A Systematic Review. *Caries Research* **56** 15–28. (doi:10.1159/000522326)

Bertram JEA & Swartz SM 1991 The 'Law of Bone Transformation': A Case of Crying Wolff ? *Biological Psychiatry* **66** 245–273.

Betsinger TK & DeWitte SN 2021 Toward a bioarchaeology of urbanization: Demography, health, and behavior in cities in the past. *American Journal of Physical Anthropology* **175** 79–118. (doi:10.1002/ajpa.24249)

Betsinger TK, DeWitte SN, Justus HM & Agnew AM 2020 Frailty, Survivorship, and Stress in Medieval Poland: A Comparison of Urban and Rural Populations. In *The Bioarchaeology of Urbanization. Bioarchaeology and Social Theory*, pp 223–243. Eds TK Betsinger & SN DeWitte. Springer, Cham.

Betsinger TK, DeWitte SN & Tracy Betsinger CK 2021 Toward a bioarchaeology of urbanization: Demography, health, and behavior in cities in the past. (doi:10.1002/ajpa.24249)

Biehler-Gomez L, Giordano G & Cattaneo C 2019 The overlooked primary: bladder cancer metastases on dry bone. A study of the 20th century CAL Milano Cemetery Skeletal Collection. *International Journal of Paleopathology* **24** 130–140. (doi:10.1016/j.ijpp.2018.10.005)

Binder M, Roberts C, Spencer N, Antoine D & Cartwright C 2014 On the antiquity of cancer: Evidence for metastatic carcinoma in a young man from ancient Nubia (c. 1200bc). *PLoS ONE* **9** 1–11. (doi:10.1371/journal.pone.0090924)

Bird RJ & Hurren BJ 2016 Anatomical and clinical aspects of Klinefelter's syndrome. *Clinical Anatomy* **29** 606–619. (doi:10.1002/ca.22695)

Bis-Worch C 2011 Zur Franziskanerkirche auf dem Knuedler. In *Unter Unseren Füssen - Archäologie in Luxemburg 1995-2010/Sous Nos Pieds - Archéologie Au Luxembourg 1995-2010*, pp 185–188. Luxembourg: Musée National d'Histoire et d'Art - Centre National de Recherche Archéologique Luxembourg.

Blackburn A & Knüsel CJ 2006 Hand Dominance and Bilateral Asymmetry of the Epicondylar Breadth of the Humerus: A Test in a Living Sample. *Current Anthropology* **47** 377–382. (doi:10.1086/503067)

Blakey ML, Leslie TE & Reidy JP 1994 Frequency and chronological distribution of dental enamel hypoplasia in enslaved African Americans: A test of the weaning hypothesis. *American Journal of Physical Anthropology* **95** 371–383. (doi:10.1002/ajpa.1330950402)

Bleasdale M, Ponce P, Radini A, Wilson AS, Doherty S, Daley P, Brown C, Spindler L, Sibun L, Speller C *et al.* 2019 Multidisciplinary investigations of the diets of two post-medieval populations from London using stable isotopes and microdebris analysis. *Archaeological and Anthropological Sciences* **11** 6161–6181. (doi:10.1007/s12520-019-00910-8)

Bocherens H & Drucker D 2003 Trophic level isotopic enrichment of carbon and nitrogen in bone collagen: Case studies from recent and ancient terrestrial ecosystems. *International Journal of Osteoarchaeology* **13** 46–53. (doi:10.1002/oa.662)

Bocherens H, Billiou D, Patou-Mathis M, Bonjean D, Otte M & Mariotti A 1997 Paleobiological Implications of the isotopic Signatures C3C, 15N) of Fossil Mammal Collagen in Scladina Cave (Sclayn, Belgium). *Quaternary Research* **48** 370–380.

Bocherens H, Drucker D, Billiou D & Moussa I 2005 A new approach for assessing the

preservation state of bone and collagen for isotopic analysis (radiocarbon dating, carbon and nitrogen stable isotopes). *Anthropologie* **109** 557–567. (doi:10.1016/j.anthro.2005.06.005)
Bocquet J-P & Masset C 1977 Estimateurs en paléodémographie. *L'homme* **17** 65–90.
Boenisch G & Bräuer G 1986 Mittelalterliche und frühneuzeitliche menschliche Skelettfunde am Dom zu Lübeck, 1: Sterblichkeitsverhältnisse und Krankheitsbelastung. *Lübecker Schriften Zur Archäologie Und Kulturgeschichte* **12** 67–111.
Bogaard A, Heaton THE, Poulton P & Merbach I 2007 The impact of manuring on nitrogen isotope ratios in cereals: archaeological implications for reconstruction of diet and crop management practices. *Journal of Archaeological Science* **34** 335–343. (doi:10.1016/j.jas.2006.04.009)
Bogin B 1999a Evolutionary Perspective on Human Growth. *Annual Review of Anthropology* **28** 109–153.
Bogin B 1999b *Patterns of Human Growth*. Cambridge: Cambridge University Press.
Bogin B 2001 *The Growth of Humanity*. New York, Chichester, Weinheim, Brisbane, Singapore, Toronto: John Wiley & Sons Ltd.
Boldsen JL 2007 Early Childhood Stress and Adult Age Mortality—A Study of Dental Enamel Hypoplasia in the Medieval Danish Village of Tirup. *American Journal of Physical Anthropology* **132** 59–66. (doi:10.1002/ajpa)
Bonar SF 2009 Bone Tumors of Miscellaneous Type or Uncertain Lineage. In *Bone and Soft Tissue Pathology: A Volume in the Foundations in Diagnostic Pathology Series, Expert Consult - Online and Print*, pp 419–445. Eds AL Folpe & CY Inwards. Elsevier. (doi:10.1016/B978-0-443-06688-7.00024-9)
Bonjour JP, Ammann P, Chevalley T & Rizzoli R 2001 Protein intake and bone growth. *Canadian Journal of Applied Physiology* **26**. (doi:10.1139/h2001-050)
Bonnick SL 2006 Osteoporosis in men and women. *Clinical Cornerstone* **8** 28–39. (doi:10.1016/S1098-3597(06)80063-3)
Boocock P, Roberts CA & Manchester K 1995 Maxillary Sinusitis in Medieval Chichester, England. *Americal Journal of Physical Anthropology* **98** 483–495.
Boulle EL 2001a Osteological features associated with ankle hyperdorsiflexion. *International Journal of Osteoarchaeology* **11** 345–349. (doi:10.1002/oa.572)
Boulle EL 2001b Evolution of two human skeletal markers of the squatting position: A diachronic study from antiquity to the modern age. *American Journal of Physical Anthropology* **115** 50–56. (doi:10.1002/ajpa.1055)
Bowers LM, Cohen DM, Bhattacharyya I, Pettigrew JC & Stavropoulos MF 2013 The Non-ossifying Fibroma: A Case Report and Review of the Literature. *Head and Neck Pathology* **7** 203–210. (doi:10.1007/s12105-012-0399-7)
Boyd DC & Boyd CC 1989 A Comparison of Tennessee Archaic and Mississippian Maximum Femoral Lengths and Midshaft Diameters : Subsistence Change and Postcranial Variability. *Southeastern Archaeology* **8** 107–116.
Branca F & Ferrari M 2002 Impact of micronutrient deficiencies on growth: The stunting syndrome. *Annals of Nutrition and Metabolism* **46** 8–17. (doi:10.1159/000066397)
Brand A, Trier JP, Unseld M, Drache D, Conrad A, Rief M, Koszik A, Steinkrauss M, Thomas M, Wuttke M *et al.* 2017 *Rettungssanitäter, Rettungshelfer*. Thieme Pädagogik.
Bräuer G 1988 Osteometrie. In *Anthropologie. Handbuch Der Vergleichenden Biologie Des Menschen. Bd. 1: Wesen Und Methoden Der Anthropologie. 1. Teil: Wissenschaftstheorie, Geschichte, Morphologische Methoden*, pp 160–231. Ed R Knussmann. Stuttgart: Fischer Verlag.
Breitinger E 1938 Zur Berechnung der Körperhöhe aus den langen Gliedmaßenknochen. *Anthropologischer Anzeiger* **14** 149–174.

Brickley MB 2006 Rib fractures in the archaeological record: A useful source of sociocultural information? *International Journal of Osteoarchaeology* **16** 61–75. (doi:10.1002/oa.809)
Brickley MB 2018 Cribra orbitalia and porotic hyperostosis: A biological approach to diagnosis. *American Journal of Physical Anthropology* **167** 896–902. (doi:10.1002/ajpa.23701)
Brickley M & Ives R 2006 Skeletal manifestations of infantile scurvy. *American Journal of Physical Anthropology* **129** 163–172. (doi:10.1002/ajpa.20265)
Brickley M & Ives R 2008 *The Bioarchaeology of Metabolic Bone Disease*. Academic Press.
Brickley MB & Mays S 2019 Metabolic disease. In *Ortner's Identification of Pathological Conditions in Human Skeletal Remains*, 3rd ed, pp 531–566. Ed JE Buikstra. Academic Press Elsevier Inc. (doi:10.1016/B978-0-12-809738-0.00015-6)
Brickley M, Mays S & Ives R 2010 Evaluation and interpretation of residual rickets deformities in adults. *International Journal of Osteoarchaeology* **20** 54–66. (doi:10.1002/oa.1007)
Bridges PS, Blitz JH & Solano MC 2000 Changes in long bone diaphyseal strength with horticultural intensification in west-central Illinois. *American Journal of Physical Anthropology* **112** 217–238. (doi:10.1002/(SICI)1096-8644(2000)112:2<217::AID-AJPA8>3.0.CO;2-E)
Britton K, Müldner G & Bell M 2008 Stable isotope evidence for salt-marsh grazing in the Bronze Age Severn Estuary, UK: implications for palaeodietary analysis at coastal sites. *Journal of Archaeological Science* **35** 2111–2118. (doi:10.1016/j.jas.2008.01.012)
Britton K, Fuller BT, Tütken T, Mays S & Richards MP 2015 Oxygen isotope analysis of human bone phosphate evidences weaning age in archaeological populations. *American Journal of Physical Anthropology* **157** 226–241. (doi:10.1002/ajpa.22704)
Britton K, McManus-Fry E, Cameron A, Duffy P, Masson-MacLean E, Czére O, Smith N, Stones J, Winfield A & Müldner G 2018 Isotopes and new norms: Investigating the emergence of early modern U.K. breastfeeding practices at St. Nicholas Kirk, Aberdeen. *International Journal of Osteoarchaeology* **28** 510–522. (doi:10.1002/oa.2678)
Brix M, Bessaguet S, Loury J, Iodice A & Lebeau J 2009 Le sinus pericranii : une anomalie veineuse transcrânienne. *Revue de Stomatologie et de Chirurgie Maxillo-Faciale* **110** 98–100. (doi:10.1016/j.stomax.2008.11.001)
Bron JL, Van Royen BJ & Wuisman PIJM 2007 The clinical significance of lumbosacral transitional anomalies. *Acta Orthopaedica Belgica* **73** 687–695.
Brooks S & Suchey J 1990 Skeletal age determination based on the os pubis. *Human Evolution* **5** 227–238.
Brothwell DR 1981 *Digging up Bones*. London & Oxford: British Museum & Oxford University Press.
Browder T, Folkman J & Pirie-Shepherd S 2000 The hemostatic system as a regulator of angiogenesis. *Journal of Biological Chemistry* **275** 1521–1524. (doi:10.1074/jbc.275.3.1521)
Brůžek J, Santos F, Dutailly B, Murail P & Cunha E 2017 Validation and reliability of the sex estimation of the human os coxae using freely available DSP2 software for bioarchaeology and forensic anthropology. *American Journal of Physical Anthropology* **164** 440–449. (doi:10.1002/ajpa.23282)
Buckberry J 2000 Missing, presumed buried? Bone diagenesis and the under-representation of Anglo-Saxon children. *Assemblage: University of Sheffield Graduate Student Journal of Archaeology*.
Buckley JD, Robison LL, Swotinsky R, Garabrant DH, LeBeau M, Manchester P, Nesbit ME, Odom L, Peters JM, Woods WG *et al.* 1989 Occupational Exposures of Parents of

Children with Acute Nonlymphocytic Leukemia: A Report from the Childrens Cancer Study Group. *Cancer Research* **49** 4030–4037.
Buckley HR, Kinaston R, Halcrow SE, Foster A, Spriggs M & Bedford S 2014 Scurvy in a tropical paradise? Evaluating the possibility of infant and adult vitamin C deficiency in the Lapita skeletal sample of Teouma, Vanuatu, Pacific islands. *International Journal of Paleopathology* **5** 72–85. (doi:10.1016/j.ijpp.2014.03.001)
Buenzli PR, Lerebours C, Roschger A, Roschger P, Buenzli PR, Lerebours C, Roschger A & Roschger P 2018 Late stages of mineralization and their signature on the bone mineral density distribution distribution. *Connective Tissue Research* **58** 74–80. (doi:10.1080/03008207.2018.1424149)
Buikstra JE 1976 The Caribou Eskimo: General and specific disease. *American Journal of Physical Anthropology* **45** 351–367. (doi:10.1002/ajpa.1330450303)
Burkhardt A 2001 Der Friedhof von Kloster Barthe, Landkreis Leer, Ostfriesland. Anthropologische Untersuchungen der Skelettfunde. *Probleme Der Küstenforschung Im Südlichen Nordseegebiet* **27** 325–393.
Burt NM 2013 Stable isotope ratio analysis of breastfeeding and weaning practices of children from medieval Fishergate House York, UK. *American Journal of Physical Anthropology* **152** 407–416. (doi:10.1002/ajpa.22370)
Burton JL 2005 A bite into the history of the autopsy. *Forensic Science, Medicine, and Pathology* **1** 277–284. (doi:10.1385/Forensic)
Büttner J 2006 Osteologische und paläodemografische Untersuchungen der mittelalterlichen und frühneuzeitlichen Skelettfunde aus Templin. Freie Universität Berlin.
Buzi C, Micarelli I, Paine RR, Profico A, Messineo D, Tafuri MA & Manzi G 2020 Digital imaging techniques applied to a case of concha bullosa from an early medieval funerary area in central Italy. *International Journal of Paleopathology* **31** 71–78. (doi:10.1016/j.ijpp.2020.10.002)
Buzon MR 2012 The bioarchaeological approach to palaeopathology. In *A Companion to Palaeopathology*, pp 58–76. Ed AL Grauer. Chichester: Wiley-Blackwell.
Bynum CW 1987 *Holy Fast and Holy Feast: The Religious Significance of Food to Medieval Women*. Berkeley, Los Angeles: University of California Press.
Byron CD, Borke J, Yu J, Pashley D, Wingard CJ & Hamrick M 2004 Effects of increased muscle mass on mouse sagittal suture morphology and mechanics. *The Anatomical Record. Part A, Discoveries in Molecular, Cellular, and Evolutionary Biology* **279** 676–684. (doi:10.1002/ar.a.20055)
Cai M, Ma L, Xu G, Gruen P, Li J, Yang M, Pan L, Guan H, Chen G, Gong J *et al.* 2012 Clinical and radiological observation in a surgical series of 36 cases of fibrous dysplasia of the skull. *Clinical Neurology and Neurosurgery* **114** 254–259. (doi:10.1016/j.clineuro.2011.10.026)
Calce SE 2012 A new method to estimate adult age-at-death using the acetabulum. *American Journal of Physical Anthropology* **148** 11–23. (doi:10.1002/ajpa.22026)
Callewaert F, Sinnesael M, Gielen E, Boonen S & Vanderschueren D 2010 Skeletal sexual dimorphism: Relative contribution of sex steroids, GH-IGF1, and mechanical loading. *Journal of Endocrinology* **207** 127–134. (doi:10.1677/JOE-10-0209)
Campillo D 1991 The possibility of diagnosing meningiomas in palaeopathology. *International Journal of Osteoarchaeology* **1** 225–230. (doi:10.1002/oa.1390010315)
Van Cant M 2019 Dyed-In-The-Wool : The Impact of Occupational Behaviour and the Environment on Small Urban and Rural Communities in Flanders , C . 1200-1860 AD. The University of Sheffield.
Capasso L 1997 Osteoma : Palaeopathology and Phylogeny. **7** 615–620.
Capasso LL 2005 Antiquity of cancer. *International Journal of Cancer* **113** 2–13.

(doi:10.1002/ijc.20610)
Capasso L, Capelli A, Frati L & Pierfelice V 1992 Absence of foramen nutricium with a probably aneurysmatic cyst of the right ilium in a medieval subject from South-West Italy. *Journal of Palaeopathology* **4** 185–192.
Cardoso HF V. 2007 Environmental Effects on Skeletal Versus Dental Development: Using a Documented Subadult Skeletal Sample to Test a Basic Assumption in Human Osteological Research. *American Journal of Physical Anthropology* **132** 223–233. (doi:10.1002/ajpa)
Cardoso FA 2018 Lives not written in bones: Discussing biographical data from identified skeletal collections. In *Identified Skeletal Collections: The Testing Ground of Anthropology?*, pp 151–167. Eds C C.Henderson & FA Cardoso. Oxford: Archeopress.
Cardoso FA & Henderson CY 2010 Enthesopathy formation in the humerus: Data from known age-at-death and known occupation skeletal collections. *American Journal of Physical Anthropology* **141** 550–560. (doi:10.1002/ajpa.21171)
Cardoso HFV & Saunders SR 2008 Two arch criteria of the ilium for sex determination of immature skeletal remains: A test of their accuracy and an assessment of intra- and inter-observer error. *Forensic Science International* **178** 24–29. (doi:10.1016/j.forsciint.2008.01.012)
Carter DR, Van Der Meulen MCH & Beaupré GS 1996 Mechanical Factors in Bone Growth and Development. *Bone* **18** 55–105.
Case DT, Burnett SE & Nielsen T 2006 Os acromiale: Population differences and their etiological significance. *HOMO- Journal of Comparative Human Biology* **57** 1–18. (doi:10.1016/j.jchb.2005.11.001)
Caselitz P 1980 Bemerkungen zur Demographie der spätmittelalterlichen und neuzeitlichen Stadt Stade, dargestellt anhand der Skelettfunde aus dem Bereich des St. Johannis-Klosters. *Stader Jahrbuch* 7–47.
Caselitz P 1981 Überlegungen zur Sexualrelation hoch- und spätmittelalterlicher Populationen am Beispiel der Bevölkerungsstichprobe aus dem Zisterzienserkloster zu Hude. *Archäologische Mitteilungen Aus Nordwestdeutschland* **4** 75–90.
Caselitz P 1982 Die menschlichen Skelettreste aus dem Paradies des Lübecker Doms. *Lübecker Schriften Zur Archäologie Und Kulturgeschichte* **6** 287–301.
Caselitz P 1983 Die menschlichen Skelettreste aus dem Dominikanerkloster zu Schleswig. In *Ausgrabungen in Schleswig. Berichte Und Studien 1*, pp 112–216. Ed V Caselitz, P.; Unverhau, D.; Vogel. Neumünster: Karl Wachholtz Verlag.
Caselitz P 1998 Caries - Ancient Plague of Humankind. In *Dental Anthropology*, pp 203–226. Eds KW Alt, FW Rösing & M Teschler-Nicola. Wien, New York: Springer.
Caselitz P & Heine HW 1979 Archäologische und anthropologische Ergebnisder Probegrabung auf dem Marktplatz zu Lingen (Ems), Kr. Emsland, 1978. *Nachrichten Aus Niedersachsens Urgeschichte* **Bd. 48** 81–112.
Casey MM & Post DM 2011 The problem of isotopic baseline: Reconstructing the diet and trophic position of fossil animals. *Earth-Science Reviews* **106** 131–148. (doi:10.1016/j.earscirev.2011.02.001)
Casna M & Schrader S 2022 Urban Beings. *Bioarchaeology International*. (doi:10.5744/bi.2022.0001)
Cave C & Oxenham MF 2007 Out of the cradle and into the grave: The children of Anglo-Saxon great Chesterford, Essex, England. In *Children, Death and Burial: Archaeological Discourses*, pp 179–196. Eds EM Murphy & M Le Roy. Oxbow Books.
Chapurlat RD & Meunier PJ 2000 Fibrous dysplasia of bone. *Bailliere's Best Practice and Research in Clinical Rheumatology* **14** 385–398. (doi:10.1053/berh.1999.0071)
Chazel JC, Valcarcel J, Tramini P, Pelissier B & Mafart B 2005 Coronal and apical lesions,

environmental factors: Study in a modern and an archeological population. *Clinical Oral Investigations* **9** 197–202. (doi:10.1007/s00784-005-0318-3)
Cheung E, Mutahar R, Assefa F, Ververs MT, Nasiri SM, Borrel A & Salama P 2003 An epidemic of scurvy in Afghanistan: Assessment and response. *Food and Nutrition Bulletin* **24** 247–255. (doi:10.1177/156482650302400303)
Chiba F, Makino Y, Motomura A, Inokuchi G, Torimitsu S, Ishii N, Sakuma A, Nagasawa S, Saitoh H, Yajima D *et al.* 2013 Age estimation by multidetector CT images of the sagittal suture. *International Journal of Legal Medicine* **127** 1005–1011. (doi:10.1007/s00414-013-0883-y)
Chinique Y, Id DA, Mavridou A, Domı JG, Hanson K & Id JL 2022 Tracking breastfeeding and weaning practices in ancient populations by combining carbon , nitrogen and oxygen stable isotopes from multiple non-adult tissues. 1–28. (doi:10.1371/journal.pone.0262435)
Chinique De Armas Y & Pestle W 2018 Assessing the association between subsistence strategies and the timing of weaning among indigenous archaeological populations of the Caribbean. *International Journal of Osteoarchaeology* **28** 492–509. (doi:10.1002/oa.2695)
Chisholm BS 1989 Variation in diet reconstruction based on stable carbon isotopic evidence. In *The Chemistry of Prehistoric Human Bone*, pp 10–37.
Chisholm BS, Nelson DE & Schwarcz HP 1982 Stable-carbon isotope ratios as a measure of marine versus terrestrial protein in ancient diets. *Science* **216** 1131–1132. (doi:10.1126/science.216.4550.1131)
Clarke S 1977 Mortality Trends in Prehistoric Populations. *Human Biology* **49** 181–186.
Clarke SK 1980 Early childhood morbidity trends in prehistoric populations. *Human Biology* **52** 79–85.
Clarke NG, Carey SE, Srikandi W, Hirsch RS & Leppard PI 1986 Periodontal disease in ancient populations. *American Journal of Physical Anthropology* **71** 173–183. (doi:10.1002/ajpa.1330710205)
Clavel B 2002 Les restes osseux médiévaux de 11 rue de la Boucherie. In *Aux Origines de La Ville de Luxembourg*, Musée nati, pp 267–276. Ed J Zimmer. Luxembourg: saint-paul.
Clayton P & Rowbotham J 2009 How the Mid-Victorians worked, Ate and Died. *International Journal of Environmental Research and Public Health* **6** 1235–1253. (doi:10.3390/ijerph6031235)
Cockburn A, Duncan H & Riddle JM 1979 Arthritis, ancient and modern: guidelines for field workers. *Henry Ford Hospital Medical Journal* **27** 74–79.
Cole TM 1994 Size and shape of the femur and tibia in northern Plains Indians. In *Skeletal Biology in the Great Plains: Migration, Warfare, Health, and Subsistence*, pp 219–233. Eds DW Owsley & RL Jantz. Washington D.C.: Smithonian Institution Press.
Cole G & Waldron T 2019 Cribra orbitalia: Dissecting an ill-defined phenomenon. *International Journal of Osteoarchaeology* **29** 613–621.
Coleman RE 2001 Metastatic bone disease: Clinical features, pathophysiology and treatment strategies. *Cancer Treatment Reviews* **27** 165–176. (doi:10.1053/ctrv.2000.0210)
Coleman RE, Roodman, Smith, Body, Suva & Vessella 2006 Clinical features of metastatic bone disease and risk of skeletal morbidity. *Clinical Cancer Research* **12** 6243–6250. (doi:10.1158/1078-0432.CCR-06-0931)
Cook DC 1981 Mortality, age structure and status in the interpretation of stress indicators in prehistoric skeletons: a dental example from the Lower Illinois Valley. In *The Archaeology of Death*. Eds R Chapman, I Kinnes & K Ransborg. Cambridge.
Cook DC & Buikstra JE 1979 Health and differential survival in prehistoric populations: Prenatal dental defects. *American Journal of Physical Anthropology* **51** 649–664.

(doi:10.1002/ajpa.1330510415)
Cooper C 1995 Occupational activity and the risk of osteoarthritis. *The Journal of Rheumatology* **43** 10–12.
Cooper C, Inskip H, Croft P, Campbell L, Smith G, McLaren M & Coggon D 1998 Individual risk factors for hip osteoarthritis: Obesity, hip injury, and physical activity. *American Journal of Epidemiology* **147** 516–522. (doi:10.1093/oxfordjournals.aje.a009482)
Corbett EM & Moore WJ 1976 Distribution of Dental Caries in Ancient British Populations. *Caries Research* **10** 401–414.
Corcino JJ, Waxman S & Herbert V 1970 Absorption and Malabsorption of Vitamin B12. *The American Journal of Medicine* **48** 562–569.
Corruccini RS, Handler JS & Jacobi KP 1985 Chronological Distribution of Enamel Hypoplasias and Weaning in a Caribbean Slave Population. *Human Biology* **57** 699–711.
Crabbe WA 1966 Intra-osseous ganglia of bone. *British Journal of Surgery* **53** 15–17. (doi:10.1002/bjs.1800530151)
Crandall JJ 2014 Scurvy in the Greater American Southwest: Modeling micronutrition and biosocial processes in contexts of resource stress. *International Journal of Paleopathology* **5** 46–54. (doi:10.1016/j.ijpp.2014.05.001)
Crosby WH 1977 Lead-Contaminated Health Food: Association With Lead Poisoning and Leukemia. *JAMA: The Journal of the American Medical Association* **237** 2627–2629. (doi:10.1001/jama.1977.03270510049022)
Crozier R, Cameron A, Mann B, Ashcroft E & Wood R 2021 Osteoarchaeological evidence for medical dissection in 18th to 19th century Aberdeen, Scotland. *Post-Medieval Archaeology* **55** 159–175. (doi:10.1080/00794236.2021.1972584)
Cucina A & Işcan MY 1997 Assessment of Enamel Hypoplasia in a High Status Burial Site. *American Journal of Human Biology* **9** 213–222. (doi:10.1002/(sici)1520-6300(1997)9:2<213::aid-ajhb7>3.0.co;2-0)
Cui L, Li X, Tian Y, Bao J, Wang L, Xu D, Zhao B & Li W 2017 Breastfeeding and early childhood caries: A meta-analysis of observational studies. *Asia Pacific Journal of Clinical Nutrition* **26** 867–880. (doi:10.6133/apjcn.082016.09)
Čuk T, Leben-Seljak P & Stefancic M 2001 Lateral asymmetry of human long bones. *Variability and Evolution* **9** 19–32.
Curto A, Mahoney P, Maurer AF, Barrocas-Dias C, Fernandes T & Fahy GE 2020 Effect of different healing stages on stable isotope ratios in skeletal lesions. *American Journal of Physical Anthropology* **171** 285–297. (doi:10.1002/ajpa.23958)
Czermak AM 2011 Soziale Stratifizierung im frühen Mittelalter - Aussage- und Nachweismöglichkeiten anhand von biologischen Indikatoren. Ludwigs-Maximilians-Universität München.
d' Hollosy M & de Meulemeester J 1999 Le cimetière de Saint-Jean et l'étude des squelettes. In *Le Passé Recomposé, Archéologie Urbaine à Luxem- Bourg. Catalogue d'exposition Du Musée National d'Histoire et d'Art Luxembourg*, pp 149–153. Ed J-L Mousset. Luxembourg: Musée National d'Histoire et d'Art Luxembourg.
Dar G, Masharawi Y, Peleg S, Steinberg N, May H, Medlej B, Peled N & Hershkovitz I 2010 Schmorl's nodes distribution in the human spine and its possible etiology. *European Spine Journal* **19** 670–675. (doi:10.1007/s00586-009-1238-8)
Dash HR, Rawat N & Das S 2020 Alternatives to amelogenin markers for sex determination in humans and their forensic relevance. *Molecular Biology Reports* **47** 2347–2360. (doi:10.1007/s11033-020-05268-y)
Davey Smith G, Hart C, Upton M, Hole D, Gillis C, Watt G & Hawthorne V 2000 Height

and risk of death among men and women: Aetiological implications of associations with cardiorespiratory disease and cancer mortality. *Journal of Epidemiology and Community Health* **54** 97–103. (doi:10.1136/jech.54.2.97)
David AR & Zimmerman MR 2010 Cancer: An old disease, a new disease or something in between? *Nature Reviews Cancer* **10** 728–733. (doi:10.1038/nrc2914)
Davies AM, Douis H & James SLJ 2015 Tumor-Like Lesions of Bone. In *Musculoskeletal Imaging*, 2nd ed, pp 959–969. Eds T Pope, HL Bloem, J Beltran, WB Morrison & DJ Wilson. Elsevier Health Sciences.
Dawson H & Robson Brown K 2012 Childhood tuberculosis: A probable case from late mediaeval Somerset, England. *International Journal of Paleopathology* **2** 31–35. (doi:10.1016/j.ijpp.2012.04.001)
Deines P 1980 The Isotopic Composition of Reduced Organic Carbon. In *Handbook of Environmental Isotope Geochemistry*, pp 329–406. Eds P Fritz & JC Fontes. Amsterdam: Elsevier.
Demirjian A 1986 Dentition. In *Human Growth 2*, 2. Aufl., pp 268–298. Eds F Falkner & JM Tanner. London: Plenum Press.
Demmelmair H, von Rosen J & Koletzko B 2006 Long-term consequences of early nutrition. *Early Human Development* **82** 567–574. (doi:10.1016/j.earlhumdev.2006.07.004)
Deniro MJ & Epstein S 1981 Influence of diet on the distribution of nitrogen isotopes in animals. *Geochimica et Cosmochimica Acta* **45** 341–351. (doi:10.1016/0016-7037(81)90244-1)
DeNiro MJ 1985 Postmortem preservation and alteration of in vivo bone collagen isotope ratios in relation to palaeodietary reconstruction. *Nature* **317** 806–809.
DeNiro MJ & Epstein S 1978 Influence of diet on the distribution of carbon isotopes in animals. *Geochimica et Cosmochimica Acta* **42** 495–506. (doi:10.1002/mop.25285)
Dennison, E. P., DesBrisay, G., & Diack HL 2002 Health in the two towns. In *Aberdeen before 1800: A New History*, pp 70–96. Eds EP Dennison, D Ditchburn & M Lynch. East Linton: Tuckwell Press.
Derums VJ 1987 Paleopathology of Bronze Age Population in Latvia. *Anthropologie (1962-)* **25** 57–61.
Dettwyler KA 2004 When to wean: Biological versus cultural perspectives. *Clinical Obstetrics and Gynecology* **47** 712–723. (doi:10.1097/01.grf.0000137217.97573.01)
DeWitte SN & Betsinger TK 2020 Introduction to the bioarchaeology of urbanization. In *The Bioarchaeology of Urbanization: The Biological, Demographic, and Social Consequences of Living in Cities*, pp 1–21. Eds SN DeWitte & TK Betsinger. Springer.
Dhaliwal K, Rando C, Reade H, Jourdan AL & Stevens RE 2020 Socioeconomic differences in diet: An isotopic examination of post-Medieval Chichester, West Sussex. *American Journal of Physical Anthropology* **171** 584–597. (doi:10.1002/ajpa.23984)
Dias G & Tayles N 1997 'Abscess cavity'—a Misnomer. *International Journal of Osteoarchaeology* **7** 548–554.
Dias GJ, Prasad K & Santos AL 2007 Pathogenesis of apical periodontal cysts: Guidelines for diagnosis in palaeopathology. *International Journal of Osteoarchaeology* **17** 619–626. (doi:10.1002/oa.902)
DiCaprio MR & Enneking WF 2005 Fibrous dysplasia: Pathophysiology, evaluation, and treatment. *Journal of Bone and Joint Surgery* **87** 1848–1864. (doi:10.2106/JBJS.D.02942)
Dimitrov M, Grafman J & Hollnagel C 1996 The effects of frontal lobe damage on everyday problem solving. *Cortex* **32** 357–366. (doi:10.1016/S0010-9452(96)80057-8)
Dittmann K & Grupe G 2000 Biochemical and palaeopathological investigations on weaning and infant mortality in the early Middle Ages. *Anthropologischer Anzeiger* **58** 345–355.

Dittmar JM, Mitchell PD, Cessford C, Inskip SA & Robb JE 2021 Medieval injuries: Skeletal trauma as an indicator of past living conditions and hazard risk in Cambridge, England. *American Journal of Physical Anthropology* **175** 626–645. (doi:10.1002/ajpa.24225)
Djurić M, Djukić K, Milovanović P, Janović A & Milenković P 2011 Representing children in excavated cemeteries: The intrinsic preserva- tion factors. *Antiquity,* **85** 250–262.
Doi H, Akamatsu F & González AL 2017 Starvation effects on nitrogen and carbon stable isotopes of animals: An insight from meta-analysis of fasting experiments. *Royal Society Open Science* **4**. (doi:10.1098/rsos.170633)
Dollhopf K-D 2002 Die verschwundenen Kinder: Bemerkungen zum Kinderdefizit bei Bestattungen auf frühmittelalterlichen Gräberfeldern. *Archäologisches Korrespondenzblatt* **32** 151–159.
Drenhaus U 1977 Paläodemographie, ihre Aufgaben, Grundlagen und Methoden. *Z. Bevölkerungswiss.* **3** 3–40.
Drtikolová Kaupová S, Cvrček J, Grossová I, Hadrava J, Půtová L & Velemínský P 2021 The impact of pathological conditions on carbon and nitrogen isotopic values in the bone collagen of individuals with known biographic data and medical history. *International Journal of Osteoarchaeology* **31** 1105–1124. (doi:10.1002/oa.3022)
Dufour E, Bocherens H & Mariotti A 1999 Palaeodietary implications of isotopic variability in Eurasian lacustrine fish. *Journal of Archaeological Science* **26** 617–627. (doi:10.1006/jasc.1998.0379)
Duncan AE, Colman RJ & Kramer PA 2012 Sex differences in spinal osteoarthritis in humans and rhesus monkeys (macaca mulatta). *Spine* **37** 915–922. (doi:10.1097/BRS.0b013e31823ab7fc)
Dupras TL & Tocheri MW 2007 Reconstructing Infant Weaning Histories at Roman Period Kellis, Egypt Using Stable Isotope Analysis of Dentition. *Americal Journal of Physical Anthropology* **134** 63–74. (doi:10.1002/ajpa)
Duray SM 1990 Deciduous enamel defects and caries susceptibility in a prehistoric ohio population. *American Journal of Physical Anthropology* **81** 27–34. (doi:10.1002/ajpa.1330810105)
Duray SM 1996 Dental indicators of stress and reduced age at death in prehistoric native Americans. *American Journal of Physical Anthropology* **99** 275–286. (doi:10.1002/(SICI)1096-8644(199602)99:2<275::AID-AJPA5>3.0.CO;2-Y)
Düring A 2014 Der Friedhof von Bärenthal auf der Scherra. Lebensverhältnisse und Bestattungsbrauch einer Dorfbevölkerung des 7. bis 10. Jahrhunderts. *Fundberichte Aus Baden-Württemberg* **34** 391–490.
Dyer C 1983 English diet in the later middle ages. In *Social Relations and Ideas*, pp 210–216. Eds TH Aston, PR Coss, C Dyer & J Thirsk. Cambridge: Cambridge University Press.
Dyer C 2006 Gardens and Garden Produce in the Later Middle Ages. In *Food in Medieval England: Diet and Nutrition*, pp 27–40. Eds CM Woolgar, D Serjeantson & T Waldron. Oxford: Oxford University Press,.
Effros B 1997 Beyond cemetery walls : early medieval funerary topography and Christian salvation. *Early Medieval Europe* **6** 1–23.
Eggleston G 2019 History of Sugar and Sweeteners. *ACS Symposium Series* **1314** 63–74. (doi:10.1021/bk-2019-1314.ch005)
Eibl F 2004 Zur Kenntnis altbayerischer älter- bis spätmittelalterlicher Bestattungen in und um Kirchen. *Archäologische Arbeitsgemeinschaft Ostbayern/West-Südböhmen* **14** 223–245.
El-Zaatari S 2010 Occlusal microwear texture analysis and the diets of historical/prehistoric hunter-gatherers. *International Journal of Osteoarchaeology* **20** 67–87. (doi:10.1002/oa.1027)

El-Najjar MY, Desanti M V. & Ozebek L 1978 Prevalence and possible etiology of dental enamel hypoplasia. *American Journal of Physical Anthropology* **48** 185–192. (doi:10.1002/ajpa.1330480210)
Elsberg CA & Schwartz CW 1924 INCREASED CRANIAL VASCULARITY IN ITS RELATION TO INTRACRANIAL DISEASE with special reference to enlargement of the veins of the diploe and its relation to the endotheliomas. *Archives of Neurology and Psychiatry* **11** 292–307.
Ennen E 1993 Die Frau in der mittelalterlichen Stadt. In *Mensch Und Umwelt Im Mittelalter*, 3rd ed, pp 35–52. Ed B Hermann. Stuttgart: Fischer verlag.
Ervynck A 2004 Orant, pugnant, laborant. The diet of the three orders in the feudal society of medieval north-western Europe. In *Behaviour Behind Bones: The Zooarchaeology of Ritual, Religion, Status and Identity*, pp 215–223. Eds A Ervynck, W Van Neer & S Jones O'Day. Oxbow Books.
Eshed V, Latimer B, Greenwald CM, Jellema LM, Rothschild BM, Wish-baratz S & Hershkovitz I 2002 Button Osteoma : Its Etiology and Pathophysiology. **230** 217–230. (doi:10.1002/ajpa.10087)
Van Esterik P 2002 Contemporary Trends in Infant Feeding Research. *Annual Review of Anthropology* **31** 257–278. (doi:10.1146/annurev.anthro.31.040402.085428)
Faccia KJ & Williams RC 2008 Schmorl's nodes: Clinical significance and implications for the bioarchaeological record. *International Journal of Osteoarchaeology* **18** 28–44. (doi:10.1002/oa.924)
Falchetti A, Masi L & Brandi ML 2010 Paget's disease of bone: There's more than the affected skeletal-a clinical review and suggestions for the clinical practice. *Current Opinion in Rheumatology* **22** 410–423. (doi:10.1097/BOR.0b013e32833af61e)
Ferembach, D.; Schwidetzky, I.; Stloukal M 1979 Empfehlungen für die Alters- und Geschlechtsdiagnose am Skelett. *Homo* **30** 1–32.
Fernandes R, Millard AR, Brabec M, Nadeau MJ & Grootes P 2014 Food reconstruction using isotopic transferred signals (FRUITS): A bayesian model for diet reconstruction. *PLoS ONE* **9** 1–9. (doi:10.1371/journal.pone.0087436)
Fewtrell MS, Morgan JB, Duggan C, Gunnlaugsson G, Hibberd PL, Lucas A & Kleinman RE 2007 Optimal duration of exclusive breastfeeding: What is the evidence to support current recommendations? *American Journal of Clinical Nutrition* **85** 635S-638S. (doi:85/2/635S [pii])
Field AP 2009 *Discovering Statistics Using SPSS: And Sex and Drugs and Rock 'n' Roll*. SAGE Publications Inc.
Fildes VA 1986 *Breasts, Bottles and Babies: A History of Infant Feeding*. Edinburgh: Edinburgh University Press.
Fildes V 1995 The culture and biology of breastfeeding: an historical review of Western Europe. In *Breastfeeding: Biocultural Perspecives.*, pp 101–126. Eds P Stuart-Macadam & KA Dettwyler. New York: Aldine de Gruyter.
Finnegan M 1978 Non-metric variation of the infracranial skeleton. *Journal of Anatomy* **125** 23–37.
Forestier J & Rotes-Querol J 1950 Senile ankylosing hyperostosis of the spine. *Annals of the Rheumatic Diseases* **9** 321–330. (doi:10.1136/ard.9.4.321)
Fornetti J, Welm AL & Stewart SA 2018 Understanding the Bone in Cancer Metastasis. *Journal of Bone and Mineral Research* **33** 2099–2113. (doi:10.1002/jbmr.3618)
Fournier P, Juárez P & Guise T 2014 Tumor-bone interactions: there is no place like bone. In *Bone Cancer: Primary Bone Cancers and Bone Metastases*, Second Edi, pp 13–28. Ed D Heymann. Waltham: Academic Press.
France RL 1995 Differentiation between littoral and pelagic food webs in lakes using stable

carbon isotopes. *Limnology and Oceanography* **40** 1310–1313. (doi:10.4319/lo.1995.40.7.1310)
Fraser RA, Bogaard A, Heaton T, Charles M, Jones G, Christensen BT, Halstead P, Merbach I, Poulton PR, Sparkes D *et al.* 2011 Manuring and stable nitrogen isotope ratios in cereals and pulses: Towards a new archaeobotanical approach to the inference of land use and dietary practices. *Journal of Archaeological Science* **38** 2790–2804. (doi:10.1016/j.jas.2011.06.024)
Freeman DW 2015 Management of Intracranial Pressure. *Neurocritical Care* **21** 1299.1323.
Freyschmidt J 2016 *Skeletterkrankungen. Klinisch-Radiologische Diagnostik Und Differenzialdiagnose.* Berlin: Springer.
Frost HM 1961 Human osteoblastic activity. *Henry Ford Hospital Medical Bulletin* **9** 87–99.
Frost HM 1969 Tetracycline-based histological analysis of bone remodeling. *Calcified Tissue Research* **3** 211–237. (doi:10.1007/BF02058664)
Frost HM 2000 The Utah paradigm of skeletal physiology : an overview of its insights for bone , cartilage and collagenous tissue organs. *Journal of Bone And Mineral Metabolism* **18** 305–316.
Fuller BT, Richards MP & Mays SA 2003 Stable carbon and nitrogen isotope variations in tooth dentine serial sections from Wharram Percy. *Journal of Archaeological Science* **30** 1673–1684. (doi:10.1016/S0305-4403(03)00073-6)
Fuller BT, Fuller JL, Sage NE, Harris DA, O'Connell TC & Hedges REM 2005 Nitrogen balance and δ15N: Why you're not what you eat during nutritional stress. *Rapid Communications in Mass Spectrometry* **19** 2497–2506. (doi:10.1002/rcm.2090)
Fuller BT, Molleson TI, Harris DA, Gilmour LT & Hedges REM 2006 Isotopic Evidence for Breastfeeding and Possible Adult Dietary Differences from Late/Sub-Roman Britain. *American Journal of Physical Anthropology* **129** 45–54. (doi:10.1002/ajpa.20244)
Fulminante F 2015 Infant Feeding Practices in Europe and the Mediterranean from Prehistory to the Middle Ages : A Comparison between the Historical Sources and Bioarchaeology. *Childhood in the Past* **8** 24–47. (doi:10.1179/1758571615Z.00000000026)
Galea S & Vlahov D 2005 Urban health: Evidence, challenges, and directions. *Annual Review of Public Health* **26** 341–365. (doi:10.1146/annurev.publhealth.26.021304.144708)
Galera V, Ubelaker DH & Hayek L a 1998 Comparison of macroscopic cranial methods of age estimation applied to skeletons from the Terry Collection. *Journal of Forensic Sciences* **43** 933–939. (doi:10.1520/JFS14337J)
Gamble JA 2020 A life history approach to stature and body proportions in medieval danes. *Anthropologischer Anzeiger* **77** 27–45. (doi:10.1127/anthranz/2019/0951)
Garcia RI, Henshaw MM & Krall EA 2001 Relationship between periodontal disease and systemic health. *Periodontology* **25** 21–36.
Garcin V, Velemínský P, Trefný P, Bagousse AA Le, Lefebvre A & Bruzek J 2010 Dental health and lifestyle in four early mediaeval juvenile populations: Comparisons between urban and rural individuals, and between coastal and inland settlements. *HOMO-Journal of Comparative Human Biology* **61** 421–439. (doi:10.1016/j.jchb.2010.06.004)
Gardner KS, Leventhal A, Cambra R, Bartelink EJ & Martinez A 2011 Mothers and Infants in the Prehistoric Santa Clara Valley: What Stable Isotopes Tell us about Ancestral Ohlone Weaning Practices. *SCA Proceedings* **25** 1–14.
Garn SM, Sullivan T V, Decker SA, Larkin FA & Hawthorne VM 1992 Continuing Bone Expansion and Increasing Bone Loss Over a Two-Decade Period in Men and Women From a Total Community Sample. *American Journal of Human Biology* **4** 57–67.
Gawlikowska-Sroka A, Szczurowski J, Kwiatkowska B, Konczewski P, Dzieciołowska-Baran E, Donotek M, Walecka A & Nowakowski D 2016 Concha bullosa in

paleoanthropological material. *Advances in Experimental Medicine and Biology* **952** 65–73. (doi:10.1007/5584_2016_62)
Geber VD 2006 Paläodontologische Untersuchungsergebnisse der Bestattungen im Kreuzgang der Stiftskirche St . Arnual , Saarbrücken. UNIVERSITÄT DES SAARLANDES.
Geber J 2014 Skeletal manifestations of stress in child victims of the Great Irish Famine (1845-1852): Prevalence of enamel hypoplasia, Harris lines, and growth retardation. *American Journal of Physical Anthropology* **155** 149–161. (doi:10.1002/ajpa.22567)
Geber J & Murphy E 2012 Scurvy in the great irish famine: Evidence of vitamin C deficiency from a mid-19th century skeletal population. *American Journal of Physical Anthropology* **148** 512–524. (doi:10.1002/ajpa.22066)
Gellrich N & Essig H 2011 Fehlbildungen des Gesichts. In *Praxis Der Plastischen Chirurgie*, pp 767–789. Berlin, Heidelberg: Springer.
Gilchrist R 2009 Rethinking later medieval masculinity: the male body in death. *Mortuary Practices and Social Identities in the Middle Ages: Essays in Honour of Heinrich Harke* 236–252.
Gilchrist R 2011 The Intimacy of Death: Interpreting Gender and the Life Course in Medieval and Early Modern Burials. In *Interpreting the Early Modern World.*, pp 159–176. Eds MC Beaudry & J Symonds. New York, Dordrecht, Heidelberg, London: Springer.
Giuffra V & Fornaciari G 2013 Breastfeeding and Weaning in Renaissance Italy: The Medici Children. *Breastfeeding Medicine* **8** 257–262. (doi:10.1089/bfm.2012.0060)
Giuffra V, Vitiello A, Caramella D, Fornaciari A, Giustini D & Fornaciari G 2015 Rickets in a High Social Class of Renaissance Italy: The Medici Children. *International Journal of Osteoarchaeology* **25** 608–624. (doi:10.1002/oa.2324)
Giuffra V, Minozzi S, Riccomi G, Naccarato AG, Castagna M, Lencioni R, Chericoni S, Mongelli V & Felici C 2019 Multiple osteomata from medieval Tuscany, Italy (ca. 10 th –12 th AD). *International Journal of Paleopathology* **25** 56–61. (doi:10.1016/j.ijpp.2019.04.003)
Gloux SA-F 2007 Latéralité manuelle et asymétrie directionnelle des membres inférieurs Test de l'hypothèse de la symétrie croisée des surfaces articulaires. University of Montréal.
Gocha TP, Ingvoldstad ME, Kolatorowicz A, Cosgriff-Hernandez MTJ & Sciulli PW 2015 Testing the applicability of six macroscopic skeletal aging techniques on a modern Southeast Asian sample. *Forensic Science International* **249** 318–318. (doi:10.1016/j.forsciint.2014.12.015)
Golghate T, Tambe S, Meshram M, Kasote A, Rahule AS & Thakre B 2014 Early Ossification of Thyroid Cartilage. *Journal of Contemporary Medicine and Dentistry* **2** 51–53. (doi:10.18049/jcmad/219a11)
Goodman AH & Armelagos GJ 1985 Factors affecting the distribution of enamel hypoplasias within the human permanent dentition. *American Journal of Physical Anthropology* **68** 479–493. (doi:10.1002/ajpa.1330680404)
Goodman AH & Armelagos GJ 1989 Infant and childhood morbidity and mortality risks in archaeological populations. *World Archaeology* **21** 225–243. (doi:10.1080/00438243.1989.9980103)
Goodman AH & Rose JC 1990 Assessment of systemic physiological perturbations from dental enamel hypoplasias and associated histological structures. *American Journal of Physical Anthropology* **33** 59–110. (doi:10.1002/ajpa.1330330506)
Goodman A & Rose JC 1991 Dental enamel hypoplasias as indicators of nutritional status. *Advances in Dental Anthropology* 279–293.
Goodman AH, Armelagos GJ & Rose JC 1980 Enamel Hypoplasias as Indicators of Stress in

Three Prehistoric Populations from Illinois A. *Human Biology* **52** 515–528.
Goodman AH, Pelto GH, Allen LH & Chavez A 1992 Socioeconomic and anthropometric correlates of linear enamel hypoplasia in children from Solis, Mexico. *Journal of Paleopathology* **Monograph** 373–380.
Goodman A H, Armelagos G J & Rose J C 1984 The Chronological Distribution Of Enamel Hypoplasias From Prehistoric Dickson Mounds Lewiston Illinois Usa Populations. *American Journal of Physical Anthropology* **65** 259–266.
Gosman JH, Stout SD & Larsen CS 2011 Skeletal biology over the life span: A view from the surfaces. *American Journal of Physical Anthropology* **146** 86–98. (doi:10.1002/ajpa.21612)
Goude G & Fontugne M 2016 Carbon and nitrogen isotopic variability in bone collagen during the Neolithic period: Influence of environmental factorsand diet. *Journal of Archaeological Science* **70** 117–131. (doi:10.1016/j.jas.2016.04.019)
Governale LS 2015 Craniosynostosis. *Pediatric Neurology* **53** 394–401. (doi:10.1016/j.pediatrneurol.2015.07.006)
Grauer AL 1993 Patterns of anemia and infection from medieval York, England. *American Journal of Physical Anthropology* **91** 203–213. (doi:10.1002/ajpa.1330910206)
Grauer AL 2019 *Circulatory, Reticuloendothelial, and Hematopoietic Disorders*. Elsevier Inc. (doi:10.1016/B978-0-12-809738-0.00014-4)
Grauer AL & Roberts CA 1996 Paleoepidemiology, healing, and possible treatment of trauma in the medieval cemetery population of St. Helen-on-the-Walls, York, England. *American Journal of Physical Anthropology* **100** 531–544. (doi:10.1002/(SICI)1096-8644(199608)100:4<531::AID-AJPA7>3.0.CO;2-T)
Grauer AL & Roberts CA 2019 *Fungal, Viral, Multicelled Parasitic, and Protozoan Infections*. Elsevier Inc. (doi:10.1016/B978-0-12-809738-0.00012-0)
Greenspan A 1993 Benign bone-forming lesions: osteoma, osteoid osteoma, and osteoblastoma - Clinical, imaging, pathologic, and differential considerations. *Skeletal Radiology* **22** 485–500. (doi:10.1007/BF00209095)
Grine FE, Jungers WL, Tobias P V. & Pearson OM 1995 Fossil Homo femur from Berg Aukas, northern Namibia. *American Journal of Physical Anthropology* **97** 151–185. (doi:10.1002/ajpa.1330970207)
De Groote K, De Maeyer W, Moens J, Quintelier K, Cleven F Van, Berghe I Vanden & Vernaeve W 2011 Het karmelietenklooster van Aalst (prov. Oost-Vl.) (1497-1797): het gebouwenbestand, de begravingen en het fysisch-antropologische onderzoek. *Relicta* **8** 83–250.
Groza V-M, Simalcsik A, Bejenaru L & Simalcsik R-D 2016 Spina Bifida Occulta in Medieval and Postmedieval Times in Eastern Romania. *Memoirs of the Scientific Sections of the Romanian Academy* **XXXIX** 103–115. (doi:10.2106/00004623-198264030-00030)
Grupe G 1986 Multielementanalyse: ein neuer Weg für die Paläodemographie. In *Materialien Zur Bevölkerungs- Wissenschaft, Sonderheft 7*. Ed B für Bevölkerungswissenschaft. Wiesbaden.
Grupe G & Harbeck M 2015 Taphonomic and Diagenetic Processes. In *Handbook of Paleoanthropology*, pp 417–439. Eds W Henke & I Tattersall. Berlin, Heidelberg: Springer.
Grupe G, Christiansen K, Schröder I & Wittwer-Backofen W 2005 *Anthropologie, Ein Einführendes Lehrbuch*. Berlin, Heidelberg: Springer Verlag.
Grupe G, Harbeck M & McGlynn GC 2015 *Prähistorische Anthropologie*. Springer Spektrum.
Gualdi-Russo E 1998 Study on Long Bones : Variation in angular traits with sex , age , and

laterality. *Anthropologischer Anzeiger* **56** 289–299.
Guangyi. L, Yin J, Gao J, Cheng TS, Pavlos NJ, Zhang C & Zheng MH 2013 Subchondral bone in osteoarthritis: Insight into risk factors and microstructural changes. *Arthritis Research and Therapy* **15**.
Guidozzi F, Maclennan M, Graham KM & Jooste CP 1992 Salivary calcium, magnesium, phosphate, chloride, sodium and potassium in pregnancy and labour. *South African Medical Journal* **81** 152–154.
Gumina S, Salvatore M, De Santis P, Orsina L & Postacchini F 2002 Coracoclavicular joint: Osteologic study of 1020 human clavicles. *Journal of Anatomy* **201** 513–519. (doi:10.1046/j.1469-7580.2002.00115.x)
Güntz E 1958 Die normale Haltung und ihre Abweichung. In *Handbuch Der Orthopädie. Band 2. Spezielle Orthopädie Rumpf (Wirbelsäule Und Becken)*, pp 27–34. Ed G et al. Hohmann. Stuttgart: Georg Thieme.
Gustafsson BE, Quensel CE, Lanke LS, Lundqvist C, Grahnen H, Bonow BE & Krasse B 1954 The Vipeholm dental caries study. The effect of different levels of carbohydrate intake on caries activity in 436 individuals observed for five years. *Acta Odontol. Scand.* **11** 232–364.
Haapasalo H, Sievanen H, Kannus P, Heinonen A, Oja P & Vuori I 1996 Dimensions and estimated mechanical characteristics of the humerus after long-term tennis loading. *Journal of Bone and Mineral Research* **11** 864–872. (doi:10.1002/jbmr.5650110619)
Haines MR & Kintner HJ 2008 ‘“ Can breast feeding help you in later life ? Evidence from German military heights in the early 20th century ”’. *Economics and Human Biology* **6** 420–430. (doi:10.1016/j.ehb.2008.06.004)
Haj-Mirzaian A, Mohajer B, Guermazi A, Roemer FW, Zikria B & Demehri S 2021 Kneeling as a risk factor of patellofemoral joint cartilage damage worsening: an exploratory analysis on the Osteoarthritis Initiative. *European Radiology* **31** 2601–2609. (doi:10.1007/s00330-020-07337-z)
Hakenbeck S, McManus E, Geisler H, Grupe G & O’Connell T 2010 Diet and mobility in early medieval bavaria: A study of carbon and nitrogen stable isotopes. *American Journal of Physical Anthropology* **143** 235–249. (doi:10.1002/ajpa.21309)
Hakim DN, Pelly T, Kulendran M & Caris JA 2015 Benign tumours of the bone: A review. *Journal of Bone Oncology* **4** 37–41. (doi:10.1016/j.jbo.2015.02.001)
Hammoud S, Weber K & McCarthy EF 2005 Unicameral bone cysts of the pelvis: a study of 16 cases. *The Iowa Orthopaedic Journal* **25** 69–74.
Hanson LÅ, Korotkova M, Lundin S, Håversen L, Silfverdal SA, Mattsby-Baltzer I, Strandvik B & Telemo E 2003 The transfer of immunity from mother to child. *Annals of the New York Academy of Sciences* **987** 199–206. (doi:10.1111/j.1749-6632.2003.tb06049.x)
Hausmair B 2017 Topographies of the afterlife: Reconsidering infant burials in medieval mortuary space. *Journal of Social Archaeology* **17** 210–236. (doi:10.1177/1469605317704347)
Hausmair B 2020 „Traufkinder“ im Mittelalter? Überlegungen zu Kleinkindbestattungen, Taufstatus und einem populären Deutungsansatz. In *Leben Mit Dem Tod Der Umgang Mit Sterblichkeit in Mittelalter Und Neuzeit Beiträge Zur Mittelalterarchäologie in Österreich 35*. Eds T Kühtreiber, R Risy, G Scharrer-Liska & C Theune. Wien.
Havelková P, Villotte S, Velemínský P, Poláček L & Dobisíková M 2011 Enthesopathies and activity patterns in the Early Medieval Great Moravian population: Evidence of division of labour. *International Journal of Osteoarchaeology* **21** 487–504. (doi:10.1002/oa.1164)
Havelková P, Hladík M & Velemínský P 2013 Entheseal Changes: Do They Reflect

Socioeconomic Status in the Early Medieval Central European Population? (Mikulčice - Klášteřisko, Great Moravian Empire, 9th - 10th century). *International Journal of Osteoarchaeology* **23** 237–251. (doi:10.1002/oa.2294)
Hawkey DE & Merbs CF 1995 Activity-induced musculoskeletal stress markers (MSM) and subsistence strategy changes among ancient Hudson Bay Eskimos. *International Journal of Osteoarchaeology* **5** 324–338. (doi:10.1002/oa.1390050403)
Haydock H, Clarke L, Craig-Atkins E, Howcroft R & Buckberry J 2013 Weaning at Anglo-Saxon raunds: Implications for changing breastfeeding practice in britain over two millennia. *American Journal of Physical Anthropology* **151** 604–612. (doi:10.1002/ajpa.22316)
Haytac MC, Ozcelik O & Mariotti A 2013 Periodontal disease in men. *Periodontology 2000* **61** 252–265.
Heaney RP, Davies KM, Ryan RA, Johnson ML & Gong G 1997 Bone Dimensional Change with Age : Interactions of Genetic, Hormonal, and Body Size Variables. *Osteoporosis International* **7** 426–431.
Heaton THE, Vogel JC, Chevallerie GVI & Collett G 1986 Climatic influence on the isotope composition of bone nitrogen. *Nature* **322** 822–823.
Hedges REM, Clement JG, Thomas DL & O'Connell TC 2007 Collagen Turnover in the Adult Femoral Mid-Shaft: Modeled From Anthropogenic Radiocarbon Tracer Measurements. *American Journal of Physical Anthropology* **133** 808–816. (doi:10.1002/ajpa)
Helmuth H 1966 The findings of human skeletons at the medieval Gertrudenfriedhof in Kiel. *Zeitschrift Fur Morphologie Und Anthropologie* **57** 272–298.
Henderson CY, Mariotti V, Pany-Kucera D, Villotte S & Wilczak C 2013 Recording Specific Entheseal Changes of Fibrocartilaginous Entheses: Initial Tests Using the Coimbra Method. *International Journal of Osteoarchaeology* **23** 152–162. (doi:10.1002/oa.2287)
Henderson RC, Lee-Thorp J & Loe L 2014 Early life histories of the London poor using δ13C and δ15N stable isotope incremental dentine sampling. *American Journal of Physical Anthropology* **154** 585–593. (doi:10.1002/ajpa.22554)
Henderson CY, Mariotti V, Pany-Kucera D, Villotte S & Wilczak C 2016 The New 'Coimbra Method': A Biologically Appropriate Method for Recording Specific Features of Fibrocartilaginous Entheseal Changes. *International Journal of Osteoarchaeology* **26** 925–932. (doi:10.1002/oa.2477)
Henke W 1972 Morphometrische Untersuchungen am Skelettmaterial des mittelalterlichen Kieler Gertrudenfriedhofs im Vergleich mit anderen nordeuropäischen Skelettserien. *Z. Morph. Anthrop.* **64** 308–347.
Hernberg S 2000 Lead poisoning in a historical perspective. *American Journal of Industrial Medicine* **38** 244–254. (doi:10.1002/1097-0274(200009)38:3<244::AID-AJIM3>3.0.CO;2-F)
Herrerín J & Garralda MD 2012 Legg-Calvé-Perthes Disease and unifocal eosinophilic granuloma in a visigoth from the Duratón necropolis (Segovia, Spain). *International Journal of Osteoarchaeology* **22** 86–97. (doi:10.1002/oa.1189)
Herring SW 2008 Mechanical influences on suture development and patency. *Frontiers of Oral Biology* **12** 41–56. (doi:10.1159/000115031)
Herrmann B, Grupe G, Hummel S, Piepenbrink H & Schutkowski H 1990 *Prähistorische Anthropologie. Leitfaden Der Feld- Und Labormethoden*. Berlin, Heidelberg: Springer-Verlag.
Herrscher E 2013 Détection isotopique des modalités d'allaitement et de sevrage à partir des ossements archéologiques. *Cahiers de Nutrition et de Dietetique* **48** 75–85. (doi:10.1016/j.cnd.2012.12.004)

Herrscher E, Bocherens H, Valentin F & Colardelle R 2001 Comportements alimentaires au Moyen Âge à Grenoble : application de la biogéochimie isotopique à la nécropole Saint-Laurent (XIIIe–XVe siècles, Isère, France). *C.R. Acad. Sci. Paris Sciences de La Vie/ Life Sciences* **324** 479–487.
Hershkovitz I, Latimer B, Dutour O, Jellema LM, Wish-Baratz S, Rothschild C & Rothschild BM 1997 Why do we fail in aging the skull from the sagittal suture? *American Journal of Physical Anthropology* **103** 393–399. (doi:10.1002/(SICI)1096-8644(199707)103:3<393::AID-AJPA8>3.0.CO;2-R)
Hershkovitz I, Rothschild BM, Dutour O & Greenwald C 1998 Clues to recognition of fungal origin of lytic skeletal lesions. *American Journal of Physical Anthropology* **106** 47–60. (doi:10.1002/(SICI)1096-8644(199805)106:1<47::AID-AJPA4>3.0.CO;2-A)
Hertz E, Trudel M, Cox MK & Mazumder A 2015 Effects of fasting and nutritional restriction on the isotopic ratios of nitrogen and carbon: A meta-analysis. *Ecology and Evolution* **5** 4829–4839. (doi:10.1002/ece3.1738)
Hesham M, Edariah A & Norhayati M 2004 Intestinal parasitic infections and micronutrient deficiency: a review. *The Medical Journal of Malaysia* **59** 284–293.
Hesketh R 2013 *Introduction to Cancer Biology*. Cambridge University Press.
Von Heyking K 2012 Anthropologie einer frühstädtischen Randgruppe morphologische und archäometrische Untersuchung eines hoch- bis spätmittelalterlichen Armenhausgräberfeldes in Regensburg. Ludwig-Maximilians-Universität München.
Hillson SW 1979 Diet and dental disease. *World Archaeology* **11** 147–162. (doi:10.1080/00438243.1979.9979758)
Hillson S 1996 *Dental Anthropology*. University Press Cambridge.
Hillson S 2001 Recording dental caries in archaeological human remains. *International Journal of Osteoarchaeology* **11** 249–289. (doi:10.1002/oa.538)
Hillson S 2008 The current state of dental decay. In *Technique and Application in Dental Anthropology*, 2nd ed, pp 111–135. Eds JD Irish & ND Greg. Cambridge University Press.
Hillson S & Bond S 1997 Relationship of enamel hypoplasia to the pattern of tooth crown growth: A discussion. *American Journal of Physical Anthropology* **104** 89–103. (doi:10.1002/(SICI)1096-8644(199709)104:1<89::AID-AJPA6>3.0.CO;2-8)
Hillson S, Grigson C & Bond S 1998 Dental Defects of Congenital Syphilis. *Americal Journal of Physical Anthropology* **107** 25–40.
Hiramoto Y 1993 Right-left differences in the lengths ofhuman arm and leg bones. *Kaibogaku Zasshi. Journal of Anatomy* **68** 536–543.
Hobsbawm E 1962 *The Age of Revolution: Europe 1789–1848*. Weidenfeld & Nicolson Ltd.
Holt B, Whittey E, Niskanen M, Sládek V, Berner M & Ruff CB 2018 Temporal and geographic variation Robusticity. In *Skeletal Variation and Adaptation in Europeans: Upper Palaeolithic to the Twentieth Century*, 1st ed, pp 91–132. Ed CB Ruff. John Wiley & Sons, Inc.
Hornig H 2002 Die spätmittelalterliche Skelettserie der Stadt Bernau (Brandenburg)– Vergleichende anthropologische Untersuchungen. Freie Universität Berlin.
Houston E & Upton J 2021 The rates of caries prevalence by sex and age from individuals in St. Mary Graces and East Smithfield cemeteries. University of Mississippi.
Howcroft R, Eriksson G & Lidén K 2012 Conformity in diversity? Isotopic investigations of infant feeding practices in two iron age populations from Southern Öland, Sweden. *American Journal of Physical Anthropology* **149** 217–230. (doi:10.1002/ajpa.22113)
Howcroft R, Eriksson G & Lidén K 2014 Infant feeding practices at the Pitted Ware Culture site of Ajvide, Gotland. *Journal of Anthropological Archaeology* **34** 42–53. (doi:10.1016/j.jaa.2014.01.001)

Huffman SL 1984 Determinants of Breastfeeding in Developing Countries: Overview and Policy Implications. *Studies in Family Planning* **15** 170. (doi:10.2307/1966134)
Hühne-Osterloh G 1989 Ursachen von Kindersterblichkeit in einer hochmittelalterlichen Skelettserie. *Anthropologischer Anzeiger* **47** 11–25.
Hühne-Osterloh G & Grupe G 1989 Causes of infant mortality in the Middle Ages revealed by chemical and palaeopathological analyses of skeletal remains. *Zeitschrift Für Morphologie Und Anthropologie* **77** 247–258.
Hühne-Osterloh G & Vogel V 1997 Pathologische und subpathologische Befunde von Kindern und Jugendlichen des Skelettkollektivs Schleswig, Ausgrabung Rathausmarkt. *Berichte Und Studien* **12** 211–236.
Humphrey LT 2014 Isotopic and trace element evidence of dietary transitions in early life. *Annals of Human Biology* **41** 348–357. (doi:10.3109/03014460.2014.923939)
Hunt DR & Bullen L 2007 The frequency of Os acromiale in the Robert J. Terry Collection. *International Journal of Osteoarchaeology* **17** 309–317. (doi:10.1002/oa.877)
Hunt KJ, Roberts C & Kirkpatrick C 2018 Taking stock: A systematic review of archaeological evidence of cancers in human and early hominin remains. *International Journal of Paleopathology* **21** 12–26. (doi:10.1016/j.ijpp.2018.03.002)
Le Huray JD & Schutkowski H 2005 Diet and social status during the La Tène period in Bohemia: Carbon and nitrogen stable isotope analysis of bone collagen from Kutná Hora-Karlov and Radovesice. *Journal of Anthropological Archaeology* **24** 135–147. (doi:10.1016/j.jaa.2004.09.002)
IARC 2006 Inorganic and organic lead compounds. *IARC Monographs on the Evaluation of Carcinogenic Risks to Humans / World Health Organization, International Agency for Research on Cancer* **87** 1–471.
Illi M 1992 *Wohin Die Toten Gingen. Begräbnis Und Kirchhof in Er Vorindustriellen Stadt*. Zürich: Chronos Verlag.
Işcan MY & Loth SR 1986a Determination of Age from the Sternal Rib in White Males: A Test of the Phase Method. *Journal of Forensic Sciences* **31** 122–132. (doi:10.1520/jfs11866j)
Işcan MY & Loth SR 1986b Determination of age from the sternal rib in white males: a test of the phase method. *Journal of Forensic Science* **31** 122–132.
Isola G, Alibrandi A, Rapisarda E, Matarese G, Williams RC & Leonardi R 2020 Association of vitamin D in patients with periodontitis: A cross-sectional study. *Journal of Periodontal Research* **55** 602–612. (doi:10.1111/jre.12746)
Ittrich H 2004 *Paläopathologische Befunde an 364 Mittelalterlichen Skeletten Aus Rostock*. Shaker Verlag.
Ives R & Humphrey LT 2020 Exploring Patterns of Appositional Growth Amongst Urban Children. In *The Bioarchaeology of Urbanization. Bioarchaeology and Social Theory*, pp 317–339. Eds TK Betsinger & SN Dewitte. Springer, Cham.
Iwamuro H, Ikeda S & Taniguchi M 2016 A rare case of diploic venous anomaly: asymptomatic venous sac expanding in the diploe. *SpringerPlus* **5** 1–7. (doi:10.1186/s40064-016-3607-1)
Jansen G & Haas J 1991 *Kompendium Der Arbeitsmedizin.* Köln: Verlag TÜV Rheinlang GmbH,.
Järvinen TLN, Kannus P, Pajamäki I, Vuohelainen T, Tuukkanen J, Järvinen M & Sievänen H 2003 Estrogen deposits extra mineral into bones of female rats in puberty, but simultaneously seems to suppress the responsiveness of female skeleton to mechanical loading. *Bone* **32** 642–651.
Jay M, Fuller BT, Richards MP, Knüsel CJ & King SS 2008 Iron age breastfeeding practices in Britain: Isotopic evidence from wetwang slack, east yorkshire. *American Journal of*

Physical Anthropology **136** 327–337. (doi:10.1002/ajpa.20815)
Jones HH, Priest, James D, Hayes WC, Tichenor CC & Nagel D 1977 Humeral hypertrophy in response to exercise. *Journal of Bone and Joint Surgery* 204–208. (doi:10.1007/978-1-4471-5451-8_104)
Joshi A, Arora A, Amadi-Mgbenka C, Mittal N, Sharma S, Malhotra B, Grover A, Misra A & Loomba M 2019 Burden of household food insecurity in urban slum settings. *PLoS ONE* **14** 1–24. (doi:10.1371/journal.pone.0214461)
Jungers WL & Minns RJ 1979 Computed tomography and biomechanical analysis of fossil long bones. *American Journal of Physical Anthropology* **50** 285–290. (doi:10.1002/ajpa.1330500219)
Jungklaus, B. & Neumann, M. & Niemitz C 2001 Lebenserwartung und Arbeitsbelastung im Mittelalter in der Mark Brandenburg - Untersuchungen an der Skelettserie aus Treskow/Neuruppin. In *Homo - Unsere Herkunft Und Zukunft: Proceedings - 4. Kongress Der Gesellschaft Für Anthropologie e.V. (GfA)*, pp 299–305. Ed M Schultz. Göttingen: Cuvillier Verlag.
Jungklaus, B. & Niemitz C 2001 Hinweise zu unterschiedlichen Lebensbedingungen im späten Mittelalter und der frühen Neuzeit am Beispiel der Skelettserie Tasdorf, Brandenburg, Deutschland. *Archaeologia Austriaca, Beiträge Zur Paläoanthropologie, Ur- Und Frühgeschichte Österreichs,* **84**–**85** 221–232.
Jungklaus B 2004 *Anthropologische Untersuchung Der Mittelalterlichen Skelette Aus Liebenwalde (Landkreis Oberhavel)*. In *Unpublizierter Abschlussbericht, Vorgelegt Dem BLDAM*.
Jungklaus B 2007 Mangelerkrankungen an Kinderskeletten im Mittelalter und der frühen Neuzeit in Brandenburg. *Mitteilungen Der Deutschen Gesellschaft Für Archäologie Des Mittelalters Und Der Neuzeit* **19** 287–290.
Jungklaus B 2008a Ein kompletter Dorffriedhof aus dem späten Mittelalter: Diepensee – ein Glücksfall für die Anthropologie. In *Einsichten 18, Archäologische Beiträge Aus Dem Süden Des Landes Brandenburg 2006/2007*, pp 123–131.
Jungklaus B 2008b Palaeodemographic and palaeopathological aspects to the late medieval village population of Diepensee (Brandenburg). In *Limping Together Trough the Ages. Joint Afflictions and Bone Infections.*, pp 81–117. Eds G Grupe, G McGlynn & J Peters. Documenta Archaeobiologiae.
Jungklaus B 2009 Zur brandenburgischen Bevölkerung im Mittelalter und ihren Lebensumständen aus anthropologischer Sicht. In *Forschungen Zur Archäologie Im Land Brandenburg 11. Tagungsband: Wie Die Mark Entstand. 850 Jahre Mark Brandenburg, Wünsdorf.*, pp 249–281.
Jungklaus B 2011 *Harte Arbeit Für Die Bauern in Brandenburg – Degenerative Gelenkveränderungen in Der Spätmittelalterlichen Population von Diepensee (Lkr. Dahme-Spreewald)*. Beier & Beran. Archäologische Fachliteratur.
Jungklaus B 2017 Wandel der Bestattumgssitten und Lebensbedingungen vom späten Mittelalter zur frühen Neuzeit aus anthropologischer Sicht. In *Feuerstein, Fibel, Fluchttunnel. Archäologie in Berlin Und Brandenburg Seit Der Wende*, pp 231–242. Ed SF& WM Meyer M. Petersberg: Michael Imhoff.
Jungklaus B & Krippner K V. 2016 Der „Grüne Friedhof“ von Freiberg (Lkr. Mittelsachsen). *Ausgrabungen in Sachsen* **5** 415–429.
Kaas L & Struijs PAA 2012 Congenital radial head dislocation with a progressive cubitus valgus: A case report. *Strategies in Trauma and Limb Reconstruction* **7** 39–44. (doi:10.1007/s11751-011-0126-z)
Kacki S, Jagu D & Durand J-P 2010 Probable unicameral bone cyst in a 4700-year-old radius. *Journal of Paleopathology* **22** 5–13.

Kairies M-S 2021 Osteologische Untersuchungen des Gräberfeldes in Ellwangen (Jagst) -. University of Tübingen.
Kalfas IH 2001 Principles of bone healing. *Neurosurgical Focus* **10** 1–4. (doi:10.3171/foc.2001.10.4.2)
Kalichman L, Kim DH, Li L, Guermazi A, Berkin V & Hunter DJ 2009 Spondylolysis and spondylolisthesis: Prevalence and association with low back pain in the adult community-based population. *Spine* **34** 199–205. (doi:10.1097/BRS.0b013e31818edcfd)
Kanisius PH & Luke DA 1994 Is the complexity of the human sagittal suture related to the size of the temporal muscle? *International Journal of Anthropology* **9** 265–272.
Katzenberg, M. A., & Waters-Rist AL 2019 Stable Isotope Analysis: a Tool for Studying Past Diet, Demography, and Life History. In *Biological Anthropology of the Human Skeleton*, 3rd ed, pp 467-504. Eds MA Katzenberg & SR Saunders. New York: John Wiley & Sons Inc.
Katzenberg MA & Lovell NC 1999 Stable isotope variation in pathological bone. *International Journal of Osteoarchaeology* **9** 316–324. (doi:10.1002/(SICI)1099-1212(199909/10)9:5<316::AID-OA500>3.0.CO;2-D)
Katzenberg MA & Weber A 1999 Stable isotope ecology and palaeodiet in the Lake Baikal region of Siberia. *Journal of Archaeological Science* **26** 651–659. (doi:10.1006/jasc.1998.0382)
Katzenberg MA, Saunders SR & Fitzgerald WR 1993 Age differences in stable carbon and nitrogen isotope ratios in a population of prehistoric maize horticulturists [published erratum appears in Am J Phys Anthropol 1993 Sep;92(1):127]. *Am J Phys Anthropol* **90** 267–281.
Katzenberg MA, Herring DA & Saunders SR 1996 Weaning and infant mortality: evaluating the skeletal evidence. *American Journal of Physical Anthropology* **39** 177–199. (doi:10.1002/(SICI)1096-8644(1996)23+<177::AID-AJPA7>3.0.CO;2-2)
Kaupová S, Brůžek J, Velemínský P & Čerńiková A 2013 Urban-rural differences in stature in the population of medieval Bohemia. *Anthropologischer Anzeiger* **70** 43–55. (doi:10.1127/0003-5548/2012/0276)
Kaupová S, Herrscher E, Velemínskÿ P, Cabut S, Polácek L & Bruzek J 2014 Urban and rural infant-feeding practices and health in early medieval Central Europe (9th-10th century, Czech Republic). *American Journal of Physical Anthropology* **155** 635–651. (doi:http://dx.doi.org/10.1002/ajpa.22620)
Kellner CM & Schoeninger MJ 2007 A Simple Carbon Isotope Model for Reconstructing Prehistoric Human Diet. *American Journal of Physical Anthropology* **133** 1112–1127. (doi:10.1002/ajpa)
Kelly DW 1981 Congenital dislocation of the radial head: Spectrum and natural history. *Journal of Pediatric Orthopaedics* **1** 295–298. (doi:10.1097/01241398-198111000-00009)
Kemkes-Grottenthaler A 1997 Das Frauendefizit archäologischer Serien — ein paläodemographisches Paradoxon ? *Anthropologischer Anzeiger* **55** 265–280.
Kemkes-Grottenthaler A 2005 The short die young: The interrelationship between stature and longevity - Evidence from skeletal remains. *American Journal of Physical Anthropology* **128** 340–347. (doi:10.1002/ajpa.20146)
Kenzler H 2015 Religion, Status and Taboo. Changing Funeral Rites in Catholic and Protestant Germany. In *The Archaeology of Death in Post-Medieval Europe*, pp 149–169. Ed S Tarlow. Warsaw, Berlin: De Gruyter Open Ltd.
Kesterke MJ & Judd MA 2019 A microscopic evaluation of Paget's disease of bone from a Byzantine monastic crypt in Jordan. *International Journal of Paleopathology* **24** 293–298. (doi:10.1016/j.ijpp.2018.08.005)

Key CA, Aiello LC & Molleson T 1994 Cranial suture closure and its implications for age estimation. *International Journal of Osteoarchaeology* **4** 193–207. (doi:10.1002/oa.1390040304)
Khoo MLC, Asa SL, Witterick IJ & Freeman JL 2002 Thyroid calcification and its association with thyroid carcinoma. *Head and Neck* **24** 651–655. (doi:10.1002/hed.10115)
Kinane DF 2000 Aetiology and pathogenesis of periodontal disease. *Annals of the Royal Australasian College of Dental Surgeons* **15** 42–50.
King T, Hillson S & Humphrey LT 2002 A detailed study of enamel hypoplasia in a post-medieval adolescent of known age and sex. *Archives of Oral Biology* **47** 29–39. (doi:10.1016/S0003-9969(01)00091-7)
King T, Humphrey LT & Hillson S 2005 Linear enamel hypoplasias as indicators of systemic physiological stress: Evidence from two known age-at-death and sex populations from postmedieval London. *American Journal of Physical Anthropology* **128** 547–559. (doi:10.1002/ajpa.20232)
Kjellström A, Storå J, Possnert G & Linderholm A 2009 Dietary patterns and social structures in medieval Sigtuna, Sweden, as reflected in stable isotope values in human skeletal remains. *Journal of Archaeological Science* **36** 2689–2699. (doi:10.1016/j.jas.2009.08.007)
Klaus HD 2014 Subadult scurvy in Andean South America: Evidence of vitamin C deficiency in the late pre-Hispanic and Colonial Lambayeque Valley, Peru. *International Journal of Paleopathology* **5** 34–45. (doi:10.1016/j.ijpp.2013.09.002)
Klaus HD 2017 Paleopathological rigor and differential diagnosis: Case studies involving terminology, description, and diagnostic frameworks for scurvy in skeletal remains. *International Journal of Paleopathology* **19** 96–110. (doi:10.1016/j.ijpp.2015.10.002)
Klaus HD, Larsen CS & Tam ME 2009 Economic intensification and degenerative joint disease: Life and labor on the postcontact north coast of Peru. *American Journal of Physical Anthropology* **139** 204–221. (doi:10.1002/ajpa.20973)
Van Klinken GJ 1999 Bone collagen quality indicators for palaeodietary and radiocarbon measurements. *Journal of Archaeological Science* **26** 687–695. (doi:10.1006/jasc.1998.0385)
Knappwost A 1951 Fluor-Hydroxyl-Su bstitution am Hydroxyla pa ti t als lonenaustauschreaktion und ihre Anwendung fur die Mikrofluoranalyse. *Angewandte Chemie* **68** 371–373.
Knipper C, Peters D, Meyer C, Maurer AF, Muhl A, Schöne BR & Alt KW 2013 Dietary reconstruction in Migration Period Central Germany: A carbon and nitrogen isotope study. *Archaeological and Anthropological Sciences* **5** 17–35. (doi:10.1007/s12520-012-0106-3)
Knüsel CJ, Göggel S & Lucy D 1997 Comparative degenerative joint disease of the vertebral column in the medieval monastic cemetery of the gilbertine priory of St. Andrew, Fishergate, York, England. *American Journal of Physical Anthropology* **103** 481–495. (doi:10.1002/(SICI)1096-8644(199708)103:4<481::AID-AJPA6>3.0.CO;2-Q)
Kölbl S 2004 Das Kinderdefizit im frühen Mittelalter - Realität oder Hypothese? - Zur Deutung demographischer Strukturen in Gräberfeldern. Eberhard-Karls-Universität Tübingen.
Komar DA & Buikstra JE 2007 *Forensic Anthropology: Contemporary Theory and Practice*. New York: Oxford University Press,.
Komlos J 2005 Anthropometric history: an overview of a quarter century of research. *Anthropologischer Anzeiger* **67** 341–356.
Kozak J & Krenz-Niedbała M 2002 The occurrence of cribra orbitalia and its association with

enamel hypoplasia in a medieval population from Kołobrzeg, Poland. *Variability and Evolution* **10** 75–82.
Kozlowski T & Witas HW 2012 Metabolic and Endocrine Diseases. In *A Companion to Palaeopathology*, 1st ed, pp 401–419. Ed AL Grauer. Blackwell Publishing Ltd.
Kramer MS & Kakuma R 2009 Optimal duration of exclusive breastfeeding (review). *The Cochrane Library*.
Kreiter SR, Schwartz RP, Kirkman HN, Charlton PA, Calikoglu AS & Davenport ML 2000 Nutritional rickets in African American breast-fed infants. *Journal of Pediatrics* **137** 153–157. (doi:10.1067/mpd.2000.109009)
Krenz-Niedbała M 2016 Did Children in Medieval and Post-medieval Poland Suffer from Scurvy? Examination of the Skeletal Evidence. *International Journal of Osteoarchaeology* **26** 633–647. (doi:10.1002/oa.2454)
Krueger HW & Sullivan CH 1984 Models for Carbon Isotope Fractionation Between Diet and Bone. In *Stable Isotopes in Nutrition*, pp 205–220. Eds J Turnlund & E Phyllis. Washington D.C.: ACS Symposium Series. (doi:10.1021/bk-1984-0258.ch014)
Krugner-Higby LA, Gendron A, Laughlin NK, Luck M, Scheffler J & Phillips B 2001 Chronic Myelocytic Leukemia in a Juvenile Rhesus Macaque (Macaca mulatta). *Contemporary Topics in Laboratory Animal Science* **40** 44–48.
Kühnel H 1986 *Alltag Im Spätmittelalter*. Wien: Styria Graz Verlag.
Kumar A & Tubbs RS 2011 Spina bifida: A diagnostic dilemma in paleopathology. *Clinical Anatomy* **24** 19–33. (doi:10.1002/ca.21058)
Kunos CA, Simpson SW, Russell KF & Hershkovitz I 1999 First rib metamorphosis: Its possible utility for human age-at-death estimation. *American Journal of Physical Anthropology* **110** 303–323. (doi:10.1002/(SICI)1096-8644(199911)110:3<303::AID-AJPA4>3.0.CO;2-O)
Kvaal SI & Derry TK 1996 Tell-tale teeth: Abrasion from the traditional clay pipe. *Endeavour* **20** 28–30. (doi:10.1016/0160-9327(96)10006-5)
Kwok CS & Keenleyside A 2015 Stable isotope evidence for infant Feeding Practices in the Greek Colony of Apollonia Pontica. *Hesperia Supplements, ARCHAEODIET IN THE GREEK WORLD: Dietary Reconstruction from Stable Isotope Analysis* **49** 147–170.
Kyere KA, Than KD, Wang AC, Rahman SU, Valdivia-Valdivia JM, Marca F La & Park P 2012 Schmorl's nodes. *European Spine Journal* **21** 2115–2121. (doi:10.1007/s00586-012-2325-9)
LaDeau SL, Allan BF, Leisnham PT & Levy MZ 2015 The ecological foundations of transmission potential and vector-borne disease in urban landscapes. *Functional Ecology* **29** 889–901. (doi:10.1111/1365-2435.12487)
Laffranchi Z, Charisi D, Jiménez-Brobeil SA & Milella M 2020 Gendered division of labor in a Celtic community? A comparison of sex differences in entheseal changes and long bone shape and robusticity in the pre-Roman population of Verona (Italy, third–first century BC). *American Journal of Physical Anthropology* **173** 568–588. (doi:10.1002/ajpa.24111)
Lagier R, Kramar C & Baud CA 1987 Femoral unicameral bone cyst in a medieval child. Radiological and pathological study. *Pediatric Radiology* **17** 498–500. (doi:10.1016/s0221-0363(04)97706-2)
Lamberti LM, Fischer Walker CL, Noiman A, Victora C & Black RE 2011 Breastfeeding and the risk for diarrhea morbidity and mortality. *BMC Public Health* **11** 1–12. (doi:10.1186/1471-2458-11-S3-S15)
Langenberg LC, Beumer ACH, The B, Koenraadt KLM & Eygendaal D 2020 Surgical treatment of chronic anterior radial head dislocations in missed Monteggia lesions in children: A rationale for treatment and pearls and pitfalls of surgery. *Shoulder and*

Elbow **12** 422–431. (doi:10.1177/1758573219839225)
Langenscheidt F 1985 Methodenkritische Untersuchungen zur Paläodemographie am Beispiel zweier fränkischer Gräberfelder. *Materialh. Bevölkerungswiss.* **Sonderh. 2**.
Lanphear KM 1990 Frequency and distribution of enamel hypoplasias in a historic skeletal sample. *American Journal of Physical Anthropology* **81** 35–43. (doi:10.1002/ajpa.1330810106)
Lantzsch J & Schuster K 2009 Socioeconomic status and physical stature in 19th-century Bavaria. *Economics and Human Biology* **7** 46–54. (doi:10.1016/j.ehb.2008.08.001)
Larsen CS 1981 Functional Implications of Postcranial Size Reduction on the Prehistoric Georgia Coast, U.S.A. *Journal of Human Evolution* **10** 489–502.
Larsen CS 1997 *Bioarchaeology: Interpreting Behavior from the Human Skeleton*. Cambridge: Cambridge University Press.
Larsen CS 2015 *Bioarchaeology: Interpreting Behavior from the Human Skeleton*. Cambridge University Press.
Larsen CS, Shavit R & Griffin MC 1991 Dental caries evidence for dietary change: an archaeological context. *Advances in Dental Anthropology* 179–202.
Layman CA, Araujo MS, Boucek R, Hammerschlag-Peyer CM, Harrison E, Jud ZR, Matich P, Rosenblatt AE, Vaudo JJ, Yeager LA *et al.* 2012 Applying stable isotopes to examine food-web structure: An overview of analytical tools. *Biological Reviews* **87** 545–562. (doi:10.1111/j.1469-185X.2011.00208.x)
Lazenby RA 2002 Skeletal Biology , Functional Asymmetry and the Origins of ‘“ Handedness ”’. 129–138. (doi:10.1006/yjtbi.3052)
Leggio A & Introna F 2021 Fully Ossified Thyroid Cartilage Found among the Skeletal Remains of A 21-Year-Old Slavic Soldier: Interpretation of a Case. *Forensic Sciences* **1** 213–219. (doi:10.3390/forensicsci1030019)
Lehnert M 1993 Stomatologische Untersuchungen an den Skelettresten der Bewohner Esslingens a. N. von der Gotik (1230 AD) bis zur Neuzeit. Eberhard Karls Universität Tübingen.
Lewis ME 2002 Impact of Industrialization : Comparative Study of Child Health in Four Sites From Medieval and Postmedieval England (A . D . 850 – 1859). *American Journal of Physical Anthropology* **119** 211–223. (doi:10.1002/ajpa.10126)
Lewis M 2007 *The Bioarchaeology of Children. Perspectives from Biological and Forensic Anthropology.* Cambridge University Press.
Lewis ME 2009 *The Bioarchaeology of Children*. (doi:10.1017/cbo9780511542473.001)
Lewis ME & Gowland R 2007 Brief and Precarious Lives: Infant Mortality in Contrasting Sites from Medieval and Post-Medieval England (AD 850–1859). *American Journal of Physical Anthropology* **134** 117–129. (doi:10.1002/ajpa)
Lewis ME, Roberts CA & Manchester K 1995a Comparative study of the prevalence of maxillary sinusitis in later Medieval urban and rural populations in Northern England. *American Journal of Physical Anthropology* **98** 497–506. (doi:10.1002/ajpa.1330980409)
Lewis ME, Roberts CA & Manchester K 1995b Inflammatory bone changes in leprous skeletons from the medieval hospital of St. James and St. Mary Magdalene, Chichester, England. *International Journal of Leprosy* **63** 77–85.
Libby WF, Berger R, Mead JF, Alexander GV & Ross JF 1964 Replacement Rates for Human Tissue from Atmospheric Radiocarbon. *Science* **146** 1170–1172.
Liebe-Harkort C 2012 Cribra orbitalia, sinusitis and linear enamel hypoplasia in Swedish Roman iron age adults and subadults. *International Journal of Osteoarchaeology* **22** 387–397. (doi:10.1002/oa.1209)
Lieberman DE, Devlin MJ & Pearson OM 2001 Articular area responses to mechanical

loading: Effects of exercise, age, and skeletal location. *American Journal of Physical Anthropology* **116** 266–277. (doi:10.1002/ajpa.1123)
Liebert H, Bach H & Felsch G 1971 Degenerative Gelenk und Wirbel- säulenerkrankungen an Skeletten aus dem 11. und 12. Jahrhundert. *Wissenschaftliche Zeitschrift Der Friedrich-Schiller- Universität Jena* **20** 813–820.
Lieverse AR 1999 Diet and the Aetiology of Dental Calculus. *International Journal of Osteoarchaeology* **9** 219–232. (doi:10.1002/(SICI)1099-1212(199907/08)9:4<219::AID-OA475>3.0.CO;2-V)
Lieverse AR, Temple DH & Bazaliiskii VI 2014 Paleopathological description and diagnosis of metastatic carcinoma in an early bronze age (4588+34 Cal. BP) forager from the cis-baikal region of eastern siberia. *PLoS ONE* **9** 1–25. (doi:10.1371/journal.pone.0113919)
Lindenhofer P 2012 'Traufkinder' - ein besonderer Umgang mit ungetauft verstorbenen Kindern in der Frühen Neuzeit - 'wahrlich, wahrlich, ich sage dir, wenn einer nicht geboren wird aus Wasser und Heiligem Geiste, so kann er nicht in das Reich Gottess eingehen' (Joh. 3,5). Universität Wien.
Linderholm A & Kjellström A 2011 Stable isotope analysis of a medieval skeletal sample indicative of systemic disease from Sigtuna Sweden. *Journal of Archaeological Science* **38** 925–933. (doi:10.1016/j.jas.2010.11.022)
Long KZ, Rosado JL & Fawzi W 2007 The comparative impact of iron, the B-complex vitamins, vitamins C and E, and selenium on diarrheal pathogen outcomes relative to the impact produced by vitamin A and zinc. *Nutrition Reviews* **65** 218–232. (doi:10.1301/nr.2007.may.218-232)
Lösch S 2009 Paläopathologisch-anthropologische und molekulare Untersuchungen an mittelalterlichen und frühneuzeitlichen Bevölkerungsgruppen: Ernährung und Gesundheitszustand süd- und nordbayerischer Bevölkerungsstichproben. In *Medizinischen Fakultät*. Ludwig-Maximilians-Universität München.
Loth SR & Henneberg M 2001 Sexually dimorphic mandibular morphology in the first few years of life. *American Journal of Physical Anthropology* **115** 179–186. (doi:10.1002/ajpa.1067)
Lovejoy CO 1985 Dental wear in the Libben population: Its functional pattern and role in the determination of adult skeletal age at death. *American Journal of Physical Anthropology* **68** 47–56. (doi:10.1002/ajpa.1330680105)
Lovejoy CO, Burstein AH & Heiple KG 1976 The biomechanical analysis of bone strength: A method and its application to platycnemia. *American Journal of Physical Anthropology* **44** 489–505. (doi:10.1002/ajpa.1330440312)
Lovejoy CO, Meindl RS, Pryzbeck TR & Mensforth RP 1985 Chronological metamorphosis of the auricular surface of the ilium: A new method for the determination of adult skeletal age at death. *American Journal of Physical Anthropology* **68** 15–28. (doi:10.1002/ajpa.1330680103)
Lovell NC 1997 Trauma Analysis in Paleopathology. *Yearbook of Physical Anthropology* **40** 139–170. (doi:10.1002/(sici)1096-8644(1997)25+<139::aid-ajpa6>3.0.co;2-#)
Lovell NC 2008 Analysis and interpretation of Skeletal Trauma. In *Biological Anthropology of the Human Skeleton: Second Edition*, 2nd ed, pp 341–386. Eds MA Katzenberg & SR Saunders. John Wiley & Sons, Inc.
Lovell NC & Grauer AL 2018 Analysis and Interpretation of Trauma in Skeletal Remains. In *Biological Anthropology of the Human Skeleton*, 3rd ed, pp 335–383. Eds MA Katzenberg & AL Grauer. John Wiley & Sons Inc. (doi:10.1002/9781119151647.ch10)
Lozano M, Jiménez-Brobeil SA, Willman JC, Sánchez-Barba LP, Molina F & Rubio Á 2021 Argaric craftswomen: Sex-based division of labor in the Bronze Age southeastern Iberia. *Journal of Archaeological Science* **127**. (doi:10.1016/j.jas.2020.105239)

Lucia A, Lima L, Oliveira PR, Carvalho VC, Cimerman S & Savio E 2014 Recommendations for the treatment of osteomyelitis. *Brazilian Journal of Infectious Diseases* **18** 526–534.
Lukacs JR 1995 The 'caries correction factor': A new method of calibrating dental caries rates to compensate for antemortem loss of teeth. *International Journal of Osteoarchaeology* **5** 151–156. (doi:10.1002/oa.1390050207)
Lukacs JR 1996 Sex Differences in Dental Caries Rates with the Origin of Agriculture in South Asia. *Current Anthropology* **37** 147–153.
Lukacs JR & Largaespada LL 2006 Explaining sex differences in dental caries prevalence: Saliva, hormones, and 'life history' etiologies. *American Journal of Human Biology* **18** 540–555. (doi:10.1002/ajhb.20530)
Lukacs JR & Thompson LM 2008 Dental caries prevalence by sex in prehistory: magnitude and meaning. *Cambridge Studies in Biological and Evolutionary Anthropology* **53** 136.
Maat GJR 2005 Two millennia of male stature development and population health and wealth in the Low Countries. *International Journal of Osteoarchaeology* **15** 276–290. (doi:10.1002/oa.785)
Maat GJR & Mastwijk RW 2000 Avulsion injuries of vertebral endplates. *International Journal of Osteoarchaeology* **10** 142–152. (doi:10.1002/(SICI)1099-1212(200003/04)10:2<142::AID-OA519>3.0.CO;2-L)
Maat GJR, Mastwijk RW & Sarfatij H 1998 *Een Fysisch Anthropologisch Onderzoek van Begravenen Bij Het Minderbroeders-Klooster Te Dordrecht, circa 1275-1572 AD*. In *Rapportage Archeologische Monumentenzorg*. Amersfoort.
Macedo F, Ladeira K, Pinho F, Saraiva N, Bonito N, Pinto L & Gonçalves F 2017 Bone metastases: An overview. *Oncology Reviews* **11**. (doi:10.4081/oncol.2017.321)
Macintosh AA, Pinhasi R & Stock JT 2014 Lower limb skeletal biomechanics track long-term decline in mobility across ~6150 years of agriculture in Central Europe. *Journal of Archaeological Science* **52** 376–390. (doi:10.1016/j.jas.2014.09.001)
Macintosh AA, Pinhasi R & Stock JT 2017 Prehistoric women's manual labor exceeded that of athletes through the first 5500 years of farming in Central Europe. *Science Advances* **3**. (doi:10.1126/sciadv.aao3893)
Mader R & Lavi I 2009 Diabetes mellitus and hypertension as risk factors for early diffuse idiopathic skeletal hyperostosis (DISH). *Osteoarthritis and Cartilage* **17** 825–828. (doi:10.1016/j.joca.2008.12.004)
Malčić AI, Vodanović M, Matijević J, Mihelić D, Mehičić GP & Krmek SJ 2011 Caries prevalence and periodontal status in 18th century population of Požega-Croatia. *Archives of Oral Biology* **56** 1592–1603. (doi:10.1016/j.archoralbio.2011.05.016)
Mann RW & Hunt DR 2005 *Photographic Regional Atlas of Bone Disease. A Guide to Pathologic and Normal Variation in the Human Skeleton.* Springfield: Charles C. Thomas Press.
Mant M & Roberts C 2015 Diet and caries prevalence in PM London. *International Journal of Historical Archaeology* **19** 188–207.
Mant M, de la Cova C & Brickley MB 2021 Intersectionality and trauma analysis in bioarchaeology. *American Journal of Physical Anthropology* **174** 583–594. (doi:10.1002/ajpa.24226)
Manton WI 1994 Editorial comment: Lead poisoning from gunshots a five century heritage. *Clinical Toxicology* **32** 387–389. (doi:10.3109/15563659409011039)
Marchi D 2008 Relationships between lower limb cross-sectional geometry and mobility: The case of a Neolithic sample from Italy. *American Journal of Physical Anthropology* **137** 188–200. (doi:10.1002/ajpa.20855)
Mariotti V, Facchini F & Belcastro MG 2004 Enthesopathies - Proposal of a standardized

scoring method and applications. *Collegium Antropologicum* **28** 145–159.
Mariotti V, Facchini F & Belcastro MG 2007 The study of entheses: Proposal of a standardised scoring method for twenty-three entheses of the postcranial skeleton. *Collegium Antropologicum* **31** 291–313.
Marks MK & Hamilton MD 2007 Metastatic carcinoma: Palaeopathology and differential diagnosis. *International Journal of Osteoarchaeology* **17** 217–234. (doi:10.1002/oa.874)
Marques C 2019 *Tumors of Bone*. Elsevier Inc. (doi:10.1016/B978-0-12-809738-0.00019-3)
Marques C, Santos AL & Cunha E 2013 Better a Broader Diagnosis Than a Misdiagnosis: The Study of a Neoplastic Condition in a Male Individual who Died in Early 20th Century (Coimbra, Portugal). *International Journal of Osteoarchaeology* **23** 664–675. (doi:10.1002/oa.1294)
Marques C, Matos V, Costa T, Zink A & Cunha E 2018 Absence of evidence or evidence of absence? A discussion on paleoepidemiology of neoplasms with contributions from two Portuguese human skeletal reference collections (19th–20th century). *International Journal of Paleopathology* **21** 83–95. (doi:10.1016/j.ijpp.2017.03.005)
Martens F & Alt KW 2019 St. Leonhard – ein Bestattungsplatz der Oberschicht? In *St. Leonhard in Der Frankfurter Altstadt: Archäologie / Anthropologie*, 1st ed, pp 195–250. Eds A Hampel, KW Alt, P Held, F Martens & L Renner. Frankfurt am Main: Verlag Henrich Editionen.
Martin R & Saller K 1957 *Lehrbuch Der Anthropologie in Systematischer Darstellung Mit Besonderer Berücksichtigung Der Anthropologischen Methoden*. Stuttgart: Gustav Fischer Verlag.
Martinez-Lage JF, Esteban JA, Perez MM & Poza M 1984 Craniostenosis Secondary to Calcified Subperiosteal Hematoma: Case Report. *Neurosurgery* **15** 703–704.
Mascard E, Gomez-Brouchet A & Lambot K 2015 Bone cysts: Unicameral and aneurysmal bone cyst. *Orthopaedics and Traumatology: Surgery and Research* **101** S119–S127. (doi:10.1016/j.otsr.2014.06.031)
Masset C 1982 Estimation de l'age de deces par les sutures craniennes. Université´ Paris VII.
Matsushima S, Shimizu T, Fukasawa N & Ojiri H 2019 Novel Characteristic Skull Magnetic Resonance Imaging Features Associated with Meningioma. *Journal of Computer Assisted Tomography* **43** 708–712. (doi:10.1097/RCT.0000000000000900)
Matussek J, Hayn T, Dingeldey E & Mellerowicz H 2022 Typische kongenitale Skelettfehlbildungen in der Kinder- und Jugendorthopädie. *Orthopädie Und Unfallchirurgie Up2date* **17** 69–96. (doi:10.1055/a-1371-9874)
Maurizi A & Rucci N 2018 The osteoclast in bone metastasis: Player and target. *Cancers* **10**. (doi:10.3390/cancers10070218)
Mays SA 1985 The relationship between harris line formation and bone growth and development. *Journal of Archaeological Science* **12** 207–220. (doi:10.1016/0305-4403(85)90021-4)
Mays SA 1997 Carbon stable isotope ratios in mediaeval and later human skeletons from Northern England. *Journal of Archaeological Science* **24** 561–568. (doi:10.1006/jasc.1996.0139)
Mays SA 2002 Asymmetry in Metacarpal Cortical Bone in a Collection of British Post-Mediaeval Human Skeletons. *Journal of Archaeological Science* **29** 435–441. (doi:10.1006/jasc.2002.0729)
Mays S 2006 Spondylolysis, Spondylolisthesis, and Lumbo-Sacral Morphology in a Medieval English Skeletal Population. *American Journal of Physical Anthropology* **131** 352–362. (doi:10.1002/ajpa)
Mays S 2008 Human remains in marine archaeology. *Environmental Archaeology* **13** 123–133. (doi:10.1179/174963108X343245)

Mays S 2009 The Osteology of Monasticism in Medieval England. In *The Social Archaeology of Funerary Remains*, pp 179–189. Eds R Gowland & CJ Knüsel. Oxford: Oxbow Books.
Mays S 2010 Archaeological Skeletons Support a Northwest European Origin for Paget ' s Disease of Bone. *Journal of Bone Mineral Research* **25** 1839–1841. (doi:10.1002/jbmr.64)
Mays S 2014 The palaeopathology of scurvy in Europe. *International Journal of Paleopathology* **5** 55–62. (doi:10.1016/j.ijpp.2013.09.001)
Mays S & Brickley MB 2018 Vitamin D deficiency in bioarchaeology and beyond: The study of rickets and osteomalacia in the past. *International Journal of Paleopathology* **23** 1–5. (doi:10.1016/j.ijpp.2018.05.004)
Mays S & Brickley MB 2022 Is dietary deficiency of calcium a factor in rickets ? Use of current evidence for our understanding of the disease in the past. *International Journal of Paleopathology* **36** 36–44. (doi:10.1016/j.ijpp.2021.11.001)
Mays S, Steele J & Ford M 1999 Directional Asymmetry in the Human Clavicle. *International Journal of Osteoarchaeology* **9** 18–28.
Mays SA, Richards MP & Fuller BT 2002 Bone stable isotope evidence for infant feeding in Mediaeval England. *Antiquity* **76** 654–656. (doi:10.1063/1.2756072)
Mays S, Brickley M & Ives R 2006 Skeletal manifestation of rickets in infants and young children in a historic population from England. *American Journal of Physical Anthropology* **129** 362–374. (doi:10.1002/ajpa.20292)
Mays S, Brickley M & Ives R 2008 Growth in an English population from the Industrial Revolution. *American Journal of Physical Anthropology* **136** 85–92. (doi:10.1002/ajpa.20780)
Mays S, Brickley M & Ives R 2009 Growth and vitamin D deficiency in a population from 19th century Birmingham, England. *International Journal of Osteoarchaeology* **19** 406–415. (doi:10.1002/oa.976)
Mays S, Vincent S, Snow M & Robson-Brown K 2011 Concha bullosa, a neglected condition in palaeopathology. *International Journal of Paleopathology* **1** 184–187. (doi:10.1016/j.ijpp.2012.02.002)
Mays S, Mavrogordato M, Lambert J & Sofaer J 2014 The Prevalence and Health Implications of Concha Bullosa in a Population from Mediaeval England. *International Journal of Osteoarchaeology* **24** 614–622. (doi:10.1002/oa.2246)
Mays S, Gowland R, Halcrow S & Murphy E 2017 Child Bioarchaeology: Perspectives on the Past 10 Years. *Childhood in the Past* **10** 38–56. (doi:10.1080/17585716.2017.1301066)
Mazza B 2019 Postcranial morphological variation between hunter-gatherers and horticulturalists from the lower Paraná River Delta, Argentina. *American Journal of Physical Anthropology* **170** 176–195. (doi:10.1002/ajpa.23889)
McDade TW 2005 Life history, maintenance, and the early origins of immune function. *American Journal of Human Biology* **17** 81–94. (doi:10.1002/ajhb.20095)
McFadden C, Muir B & Oxenham MF 2022 Determinants of infant mortality and representation in bioarchaeological samples: A review. *American Journal of Biological Anthropology* **177** 196–206. (doi:10.1002/ajpa.24406)
McHenry HM 1992 Body size and proportions in early hominids. *American Journal of Physical Anthropology* **87** 407–431. (doi:10.1002/ajpa.1330870404)
McKinnell RG 2006 Invasion and metastasis. In *The Biological Basis of Cancer*, pp 51–79. Eds RG McKinnell, RE Parchment, AO Perantoni, I Damjanov & GB Pierce. Cambridge: Cambridge University Press. (doi:10.1002/9780470719985.ch15)
McQuirter J, Rothenberg SJ, Dinkins GA, Manalo M, Kondrashov V & Todd AC 2001 The

Effects of Retained Lead Bullets on Body Lead Burden. *The Journal of Trauma: Injury, Infection, and Critical Care* **50** 892–899.
Van Meijeren-Van Lunteren AW, Voortman T, Elfrink MEC, Wolvius EB & Kragt L 2021 Breastfeeding and Childhood Dental Caries: Results from a Socially Diverse Birth Cohort Study. *Caries Research* **55** 153–161. (doi:10.1159/000514502)
Meindl RS & Lovejoy CO 1985a Ectocranial suture closure: A revised method for the determination of skeletal age at death based on the lateral-anterior sutures. *American Journal of Physical Anthropology* **68** 57–66. (doi:10.1002/ajpa.1330680106)
Meindl RS & Lovejoy CO 1985b Ectocranial Suture Closure: A revised method for the determination of sketetal age at death based on the lateral-aneterior sutures. *Americal Journal of Physical Anthropology* **68** 57–66.
Melanson KJ 2007 Diet, Nutrition, and Osteoarthritis. *American Journal of Lifestyle Medicine* **1** 260–263. (doi:10.1177/1559827607302033.)
Melzer K 2005 Die Skelette der Wüstung Dahmsdorf (Teltow/Fläming) des 13. bis 15. Jahrhunderts - osteologische und paläopathologische Untersuchung. Freie Universität Berlin.
Mendenhall WM, Zlotecki RA, Scarborough MT, Gibbs CP & Mendenhall NP 2006 Giant cell tumor of bone. *American Journal of Clinical Oncology: Cancer Clinical Trials* **29** 96–99. (doi:10.1097/01.coc.0000195089.11620.b7)
Méndez Collí C, Sierra Sosa TN, Tiesler V & Cucina A 2009 Linear enamel hypoplasia at Xcambó, Yucatán, during the Maya Classic period: An evaluation of coastal marshland impact on ancient human populations. *HOMO- Journal of Comparative Human Biology* **60** 343–358. (doi:10.1016/j.jchb.2009.04.001)
Menninger M & Waibel O 1996 Spondylopathien. In *Stumme Zeugen Ihrer Leiden*, pp 7–39. Ed A Czarnetzski. Tübingen: Attempto Verlag.
Merashli M, Chowdhury TA & Jawad ASM 2015 Musculoskeletal manifestations of diabetes mellitus. *QJM: An International Journal of Medicine* **108** 853–857. (doi:10.1093/qjmed/hcv106)
Mestekova S, Bruzek J, Veleminska J & Chaumoitre K 2015 A Test of the DSP Sexing Method on CT Images from a Modern French Sample. *Journal of Forensic Sciences* **60** 1295–1299. (doi:10.1111/1556-4029.12817)
Micarelli I, Paine RR, Tafuri MA & Manzi G 2019 A possible case of mycosis in a post-classical burial from La Selvicciola (Italy). *International Journal of Paleopathology* **24** 25–33. (doi:10.1016/j.ijpp.2018.09.001)
Michopoulou E, Nikita E & Valakos ED 2015 Evaluating the efficiency of different recording protocols for entheseal changes in regards to expressing activity patterns using archival data and cross-sectional geometric properties. *American Journal of Physical Anthropology* **158** 557–568. (doi:10.1002/ajpa.22822)
Michou L & Orcel P 2016 The changing countenance of Paget's Disease of bone. *Joint Bone Spine* **83** 650–655. (doi:10.1016/j.jbspin.2016.02.011)
Milella M, Giovanna Belcastro M, Zollikofer CPE & Mariotti V 2012 The effect of age, sex, and physical activity on entheseal morphology in a contemporary Italian skeletal collection. *American Journal of Physical Anthropology* **148** 379–388. (doi:10.1002/ajpa.22060)
Miles AEW 1963 The dentition in the assessment of individual age in skeletal material. pp 191–209. Ed DR Brothwell.
Miles A, White W & Tankard D 2008 *Burial at the Site of the Parish Church of St Benet Sherehog before and after the Great Fire: Excavations at 1 Poultry, City of London*. London: Museum of London Archaeology Service.
Miliauskiene Ž & Jankauskas R 2015 Social differences in oral health: Dental status of

individuals buried in and around Trakai Church in Lithuania (16th-17th c.c.). *Anthropologischer Anzeiger* **72** 89–106. (doi:10.1127/anthranz/2014/0407)
Milner GR & Boldsen JL 2012 Humeral and femoral head diameters in recent white american skeletons. *Journal of Forensic Sciences* **57** 35–40. (doi:10.1111/j.1556-4029.2011.01953.x)
Milward A & Samuel SB 2013 *The Economic Development of Continental Europe 1780-1870*. Routledge.
Minozzi S, Caldarini C, Pantano W, di Giannantonio S, Catalano P & Giuffra V 2020 Enamel hypoplasia and health conditions through social status in the Roman Imperial Age (First to third centuries, Rome, Italy). *International Journal of Osteoarchaeology* **30** 53–64. (doi:10.1002/oa.2830)
Miracle VA 2017 Lead Poisoning in Children and Adults. *Dimensions of Critical Care Nursing* **36** 71–73. (doi:10.1097/DCC.0000000000000227)
Miszkiewicz JJ 2015 Linear enamel hypoplasia and age-at-death at medieval (11th-16th centuries) St. Gregory's priory and cemetery, Canterbury, UK. *International Journal of Osteoarchaeology* **25** 79–87. (doi:10.1002/oa.2265)
Mitchell PD & Redfern RC 2011 Brief communication: Developmental dysplasia of the hip in medieval London. *American Journal of Physical Anthropology* **144** 479–484. (doi:10.1002/ajpa.21448)
Moggi-Cecchi J, Pacciani E & Pinto-Cisternas J 1994 Enamel hypoplasia and age at weaning in 19th-century Florence, Italy. *American Journal of Physical Anthropology* **93** 299–306. (doi:10.1002/ajpa.1330930303)
Molleson T & Cox M 1993 The Spitalfields project: Vol. 2: The anthropology, the middling sort. In *Council for British Archaeology*.
Molleson T, Cruse K & Mays S 1998 Some Sexually Dimorphic Features of the Human Juvenile. *Journal of Archaeological Science* **25** 719–728.
Molnar P 2008 Dental wear and oral pathology: Possible evidence and consequences of habitual use of teeth in a Swedish neolithic sample. *American Journal of Physical Anthropology* **136** 423–431. (doi:10.1002/ajpa.20824)
Molto JE, Kirkpatrick CL & Keron J 2019 The paleoepidemiology of Sacral Spina Bifida Occulta in population samples from the Dakhleh Oasis, Egypt. *International Journal of Paleopathology* **26** 93–103. (doi:10.1016/j.ijpp.2019.06.006)
Montford A 2002 Fit to Preach and Pray: Considerations of Occupational Health in the Mendicant Orders. *Studies in Church History* **37** 95–106. (doi:10.1017/S0424208400014674)
Moon SM, Yoder JH, Wright AC, Smith LJ, Vresilovic EJ & Elliott DM 2013 Evaluation of intervertebral disc cartilaginous endplate structure using magnetic resonance imaging. *European Spine Journal* **22** 1820–1828. (doi:10.1007/s00586-013-2798-1)
Moore JW & Semmens BX 2008 Incorporating uncertainty and prior information into stable isotope mixing models. *Ecology Letters* **11** 470–480. (doi:10.1111/j.1461-0248.2008.01163.x)
Morgan JWM, Adcock KA & Donohue RE 1990 Distribution of skeletal metastases in prostatic and lung cancer. Mechanisms of skeletal metastases. *Urology* **36** 31–34. (doi:10.1016/0090-4295(90)80308-A)
Morrone A, Tõrv M, Piombino-Mascali D, Malve M, Valk H & Oras E 2021 Hunger, disease, and subtle lesions: Insights into systemic metabolic disease in fetal and perinatal remains from 13th- to 15th-century Tartu, Estonia. *International Journal of Osteoarchaeology* **31** 534–555. (doi:10.1002/oa.2970)
Moss ML 1960 Inhibition and Stimulation of Sutural Fusion in the Rat Calvaria. *The Anatomical Record* **136** 457–467. (doi:10.1002/ar.1091360405)

Mousset J-L 1999 Les sites archéologiques. Les cimetières de l'église Saint-Nicolas, de l'église Saint-Jean et du couvent des Franciscains. In *Le Passé ReComposé. Archöologie Urbaine à Luxembourg*, pp 277–280. Ed J Zimmer. Luxembourg: Musée National d'Histoire et d'Art Luxembourg.
Müldner G 2016 Marine Fish Consumption in Medieval Britain: The Isotope Perspective from Human Skeletal Remains. In *Cod and Herring: The Archaeology and History of Medieval Sea Fishing*, pp 239–249. Eds J Barrett & D Orton. Oxford: Oxbow Books.
Müldner G & Richards MP 2005 Fast or feast: Reconstructing diet in later medieval England by stable isotope analysis. *Journal of Archaeological Science* **32** 39–48. (doi:10.1016/j.jas.2004.05.007)
Müldner G & Richards MP 2007a Diet and Diversity at Later Medieval Fishergate: The Isotopic Evidence. *American Journal of Physical Anthropology* **134** 162–174. (doi:10.1002/ajpa)
Müldner G & Richards MP 2007b Stable Isotope Evidence for 1500 Years of Human Diet at the City of York, UK. *American Journal of Physical Anthropology* **133** 682–697. (doi:10.1002/ajpa)
Müller A & Hussein K 2017 Meta-analysis of teeth from European populations before and after the 18th century reveals a shift towards increased prevalence of caries and tooth loss. *Archives of Oral Biology* **73** 7–15. (doi:10.1016/j.archoralbio.2016.08.018)
Mummert A, Esche E, Robinson J & Armelagos GJ 2011 Stature and robusticity during the agricultural transition: Evidence from the bioarchaeological record. *Economics and Human Biology* **9** 284–301. (doi:10.1016/j.ehb.2011.03.004)
Murail P, Bruzek J, Houët F & Cunha E 2005 DSP: A tool for probabilistic sex diagnosis using worldwide variability in hip-bone measurements. *Bulletins et Mémoires de La Société d'anthropologie de Paris* **17** 167–176. (doi:10.4000/bmsap.1157)
Nagaoka T, Ishida H, Tsurumoto T, Wakebe T, Saiki K & Hirata K 2019 A health crisis during the Japanese Medieval Period: A new paleodemographic perspective. *International Journal of Paleopathology* **26** 145–156. (doi:10.1016/j.ijpp.2019.03.005)
Nakayama N 2016 The Relationship Between Linear Enamel Hypoplasia and Social Status in 18th to 19th Century Edo, Japan. *International Journal of Osteoarchaeology* **26** 1034–1044. (doi:10.1002/oa.2515)
Nater C 2018 Social differences in burial practices in the medieval cemetery of Reusel: An osteoarchaeological and mortuary archaeological study of burial practices in the southern Netherlands during the Central Middle Ages. In *The Urban Graveyard: Archaeological Perspectives*, pp 51–87. Eds RMR Van Oosten, R Schats, K Fast, N Arts & HMP Bowmeester. Leiden: Sidestone Press.
Van Neer W & Ervynck A 2004 Remains of traded fish in archaeological sites: indicators of status, or bulk food? In *Behaviour Behind Bones: The Zooarchaeology of Ritual, Religion, Status and Identity*, pp 203–214. Eds S Jones O'Day, W Van Neer & A Ervynck. New York: Oxbow Books.
Newman SL & Gowland RL 2017 Dedicated Followers of Fashion? Bioarchaeological Perspectives on Socio-Economic Status, Inequality, and Health in Urban Children from the Industrial Revolution (18th–19th C), England. *International Journal of Osteoarchaeology* **27** 217–229. (doi:10.1002/oa.2531)
Nicholls R, Buckberry J, Beaumont J, Črešnar M, Mason P, Armit I & Koon H 2020 A carbon and nitrogen isotopic investigation of a case of probable infantile scurvy (6th–4th centuries BC, Slovenia). *Journal of Archaeological Science: Reports* **30**. (doi:10.1016/j.jasrep.2020.102206)
Niinimäki S & Baiges Sotos L 2013 The Relationship Between Intensity of Physical Activity and Entheseal Changes on the Lower Limb. *International Journal of Osteoarchaeology*

23 221–228. (doi:10.1002/oa.2295)
Nikiforuk G & Fraser D 1981 The etiology of enamel hypoplasia: A unifying concept. *The Journal of Pediatrics* **98** 888–893. (doi:10.1016/S0022-3476(81)80580-X)
Nikulka F 2016 *Archäologische Demographie. Methoden, Daten Und Bevölkerung Der Europäischen Bronze- Und Eisenzeiten*. Hamburg: Sidestone Press.
Nitsch EK, Humphrey LT & Hedges REM 2011 Using stable isotope analysis to examine the effect of economic change on breastfeeding practices in Spitalfields, London, UK. *American Journal of Physical Anthropology* **146** 619–628. (doi:10.1002/ajpa.21623)
Nothwang U & Rehbach N-J 2006 Abschlussbericht zur anthropologischen Untersuchung der Skelette aus der Kirchengrabung Fentingen. *ADAG Nothwang u. Partner, Frankfurt/Main* **2. Auflage**.
Nothwang U, Rehbach N-J & Flohr S 2004 Die "Gräberserie 'Hospice civil' - eine Bestandsaufnahme aus dem Barock. *Bulletin d'Information Du Musée National d'histoire et d'art, Luxembourg* **17** 67–68.
Novak M, Šlaus M & Pasarić M 2010 Subadult Stress in the Medieval and Early Modern Populations of Continental Croatia. *Prilozi Instituta Za Arheologiju* **26** 247–270.
O'Donnell L & Moes E 2021 Sex differences in linear enamel hypoplasia prevalence and frailty in Ancestral Puebloans. *Journal of Archaeological Science: Reports* **39** 103153. (doi:10.1016/j.jasrep.2021.103153)
O'Donnell L, Hill EC, Anderson ASA & Edgar HJH 2020 Cribra orbitalia and porotic hyperostosis are associated with respiratory infections in a contemporary mortality sample from New Mexico. *American Journal of Physical Anthropology* **173** 721–733. (doi:10.1002/ajpa.24131)
Obert M, Schulte-Geers C, Schilling RL, Harth S, Kläver M, Traupe H, Ramsthaler F & Verhoff MA 2010 High-resolution flat-panel volumetric CT images show no correlation between human age and sagittal suture obliteration-Independent of sex. *Forensic Science International* **200**. (doi:10.1016/j.forsciint.2010.04.006)
Obertová Z & Thurzo M 2008 Relationship between cribra orbitalia and enamel hypoplasia in the early medievel Slavic populaton at Borovce, Slovakia. *International Journal of Osteoarchaeology* **18** 280–292. (doi:10.1002/oa.937)
Obertová Z, Menninger M, Wahl J & Bis-Worch C 2008 Die „Traufkinder" von der Nordseite der „Kirche 10" in Grevenmacher (Luxemburg) – anthropologische Auswertung der Skelettreste. *Empreintes Annuaire Du Musée National d'histoire et d'art* **1** 92–99.
Odri GA, Tchicaya-Bouanga J, Yoon DJY & Modrowski D 2022 Metastatic Progression of Osteosarcomas: A Review of Current Knowledge of Environmental versus Oncogenic Drivers. *Cancers* **14** 1–16. (doi:10.3390/cancers14020360)
Ogden A 2007 Advances in the Palaeopathology of Teeth and Jaws. In *Advances in Human Palaeopathology*, pp 283–307. Eds R Pinhasi & S Mays. John Wiley & Sons, Ltd.
Oka K, Murase T, Moritomo H, Sugamoto K & Yoshikawa H 2010 Morphologic evaluation of chronic radial head dislocation: Three-dimensional and quantitative analyses. *Clinical Orthopaedics and Related Research* **468** 2410–2418. (doi:10.1007/s11999-010-1283-y)
Olivares JL, Fernández R, Fleta J, Ruiz MY & Clavel A 2002 Vitamin B12 and Folic Acid in Children with Intestinal Parasitic Infection. *Journal of the American College of Nutrition* **21** 109–113. (doi:10.1080/07315724.2002.10719202)
Olsen KC, White CD, Longstaffe FJ, Von Heyking K, McGlynn G, Grupe G & Rühli FJ 2014 Intraskeletal isotopic compositions (δ13C, δ15N) of bone collagen: Nonpathological and pathological variation. *American Journal of Physical Anthropology* **153** 598–604. (doi:10.1002/ajpa.22459)
Olsen KC, White CD, Longstaffe FJ, Rühli FJ, Warinner C & Salazar-García DC 2018

Isotopic anthropology of rural German medieval diet: intra- and inter-population variability. *Archaeological and Anthropological Sciences* **10** 1053–1065. (doi:10.1007/s12520-016-0432-y)
Onisto N, Maat GJR & Bult EJ 1998 Human Remains form the Infirmary 'Oude en Nieuwe Gasthuis' of the City of Delft in the Netherlands 1265-1652 AD. *Barge's Anthropologica* **2** 1998.
Opitz C 2006 Frauenalltag im Spätmittelalter (1250-1500). In *Geschichte Der Frauen. Band 2: Mittelalter*, pp 283–344. Ed C Klapisch-Zuber. Frankfurt am Main: Campus Verlag.
Orme N 2003 *Medieval Children*. New Haven: Yale University Press.
Ortner DJ 2003a *Identification of Pathological Conditions in Human Skeletal Remains*. Elsevier Academic Press.
Ortner DJ 2003b Tumors and tumor-like lesions of bone. In *Identification of Pathological Conditions in Human Skeletal Remains*, Second Edi, pp 503–544. Ed DJ Ortner. Elsevier Inc. (doi:10.1007/88-470-0339-3_10)
Ortner DJ 2003c Infectious diseases: Tuberculosis and leprosy. In *Identification of Pathological Conditions in Human Skeletal Remains*, pp 227–271. Ed DJ Ortner. Academic Press.
Ortner DJ & Ericksen MF 1997 Bone Changes in the Human Skull Probably Resulting from Scurvy in Infancy and Childhood. *International Journal of Osteoarchaeology* **7** 212–220. (doi:10.1002/(sici)1099-1212(199705)7:3<212::aid-oa346>3.0.co;2-5)
Ortner DJ & Mays S 1998 Dry-bone Manifestations of Rickets in Infancy and Early Childhood. *International Journal of Osteoarchaeology* **8** 45–55. (doi:10.1002/(SICI)1099-1212(199801/02)8:1<45::AID-OA405>3.0.CO;2-D)
Ortner DJ, Kimmerle EH & Diez M 1999 Probable evidence of scurvy in subadults from archeological sites in Peru. *American Journal of Physical Anthropology* **108** 321–331. (doi:10.1002/(SICI)1096-8644(199903)108:3<321::AID-AJPA7>3.0.CO;2-7)
Ortner DJ, Butler W, Cafarella J & Milligan L 2001 Evidence of probable scurvy in subadults from archeological sites in North America. *American Journal of Physical Anthropology* **114** 343–351. (doi:10.1002/ajpa.1046)
Osterberg PH, Wallace RGH, Adams DA, Crone RS, Dickson GR, Kanis JA, Mollan RAB, Nevin NC, Sloan J & Toner PG 1988 Familial expansile osteolysis. A new dysplasia. *Journal of Bone and Joint Surgery - Series B* **70** 255–260. (doi:10.1302/0301-620x.70b2.3346299)
Oxenham, M., & Willis A 2017 Towards a bioarchaeology of Care of Children. In *New Developments in the Bioarchaeology of Care: Further Case Studies and Expanded Theory*, pp 219–236. Eds L Tilley & AA Schrenk. Springer International Publishing.
Oxenham MF & Cavill I 2011 Porotic hyperostosis and cribra orbitalia: The erythropoietic response to iron-deficiency anaemia. *Anthropological Science* **118** 199–200. (doi:10.1537/ase.100302)
Özener B 2007 Biomechanical Pressures and Upper Extremity Asymmetry : A Study on Young Laborers. *Collegium Anthropologium* **31** 693–699.
Ozmen H, Akarsu S, Polat F & Cukurovali A 2013 The levels of calcium and magnesium, and of selected trace elements, in whole blood and scalp hair of children with growth retardation. *Iranian Journal of Pediatrics* **23** 125–130.
Paladin A, Wahl J & Zink A 2018 Evidence of probable subadult scurvy in the Early Medieval cemetery of Castel Tirolo, South Tyrol, Italy. *International Journal of Osteoarchaeology* **28** 714–726. (doi:10.1002/oa.2694)
Paladin A, Moghaddam N, Stawinoga AE, Siebke I, Depellegrin V, Tecchiati U, Lösch S & Zink A 2020 Early medieval Italian Alps: reconstructing diet and mobility in the valleys. *Archaeological and Anthropological Sciences* **12**. (doi:10.1007/s12520-019-00982-6)

Palmer AR 1994 Fluctuating Asymmetry Analyses: A Primer. In *Developmental Instability: Its Origins and Evolutionary Implications.*, pp 335–364. Ed TA Markow. Dordrecht, Netherlands: Kluwer.
Palmer JLA & Waters-Rist AL 2019 Acts of life: Assessing entheseal change as an indicator of social differentiation in postmedieval Aalst (Belgium). *International Journal of Osteoarchaeology* **29** 303–313. (doi:10.1002/oa.2740)
Palmer JLA, Hoogland MHL & Waters-Rist AL 2016 Activity Reconstruction of Post-Medieval Dutch Rural Villagers from Upper Limb Osteoarthritis and Entheseal Changes. *International Journal of Osteoarchaeology* **26** 78–92. (doi:10.1002/oa.2397)
Palmer JLA, Quintelier K, Inskip S & Waters-Rist AL 2019 A Comparison of Two Methods for Recording Entheseal Change on a Post-Medieval Urban Skeletal Collection from Aalst (Belgium). *Archaeometry* **61** 211–225. (doi:10.1111/arcm.12409)
Palubeckaitė Ž, Jankauskas R & Boldsen J 2002 Enamel hypoplasia in Danish and Lithuanian Late Medieval/early modern samples: A possible reflection of child morbidity and mortality patterns. *International Journal of Osteoarchaeology* **12** 189–201. (doi:10.1002/oa.607)
Palubeckaitė Ž, Jankauskas R, Ardagna Y, Macia Y, Rigeade C, Signoli M & Dutour O 2006 Dental status of Napoleon's Great Army's (1812) mass burial of soldiers in Vilnius: Childhood peculiarities and adult dietary habits. *International Journal of Osteoarchaeology* **16** 355–365. (doi:10.1002/oa.846)
Panchal J & Uttchin V 2003 Management of Craniosynostosis. *Plastic and Reconstructive Surgery* **111** 2032–2049. (doi:10.1055/s-0036-1582228)
Panhuysen RGAM, Coenen V & Bruintjes TD 1997 Chronic Maxillary Sinusitis in Medieval Maastricht, the Netherlands. *International Journal of Osteoarchaeology* **7** 610–614. (doi:10.1002/(SICI)1099-1212(199711/12)7:6<610::AID-OA366>3.0.CO;2-Q)
Paraskevas G, Stavrakas ME & Stoltidou A 2009 Coracoclavicular joint, an osteological study with clinical implications: A case report. *Cases Journal* **2**. (doi:10.4076/1757-1626-2-8715)
Parfitt AM 2002 Misconceptions (2): Turnover Is Always Higher in Cancellous Than in Cortical Bone. *Bone* **30** 807–809.
Park Y-K 2015 Enchondroma. In *Tumors and Tumor-Like Lesions of Bon*, pp 243–251. Eds E Santini-Araujo, R Kalil, F Bertoni & Y Park. London: Springer.
Parker K 2019 Health and Aging in Medieval and Post-medieval Denmark. University of Manitoba.
Patnaik S, Jyotsnarani Y, Uppin SG & Susarla R 2016 Imaging features of primary tumors of the spine: A pictorial essay. *Indian Journal of Radiology and Imaging* **26** 279–289. (doi:10.4103/0971-3026.184413)
Pauly M 1994 Le bas Moyen Age. Chance et handicaps d'une ville et de ses habitants. In *La Ville de Luxembourg- Du Château Des Comtes à La Métropole Européenne*, pp 61–79. Ed G Trausch. Fonds Mercator Anvers.
Pauly M 2011 *Geschichte Luxemburgs*. München: Verlag C.H. Beck oHG.
Pauly M 2020 Pestepidemien in Luxemburg. In *Self and Society in the Corona Crisis.Perspectives from the Humanities and Social Sciences*. Eds G Mein & J Pause. Luxembourg: Melusina Press.
Pauly M 2022a Eine Urbanismusdebatte aus dem Jahr 1561. In *Die Geschichte Der Stadt Luxemburg in 99 Objekten*, pp 117–118. Ed M Pauly. Luxembourg: Capybara Books.
Pauly M 2022b Stadtbrände und ein neues Rathaus. In *Die Geschichte Der Stadt Luxemburg in 99 Objekten*, pp 125–126. Ed M Pauly. Luxembourg: Capybara Books.
Pauly M 2022c Wou d'Uelzecht (net) duerch d'Wisen zéit... In *Fecit. W: Callot. Die Stadtansicht Luxemburgs von Wenzel Callot Aus Dem Jahr 1753*, 1st ed, pp 275–293.

Eds G Genot & Ä Bruns. Luxembourg: Lëtzebuerg City Museum.
Pearson K 1899 On the reconstruction of the stature of prehistoric races. Mathematical contributions to the theory of evolution. *Physical Transactions of the Royal Society of London* **192** 169–244.
Pearson MP 1999 *Archaeology of Death and Burial*. Sutton: Phoenix Mill.
Pearson OM 2000 Activity, climate, and postcranial robusticity: Implications for modern human origins and scenarios of adaptive change. *Current Anthropology* **41** 569–607. (doi:10.1086/317382)
Pearson JA, Hedges REM, Molleson TI & Özbek M 2010 Exploring the relationship between weaning and infant mortality: An isotope case study from Aşikli Höyük and Çayönü Tepesi. *American Journal of Physical Anthropology* **143** 448–457. (doi:10.1002/ajpa.21335)
Peres KG, Chaffee BW, Feldens CA, Flores-Mir C, Moynihan P & Rugg-Gunn A 2018 Breastfeeding and Oral Health: Evidence and Methodological Challenges. *Journal of Dental Research* **97** 251–258. (doi:10.1177/0022034517738925)
Perez-Arzak U, Villotte S, Arrizabalaga A & Trancho GJ 2022 Looking for the most suitable method for the study of entheseal changes: Application to upper limb's fibrocartilaginous entheses in a human medieval sample. *International Journal of Osteoarchaeology* **32** 595–606. (doi:10.1002/oa.3085)
Perizonius WRK 1984 Closing and non-closing sutures in 256 crania of known age and sex from Amsterdam (a.d. 1883-1909). *Journal of Human Evolution* **13** 201–216. (doi:10.1016/S0047-2484(84)80065-2)
Perry EM 2004 Bioarchaeology of labor and gender in the prehispanic American Southwest. University of Arizona, Tucson.
Pētersone-Gordina E & Gerhards G 2012 Dental disease in a 17th–18th century German community in Jelgava, Latvia. *Papers on Anthropology* **20** 327. (doi:10.12697/poa.2011.20.31)
Pētersone-Gordina E, Gerhards G & Jakob T 2013 Nutrition-related health problems in a wealthy 17-18th century German community in Jelgava, Latvia. *International Journal of Paleopathology* **3** 30–38. (doi:10.1016/j.ijpp.2013.01.002)
Pētersone-Gordina E, Roberts C, Millard AR, Montgomery J & Gerhards G 2018 Dental disease and dietary isotopes of individuals from St Gertrude Church cemetery, Riga, Latvia. *PLoS ONE* **13** 1–26. (doi:10.1371/journal.pone.0191757)
Pfeiffer S 1980 Age changes in the external dimensions of adult bone. *American Journal of Physical Anthropology* **52** 529–532. (doi:10.1002/ajpa.1330520409)
Phenice TW 1969 A newly developed visual method of sexing the os pubis. *American Journal of Physical Anthropology* **30** 297–301. (doi:10.1002/ajpa.1330300214)
Philippart R 1994 Témoins du passé. Demeures seignorales et bourgeoises. In *La Ville de Luxembourg- Du Château Des Comtes à La Métropole Européenne*, pp 155–165. Ed G Trausch. Fonds Mercator Anvers.
Pieper H-G 1998 Retrotorsion of the Humerus in the Throwing Arm of Handball Player - An Adaptation to Unilateral Strain. *16th International Symposium on Biomechanics in Sports* 321–324.
Pietrokovski J, Starinsky R, Arensburg B & Kaffe I 2007 Morphologic characteristics of bony edentulous jaws. *Journal of Prosthodontics* **16** 141–147. (doi:10.1111/j.1532-849X.2007.00165.x)
Pinhasi R & Mays S 2007 *Advances in Human Palaeopathology*. (doi:10.1002/9780470724187)
Plochocki JH 2004 Article Bilateral Variation in Limb Articular Surface Dimensions. *American Journal of Human Biology* **16** 328–333. (doi:10.1002/ajhb.20023)

Polet C & Katzenberg MA 2003 Reconstruction of the diet in a mediaeval monastic community from the coast of Belgium. *Journal of Archaeological Science* **30** 525–533. (doi:10.1016/S0305-4403(02)00183-8)
Portales F, Thézenas S, Samalin E, Assenat E, Mazard T & Ychou M 2015 Bone metastases in gastrointestinal cancer. *Clinical and Experimental Metastasis* **32** 7–14. (doi:10.1007/s10585-014-9686-x)
Posselt J-U 1997 Die Arthrosis deformans – Unter-suchungen an einer Bevölkerung des 16. bis 18. Jahr-hunderts aus Brandenburg an der Havel. Freie Universität Berlin.
Powers N 2008 Human osteology method statement. *Mola*.
Primeau C, Homøe P & Lynnerup N 2018 Childhood health as reflected in adult urban and rural samples from medieval Denmark. *Homo* **69** 6–16. (doi:10.1016/j.jchb.2018.03.004)
Privat KL, O'connell TC & Richards MP 2002 Stable isotope analysis of human and faunal remains from the Anglo-Saxon Cemetery and Berinsfield, Oxfordshire: Dietary and social implications. *Journal of Archaeological Science* **29** 779–790. (doi:10.1006/jasc.2001.0785)
Prowse TL, Saunders SR, Schwarcz HP, Garnsey P, Macchiarelli R & Bondioli L 2008 Isotopic and dental evidence for infant and young child feeding practices in an imperial roman skeletal sample. *American Journal of Physical Anthropology* **137** 294–308. (doi:10.1002/ajpa.20870)
Quatrehomme G, Radoman I, Nogueira L, du Jardin P & Alunni V 2017 Sex determination using the DSP (probabilistic sex diagnosis) method on the coxal bone: Efficiency of method according to number of available variables. *Forensic Science International* **272** 190–193. (doi:10.1016/j.forsciint.2016.10.020)
Quigley MA, Kelly YJ & Sacker A 2007 Breastfeeding and Hospitalization for Diarrheal and Respiratory Infection in the United Kingdom Millennium Cohort Study. *Pediatrics* **119** e837–e842. (doi:10.1542/peds.2006-2256)
Quinlan RJ 2007 Human parental effort and environmental risk. *Proceedings of the Royal Society B: Biological Sciences* **274** 121–125. (doi:10.1098/rspb.2006.3690)
Quintelier K, Ervynck A, Müldner G, Van Neer W, Richards MP & Fuller BT 2014 Isotopic examination of links between diet, social differentiation, and DISH at the post-medieval Carmelite Friary of Aalst, Belgium. *American Journal of Physical Anthropology* **153** 203–213. (doi:10.1002/ajpa.22420)
Ragsdale BD, Campbell RA & Kirkpatrick CL 2018 Neoplasm or not? General principles of morphologic analysis of dry bone specimens. *International Journal of Paleopathology* **21** 27–40. (doi:10.1016/j.ijpp.2017.02.002)
Rajkumar SV & Kumar S 2016 Multiple Myeloma: Diagnosis and Treatment. *Mayo Clinic Proceedings* **91** 101–119. (doi:10.1016/j.mayocp.2015.11.007)
Rana RS, Wu JS & Eisenberg RL 2009 Periosteal reaction. *American Journal of Roentgenology* **193** 259–278. (doi:10.2214/AJR.09.3300)
Rao VM & Karasick D 1982 Hypercementosis - An Important Clue to Paget Disease of the Maxilla. *Skeletal Radiology* **9** 126–128.
Raxter MH, Auerbach BM & Ruff CB 2006 Revision of the fully technique for estimating statures. *American Journal of Physical Anthropology* **130** 374–384. (doi:10.1002/ajpa.20361)
Redfern R & Roberts CA 2019 *Trauma*. Elsevier Inc. (doi:10.1016/B978-0-12-809738-0.00009-0)
Redfern RC, DeWitte SN, Beaumont J, Millard AR & Hamlin C 2019 A new method for investigating the relationship between diet and mortality: hazard analysis using dietary isotopes. *Annals of Human Biology* **46** 378–387. (doi:10.1080/03014460.2019.1662484)

Reeves NM, Auerbach BM & Sylvester AD 2016 Fluctuating and directional asymmetry in the long bones of captive cotton-top tamarins (Saguinus oedipus). *American Journal of Physical Anthropology* **160** 41–51. (doi:10.1002/ajpa.22942)
Rehbach N-J 2008 Abschlußbericht zur anthropologischen Untersuchung der Gräberserie aus dem ehemaligen Kloster St. Esprit/Luxemburg. *ADFG Nothwang u. Partner, Frankfurt/Main*.
Rehbach N-J & Bis-Worch C 2006 Das Kloster St.Esprit in Luxemburg und seine Toten. *Beiträge Zur Archäozoologie Und Prähistorischen Anthropologie V* 110–117.
Rehbach N-J, Nothwang U & Flohr S 2005 Die menschlichen Skelettfunde aus Fentingen – ein Vorbericht. *Bulletin d'Information de Musée National d'histoire et d'art, Luxembourg* **18** 70–72.
Rehbach N-J, Nothwang U, Weidig I & Sindermann A 2009 Abschlussbericht zur anthropologischen Untersuchung einer Givenicher Skelettserie aus dem 8.-15. Jahrhundert. *ADFG Nothwang u. Partner, Frankfurt/Main* **3. korrigi**.
Reid DJ & Dean MC 2000 Brief communication: The timing of linear hypoplasias on human anterior teeth. *American Journal of Physical Anthropology* **113** 135–139. (doi:10.1002/1096-8644(200009)113:1<135::aid-ajpa13>3.0.co;2-a)
Reid DJ & Dean MC 2006 Variation in modern human enamel formation times. *Journal of Human Evolution* **50** 329–346. (doi:10.1016/j.jhevol.2005.09.003)
Reitsema LJ 2013 Beyond diet reconstruction: Stable isotope applications to human physiology, health, and nutrition. *American Journal of Human Biology* **25** 445–456. (doi:10.1002/ajhb.22398)
Reitsema LJ & Vercellotti G 2012 Stable isotope evidence for sex- and status-based variations in diet and life history at medieval Trino Vercellese, Italy. *American Journal of Physical Anthropology* **148** 589–600. (doi:10.1002/ajpa.22085)
Reitsema LJ, Crews DE & Polcyn M 2010 Preliminary evidence for medieval Polish diet from carbon and nitrogen stable isotopes. *Journal of Archaeological Science* **37** 1413–1423. (doi:10.1016/j.jas.2010.01.001)
Reitsema LJ, Kozłowski T & Makowiecki D 2013 Human-environment interactions in medieval Poland: A perspective from the analysis of faunal stable isotope ratios. *Journal of Archaeological Science* **40** 3636–3646. (doi:10.1016/j.jas.2013.04.015)
Reuter J 1966 Die Kirche in der tausendjährigen Geschichte der Stadt Luxemburg - Die Franziskaner in Luxemburg (1250-1796). *Hémecht* **18** 405–431.
Rhodes JA & Knüsel CJ 2005 Activity-related skeletal change in medieval humeri: Cross-sectional and architectural alterations. *American Journal of Physical Anthropology* **128** 536–546. (doi:10.1002/ajpa.20147)
Ribot I & Roberts C 1996 A study of non-specific stress indicators and skeletal growth in two mediaeval subadult populations. *Journal of Archaeological Science* **23** 67–79. (doi:10.1006/jasc.1996.0006)
Ricci R, Lama R, Di Tota G, Capelli A & Capasso L 1995 Some Considerations about the Incidence of Neoplasms in the Human History. *Journal of Palaeopathology* **7** 5–12.
Riccomi G, Fornaciari G & Giuffra V 2019 Multiple myeloma in paleopathology: A critical review. *International Journal of Paleopathology* **24** 201–212. (doi:10.1016/j.ijpp.2018.12.001)
Richards MP & Hedges REM 1999 Stable isotope evidence for similarities in the types of marine foods used by late Mesolithic humans at sites along the Atlantic coast of Europe. *Journal of Archaeological Science* **26** 717–722. (doi:10.1006/jasc.1998.0387)
Richards MP, Pettitt PB, Stiner MC & Trinkaus E 2001 Stable isotope evidence for increasing dietary breadth in the European mid-Upper Paleolithic. *Proceedings of the National Academy of Sciences of the United States of America* **98** 6528–6532.

(doi:10.1073/pnas.111155298)
Richards MP, Mays S & Fuller BT 2002 Stable carbon and nitrogen isotope values of bone and teeth reflect weaning age at the Medieval Wharram Percy site, Yorkshire, UK. *American Journal of Physical Anthropology* **119** 205–210. (doi:10.1002/ajpa.10124)
Richards MP, Fuller BT & Molleson TI 2006 Stable isotope palaeodietary study of humans and fauna from the multi-period (Iron Age, Viking and Late Medieval) site of Newark Bay, Orkney. *Journal of Archaeological Science* **33** 122–131. (doi:10.1016/j.jas.2005.07.003)
Rinaldo N, Zedda N, Bramanti B, Rosa I & Gualdi-Russo E 2019 How reliable is the assessment of Porotic Hyperostosis and Cribra Orbitalia in skeletal human remains? A methodological approach for quantitative verification by means of a new evaluation form. *Archaeological and Anthropological Sciences* **11** 3549–3559. (doi:10.1007/s12520-019-00780-0)
Ritchie H, Spooner F & Roser M 2018 Causes of death. In *Our World in Data*.
Rivera F & Mirazón Lahr M 2017 New evidence suggesting a dissociated etiology for cribra orbitalia and porotic hyperostosis. *American Journal of Physical Anthropology* **164** 76–96. (doi:10.1002/ajpa.23258)
Rizzoli R 2008 Nutrition: its role in bone health. *Best Practice and Research: Clinical Endocrinology and Metabolism* **22** 813–829. (doi:10.1016/j.beem.2008.08.005)
Robb J, Bigazzi R, Lazzarini L, Scarsini C & Sonego F 2001 Social 'status' and biological 'status': A comparison of grave goods and skeletal indicators from Pontecagnano. *American Journal of Physical Anthropology* **115** 213–222. (doi:10.1002/ajpa.1076)
Roberts CA 2019 *Infectious Disease*. Elsevier Inc. (doi:10.1016/B978-0-12-809738-0.00010-7)
Roberts CA & Buikstra JE 2019 *Bacterial Infections*. Elsevier Inc. (doi:10.1016/B978-0-12-809738-0.00011-9)
Roberts CA & Cox M 2003 *Health and Disease in Britain: From Prehistory to the Present Day*. Sutton Publishing Limited. (doi:10.1002/oa.742)
Roberts C & Manchester K 2010 *The Archaeology of Disease*. The History Press.
Roches E, Blondiaux J, Cotten A, Chastanet P & Flipo RM 2002 Microscopic evidence for Paget's disease in two osteoarchaeological samples from early northern France. *International Journal of Osteoarchaeology* **12** 229–234. (doi:10.1002/oa.617)
Rogers J & Waldron T 2001 DISH and the monastic way of life. *International Journal of Osteoarchaeology* **11** 357–365. (doi:10.1002/oa.574)
Rogers J, Watt I & Dieppe P 1985 Palaeopathology of spinal osteophytosis, vertebral ankylosis, ankylosing spondylitis, and vertebral hyperostosis. *Annals of the Rheumatic Diseases* **44** 113–120. (doi:10.1136/ard.44.2.113)
Rollet E 1888 *De La Mensuration Des Os Longs Des Membres, Dans Ses Rapports Avec l'anthropologie, La Clinique et La Médicine Judiciare*. Lyon: Storck.
Rösener W 2001 Stadt-Land-Beziehungen im Mittelalter. In *Dorf Und Stadt*, pp 35–65. Ed C Zimmermann. Frankfurt am Main: DLG-Verlag.
Rosenstock E 2014 Eiweißversorgung und Körperhöhe : zur Übertragbarkeit anthropometrischer Ansätze auf die Archäologie. In *Vom Nil Bis an Die Elbe. Forschungen Aus Fünf Jahrzehnten Am Institut Für Prähistorische Archäologie Der Freien Universität Berlin*, pp 147–164. Eds W Schier & M Meyer. Berlin: VML Maries Leidorf Verlag.
Rösing FW 1988 Körperhöhenrekonstruktion aus Skelettmaßen. In *Anthropologie: Handbuch Der Vergleichenden Biologie Des Menschen 1*, pp 586–600. Ed R Knussmann. Stuttgart: Spektrum Akademischer Verlag.
Roßbach AES 2015 Leben und Sterben im Mittelalter und der Frühen Neuzeit im Vergleich

von Bevölkerungen aus Hettstedt (Sachsen-Anhalt) und Völklingen (Saarland).
Rössler H & Rüther W 2005 *Orthopädie Und Unfallchirurgie*. Elsevier Urban & Fischer.
Rothschild BM & Rothschild C 1997 Congenital Syphilis in the Archaeological Record: Diagnostic Insensitivity of Osseous Lesions. *International Journal of Osteoarchaeology* **7** 39–42. (doi:10.1002/(sici)1099-1212(199701)7:1<39::aid-oa313>3.0.co;2-j)
Rothschild BM, Hershkovitz I, Dutour O, Latimer B, Rothschild C & Jellema LM 1997 Recognition of leukemia in skeletal remains: Report and comparison of two cases. *American Journal of Physical Anthropology* **102** 481–496. (doi:10.1002/(SICI)1096-8644(199704)102:4<481::AID-AJPA5>3.0.CO;2-V)
Rothschild BM, Hershkovitz I & Dutour O 1998 Clues potentially distinguishing lytic lesions of multiple myeloma from those of metastatic carcinoma. *American Journal of Physical Anthropology* **105** 241–250. (doi:10.1002/(SICI)1096-8644(199802)105:2<241::AID-AJPA10>3.0.CO;2-0)
Rothschild BM, Zdilla MJ, Jellema LM & Lambert HW 2021 Cribra orbitalia is a vascular phenomenon unrelated to marrow hyperplasia or anemia: Paradigm shift for cribra orbitalia. *Anatomical Record* **304** 1709–1716. (doi:10.1002/ar.24561)
Round JM, Jones DA, Honour JW & Nevill AM 1999 Hormonal factors in the development of differences in strength between boys and girls during adolescence : a longitudinal study. *Annals of Human Biology* **26** 49–62. (doi:10.1080/030144699282976)
Roy TA, Ruff CB & Plat CC 1994 Hand Dominance and Bilateral Asymmetry in the Structure of the Second Metacarpal. *American Journal of Physical Anthropology* **94** 203–211.
Rubio Salvador Á, Jiménez-Brobeil SA, Sánchez-Barba Muñoz LP & Molina F 2019 New case of concha bullosa from Bronze Age Iberia (Granada, Spain). *International Journal of Paleopathology* **24** 154–157. (doi:10.1016/j.ijpp.2018.10.009)
Ruff CB 1994 Biomechanical analysis of northern and southern Plains femora: behavioral implications. In *Skeletal Biology in the Great Plains: Migration, Warfare, Health, and Subsistence*. Eds DW Owsley & RL Jantz. Washington D.C.: Smithonian Institution Press.
Ruff CB 2000 Body size, body shape, and long bone strength in modern humans. *Journal of Human Evolution* **38** 269–290. (doi:10.1006/jhev.1999.0322)
Ruff CB 2007 Biomechanical Analyses of Archaeological Human Skeletons. In *Biological Anthropology of the Human Skeleton: Second Edition*, 3rd ed, pp 183–206. Eds AM Katzenberg & AL Grauer. John Wiley & Sons, Inc. (doi:10.1002/9780470245842.ch6)
Ruff CB & Jones HH 1981 Bilateral asymmetry in cortical bone of the humerus and tibia — sex and age factors. *Human Biology* **53** 69–86.
Ruff CB, Larsen CS & Hayes WC 1984 Structural changes in the femur with the transition to agriculture on the Georgia coast. *American Journal of Physical Anthropology* **64** 125–136. (doi:10.1002/ajpa.1330640205)
Ruff CB, Scott WW & Liu AY-. 1991 Articular and diaphyseal remodeling of the proximal femur with changes in body mass in adults. *American Journal of Physical Anthropology* **86** 397–413. (doi:10.1002/ajpa.1330860306)
Ruff CB, Trinkaus E & Holliday TW 1997 Body mass and encephalization in Pleistocene Homo. *Nature* **387** 173–176.
Ruff CB, Holt BM, Niskanen M, Sladék V, Berner M, Garofalo E, Garvin HM, Hora M, Maijanen H, Niinimäki S *et al.* 2012 Stature and body mass estimation from skeletal remains in the European Holocene. *American Journal of Physical Anthropology* **148** 601–617. (doi:10.1002/ajpa.22087)
Rusu MC, Măru N, Sava CJ, Săndulescu M & Dincă D 2019a Rare anatomic variation: Giant unilateral concha bullosa superior. *Morphologie* **103** 54–59.

(doi:10.1016/j.morpho.2018.12.001)
Rusu I, Radu C, Țentea O, Popescu O & Kelemen B 2019b A probable case of infantile cortical hyperostosis in 2nd–4th centuries AD Romania. *International Journal of Paleopathology* **26** 8–13. (doi:10.1016/j.ijpp.2019.05.004)
Rutgers L V., van Strydonck M, Boudin M & van der Linde C 2009 Stable isotope data from the early Christian catacombs of ancient Rome: new insights into the dietary habits of Rome's early Christians. *Journal of Archaeological Science* **36** 1127–1134. (doi:10.1016/j.jas.2008.12.015)
Sabnis A & Mane P 2020 A case report on ossified thyroid cartilage. *The Journal of Medical Research* **6** 7–8. (doi:10.31254/jmr.2020.6103)
Sahni D, Jit I, Neelam & Sanjeev 2005 Time of closure of cranial sutures in northwest Indian adults. *Forensic Science International* **148** 199–205. (doi:10.1016/j.forsciint.2004.06.002)
Sakai T, Sairyo K, Suzue N, Kosaka H & Yasui N 2010 Incidence and etiology of lumbar spondylolysis: Review of the literature. *Journal of Orthopaedic Science* **15** 281–288. (doi:10.1007/s00776-010-1454-4)
Sakamoto A, Oda Y & Iwamoto Y 2013 Intraosseous ganglia: A series of 17 treated cases. *BioMed Research International* **2013** 3–6. (doi:10.1155/2013/462730)
Sakaue K 1998 Bilateral Asymmetry of the Humerus in Jomon People and Modern Japanese. *Anthropological Science* **105** 231–246.
Salamon M, Coppa A, McCormick M, Rubini M, Vargiu R & Tuross N 2008 The consilience of historical and isotopic approaches in reconstructing the medieval Mediterranean diet. *Journal of Archaeological Science* **35** 1667–1672. (doi:10.1016/j.jas.2007.11.015)
Salva JE & Merrill AE 2017 Signaling networks in joint development. *Developmental Dynamics* **246** 262–274. (doi:10.1002/dvdy.24472)
Salvolini E, Di Giorgio R, Curatola A, Mazzanti L & Fratto G 1998 Biochemical modifications of human whole saliva induced by pregnancy. *BJOG: An International Journal of Obstetrics and Gynaecology* **105** 656–660. (doi:10.1111/j.1471-0528.1998.tb10181.x)
Santos AL & Roberts CA 2001 A picture of tuberculosis in young Portuguese people in the early 20th century: A multidisciplinary study of the skeletal and historical evidence. *American Journal of Physical Anthropology* **115** 38–49. (doi:10.1002/ajpa.1054)
Satter EK & High WA 2008 Langerhans cell histiocytosis: A review of the current recommendations of the histiocyte society. *Pediatric Dermatology* **25** 291–295. (doi:10.1111/j.1525-1470.2008.00669.x)
Schaaf C & Zschocke J 2013 *Basiswissen Humangenetik*. Springer.
Schaefer M, Black S & Scheuer L 2009 *Juvenile Osteology: A Laboratory and Field Manual*. Academic Press. (doi:10.1016/b978-0-12-374635-1.x0001-x)
Schajowicz F, Clavel Sainz M & Slullitel JA 1979 Juxta-articular bone cysts (intra-osseous ganglia). A clinicopathological study of eighty-eight cases. *Journal of Bone and Joint Surgery - Series B* **61** 107–116. (doi:10.1302/0301-620x.61b1.422629)
Schattmann A, Bertrand B, Vatteoni S & Brickley M 2016 Approaches to co-occurrence: Scurvy and rickets in infants and young children of 16-18th century Douai, France. *International Journal of Paleopathology* **12** 63–75. (doi:10.1016/j.ijpp.2015.12.002)
Schäuble A 2007 Ernährungsrekonstruktion zweier mittelalterlicher Bevölkerungen aus Brandenburg anhand der Analyse stabiler Isotope. *Mitteilungen Der DGAMN: Küche-Knochen-Ernährung* **Bd. 19** 269–286.
Scheuer L & Black S 2000 *Developmental Juvenile Osteology*. Elsevier Academic Press.
Schiebler TH, Schmidt W & Zilles K 1995 *Anatomie. Zytologie, Histologie, Entwicklungsgeschichte, Makroskopische Und Mikroskopische Anatomie Des*

Menschen. Springer.
Schmidt J, Kwok C & Keenleyside A 2016 Infant feeding practices and childhood diet at Apollonia Pontica: Isotopic and dental evidence. *American Journal of Physical Anthropology* **159** 284–299. (doi:10.1002/ajpa.22874)
Schmitt M 1994 Luxembourg, métropole religieuse d'un duché. In *La Ville de Luxembourg-Du Château Des Comtes à La Métropole Européenne*, pp 143–154. Ed G Trausch. Fonds Mercator Anvers.
Schoch T, Staub K & Pfister C 2012 Social inequality and the biological standard of living: An anthropometric analysis of Swiss conscription data, 1875-1950. *Economics and Human Biology* **10** 154–173. (doi:10.1016/j.ehb.2011.05.001)
Schoeninger MJ & DeNiro MJ 1984 Nitrogen and carbon isotopic composition of bone collagen from marine and terrestrial animals. *Geochimica et Cosmochimica Acta* **48** 625–639. (doi:10.1016/0016-7037(84)90091-7)
Schoeninger MJ, Deniro MJ & Tauber H 1983 Stable nitrogen isotope ratios of bone collagen reflect marine and terrestrial components of prehistoric human diet. *Science* **220** 1381–1383. (doi:10.1126/science.6344217)
Scholkmann B 2009 Das Mittelalter im Fokus der Archäologie. In *Archäologie in Deutschland*. Stuttgart.
Schott L 1960 Zur Kraniologie von Leipziger Mönchen des ausgehenden Mittelalters. Ein Beitrag zur Frage der Mitteldeutschen Brachycephalisation. *Arbeits- Und Forschungs-Berichte Zur Sächsischen Bodendenkmalpflege.* **9** 59–206.
Schott L 1964 Die Sexualrelation bei einigen hochmittelalterlichen Siedlungen nach ihrer palaodemographischen Rekonstruktion. *Zeitschrift Für Morphologie Und Anthropologie* **55** 60–71.
Schour I & Massler M 1941 Development of human dentition chart. *American Dental Association.* **2nd ed.**
Schrader SA 2015 Elucidating inequality in Nubia: An examination of entheseal changes at Kerma (Sudan). *American Journal of Physical Anthropology* **156** 192–202. (doi:10.1002/ajpa.22637)
Schrader S 2019 Bioarchaeological Approaches to Activity Reconstruction. In *Bioarchaeology and Social Theory*, pp 55–126. (doi:10.1007/978-3-030-02544-1_3)
Schroeder HE 1997 *Pathobiologie Oraler Strukturen, Zähne, Pulpa, Parodont*. Karger Medical and Scientific Publishers.
Schultz M 1982 Umwelt und Krankheit des vor- und frühgeschichtlichen Menschen. In *Kindler Enzyklopädie Der Mensch*, Band 2, pp 251–312. Eds H Wendt & N Loacker. Zürich: Kindler Verlag AG.
Schultz M 1988 Paläopathologische Diagnostik. In *Anthropologie. Handbuch Der Vergleichenden Biologie Des Menschen. Bd. 1: Wesen Und Methoden Der Anthropologie. 1. Teil: Wissenschaftstheorie, Geschichte, Morphologische Methoden*, pp 480–496. Ed R Knussmann.
Schultz H 1991 Social differences in mortality in the eighteenth century: An analysis of berlin church registers. *International Review of Social History* **36** 232–248. (doi:10.1017/S002085900011051X)
Schultz M, Carli-Thiele P, Schmidt-Schultzf TH, Kierdorf U, Kierdorf H, Teegen W-R & Kreutz K 1998 Enamel Hypoplasias in Archaeological Skeletal Remains. In *Dental Anthropology*, pp 293–311. Eds Alt, Kurt W., FW Rösing & M Teschler-Nicola. Wien, New York: Springer. (doi:10.1007/978-3-7091-7496-8_16)
Schurr MR 1997 Stable Nitrogen Isotopes as Evidence for the Age of Weaning at the Angel Site: A Comparison of Isotopic and Demographic Measures of Weaning Age. *Journal of Anthropological Science* **27** 919–927. (doi:10.1006/jasc.1996.0171)

Schurr MR 1998 Using stable nitrogen-isotopes to study weaning behavior in past populations. *World Archaeology* **30** 327–342. (doi:10.1080/00438243.1998.9980413)
Schutkowski H 1989 Beitrag zur Alters- und Geschlechtsdiagnose am Skelett nichterwachsener Individuen. *Anthropologischer Anzeiger* **47** 1–9.
Schutkowski H 1990 Zur Geschlechtsdiagnose von Kinderskeletten. Morphologische, metrische und diskriminanzanalytische Untersuchungen. Universität Göttingen.
Schutkowski H 1993 Sex determination of infant and juvenile skeletons: I. Morphognostic features. *American Journal of Physical Anthropology* **90** 199–205. (doi:10.1002/ajpa.1330900206)
Schutkowski H, Herrmann B, Wiedemann F, Bocherens H & Grupe G 1999 Diet, status and decomposition at Weingarten: Trace element and isotope analyses on early mediaeval skeletal material. *Journal of Archaeological Science* **26** 675–685. (doi:10.1006/jasc.1998.0384)
Schwarcz HP & Schoeninger MJ 2012 Stable isotopes of carbon and nitrogen as tracers for paleo-diet reconstruction. In *Handbook of Environmental Isotope Geochemistry. Advances of Geochemistry*, pp 725–742. Ed M Baskaran. Berlin, Heidelberg: Springer.
Scott AB & Hoppa RD 2018 The subtleties of stress: A comparative analysis of skeletal lesions between the Medieval and post-Medieval Black Friars cemetery population (13th to 17th centuries). *International Journal of Osteoarchaeology* **28** 695–702. (doi:10.1002/oa.2691)
Scott GR & Turner CG 1988 Dental Anthropology. *Annual Review of Anthropology* **17** 99–126.
Segura Marcenes W & Sheiham A 1992 The relationship between work stress and oral health status. *Social Science and Medicine* **35** 1511–1520. (doi:10.1016/0277-9536(92)90054-T)
Sellam J & Berenbaum F 2012 Osteoarthritis and Obsity. *La Revue Du Practicien* **62** 621–624.
Sellen DW 2001 Comparison of infant feeding patterns reported for nonindustrial populations with current recommendations. *Journal of Nutrition* **131** 2707–2715. (doi:10.1093/jn/131.10.2707)
Selwitz RH, Ismail A & Pitts NB 2007 Dental caries. *Lancet* **369** 51–59.
Sencan D, Elden H, Nacitarhan V, Sencan M & Kaptanoglu E 2005 The prevalence of diffuse idiopathic skeletal hyperostosis in patients with diabetes mellitus. *Rheumatology International* **25** 518–521. (doi:10.1007/s00296-004-0474-9)
Senol RGT & Yucel AH 2019 Evaluation and Categorization of Femur Morphometry with Digital Measurement Method. *Journal of Evolution of Medical and Dental Sciences* **8** 3064–3069. (doi:10.14260/jemds/2019/666)
Seton M, Moses AM, Bode RK & Schwartz C 2011 Paget's disease of bone: The skeletal distribution, complications and quality of life as perceived by patients. *Bone* **48** 281–285. (doi:10.1016/j.bone.2010.09.021)
Shaw CN & Stock JT 2009 Habitual throwing and swimming correspond with upper limb diaphyseal strength and shape in modern human athletes. *American Journal of Physical Anthropology* **140** 160–172. (doi:10.1002/ajpa.21063)
Shiau HJ & Reynolds MA 2010a Sex Differences in Destructive Periodontal Disease: A Systematic Review. *Journal of Periodontology* **81** 1379–1389. (doi:10.1902/jop.2010.100044)
Shiau HJ & Reynolds MA 2010b Sex Differences in Destructive Periodontal Disease: Exploring the Biologic Basis. *Journal of Periodontology* **81** 1505–1517. (doi:10.1902/jop.2010.100045)
Siddartha, Bhat V, Bhandary SK, Shenoy V & Rashmi 2011 Otitis Media with Effusion in

Relation to Socio Economic Status: A Community Based Study. *Association of Otolaryngologists of India* 56–58.
Siegmund F 2010a Körpergewicht und BMI bezeugen einen hohen Lebensstandard im europäischen Mittelalter. *Ethnographisch-Archäologische Zeitschrift* **51** 258–282.
Siegmund F 2010b *Die Körpergröße Der Menschen in Der Ur- Und Frühgeschichte Mitteleuropas Und Ein Vergleich Ihrer Anthropologischen Schätzmethoden*. Norderstedt: Books on Demand GmbH.
Siek TJ 2019 Reconsidering Palaeoepidemiological Investigations in Palaeo-Oncology. University College London.
Siek T 2020 In defence of the osteoma: The relevance of benign tumours in bioarchaeology and palaeo-oncology. *International Journal of Osteoarchaeology* **30** 281–283. (doi:10.1002/oa.2839)
Siek TJ & Spinek AE 2021 A differentially diagnosed simple bone cyst from a medieval Polish osteological collection. *International Journal of Osteoarchaeology* **32** 910–915. (doi:10.1002/oa.3086)
Siek TJ, Rando C, Spinek AE, Cieślik A & Waldron T 2021a Malignancy in three medieval Polish osteological collections. *Journal of Archaeological Science: Reports* **40**. (doi:10.1016/j.jasrep.2021.103246)
Siek T, Rando C, Cieślik A, Spinek A & Waldron T 2021b A palaeoepidemiological investigation of osteomata, with reference to medieval Poland. *International Journal of Osteoarchaeology* **31** 154–161. (doi:10.1002/oa.2935)
Sillen A & Smith P 1984 Weaning patterns are reflected in strontium-calcium ratios of juvenile skeletons. *Journal of Archaeological Science* **11** 237–245. (doi:10.1016/0305-4403(84)90004-9)
Silventoinen K 2003 Determinants of variation in adult body height. *Journal of Biosocial Science* **35** 263–285. (doi:10.1017/S0021932003002633)
Silventoinen K, Kaprio J, Lahelma E & Koskenvuo M 2000 Relative effect of genetic and environmental factors on body height: Differences across birth cohorts among finnish men and women. *American Journal of Public Health* **90** 627–630. (doi:10.2105/AJPH.90.4.627)
Silventoinen K, Sammalisto S, Perola M, Boomsma DI, Cornes BK, Davis C, Dunkel L, De Lange M, Harris JR, Hjelmborg JVB *et al.* 2003 Heritability of Adult Body Height: A Comparative Study of Twin Cohorts in Eight Countries. *Twin Research* **6** 399–408. (doi:10.1375/136905203770326402)
Šlaus M 2000 Biocultural analysis of sex differences in mortality profiles and stress levels in the late medieval population from Nova Raca, Croatia. *American Journal of Physical Anthropology* **111** 193–209. (doi:10.1002/(SICI)1096-8644(200002)111:2<193::AID-AJPA6>3.0.CO;2-0)
Šlaus M, Bedić Ž, Rajić Šikanjić P, Vodanović M & Domić Kunić A 2011 Dental health at the transition from the Late Antique to the early Medieval period on Croatia's eastern Adriatic coast. *International Journal of Osteoarchaeology* **21** 577–590. (doi:10.1002/oa.1163)
Slavin JL 2013 Carbohydrates, dietary fiber, and resistant starch in white vegetables: Links to health outcomes. *Advances in Nutrition* **4** 351–355. (doi:10.3945/an.112.003491)
Smith BH 1991 Standards of human tooth formation and dental age assessment. In *Advances in Dental Anthropology*, pp 143–168. Eds MA Kelley & CS Larsen. New York: Wiley-Liss.
Smith AF 2015 *Sugar: A Global History*. Reaktion Books.
Smrcka V, Marik I, Svenssonova M & Likovsky J 2009 Case reports: Legg-calvé-perthes disease in czech archaeological material. *Clinical Orthopaedics and Related Research*

467 293–297. (doi:10.1007/s11999-008-0527-6)
Snoddy AME, Halcrow SE, Buckley HR, Standen VG & Arriaza BT 2017 Scurvy at the agricultural transition in the Atacama desert (ca 3600–3200 BP): nutritional stress at the maternal-foetal interface? *International Journal of Paleopathology* **18** 108–120. (doi:10.1016/j.ijpp.2017.05.011)
Snoddy AME, Buckley HR, Elliott GE, Standen VG, Arriaza BT & Halcrow SE 2018 Macroscopic features of scurvy in human skeletal remains: A literature synthesis and diagnostic guide. *American Journal of Physical Anthropology* **167** 876–895. (doi:10.1002/ajpa.23699)
Sofaer J 2005 *The Body as Material Culture. A Theoretical Osteoarchaeology*. Cambridge: Cambridge University Press.
Sofaer Derevenski JR 2000 Sex differences in activity-related osseous change in the spine and the gendered division of labor at Ensay and Wharram Percy, UK. *American Journal of Physical Anthropology* **111** 333–354. (doi:10.1002/(SICI)1096-8644(200003)111:3<333::AID-AJPA4>3.0.CO;2-K)
Sono T, Ware AD, McCarthy EF & James AW 2019 Chondromyxoid Fibroma of the Pelvis: Institutional Case Series With a Focus on Distinctive Features. *International Journal of Surgical Pathology* **27** 352–359. (doi:10.1177/1066896918820446)
Sowers MR & Karvonen-Gutierrez CA 2010 The evolving role of obesity in knee osteoarthritis. *Current Opinion in Rheumatology* **22** 533–537. (doi:10.1097/BOR.0b013e32833b4682)
Sparacello V & Marchi D 2008 Mobility and subsistence economy: A diachronic comparison between two groups settled in the same geographical area (Liguria, Italy). *American Journal of Physical Anthropology* **136** 485–495. (doi:10.1002/ajpa.20832)
Sparacello VS, Pearson OM, Coppa A & Marchi D 2011 Changes in skeletal robusticity in an iron age agropastoral group: The samnites from the Alfedena necropolis (Abruzzo, Central Italy). *American Journal of Physical Anthropology* **144** 119–130. (doi:10.1002/ajpa.21377)
Spradley MK & Jantz RL 2011 Sex estimation in forensic anthropology: Skull versus postcranial elements. *Journal of Forensic Sciences* **56** 289–296. (doi:10.1111/j.1556-4029.2010.01635.x)
Srejic MD 2001 Dental Paleopathology in a Serbian Medieval Population. *Anthropologischer Anzeiger* **59** 113–122.
Stallman JS, Lobo JN & Som PM 2004 The incidence of concha bullosa and its relationship to nasal septal deviation and paranasal sinus disease. *American Journal of Neuroradiology* **25** 1613–1618.
Stantis C, Soltysiak A & Schutkowski H 2020 Reconstructing breastfeeding and weaning practices in the Bronze Age Near East using stable nitrogen isotopes. *Americal Journal of Physical Anthropology* **172** 58–69. (doi:10.1002/ajpa.23980)
Stark RJ 2014 A proposed framework for the study of paleopathological cases of subadult scurvy. *International Journal of Paleopathology* **5** 18–26. (doi:10.1016/j.ijpp.2014.01.005)
Starling AP & Stock JT 2007 Dental indicators of health and stress in early Egyptian and Nubian agriculturalists: A difficult transition and gradual recovery. *American Journal of Physical Anthropology* **134** 520–528. (doi:10.1002/ajpa.20700)
Stech K 2009 Wie lebte die Oberschicht im historischen Emden ? Osteologische Untersuchungen von Kircheninnenbestattungen zur Rekonstruktion der Lebensbedingungen in einer ostfriesischen Seehafenstadt. Freie Universität Berlin.
Steckel RH 2004 New Light on the 'Dark Ages': The Remarkably Tall Stature of Northern European Men during the Medieval Era. *Social Science History* **28** 211–229.

(doi:10.1215/01455532-28-2-211)
Steckel RH, Larsen CS, Sciulli PW & Walker PL 2006 Data Collection Codebook. *The Global History of Health Project* 1–41. (doi:10.1017/9781108379830.016)
Steele DG 1976 The estimation of sex on the basis of the talus and calcaneus. *American Journal of Physical Anthropology* **45** 581–588. (doi:10.1002/ajpa.1330450323)
Steele J & Mays S 1995 Handedness and Directional Asymmetry in the Long Bones of the Human Upper Limb. *International Journal of Osteoarchaeology* **5** 39–49.
Stevens RE, Lightfoot E & Hamilton J 2013 One for the master and one for the dame : stable isotope investigations of Iron Age animal husbandry in the Danebury Environs. *Archaeological and Anthropological Sciences* **5** 95–109. (doi:10.1007/s12520-012-0114-3)
Stirland AJ 1993 Asymmetry and activity-related change in the male humerus. *International Journal of Osteoarchaeology* **3** 105–113. (doi:10.1002/oa.1390030207)
Stirland A 2000 *Raising the Dead: The Skeleton Crew of Henry VIII's Great Ship, the Mary Rose*. John Wiley & Sons Incorporated.
Stirland AJ & Waldron T 1997 Evidence for activity related markers in the vertebrae of the crew of the Mary Rose. *Journal of Archaeological Science* **24** 329–335. (doi:10.1006/jasc.1996.0117)
Stloukal M & Hanáková H 1978 Die Länge der Längsknochen altslawischer Bevölkerungen unter besonderer Berücksichtigung von Wachstumsfragen. *Homo* **29** 53–69.
Stloukal M & Vyhnánek L 1975 Die Arthrose der grossen Gelenke. *Homo* **26** 121–136.
Stock JT & Pfeiffer SK 2004 Long bone robusticity and subsistence behaviour among Later Stone Age foragers of the forest and fynbos biomes of South Africa. *Journal of Archaeological Science* **31** 999–1013. (doi:10.1016/j.jas.2003.12.012)
Stock JT & Shaw CN 2007 Which measures of diaphyseal robusticity are robust? A comparison of external methods of quantifying the strength of long bone diaphyses to cross-sectional geometric properties. *American Journal of Physical Anthropology* **134** 412–423. (doi:10.1002/ajpa.20686)
Stone DJ 2006 The consumption of field crops in late medieval England. In *Food in Medieval England: Diet and Nutrition*, pp 11–26. Eds CM Woolgar, D Serjeantson & T Waldron. Oxford: Oxford University Press,.
Streckfus CF, Baur U, Brown LJ, Bacal C, Metter J & Nick T 1998 Effects of estrogen status and aging on salivary flow rates in healthy Caucasian women. *Gerontology* **44** 32–39. (doi:10.1159/000021980)
Strott N 2006 Paläodemographie frühmittelalterlicher Bevölkerungen Altbaierns – Diachrone und allopatrische Trends. Ludwig-Maximilians-Universität München.
Stuart-Macadam P & Dettwyler KA 1995 *Breastfeeding: Biocultural Perspectivesg*. London, New York: Routledge.
Stuart-Macadam P 1985 Porotic hyperostosis: Representative of a childhood condition. *American Journal of Physical Anthropology* **66** 391–398. (doi:10.1002/ajpa.1330660407)
Stuart-Macadam P 1992 Porotic hyperostosis: A new perspective. *American Journal of Physical Anthropology* **87** 39–47. (doi:10.1002/ajpa.1330870105)
Sumner DR & Andriacchi TP 1996 Adaptation to Differential Loading : Comparison of Growth-Related Changes in Cross-Sectional Properties of the Human Femur and Humerus. *Bone* **19** 121–126.
Sun Z, Lee E & Herring SW 2004 Cranial sutures and bones: growth and fusion in relation to masticatory strain. *The Anatomical Record. Part A, Discoveries in Molecular, Cellular, and Evolutionary Biology* **276** 150–161. (doi:10.1002/ar.a.20002)
Sutton PR 1990 Acute dental caries, mental stress, immunity and the active passage of ions

through the teeth. *Medical Hypotheses* **31** 17.
Sykes NJ 2006 From cu and sceap to beffe and motton: The management, distribution, and consumption of cattle and sheep in medieval England. In *Food in Medieval England: Diet and Nutrition*, pp 56–71.
Szilvássy J 1988 Altersdiagnose am Skelett. In *Anthropologie. Handbuch Der Vergleichenden Biologie Des Menschen. Bd. 1: Wesen Und Methoden Der Anthropologie. 1. Teil: Wissenschaftstheorie, Geschichte, Morphologische Methoden*, 4. Aufl., pp 421–443. Ed R Knußmann. Stuttgart, New York: Gustav-Fischer-Verlag.
Tabani H, Tayebi Meybodi A & Benet A 2020 *Venous Anatomy of the Supratentorial Compartment*. Elsevier B.V. (doi:10.1016/B978-0-12-804280-9.00003-2)
Tacail T, Thivichon-Prince B, Martin JE, Charles C, Viriot L & Balter V 2017 Assessing human weaning practices with calcium isotopes in tooth enamel. *Proceedings of the National Academy of Sciences* **114** 6268–6273. (doi:10.1073/pnas.1704412114)
Tada A & Miura H 2019 The relationship between vitamin C and periodontal diseases: A systematic review. *International Journal of Environmental Research and Public Health* **16**. (doi:10.3390/ijerph16142472)
Tagesson G 2015 The Human Body as Material Culture – Linköping Cathedral Churchyard in the Early Modern Period. In *The Archaeology of Death in Post-Medieval Europe*, pp 19–38. Ed S Tarlow. Warsaw, Berlin: De Gruyter Open Ltd.
Tanner JM 1989 *Growth before Birth. Foetus into Man: Physical Growth from Conception to Maturity*. Ware, England: Castlemead Publications.
Targino A, Rosenblatt A, Oliveira A, Chaves A & Santos V 2011 The relationship of enamel defects and caries: A cohort study. *Oral Diseases* **17** 420–426. (doi:10.1111/j.1601-0825.2010.01770.x)
Tauber H 1981 13C evidence for dietary habits of prehistoric man in Denmark. *Nature* **292** 332–333. (doi:10.1038/292332a0)
Telkkä A, Palkama A & Virtama P 1962 Estimation of stature from radiographs of long bones in children. *Ann Med Exp Biol Fenn.* **40** 91–96.
Tessone A, García Guraieb S, Goñi RA & Panarello HO 2015 Isotopic evidence of weaning in hunter-gatherers from the late holocene in Lake Salitroso, Patagonia, Argentina. *American Journal of Physical Anthropology* **158** 105–115. (doi:10.1002/ajpa.22768)
Tham R, Bowatte G, Dharmage S, Tan D, Lau M, Dai X, Allen K & Lodge C 2015 Breastfeeding and the risk of dental caries: A systematic review and meta-analysis. *Acta Paediatrica, International Journal of Paediatrics* **104** 62–84. (doi:10.1111/apa.13118)
Theureau C 1985 Anthropologie des squelettes du cimetière paroissial de Saint-Pierre-le-Puellier (XIe-XVIIe siècle). *Recherches Sur Tours: Laboratoire d'archéologie Urbaine* **3** 5–62.
Thewes G 1994 De l'Ancien Régime au Luxembourg moderne. La bourgeoisie de la ville au XVIIIe siècle. In *La Ville de Luxembourg- Du Château Des Comtes à La Métropole Européenne*, pp 195–199. Ed G Trausch. Fonds Mercator Anvers.
Thewes G 2011 Luxembourg, ville forteresse. L'impact de la fortification sur l'organisation de l'espace urbain (XVIe-XIXe siècle). *Revue Belge de Philologie et d'histoire* **89** 787–801. (doi:10.3406/rbph.2011.8135)
Thewes G 2013 Le logement des soldats dans la forteresse de Luxembourg. *Ons Staadt* 14–17.
Thewes G 2017 *Grand Duché de Luxembourg à Propos*. Imprimerie Exe.
Thirsk J 2007 *Food in Early Modern England: Phases, Fads, Fashions, 1500-1760*. Continuum.
Thompson-Schill SL, Jonides J, Marshuetz C, Smith EE, D'Esposito M, Kan IP, Knight RT & Swick D 2002 Effects of frontal lobe damage on interference effects in working

memory. *Cognitive, Affective and Behavioral Neuroscience* **2** 109–120.
Thorimbert S & Hervé C 2015 Luxembourg-Ville: fouilles de la place Guillaume II. Résultats préliminaires documentant l'évolution entre le XIIIe et le XIXe siècle d'un ensemble ecclésiastique. *Archaeologia Luxemburgensis* **2** 187–197.
Timmermann M 2009 Das Ihlower Zisterzienserkloster : Beten , Arbeiten und heilsames Leben im Mittelalter ! - Eine anthropologische Untersuchung -.
Tomczyk, Jacek, Soltysiak Arkadiusz T-GM 2007 Temproal changes in frequency of enamel hypoplasia Syria. *Human Biology Budapest* **30** 87–97.
Tomkins JL & Andrews S 2001 Fluctuating Asymmetry. *Encyclopedia of Life Sciences* 1–5. (doi:10.1055/s-0031-1275301)
Tonina E, Licata M, Pangrazzi C, Maspero U, Romano L & Larentis O 2018 A case of Concha Bullosa and potentially related evidences. Concha bullosa discovered in the bones of a medieval skeleton from Brentonico, northeast Italy: A case report. *Medicina Historica* **2** 94–98.
Toso A, Gaspar S, Banha da Silva R, Garcia SJ & Alexander M 2019 High status diet and health in Medieval Lisbon: a combined isotopic and osteological analysis of the Islamic population from São Jorge Castle, Portugal. *Archaeological and Anthropological Sciences* **11** 3699–3716. (doi:10.1007/s12520-019-00822-7)
Touger-Decker R & van Loveren C 2003 Sugars and dental caries. *The American Journal of Clinical Nutrition* **78**. (doi:10.1093/ajcn/78.4.881s)
Trammell LH & Kroman AM 2013 *Bone and Dental Histology*. Elsevier Inc. (doi:10.1016/B978-0-12-385189-5.00013-3)
Trausch G 1993 Du Chateau du Bock au Gibraltar du Nord. Luxembourg et sa forteresse.
Trautmann B 2012 Luxembourg in the Middle Ages - An Anthropological Study of the Living Conditions of the Rural Society of Grevenmacher. Eberhard Karls Universität Tübingen.
Trautmann M & Trautmann I 2011 *Ausgrabung in Grund „Wenzelsmauer" 2008 – Die Bestattungen*.
Trautmann B, Wißing C, Díaz-Zorita Bonilla M, Bis-Worch C & Bocherens H 2017 Reconstruction of Socioeconomic Status in the Medieval (14th–15th Century) Population of Grevenmacher (Luxembourg) Based on Growth, Development and Diet. *International Journal of Osteoarchaeology* **27** 947–957. (doi:10.1002/oa.2606)
Trickett MA 2006 A Tale of Two Cities: Diet, Health and Migration in Post-Medieval Coventry and Chelsea through Biographical Reconstruction, Osteoarchaeology and Isotope Biogeochemistry. Durham: Durham University.
Trinkaus E, Churchill SE & Ruff CB 1994 Postcranial robusticity in Homo. II: Humeral bilateral asymmetry and bone plasticity. *American Journal of Physical Anthropology* **93** 1–34. (doi:10.1002/ajpa.1330930102)
Trombelli L, Farina R, Marzola A, Bozzi L, Liljenberg B & Lindhe J 2008 Modeling and remodeling of human extraction sockets. *Journal of Clinical Periodontology* **35** 630–639. (doi:10.1111/j.1600-051X.2008.01246.x)
Trotter M & Gleser GC 1952 Estimation of stature from long bones of American White and Negroes. *American Journal of Physical Anthropology* **10** 463–514 and 355–356.
Trotter M & Gleser GC 1958 A re-evaluation of estimation of stature based on measurements of stature taken during life and of long bones after death. *American Journal of Physical Anthropology* **16** 79–123.
Tsutaya T 2017 Post-weaning diet in archaeological human populations: A meta-analysis of carbon and nitrogen stable isotope ratios of child skeletons. *American Journal of Physical Anthropology* **164** 546–557. (doi:10.1002/ajpa.23295)
Tsutaya T 2019 Package ' WARN '. 1–17.

Tsutaya T & Yoneda M 2013a Quantitative Reconstruction of Weaning Ages in Archaeological Human Populations Using Bone Collagen Nitrogen Isotope Ratios and Approximate Bayesian Computation. *PLoS ONE* **8** 1–10. (doi:10.1371/journal.pone.0072327)
Tsutaya T & Yoneda M 2013b *WARN: An R Package for Quantitative Reconstruction of Weaning Ages in Archaeological Populations Using Bone Collagen Nitrogen Isotope Ratios*.
Tsutaya T & Yoneda M 2015 Reconstruction of breastfeeding and weaning practices using stable isotope and trace element analyses: A review. *American Journal of Physical Anthropology* **156** 2–21. (doi:10.1002/ajpa.22657)
Tsutaya T, Shimomi A, Fujisawa S, Katayama K & Yoneda M 2016 Isotopic evidence of breastfeeding and weaning practices in a hunter-gatherer population during the Late/Final Jomon period in eastern Japan. *Journal of Archaeological Science* **76** 70–78. (doi:10.1016/j.jas.2016.10.002)
Tuck SP, Layfield R, Walker J, Mekkayil B & Francis R 2017 Adult Paget's disease of bone: A review. *Rheumatology (United Kingdom)* **56** 2050–2059. (doi:10.1093/rheumatology/kew430)
Turcotte RE 2006 Giant cell tumor of bone. *Orthopedic Clinics of North America* **37** 35–51. (doi:10.1016/j.ocl.2005.08.005)
Ubelaker DH 1978 *Human Skeletal Remains: Excavation, Analysis, Interpretation*. Chicago: Aldine Publishing Co. Inc.
Ubelaker DH 1979 Skeletal evidence for kneeling in prehistoric Ecuador. *American Journal of Physical Anthropology* **51** 679–685. (doi:10.1002/ajpa.1330510417)
Ulrich-Bochsler S 1997 *Anthropologische Befunde Zur Stellung von Frau Und Kind in Mittelalter Und Neuzeit*. Bern: Berner Lehrmittel- und Medienverlag.
Ulrich-Bochsler SCC&. SL 2008 Part I: Palaeopathological examination of human skeketons: Stress markers in three populations from medieval and postmedieval Bern - a comparison of pre-alpine and midland regions in Switzerland. *Limping Together Trough the Ages. Joint Afflictions and Bone Infections* **6** 15–37.
Ulrich-Bochsler S & Meyer L 1993 Anthropologische Befunde zu den Gräbern aus dem Kreuzgang. In *Bern Französiche Kirche. Ehemaliges Predigerkloster*, pp 187–202. Eds G Descoeudres & K Utz Tremp. Bern, Stuttgart: Verlag Paul Haupt.
Üstündag H 2009 Schmorl's Nodes in a Post- Medieval Skeletal Sample from. *International Journal of Osteoarchaeology* **19** 695–710. (doi:10.1002/oa)
Van Valen L 1962 A study of Fluctuating Asymmetry. *International Journal of Organic Evolution* **16** 125–142.
Varshney MK 2016 *Essential Orthopedics. Principles & Practice*. New Delhi, London, Philadelphia, Panama: The Health Sciences Publisher.
Venkataramana NK 2011 Spinal dysraphism. *Journal of Pediatric Neuroscience* **6** 31–40.
Vercellotti G, Stout SD, Boano R & Sciulli PW 2011 Intrapopulation variation in stature and body proportions: Social status and sex differences in an Italian medieval population (Trino Vercellese, VC). *American Journal of Physical Anthropology* **145** 203–214. (doi:10.1002/ajpa.21486)
Verna E, Piercecchi-Marti MD, Chaumoitre K, Panuel M & Adalian P 2014 Mise au point sur les caractères discrets du membre inférieur: définition, épidémiologie, étiologies. *Bulletins et Memoires de La Societe d'Anthropologie de Paris* **26** 52–66. (doi:10.1007/s13219-013-0090-x)
Victora CG, Bahl R, Barros AJD, França GVA, Horton S, Krasevec J, Murch S, Sankar MJ, Walker N, Rollins NC *et al.* 2016 Breastfeeding in the 21st century: Epidemiology, mechanisms, and lifelong effect. *The Lancet* **387** 475–490. (doi:10.1016/S0140-

6736(15)01024-7)
Van de Vijver K 2018 Past life and death in a Flemish town. An archaeo-anthropological study of burials from the medieval and post-medieval St. Rombout's cemetery in Mechelen, Belgium (10th–18th centuries CE). *Journal of Archaeological Science: Reports* **20** 524–555. (doi:10.1016/j.jasrep.2018.05.007)
Vilkama R, Kylli R & Salmi AK 2016 Sugar Consumption, Dental Health and Foodways in Late Medieval Iin Hamina and Early Modern Oulu, Northern Finland. *Scandinavian Journal of History* **41** 2–31. (doi:10.1080/03468755.2015.1106974)
Villotte S 2006 Connaissances médicales actuelles, cotation des enthésopathies : nouvelle méthode. *Bulletins et Mémoires de La Société d'anthropologie de Paris* **18** 65–85. (doi:10.4000/bmsap.1325)
Villotte S 2008 Enthésopathies et activités des hommes préhistoriques: Recherche méthodologique et application aux fossiles européens du Paléolithique supérieur et du Mésolithique. In *Enthésopathies et Activités Des Hommes Préhistoriques: Recherche Méthodologique et Application Aux Fossiles Européens Du Paléolithique Supérieur et Du Mésolithique*. Université Sciences et Technologies - Bordeaux 1. (doi:10.30861/9781407305264)
Villotte S, Castex D, Couallier V, Dutour O, Knüsel CJ & Henry-Gambier D 2010 Enthesopathies as occupational stress markers: Evidence from the upper limb. *American Journal of Physical Anthropology* **142** 224–234. (doi:10.1002/ajpa.21217)
Vossler-Wolf C 2016 Klosterarchäologie. In *Archäologie Des Mittelalters Und Der Neuzeit : Grundwissen*, pp 210–217. Eds B Scholkmann, H Kenzler & R Schreg. Darmstadt: Wissenschaftliche Buchgesellschaft.
Wade AD, Holdsworth DW & Garvin GJ 2011 CT and micro-CT analysis of a case of Paget's disease (osteitis deformans) in the Grant skeletal collection. *International Journal of Osteoarchaeology* **21** 127–135. (doi:10.1002/oa.1111)
Wahl J 1994 Zur Ansprache und Definition von Sonderbestattungen. In *Beiträge Zur Archäozoologie Und Prähistorischen Anthropologie. Forschung Und Berichte Zur Vor- Und Frühgeschichte in Baden-Württemberg*, pp 85–106. Eds M Kokabi & J Wahl. Stuttgart.
Wahl J 2007 Karies, Kampf und Schädelkult. 150 Jahre anthropologische Forschung in Südwestdeutschland. In *Materialhefte Zur Archäologie in Baden-Württemberg*. Stuttgart: Theiss Verlag.
Wahl J 2022 Grundzüge der Prähistorischen Anthropologie. In *Osteologische Paläopathologie: Ein Handbuch Für Anthropologen, Mediziner Und Archäologen*, Berlin, pp 33–60. Eds J Weber, J Wahl & A Zink. Lehmanns Media GmbH.
Wahl J & Zink A 2013 Karies, Pest und Knochenbrüche. Was Skelette über Leben und Sterben in alter Zeit verraten. *Sonderheft Archäologie Baden-Württemberg*.
Waidhofer M 2013 „Direktionale Asymmetrien an Clavicula, Humerus, Ulna und Radius bei Awaren und Khoisan.
Waldron T 1985 DISH at Merton Priory: Evidence for a "new" occupational disease? *British Medical Journal (Clinical Research Ed.)* **291** 1762–1763. (doi:10.1136/bmj.291.6511.1762)
Waldron T 1994 *Counting the Dead – The Epidemiology of Skeletal Populations.* Chichester: Wiley.
Waldron T 1998 An Unusual Cluster of Meningiomas? *International Journal of Osteoarchaeology* **8** 213–217. (doi:10.1002/(sici)1099-1212(199805/06)8:3<213::aid-oa418>3.0.co;2-a)
Waldron T 2009 *Palaeopathology*. Cambridge University Press.
Walker D 2012 *Disease in London, 1st-19th Centuries*. Museum of London Archaeology.

Walker D & Henderson M 2010 Smoking and health in London's East End in the first half of the 19th century. *Post-Medieval Archaeology* **44** 209–222. (doi:10.1179/174581310X12662382629373)
Walker PL, Bathurst RR, Richman R, Gjerdrum T & Andrushko VA 2009 The causes of porotic hyperostosis and cribra orbitalia: A reappraisal of the iron-deficiency-anemia hypothesis. *American Journal of Physical Anthropology* **139** 109–125. (doi:10.1002/ajpa.21031)
Walter BS & DeWitte SN 2017 Urban and rural mortality and survival in Medieval England. *Annals of Human Biology* **44** 338–348. (doi:10.1080/03014460.2016.1275792)
Wapler U, Crubézy E & Schultz M 2004 Is Cribra Orbitalia Synonymous with Anemia? Analysis and Interpretation of Cranial Pathology in Sudan. *American Journal of Physical Anthropology* **123** 333–339. (doi:10.1002/ajpa.10321)
Ward C V., Mays SA, Child S & Latimer B 2009 Lumbar vertebral morphology and isthmic spondylolysis in a British medieval population. *American Journal of Physical Anthropology* **280** NA-NA. (doi:10.1002/ajpa.21142)
Wasterlain SN & Umbelino C 2014 Legg-Calvé-Perthes disease and slipped femoral capital epiphysis in the skeletal remains of the Mediaeval Necropolis of Santa Maria (Sintra, Portugal). *Cadernos Do GEEvH* **2** 27–39.
Wasterlain SN, Ascenso BF & Silva AM 2011 Skeletal metastatic carcinoma: A case from 15th-20th century Coimbra, Portugal. *International Journal of Osteoarchaeology* **21** 336–346. (doi:10.1002/oa.1130)
Waters-Rist AL & Katzenberg MA 2010 The effect of growth on stable nitrogen isotope ratios in subadult bone collagen. *International Journal of Osteoarchaeology* **20** 172–191. (doi:10.1002/oa.1017)
Waters-Rist AL, Bazaliiskii VI, Weber AW & Katzenberg MA 2011 Infant and child diet in Neolithic hunter-fisher-gatherers from cis-baikal, Siberia: Intra-long bone stable nitrogen and carbon isotope ratios. *American Journal of Physical Anthropology* **146** 225–241. (doi:10.1002/ajpa.21568)
Waters-Rist AL, de Groot K & Hoogland MLP 2022 Isotopic reconstruction of short to absent breastfeeding in a 19th century rural Dutch community. *PLoS ONE* **17** 1–29. (doi:10.1371/journal.pone.0265821)
Wedel VL & Galloway A 2014 *Broken Bones: Anthropological Analysis of Blunt Force Trauma*. Springfield: Charles C. Thomas Publisher LTD. (doi:10.1002/ajhb.1069.abs)
Weidig I, Sindermann A, Rehbach N-J & Nothwang U 2009 A medieval skeletal series from Givenich (Luxembourg) and its pathologies. *Beiträge Zur Archäozoologie Und Prähistorischen Anthropologie VIII* 165–169.
Weis M 2004 Nourrir les armées de Philippe II. La ville et le duché de Luxembourg face aux défis de la logistique militaire pendant la Révolte des Pays-Bas. In *L'armée et La Ville Dans l' Europe Du Nord et Du Nord-Ouest. Du XVe Siècle à Nos Jours*, Temps & Es, pp 263–274. Eds P Bragard, J-F Chanet, C Denys & P Guignet. Lille: presses universitaires de louvain.
Weiss KM 1973 Demographic Models for Anthropology. *American Antiquity* **38** 1–186.
Weiss E 2009 Sex differences in humeral bilateral asymmetry in two hunter-gatherer populations: California Amerinds and British Columbian Amerinds. *American Journal of Physical Anthropology* **140** 19–24. (doi:10.1002/ajpa.21025)
Weiss E & Jurmain R 2007 Osteoarthritis revisited : A contemporary review of aetiology. *International Journal of Osteoarchaeology* **17** 437–450. (doi:10.1002/oa.889)
Weiss NM, Vercellotti G, Boano R, Girotti M & Stout SD 2019 Body size and social status in medieval Alba (Cuneo), Italy. *American Journal of Physical Anthropology* **168** 595–605. (doi:10.1002/ajpa.23776)

Welte B & Wahl J 2010 Auxologische Studien an Skelettresten frühneolithischer Kinder und Jugendlicher aus Südwestdeutschland. *Fundberichte Aus Baden-Württemberg* **31** 7–28.
Wescott DJ 2006 Effect of Mobility on Femur Midshaft External Shape and Robusticity. *American Journal of Physical Anthropology* **130** 201–213. (doi:10.1002/ajpa)
West JA & Louis TH 2015 Radiographic Findings in the Nail-Patella Syndrome. *Baylor University Medical Center Proceedings* **28** 334–336. (doi:10.1080/08998280.2015.11929265)
Western AG & Bekvalac JJ 2017 Hyperostosis frontalis interna in female historic skeletal populations: Age, sex hormones and the impact of industrialization. *American Journal of Physical Anthropology* **162** 501–515. (doi:10.1002/ajpa.23133)
Weston DA 2008 Investigating the specificity of periosteal reactions in pathology museum specimens. *American Journal of Physical Anthropology* **137** 48–59. (doi:10.1002/ajpa.20839)
White TD & Folkens PA 2005 *The Human Bone Manual*. Elsevier Academic Press.
White TD, Black MT & Folkens PA 2012 *Human Osteology*. Amsterdam; Boston; Heidelberg; London; New York; Oxford; Paris; San Diego; San Fransisco; Singapore; Sydney; Tokyo: Elsevier Academic Press.
Whitehead TP, Ward MH, Colt JS, Dahl G, Ducore J, Kyndaron R, Gunier RB, Hammond SK, Rappaport SM & Metayer C 2015 Dust-metal Loadings and the Risk of Childhood Acute Lymphoblastic Leukemia. *Journal of Exposure Science & Environmental Epidemiology* **25** 593–598. (doi:10.1038/jes.2015.9.Dust-metal)
Whittaker DK & Molleson T 1996 Caries prevalence in the dentition of a late eighteenth century population. *Archives of Oral Biology* **41** 55–61. (doi:10.1016/0003-9969(95)00096-8)
WHO 2010 A healthy lifestyle - WHO recommendations.
Widmaier J 2016 Kirche und Gesellschaft. In *Archäologie Des Mittelalters Und Der Neuzeit : Grundwissen*, pp 203–209. Eds B Scholkmann, H Kenzler & R Schreg. Darmstadt: Wissenschaftliche Buchgesellschaft.
Williams JS, White CD & Longstaffe FJ 2005 Trophic level and macronutrient shift effects associated with the weaning process in the postclassic maya. *American Journal of Physical Anthropology* **128** 781–790. (doi:10.1002/ajpa.20229)
Willman JC, Valera AC & Silva AM 2020 The embodiment of craft production in Bronze Age Portugal: Exceptional dental wear grooves in an individual from Monte do Vale do Ouro 2 (Ferreira do Alentejo, Portugal). *International Journal of Osteoarchaeology* **2** 0–2. (doi:10.1002/oa.2944)
Wilson CA 1973 *Food and Drink in Britain*. Constable & Co. Ltd.
Wolff J 1892a *Das Gesetz Der Transformation Der Knochen*. Berlin: A Hirschwald.
Wolff J 1892b *Das Gesetz Der Transformation Der Knochen*. Stuttgart: Schattauer.
Wolff K, Vas Z, Sótonyi P & Magyar LG 2012 Skeletal age estimation in Hungarian population of known age and sex. *Forensic Science International* **223**. (doi:10.1016/j.forsciint.2012.08.033)
Wood L 1996 Frequency and chronological distribution of linear enamel hypoplasia in a North American colonial skeletal sample. *American Journal of Physical Anthropology* **100** 247–259. (doi:10.1002/(SICI)1096-8644(199606)100:2<247::AID-AJPA6>3.0.CO;2-U)
Wood JW, Milner GR, Harpending HC, Weiss KM, Cohen MN, Eisenberg LE, Hutchinson DL, Jankauskas R, Cesnys G, Katzenberg MA *et al.* 1992 The Osteological Paradox: Problems of Inferring Prehistoric Health from Skeletal Samples [and Comments and Reply]. *Current Anthropology* **33** 343–370. (doi:10.1086/204084)
Wright LE & Schwarcz HP 1998 Stable carbon and oxygen isotopes in human tooth enamel:

Identifying breastfeeding and weaning in prehistory. *American Journal of Physical Anthropology* **106** 1–18. (doi:10.1002/(SICI)1096-8644(199805)106:1<1::AID-AJPA1>3.0.CO;2-W)
Wu S, Pan Y, Mao Y, Chen Y & He Y 2021 Current progress and mechanisms of bone metastasis in lung cancer: A narrative review. *Translational Lung Cancer Research* **10** 439–451. (doi:10.21037/tlcr-20-835)
Wurm H 1985 Über die durchschnittlichen Körperhöhen der sozialen Mittel- und Unterschichten im mitteleuropäischen germanischen Siedlungsraum vom Frühmittelalter bis zur Neuzeit Author (s): H . Wurm Published by : E . Schweizerbart ' sche Verlagsbuchhandlung Stable. *Anthropologischer Anzeiger* **43** 11–30.
Wurm H 1987 Zum Einfluss von Ernährung, insbesondere zum Einfluss von Nahrungseiweiß unterschiedlicher Quantität und Qualität auf die Konstitution nach Ernährungsversuchen – ein Vorbericht. *Homo* **38** 34–58.
Xinyun HA, Razak HRBA & Chye TH 2014 The Truth Behind Subchondral Cysts in Osteoarthritis of the Knee. *The Open Orthopaedics Journal* **8** 7–10.
Yegles-Becker I 2002 *De Fëschmaart*. Esch-sur-Alzette: Fonds de la Vieille Ville.
Yoder C 2012 Let them eat cake? Status-based differences in diet in medieval Denmark. *Journal of Archaeological Science* **39** 1183–1193. (doi:10.1016/j.jas.2011.12.029)
You T, Frostick S, Zhang W tao & Yin Q 2019 Os Acromiale: Reviews and Current Perspectives. *Orthopaedic Surgery* **11** 738–744. (doi:10.1111/os.12518)

12 List of Tables

TABLE 1 RADIOCARBON DATES FOR SAMPLES FROM ALL THREE EXCAVATION CAMPAIGNS 29
TABLE 2 COMPOSITION OF SKELETAL AREAS USED IN ANALYSIS OF REPRESENTATION 36
TABLE 3 DESCRIPTION OF BONE PRESERVATION STAGES AFTER TRAUTMANN (2012) 37
TABLE 4 BONE PRESERVATION STATUS OF THE KNUEDLER CEMETERY 38
TABLE 5 AGE CATEGORIES USED IN ALL ANALYSES OF THIS STUDY 41
TABLE 6 AGE DISTRIBUTION BY LAYER AND LOCATION 46
TABLE 7 COMPARISON OF AGE DISTRIBUTIONS BETWEEN THE KNUEDLER CEMETERY AND 9 URBAN GERMAN SITES, 6 EUROPEAN MONASTIC SITES AND 8 LUXEMBOURGISH RURAL AND MONASTIC SITES 50
TABLE 8 MASCULINITY INDICES (MI) FROM THE KNUEDLER CEMETERY COMPARED TO OTHER EUROPEAN AND LUXEMBOURGISH URBAN AND MONASTIC SITES 61
TABLE 9 FORMULAS FOR THE CALCULATION OF MORTALITY TABLES 64
TABLE 10 COMPARISON OF LIFE EXPECANCY AT BIRTH AND 20 YEARS TO OTHER EUROPEAN URBAN, RURAL AND MONASTIC SITES 79
TABLE 11 NUMBER OF INDIVIDUALS IN EACH AGE CATEGORY FOR EACH MEASUREMENT (DUE TO OVERLAPPING AGE ESTIMATIONS, SEVERAL AGE GROUPS SHARE THE SAME PARTICIPANTS) 82
TABLE 12 BMI CLASSIFICATION AFTER WHO (2010) 84
TABLE 13 WITHIN SITE COMPARISONS OF BODY HEIGHT RECONSTRUCTION (CM) AFTER PEARSON (1899), TROTTER AND GLESER (1952) AND RUFF ET AL. (2012) 88
TABLE 14 WITHIN SITE COMPARISONS OF BODY MASS (IN KG) RECONSTRUCTIONS AFTER AUERBACH AND RUFF (2004) AND RUFF ET AL. (2012) 89
TABLE 15 COMPARISON OF ADULT STATURE WITH RURAL, URBAN AND MONASTIC SITES ACROSS NORTHERN EUROPE 95
TABLE 16 COMPARISON OF ADULT BODY MASS WITH RURAL, URBAN AND MIXED SITES ACROSS NORTHERN EUROPE 98
TABLE 17 RAW MEASUREMENTS WITH RESULTS OF WILCOXON SIGNED RANKS TESTS FOR MALES AND FEMALES 104
TABLE 18 SIGNIFICANT %AA BETWEEN MALES AND FEMALES. 109
TABLE 19 %AA BETWEEN THE THREE AGE GROUPS IN MALES AND FEMALES 110
TABLE 20 %AA BETWEEN CLOISTER AND CEMETERY BURIALS IN MALES AND FEMALES 112
TABLE 21 %AA BETWEEN BURIALS FROM, CLOSE TO, MIDWAY TO AND FAR FROM THE CHURCH IN MALES AND FEMALES 113
TABLE 22 %AA BETWEEN BURIALS FROM THE CLOISTER AND THE CEMETERY IN LAYER 1 AND 2 114
TABLE 23 %AA BETWEEN LAYER 1 AND 2 IN MALES AND FEMALES 115
TABLE 24 %AA BETWEEN LAYER 1 AND 2 IN CLOISTER AND CEMETERY BURIALS 116
TABLE 25 CUT-OFF VALUES AND SHAPE DESCRIPTIONS OF THE PLATYMERIC INDEX 127
TABLE 26 CUT-OFF VALUES AND SHAPE DESCRIPTIONS OF THE PILASTRIC INDEX 128
TABLE 27 CUT-OFF VALUES AND SHAPE DESCRIPTIONS OF THE CNEMIC INDEX 129
TABLE 28 PREVALENCE OF BONE DIAPHYSEAL SHAPES AMONG MALES AND FEMALES 131
TABLE 29 PREVALENCE OF BONE DIAPHYSEAL SHAPES AMONG ADULTS, MATURES AND SENILES 132
TABLE 30 PREVALENCE OF BONE DIAPHYSEAL SHAPES AMONG CLOISTER AND CEMETERY 134
TABLE 31 PREVALENCE OF BONE DIAPHYSEAL SHAPES AMONG THE UPPER AND LOWER LAYERS 135
TABLE 32 RESULTS OF THE MANN-WHITNEY U TEST FOR ALL BONE INDICES COMPARING MEN TO WOMEN ON UNPAIRED DATA. 137
TABLE 33 RESULTS OF THE MANN-WHITNEY U TEST FOR ALL BONE INDICES COMPARING ALL THE AGE GROUPS ON UNPAIRED DATA 138
TABLE 34 RESULTS OF THE MANN-WHITNEY U TEST FOR ALL BONE INDICES COMPARING CLOISTER TO CEMETERY BURIALS ON UNPAIRED DATA 140
TABLE 35 RESULTS OF THE MANN-WHITNEY U TEST FOR ALL BONE INDICES COMPARING BURIAL FROM LAYER 1 TO THOSE FROM LAYER 2 ON UNPAIRED DATA 142
TABLE 36 RESULTS OF THE WILCOXON SIGNED RANKS TEST FOR BONE INDICES 144
TABLE 37 INDICES SHOWING A SIGNIFICANT DIFFERENCE IN %DA BETWEEN MEN AND WOMEN 146
TABLE 38 INDICES SHOWING A SIGNIFICANT DIFFERENCE IN %AA BETWEEN MEN AND WOMEN 146
TABLE 39 INDICES SHOWING A SIGNIFICANT DIFFERENCE IN %AA BETWEEN THE DIFFERENT AGE GROUPS 147

TABLE 40 INDICES SHOWING A SIGNIFICANT DIFFERENCE IN %DA BETWEEN CLOISTER AND CEMETERY BURIALS 147
TABLE 41 INDICES SHOWING A SIGNIFICANT DIFFERENCE IN %AA BETWEEN CLOISTER AND CEMETERY BURIALS 148
TABLE 42 INDICES SHOWING A SIGNIFICANT DIFFERENCE IN %DA BETWEEN INDIVIDUALS BURIED INSIDE, CLOSE AND MIDWAY TO AND FAR FROM THE CHURCH COMPLEX 148
TABLE 43 COMPARISON OF MEAN INDEX VALUES BETWEEN OLDER AND CONTEMPORANEOUS LUXEMBOURGISH SITES 150
TABLE 44 MUSCLE ATTACHMENT SITES SORTED BY FUNCTIONAL COMPLEX (AFTER MARIOTTI ET AL.2007) 156
TABLE 45 DIFFERENCES BY SEX FOR ALL FUNCTIONAL AREAS 158
TABLE 46 DIFFERENCES BY AGE FOR ALL FUNCTIONAL AREAS 160
TABLE 47 DIFFERENCES BY BURIAL LOCATION FOR ALL FUNCTIONAL AREAS 163
TABLE 48 DIFFERENCES BY LAYER FOR ALL FUNCTIONAL AREAS 164
TABLE 49 FREQUENCY OF SQUATTING FACETS BY SCOREABLE INDIVIDUAL COMPARED BY SEX, AGE, BURIAL LOCATION, AND SIDE 172
TABLE 50 PRESENCE OF SQUATTING FACETS BY SIDE, SEX, AGE, BURIAL LOCATION, AND LAYER, INCLUDING RESULTS OF THE PEARSON'S CHI SQUARE AND FISHER'S EXACT TESTS FOR EACH GROUP COMPARISON. 173
TABLE 51 RECORDING SCHEME FOR DEGENERATIVE JOINT DISEASES (AFTER SCHULTZ, 1988) 179
TABLE 52 LIST OF JOINTS AND THE JOINT SURFACES THAT THEY ARE COMPOSED OF 179
TABLE 53 SIMPLIFIED OVERALL JOINT SCORES USED FOR REPRESENTATION IN THE GRAPHS 180
TABLE 54 SCORES OF DEGENERATIVE JOINT DISEASE FOR EACH JOINT OF THE RIGHT BODY SIDE 184
TABLE 55 KRUSKAL-WALLIS AND MANN-WHITNEY U TESTS FOR THE SCORES OF DEGENERATIVE JOINT DISEASE FOR EACH JOINT OF THE RIGHT BODY SIDE 185
TABLE 56 SCORES OF DEGENERATIVE JOINT DISEASE FOR EACH JOINT OF THE LEFT BODY SIDE 185
TABLE 57 KRUSKAL-WALLIS AND MANN-WHITNEY U TESTS FOR THE SCORES OF DEGENERATIVE JOINT DISEASE FOR EACH JOINT OF THE LEFT BODY SIDE 186
TABLE 58 FREQUENCIES OF DEGENERATIVE JOINT DISEASE FOR EACH JOINT OF THE RIGHT BODY SIDE 187
TABLE 59 FREQUENCIES OF DEGENERATIVE JOINT DISEASE FOR EACH JOINT OF THE RIGHT BODY SIDE (CONTINUATION) 188
TABLE 60 FREQUENCIES OF DEGENERATIVE JOINT DISEASE FOR EACH JOINT OF THE LEFT BODY SIDE 189
TABLE 61 FREQUENCIES OF DEGENERATIVE JOINT DISEASE FOR EACH JOINT OF THE LEFT BODY SIDE (CONTINUATION) 190
TABLE 62 PERCENTAGE OF INDIVIDUALS AFFECTED BY ANY DEGREE OF AND ONLY MODERATE AND SEVERE DJD BY SEX, AGE, BURIAL LOCATION, DISTANCE TO CHURCH, AND BURIAL LAYER 193
TABLE 63 MEAN INDEX SCORES FOR DEGENERATIVE JOINT DISEASE FOR ALL MAJOR JOINTS COMPARED TO OTHER MEDIEVAL AND POSTMEDIEVAL EUROPEAN SITES 201
TABLE 64 MEAN FREQUENCIES FOR DEGENERATIVE JOINT DISEASE FOR ALL MAJOR JOINTS COMPARED TO OTHER MEDIEVAL AND POSTMEDIEVAL EUROPEAN SITES 201
TABLE 65 CASES OF ANKYLOSIS WITH POSSIBLE AETIOLOGY 202
TABLE 66 INDIVIDUALS WITH OSTEOCHONDRITIS DISSECANS LESIONS 203
TABLE 67 RECORDING SCHEME FOR SPONDYLOSIS DEFORMANS (AFTER TRAUTMANN 2012 SIMPLIFIED FROM SCHULTZ 1988) 205
TABLE 68 RECORDING SCHEME FOR SPONDYLARTHROSIS DEFORMANS (AFTER TRAUTMANN 2012 SIMPLIFIED FROM SCHULTZ 1988) 205
TABLE 69 SIMPLIFIED OVERALL JOINT SCORES USED FOR REPRESENTATION IN THE GRAPHS 206
TABLE 70 SUMMARY AND TEST RESULTS FOR THE SEVERITY CODE COMBINING DATA FOR SPONDYLARTHROSIS AND SPONDYLOSIS DEFORMANS BY SPINAL SECTION 219
TABLE 71 FREQUENCY OF SPONDYLOSIS AND SPONDYLARTHROSIS BY SPINAL SECTIONS 220
TABLE 72 PERCENTAGE OF INDIVIDUALS AFFECTED BY SCHMORL'S NODES BY SPINAL SECTION 224
TABLE 73 LIST OF INDIVIDUALS WITH PARTIAL OR COMPLETE SPINA BIFIDA OCCULTA 232
TABLE 74 LIST OF LUMBOSACRAL TRANSITIONAL VERTEBRAE 233
TABLE 75 LIST OF SPONDYLOLYSIS CASES 235
TABLE 76 LIST OF ALL INDIVIDUALS WITH OSTEOMATA AND THEIR LOCATION 252
TABLE 77 LIST OF INDIVIDUALS WITH BONE FRACTURES 297
TABLE 78 TRAUMA FREQUENCIES ACROSS MEDIEVAL AND POTMEDIEVAL EUROPE 313
TABLE 79 DESCRIPTION OF PERIOSTEAL REACTION SCORES FROM STECKEL ET AL. (2006) WITH ADDITION OF SCORE FOR "ACTIVE" LESION BY THE AUTHOR 316
TABLE 80 SCORES FOR RECORDING ENAMEL DEFECTS 331

TABLE 81 SUMMARY AND TEST RESULT FOR ADULT ENAMEL HYPOPLASIA TRUE AND CRUDE FREQUENCY 334
TABLE 82 SUMMARY AND TEST RESULTS FOR SUBADULT ENAMEL HYPOPLASIA TRUE AND CRUDE FREQUENCY .337
TABLE 83 OVERVIEW OF ENAMEL HYPOPLASIA PREVALENCE IN MEDIEVAL-POSTMEDIEVAL EUROPEAN SITES ..343
TABLE 84 SCORING SYSTEM FOR CRIBRA ORBITALIA (ADAPTED FROM (STECKEL ET AL. 2006)).....346
TABLE 85 SCORING SYSTEM FOR CRIBRA CRANII (ADAPTED FROM (STECKEL ET AL. 2006)).....348
TABLE 86 SUMMARY AND TEST RESULTS FOR CRIBRA CRANII AND CRIBRA ORBITALIA 349
TABLE 87 CRITERIA FOR DIAGNOSIS OF SCURVY FROM HUMAN REMAINS (TAKEN FROM AND ACCUMULATED BY SNODDY ET AL. (2018)) 355
TABLE 88 SUGGESTIVE AND DIAGNOSTIC CRITERIA FOR RICKETS (TAKEN FROM AND ACCUMULATED BY BRICKLEY AND IVES (2008)).....356
TABLE 89 LIST OF DIFFERENTIAL DIAGNOSES AND THEIR CRITERIA FOR POROUS LESIONS AND SPNB (SOURCED FROM MORRONE ET AL. 2021, BRICKLEY AND IVES (2008, MAYS AND BRICKLEY (2022) AND BRICKLEY AND MAYS (2019)) 357
TABLE 90 DIAGNOSTIC LESIONS AND DIFFERENTIAL DIAGNOSIS FOR INDIVIDUALS WITH POTENTIAL RICKETS....359
TABLE 91 CASES OF PROBABLE AND POSSIBLE SCURVY WITH DIAGNOSTIC AND SUGGESTIVE CRITERIA 363
TABLE 92 LIST OF INDIVIDUALS WITH LESIONS SUGGESTIVE OF METABOLIC DISEASE, WITH ABSENCE OF DIAGNOSTIC CRITERIA QUALIFYING FOR A FINAL DIAGNOSIS 364
TABLE 93 SCORING SYSTEM FOR DENTAL CALCULUS BASED ON (BROTHWELL 1981) 380
TABLE 94 SUMMARY AND TEST RESULTS FOR ADULT CALCULUS TRUE AND CRUDE FREQUENCY 382
TABLE 95 SUMMARY AND TEST RESULTS FOR SUBADULT CALCULUS TRUE AND CRUDE FREQUENCY 385
TABLE 96 CALCULUS DISTRIBUTION ACROSS LATE MEDIEVAL AND POSTMEDIEVAL EUROPE.....386
TABLE 97 SCORING SYSTEM FOR DENTAL CARIES SEVERITY AFTER TRAUTMANN 2012 389
TABLE 98 SUMMARY AND TEST RESULTS FOR ADULT CARIES TRUE AND CRUDE FREQUENCY.....393
TABLE 99 DISTRIBUTION OF CARIES DIRECTION IN THE ADULT PERMANENT DENTITION.....395
TABLE 100 SUMMARY AND TEST RESULTS FOR SUBADULT CARIES TRUE AND CRUDE FREQUENCY.....396
TABLE 101 CARIES TRUE AND CRUDE FREQUENCIES ACROSS EUROPE (COMPILED PARTIALLY FROM (MÜLLER & HUSSEIN 2017; BERTILSSON ET AL. 2022)) 400
TABLE 102 SCORES FOR THE EVALUATION OF PERIODONTAL DISEASE BASED ON (BROTHWELL 1981).....403
TABLE 103 SUMMARY AND RESULTS OF PERIODONTAL DISEASE CRUDE FREQUENCY.....404
TABLE 104 SUMMARY AND TEST RESULTS FOR SUBADULT PERIODONTAL DISEASE CRUDE FREQUENCY.....406
TABLE 105 OVERVIEW OF PERIODONTAL DISEASE PREVALENCE IN MEDIEVAL-POSTMEDIEVAL EUROPEAN SITES 408
TABLE 106 SCORES FOR RECORDING PERIAPICAL LESIONS AFTER (DIAS & TAYLES 1997).....410
TABLE 107 SUMMARY AND TEST RESULTS FOR ADULT PERIAPICAL LESIONS CRUDE FREQUENCY.....412
TABLE 108 SUMMARY AND TEST RESULTS FOR SUBADULT PERIAPICAL LESIONS CRUDE FREQUENCY 413
TABLE 109 OVERVIEW OF PERIAPICAL LESION PREVALENCE IN MEDIEVAL-POSTMEDIEVAL EUROPEAN SITES 414
TABLE 110 SUMMARY AND TEST RESULTS FOR ADULT ANTEMORTEM TOOTH LOSS TRUE AND CRUDE FREQUENCY 418
TABLE 111 SUMMARY AND TEST RESULTS FOR SUBADULT ANTEMORTEM TOOTH LOSS TRUE AND CRUDE FREQUENCY 420
TABLE 112 OVERVIEW OF ANTE MORTEM TOOTH LOSS (AMTL) PREVALENCE IN MEDIEVAL-POSTMEDIEVAL EUROPEAN SITES (COMPILED PARTIALLY FROM (MÜLLER & HUSSEIN 2017; BERTILSSON ET AL. 2022))...421
TABLE 113 SCORES FOR DENTAL ATTRITION BASED ON TRAUTMANN (2012).....424
TABLE 114 MEAN ATTRITION SCORES FOR ADULTS BY SEX, AGE, BURIAL LOCATION AND LAYER 426
TABLE 115 MEAN ATTRITION SCORES FOR SUBADULTS BY SEX, AGE, BURIAL LOCATION AND LAYER 428
TABLE 116 EARLIEST ONSET OF CARIES AND ATTRITION IN SUBADULTS 448
TABLE 117 STABLE ISOTOPE VALUES FROM MIDSHAFT AND METAPHYSIS FROM SUBADULTS WITH INFERRED WEANING STATUS.....453
TABLE 118 RESULTS OF DENTAL STATUS WITH FEEDING STATUS BASED ON $\delta^{15}N$ VALUES 455
TABLE 119 RESULTS OF THE WARN MODEL FOR THE MIDSHAFT SAMPLES.....458
TABLE 120 RESULTS OF THE WARN MODEL FOR THE METAPHYSIS SAMPLES 458
TABLE 121 RESULTS FOR THE GROUP COMPARISONS OF $\delta^{15}N$ AND $\delta^{13}C$ 477

13 List of Figures

FIGURE 1 MAP OF LUXEMBOURG CITY AROUND 1560AD (BY JACQUES DEVENTER) SOURCED FROM TRAUSCH (1993), MODIFIED BY A. KREMMER TO SHOW THE LOCATION OF THE FRANCISCAN FRIARY (BLUE ARROW).15
FIGURE 2 MAP OF LUXEMBOURG CITY WITH FOCUS ON THE FORTIFICATIONS FROM THE MID 18TH CENTURY (BY PETER MARTELL, LONDON ~1745) SOURCED FROM TRAUSCH (1993), MODIFIED BY A. KREMMER TO SHOW THE LOCATION OF THE FRANCISCAN FRIARY (BLUE ARRO 17
FIGURE 3 SUPERIMPOSITION OF THE OUTLINES OF THE REMNANTS OF THE FRIARY BUILDINGS FROM OLD CADASTRAL MAPS (1820/24) ON THE DRAWING OF THE FRIARY ON THE PLAN DE GOUGEON FROM 1691 (SOURCED FROM BIS-WORCH (2011) 20
FIGURE 4 EXCAVATION MAP OF THE EXCAVATION CAMPAIGN 2008-2011 (KINDLY PROVIDED BY MME BIS-WORCH OF THE INRA) 26
FIGURE 5 EXCAVATION MAP OF THE EXCAVATION CAMPAIGN 2013-15 (KINDLY PROVIDED BY ARCHEODUNUM SA), MODIFIED BY A.KREMMER TO INDICATE APPROXIMATE PLACEMENT OF THE 4 SURVEYS WITH INHUMATIONS FROM CAMPAIGN 2016 (MAUVE OVALS) AND INDICATING THE POSITION OF CAMPAIGN 2008-11(PALE BLUE ARROWS) (SKELETONS FROM 2013-15 MISSING (YELLOW RECTANGLE 28
FIGURE 6 SUPERIMPOSITION OF THE RECONSTRUCTION FROM ARCHAEOLOGICAL VESTIGES OF THE FIRST FRANCISCAN CHURCH (GREEN) WITH THE CEMETERY AREA (RED) AND THE OUTLINE OF THE FRIARY BUILDINGS AND 17TH CENTURY CHURCH AND MARIENTHAL REFUGIUM FROM CADASTRAL MAPS (1820/24) (MAUVE) AND THE MANSFELD CHAPEL (GREEN DASHES) SOURCED FROM BIS-WORCH (2011), MODIFIED BY A. KREMMER TO SHOW APPROXIMATE LOCATION OF INHUMATION AREAS OF CAMPAIGN 2008-11 (BLUE RECTANGLE) TO CAMPAIGN 2013-15 (YELLOW RECTANGLE) AND 2016 (PINK RECTANGLE) 29
FIGURE 7 EXAMPLE OF A TYPICAL BURIAL ORIENTED WEST-EAST WITH ARMS FOLDED OVER ABDOMEN (2008-78/885; 161B444) BY OLIVER HAFFNER PROVIDED BY CNRA (SCALE 1:10) 31
FIGURE 8 THE INDIVIDUAL RESTING ON THE LEFT SIDE WITH BENT KNEES, ORIENTED WEST-EAST (2008-78/1340; 241B594) BY OLIVER HAFFNER PROVIDED BY CNRA (SCALE 1:10) 31
FIGURE 9 A-E DEPICT THE DIFFERENT ARM POSITIONS RECORDED FOR THE KNUEDLER CEMETERY. THE POSITION DESCRIPTIONS AND LABELLING ARE RECORDED AFTER TAGESSON (2015) BUT THE ILLUSTRATIONS ARE SOURCED FROM EIBL (2015) 32
FIGURE 10 FREQUENCY OF ARM POSITIONS OVERALL 32
FIGURE 11 FREQUENCY OF ARM POSITIONS BY LAYER 32
FIGURE 12 FREQUENCY OF ARM POSITIONS BY BURIAL LOCATION 33
FIGURE 13 FREQUENCY OF ARM POSITIONS BY SEX 33
FIGURE 14 AVERAGE REPRESENTATION OF THE WHOLE SKELETON AND BY SKELETAL AREA 37
FIGURE 15 REPRESENTATION CLASSIFICATION FOR THE WHOLE SKELETON AND BY SKELETAL AREA (DARK RED: 1-25%, DARK ORANGE: 25-50%, ORANGE: 50-75%, LIGHT ORANGE: 75-100%) 38
FIGURE 16 NUMBER OF INDIVIDUALS IN EACH AGE CATEGORY 46
FIGURE 17 FREQUENCY OF INDIVIDUALS FOR THE 20-YEAR SPAN AGE CATEGORIES WITHOUT ADULTUS 46
FIGURE 18 NUMBER OF INDIVIDUALS BY AGE AND SEX 54
FIGURE 19 MORTALITY PEAKS OF WOMEN FROM LAYER 1 BY BURIAL LOCATION (P=0.8926) 55
FIGURE 20 MORTALITY PEAKS OF WOMEN FROM LAYER 2 BY BURIAL LOCATION (P=0.9529) 55
FIGURE 21 MORTALITY PEAKS OF MEN FROM LAYER 1 BY BURIAL LOCATION (P=0.0001) 55
FIGURE 22 MORTALITY PEAKS OF MEN FROM LAYER 2 BY BURIAL LOCATION (P=0.3526) 55
FIGURE 23 LIFE EXPECTANCY OVERALL 68
FIGURE 24 LIFE EXPECTANCY BY SEX 68
FIGURE 25 LIFE EXPECTANCY BY BURIAL LOCATION 68
FIGURE 26 LIFE EXPECTANCY BY BURIAL LOCATION AND SEX 68
FIGURE 27 LIFE EXPECTANCY BY BURIAL LAYER 69
FIGURE 28 LIFE EXPECTANCY BY BURIAL LAYER AND SEX 69
FIGURE 29 PROBABILITY OF DEATH OVERALL 70
FIGURE 30 PROBABILITY OF DEATH BY SEX 70
FIGURE 31 PROBABILITY OF DEATH BY BURIAL LOCATION 71
FIGURE 32 PROBABILITY OF DEATH BY BURIAL LOCATION AND SEX 71
FIGURE 33 PROBABILITY OF DEATH BY BURIAL LAYER 72
FIGURE 34 PROBABILITY OF DEATH BY BURIAL LAYER AND SEX 72
FIGURE 35 LIFE EXPECTANCY FOR 10-YEAR STEPS FOR THE KNUEDLER AD ST. ESPRIT BURIAL GROUNDS 78

FIGURE 36 GROWTH CURVE OF MAXIMUM HUMERAL LENGTH (H3/HU1) (DARK GREEN LINE) AND HUMERAL MIDSHAFT CIRCUMFERENCE (H6/HU7) (LIGHT GREEN LINE) BY AGE IN YEARS. THE LINES CONNECT THE AVERAGE VALUES OF EACH MEASUREMENT BY AGE GROUP 85
FIGURE 37 ADDITIONAL GROWTH IN ANNUAL STEPS OF MAXIMUM HUMERAL LENGTH (H3/HU1) (DARK GREEN LINE) AND HUMERAL MIDSHAFT CIRCUMFERENCE (H6/HU7) (LIGHT GREEN LINE) 85
FIGURE 38 GROWTH CURVE OF MAXIMUM RADIAL LENGTH (R7/RA1) (DARK GREEN LINE) AND MAXIMUM BREADTH OF DISTAL DIAPHYSIS (R8/RA5(6)) (LIGHT GREEN LINE) BY AGE IN YEARS. THE LINES CONNECT THE AVERAGE VALUES OF EACH MEASUREMENT BY AGE GROUP 86
FIGURE 39 ADDITIONAL GROWTH IN ANNUAL STEPS OF MAXIMUM RADIAL LENGTH (R7/RA1) (DARK GREEN LINE) AND MAXIMUM BREADTH OF DISTAL DIAPHYSIS (R8/RA5(6)) (LIGHT GREEN LINE) 86
FIGURE 40 GROWTH CURVE OF MAXIMUM FEMORAL LENGTH (F10/FE1) (DARK GREEN LINE) AND FEMORAL MIDSHAFT CIRCUMFERENCE (F13/FE8) (LIGHT GREEN LINE) BY AGE IN YEARS THE LINES CONNECT THE AVERAGE VALUES OF EACH MEASUREMENT BY AGE GROUP 86
FIGURE 41 ADDITIONAL GROWTH IN ANNUAL STEPS OF MAXIMUM FEMORAL LENGTH (F10/FE1) (DARK GREEN LINE) AND FEMORAL MIDSHAFT CIRCUMFERENCE (F13/FE8) (LIGHT GREEN LINE) 86
FIGURE 42 GROWTH CURVE OF MAXIMUM TIBIAL LENGTH (T14/TI1) (DARK GREEN LINE) AND TIBIAL LEAST CIRCUMFERENCE (T16/TI10B) (LIGHT GREEN LINE) BY AGE IN YEARS. THE LINES CONNECT THE AVERAGE VALUES OF EACH MEASUREMENT BY AGE GROUP 86
FIGURE 43 ADDITIONAL GROWTH IN ANNUAL STEPS OF MAXIMUM TIBIAL LENGTH (T14/TI1) (DARK GREEN LINE) AND TIBIAL LEAST CIRCUMFERENCE (T16/TI10B) (LIGHT GREEN LINE) 86
FIGURE 44 GROWTH CURVE OF RECONSTRUCTED BODY HEIGHT BY AGE IN YEARS. THE LINES CONNECT THE AVERAGE VALUES OF EACH MEASUREMENT BY AGE GROUP 87
FIGURE 45 ADDITIONAL GROWTH IN ANNUAL STEPS RECONSTRUCTED BODY HEIGHT 87
FIGURE 46 DISTRIBUTION OF BMI CLASSES BETWEEN CLOISTER AND CEMETERY BURIALS FOR MALES AND FEMALES BASED ON RUFF ET AL. (2012) 90
FIGURE 47 DISTRIBUTION OF BMI CLASSES BETWEEN LAYER 1 AND LAYER 2 BURIALS FOR MALES AND FEMALES BASED ON RUFF ET AL. (2012) 90
FIGURE 48 COMPARISON OF AVERAGE BMI BY PERIOD BETWEEN DANISH SITES AND THE KNUEDLER CEMETERY (LAYER 2 = LATE MEDIEVAL-EARLY POSTMEDIEVAL, LAYER 1 = POSTMEDIEVAL, M = MEDIEVAL, PM = POSTMEDIEVAL) (KNU AFTER RUFF ET AL. 2012) 100
FIGURE 49 COMPARISON OF BMI CLASS FREQUENCIES BY PERIOD BETWEEN DANISH SITES AND THE KNUEDLER CEMETERY (LAYER 2 = LATE MEDIEVAL-EARLY POSTMEDIEVAL, LAYER 1 = POSTMEDIEVAL, M = MEDIEVAL, PM = POSTMEDIEVAL) (KNU AFTER RUFF ET AL. 2012) 100
FIGURE 50 COMPARISON OF AVERAGE BMI BY PERIOD BETWEEN DANISH SITES AND THE KNUEDLER CEMETERY (LAYER 2 = LATE MEDIEVAL-EARLY POSTMEDIEVAL, LAYER 1 = POSTMEDIEVAL, M = MEDIEVAL, PM = POSTMEDIEVAL) (KNU AND EUROPE MIX AFTER AUERBACH AND RUFF (2004) & (TROTTER AND GLESER (1952)) 100
FIGURE 51 COMPARISON OF BMI CLASS FREQUENCIES BY PERIOD BETWEEN DANISH SITES, A MIX OF EUROPEAN SITES AND THE KNUEDLER CEMETERY (LAYER 2 = LATE MEDIEVAL-EARLY POSTMEDIEVAL, LAYER 1 = POSTMEDIEVAL, M = MEDIEVAL, PM = POSTMEDIEVAL) (KNU AND EUROPE MIX AFTER AUERBACH AND RUFF (2004) & (TROTTER AND GLESER (1952)) 100
FIGURE 52 BAR CHARTS ILLUSTRATING THE FREQUENCY OF LOW, MEDIUM AND STRONG DEGREES OF ENTHESEAL DEVELOPMENT AMONG MEN AND WOMEN OF ALL AGE GROUPS 159
FIGURE 53 BAR CHARTS ILLUSTRATING THE FREQUENCY OF LOW, MEDIUM AND STRONG DEGREES OF ENTHESEAL DEVELOPMENT AMONG MEN AND WOMEN AGED BETWEEN 20-39Y 159
FIGURE 54 BAR CHARTS ILLUSTRATING THE FREQUENCY OF LOW, MEDIUM, AND STRONG DEGREES OF ENTHESEAL DEVELOPMENT AMONG ALL INDIVIDUALS AGED 20-40Y 161
FIGURE 55 BAR CHARTS ILLUSTRATING THE FREQUENCY OF LOW, MEDIUM, AND STRONG DEGREES OF ENTHESEAL DEVELOPMENT BETWEEN CEMETERY AND CLOISTER BURIALS AMONG ALL AGE GROUPS 162
FIGURE 56 BAR CHARTS ILLUSTRATING THE FREQUENCY OF LOW, MEDIUM, AND STRONG DEGREES OF ENTHESEAL DEVELOPMENT BETWEEN CEMETERY AND CLOISTER BURIALS AMONG THE YOUNGER ADULTS 162
FIGURE 57 BAR CHARTS ILLUSTRATING THE FREQUENCY OF LOW, MEDIUM, AND STRONG DEGREES OF ENTHESEAL DEVELOPMENT BETWEEN BURIALS FROM THE UPPER LAYER (LAYER 1) AND THE LOWER LAYER (LAYER 2) AMONG ALL AGE GROUPS 164
FIGURE 58 BAR CHARTS ILLUSTRATING THE FREQUENCY OF LOW, MEDIUM, AND STRONG DEGREES OF ENTHESEAL DEVELOPMENT BETWEEN BURIALS FROM THE UPPER LAYER (LAYER 1) AND THE LOWER LAYER (LAYER 2) AMONG ALL AGE GROUPS 164
FIGURE 59 DISTRIBUTION OF ALL EF LESIONS OF ALL ENTHESES WITHIN ONE JOINT AREA BY SIDE, SEX, AGE, BURIAL LOCATION AND LAYER 166

FIGURE 60 DISTRIBUTION OF ALL OL LESIONS OF ALL ENTHESES WITHIN ONE JOINT AREA BY SIDE, SEX, AGE, BURIAL LOCATION AND LAYER 167
FIGURE 61 SQUATTING FACETS IN THE TIBIAE OF 2016-082/452 175
FIGURE 62 ILLUSTRATION OF THE DIFFERENT JOINT TYPES SOURCED FROM (BRAND ET AL. 2017)....177
FIGURE 63 FREQUENCY AND SEVERITY OF DEGENERATIVE JOINT DISEASE IN THE DIFFERENT JOINTS FOR THE RIGHT AND LEFT SIDES....192
FIGURE 64 FREQUENCY AND SEVERITY OF DEGENERATIVE JOINT DISEASE IN THE DIFFERENT JOINTS FOR THE RIGHT AND LEFT SIDES DIFFERENTIATED BY SEX 192
FIGURE 65 FREQUENCY AND SEVERITY OF DEGENERATIVE JOINT DISEASE IN THE DIFFERENT JOINTS FOR THE RIGHT AND LEFT SIDES DIFFERENTIATED BY AGE....192
FIGURE 66 STRIATED EBURNATION (OSTEOARTHRITIS) ON LEFT DISTAL FEMORAL EPIPHYSIS (2008-78/1154) ...200
FIGURE 67 DJD WITHOUT EBURNATION IN RA +UL R OF 2008-78/215 200
FIGURE 68 ANKYLOSIS OF MT3 WITH LATERAL CUBOID (2008-78/666)....202
FIGURE 69 OSTEOCHONDRITIS DISSECANS IN THE LATERAL CONDYLE OF THE RIGHT TIBIA (2008-78/668) 203
FIGURE 70 OSTEOCHONDRITIS DISSECANS AT THE DISTAL EPIPHYSIS OF A SUBADULT TIBIA (2008-78/1424)....203
FIGURE 71 FREQUENCY OF SPONDYLOSIS DEFORMANS IN THE CERVICAL SPINE DIFFERENTIATED BY SEX 207
FIGURE 72 FREQUENCY OF SPONDYLOSIS DEFORMANS IN THE CERVICAL SPINE DIFFERENTIATED BY AGE 209
FIGURE 73 FREQUENCY OF SPONDYLOSIS DEFORMANS IN THE THORACIC SPINE DIFFERENTIATED BY SEX....210
FIGURE 74 FREQUENCY OF SPONDYLOSIS DEFORMANS IN THE THORACIC SPINE DIFFERENTIATED BY AGE 211
FIGURE 75 FREQUENCY OF SPONDYLOSIS DEFORMANS IN THE LUMBAR SPINE DIFFERENTIATED BY SEX 212
FIGURE 76 FREQUENCY OF SPONDYLOSIS DEFORMANS IN THE LUMBAR SPINE DIFFERENTIATED BY AGE....213
FIGURE 77 FREQUENCY OF SPONDYLARTHROSIS DEFORMANS IN THE CERVICAL SPINE DIFFERENTIATED BY SEX 214
FIGURE 78 FREQUENCY OF SPONDYLARTHROSIS DEFORMANS IN THE CERVICAL SPINE DIFFERENTIATED BY AGE215
FIGURE 79 FREQUENCY OF SPONDYLARTHROSIS DEFORMANS IN THE THORACIC SPINE DIFFERENTIATED BY SEX 215
FIGURE 80 FREQUENCY OF SPONDYLARTHROSIS DEFORMANS IN THE THORACIC SPINE DIFFERENTIATED BY AGE216
FIGURE 81 FREQUENCY OF SPONDYLARTHROSIS DEFORMANS IN THE LUMBAR SPINE DIFFERENTIATED BY SEX...217
FIGURE 82 FREQUENCY OF SPONDYLARTHROSIS DEFORMANS IN THE LUMBAR SPINE DIFFERENTIATED BY AGE ..218
FIGURE 83 PREVALENCE OF SCHMORL'S NODES IN THE CERVICAL SPINE, DIFFERENTIATED BY SEX 222
FIGURE 84 PREVALENCE OF SCHMORL'S NODES IN THE CERVICAL SPINE, DIFFERENTIATED BY AGE 222
FIGURE 85 PREVALENCE OF SCHMORL'S NODES IN THE THORACIC SPINE, DIFFERENTIATED BY SEX....223
FIGURE 86 PREVALENCE OF SCHMORL'S NODES IN THE THORACIC SPINE, DIFFERENTIATED BY SEX AND AGE....223
FIGURE 87 PREVALENCE OF SCHMORL'S NODES IN THE LUMBAR SPINE, DIFFERENTIATED BY SEX 224
FIGURE 88 PREVALENCE OF SCHMORL'S NODES IN THE LUMBAR SPINE, DIFFERENTIATED BY SEX AND AGE 224
FIGURE 89 DISH IN 2008-78/536 WITH SPARING OF THE INTERVERTEBRAL DISC SPACE (ANTERIOR VIEW)....226
FIGURE 90 DISH IN 2008-78/536 (RIGHT LATERAL VIEW)....226
FIGURE 91 OSTEOARTHRITIS IN THE RIGHT INFERIOR INTERVERTEBRAL JOINT OF A LUMBAR VERTEBRA (2008-78/670) 228
FIGURE 92 DEGENERATIVE CHANGES IN THE LOWER THORACIC VERTEBRAE (SPONDYLOPHYTES) (2008-78/1021) 228
FIGURE 93 PARTIAL SACRALISATION OF LV5 (2008-78/200) 245
FIGURE 94 PARTIAL BILATERAL SACRALISATION WITH PSEUDOARTHROSES OF 2008-78/1300....245
FIGURE 95 SPINA BIFIDA OCCULTA OF INDIVIDUAL 2008-78/380 246
FIGURE 96 SPONDYLOLYSIS OF LV5 AND NON-FUSION OF ARCH OF S1 (2008-78/1354)....246
FIGURE 97 SPONDYLOLYSIS OF LV5 OF 2008-78/1390....246
FIGURE 98 CONCHA BULLOSA....246
FIGURE 99 FACET FOR OS ACROMIALE ON THE RIGHT SCAPULA OF 2008-78/1312....246
FIGURE 100 UNILATERAL CORACOCLAVICULAR JOINT ON CLAVICULA L OF 2013-015/183 246
FIGURE 101 UNILATERAL CORACOCLAVICULAR JOINT ON CLAVICULA L OF 2008-78/885 247
FIGURE 102 CRANIOSYNOSTOSIS OF THE LEFT SIDE OF THE CORONAL SUTURE CAUSING PLAGIOCEPHALY (2008-78/818) 247
FIGURE 103 UNILATERAL CONGENITAL HIP DYSPLASIA IN 2008-78/1342 VIEW OF RIGHT FEMUR WITH SMALL, FLATTENED HEAD....247
FIGURE 104 UNILATERAL CONGENITAL HIP DYSPLASIA IN 2008-78/1342 VIEW OF RIGHT OS COXA WITH TRIANGULAR ACETABULUM 247
FIGURE 105 BILATERAL CONGENITAL HIP DYSPLASIA IN 2008-78/1440 VIEW OF THE FEMORA WITH DYSPLASTIC HEADS 247

FIGURE 106 BILATERAL CONGENITAL HIP DYSPLASIA IN 2008-78/1440 VIEW OF THE OSSA COXA WITH DYSPLASTIC ACETABULUM 247
FIGURE 107 RADIOGRAPH OF THE LEFT FEMUR OF 2008-78/1487 (PROBABLE CONGENITAL HIP DYSPLASIA) 248
FIGURE 108 FORMATION OF PROMINENT SECONDARY ACETABULUM IN 2008-78/1487 248
FIGURE 109 BILATERAL CONGENITAL HIP DYSPLASIA OF 2008-78/1487 VIEW OF FEMURS WITH FLATTENED, ELONGATED HEADS 248
FIGURE 110 BILATERAL CONGENITAL HIP DYSPLASIA OF 2008-78/1487 VIEW OF SHALLOW ACETABULUM LEFT 248
FIGURE 111 EPIPHYSIOLYSIS OR PERTHE'S DISEASE OF THE LEFT FEMORAL HEAD (SLIPPED FEMORAL EPIPHYSIS) OF 2008-78/150 SHOWING AN ENLARGED AND DISPLACED HEAD WITH NO DEGENERATIVE CHANGES AND OSTEOCHONDRITIS DISSECANS IN THE DISTAL EPIPHYSIS 249
FIGURE 112 MODIFICATION OF THE FEMORAL HEAD WITH OSTEOARTHRITIS LIKELY FROM PERTHE'S DISEASE OR SCFE, BUT TRAUMA CANNOT BE EXCLUDED (2008-78/1471) 249
FIGURE 113 RADIOGRAPH OF THE EPIPHYSIOLYSIS/PERTHE'S DISEASE OF 2008-78/150, SHOWING NO SIGNS OF FRACTURE 249
FIGURE 114 RADIOGRAPH OF FEMUR OF 2008-78/1471 249
FIGURE 115 ENLARGED RIGHT ELBOW JOINT OF 2008-78/1080 249
FIGURE 116 RADIOGRAPH OF ENLARGED HUMERAL DISTAL EPIPHYSIS (2008-78/1080) 249
FIGURE 117 COMPARISON OF THE RIGHT AND LEFT RADIUS OF INDIVIDUAL 2008-78/1080 SHOWING THE SLIGHTLY ENLARGED AND DOMED HEAD AND SLIGHTLY ELONGATED AND THINNED NECK OF THE RIGHT RADIUS. THE LEFT RADIUS PRESENTS A DEEP SMOOTH DIP IN THE CENTER OF THE RADIAL TUBEROSITY BUT SHOWS NO OTHER PATHOLOGICAL CHANGES OR ANATOMICAL VARIATIONS 249
FIGURE 118 TWO SMALL OSTEOMATA INSIDE THE FRONTAL SINUS OF INDIVIDUAL 2008-78/1361 253
FIGURE 119 LARGE OSTEOMA ON THE ENDOCRANIAL SIDE OF THE OCCIPITAL NEXT TO THE LAMBDOID SUTURE OF INDIVIDUAL 2008-78/1368 253
FIGURE 120 RADIOGRAPH OF THE LEFT ILIUM WITH PROBABLE INTRAOSSEOUS GANGLION ABOVE THE ACETABULUM (2008-78/655) 260
FIGURE 121 CLOSE-UP OF THE CAVITY ABOVE THE ACETABULUM PROBABLY CAUSED BY AND INTRAOSSEOUS GANGLION, SHOWING THE SMOOTH BORDERS (2008-78/655) 260
FIGURE 122 VENTRAL VIEW OF THE CAVITY PROBABLY CAUSED BY AN INTRAOSSEOUS GANGLION (2008-78/655) 260
FIGURE 123 TOP VIEW OF THE LEFT ILIUM WITH THE CAVITY VISIBLE IN THE LOWER RIGHT CORNER SUPERIOR TO THE ACETABULUM (2008-78/655) 260
FIGURE 124 PRIMARY SOFT TISSUE CARCINOMAS AND THE TYPE OF METASTATIC LESIONS THEY PRODUCE (FROM COLEMAN (2001)) 271
FIGURE 125 TOP VIEW OF THE FRONTAL BONE AND PART OF THE RIGHT AND LEFT PARIETAL WITH THE LYTIC LESION 276
FIGURE 126 CLOSE-UP OF THE LYTIC LESION ON THE ENDOCRANIAL SURFACE OF THE RIGHT PARIETAL BONE CLOSE TO THE CORONAL AND SAGITTAL SUTURES 276
FIGURE 127 SMALLER LYTIC LESION WITH BONE REACTION IN MAXILLA AT THE ZYGOMATICOMAXILLARY SUTURE 277
FIGURE 128 LARGE LYTIC LESION WITH EXTENSIVE NEW BONE FORMATION INSIDE LEFT ZYGOMATIC PROCESS OF FRONTAL BONE 277
FIGURE 129 ECTOCRANIAL VIEW OF RADIOGRAPH SHOWING LYTIC LESIONS AND THE CLOUDY UNDEFINED LYTIC LESION IN THE LEFT FRONTAL PROCESS, REFLECTING THE OSTEOBLASTIC BONE GROWTH ON THE LESION WALLS 277
FIGURE 130 LYTIC LESION WITH BONE REACTION INSIDE FRONTAL PROCESS OF LEFT ZYGOMATIC BONE 277
FIGURE 131 STRONG IRREGULAR PERIOSTEAL REACTION COVERING AN UNDERLYING OSTEOLYTIC LESION ON THE LATERAL SIDE OF THE LEFT ILIUM 278
FIGURE 132 VIEW INTO THE OSTEOLYTIC LESION COVERED BY IRREGULAR NEW BONE, SHOWCASING ALSO INTENSE NEW BONE FORMATION INSIDE CAVITY (LEFT ILIUM) 278
FIGURE 133 LARGE AREA OF AGGRESSIVE IRREGULAR PERIOSTEAL REACTION ON THE LATERAL SIDE OF THE RIGHT ILIUM 278
FIGURE 134 OSTEOLYTIC LESIONS SURROUNDED BY REACTIVE BONE ON THE AURICULAR SURFACE OF THE LEFT ILIUM 278
FIGURE 135 LATERAL SIDE OF THE RIGHT ILIUM WITH OSTEOLYTIC LESIONS AND AGGRESSIVE PERIOSTEAL REACTIONS 279
FIGURE 136 LATERAL SIDE OF THE RIGHT ILIUM WITH OSTEOLYTIC LESIONS AND AGGRESSIVE PERIOSTEAL REACTION 279

FIGURE 137 LARGE OSTEOLYTIC LESION WITH AGGRESSIVE NEW BONE FORMATION INSIDE THE TRABECULAR BONE AT THE RIGHT ILIAC CREST....279
FIGURE 138 RADIOGRAPH OF THE LEFT OS COXAE SHOWING SEVERAL OSTEOLYTIC FOCI WITH DIFFUSE MARGINS THAT WERE NOT VISIBLE MACROSCOPICALLY....279
FIGURE 139 CLOSE-UP OF THE OSTEOLYTIC LESION IN THE SCAPULAR SPINE, SURROUNDED BY LIGHT REACTIVE BONE LESIONS....280
FIGURE 140 POSTERIOR VIEW OF THE RIGHT SCAPULA WITH LYTIC LESIONS....280
FIGURE 141 RADIOGRAPH OF THE RIGHT SCAPULA REVEALING THE PRESENCE OF FURTHER OSTEOLYTIC LESIONS IN THE APEX....280
FIGURE 142 OSTEOLYTIC LESIONS IN THE RIGHT HUMERUS THAT WERE NOT VISIBLE MACROSCOPICALLY....280
FIGURE 143 OSTEOLYTIC LESIONS INSIDE THE LEFT PARIETAL AND OCCIPITAL THAT WERE NOT VISIBLE MACROSCOPICALLY....280
FIGURE 144 OSTEOLYTIC LESION WITH AGGRESSIVE NEW BONE FORMATION INSIDE THE DIPLOE OF THE LEFT PARIETAL....281
FIGURE 145 OSTEOLYTIC LESION ON THE INNER SIDE OF THE LEFT MANDIBULAR RAMUS....281
FIGURE 146 OSTEOLYTIC LESION AT THE ENDOCRANIAL SIDE OF THE OCCIPITAL BASE....281
FIGURE 147 OSTEOLYTIC LESION AND REACTIVE BONE ON THE ECTOCRANIAL SIDE OF THE LEFT GREATER SPHENOID WING....281
FIGURE 148 OSTEOLYTIC LESION WITH "MOTH-EATEN" APPEARANCE IN S1 OF THE SACRUM WITH AGGRESSIVE PERIOSTEAL REACTION AT THE MARGINS (FURTHER OSTEOLYTIC LESION ON THE S1 VERTEBRAL PLATE)..281
FIGURE 149 OSTEOLYTIC LESIONS IN THE VERTEBRAL ARCH OF A CERVICAL VERTEBRA....281
FIGURE 150 RIGHT OF COXAE WITH OSTEOLYTIC LESIONS AND AGGRESSIVE PERIOSTEAL REACTION....282
FIGURE 151 LEFT OF COXAE WITH OSTEOLYTIC LESIONS AND LIHGHT AGGRESSIVE PERIOSTEAL REACTION (SURFACE CHANGE OF THE AURICULAR SURFACE)....282
FIGURE 152 CLOSE-UP OF THE LESION ON THE RIGHT ILIAC BLADE SHOWING COALESCED LYTIC LESIONS WITH AGGRESSIVE PERIOSTEAL REACTION....282
FIGURE 153 MULTIPLE OSTEOLYTIC LESIONS ON THE LEFT OS PUBIS....282
FIGURE 154 RIGHT HUMERUS WITH OSTEOLYTIC LESIONS AT THE PROXIMAL META- AND EPIPHYSIS AND A HEALED FRACTURE AT THE DISTAL EPIPHYSIS....282
FIGURE 155 CLOSE-UP OF THE OSTEOLYTIC LESIONS IN THE RIGHT PROXIMAL HUMERAL META- AND EPIPHYSIS WITH LIGHT AGGRESSIVE PERIOSTEAL REACTION....283
FIGURE 156 RADIOGRAPH OF THE RIGHT RADIUS, ULNA AND HUMERUS SHOWING LEAD SHRAPNEL IN THE DISTAL HUMERAL FRACTURE AND INSIDE THE ULNAR OLECRANON....283
FIGURE 157 RADIOGRAPH SHOWING AN OSTEOLYTIC LESION IN THE RIGHT AND LEFT CLAVICLES....283
FIGURE 158 SMALL OSTEOLYTIC LESIONS IN THE STERNUM....283
FIGURE 159 OSTEOLYTIC LESIONS ON THE LEFT SCAPULA WITH PERIOSTEAL REACTION....283
FIGURE 160 CLOSE-UP OF ONE OF THE OSTEOLYTIC LESIONS ON THE LEFT SCAPULA WITH THICK IRREGULAR BUT SMOOTH PERIOSTEAL REACTION....283
FIGURE 161 RIGHT RIBS WITH OSTEOLYTIC LESIONS AND PERIOSTEAL REACTION....284
FIGURE 162 LEFT RIBS WITH MIXED OSTEOLYTIC LESIONS AND PERIOSTEAL REACTION....284
FIGURE 163 CLOSE-UP OF OSTEOLYTIC LESIONS WITH EXTENSIVE AGGRESSIVE PERIOSTEAL REACTION ON LEFT RIB VENTRAL SIDE....284
FIGURE 164 CLOSE-UP OF MIXED LESIONS WITH EXTENSIVE AGGRESSIVE PERIOSTEAL REACTION ON LEFT RIB TOP VIEW....284
FIGURE 165 LIGHT OSTEOLYTIC LESIONS WITH PERIOSTEAL REACTION ON RIGHT RIB VENTRAL SIDE....284
FIGURE 166 OSTEOLYTIC LESIONS WITH AGGRESSIVE PERIOSTEAL REACTION ON RIGHT RIB BOTTOM VIEW....284
FIGURE 167 CLOSE-UP ON LARGE AREA WITH MANY LYTIC FOCI ON THE ECTOCRANIAL SIDE OF THE SPHENOID .284
FIGURE 168 CLOSE-UP OF AN OSTEOLYTIC LESION ON THE LEFT PARIETAL NEXT TO THE SAGITTAL SUTURE....284
FIGURE 169 CLOSE-UP OF AN OSTEOLYTIC LESION AT THE CORONAL SUTURE (RATHER A DENSE POROUS SPOT).285
FIGURE 170 OSTEOLYTIC LESION OF "MOTH-EATEN" APPEARANCE AND EXTENSIVE AND AGGRESSIVE NEW BONE FORMATION THROUGHOUT THE RIGHT ORBIT....285
FIGURE 171 OSTEOLYTIC LESION OF "MOTH-EATEN" APPEARANCE AT THE BASE OF THE LEFT TEMPORAL AND SPHENOID....285
FIGURE 172 OBLIQUE-BASAL VIEW OF THE CRANIUM SHOWCASING SEVERAL OSTEOLYTIC LESIONS AND PERIOSTEAL REACTIONS....285
FIGURE 173 CT-SCAN OF THE CRANIUM WITH LARGE OSTEOLYTIC LESION IN THE LEFT SPHENOID AND A SMALLER ONE IN THE RIGHT ORBIT, AND THE NEW BONE DEPOSITION ON THE ORBITAL ROOF....285

FIGURE 174 LATERAL VIEW OF THE CRANIUM SHOWING AN OSTEOLYTIC LESION IN THE DIPLOE OF THE FRONTAL AND INSIDE THE SPHENOID AND ORBITAL ROOF....285
FIGURE 175 MANDIBLE WITH OSTEOLYTIC LESION ON THE RIGHT ALVEOLAR PROCESS AND A HEALED FRACTURE ON THE LEFT BODY....286
FIGURE 176 HEALED FRACTURE OF THE LEFT MANDIBULAR BODY WITH PATCH OF PERIOSTEAL NEW BONE FORMATION ON THE RAMUS....286
FIGURE 177 RADIOGRAPH OF RIBS SHOWING OSTEOLYTIC LESIONS AND SCLEROTIC AREAS (GREEN ARROW) INDICATIVE OF OSTEOBLASTIC REACTION....286
FIGURE 178 PROBABLE OSTEOBLASTIC LESION COVERING THE COMPLETE AURICULAR SURFACE OF THE LEFT ILIUM....286
FIGURE 179 SPONGIOSCLEROSIS INDICATIVE OF AN OSTEOBLASTIC LESION WITHIN THE TRABECULAE OF THE LEFT OS ILIUM, PROBABLY IN RELATION TO THE LESION IN FIGURE 178....286
FIGURE 180 TOP VIEW ON THE LYTIC LESIONS OF THE SPINOUS PROCESS OF THE 10TH VERTEBRA....287
FIGURE 181 BOTTOM VIEW ON THE LYTIC LESIONS OF THE SPINOUS PROCESS OF THE 10TH VERTEBRA....287
FIGURE 182 ABSENCE OF LYTIC LESIONS IN THE 9TH THORACIC VERTEBRA....287
FIGURE 183 POSSIBLE LYTIC LESION (ILL-DEFINED RADIOLUCENCY WITHOUT SCLEROTIC MARGIN) IN THE METAPHYSIS OF THE LEFT HUMERUS....287
FIGURE 184 ENLARGED AND SCLEROTISED DIPLOIC VEINS (2016_082/403)....292
FIGURE 185 LARGE GROOVE INSIDE CRUCIFORM EMINENCE ON OCCIPITAL, LIKELY AN ENLARGED DIPLOIC VEIN (2013-015/403)....292
FIGURE 186 ENDOCRNIAL BONE DEPOSITS ON PARIETAL OF 2016-082/403....292
FIGURE 187 ENDOCRNIAL BONE DEPOSITS ON FRONTAL OF 2016-082/403....292
FIGURE 188 ENLARGED AND SCLEROTISED DIPLOIC VEIN IN THE FRONTAL BONE (2016_082/403)....293
FIGURE 189 RADIOGRAPH REVEALING ENLARGED AND SCLEROTISED DIPLOIC VEINS IN FRONTAL BONE R SIDE AND CENTRAL PART (2016_082/403)....293
FIGURE 190 PARTIALLY OSSIFIED CARTILLAGE OF INDIVIUAL 2008-78/194....293
FIGURE 191 RADIOGRAPH OF THE LEFT ULNA DISPLAYING CLEARLY THE LAMELLAR STRUCTURE OF THE PERIOSTEAL NEW BONE DEPOSIT AND SHOWING NO EVIDENCE OF LYTIC LESIONS INSIDE THE BONE (2013-15/161)....293
FIGURE 192 HEALED COLLES FRACTURE OF THE LEFT RADIUS OF 2008-78/793....299
FIGURE 193 MISALIGNED PARRY FRACTURE IN THE RIGHT ULNA OF 2008-78/800....299
FIGURE 194 OBLIQUE FRACTURE OF THE LEFT FEMUR OF A SUBADULT (2008-78/153) MIMICKING RICKETS....299
FIGURE 195 RADIOGRAPH OF OBLIQUE FRACTURE OF THE LEFT FEMUR OF A SUBADULT (2008-78/153) MIMICKING RICKETS....299
FIGURE 196 HEALED COMMINUTED FRACTURE OF THE RIGHT TIBIA DIAPHYSIS WITH PERIOSTEAL REACTIONS ON THE FIBULA AS WELL (2008-78/1476)....299
FIGURE 197 HEALED OBLIQUE FRACTURE OF THE RIGHT TIBIA OF 2008-78/1431....299
FIGURE 198 HEALED FRACTURE OF BOTH OSSA NASALIA OF 2008-78/1317....299
FIGURE 199 NON-FUSION OF FRACTURES ON TWO CONSECUTIVE LEFT RIBS OF 200-78/1001....299
FIGURE 200 DISTRIBUTION OF FRACTURES BY BODY PART....300
FIGURE 201 MYOSITIS OSSIFICANS TRAUMATICA LEFT FEMUR OF 2008-78/148....302
FIGURE 202 MYOSITIS OSSIFICANS TRAUMATICA LEFT FEMUR OF 2008-78/193....302
FIGURE 203 LARGE HEALED BLUNT FORCE TRAUMA ON FRONTAL 2008-78/603....306
FIGURE 204 CLOSE-UP OF THE ARGE HEALED BLUNT FORCE TRAUMA ON FRONTAL 2008-78/603....306
FIGURE 205 LARGE UNHEALED SHARP FORCE TRAUMA CROSSING THE LEFT PARIETAL OF 2008-78/99....306
FIGURE 206 CLOSE-UP OF UNHEALED SHARP FORCE TRAUMA CROSSING THE LEFT PARIETAL OF 2008-78/99....306
FIGURE 207 HEALED SHARP FORCE TRAUMA AT POSTERIOR RIGHT PARIETAL OF 2008-78/344 (FROM GRAVE FILL).....306
FIGURE 208 HEALED GUNSHOT WOUND WITH BULLET STUCK IN ORBITAL ROOF (2013-015/353)....306
FIGURE 209 AMPUTATION AT THE RIGHT HUMERUS (2008-78/729)....309
FIGURE 210 AMPUTATION AT THE RIGHT HUMERUS (2008-78/729) VIEW OF THE CUTTING SURFACE....309
FIGURE 211 EVIDENCE OF TREPHINATION WITH CUTMARKS (ARROWS) AT THE MARGINS OF 2008-78/1040....309
FIGURE 212 PENETRATING BLUNT FORCE TRAUMA OR TREPHINATION CLOSE TO BREGMA OF 2013-015/357 (FROM GRAVE FILL)....309
FIGURE 213 CUT MARKS (PROBABLY FOR FLESHING) AT THE RIGHT TEMPORALIS MUSCLE ATTACHMENT OF 2008-78/765 AN AUTOPSIED INDIVIDUAL....309
FIGURE 214 CUTTING MARKS ON THE FRONTAL OF AN AUTOPSIED INDIVIDUAL (2008-78/765)....309
FIGURE 215 AUTOPSY OF 2008-78/343....309

FIGURE 216 STAGES FOR SCORING PERIOSTEAL REACTION (FROM STECKEL ET AL. (2006)) 316
FIGURE 217 SEVERE PERIOSTITIS ON THE RIGHT TIBIA AND FIBULA OF 2008-78/1001 317
FIGURE 218 DISTRIBUTION OF ACTIVE AND HEALED PERIOSTEAL REACTIONS BY BONE TYPE....318
FIGURE 219 OSTEOMYELITIS IN THE PROXIMAL EPIPHYSIS OF THE RIGHT TIBIA OF 2008-78/838....323
FIGURE 220 LARGE DESTRUCTIVE OSTEOLYTIC LESION ON THE SUPERIOR VERTEBRAL PLATE OF TV4 OF 2008-78/585 323
FIGURE 221 PROBABLY OSTEOMYELITIS IN THORACIC VERTEBRAE OF 2008-78/1021 323
FIGURE 222 OSTEOMYELITIS IN THE RIGHT SCAPULA OF 2008-78/1021 323
FIGURE 223 OSTEOMYELITIS IN THE LEFT FEMUR OF 2008-78/1021 WITH ANKYLOSIS OF PATELLA AND TIBIA ...323
FIGURE 224 EVIDENCE FOR CHRONIC SINUSITIS IN RIGHT MAXILLARY SINUS OF 2008-78/1704 327
FIGURE 225 DIFFERENT TYPES OF ENAMEL DEFECTS (TAKEN FROM PINHASI AND MAYS, 2007) 330
FIGURE 226 TEMPLATE FOR AGEING LINEAR ENAMEL DEFECTS ON FRONT TEETH (TAKEN FROM (REID & DEAN 2000)) 332
FIGURE 227 TEMPLATE FOR AGEING LINEAR ENAMEL DEFECTS ON MOLARS (TAKEN FROM (REID & DEAN 2006)) 332
FIGURE 228 PITTED ENAMEL DEFECT ON RIGHT MANDIBULAR M1 OF 2008-78/731 332
FIGURE 229 TWO STRONG BANDS OF LINEAR ENAMEL HYPOPLASIA ACROSS SEVERAL TEETH (2008-78/1342) ...332
FIGURE 230 NUMBER OF LEH BY AGE FOR THE COMPLETE SAMPLE 338
FIGURE 231 NUMBER OF LEH BY AGE DIFFERENTIATED BY SEX 338
FIGURE 232 NUMBER OF LEH BY AGE DIFFERENTIATED BY BURIAL LOCATION 338
FIGURE 233 NUMBER OF LEH BY AGE DIFFERENTIATED BY BURIAL LAYER....338
FIGURE 234 ILLUSTRATION OF THE SCORING SYSTEM FOR CRIBRA ORBITALIA AFTER (STECKEL ET AL. 2006) ...346
FIGURE 235 ILLUSTRATION OF THE SCORING SYSTEM FOR CRIBRA CRANII AFTER (STECKEL ET AL. 2006) 348
FIGURE 236 CLOSE-UP OF CRIBRA ORBITALIA IN LEFTT ORBIT OF 2008-78/818....350
FIGURE 237 CLOSE-UP OF POROTIC HYPEROSTOSIS ALONG SAGITTAL SUTURE OF 2008-78/809 350
FIGURE 238 FACTORS THAT MAY HAVE AN IMPACT ON THE DEVELOPMENT OF METABOLIC DISEASE (FROM (BRICKLEY & IVES 2008)) 353
FIGURE 239 THICK LAMELLATED PERIOSTEAL NEW BONE DEPOSITION ON PROXIMAL ULNA OF INDIVIDUAL 2016-082/161 365
FIGURE 240 STRONG ENAMEL DEFECT ON LEFT PERMANENT P3 OF INDIVIDUAL 2016-082/161 365
FIGURE 241 SACRUM WITH STRONG BEND AT THE S1-S2 JUNCTION OF INDIVIDUAL 2008-78/190....365
FIGURE 242 LIGHT PERIOSTEAL NEW BONE FORMATION ON THE DISTAL METAPHYSIS OF THE RIGHT FEMUR OF INDIVIDUAL 2008-78/190....365
FIGURE 243 CRIBRA ORBITALIA IN RIGHT ORBIT OF INDIVIDUAL 2008-78/248 369
FIGURE 244 POROUS LESION ON MAXILLARY PALATE OF INDIVIDUAL 2008-78/248 369
FIGURE 245 STRONG POROUS LESION ON OCCIPITAL BASE OF INDIVIDUAL 2008-78/522 369
FIGURE 246 POROUS LESION IN THE SUPRASPINOUS FOSSA OF THE RIGHT SCAPULA OF INDIVIDUAL 2008-78/522 369
FIGURE 247 POROUS NEW BONE FORMATION ABOVE THE MANDIBULAR FORAMEN IN INDIVIDUAL 2008-78/673.369
FIGURE 248 POROUS NEW BONE FORMATION ON THE LATERAL ASPECT OF THE RIGHT ZYGOMATIC BONE OF INDIVIDUAL 2008-78/728....369
FIGURE 249 EXTENSIVE POROUS NEW BONE FORMATION ON RIGHT TEMPORAL OF INDIVIDUAL 2016-082/419 ...370
FIGURE 250 EXTENSIVE ECTOCRANIAL POROUS LESION AND NEW BONE FORMATION ON THE LEFT PARIETAL OF INDIVIDUAL 2016-082/419....370
FIGURE 251 EXTENSIVE POROUS NEW BONE FORMATION ON POSTERIOR SIDE OF DISTAL RIGHT HUMERUS OF INDIVIDUAL 2008-78/728....370
FIGURE 252 PERIOSTEAL NEW BONE FORMATION ON ANTERIOR SIDE OF MAXILLA AND AROUND INFRAORBITAL FORAMEN OF INDIVIDUAL 2013-015/179 370
FIGURE 253 EXTENSIVE POROUS NEW BONE FORMATION THE PROXIMAL METAPHYSIS AND DIAPHYSIS OF THE RIGHT ULNA OF INDIVIDUAL 2008-78/728 370
FIGURE 254 VASCULAR IMPRESSIONS INSIDE OCCIPITAL OF INDIVIDUAL 2008-78/1099....371
FIGURE 255 PERIOSTEAL NEW BONE FORMATION ON LEFT SCAPULAR BLADE ANTERIOR SIDE OF INDIVIDUAL 2016-082/419 371
FIGURE 256 EXTENSIVE PERIOSTEAL NEW BONE FORMATION ALONG ALL OF DIAPHYSIS AND METAPHYSIS OF THE LEFT AND RIGHT HUMERUS OF INDIVIDUAL 2016-082/419 371
FIGURE 257 FLARING OF THE CHOBN^NDRAL RIB END WITH EXOSTOSIS AT MARGIN AND VERY POROUS SURFACES OF INDIVIDUAL 2016-082/419....371
FIGURE 258 POROUS LESIONS AROUND FORAMEN ROTUNDUM ON SPHENOID OF INDIVIDUAL 2008-78/728.....371

FIGURE 259 POROUS LESIONS ON ECTOCRANIAL SIDE OF THE ALA MAJOR OF THE SPHENOID FROM INDIVIDUAL 2008-78/728 371
FIGURE 260 ANTERIOR BOWING IN RIGHT FEMUR OF INDIVIDUAL 2008-78/1038 INDICATIVE OF POSSIBLE RESIDUAL RICKETS OR OSTEOMALACIA 374
FIGURE 261 LATERAL BOWING OF TIBIA R OF INDIVIDUAL 2008-78/820 INDICATIVE OF POSSIBLE RESIDUAL RICKETS OR OSTEOMALACIA 374
FIGURE 262 ANTEROPOSTERIOR FLATTENING OF FIBULA R OF INDIVIDUAL 2008-78/350 374
FIGURE 263 MEDIAL ANGULATION OF THE MANDIBULAR CONDYLES IN INDIVIDUAL 2008-78/1141 WITH RICKETS 374
FIGURE 264 PLANE ENAMEL DEFECT ON UNERUPTED M2 OF INDIVIDUAL 2008-78/1141 374
FIGURE 265 FLARING OF DISTAL METAPHYSIS AND COXA VARA OF THE LEFT FEMUR AND METAPHYSEAL CORTICAL THINNING IN INDIVIDUAL 2008-78/1141 374
FIGURE 266 ENDOCRANIAL VIEW OF THICKENED PARIETAL BONES (POSTERIOR PART OF LEFT AND RIGHT PARIETAL WITH ENDOCRANIALLY OBLITERATED SAGITTAL SUTURE IN THE CENTER) 378
FIGURE 267 CLOSE-UP OF THICKENED SKULL VAULT ON PARIETAL R SHOWCASING LOSS OF SPONGE-LIKE STRUCTURE OF THE DIPLOE 378
FIGURE 268 ILLUSTRATION OF THE SCORING SYSTEM FOR CALCULUS INTENSITY AFTER BROTHWELL 1981 (TAKEN FROM HILLSON 1996 REPRODUCED FROM BROTHWELL 1981) 380
FIGURE 269 DISTRIBUTION OF DENTAL CALCULUS INFESTATION BY AGE 382
FIGURE 270 DISTRIBUTION OF DENTAL CALCULUS INFESTATION BY AGE FOR MALES AND FEMALES 382
FIGURE 271 DISTRIBUTION OF DENTAL CALCULUS INFESTATION FOR THE UPPER AND LOWER JAW AS WELL AS RIGHT AND LEFT BODY SIDE 384
FIGURE 272 DISTRIBUTION OF CARIES INFESTATION BY BURIAL LOCATION 391
FIGURE 273 DISTRIBUTION OF CARIES INFESTATION BY AGE 392
FIGURE 274 DISTRIBUTION OF CARIES INFESTATION FOR MALES AND FEMALES BY AGE 392
FIGURE 275 DISTRIBUTION OF CARIES INFESTATION BY TOOTH FOR THE UPPER AND LOWER JAW AS WELL AS RIGHT AND LEFT BODY SIDE 395
FIGURE 276 DISTRIBUTION OF SEVERITY OF ALVEOLAR DISEASE BY AGE 406
FIGURE 277 ILLUSTRATION OF THE DIFFERENT TYPES OF PERIAPICAL LESIONS (TAKEN FROM PINHASI AND MAYS, 2007) 409
FIGURE 278 PERCENTAGE OF GRANULOMAS AND CYSTS BY AGE 411
FIGURE 279 RATES OF ANTEMORTEM TOOTH LOSS CALCULATED ON ALL TOOTH SOCKETS FOR MALES AND FEMALES BY AGE 417
FIGURE 280 COMPARISON OF TRUE CARIES AND ANTEMORTEM TOOTH LOSS RATES FOR MALES AND FEMALES BY AGE 417
FIGURE 281 DENTAL ATTRITION SEVERITY BY TOOTH FOR THE UPPER AND LOWER JAW OF THE LEFT AND RIGHT BODY SIDE OF THE ADULT PERMANENT DENTITION 425
FIGURE 282 DISTRIBUTION OF DENTAL ATTRITION SEVERITY BY TOOTH FOR THE SUBADULT PERMANENT DENTITION DIFFERENTIATED FOR RIGHT AND LEFT BODY SIDE 428
FIGURE 283 DISTRIBUTION OF DENTAL ATTRITION SEVERITY BY TOOTH FOR THE ADULT PERMANENT DENTITION, DIFFERENTIATED FOR RIGHT AND LEFT BODY SIDE 428
FIGURE 284 EXAMPLE OF A PIPE HOLE FROM THE KNUEDLER CEMETERY 430
FIGURE 285 AMOUNT OF CHILDREN AGED 0-6Y WITH CARIES LESIONS 447
FIGURE 286 NB OF CHILDREN AGED 0-6Y WITH OR WITHOUT CARIES LESIONS BY AGE 447
FIGURE 287 NUMBER OF CHILDREN AGED 0-6Y WITH AND WITHOUT DENTAL ATTRITION BY AGE 447
FIGURE 288 NUMBER OF CHILDREN AGED 0-6Y WITH LIGHT AND MODERATE ATTRITION BY AGE 447
FIGURE 289 NUMBER OF LEH BY AGE FOR ALL TEETH EXCEPT PREMOLARS. WHEN CONSIDERING ALL TEETH, ENAMEL HYPOPLASIA PEAKS ABRUPTLY AT 2-2.4 YEARS AND SLIGHTLY LESS AROUND 2.5-2.9 YEARS AND FREQUENCY THEN DROPS GRADUALLY WITH AGE. 449
FIGURE 290 NUMBER OF LEH LINES BY AGE FOR INCISORS AND CANINES ONLY. WHEN CONSIDERING ONLY INCISORS AND CANINES, THE PEAK AGE OF ENAMEL DEFECT FORMATION LIES BETWEEN 2-2.9 YEARS, FOLLOWED CLOSELY BY A PEAK AT 3-3.4 YEARS, AFTER WHICH FREQUENCY DROPS QUICKLY WITH INCREASING AGE. 449
FIGURE 291 NUMBER OF SINGLE LEH LINES BY AGE FOR INCISORS AND CANINES. LEH PEAKS ABRUPTLY BETWEEN 2-2.4 YEARS AND DECREASES GRADUALLY BUT STRONGLY WITH INCREASING AGE. 449
FIGURE 292 FITTED 4TH ORDER POLYNOMIAL TREND LINES FOR $\delta^{13}C$ OF MIDSHAFT AND METAPHYSIS SHOWING DIFFERENT DECREASING TRENDS BY AGE IN CHILDREN 1-6 YEARS 451

FIGURE 293 FITTED 2ND AND 3RD ORDER POLYNOMIAL TREND LINES FOR δ15N OF MIDSHAFT AND METAPHYSIS RESPECTIVELY SHOWING DIFFERENT DECREASING TRENDS BY AGE IN CHILDREN 1-6 YEARS 451
FIGURE 294 DATA SPREAD AND FITTED 4TH ORDER POLYNOMIAL CURVE FOR THE D15N DIFFERENCES BETWEEN MIDSHAFT AND METAPHYSIS OF CHILDREN AGED 1-6 YEARS 452
FIGURE 295 STACKED BAR CHART SHOWING THE NUMBER OF INDIVIDUALS OF DIFFERENT FEEDING STATUS BASED ON D15N DIFFERENCES BETWEEN MIDSHAFT AND METAPHYSIS (BF=BREASTFEEDING, WNG=WEANING, WN=WEANED, IN=INDETERMINATE).....453
FIGURE 296 TRANSVERSE COMPARISON OF δ15N (‰ AIR) VALUES BY NONADULT AGE CALCULATED FROM RECONSTRUCTED MAXIMUM DENSITY ESTIMATORS (MDES). MEAN AND SD RANGE FOR ADULT FEMALES IS INDICATED WITH AN OPEN CIRCLE. RESULTS ARE SHOWN FOR SAMPLES FROM THE MID-SHAFT OF SUBADULTS FROM LUXEMBOURG CITY 457
FIGURE 297 TRANSVERSE COMPARISON OF δ15N (‰ AIR) VALUES BY NONADULT AGE CALCULATED FROM RECONSTRUCTED MAXIMUM DENSITY ESTIMATORS (MDES). MEAN AND SD RANGE FOR ADULT FEMALES IS INDICATED WITH AN OPEN CIRCLE. RESULTS ARE SHOWN FOR SAMPLES FROM THE DISTAL METAPHYSIS OF SUBADULTS FROM LUXEMBOURG CITY.....458
FIGURE 298 SCATTERPLOT OF δ13C AND δ15N VALUES OF MALES AND FEMALES.....469
FIGURE 299 BOXPLOT OF δ15N VALUES OF MALES AND FEMALES SHOWING THE NARROWER RANGE OF FEMALE VALUES COMPARED TO MEN'S 469
FIGURE 300 BOXPLOT OF δ13C VALUES OF MEN AND WOMEN SHOWING THE OVERALL HIGHER VALUES δ13C OF MEN 469
FIGURE 301 SCATTERPLOT OF δ13C AND δ15N VALUES BY AGE.....471
FIGURE 302 BOXPLOT OF δ15N VALUES OF ADULTS, MATURES AND SENILES SHOWING SLIGHTLY BUT NOT SIGNIFICANTLY LOWER VALUES IN ADULTS.....471
FIGURE 303 BOXPLOT OF δ13C VALUES OF MALES AND FEMALES SHOWING NO DIFFERENCE BETWEEN THE AGE GROUPS 471
FIGURE 304 SCATTERPLOT OF δ13C AND δ15N VALUES BY LAYER.....472
FIGURE 305 BOXPLOT OF δ15N VALUES OF MALES AND FEMALES SHOWING NO SIGNIFICANT DIFFERENCE BETWEEN THE LAYERS.....472
FIGURE 306 BOXPLOT OF δ13C VALUES OF MALES AND FEMALES SHOWING NO SIGNIFICANT DIFFERENCE BETWEEN THE LAYERS.....472
FIGURE 307 SCATTERPLOT OF δ13C AND δ15N VALUES BY BURIAL LOCATION 474
FIGURE 308 BOXPLOT OF δ15N VALUES SHOWING THE SIGNIFICANT DIFFERENCE BETWEEN CLOISTER AND CEMETERY BURIALS 474
FIGURE 309 BOXPLOT OF δ13C VALUES SHOWING THE SIGNIFICANT DIFFERENCE BETWEEN CLOISTER AND CEMETERY BURIALS 474
FIGURE 310 SCATTERPLOT OF δ13C AND δ15N VALUES BY DISTANCE TO THE CHURCH.....476
FIGURE 311 BOXPLOT OF δ15N VALUES SHOWING THE GRADUAL DECREASE IN δ15N FROM CLOISTER BURIALS TO BURIALS FAR AWAY FROM CHURCH.....476
FIGURE 312 BOXPLOT OF δ13C VALUES SHOWING THE GRADUAL DECREASE IN δ13C 15N FROM CLOISTER BURIALS TO BURIALS FAR AWAY FROM CHURCH 476
FIGURE 313 SCATTERPLOT OF MEAN $\delta^{13}C$ AND $\delta^{15}N$ VALUES WITH SD OF THE KNUEDLER SAMPLE SEPARATED BY BURIAL LOCATION COMPARED TO FAUNAL REMAINS FROM CONTINENTAL EUROPE 483
FIGURE 314 SCATTERPLOT ILLUSTRATING THE DIFFERENCES IN $\delta^{13}C$ AND $\delta^{15}N$ VALUES BETWEEN CEMETERY AND CLOISTER/CHURCH BURIALS AT THE KNUEDLER SITE (LUXEMBOURG), AT AALST (BELGIUM) AND AT GREVENMACHER (LUXEMBOURG) 488

14 Acknowledgments

Foremost, I want to thank my supervisors for their ongoing support while writing this dissertation, Prof. J. Wahl for answering my questions on interpretations of the anthropological data, and Prof. H. Bocherens for providing helpful guidance on the interpretation of the results of the stable isotope analysis.

Additionally, I want to thank Mme. Bis-Worch and the Institut National de Recherches Archéologiques (INRA) of Luxembourg for providing the human remains analysed in this study, for providing me with the rooms and equipment to clean all the remains before analysis and for supporting some of the laboratory analyses.

Furthermore, this work would not have been possible without the AFR-PhD funding granted by the FNR (Fondation Nationale de Recherche) in Luxembourg.

I also want to thank Dr. M. Francken for access to the osteological collections at the start of my PhD when I did not have an office yet and for the invaluable help in identifying some of the trickier pathological lesions observed in the skeletal remains. In the same way I also want to thank Dr. J. Gresky and Dr. E. Petiti as well Dr. M. Díaz Zorita-Bonilla for providing guidance on some pathological lesions and the former as well for allowing me to use the equipment at the DAI (Deutsches Archäologisches Institut) to take radiographs of some pathologically altered bones.

I want to thank Dr. S. Afad from the KRONA clinic, Mr. A. Tröscher, Dr. G. Ferreira and Mrs. C. Kyriakouli from the palaeontology department at the University of Tübingen for granting me access to and assisting with medical, respectively Micro-Ct-scanning of pathological bone lesions.

Furthermore, I want to thank all my friends, my WG past and present as well as the Everest/Hölderlinstrasse Stammtisch for the wonderful moments spent together and their support throughout this PhD journey. Special thanks go to Monice Timm who also assisted me with photography and editing (all photos on black background) and let me borrow her photographic equipment.

Lastly, I want to thank my parents and my sister for their unwavering support and encouragements and for taking the time to proofread parts of the thesis.